ARTICLE *Multiple Sclerosis* 2006; **12**: 309–320

A prospective open-label study of glatiramer acetate: over a decade of continuous use in multiple sclerosis patients

CC Ford[1], KP Johnson[2], RP Lisak[3], HS Panitch[4], G Shifroni[5], JS Wolinsky[6] and The Copaxone® Study Group

A decade of continuous glatiramer acetate (GA) use by relapsing remitting multiple sclerosis (RRMS) patients was evaluated in this ongoing, prospective study, and the neurological status of 'Withdrawn' patients was assessed at a 10-year long-term follow-up (LTFU) visit. Modified intention-to-treat (mITT, $n = 232$) patients received ≥ 1 GA dose since 1991; 'Ongoing' patients ($n = 108$) continued in November 2003. Of 124 patients, 50 Withdrawn patients returned for LTFU. Patients were evaluated every six months (EDSS). Mean GA exposure was 6.99, 10.1 and 4.26 years for mITT, Ongoing, and Withdrawn/LTFU patients, respectively. While on GA, mITT relapse rates declined from 1.18/year prestudy to ~ 1 relapse/5 years; median time to ≥ 1 EDSS point increase was 8.8 years; mean EDSS change was 0.73 ± 1.66 points; 58% had stable/improved EDSS scores; and 24, 11 and 3% reached EDSS 4, 6 and 8, respectively. For Ongoing patients, EDSS increased 0.50 ± 1.65; 62% were stable/improved; and 24, 8 and 1% reached EDSS 4, 6 and 8, respectively. For Withdrawn patients at 10-year LTFU, EDSS increased 2.24 ± 1.86; 28% were stable/improved; and 68, 50 and 10% reached EDSS 4, 6 and 8, respectively. While on GA nearly all patients (mean disease duration 15 years) remained ambulatory. At LTFU, Withdrawn patients had greater disability than Ongoing patients. *Multiple Sclerosis* 2006; **12**: 309–320. www.multiplesclerosisjournal.com

Key words: disability; disease modifying therapy; EDSS; glatiramer acetate; immunomodulator; relapse; relapsing-remitting multiple sclerosis

Introduction

Currently, the best therapeutic options for relapsing remitting multiple sclerosis (RRMS) patients are the disease-modifying therapies: glatiramer acetate (GA) and the beta-interferons, subcutaneous (SC) IFNβ-1b, SC IFNβ-1a, and intramuscular (IM) IFNβ-1a [1]. There is growing consensus that immunomodulatory therapy should begin shortly after RRMS diagnosis, and to prevent or delay progression of disability, continuous therapy may be recommended for many years [1–3]. However, evidence of long-term clinical efficacy, safety, and patient acceptance of immunomodulatory therapy is scarce. Indeed, the designation 'long-term' to describe clinical data for immunomodulators is arbitrary – three to five years [4–6], is a relatively short interval considering the predicted treatment duration and disease course noted in MS natural history studies [2].

The ongoing US Glatiramer Acetate Trial began in 1991 and is unique in that it is the only organized, ongoing, open-label study of more than 10 years duration to prospectively evaluate

[1] MIND Imaging Center, Albuquerque, NM, USA
[2] Maryland Center for MS, Baltimore, MD, USA
[3] Wayne State University, Detroit, MI, USA
[4] University of Vermont, Burlington, VT, USA
[5] Teva Pharmaceutical Industries Ltd., Petah Tiqva, Israel
[6] University of Texas Health Science Center at Houston, Houston, TX, USA
Author for correspondence: Kenneth P Johnson, MD, Maryland Center for Multiple Sclerosis, 11 S. Paca Street, 4th Floor, Baltimore, MD 21201, USA. E-mail: kjohnson@som.umaryland.edu
Received 30 June 2005; accepted 22 November 2005

© 2006 Edward Arnold (Publishers) Ltd 10.1191/135248506ms1318oa

continuous immunomodulatory therapy in RRMS patients. Prospective clinical efficacy data were reported for continuous IFNβ-1b (Betaseron®) use at four to five years, continuous IFNβ-1a SC (Rebif®) at four years, and continuous IFNβ-1a IM (Avonex®) at approximately two years after initiation of their respective pivotal double-blind trials [4–6]. Further data have since been collected in non-continuous and/or retrospective, open-label extensions of these studies. In some cases, data were collected retrospectively after considerable intervals in which patients were not monitored and during which they may have discontinued, switched, or added other medications to the immunomodulatory therapy under study. Another MS treatment, natalizumab (Tysabri®) remains under investigation; reported efficacy data reflect only two years of clinical experience and the full serious side effect profile of this drug remains uncertain [7].

This GA study began with a double-blind, placebo-controlled phase in which 251 RRMS patients were randomized to receive GA (20 mg) or placebo by SC injection daily [8,9]. After double-blind treatment for a mean of 30 months, all patients were offered active treatment as part of an ongoing, prospective, open-label study. Reported clinical efficacy results six and eight years after randomization of GA therapy comparing differences in clinical outcomes between patients who received GA from study inception versus those in patients who began treatment approximately 2.5 years later (ie, patients originally randomized to placebo), demonstrate the benefits of early GA therapy compared with delayed therapy [10–12].

This paper describes long-term experience with GA in all patients who received it during the double-blind and/or open-label phases of the study. The primary aim was to determine the long-term effects of GA in carefully monitored patients who had received continuous GA for a mean of 10 years. A secondary goal was to gather information on patients who had withdrawn from the study – their disease course while in the study and why they discontinued. Those who agreed to return for the long-term follow-up (LTFU) visit were evaluated for their neurologic status approximately 10 years after they had initiated GA therapy.

Methods

Patients in this study were originally enrolled in the US Glatiramer Acetate Pivotal Trial, a double-blind, randomized, placebo-controlled study that began in October 1991. RRMS patients who had experienced two or more medically documented relapses in the previous two years and had EDSS scores between 0 and 5 at entry, were randomized to receive SC GA (20 mg) or placebo daily, administered by self-injection. After double-blind treatment, all patients who had entered the study were given the option to continue in an open-label extension phase. Those patients originally randomized to GA continued to take the drug and those randomized to placebo switched to GA. Details of the double-blind and open-label phases of the study are described elsewhere [8–12]. The modified intention-to-treat (mITT) population in the study reported here differs from the original ITT cohort in the pivotal trial [8], in that this analysis includes only patients who have received at least one dose of GA (19 patients initially randomized to placebo in the pivotal study declined entry into the open-label extension and are excluded from this mITT cohort).

Data cut-off for this analysis occurred in November 2003, a mean of 10.1 years from the beginning of GA therapy for the 108 patients continuing in the ongoing study. Because 10 years was the *mean* treatment duration, patients who had received GA from randomization had been treated for up to 12 years and patients originally randomized to placebo had been actively treated for approximately eight to nine years.

This organized, prospective study is ongoing. The 11 original US academic centers continue to participate, and the Institutional Review Boards at all centers continue to approve the study.

Study design

Ongoing study procedure

Briefly, in the open-label study, neurological status is evaluated in the clinic every six months using the Kurtzke Expanded Disability Status Scale (EDSS) [13]. Patients are examined, usually within seven days, if they experience symptoms suggestive of a relapse (appearance or reappearance of one or more neurologic abnormalities persisting for at least 48 hours, preceded by a stable or improving neurological state of at least 30 days duration [8–12]). Incidence, severity, and potential cause of adverse events are recorded; serious adverse events are reported to the sponsor and to the FDA as required by protocol. The safety of GA therapy in these patients at 2 [8], 3 [9], 6 [10], and 8 [12], years has been reported previously. During the open-label phase, laboratory assessments (chemistry panel) and vital signs are documented at six-month study visits. In most cases, the same neurologists and study co-ordinators continue to assess patients at each visit.

Any patient who discontinued daily GA, for whatever reason, and/or took another immunomodulator was withdrawn. Therefore, those who remain in the study represent a group of RRMS patients receiving only continuous GA monotherapy for disease modification.

Upon withdrawal, patients were classified by study personnel as: (1) withdrawal due to adverse event; (2) lost-to-follow-up, which included withdrawal from the study without attending a final visit or providing a reason for withdrawal; (3) withdrawal due to 'patient decision'; or (4) withdrawal for other reason(s). Because of overlap in reasons for leaving, the 'patient decision' and 'other' categories were combined. The 'patient decision/other' category was divided into subcategories based on comments patients provided at termination. Subcategories included (but were not limited to) pregnancy, inability to adhere to study protocol (eg, lack of transportation or moving away), a desire to switch or combine therapies, and perceptions of disease worsening. Patients were assigned to a subcategory based on the consensus judgment of three study personnel who independently reviewed patient comments provided at the final visit.

Long-term follow-up visit procedure

Personnel at each center made repeated attempts to contact all study patients who had received GA and withdrawn, to invite them to return for a single LTFU visit at approximately 10 years after GA start. LTFU visits were conducted between July and December 2003. At the LTFU visit, patients underwent neurological evaluation by EDSS, medical history during the time between study discontinuation and LTFU was recorded, and patients were asked what MS medications they had taken during the period between withdrawal and the LTFU visit.

Patient cohorts

The mITT cohort ($n = 232$) included all patients who had received at least one GA dose since study inception. Data reported for the mITT cohort reflect outcomes measured while patients were receiving GA. The mITT cohort was subdivided into the following cohorts: Ongoing, which comprised patients continuing in the study (and, by definition, continuing on GA) at the time of data cut-off, November 2003; Withdrawn Total, which comprised all patients who withdrew from the study before November 2003; Withdrawn with LTFU cohort, which included patients who withdrew from the study and returned for a single LTFU visit 10 years after GA start; and Withdrawn without LTFU cohort, which included patients who withdrew from the study and could not be reached or declined LTFU.

Statistical methods

Baseline demographic and disease characteristics were analysed using descriptive statistics and statistical inference tests (SAS® software, SAS Institute, Cary, NC, USA); comparisons among cohorts were performed using χ^2 for categorical variables and the Wilcoxon non-parametric test for continuous variables. Time to study withdrawal was estimated using Kaplan–Meier survival analysis.

Outcome measures

The yearly relapse rate was calculated by dividing the total number of relapses by the total number of patients in the mITT cohort entering a given treatment year. Accumulated disability was measured by mean EDSS and mean change in EDSS from GA start to the last observation while on GA in all study cohorts, and at LTFU in the Withdrawn with LTFU cohort. Confirmed progression of disability was defined as an increase of ≥ 1.0 EDSS point sustained for at least two clinical assessments, six months apart. Categorical analyses of patients' neurological status were performed; patients were classified as 'stable/improved' if EDSS scores increased by ≤ 0.5 EDSS points, did not change, or decreased from onset of treatment. Categorical analyses were repeated with patients stratified by entry EDSS score (0–2 or ≥ 2.5).

The number of patients who reached confirmed scores of EDSS 4, 6 or 8 while on GA were obtained for the mITT, Ongoing, and Withdrawn Total cohorts (only patients who began GA therapy with EDSS scores lower than the endpoint were included in these analyses). Additionally, Kaplan–Meier survival analysis was used to estimate the time to EDSS 4, 6 and 8 while on GA.

For comparison at 10 years between Ongoing and Withdrawn with LTFU patients, numbers of patients who reached predefined EDSS thresholds by the last observation for Ongoing patients and at the single LTFU visit for Withdrawn with LTFU patients were assessed. Efficacy comparisons at 10 years were made using analysis of covariance (ANCOVA) for change from GA start in EDSS, in which EDSS at GA start was a covariate in the model; χ^2; and when appropriate, Fisher's Exact

Test for categorical change in EDSS and for attainment of predefined EDSS thresholds.

Results

Patient characteristics

A total of 232 patients from 11 US study sites who had received at least one dose of GA since study inception comprised the mITT cohort (Figure 1). One patient discontinued after receiving GA but before undergoing neurological evaluation; therefore, the efficacy evaluable mITT cohort included 231 patients. As of November 2003, 108/232 patients (47%) remained in the study and comprised the Ongoing cohort. Of 124 (53%) patients in the Withdrawn Total cohort, 50 returned for the LTFU visit (Withdrawn with LTFU cohort). In the Withdrawn without LTFU cohort ($n=74$), 27 patients declined the LTFU visit and 47 could not be reached, including five patients known to have died. Deaths occurred one to six years after study withdrawal; three deaths were at least partly attributed to MS complications, there was no information about one death, and one death was listed as sudden and unexplained.

There were no differences among study cohorts in age, gender, disease duration, or annualized relapse rate in the two years before beginning GA (Table 1). Mean MS disease duration at GA start was 8.3 years in the mITT cohort.

Patient withdrawal

The Kaplan–Meier estimate of the median time from GA start to withdrawal in the mITT cohort was 9.2 years. Patients who withdrew had slightly higher EDSS scores at GA start than those who remained in the study (3.00 ± 1.59 [SD] versus 2.56 ± 1.35, respectively; $P=0.03$). Mean duration of GA treatment was 4.26 ± 3.13 [SD] years (range: 0.2–11.5 years) in the Withdrawn Total cohort (Table 2). When separated into subcohorts, GA exposure was 4.47 ± 2.95 years (range: 0.2–10.4) in the Withdrawn with LTFU cohort, and 4.13 ± 3.26 years (range: 0.2–11.5) in the Withdrawn without LTFU cohort. There were no statistical differences in demographic or disease characteristics at GA start between Withdrawn patients who returned for LTFU and Withdrawn patients who did not return (Table 1).

Reasons for patient withdrawal are listed in Table 3. The most common ($\geq1\%$) adverse events leading to discontinuation were local injection-site reactions (eg, erythema, pain), vasodilation, dyspnea, and urticaria. Patients who left due to the perception that their disease was worsening were not evaluated by objective neurological testing at the time of withdrawal; therefore, whether individual patients had worsened by objective criteria is unknown. The mean change in EDSS score from GA start to the last observed on-treatment EDSS value for all patients in the patient decision/other category ($n=87$) was 1.16 ± 1.65 [SD] and mean EDSS changes in the Withdrawn Total and

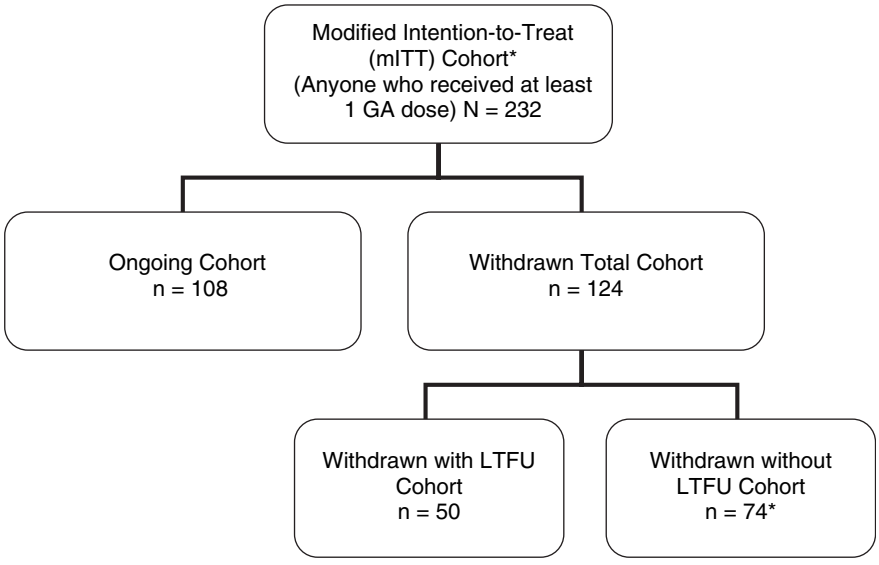

Figure 1 Study cohorts. One patient (in the Withdrawn without LTFU cohort) withdrew after a single GA dose and before an on-treatment neurological evaluation; therefore, 231 patients comprised the efficacy evaluable mITT cohort.

Table 1 Patient characteristics at GA start

	mITT ($n=232$)	Ongoing ($n=108$)	Withdrawn total ($n=124$)	*P* value[a]	Withdrawn with LTFU ($n=50$)	Withdrawn without LTFU ($n=74$)	*P* value[b]
Age (years)							
Mean ± SD	35.5 ± 6.4	36.6 ± 5.7	34.8 ± 6.8	0.0918	35.2 ± 6.6	34.6 ± 7.0	0.6787
Range	19.0–48.6	22.0–48.6	19.0–47.9		19.0–46.7	19.0–47.9	
Female *n* (%)	170 (73%)	77 (71%)	93 (75%)	0.5248	33 (66%)	60 (81%)	0.0581
Disease duration (years) at GA start							
Mean ± SD	8.3 ± 5.1	8.4 ± 5.1	8.1 ± 5.2	0.8013	8.6 ± 6.2	7.8 ± 4.3	0.7373
Median	7.23	6.85	7.49		7.34	7.66	
Range	0.6–25.7	1.1–23.9	0.6–25.7		0.6–25.7	0.6–18.0	
Annualized relapse rate two years before GA start							
Mean ± SD	1.18 ± 0.82	1.11 ± 0.82	1.24 ± 0.83	0.2286	1.09 ± 0.68	1.34 ± 0.90	0.0760
Median	1.00	1.00	1.00		1.00	1.00	
Range	0–5.5	0–3.5	0–5.5		0–3.0	0–5.5	

[a]Ongoing versus Withdrawn Total.
[b]Withdrawn with LTFU versus Withdrawn without LTFU.

mITT cohorts were 0.94 ± 1.65 and 0.73 ± 1.66, respectively (Table 2).

The LTFU visit for Withdrawn patients occurred at a mean of 10.0 years after GA start. These patients were asked about other disease modifying therapies they had taken for MS in the interval between leaving the study and the LTFU visit. Of the 50 Withdrawn with LTFU patients, four patients reported taking no medications, no data were available for eight patients, and 38 reported they took a variety of agents over the interval, often in combination, for varying lengths of time: 13 patients took GA, 32 took an IFNβ drug, 14 took an immunosuppressive agent (mitoxantrone, methotrexate, azathioprine, cyclophosphamide), 10 took corticosteroids, and five took 'other' drugs for MS. At the time of the LTFU visit, 10 patients were taking GA, 16 were taking an IFNβ drug, four were taking an immunosuppressor agent (mitoxantrone, methotrexate), and one was receiving intravenous immunoglobulin (IVIg).

Efficacy

mITT cohort while on GA

Relapse rate. The medically documented annualized relapse rate in the mITT cohort during the two years before beginning GA therapy was 1.18 ± 0.82 [SD] (Table 1). While on GA, yearly relapse rates declined approximately 50% to 0.61 ± 0.85 in treatment year 1 and continued to decline so that in treatment year 4, patients experienced the equivalent of one relapse every four years. Yearly relapse rates are shown in Figure 2 (after year 9, the mITT cohort comprised only patients who had received GA from randomization). Low relapse rates were maintained over all subsequent years; relapse rates were reduced by >80% from rates at GA start to approximately one relapse every five years.

Accumulated disability. Mean and median GA treatment durations for the mITT, Ongoing, and Withdrawn Total cohorts, overall and according to drug assignment at randomization, are shown in Table 2. Mean GA exposure time in the Ongoing cohort was 10.1 ± 1.32 years and in the Withdrawn Total cohort was 4.26 ± 3.13 years. Also shown are EDSS scores and changes in EDSS scores from GA start to the last measurement while on GA.

The Kaplan–Meier estimate of the median time to confirmed (verified at two six-month clinical visits) progression of ≥1.0 EDSS point while on GA was 8.82 years in the mITT cohort. Proportions of patients with at least one confirmed progression of 1.0 EDSS point while on GA were 42% of the mITT cohort, 42% of the Ongoing cohort, and 43% of the Withdrawn Total cohort.

Categorical analysis showed 58% of patients in the mITT cohort maintained stable/improved EDSS scores between GA start and their last on-treatment EDSS assessment. Proportions of patients in the Ongoing and Withdrawn Total cohorts with stable/improved EDSS scores while on GA were 62 and 55%, respectively. When patients were stratified by entry EDSS (0–2 and ≥2.5), proportions of patients with stable/improved EDSS scores while on GA were similar in both strata in all cohorts (Table 2), indicating no difference in GA effect regardless of disability level at GA start. Figure 3 shows a high proportion of patients (59–79%) in the mITT cohort (cohort size each year shown in Figure 2) had stable/improved EDSS scores each treatment year.

Table 4 shows the number of patients in each cohort who reached predefined EDSS thresholds.

Table 2 GA exposure and EDSS measures while on GA

While on GA	mITT ($n=232$)		Ongoing ($n=108$)		Withdrawn Total ($n=124$)	
GA exposure (years)						
Mean ± SD	6.99 ± 3.82		10.12 ± 1.32		4.26 ± 3.13	
Median	8.62		9.16		3.55	
Range	0.2–11.9		7.9–11. 9		0.2–11.5	
GA exposure based on drug assignment at randomization (years)	PL[a] ($n=107$)	GA ($n=125$)	PL ($n=55$)	GA ($n=53$)	PL ($n=52$)	GA ($n=72$)
Mean ± SD	6.25 ± 3.30	7.63 ± 4.13	8.84 ± 0.23	11.44 ± 0.20	3.50 ± 2.75	4.81 ± 3.28
Median	8.50	9.22	8.90	11.44	2.62	4.26
Range	0.2–9.2	0.2–11.9	7.9–9.2	10.9–11.9	0.2–8.9	0.2–11.5
EDSS score at GA start						
Mean ± SD	2.79 ± 1.50		2.56 ± 1.35		3.00 ± 1.59	
Median	2.50		2.25		3.00	
Range	0.0–7.0		0.0–6.0		0.0–7.0	
EDSS at last observation[c]						
Mean ± SD	3.53 ± 2.08		3.06 ± 1.78		3.94 ± 2.25	
Median	3.00		2.50		3.50	
Range	0.0–9.0		0.0–8.0		0.0–9.0	
EDSS change from GA start to last observation[b]						
Mean ± SD	0.73 ± 1.66		0.50 ± 1.65		0.94 ± 1.65	
Median	0.50		0.50		0.50	
Range	−3.5 to 5.5		−3.5 to 5.5		−3.5 to 5.5	
Clinically stable/improved EDSS[c] score while on GA[b]						
Overall	134/231 (58%)		67/108 (62%)		67/123 (55%)	
EDSS 0–2 at GA start	58/103 (56%)		30/54 (56%)		28/49 (57%)	
EDSS ≥2.5 at GA start	76/128 (59%)		37/54 (69%)		39/74 (53%)	

[a]PL, placebo.
[b]$n=231$ in mITT cohort and $n=123$ in Withdrawn total cohort (one patient had no post-GA-start EDSS score).
[c]Defined as an increase of ≤0.5 point, no change, or decrease in EDSS score from onset of treatment.

Table 3 Reasons for patient withdrawal

Reason for withdrawal	*n*	Patient decision/other subcategories[a]	*n*
Total	124	Total	87
Lost-to-follow-up	14	Patient perception of disease worsening	27
Adverse event	23	Desire to switch or combine therapies	22
Patient decision/other	87	Difficulty, inability, or unwillingness to adhere to study protocol	30
		Pregnancy	8

[a]Patient decision/other subcategories were derived from written comments provided by Withdrawn patients at their final visit.

These analyses include only patients with EDSS scores at GA start below EDSS 8 (all patients), EDSS 6 ($n=221$), or EDSS 4 ($n=169$). Inclusion criteria in the original double-blind phase of the study was limited to patients with EDSS ≤ 5, however, 10 original placebo patients had an EDSS ≥ 6 when they started GA therapy in the open-label phase of the study. Mean EDSS scores at GA start were 2.07 ± 0.95 [SD], 2.64 ± 1.34, and 2.79 ± 1.50 in patient groups with EDSS scores at GA start below EDSS 4, 6 and 8, respectively. In the mITT cohort, fewer than 25% of patients reached a score of EDSS 4, approximately 11% reached EDSS 6, and 3% reached EDSS 8 while on GA. Due to differences in GA exposure among cohorts, Kaplan–Meier survival analysis was used to estimate the time to the predefined EDSS thresholds (mITT cohort shown in Figure 4). The time to 25% of patients reaching EDSS 4 was 6.58 years in the mITT cohort, 9.08 years in the Ongoing cohort, and 5.47 years in the Withdrawn Total cohort. In the Withdrawn Total cohort, median time to EDSS 4 occurred at 9.91 years. Fewer than 25% of patients in the mITT, Ongoing, and Withdrawn Total cohorts reached EDSS 6 or 8 by the end of the analysis period.

Clinical comparison between Ongoing and Withdrawn patients at ten years/LTFU

Accumulated disability

The occurrence of relapse after leaving the study was not systematically documented by prospective neurological assessments; therefore, these data were not available. Neurological assessments of disability at LTFU for Withdrawn patients were made at a mean of 10.0 years from starting GA therapy. For Ongoing patients, EDSS data reflected the last observation before data cut-off.

At LTFU, patients who had withdrawn showed significantly increased disability compared with

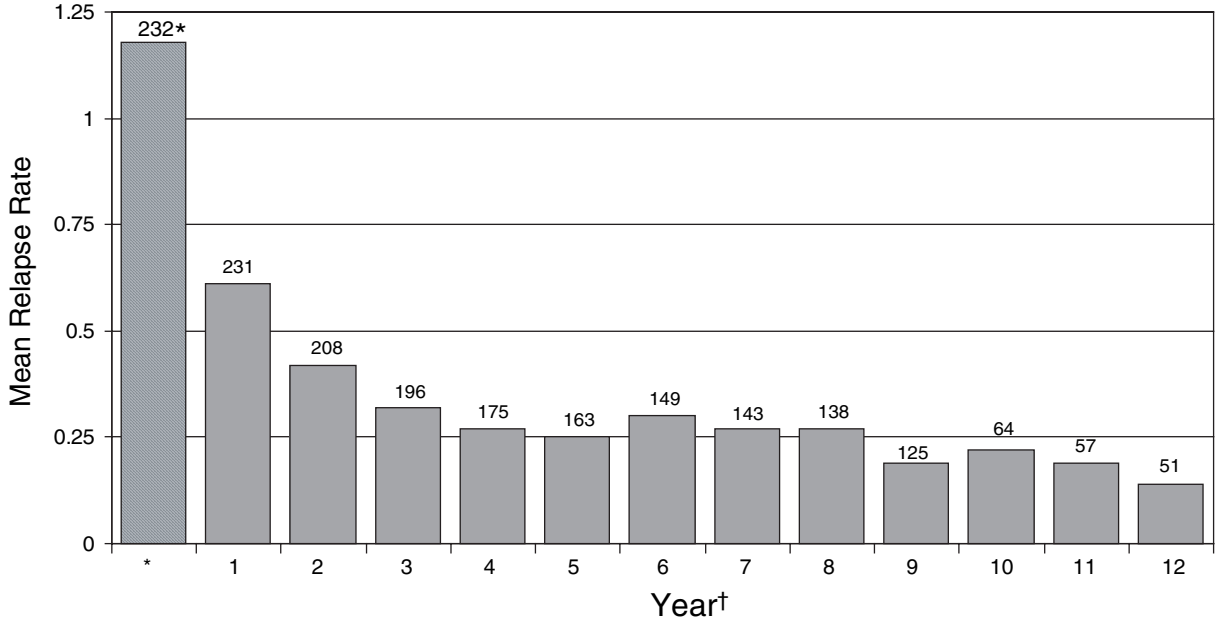

Figure 2 Yearly Relapse Rate from GA Start (mITT Cohort, *n*=231). *Mean [SD] annualized relapse rate in the mITT cohort in the 2 years before GA start was 1.18 ± 0.82. †Reflects treatment duration from GA start to the year listed. Numbers of patients evaluated in each treatment year are shown above bars; after year 9, the mITT cohort comprised only patients randomized to GA in the double-blind phase of the study (placebo/active group had a shorter duration of GA exposure).

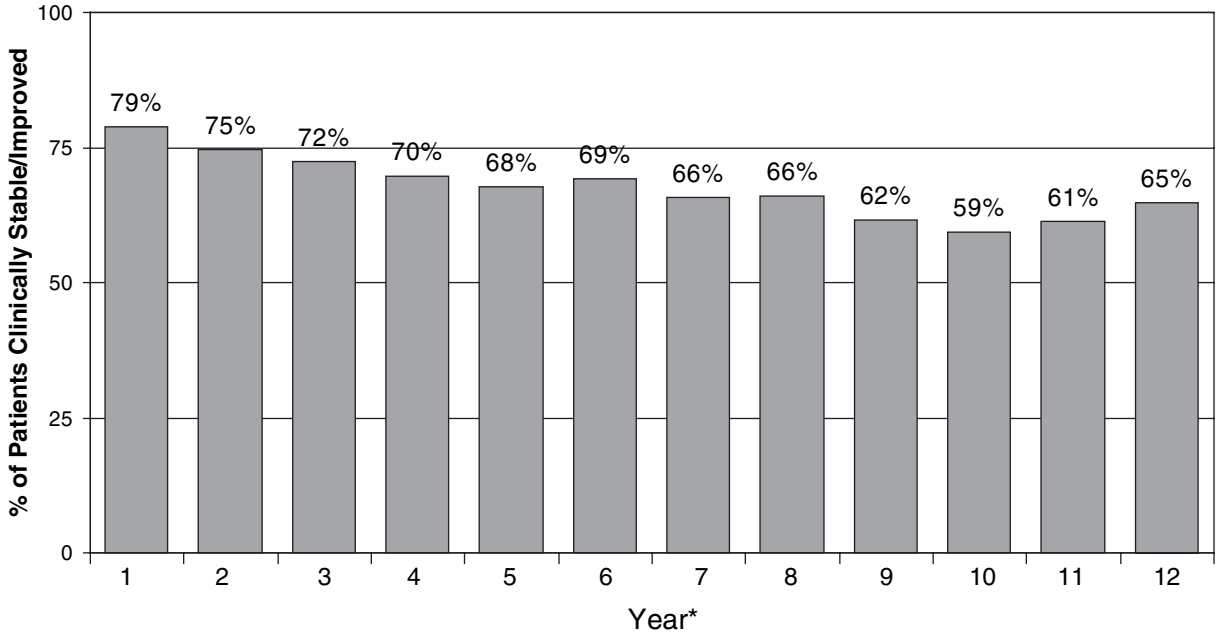

Figure 3 Yearly Percent of Patients on GA with stable/improved EDSS. Scores from GA start (mITT cohort: $n = 231$). *Reflect treatment duration from GA start to the year listed (the number of patients in the mITT cohort each treatment year is shown in Figure 2). Clinically stable/improved = an increase of ≤ 0.5 point, no change, or decrease in EDSS score from onset of GA treatment.

Ongoing patients (Table 5). The mean increase in EDSS score was 2.24 ± 1.86 [SD] points in the Withdrawn with LTFU cohort compared with a 0.50 ± 1.65 point increase in Ongoing patients. Similarly, 62% of Ongoing patients had stable or improved EDSS scores compared with 28% of Withdrawn with LTFU patients (while receiving GA, 56% of patients in the Withdrawn with LTFU cohort had stable/improved EDSS scores). Finally, at 10 years, 24% of patients in the Ongoing cohort had reached EDSS 4, 8% had reached EDSS 6, and 1% had reached EDSS 8, compared with 68, 50 and 10%, respectively, in the Withdrawn with LTFU cohort.

Safety

The most commonly reported adverse events in patients receiving long-term GA, regardless of whether the investigator judged them to be related to GA therapy or not, were accidental injury, asthenia, paresthesia, upper respiratory and urinary tract infections, headache, and pain. Adverse events thought to be associated with GA therapy included local injection-site reactions (eg, erythema, pain, mass, edema) and symptoms associated with an immediate post-injection reaction (IPIR), which may have included vasodilation, chest pain, palpitation, tachycardia, or dyspnea. Reporting of injection-site reactions and symptoms associated with IPIR declined over time. No apparent time-dependent adverse events emerged. Moreover, no evidence of hematologic, hepatic, or renal dysfunction; immunosuppression; emergence of malignancy; or development of other autoimmune disease was observed.

Table 4 Number of patients reaching EDSS 4, 6 and 8 while on GA (confirmed)

While on GA	mITT[a] n/N[b] (%)	Ongoing n/N[b] (%)	Withdrawn Total n/N[b] (%)	Disease duration at GA start mITT[a] mean years $\pm$ SD	GA exposure mITT[a] mean years $\pm$ SD
EDSS 4	40/169 (24%)	20/84 (24%)	20/85 (24%)	7.79 ± 5.00	7.16 ± 3.77
EDSS 6	24/221 (11%)	8/106 (8%)	16/115 (14%)	8.10 ± 5.01	7.11 ± 3.81
EDSS 8	6/231 (3%)	1/108 (1%)	5/123 (4%)	8.26 ± 5.12	6.99 ± 3.82

[a]mITT cohorts included all patients below the EDSS threshold at GA start.
[b]n = number of patients who reached EDSS endpoint (confirmed); N = number of patients who were below the EDSS threshold at GA start.

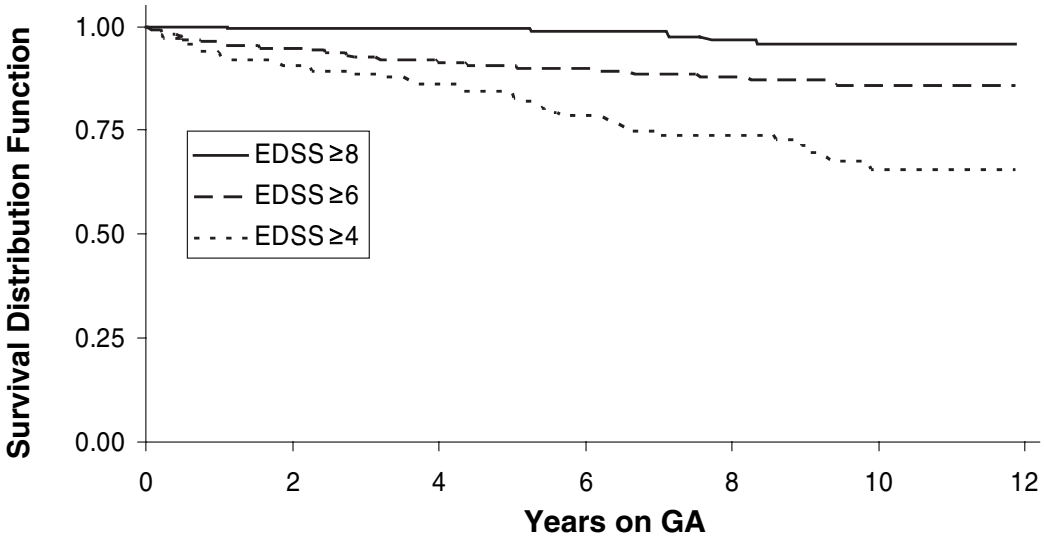

Cumulative Number of Patients Reaching Endpoint

EDSS 4	0	15	21	30	35	40	40
EDSS 6	0	11	17	19	22	24	24
EDSS 8	0	1	1	2	5	6	6

Figure 4 Time to confirmed EDSS 4, 6 and 8 while on GA (mITT cohort: $n = 231$). The mean disease duration in the mITT cohort was 8.3 years at GA Start.

Discussion

This ongoing study is the longest prospective, organized evaluation of continuous immunomodulatory therapy in MS [4,5,14,15]. In November 2003, nine to 12 years after beginning GA therapy, 47% of all patients who ever received GA remained in the study. These data provide an opportunity to evaluate the level of neurologic disability in patients who have continued to take GA for an

Table 5 EDSS data at 10 years/LTFU

EDSS measure	Ongoing ($n = 108$)	Withdrawn with LTFU[a] ($n = 50$)	*P* value
EDSS score			
Mean ± SD	3.06 ± 1.78	5.22 ± 2.21	<0.0001[c]
Median	2.50	6.00	
Range	0.0–8.0	1.0–9.0	
EDSS change from GA start			
Mean ± SD	0.50 ± 1.65	2.24 ± 1.86	<0.0001[c]
Median	0.50	2.25	
Range	−3.5 to 5.5	3.0–5.5	
Categorical analysis			
Clinically stable/improved	67/108 (62%)	14/50 (28%)	<0.0001[d]
Patients reaching EDSS 4, 6, or 8[b]			
EDSS 4 *n/N* (%)	20/84 (24%)	25/37 (68%)	<0.0001[d]
EDSS 6 *n/N* (%)	8/106 (8%)	23/46 (50%)	<0.0001[d]
EDSS 8 *n/N* (%)	1/108 (1%)	5/50 (10%)	<0.0125[e]

[a]EDSS level was not confirmed at six months in Withdrawn with LTFU patients, since LTFU comprised a single visit.
[b]n = number of patients who reached EDSS threshold (confirmed in Ongoing patients) and N = number of patients who were below the EDSS threshold at GA start.
[c]From ANCOVA adjusted for EDSS score at GA start.
[d]χ^2 Test.
[e]Fisher's Exact Test.

average of 10 years and compare it with that of patients who withdrew from the study (and may have used other MS therapies) then returned for neurological evaluation 10 years after beginning GA therapy.

Results of this study are consistent with mechanisms of action of GA, which address both the inflammatory and neurodegenerative aspects of MS pathology within the CNS. GA-reactive Th2 cells induce 'bystander' suppression of inflammation within the CNS by increasing anti-inflammatory cytokine production, and facilitate neuroprotection via enhanced secretion of neurotrophins [16–20]. Immunological effects of GA persist in MS patients for at least six to nine years with continued use [18,20].

Multiple measures demonstrated the majority of patients who remain on long-term GA therapy continued to do well. Relapse rates dropped by approximately one half in the first year of treatment and by years nine to 12, had declined more than 80% (Figure 2). A decline in relapse rate could signal transition to secondary progressive MS (SPMS). However, if this were the cause of the observed decline in relapse rates, a commensurate increase in disability would be expected over time. Although there was a slight trend toward increasing mean EDSS score over 10 years, the majority of patients in the mITT cohort (Figures 3 and 4) and in the Ongoing cohort exhibited stable or improved EDSS scores while on long-term GA therapy. The mean EDSS score in Ongoing patients increased only 0.50 points over 10 treatment years. Moreover, proportions of patients who progressed to predefined EDSS thresholds (Table 4) were much lower than what would be predicted based on MS natural history data [2,21,22]. Thus, the decline in relapse rate probably reflects treatment-related stabilization or improvement of the underlying disease process.

Although it would be of considerable interest to compare the long-term treatment effects of GA with similarly collected data for other available immunomodulators, the present study is the only prospective study with stipulated six-month assessments of neurologic status and safety to extend beyond four years. Furthermore, it is the only study in which patients must remain on the study drug and not switch or add concomitant immunotherapy. Additional deficiencies of other studies include involvement of very few patients [23], potential use of multiple therapies during unmonitored time periods [24], inclusion of different patient populations [25], or lack of information regarding disability or relapses [23,26].

An alternative method to evaluate these results in context is to use MS natural history data. Comparisons with published natural history reports must be made cautiously, since patient assessments are relatively infrequent and patient populations are likely to be less well defined. Furthermore, disability data in some cases reflect 'snapshot' assessments; whereas any accumulated disability was confirmed in this study at two clinical examinations six-months apart for patients while on GA therapy (withdrawal patient data at LTFU visit was not confirmed). Nevertheless, similarities between this study group and reported natural history cohorts, with respect to patients' disease duration and measures of disease progression, allow for general comparisons.

Before the availability of immunomodulatory therapies, Weinshenker *et al*. reported data from a geographically-based natural history cohort in Middlesex County, Ont., Canada ($n = 1099$ RRMS patients) [2]. This prospective study included yearly patient evaluations; by 15 years after disease onset, 50% of untreated patients had reached EDSS 6 and 10% had reached EDSS 8. In the current study, at the start of GA therapy the mITT cohort already had a mean disease duration since diagnosis of 8.3 years and mean EDSS score of 2.79. At the last observation on GA (mean disease duration approximately 15 years), only 11% of patients in the mITT cohort had reached a confirmed score of EDSS 6 and 3% had reached EDSS 8. Moreover, in the Ongoing cohort, only 8% of patients reached EDSS 6 and 1% reached EDSS 8 after 10 years of continuous GA therapy (Table 4). In another natural history cohort of RRMS patients ($n = 1562$) with approximately the same disease duration (median 11.4 years from diagnosis), Confavreux *et al*. [21], reported that almost half (48%) of the patients had reached EDSS 4. In the current study, only 24% of mITT patients, with a median disease duration of 15.2 years, reached a score of EDSS 4 while taking GA (Table 4).

Recently, data were reported from a population-based cohort evaluated for 10 years in Olmsted County, Minnesota ($n = 161$ patients with RRMS, SPMS, or primary progressive MS) [22]. Unlike the present study, patients were evaluated only twice – at the beginning and at the end of the 10-year period. Ten-year disability outcomes for Olmsted County patients with disease characteristics similar to this study's patients (RRMS and entry EDSS 0–5) compare less favorably with 10-year outcomes in Ongoing GA patients. Overall, 28% of patients in the Olmsted County cohort had reached a score of EDSS 6 and 7% had reached a score of EDSS 8 at 10 years, compared with 8 and 1%, respectively, of patients in this study.

Ongoing versus Withdrawn patients

Long-term study data provided an opportunity to evaluate reasons for patient withdrawal and how these patients fared during and after study participation. Patients who withdrew from this study did so for multiple reasons (Table 3). Comments reported in the 'patient decision/other' category suggest many patients withdrew for non-MS-related issues, such as lack of transportation to the study site or pregnancy, while some patients withdrew because they believed their disease was worsening. Although this was undoubtedly true in some cases, mean changes in EDSS scores while on GA in the 'patient decision/other' category were not substantially different from those of the Withdrawn Total or mITT cohort. In addition, many patients who withdrew fared well before leaving the study; more than half of all Withdrawn Total patients (55%) had improved or stable EDSS scores while on GA.

It is possible that withdrawal was influenced by the introduction of newly approved immunomodulatory therapies. During the early years of the study, patients participating in the placebo-controlled GA trial may have wanted to try an approved medication (Betaseron® and Avonex® were approved in 1993 and 1995, respectively) instead of continuing to take either an experimental drug or a placebo.

Findings at 10-year LTFU

Inferences regarding differences in GA treatment effects between Ongoing and Withdrawal with LTFU patients at a mean of 10.0 years from GA start must also be made cautiously. At LTFU, the majority of returning patients reported having taken multiple medications after leaving the study, frequently switching and/or combining disease modifying therapies.

At 10 years after beginning GA therapy, all measures indicated that Withdrawn with LTFU patients fared significantly worse than Ongoing patients (Table 5). At LTFU, only 28% of Withdrawal with LTFU patients had stable/improved EDSS scores, whereas, while they were active in the study (ie, taking GA for an average of 4.5 years), the proportion was twice as high (56%). Compared with Ongoing patients, EDSS increases were significantly higher in Withdrawn with LTFU patients and more patients in the latter cohort reached EDSS 4, 6 and 8. Thus, disability measures indicated these Withdrawn patients worsened over time, regardless of whether, how long, or which immunomodulatory therapy they took after leaving the study.

The favorable safety profile of GA therapy was maintained over long-term use. The most common adverse events associated with GA over the course of the study were local injection-site reactions and IPIR, which were reported with decreasing frequency as treatment duration increased. No other immune-mediated disorders, infections, or malignancies have been associated with long-term GA treatment. The willingness of RRMS patients to continue to self-administer daily GA SC injections for more than a decade attests to the excellent tolerability of the drug.

This study is the longest ever conducted to prospectively evaluate the efficacy and safety of continuous immunomodulator use in MS. Reduction of relapses over 10 years of GA therapy was sustained with minimal increase (<1 EDSS point) in confirmed disability. Patients continuing GA therapy for 10 years had an average disease duration of more than 18 years, yet nearly all remained ambulatory.

Acknowledgements

The authors acknowledge the assistance of Pippa Loupe, PhD, Teva Neuroscience, Kansas City, Missouri; Frederic Deutsch, BS, Teva Pharmaceutical Industries Ltd., Petah Tiqva, Israel; Sheila Owens, BS, Medical Communication Co., Inc., Sarasota, Florida; and The Copaxone® Study Group in the development of this manuscript. The Copaxone® Study Group includes the following investigative teams: University of Pennsylvania Medical Center, Clyde Markowitz, MD, Amy Pruitt, MD, Dorothea Pfohl, RN, BS, MSCN; University of New Mexico School of Medicine, Gary A Rosenberg, MD, Elida Greinel, RN; Wayne State University School of Medicine, Omar A Khan, MD, Deena Lisak, BS, MA, RN, Alexandros Tselis, MD, PhD, John Kamholz, MD, PhD, Christina Caon, MSN, RN; UCLA School of Medicine, Lawrence Myers, MD, W Baumhefner, MD, Ricki Klutch, RN; University of Maryland School of Medicine, Christopher Bever, MD, Eleanor Katz, RN; VASLCHCS/University of Utah, John Rose, MD, James B Burns, MD, Connie Kawai, RN; University of Rochester, Andrew Goodman, MD, Steven R Schwid, MD, Mary D Petrie, RN; Yale University School of Medicine, Jana Preiningerova, MD, Silva Markovic Plese, MD, George Blanco, MD; University of Southern California School of Medicine, Norman Kachuck, MD; University of Texas Health Science Center at Houston, Staley Brod, MD, PhD, J William Lindsey, MD, Myrna Koh, RN; University of Wisconsin Hospital and Clinic, Benjamin Brooks, MD, Jennifer Parnell, BA, Kathy Roelke, RN. Teva Pharmaceuticals Industries Ltd., David Ladkani, PhD, Shaul Kadosh, MS, Yafit Stark, PhD. This study was supported by grants from the Federal Food and Drug Administration

Orphan Drug Program No. FD-4000559-01, the National Multiple Sclerosis Society No. RG 2202-A-6 and Teva Pharmaceutical Industries Ltd., Petah Tiqva, Israel.

References

1. **Oger J, Freedman M.** Consensus statement of the Canadian MS Clinics Network on the use of disease modifying agents in multiple sclerosis. *Can J Neurol Sci* 1999; **26**: 274–75.
2. **Weinshenker BG.** The natural history of multiple sclerosis. *Neurol Clin* 1995; **13**: 119–46.
3. **Miller A, Cohen J, Ford C, Garmany G, Goodman A, Green B** *et al*. *National Multiple Sclerosis Society (NMSS): disease management consensus statement*. National MS Society, 2005.
4. **The PRISMS (Prevention of Relapses and Disability by Interferon-B-1a Subcutaneously in Multiple Sclerosis) Study Group, and the University of British Columbia MS/MRI Analysis Group**. PRISMS-4: long-term efficacy of interferon-β1a in relapsing MS. *Neurology* 2001; **56**: 1628–36.
5. **The IFNβ Multiple Sclerosis Study Group and The University of British Columbia MS/MRI Analysis Group**. Interferon beta-1b in the treatment of multiple sclerosis: final outcome of the randomized controlled trial. *Neurology* 1995; **45**: 1277–85.
6. **Jacobs LD, Cookfair DL, Rudick RA, Herndon RM, Richert JR, Salazar AM** *et al*. Intramuscular interferon beta-1a for disease progression in relapsing multiple sclerosis. The Multiple Sclerosis Collaborative Research Group (MSCRG). *Ann Neurol* 1996; **39**: 285–94.
7. **FDA Public Health Advisory**. Suspended marketing of Tysabri (natalizumab). Retrieved 31 March 2005, from http://www.fda.gov/cder/drug/advisory/natalizumab.htm
8. **Johnson KP, Brooks BR, Cohen JA, Ford CC, Goldstein J, Lisak RP** *et al*. Copolymer 1 reduces relapse rate and improves disability in relapsing-remitting multiple sclerosis: results of a phase III multicenter, double-blind placebo-controlled trial. The Copolymer 1 Multiple Sclerosis Study Group. *Neurology* 1995; **45**: 1268–76.
9. **Johnson KP, Brooks BR, Cohen JA, Ford CC, Goldstein J, Lisak RP** *et al*. Extended use of glatiramer acetate (Copaxone) is well tolerated and maintains its clinical effect on multiple sclerosis relapse rate and degree of disability. *Neurology* 1998; **50**: 701–708.
10. **Johnson KP, Brooks BR, Ford CC, Goodman A, Lisak RP, Meyers LW** *et al*. Glatiramer acetate (Copaxone): comparison of continuous versus delayed therapy in a six-year organized multiple sclerosis trial. *Mult Scler* 2003; **9**: 585–91.
11. **Johnson KP, Brooks BR, Ford CC, Goodman A, Guarnaccia J, Lisak RP** *et al*. Sustained clinical benefits of glatiramer acetate in relapsing remitting multiple sclerosis patients observed for 6 years. *Mult Scler* 2000; **6**: 255–66.
12. **Johnson KP, Ford CC, Lisak RP, Wolinsky JS.** Glatiramer acetate (Copaxone®): neurologic consequence of delaying glatiramer acetate therapy for multiple sclerosis: 8-year data. *Acta Neurol Scand* 2005; **111**: 42–47.
13. **Kurtzke JF.** Rating neurologic impairment in multiple sclerosis: an expanded disability status scale (EDSS). *Neurology* 1983; **33**: 1444–52.
14. **Clanet M, Kappos L, Hartung H-P, Hohlfeld R.** The European IFNβ-1a dose-comparison study. *Mult Scler* 2004; **10**: 139–44.
15. **Kappos L, Stam Moraga M, Alsop J, The PRISMS Study Group.** Long-term tolerability of interferon Beta-1a in relapsing-remitting multiple sclerosis: 6-year safety follow-up of the PRISMS study. Presented at the Joint Meeting of the American/European Committee for Treatment and Research in Multiple Sclerosis (ECTRIMS/ACTRIMS), Baltimore, MD, USA, 18–22 September, 2002: 334.
16. **Yong VW.** Differential mechanisms of action of interferon-β and glatiramer acetate in MS. *Neurology* 2002; **59**: 802–808.
17. **Gran B, Tranquill LR, Chen M, Bielekova B, Zhou W, Dhib-Jalbut S** *et al*. Mechanisms of immunomodulation by glatiramer acetate. *Neurology* 2000; **55**: 1704–14.
18. **Ragheb S, Abramczyk S, Lisak D, Lisak R.** Long-term therapy with glatiramer acetate in multiple sclerosis: effect on T cells. *Mult Scler* 2001; **7**: 43–47.
19. **Neuhaus O, Farina C, Wekerle H, Hohlfeld R.** Mechanisms of action of glatiramer acetate in multiple sclerosis. *Neurology* 2001; **56**: 702–708.
20. **Chen M, Conway K, Johnson KP, Martin R, Dhib-Jalbut S.** Sustained immunological effects of glatiramer acetate in patients with multiple sclerosis treated for over 6 years. *J Neurologic Sci* 2002; **201**: 71–77.
21. **Confavreux C, Vukusik S, Moreau T, Adeline P.** Relapses and progression of disability in multiple sclerosis. *N Engl J Med* 2000; **343**: 1430–38.
22. **Pittock SJ, Mayr WT, McClelland RL, Jorgensen NW, Weigand SD, Noseworthy JH** *et al*. Change in MS-related disability in a population-based cohort. *Neurology* 2004; **62**: 51–59.
23. **Karlik S, Kirk S, Nicolle E, Kremenchutzky M, Rice GPA.** Evidence for very long-term efficacy of interferon Beta 1B in relapsing remitting MS patients. Proceedings of the Seventeenth Annual Meeting of the European Committee for Treatment and Research in Multiple Sclerosis (ECTRIMS), Dublin, Ireland, 2001: 139.
24. **Paty D, Kappos L, Stam Moraga M, Alsop J, Abdalla J.** Long-term observational efficacy and safety follow-up of the PRISMS cohort. Proceedings of the Nineteenth Annual Meeting of the European Committee for Treatment and Research in Multiple Sclerosis (ECTRIMS), Milan, Italy, 2003: 555.
25. **Kinkel RP, Kollman C, Glassman A, Simon J, O'Connor P, Murray TJ** *et al*. Interferon beta-1a (Avonex®) delays the onset of clinically definite MS over 5 years of treatment: results from the CHAMPIONS study. Presented at the Fifty-sixth Annual Meeting of the American Academy of Neurology, San Francisco, CA, USA, 2004: D29.006.
26. **Fisher E, Rudick RA, Simon JH, Cutter G, Baier M, Lee J-C** *et al*. Eight-year follow-up study of brain atrophy in patients with MS. *Neurology* 2002; **59**: 1412–20.

ELSEVIER

Clinical Neurology and Neurosurgery 108 (2006) 250–254

Clinical Neurology and Neurosurgery

www.elsevier.com/locate/clineuro

Neuroprotection in multiple sclerosis

Dimitrios Karussis [a,*], Savas Grigoriadis [b,c], Eleni Polyzoidou [c], Nikolaos Grigoriadis [c], Shimon Slavin [d], Oded Abramsky [a]

[a] *Department of Neurology and the Agnes Ginges Center for Neurogenetics, Laboratory of Neuroimmunology, Hadassah University Hospital, Jerusalem, Ein-Karem IL-91120, Israel*

[b] *Department of Bone Marrow Transplantation, Hadassah University Hospital, Jerusalem, Ein-Karem IL-91120, Israel*

[c] *Department of Neurosurgery, AHEPA University Hospital, Aristotle University of Thessaloniki, 1 Stilp Kyriakidi Str., 54636 Thessaloniki, Greece*

[d] *Department of Neurology, Laboratory of Experimental Neurology and Neuroimmunology, AHEPA University Hospital, Aristotle University of Thessaloniki, 1 Stilp Kyriakidi Str., 54636 Thessaloniki, Greece*

Abstract

In chronic inflammatory diseases like multiple sclerosis (MS), neuroprotection refers to strategies aimed at prevention of the irreversible damage of various neuronal and glial cell populations, and promoting regeneration. It is increasingly recognized that MS progression, in addition to demyelination, leads to substantial irreversible damage to, and loss of neurons, resulting in brain atrophy and cumulative disability. One of the most promising neuroprotective strategies involves the use of bone marrow derived stem cells. Both hematopoietic and non-hematopoietic (stromal) cells can, under certain circumstances, differentiate into cells of various neuronal and glial lineages. Neuronal stem cells have also been reported to suppress EAE by exerting direct in situ immunomodulating effects, in addition to their ability to provide a potential source for remyelination and neuroregeneration. Preliminary results from our laboratory indicate that intravenous or intracerebral/intraventricular injection of bone marrow derived stromal cells could differentiate in neuronal/glial cells and suppress the clinical signs of chronic EAE. Both bone marrow and neuronal stem cells may therefore have a therapeutic potential in MS. It seems that future treatment strategies for MS should combine immunomodulation with neuroprotective modalities to achieve maximal clinical benefit.
© 2005 Elsevier B.V. All rights reserved.

Keywords: Multiple sclerosis; Neuroprotection; Stem cells; Bone marrow mesenchymal stromal cells

1. Introduction

Current treatments for MS are only partially effective, probably due to defective remyelinating-regenerating mechanisms, including insufficient growth factors and multipotential stem cells [1], resulting in chronic, cumulative disability and irreversible axonal/neuronal damage [2–4]. It has also been suggested that the course of MS proceeds in two phases [5,6], an initial inflammatory one and a degenerative one; thus, in order to improve treatment outcome in MS, additional therapeutic interventions are urgently needed other than immunomodulation.

First, it is essential to further explore the complicated relationship between the three key pathogenetic elements of MS, inflammation, demyelination and axonal damage. Inflammation can cause demyelination [7] and both inflammation and myelin destruction can damage the axons, inducing neurodegeneration [4,8–10]. It is increasingly recognized that certain aspects of inflammation may be beneficial for MS [11], causing neuroprotection via the local production of growth factors [12] or by direct cell to cell interactions with oligodendrocyte progenitors [6].

There are also significant indications of neurodegeneration in MS. Among them are amyloid precursor protein (APP) accumulation in neurons [13], reduction in the NAA/Cr ratio by MR spectroscopy (MRS) [14] (which correlates well with the degree of disability [2,15,16] even in the normally appearing white matter (NAWM) [17]), the presence of axonal ovoids/transected axons at the edge of and in the core of active lesions [2,18], along with the oxidative damage [19] of mitochondrial DNA and impaired activity

* Corresponding author. Tel.: +972 2 6776939/41; fax: +972 2 6437782.
E-mail address: karus@cc.huji.ac.il (D. Karussis).

0303-8467/$ – see front matter © 2005 Elsevier B.V. All rights reserved.
doi:10.1016/j.clineuro.2005.11.007

of mitochondrial enzyme complexes [20]. Furthermore, the reduction in axonal density in MS plaques [3] and in NAWM early in MS, and a more prominent reduction of axonal density in spinal cord NAWM in progressive MS patients [3,21] indicate that neurodegeneration appears early and is widespread in the CNS. Another sign of a late degenerative phase is that the time for EDSS progression from 0 to 4 is very variable, whereas from 4 to 7, it is very homogeneous.

2. Neuroprotective regimens

The goal of neuroprotection is to prevent an original insult to the nervous system and/or to prevent the consequences of endogenous or exogenous noxious processes causing damage to axons, neurons, synapses and dendrites. Neuroregeneration aims to induce recovery of neuronal cells or functional neuronal connections following injury [1].

Possible neurotoxic mechanisms in MS [22], include glutamate-mediated cytotoxicity (excitotoxicity) [23–25], CD8 T-cell-mediated toxicity [26,27], neurotoxicity by inflammatory mediators such as TNFα, cytokines, nitrous oxide [28–30], increased oxidative damage [31] by reactive oxygen species [32], mitochondrial damage [20], enhanced influx of Ca^{2+} [32–36] and Na^{+} increase in Ca^{2+}-dependent enzymes such as calpain [37], and enhanced apoptosis of oligodendrocytes via the caspase pathway [38].

Therefore, possible neuroprotective strategies in MS [39] (Table 1) are similar to those proposed for cerebrovascular disease, and may include, anti-excitotoxic agents (e.g., glutamate receptor antagonists) [23,40] nitric oxide and iNOS inhibitors [41], Ca-dependent neuroprotease (calpain) inhibitors [37,42], anti-oxidants (including vitamin E, prostaglandins, green tea and riluzole) [22,43–45], COX-2 inhibitors [46], anti-apoptotic agents (e.g., caspase inhibitors) [47], vitamin D [48], Ca^{2+}-channel blockers [36], Na^{+} channel blockers [49] or Na^{+}/Ca^{2+}-exchanger inhibitors and growth/neurotrophic factors [28,50,51]. Neuroprotective effects were also induced by cannabinoids in EAE [52] and in MS [53]. Axonal protection was also reported in EAE by the antiepileptic agents lamotrigine and phenytoin [54]. These reported neuroprotective effects do not appear to be related to immunomodulatory or anti-inflammatory mechanisms.

Table 1
Future neuroprotective strategies in MS

1	Anti-excitotoxic agents: e.g., glutamate receptor antagonists
2	NO and iNOS inhibitors
3	Calpain inhibitors
4	Anti-oxidants and free radical scavengers
5	COX-2 inhibitors
6	Cannabinoids
7	Anti-apoptotic therapies: e.g., caspase inhibitors
8	Na^{+} channel- or Na^{+}/Ca^{++}-exchanger inhibitors
9	Ca^{++}-channel blockers
10	Neurotrophic factors
11	Neuronal stem cell transplantation
12	Bone marrow stromal cell transplantation/infusion

3. Neuroprotective effects of currently available disease modifying drugs

It has been shown that IFNα/β sustain neuronal cell growth in vitro and that IFN-β stimulates nerve growth factor (NGF) production by astrocytes both in vitro [55] and in vivo in MS patients [56]. In addition, IFN-β was reported to inhibit astrocyte proliferation [57], microglia activation and the production of neurotoxic factors by inflammatory cells, indirectly protecting neurons and axons. The proposed "neuroprotective" effect of IFN-β is most likely by suppression of microglia activation and gliosis, and inhibition of myelin and axonal destruction.

Glatiramer acetate (GA) induces the formation of GA-specific T-cell lines with a Th2 cytokine production profile. Those cells may enter the CNS and accelerate the local production of growth factors [58,59], enhancing intrinsic neuroprotective/neuroregenerating mechanisms, thus inducing a type of "beneficial neuroprotective-inflammation." In general, the concept of the beneficial aspects of inflammation is gaining ground, following the pivotal works by Schwartz et al. [60,61], who showed that myelin-specific lymphocytes can induce neuroprotection/neuroregeneration in models of neuronal trauma or optic nerve damage. Pilot experiments in our laboratory have supported this theory and indicated that the injection of MOG-specific lymphocytes, especially the CD4+CD25+ regulatory cells, can suppress chronic EAE.

4. Neuroprotection by induction of axonal regeneration and remyelination: stem cell transplantation

Whilst many current neuroprotective methods aim to prevent axonal injury, another possibility might be to encourage remyelination; one method by which this may be achieved is by stem cell transplantation.

It was previously shown that neuronal stem cells (injected intraventricularly as "neuronal spheres") can suppress EAE by exerting peripheral and in situ immunomodulating effects, in addition to being a possible source for remyelination and neuroregeneration [62–64].

Another potential source for stem cells could be the bone marrow (BM) non-hematopoietic, mesenchymal stromal cells (MSC). These cells can exhibit stem cell features and differentiate, under certain circumstances, into cells of various tissue lineages, including neurons and glia [65,66]. Therefore, both BM and neuronal stem cells could have therapeutic potential in various neurodegenerative diseases. BM derived MSCs offer practical advantages over conventional embryonic neuronal stem cells: (1) they can easily be obtained from adult bone marrow, (2) they can

easily be cultured and expanded and (3) they can be injected autologously without the need for immunosuppression.

4.1. Neuronal stem cell transplantation

Oligodendrocyte lineage cells can be expanded from various sources, such as neural stem cells from the developing brain, and embryonic stem cells. We have shown that neurospheres grown from newborn mouse brain can express PSA-NCAM and nestin that are markers of undifferentiated neural precursor cells. In vitro, these spheres generate NG2+ oligodendrocyte progenitors that mature into GalC+ oligodendrocytes. Following intraventricular transplantation of undifferentiated neurospheres into rodents with EAE, the cells migrate into the inflamed white matter and acquire glial lineages markers. Staining of cells that have been tagged with BrdU prior to transplantation showed their migration in the corpus callosum of EAE animals [62,64], while double labeling with GalC indicated that the transplanted cells differentiated into mature oligodendrocytes. Intraventricular transplantation of neurospheres into mice with chronic EAE attenuated the clinical course of the paralytic disease. This was associated with reduction of demyelination and of axonal injury in the cell-transplanted animals compared to sham-transplanted mice [62,64]. In general, stem cell transplantation can be useful in several white matter and neurodegenerative diseases, as well as congenital dysmyelination and CNS trauma, since it induces the generation of glial precursors that can rebuild the destroyed myelin and produce growth factors. These cells seem to be safely suitable for human transplantation. They may also serve as vectors for the delivery of therapeutic genes and proteins via precursor cells utilizing their capacity for stable integration in the CNS.

4.2. Mesenchymal bone marrow stromal cell transplantation

In a series of preliminary experiments, we tested the therapeutic potential of BM MSCs in chronic progressive EAE, induced in C57Bl mice with MOG 35–50 peptide. BM cells were obtained by flashing the long limb bones of C57Bl, GFP-transgenic naive mice. GFP-expressing transgenic mice are used as donors in order to easily detect the transplanted cells. The cells were used either as a crude inoculum or cultured with specific MEM-alpha medium enriched with 20% FCS, after depleting non-adhesing hematopoietic progenitors to develop a pure stromal cell population. The MSCs were then injected intravenously or intraventricularly in EAE animals, on day 10, just before the clinical onset of the disease. Our preliminary results indicate a significant clinical and pathological beneficial effect on EAE. In six separate experiments, 75 C57Bl mice were immunized with MOG for induction of chronic EAE; 38 controls received saline injection intraventricularly; 25 animals were injected with unmanipulated BMSCs on day 10–11 post EAE induction and 12 received purified BMSCs after 14 days in culture. Both the unmanipulated and the purified BMSCs migrated into the inflamed lesions and showed morphological and immunohistological features indicating differentiation into astrocytes, neuronal and glial cells. The clinical course of EAE was significantly ameliorated in animals treated with BMSCs or purified BMSCs. Histopathologic study supported the clinical observations and showed a decrease in lymphocytic infiltrations in mice transplanted with BMSCs with a significant preservation of the axons (Karussis et al., unpublished observations). Recently, other groups have stressed the therapeutic potential of mouse and human BMSCs in the animal model of MS, EAE, focusing mainly on the immunomodulatory properties of these cells when administered intravenously [67,68].

In summary, it is obvious that in order to improve the therapeutic outcome in MS, a combined approach of immunomodulation and neuroprotection is needed [69]. Since MS probably has two phases and two faces, inflammatory and degenerative, our efforts should now focus on improving and making feasible neuroprotective techniques (Table 1), including embryonic neuronal stem cells and BM MSCs transplantation.

References

[1] Lubetzki C, Williams A, Stankoff B. Promoting repair in multiple sclerosis: problems and prospects. Curr Opin Neurol 2005;18:237–44.
[2] Trapp B, Ransohoff R, Rudick R. Axonal pathology in multiple sclerosis: relationship to neurologic disability. Curr Opin Neurol 1999;12:295–302.
[3] Lovas G, Szilagyi N, Majtenyi K, et al. Axonal changes in chronic demyelinated cervical spinal cord plaques. Brain 2000;123:308–17.
[4] Grigoriadis N, Ben-Hur T, Karussis D, et al. Axonal damage in multiple sclerosis: a complex issue in a complex disease. Clin Neurol Neurosurg 2004;106:211–7.
[5] Steinman L. Multiple sclerosis: a two-stage disease. Nat Immunol 2001;2:762–4.
[6] Owens T. The enigma of multiple sclerosis: inflammation and neurodegeneration cause heterogeneous dysfunction and damage. Curr Opin Neurol 2003;16:259–65.
[7] Felts P, Woolston A, Fernando H, et al. Inflammation and primary demyelination induced by the intraspinal injection of lipopolysaccharide. Brain 2005;128:1649–66.
[8] Bitsch A, Schuchardt J, Bunkowski S, et al. Acute axonal injury in multiple sclerosis. Correlation with demyelination and inflammation. Brain 2000;123:1174–83.
[9] Bjartmar C, Trapp B. Axonal and neuronal degeneration in multiple sclerosis: mechanisms and functional consequences. Curr Opin Neurol 2001;14:271–8.
[10] Buntinx M, Stinissen P, Steels P, et al. Immune-mediated oligodendrocyte injury in multiple sclerosis: molecular mechanisms and therapeutic interventions. Crit Rev Immunol 2002;22:391–424.
[11] Hohlfeld R, Kerschensteiner M, Stadelmann C, et al. The neuroprotective effect of inflammation: implications for the therapy of multiple sclerosis. J Neuroimmunol 2000;107:161–6.
[12] Villoslada P, Genain C. Role of nerve growth factor and other trophic factors in brain inflammation. Prog Brain Res 2004;146:403–14.
[13] Gehrmann J, Banati R, Cuzner M, et al. Amyloid precursor protein (APP) expression in multiple sclerosis lesions. Glia 1995;15:141–51.

[14] De Stefano N, Narayanan S, Mortilla M, et al. Imaging axonal damage in multiple sclerosis by means of MR spectroscopy. Neurol Sci 2000;21:S883–7.
[15] De Stefano N, Matthews P, Fu L, et al. Axonal damage correlates with disability in patients with relapsing-remitting multiple sclerosis. Results of a longitudinal magnetic resonance spectroscopy study. Brain 1998;121:1469–77.
[16] Sastre-Garriga J, Ingle G, Chard D, et al. Metabolite changes in normal-appearing gray and white matter are linked with disability in early primary progressive multiple sclerosis. Arch Neurol 2005;62:569–73.
[17] Ruiz-Pena J, Pinero P, Sellers G, et al. Magnetic resonance spectroscopy of normal appearing white matter in early relapsing-remitting multiple sclerosis: correlations between disability and spectroscopy. BMC Neurol 2004;4:8.
[18] Trapp B, Peterson J, Ransohoff R, et al. Axonal transection in the lesions of multiple sclerosis. N Engl J Med 1998;338:278–85.
[19] Gilgun-Sherki Y, Melamed E, Offen D. The role of oxidative stress in the pathogenesis of multiple sclerosis: the need for effective antioxidant therapy. J Neurol 2004;251:261–8.
[20] Andrews H, Nichols P, Bates D, et al. Mitochondrial dysfunction plays a key role in progressive axonal loss in multiple sclerosis. Med Hypotheses 2005;64:669–77.
[21] Evangelou N, Esiri M, Smith S, et al. Quantitative pathological evidence for axonal loss in normal appearing white matter in multiple sclerosis. Ann Neurol 2000;47:391–5.
[22] Stys P. General mechanisms of axonal damage and its prevention. J Neurol Sci 2005;233:3–13.
[23] Rosin C, Bates T, Skaper S. Excitatory amino acid induced oligodendrocyte cell death in vitro: receptor-dependent and -independent mechanisms. J Neurochem 2004;90:1173–85.
[24] Sarchielli P, Greco L, Floridi A, et al. Excitatory amino acids and multiple sclerosis: evidence from cerebrospinal fluid. Arch Neurol 2003;60:1082–8.
[25] Pitt D, Werner P, Raine C. Glutamate excitotoxicity in a model of multiple sclerosis. Nat Med 2000;6:67–70.
[26] Steinman L. Myelin-specific CD8 T cells in the pathogenesis of experimental allergic encephalitis and multiple sclerosis. J Exp Med 2001;194:F27–30.
[27] Skulina C, Schmidt S, Dornmair K, et al. Multiple sclerosis: brain-infiltrating CD8+ T cells persist as clonal expansions in the cerebrospinal fluid and blood. Proc Natl Acad Sci USA 2004;101:2428–33.
[28] Bitsch A, Kuhlmann T, Da Costa C, et al. Tumour necrosis factor alpha mRNA expression in early multiple sclerosis lesions: correlation with demyelinating activity and oligodendrocyte pathology. Glia 2000;29:366–75.
[29] Andrews T, Zhang P, Bhat N. TNFalpha potentiates IFNgamma-induced cell death in oligodendrocyte progenitors. J Neurosci Res 1998;54:574–83.
[30] Boullerne A, Nedelkoska L, Benjamins J. Role of calcium in nitric oxide-induced cytotoxicity: EGTA protects mouse oligodendrocytes. J Neurosci Res 2001;63:124–35.
[31] Vladimirova O, O'Connor J, Cahill A, et al. Oxidative damage to DNA in plaques of MS brains. Mult Scler 1998;4:413–8.
[32] Facchinetti F, Dawson V, Dawson T. Free radicals as mediators of neuronal injury. Cell Mol Neurobiol 1998;18:667–82.
[33] Butcher P. Calcium intake and the protein composition of mouse brain: relevance to multiple sclerosis. Med Hypotheses 1992;39:275–80.
[34] Peterlik M, Cross H. Vitamin D and calcium deficits predispose for multiple chronic diseases. Eur J Clin Invest 2005;35:290–304.
[35] Kurnellas M, Nicot A, Shull G, et al. Plasma membrane calcium ATPase deficiency causes neuronal pathology in the spinal cord: a potential mechanism for neurodegeneration in multiple sclerosis and spinal cord injury. FASEB J 2005;19:298–300.
[36] Brand-Schieber E, Werner P. Calcium channel blockers ameliorate disease in a mouse model of multiple sclerosis. Exp Neurol 2004;189:5–9.
[37] Shields D, Tyor W, Deibler G, et al. Increased calpain expression in activated glial and inflammatory cells in experimental allergic encephalomyelitis. Proc Natl Acad Sci USA 1998;95:5768–72.
[38] Hisahara S, Okano H, Miura M. Caspase-mediated oligodendrocyte cell death in the pathogenesis of autoimmune demyelination. Neurosci Res 2003;46:387–97.
[39] Trembly B. Clinical potential for the use of neuroprotective agents. A brief overview. Ann N Y Acad Sci 1995;765:1–20 [discussion 26–7].
[40] Smith T, Groom A, Zhu B, et al. Autoimmune encephalomyelitis ameliorated by AMPA antagonists. Nat Med 2000;6:62–6.
[41] Okuda Y, Sakoda S, Fujimura H, et al. Nitric oxide via an inducible isoform of nitric oxide synthase is a possible factor to eliminate inflammatory cells from the central nervous system of mice with experimental allergic encephalomyelitis. J Neuroimmunol 1997;73:107–16.
[42] Ye P, D'Ercole A. Insulin-like growth factor I protects oligodendrocytes from tumor necrosis factor-alpha-induced injury. Endocrinology 1999;140:3063–72.
[43] Hong J, Ryu S, Kim H, et al. Neuroprotective effect of green tea extract in experimental ischemia-reperfusion brain injury. Brain Res Bull 2000;53:743–9.
[44] Zhuang H, Kim YS, Namiranian K, et al. Prostaglandins of J series control heme oxygenase expression: potential significance in modulating neuroinflammation. Ann N Y Acad Sci 2003;993:208–16 [discussion 287–8].
[45] Gilgun-Sherki Y, Panet H, Melamed E, et al. Riluzole suppresses experimental autoimmune encephalomyelitis: implications for the treatment of multiple sclerosis. Brain Res 2003;989:196–204.
[46] Salzberg-Brenhouse H, Chen E, Emerich D, et al. Inhibitors of cyclooxygenase-2, but not cyclooxygenase-1 provide structural and functional protection against quinolinic acid-induced neurodegeneration. J Pharmacol Exp Ther 2003;306:218–28.
[47] Cid C, Alvarez-Cermeno J, Regidor I, et al. Caspase inhibitors protect against neuronal apoptosis induced by cerebrospinal fluid from multiple sclerosis patients. J Neuroimmunol 2003;136:119–24.
[48] Deluca H, Cantorna M. Vitamin D: its role and uses in immunology. FASEB J 2001;15:2579–85.
[49] Waxman S. Sodium channels as molecular targets in multiple sclerosis. J Rehabil Res Dev 2002;39:233–42.
[50] Webster H. Growth factors and myelin regeneration in multiple sclerosis. Mult Scler 1997;3:113–20.
[51] Linker R, Maurer M, Gaupp S, et al. CNTF is a major protective factor in demyelinating CNS disease: a neurotrophic cytokine as modulator in neuroinflammation. Nat Med 2002;8:620–4.
[52] Ni X, Geller E, Eppihimer M, et al. Win 55212-2, a cannabinoid receptor agonist, attenuates leukocyte/endothelial interactions in an experimental autoimmune encephalomyelitis model. Mult Scler 2004;10:158–64.
[53] Croxford J. Therapeutic potential of cannabinoids in CNS disease. CNS Drugs 2003;17:179–202.
[54] Lo A, Saab C, Black J, et al. Phenytoin protects spinal cord axons and preserves axonal conduction and neurological function in a model of neuroinflammation in vivo. J Neurophysiol 2003;90:3566–71.
[55] Boutros T, Croze E, Yong V. Interferon-beta is a potent promoter of nerve growth factor production by astrocytes. J Neurochem 1997;69:939–46.
[56] Biernacki K, Antel J, Blain M, et al. Interferon beta promotes nerve growth factor secretion early in the course of multiple sclerosis. Arch Neurol 2005;62:563–8.
[57] Malik O, Compston A, Scolding J. Interferon-beta inhibits mitogen induced astrocyte proliferation in vitro. J Neuroimmunol 1998;86:155–62.

[58] Aharoni R, Kayhan B, Eilam R, et al. Glatiramer acetate-specific T cells in the brain express T helper 2/3 cytokines and brain-derived neurotrophic factor in situ. Proc Natl Acad Sci USA 2003;100:14157–62.

[59] Ziemssen T, Kumpfel T, Schneider H, et al. Secretion of brain-derived neurotrophic factor by glatiramer acetate-reactive T-helper cell lines: implications for multiple sclerosis therapy. J Neurol Sci 2005;233:109–12.

[60] Kipnis J, Mizrahi T, Hauben E, et al. Neuroprotective autoimmunity: naturally occurring CD4+CD25+ regulatory T cells suppress the ability to withstand injury to the central nervous system. Proc Natl Acad Sci USA 2002;99:15620–5.

[61] Schwartz M, Kipnis J. Autoimmunity on alert: naturally occurring regulatory CD4(+)CD25(+) T cells as part of the evolutionary compromise between a 'need' and a 'risk'. Trends Immunol 2002;23:530–4.

[62] Einstein O, Karussis D, Grigoriadis N, et al. Intraventricular transplantation of neural precursor cell spheres attenuates acute experimental allergic encephalomyelitis. Mol Cell Neurosci 2003;24:1074–82.

[63] Pluchino S, Quattrini A, Brambilla E, et al. Injection of adult neurospheres induces recovery in a chronic model of multiple sclerosis. Nature 2003;422:688–94.

[64] Ben-Hur T, Einstein O, Mizrachi-Kol R, et al. Transplanted multipotential neural precursor cells migrate into the inflamed white matter in response to experimental autoimmune encephalomyelitis. Glia 2003;41:73–80.

[65] Prockop D. Marrow stromal cells as stem cells for nonhematopoietic tissues. Science 1997;276:71–4.

[66] Bonnet D. Biology of human bone marrow stem cells. Clin Exp Med 2003;3:140–9.

[67] Zhang J, Li Y, Chen J, et al. Human bone marrow stromal cell treatment improves neurological functional recovery in EAE mice. Exp Neurol 2005;195:16–26.

[68] Zappia E, Casazza S, Pedemonte E, et al. Mesenchymal stem cells ameliorate experimental autoimmune encephalomyelitis inducing T cell anergy. Blood 2005;106:1755–61.

[69] Kanwar J, Kanwar R, Krissansen G. Simultaneous neuroprotection and blockade of inflammation reverses autoimmune encephalomyelitis. Brain 2004;127:1313–31.

17

The Use of Glatiramer Acetate in the Treatment of Multiple Sclerosis

Jerry S. Wolinsky

Bartels Family and Opal Rankin Professorships in Neurology, University of Texas Health Science Center at Houston, Texas

ABSTRACT

Glatiramer acetate is a collection of synthetic polypeptides indicated as therapy for relapsing a remitting multiple sclerosis (MS). Current understanding of the immunological and neuroprotective mechanisms of action of GA makes it unique among current MS therapies. The clinical efficacy of GA appears similar to that of the recombinant beta interferons. GA has a favorable side effect profile with excellent patient compliance and long-term acceptance. The results of pivotal controlled clinical trials and long-term data derived from organized extension studies are reviewed. Supportive data from open-label comparison, combination treatment and therapeutic switch studies are also provided to enable informed decisions on the appropriate place for GA among other immunomodulatory treatments for relapsing MS.

INTRODUCTION

Multiple sclerosis (MS) is a central nervous system (CNS) disease characterized pathologically by an inflammatory destruction of myelin with variable axonal loss. It is the most common, nontraumatic, disabling neurological disorder in young adults. The etiology of MS remains unknown, but its pathogenesis likely includes altered immune reactivity to myelin components, placing it among the organ-specific autoimmune diseases. The clinical course of relapsing-remitting MS (RRMS) includes exacerbations or episodic neurologic worsening followed by complete or partial remissions. These attacks, or relapses, are followed within weeks to a few months by resolution of clinical symptoms. However, recovery from up to 40% of all relapses is incomplete, leaving measurable, residual neurologic deficits, sometimes including functional disability (1). After a variable interval of relapsing-remitting disease, a substantial proportion of RRMS patients begin to exhibit more continuous deterioration [secondary progressive MS (SPMS)] with or without continued attacks. Less commonly, more purely progressive forms of MS are encountered that begin with gradual neurological deterioration, often insidious in onset, continuing over many months to years without remission. These patients acquire increasing clinical deficits in the absence of any discernible attacks [primary progressive MS (PPMS)], or with an occasional defined attack after the progressive disease is well-established [progressive relapsing MS (PRMS)] (2).

Currently approved immunomodulator therapies for RRMS include glatiramer acetate (GA) and the recombinant interferons (IFN), (IFNβ-1a, Avonex, Biogen, Inc., Cambridge, MA; IFNβ-1a, Rebif, Serono, Inc., Geneva; IFNβ-1b, Betaseron, Berlex Laboratories, Montville, NJ), with natalizumab (Antegren, Biogen Idec, Inc., Cambridge, MA) possibly on the near horizon (3). All immunomodulatory treatments reduce disease activity and the accumulation of disability in RRMS. The National Multiple Sclerosis Society recommends initiation of therapy with an immunomodulator as soon as possible following diagnosis of RRMS. Mitoxantrone (Novantrone), an antineoplastic agent, is also approved for treatment of relapsing MS, but is generally reserved for secondary progressive and severe relapsing-remitting forms of the disease (4,5).

GA (formerly known as copolymer 1 or Cop 1), the subject of this chapter, is indicated for the reduction of the frequency of relapses in RRMS. The drug is approved in 42 countries worldwide, including the United States, Canada, Australia, Europe, and Israel. A number of excellent reviews of GA are available (6,7). GA is the acetate salt of a synthetic mixture of polypeptides that consists of random sequences of four naturally occurring amino acids: L-glutamic acid, L-lysine, L-alanine, and L-tyrosine in racemic form (molar ratio of 1.4:3.4:4.2:1.0). The copolymer was first synthesized in 1967 by Drs. Arnon and colleagues at the Weizmann Institute of Science in an attempt to simulate some of the then-known physicochemical properties of myelin basic protein (MBP) to induce and then dissect experimental allergic encephalomyelitis (EAE) (8). EAE is a laboratory animal model of organ-specific autoimmune CNS inflammatory disease with some similarities to MS. GA was incapable of inducing EAE, but had a marked effect in suppressing EAE when animals were subsequently challenged with MBP.

MECHANISMS OF ACTION

The immunopharmacology of GA in humans remains incompletely understood, but substantial preclinical and clinical data support immunomodulatory and neuroprotective effects that may contribute to the activity of the drug. At least five interdependent processes are thought to contribute to the effects of GA (Fig. 17-1): (a) high-affinity binding to the major histocompatibility complex (MHC) within the antigen binding pocket; (b) competition with MBP at the antigen-presenting cell (APC) level for binding to MHC and subsequent inhibition of MBP-specific T cell activation through competition with MBP/MHC complexes for the T cell receptor; (c) induction of a shift in GA-reactive T cells

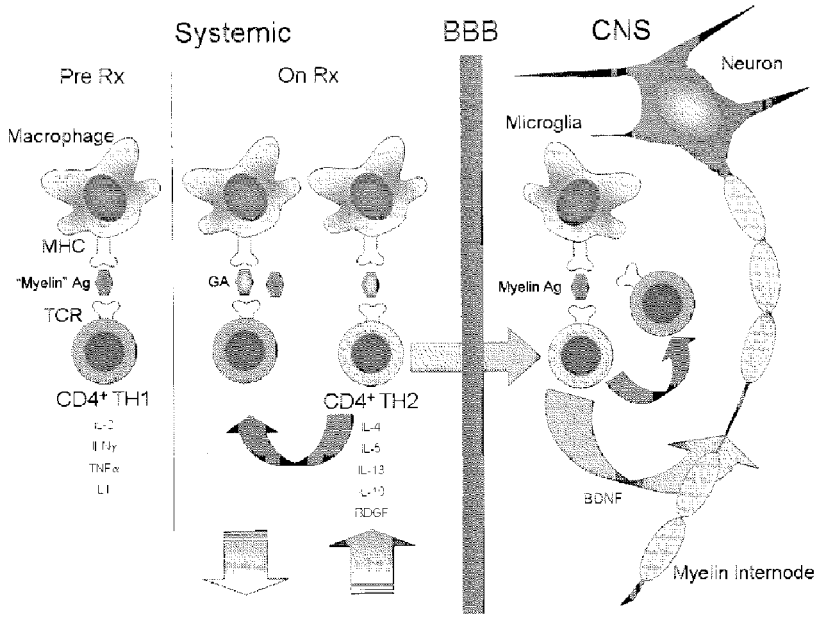

FIG. 17-1 Simplified diagrammatic representation of the immunopharmacology of GA in MS therapeutics. The pretreatment *(Pre-Rx)* portion of the panel emphasizes the baseline state in MS with $CD4^+$ TH1 myelin antigen-reactive cells being activated by systemic antigen processing cells, including macrophages that present foreign antigens that are myelin-like ("myelin" Ag) in the context of surface major histocompatibility complex (MHC) to the T cell receptor (TCR); invoking the concept of molecular mimicry. Stimulated $CD4^+$ TH1 "myelin" Ag-reactive cells secrete a number of proinflammatory cytokines (IL-2, IFNγ, TNFα, LT). On GA therapy, GA may displace some "myelin" Ag. More important, on presentation and stimulation of GA and "myelin" Ag-reactive $CD4^+$ TH1 cells, GA silences cross-reacting $CD4^+$ TH1 "myelin" Ag-reactive cells through anergy, apoptosis, or antigen-specific mechanisms. Concomitantly, GA stimulates and expands a population of GA-reactive $CD4^+$ TH2 cells that secrete anti-inflammatory cytokines (IL-4, IL-5, IL-13, IL-10) to systemically inhibit "myelin" Ag-reactive $CD4^+$ TH1 cells *(red arrow)*. With continued therapy, the net result is a reduced proportion of $CD4^+$ TH1 and an increased proportion of GA and "myelin" cross-reactive $CD4^+$ TH2 cells. When these GA and "myelin" cross-reactive $CD4^+$ TH2 cells gain access to the central nervous system (CNS) by trafficking across the blood–brain barrier (BBB), they are restimulated by true myelin antigens processed and presented by microglia, a brain-resident macrophage. On restimulation, the GA-reactive $CD4^+$ TH2 cells secrete anti-inflammatory cytokines to inhibit "myelin" Ag reactive $CD4^+$ TH1 cells within the CNS, and also secrete trophic factors such as brain-derived neurotrophic factor (BDNF) that may facilitate neuronal survival *(green arrow)*. (From Wolinsky JS. Glatiramer acetate for the treatment of multiple sclerosis. *Expert Opin Pharmacother.* 2004;5:875–891,with permission.)

from a TH1 to a TH2 phenotype; (d) migration of GA-specific T cells into the CNS; and (e) neuroprotection induced via promotion of neurotrophic factors. Immunization with GA also consistently induces GA antibodies.

High-Affinity Binding to MHC

Before any antigen-specific, T-cell-dependent immune response can take place, there must be processing and presentation of a fragment of the antigen by an APC to a T cell precursor. Ordinarily, the appropriately processed antigen is bound by physicochemical interactions to the antigen-binding cleft of the MHC within an APC, and the resulting unique structure cycled to the cell surface for presentation where it can interact with complementary, hypervariable portions of the T cell receptors of appropriate T cells. The resulting trimolecular complex is essential, but not necessarily sufficient to activate and condition subsequent T cell "education" and behavior.

Intact GA can directly bind to MHC. This can be blocked by anti-DR, but not anti-DQ or anti-class I antibodies. The binding of GA to class II

occurs at, or very near to, the peptide-binding cleft (9). This is a high-avidity interaction demonstrated to occur for all common MS-associated DR haplotypes. The molecular structure of the immunodominant peptide of MBP and DR2 has been resolved by crystallography (10). Based on that information, it is likely that the repeated alanines and tyrosines in GA facilitate its anchoring within binding pockets of class II molecules. The inherent variation in amino acid sequence of GA could account its binding to different class II haplotypes. The high-affinity interaction between GA and class II antigen is probably central to its in vivo activity, as it would seem to ensure that some of the drug will interact with any available APC at the subcutaneous site of injection. However, this alone cannot explain the drug's mechanism of action, as the immunobiologically inert dextrorotatory form of GA binds with similar avidity to DR.

Competition with MBP

The substantial MHC-binding affinity of GA allows it to compete with MBP and other myelin-associated proteins at the level of APC binding in vitro (11). GA efficiently displaces MBP, proteolipid protein (PLP), and myelin oligodendrocyte glycoprotein (MOG)-derived peptides from the MHC binding site, but is not displaced by these antigens once it is bound (12). GA isomers behave similarly, but do not suppress EAE (13). Once bound, the GA/MHC complex competes with available MBP/MHC molecules for binding to T cell receptors, rendering some of the myelin-specific pathogenic T cells anergic or otherwise altered (14).

TH1 to TH2 Lymphocyte Shift

Exposure to GA induces a relative anti-inflammatory state by causing a shift in the GA-reactive lymphocyte population from a dominant type-1 T helper (TH1) state to a type-2 (TH2) dominant state (15,16). TH1 cells produce interleukin (IL)-2, IL-12, IFN-γ, and tumor necrosis factor (TNF)-α, which generally are proinflammatory cytokines, while TH2 cells produce IL-4, IL-5, IL-6, IL-10, and IL-13 with anti-inflammatory effects. GA-reactive peripheral blood lymphocytes from untreated MS patients express mostly TNF-α mRNA, while those harvested from GA-treated patients mainly express IL-10, transforming growth factor (TGF)-β, and IL-4 mRNA (17). The shift toward a TH2 bias is reflected by diminished ratios of IFN-γ/IL-5 secretion of GA-reactive T cell lines isolated from MS patients on therapy (16,18). The GA-reactive TH2 cells presumably are regulatory cells that modulate myelin antigen-directed pathogenic immune reactions. Many T cell lines reactive to a number of potentially encephalitogenic myelin proteins, when stimulated in vitro with GA, do not proliferate but predominantly secrete anti-inflammatory cytokines (19).

Naive and memory GA-reactive $CD4^+$ T cells are part of the resident T cell repertory (20). Two phenomena occur in concert on initiating GA therapy. First, after a transient increase within the first month, the number of GA-reactive T cells found using proliferation assays falls within 3 to 6 months, is substantial at 12 months, and decreases by 75% from baseline to 24 months (21). Those without an in vitro proliferative response to GA increased from 5% at baseline to 40% at two years. Second, GA therapy results in increased apoptosis of a substantial percentage of activated ($CD69^+$) $CD4^+$ T cells (22), and long-term treatment showed a 2.9-fold decrease in the estimated precursor frequency of GA-reactive T cells (23). Nevertheless, the ex vivo assayed response to GA remained TH2-biased and, in part, cross-reactive with MBP and MBP (83–99) for up to nine years following initiation of GA (23). Thus, as the shift from a TH1 to a TH2 state develops, TH1 GA-reactive cells are also lost. These ex vivo observed effects likely occur systemically in the MS treated patient, with the result that there is a diminished systemic pool of autoaggressive cells; an effect that appears quite sustained.

Activated T Cell Migration into the CNS

White matter plaques with active CNS demyelination and axonal loss contain numerous inflammatory cells. GA is unlikely to directly inhibit the transmigration of inflammatory cells into the

brain. TH2 cells can penetrate the brain endothelium in vitro (24). Syngeneic GA-reactive murine TH2 cells, when systemically administered in adoptive transfer experiments, will enter the CNS (25,26). Once in the brain, these cells are postulated to decrease local inflammation through so-called bystander suppression. Presumably, products of normal myelin turnover or active demyelination are presented by local APCs to locally restimulated, transmigrating, GA-specific TH2. The presented antigen within-brain cannot be GA, since the drug is rapidly metabolized at the site of administration and does not circulate systemically as a free molecule. Local reactivation of GA-specific T cells in brain stimulates the release of anti-inflammatory cytokines such as IL-4, IL-6, IL-10, TGF-β and brain-derived neurotrophic factor (BDNF), but not IFN-γ (26,27). Proinflammatory cytokine production is then inhibited through this bystander effect (28). Bystander suppression could make GA useful in other CNS diseases where TH1 cells might contribute to the disorder (29,30).

Neuroprotection

Subsets of autoreactive TH1 and TH2 cells have neuroprotective effects in models of axonal injury. In a rodent optic nerve crush injury model with predictable retinal-ganglion neuron loss, injection of MBP-reactive T cells immediately after the injury resulted in an attenuated loss of retinal ganglion neurons, but also the expected undesired consequence of adoptive transfer EAE (31). However, when similarly injured rats were injected with GA-specific T cells they showed improved retinal ganglion neuron survival without developing EAE (32). In related experiments, intraocular injection of glutamate destroyed mouse retinal ganglion neurons. Here, glutamate toxicity was reduced by GA preimmunization, but not in mice immunized with MBP or MOG (33). Reduced axonal damage in C57/bl mice with chronic EAE may reflect the neuroprotective rather than a more conventional anti-inflammatory effect of GA (34).

Several possible mechanisms could account for the neuroprotective effect of GA. Nitric oxide (NO) is an inflammatory mediator that affects regulation immune responses, permeability of the blood–brain barrier, and neural trafficking of cells. It is implicated in primary demyelination via nonspecific damage to the myelin sheath of axons, and may directly promote oligodendrocyte death (35). NO is markedly increased in murine EAE, and GA therapy leads to a significant decrease in NO secretion by encephalitogen stimulated splenocytes (36).

BDNF is a neurotrophic factor that plays a prominent role in CNS development and plasticity (28,37). Some GA-specific TH2 and TH1 T cell lines on stimulation produce BDNF (38). Others have shown that secreted BDNF levels of GA-specific T cells generated on GA therapy were higher than those generated before treatment was started (27), and that high levels of BDNF were secreted by TH2 biased T cell lines. Tyrosine kinase receptor (trk) B is the signal transducing receptor for BDNF and trk B is expressed on neurons and astrocytes in MS lesions (39). Thus, BDNF secreted by GA-reactive TH2 cells in the CNS might exert neurotrophic effects directly in target tissues.

Alternatively, the GA-reactive TH2 cells may induce BDNF within the lesions indirectly by other cytokine-mediated effects on astrocytes, and may limit damage that might otherwise be orchestrated by activated microglia. In an intriguing murine model of 1-methyl-4-phenyl-1,2,3,6-tetrahydropyridine (MPTP) nigrostriatal toxicity, adoptive transfer of GA-TH2 cells attenuated neuronal loss and dopamine depletion. In this model, the extent of microglia activation was markedly reduced and BDNF increased in the substantia nigra pars compacta, which was a site of accumulation of transferred T cells. However, it appeared that astrocytes (and not the transferred cells) were the dominant source of BDNF (30). It is of interest that in vitro, GA-reactive T cells also have a reduced ability to transform bipolar microglia into morphologically activated forms (40). Recent observations on cells harvested from treated patients also show both indirect reciprocal effects of GA-reactive T cells on APCs (41) and direct effects of GA on APCs (42).

GA-specific Antibody Induction

Immunization with GA results in polyclonal anti-GA antibody formation with little evidence that these cross-react with MBP or other myelin proteins. However, some murine IgM monoclonal antibodies (mAb) generated to GA or MBP show substantial cross-reactivity in binding and competition assays (43). In a murine model of virus-associated inflammatory demyelination, polyclonal murine GA IgG antibodies stimulated remyelination (44).

Patients develop demonstrable levels of GA-binding antibodies within 1 month of starting treatment that peak within 3 months, reaching levels 8- to 20-fold higher than baseline and greatly exceeding background levels in controls. Titers decrease by month 6 of therapy, but are detected to persist with continued treatment (21). Consistent with a TH2-driven response, the antibodies are IgG class restricted, with IgG_1 levels several-fold higher than IgG_2 and with low IgG_4 (45). Patients who were relapse-free at 18 and 24 months of therapy had statistically higher GA antibody titers than those treated patients with one or more on-trial relapses (21).

Extended attempts failed to show that IgG class GA mAbs inhibit cellular responses to GA either in vitro or in vivo (46). These included various in vitro and in vivo approaches attempting to block the binding of GA to isolated MHC molecules, to inhibit the proliferative and secretory responses of GA-specific T cell lines to stimulation by GA, and to inhibit GA protection in EAE. Negative results also occurred with high-titer human GA-antibody sera, and sera from 34 GA-treated patients failed to reduce the proliferative response of a murine GA-specific T cell clone to GA, or reduce the competitive inhibition of proliferation of an MBP-specific human T cell clone by GA. In a small study, GA antibodies were found in only 48% of 42 GA-treated RRMS patients, with most antibody-positive patients seen after 1 year on therapy (47). Six of 14 high-titer sera inhibited the proliferation of normal donor peripheral blood cells to GA and, at low dilution, these six sera variably inhibited the proliferate responses of a panel of GA-specific T cell lines. However, the predominance of available data does not suggest GA antibodies influence the drug's therapeutic effect.

CLINICAL EFFICACY IN CONTROLLED TRIALS

Bornstein Single-Center RRMS Study (1980–1985)

The first double-blind, randomized, placebo-controlled trial of GA was done in the 1980s as a single-center study at Albert Einstein College of Medicine in the Bronx, NY (48). Fifty relatively young, clinically active, and modestly disabled RRMS patients were recruited (ages 20 to 35, mean 30.5 years; ≥ 2 relapses in the 2 years before entry, average 3.9 relapses; Kurtzke Disability Status Scale (DSS) score ≤ 6, mean score 3) and assigned to subcutaneously (SC) daily GA 20 mg or placebo (PBO) for 2 years. The treatment groups were matched for sex, prior relapses, and disability (DSS 0 to 2 or 3 to 6). The proportion of relapse-free patients was selected as the primary endpoint; secondary endpoints included relapse frequency, change in DSS score from baseline, and time to progression (defined as ≥ 1 DSS point increase maintained for ≥ 3 months).

Relapse-free patients were significantly more common with GA treatment (14/25 or 56% GA versus 6/23 or 26% PBO; $p = 0.045$). The overall two-year relapse frequencies were 0.6 in the GA and 2.7 in the PBO groups. A lower entry disability score increased the likelihood of remaining relapse-free on study ($p = 0.003$). By study's end, 84.6% of GA-treated patients in the lower DSS stratum (0 to 2) were stable or improved versus 30% of the PBO-treated group. Mean improvement was 0.5 DSS units with GA, while those on PBO worsened by 1.2 DSS units ($p = 0.012$). At the higher DSS stratum (3 to 6), similar proportions of patients were stable, improved, or worsened.

The Pivotal Multicenter American Trial [1991–Present (2005)]

This study had three phases: a randomized, PBO-controlled, 24-month, double-blind treat-

ment phase (core study); a blinded extension phase of up to 36 months that preserved the original treatment assignments; and an open-label extension phase in which patients received GA. In 2005, the latter phase is ongoing into its twelfth year. The primary endpoint (for all study phases) was relapse number. Secondary endpoints included the proportion of relapse-free patients, time to first relapse, change in Expanded Disability Status Scale (EDSS) score from entry, and proportion of patients with sustained disease progression (defined as ≥ 1 point increase in EDSS persisting for ≥ 3 months). EDSS evaluations were made every three months during the blinded core and extension phases and every six months thereafter. Patients were seen within seven days of each suspected relapse. When possible, the same neurologist and nurse coordinator completed the assessments of each patient.

Core Study (1991–1994)

Two hundred fifty-one RRMS patients, ages 18 to 45 (mean age 34 years), were enrolled and randomized to GA or PBO (49). Eligible patients had ≥ two relapses in the 2 years before entry (mean 2.9), and an EDSS score of ≤ 5 (mean 2.5). At 24 months there was a 29% relapse rate reduction in favor of GA (1.19 ± 0.13 GA, 1.68 ± 0.13 PBO, p = 0.007; annualized rates were 0.59 and 0.84, respectively). A total of 33.6% of GA-treated patients and 27.0% of PBO patients were relapse-free (p = 0.098). The proportions of patients improved, unchanged, or worsened by ≥ 1 EDSS steps from entry to 2 years of treatment favored GA (p = 0.037). A post hoc analysis suggested a better therapeutic effect of GA in patients with lower entry EDSS scores (≤ 2).

Double-Blind Extension Phase (1991–1994)

Two hundred and three core patients entered the blinded extension (50). After approximately 35 months of treatment there was a 32% relapse rate reduction with GA (mean 1.34 GA, 1.98 PBO, p = 0.002; annualized rates were 0.58 and 0.81, respectively). More GA-treated patients remained relapse-free over the extended trial (33.6% GA-treated, 24.6% PBO-treated, p = 0.035). No GA-treated patient who was relapse-free during the core relapsed during the extension. The median time to first relapse was prolonged by active treatment (287 days with GA, 198 days with PBO, p = 0.057). Placebo-assigned subjects experienced more multiple relapses (p = 0.008). The proportion of patients who improved by ≥ 1 EDSS steps from entry favored GA (27.2% GA, 12.0% PBO, p = 0.001). Worsening by ≥ 1.5 EDSS steps was more frequent with PBO (21.6% GA, 41.6% PBO, p = 0.001). The mean EDSS score improved by −0.11 on GA and worsened by +0.34 with PBO (p = 0.006).

Open-Label Extension [1991–Present (2005)]

All patients who were enrolled in the pivotal trial were invited into the open-label study as long as they had not violated the original study's exclusion criteria; 208 of the original 251 patients chose to do so. At ≥ 6 years of continuous GA therapy from randomization, 26 of 101 (25.7%) remained relapse-free. The relapse rate of all patients treated from the beginning of the study dropped annually, with an overall annualized relapse rate from randomization of 0.42 (95% CI: 0.34 to 0.51), which reached 0.23 during year 6 (51,52). 69.3% of those on GA from study inception were neurologically unchanged (within 0.5 EDSS steps of baseline), or had improved.

Data beyond 6 years remains published only as abstracts. One hundred forty two patients (56.6% of the original cohort) remained on study at eight years (51). The annual relapse rate had declined to 0.2 with a mean EDSS 3.14, reflecting an increase of 0.5 steps from randomization. Patient attrition and the lack of a true placebo group complicate drawing firm conclusions from this long-term cohort. Still, natural history studies predict a higher level of neurological disability within 12 years of disease onset, with 50% of RRMS patients reaching EDSS 6 (53). When the 72 patients always on GA were compared to those originally random-

ized to PBO (oPBO), the disability differences seen at the end of the controlled extension phase were still evident at year 6.

Of the 208 patients who entered the open-label study, 133 began year 10 (64 always on GA and 69 oPBO). Before randomization, their annualized relapse rates were comparable at 1.52 and 1.46, respectively; by year 10, these had fallen to 0.22 and 0.23. The mean EDSS score for the group always on GA was 3.67; an increase from randomization of 0.9. However, 64.4% remained stable or improved (54). When oPBO patients on active treatment were compared to those always on GA, the proportions with confirmed progression over the entire 10 years differed significantly (50 always GA, 72 oPBO, $p = 0.015$).

European/Canadian MRI Study (1997–1998)

This multicenter, double-blind, randomized, placebo-controlled study sought to study RRMS subjects similar to those enrolled in the pivotal American trial, but was designed specifically to define the onset, magnitude, and durability of the effect of GA on MRI-monitored disease (55). Major entry criteria differences were that only one relapse was required in the 2 years before study entry, and all randomized subjects had at least one enhancing lesion on a screening cranial MRI scan after administration of gadolinium (Gd). Altogether, 485 subjects were screened to accumulate 252 meeting all entry criteria, and most were randomized into the initial nine-month placebo-controlled phase of the study (119 to GA and 120 to PBO). Thus, these RRMS subjects were enriched for the primary outcome variable of interest. At entry, these patients were of similar age (mean 34.1 years), but shorter disease duration (mean 4.9 years), lower prior 2-year relapse rates (mean 2.6), and slightly lower entry neurological deficits (mean EDSS 2.3) than in the pivotal American trial. The primary MRI outcomes will be provided below. Clinically, at 9 months there was a 33% relapse rate reduction in favor of GA (0.51 GA, 0.76 PBO, $p = 0.012$; annualized rates were 0.81 and 1.21, respectively). There was little change in EDSS over the short study.

Meta-analysis of the Double-blind, Placebo-controlled Clinical Trials in RRMS

Data was pooled from all 540 patients in the above randomized, PBO-controlled trials over the double-blind phase of each (56). Estimates of the annualized relapse rate, total number of on-trial relapses, and time to first relapse were based on regression models. Also explored were the effect of GA on accumulated disability and the potential role of clinical variables as predictors of relapse rate and treatment efficacy (57). The average annualized relapse rate reduction was 28% in the pooled data set (mean adjusted annual relapse rate 1.14 ± 0.09 PBO, 0.82 ± 0.09 GA, treatment effect 0.31, 95% CI: 0.10 to 0.52, $p = 0.004$). A 36% reduction in on-trial relapses occurred with GA therapy (risk ratio = 0.64, CI: 0.52 to 0.78, $p < 0.0001$). Median time to first relapse favored GA (GA = 322 days, CI: 243 to 433, PBO = 219 days, CI: 170 to 255, $p = 0.01$). Entry patient demographic predictors of on-trial relapse rate included drug assignment ($p = 0.004$), baseline EDSS score ($p = 0.02$), and the number of relapses during the two years prior to study entry ($p = 0.002$) (56).

The risk of accumulating disability was reduced with GA therapy (risk ratio 0.57, CI: 0.39 to 0.91, $p = 0.02$). Accumulation of disability was more rapid among male patients (the proportion with increased disability over the placebo-controlled duration of the pooled data) with a similar magnitude of the treatment effect size for both sexes (Fig. 17-2). A Kaplan–Meier estimate of the time 25% of PBO patients accumulated sustained disability (≥ 1 EDSS step sustained for 90 days) was 521 days; GA-treated patients did not reach this milestone ($p = 0.03$). GA nearly doubled the time to confirmed progression (ratio estimate 1.88; $p = 0.02$) (57). Independent of treatment assignment, patients with on-trial relapses were more likely to accumulate deficits (odds ratio 4.3, CI: 2.4 to 7.6, $p < 0.0001$). This finding reemphasizes that relapse reduction limits accumulating disability in RRMS. Age, as a categorical variable, was also associated with accumulation of disability, supporting the concept of early initiation of immunomodulatory therapy to maximize benefit.

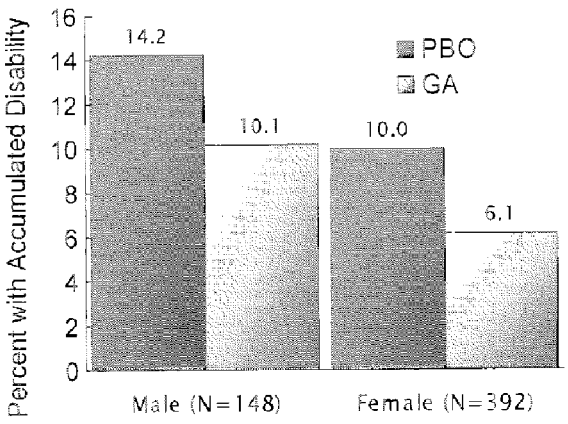

FIG. 17-2 Effect of gender on accumulated disability in RRMS. A meta-analysis was conducted of data from three PBO-controlled trials of GA in RRMS. When stratified by gender, the analysis suggests that the risk of RRMS patients accumulating new disability is greater for male patients regardless of treatment assignment (Wolinsky and Ladkani, unpublished data). However, both male and female patients appeared to benefit from glatiramer acetate therapy (male odds ratio = 0.62, 95% CI: 0.29 to 1.32; female odds ratio = 0.58, 95% CI: 0.33 to 1.00).

Another meta-analysis was communicated based on data in published reports that considered a different selection of trials for inclusion in their analysis. The authors' dissection of the data was constrained by the lack of access to primary data. Nevertheless, were relatively comparable, they reported generally similar relative risk ratios to those just provided that were developed on the primary data, but they ignored all favorable analyses in their conclusions (58).

Bornstein Chronic Progressive Trial (1981–1988)

This trial was conducted through the Albert Einstein College of Medicine in the Bronx, NY, with the aid of Baylor College of Medicine in Houston, TX. The two centers enrolled 169 subjects who would now be classified as having a mix of SPMS and PPMS. Recruitment extended over nearly a 4-year screening interval. The trial was both unique and groundbreaking; it was unique in that it required direct observation and confirmation of sustained progression over an interval of at least 6 to a maximum of 15 months by the investigators prior to randomization to the double-blind, placebo-controlled, treatment phase of the study. Consequently, only 106 of the recruited and followed subjects were randomized. It was groundbreaking in that it defined time to sustained progression of disability as a primary endpoint of an MS trial (59). In this case patients were required to advance ≥ 1.5 EDSS steps when entered at EDSS < 5, and ≥ 1 if entered a level of ≥ 5.0 that was sustained for 3 months; this was a more substantial extent of worsening than that used in subsequent SPMS trials. Subjects injected 15 mg GA twice daily in the only controlled trial that deviated from the 20-mg daily dose. Deterioration occurred in 9 GA and 14 PBO patients, but the overall survival curves did not significantly differ. Two-year progression rates for the secondary outcomes of unconfirmed progression, and progression of 0.5 EDSS units, were significant ($p = 0.03$). A subsequent post hoc analysis suggested that patients retrospectively classified as PPMS or transitional MS (a PPMS course developing at least a decade after a single, isolated attack) were significantly delayed in progressing when on GA rather than PBO; this helped to launch a subsequent, large trial in PPMS.

Oral Copaxone in RRMS (Coral Study, 2000–2001)

Dosing GA by mouth either before or after induction of EAE protects or attenuates clinical disease in a variety of animal models (60,61). Based on these observations and the highly inviting concept of oral tolerance as a potential means of controlling many organ-specific autoimmune diseases, a global, multicenter, double-blind, placebo-controlled trial testing the effects of enteric-released oral formulations of 5 mg and 50 mg GA was mounted. Altogether 1,651 RRMS patients were recruited and MRI was performed in a subset of 486 subjects. The results, which have yet (2005) to be formally communicated, showed that while the drug was safe when administered as formulated, no statistically significant clinical or MRI effect could be found at either dose. It remains uncertain whether the discrepancy between the effects of GA in the animal model and in humans reflects

some aspect of trial design (e.g., dosing, site of drug release), or a flaw in the translation of the concept of oral tolerance to humans.

PROMISE Study (1999–2003)

This was a double-blind, placebo-controlled trial of GA in PPMS that enrolled 943 patients (460 male patients) with progressive disease, the absence of relapse, and EDSS scores between 3 and 6.5, to receive either GA or PBO at a 2:1 allocation ratio. The study's objective was to determine whether GA could slow confirmed disease progression in the absence of the confounding effects of relapses (62). The primary endpoint was the time to confirmed progression (increase of 1 EDSS point sustained for three months for entry EDSS 3.0 to 5.0, or 0.5 EDSS for entry EDSS 5.5 to 6.5). This was originally conceived as a 3-year trial with quarterly clinical evaluations and annual MRI monitoring. Early after enrollment was completed, a blinded extension on assigned study medication until the last subject completed 3 years of study, and drug exposure and data were locked and analyzed, was added.

The Data Safety Monitoring Committee (DSMC) for the trial convened as part of a preplanned second-interim analysis when at least 600 subjects had completed ≥ 2 years of therapy or had prematurely withdrawn from study. Safety data were available for all patients and intention-to-treat (ITT) efficacy data were available for 757 subjects, of whom 620 had completed ≥ 2 years of treatment. The DSMC found no safety concerns. However, their unblinded review of the efficacy data and the results of a futility analysis led them to conclude it was improbable that the study would reach statistical significance for its primary outcome. Based on the conclusions and recommendations of the DSMC, and recognizing the scientific importance of this large cohort of PPMS subjects, all patients remaining in the trial were taken off study medication in an organized fashion and offered entry into a natural history study until the originally projected conclusion of the trial in October 2003; all investigators and patients remained blinded to the original study medication assignments.

An ITT analysis was performed following closure of the study in October, 2004, using all available trial data, and thus far (2005) published only in abstract form (63). A trend was found for a delay in the time to progression and there was a lower proportion with progression for those randomized to GA compared to the PBO-assigned group [hazard ratio (HR) = 0.860, 95% CI: 0.699 to 1.057, p = 0.152]. Most sensitivity and subcohort analyses supported the trend. The survival curve for male patients assigned to GA diverged early and widened over time from that of the group assigned to PBO (HR = 0.695, CI: 0.523 to 0.924, p = 0.012). Analyses of MRI-monitored enhancements and plaque burden favored GA treatment for both genders. The results suggest different time-dependent effects of GA on the endpoints.

The premature stopping of study medication and unanticipated low progression rates greatly complicate interpretation of the trial. Nevertheless, it appears that GA has benefit in retarding progression in the absence of relapses, an effect most evident in the subcohort of PPMS patients where the PBO group had the most rapid progression.

MRI Studies

MRI provides a noninvasive estimate of ongoing pathologic change within the brains of MS patients. The first indication of the effect of GA on MRI was from a small crossover trial of 10 RRMS patients in whom monthly Gd-enhanced MRI scans were obtained over 9 to 27 months before initiation of GA therapy, and then for 10 to 14 months on therapy. There were overall trends found in the frequency of new Gd-enhanced lesions (0.92 versus 2.20 lesions/month; p = 0.10), and in the rate of T2-weighted lesion volume increase for a subset of six patients with the longer pretreatment observations of 25 to 27 months (p = 0.05) compared to the interval on GA treatment (64).

American Multicenter Study

MRI was not included in the original multicenter study design. However, a cohort of 14 GA

and 13 PBO patients followed at the University of Pennsylvania was studied as part of a National Multiple Sclerosis Society pilot program to explore MRI as an adjunct outcome measure for clinical trials (65). Annual decreases from baseline to 24 months in Gd-enhanced lesion number (GA = −1.2, PBO = 0.5; p = 0.03) and Gd-enhanced tissue volume (GA = −83.5 mm^3, PBO = 147.5 mm^3; p = 0.003) were found. Annualized brain volume loss was also three-fold lower (GA = −0.6%, PBO = −1.8%; p < 0.008). No significant differences were found the number of new T2 lesions or percentage increase in T2 volumes.

Cross-sectional MRI data were obtained on 135 of the 147 patients available in the open-label phase of the American Multicenter Study (66). At imaging, 66 oPBO patients had taken GA for 1,467 ± 63 days, and 69 always-GA patients were on the drug for 2,433 ± 59 days. The annualized relapse rate in the two years just prior to beginning the drug was, as expected, higher in oPBO patients (oPBO = 0.93 ± 0.89, GA = 0.51 ± 0.64; p = 0.002), but similar for both groups during open-label treatment (oPBO = 0.27 ± 0.45, GA = 0.28 ± 0.40). The rate reduction was greater for those crossed over from PBO (oPBO reduced by 0.66 ± 0.71, GA reduced 0.23 ± 0.58; p = 0.0002). Consistent with these clinical findings, the proportion of patients with Gd-enhancements was higher in the oPBO cohort (oPBO = 36.4%, GA = 18.8%, p = 0.02). The risk of having an enhancement, regardless of original treatment assignment, was higher in those with open-label phase relapses (odds ratio 4.65, 95% CI: 2.0 to 10.7; p = 0.001), and 2.5 times higher for the oPBO group (CI: 1.1 to 5.4; p = 0.02). Atrophy was worse for those originally on PBO.

European/Canadian MRI Study

This study had two prospectively defined stages: a 9-month, PBO-controlled phase with monthly imaging, and a 9-month, open-label phase with quarterly MRI. The open-label phase was designed to determine if any MRI-related treatment effects found in the first 9 months were reproduced on initiation of GA in the PBO subjects, and to learn whether they were sustained with continued active therapy (55,67).

Controlled Phase

The treatment groups were comparable at baseline for all demographic, clinical, and MRI variables. Mean baseline enhancing lesion numbers (PBO = 4.4, GA = 4.2) were relatively high, reflecting enrichment for this activity. Results of the 9-month, double-blind phase (Fig. 17-3) showed that GA reduced total enhancements (−10.8, CI: −18.0 to −3.7; p = 0.003). Treatment effects increased over the 9-month period (55). The cumulative number of Gd-enhanced lesions was highly correlated with clinical relapses in both treatment groups (Spearman rank correlation coefficient in PBO = 0.35, p = 0.001 and in GA = 0.24, p = 0.01). Differences favoring GA were found for all secondary outcomes: number of new enhancements (−33%, p < 0.003), change in enhanced lesion volumes (−57%, p = 0.01), new T2 lesion numbers (−30%; p < 0.003), and change in T2 lesion volumes (−36%; p = 0.006).

Newly detected T2 lesions are nearly always accompanied by T1 enhancements, and ~65% of these new lesions appear hypointense on unenhanced T1 images. Once enhancement ceases, nearly one-third of new lesions remain hypointense lesions on T1-weighted images. These so-called black holes indicate more severe and permanent tissue damage, with better correlations found between the extent of black holes in the brain and MS-related disability than for the total T2-defined disease burden. In a post hoc analysis, newly formed T2 lesions (defined as a T2 lesion arising from an area of previously normal white matter with associated T1 enhancement) were identified from scans taken between study months 1 and 6 that could be followed over at least three to up to eight subsequent monthly scans to evaluate new lesion evolution (68). GA treatment reduced the proportion of new MS lesions that evolved into black holes and the recurrence of enhancements (Fig. 17-4). A total 1,251 new lesions (515 GA, 736 PBO) were found suitable for serial evaluation over a mean follow-up of 5.6 months. The proportion of persisting black holes on follow-

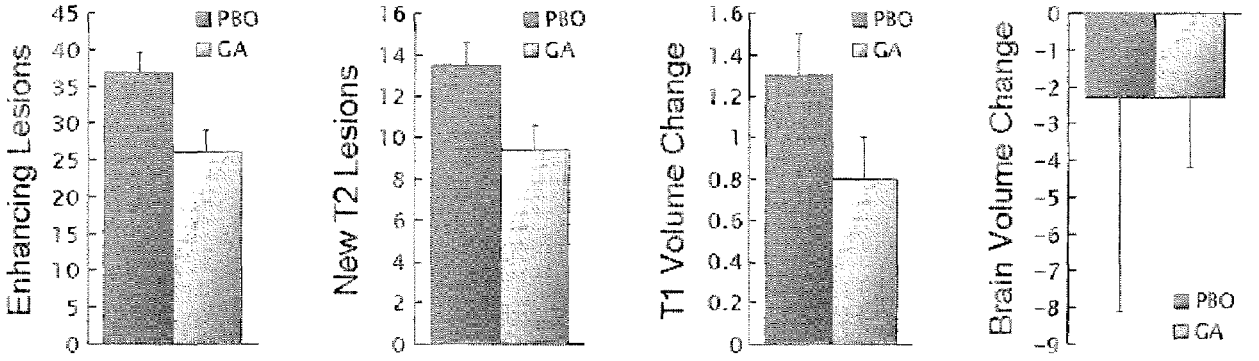

FIG. 17-3 Short-term effects of GA therapy on MRI measures in RRMS. Monthly MRI scans were obtained for 119 GA- and 120 PBO-randomized RRMS patients who were required to have at least one enhanced lesion documented on an MRI done within 30 days of randomization and initiation of study drug. The *far left panel* shows the mean number of total enhancing lesions per subject over the entire nine-month study; a 29% difference that favored GA ($p = 0.003$). The *left middle panel* displays the mean number of new T2 lesions per subject over the nine-month study, a 30% difference that favored GA ($p < 0.003$). The *middle right panel* displays the mean change from baseline in total T1 hypointense lesion volume per subject (in mL) from baseline to nine months ($p = 0.14$). (After data in Comi G, Filippi M, Wolinsky JS. European/Canadian multicenter, double-blind, randomized, placebo-controlled study of the effects of glatiramer acetate on magnetic resonance imaging—measured disease activity and burden in patients with relapsing multiple sclerosis. European/Canadian Glatiramer Acetate Study Group. *Ann Neurol.* 2001;49:290–297.) The *far right panel* shows the mean change from baseline in central brain volume per subject (in mL) from baseline to nine months (not significant). (Developed from Rovaris M, Comi G, Rocca MA, et al. Short-term brain volume change in relapsing-remitting multiple sclerosis: effect of glatiramer acetate and implications. *Brain* 2001;124:1803–1812.)

up scans was lower in GA-treated patients at all times, became significant at month 7, and by month 8 was nearly half that of the PBO group (GA = 15.6%, PBO = 31.4%, $p = 0.002$). The frequency of re-enhancing lesions was also lower in GA-treated patients (GA = 5.0%, PBO = 8.5%, $p = 0.002$).

Open-label Phase

Fully 94% of randomized patients began or continued GA for an additional 9 months (67). There were 35% fewer enhancements ($p = 0.03$) over the entire 18-month trial for those always on GA (Fig. 17-5), or six enhancing lesions per oPBO patient that might have been preventable. The intent-to-treat (with the last observation carried forward) imputation analysis favored patients always on GA over the entire study and its two phases. Enhanced lesion numbers on quarterly imaging were always lower for those always on GA, with a trend seen at 3 months that strengthened by months 6 and 9 (both $p < 0.001$) during the double-blind phase, and with the proportion of enhanced-lesion-free patients increasing to 63% at month 18. Within 3 months of crossover to GA, the proportion of enhanced-lesion-free oPBO patients increased from 31% to 45% and rose to 60% by the end of the trial.

The T2 disease burden showed little change during the open-label phase for either group, but was greatest in the oPBO group. An increase in T1 hypointense volume was found for both groups over both trial phases. However, the 9-month delay in the initiation of GA treatment was associated with a 2.2-fold increase in the accumulated hypointense lesion volume over the entire 18-month study (67).

Initially, a semiautomated segmentation method based on local thresholding was used to estimate brain volume—seven contiguous, periventricular slices from the MRI obtained at entry and at the end of the placebo-controlled and open-label phases of the study. With this measure, brain volume correlated significantly with the patients' disability at each timepoint; while there was a trend for a reduced rate of brain volume loss for those always on GA over the last

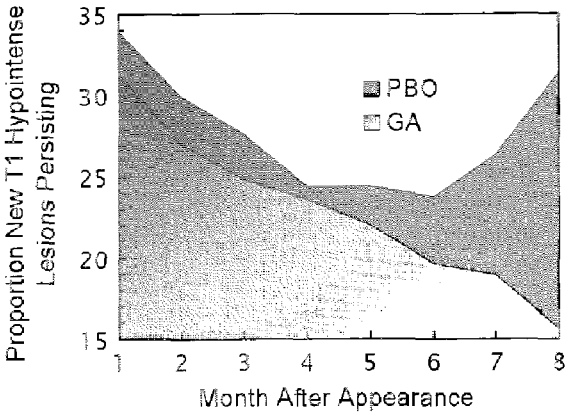

FIG. 17-4 Effect of GA on newly formed T1 hypointense lesion evolution. Monthly MRI scans were reviewed for evolution over at least three to eight months of all newly formed T1 hypointense lesions (defined as a low-signal-intensity region on a T1-weighted image that had appeared one month earlier with enhancement in a previously normal-appearing white matter region, but no longer enhanced and was not already isointense at month 1). A total of 1,722 lesions among 239 patients were available for serial evaluation. Between 31% and 34% of newly enhanced lesions persisted for 30 days as T1 hypointensities; this proportion fell progressively on GA therapy. For those treated with PBO, the decline stabilized at four months and began to rise again after six months. Difference in the evolution of these lesions between the groups was significant at months 7 and 8 ($p = 0.04$ and $p = 0.002$, respectively). (Modified from Filippi M, Rovaris M, Rocca MA, et al. Glatiramer acetate reduces the proportion of new MS lesions evolving into "black holes." *Neurology* 2001;57:731–733.)

nine months of the entire trial, it was not statistically significant (69). When the analysis was repeated using an automated technique that measured the entire intracranial contents with less variability than the prior study, the differences in loss of brain parenchyma over time were statistically significant, favoring treatment with GA at nine months ($p = 0.015$) and over the entire 18-month trial ($p = 0.037$). The overall proportional magnitude of the effect was similar with the two analytic measurement systems (70).

UNCONTROLLED CLINICAL STUDIES

The relative efficacy of currently approved, disease-modifying therapies for use in RRMS is contentious, but of considerable practical concern. Randomized, blinded, direct comparison clinical trials pose methodological, logistical, and cost problems (71). While several industry-sponsored trials are now underway to directly look at the efficacy of subcutaneous interferon (IFN) β-1a and IFNβ-1b relative to GA, these studies are not fully blinded and the results will not be available for several years. Until they are completed and reported, nonrandomized, open-label prospective and retrospective observational studies, and therapeutic "switch" studies provide the only insight into this issue for physicians and patients to judge therapeutic choice in the day-to-day clinical setting.

Comparative Studies

Khan et al. organized a prospective, nonrandomized, open-label trial of 156 RRMS patients to compare the effects of various regimens on annualized relapse rates and disability status (72), as follows: 30 μg IFNβ-1a intramuscularly and weekly ($n = 40$); 250 μg IFNβ-1b every other day ($n = 41$); GA 20 mg daily ($n = 42$); and no treatment ($n = 33$). The treating physicians and patients were directly involved in selecting treatment choices. Eligible patients were treatment-naive with at least one relapse in the previous 2 years and had a Kurtzke EDSS score ≤ 4 when starting therapy. Relapses were defined as in the pivotal American trial of GA. Mean annualized relapse rates in the 2 years similar before starting therapy (untreated = 1.08; IFNβ-1a = 1.20; IFNβ-1b = 1.21; GA = 1.10). Twelve months after initiating or declining treatment, relapse rates were 0.97 without therapy, and 0.85 [not significant, (NS)], 0.61 ($p = 0.002$), and 0.62 ($p = 0.003$) in the IFNβ-1a, IFNβ-1b, and GA groups compared to untreated patients, respectively. At 18 months of follow-up, 122 of 156 patients remained on their original treatments with similar results on relapse rate declines compared to those untreated (GA = 0.49, $p < 0.0001$; IFNβ-1b = 0.55, $p = 0.001$; IFNβ-1a = 0.81, $p = 0.11$). Mean EDSS increased in untreated patients (0.60) and those on IFNβ-1a (0.19, NS), but decreased for those on the GA (−0.44, $p = 0.003$) and IFNβ-1b (−0.25, $p = 0.01$); all inferences relative to the untreated cohort (73).

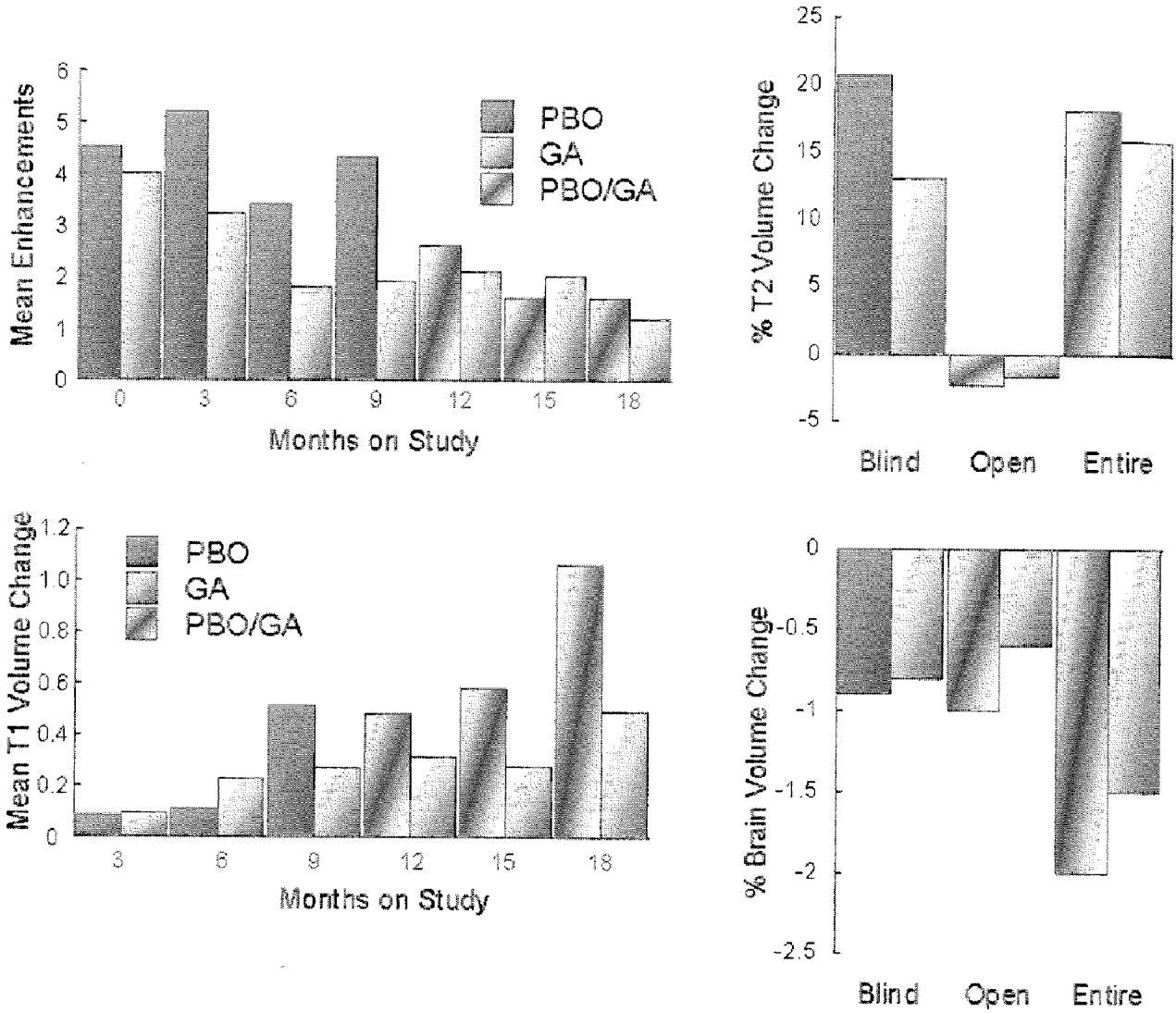

FIG. 17-5 Effect of GA therapy on MRI measures in RRMS. Following nine months of placebo-controlled study, all patients in the European/Canadian study were offered continued quarterly follow-up on open-label glatiramer acetate (67). The *upper left panel* shows the mean change from baseline in the number of enhanced lesions found on quarterly images, with significant differences noted in favor of active treatment at months 6 and 9. When switched to active treatment, a significant reduction in enhancements for those previously treated with placebo was seen within three months. Similarly, a reduction in percentage change from baseline that favored treatment was seen during the controlled phase for patients on glatiramer acetate that was reproduced during the open-label treatment phase, as seen in the *upper right panel*. In the *lower left panel*, the change in mean T1-hypointense lesion volume from baseline was significantly retarded by glatiramer acetate treatment during the controlled phase ($p = 0.035$), a finding that was reproduced over the next nine months for those with a late initiation of therapy. The *lower right panel* shows that the rate of atrophy was significantly reduced over the open label and entire study for those continuously exposed to glatiramer acetate compared to those initially randomized to placebo when total brain contents were measured (70).

Generally, similar results were found in an observational, retrospective analysis of outcomes in a sequential cohort of Argentine RRMS patients (71). Here patients were treated for 16 months with 30 μg IFNβ-1a weekly (n = 26), 44 μg IFNβ-1a three times per week (n = 20), 250 μg IFNβ-1b every other day (n = 20), or GA (n = 30), and compared with a group of untreated patients (n = 38). Socioeconomic factors influenced the latter choice, but most other demographic and clinical variables were otherwise similar between the groups. There was

considerable variation in baseline annual relapse rates between the groups (IFNβ-1a weekly = 0.77; IFNβ-1a = 1.28; IFNβ-1b = 1.13; GA = 1.02; untreated = 0.54), likely reflecting substantial selection bias. Significant declines in annual relapse rate were seen for all treated patients (IFNβ-1a weekly = 49.4%; IFNβ-1a = 65.6%; IFNβ-1b = –64.6%; GA = –81.4%), but rose for those not on therapy (131.5%). The proportion of patients who remained relapse-free over the entire treatment period varied from 37% of untreated to 83% of GA treated patients. Slight differences in EDSS score changes over the study were found, but none was significant.

Haas communicated results from a 24-month prospective, controlled, open-label clinical trial comparing the efficacy of 30 μg IFNβ-1a IM weekly (n = 79), 22 μg IFNβ-1a SC three times weekly (n = 48), 250 μg IFNβ-1b SC every other day (n = 77), and GA (n = 79) (74). RRMS patients with EDSS < 3.5 who were treated for ≥ 6 months were included an ITT-like analysis, with missing values handled as "last observation carried forward." The effect of GA on relapse reduction from prestudy rates was significant at six months (–0.71, $p < 0.001$), and remained similar at months 12 and 24. Significant reductions from prestudy to on-study relapse rates for all of the IFN preparations tested were also found, but the reduction in relapse rate with GA appeared to be superior to all beta-interferons at month 24 ($p < 0.05$).

All of the above studies must be regarded with caution. Nevertheless, the treatment effects seen were generally comparable with those found in randomized clinical trials. All of the studies confirm the importance of treatment in reducing relapse rates in RRMS and suggest possible differences in efficacy among immunomodulatory treatments worthy of rigorous study.

Dose Comparison Studies

The optimal dose or frequency of dosing of GA is relatively unexplored. In one study, 58 consecutive RRMS patients were randomly assigned to 20 mg GA daily, 20 mg GA on alternate days, or alternate-day INFβ-1b (75). After 2 years of therapy, all three cohorts showed a similar significant reduction of relapses compared to their prior 2-year relapse rates. Mean disability scores worsened by the study's end for all three cohorts—significantly so for both GA-treated groups. In another study, 68 RRMS patients were followed over two years on open-label, alternate-day GA therapy with no comparator group (76). The mean relapse rate declined by 80.8% with treatment (before = 2.91 ± 1.10; after = 0.56 ± 1.02, $p < 0.0001$). No firm conclusions can be drawn from this limited view of alternative-day GA therapy, but it does provide some guidance for alternatives for patients on GA therapy whose injection site reactions are problematic.

Therapeutic "Switch" Studies

Preliminary data were presented based on 85 RRMS patients who received 30 μg IFNβ-1a weekly over a mean of 19.7 months before switching to GA; 73% for a lack of efficacy, the rest for intolerable side effects (77). Their annual relapse rates while on IFNβ-1a declined 53% over 18 months of GA. Most of the relapse rate reduction could be attributed to those subjects who switched to GA therapy for a perceived lack of IFNβ-1a efficacy. After 3 years of follow-up from the start of GA, the mean EDSS of the group had slightly improved (78).

In a postmarketing study, the Copaxone Treatment IND Study Group developed data from 805 RRMS patients, 247 of whom had been initially treated with IFNβ-1b, the remainder being treatment naive (79). The subjects with prior exposure to IFNβ-1b had somewhat more disability on entry. All patients received GA and were clinically evaluated every 6 months and within 7 days of any relapse. The mean duration of GA exposure was 20 months. Annualized relapse rates were similar in both treatment-naive (0.3) and prior IFNβ-1b-treated patients (0.4), with both cohorts achieving a 75% relapse rate reduction. The safety and tolerability of GA therapy were similar regardless of prior treatment status.

Combination Therapy

Recombinant interferons have mechanisms of action that include antagonism of proinflammatory cytokines, reduction in T cell activation, and inhibition of blood–brain barrier transmigration and leakage that differ from those of GA (80–82). It is justified to pursue the potential effectiveness of combination therapy. The combination has an additive effect on reducing proliferation of MBP-specific T cells in vitro (83). A 12-month safety study monitored the clinical and MRI effects of adding GA after a three-month run-in period in 33 RRMS patients already taking 30 μg IFNβ-1a IM weekly for ≥ 6 months (84). The combination was safe and a decline in number and volume of Gd-enhanced lesions suggested possible increased effectiveness. Study of the behavior of GA-reactive T cell lines isolated from subjects at one participating site found no evidence to suggest that IFNβ-1a interfered with the immune response to GA. A definitive National Institutes of Health-sponsored trial is underway (2005) to confirm these observations.

Observational Biomarker Studies as Potential Clinical Response Predictors

In MS, where clinical indicators of success (reductions in relapses and accumulated disability and contained MRI activity) are relatively infrequent, delayed or difficult to quantitate), and where available therapies may be only partially effective, prediction or early identification of responders and nonresponders to therapy is a noble goal. In what may prove to have been a signal retrospective study, 44 RRMS patients (29 GA-treated, the rest with weekly 30 μg IFNβ-1a), the subject's MHC haplotype had little, if any, influence on the apparent clinical response to IFNβ-1a. In stark contrast, while all patients on GA had an apparent response to therapy, those who were DRB1*1501+ had a far greater reduction of relapses (twice as many were retrospectively classified as responders than those on GA, who lacked this haplotype). GA binds promiscuously to all common MHC haplotypes. However, the efficiency of presentation of GA complexed to different haplotypes to T cells of appropriate specificity is not well-known. If independently confirmed, this observation would establish that host genetic factors can condition the extent of responsiveness to GA.

In preliminary work requiring prospective confirmation, a highly selected cohort of MS patients failing therapy with GA differed in their in vitro immune response profile to GA compared with GA clinical responders (85). Clearly, there is the suggestion that a combination of genetic profiling, early drug immune response, and sentinel MRI parameters might differentiate those unlikely to respond to GA from the potential responders. Such relative risk response profiles could lead to rational drug selection and knowledge-based decisions on switching therapy before clinical failure becomes obvious.

Experience in Childhood MS

The pivotal trials of GA excluded subjects under 18 years of age. Childhood- and juvenile-onset cases account for only about 5% to 7% of all MS cases, but there is little evidence to suggest that they differ in immunopathogenesis from adult-onset cases. A preliminary communication (86) and other published anecdotal experience suggests that the drug is well-tolerated in children (87); no conclusions on efficacy can be drawn from these anecdotal reports.

TOLERABILITY

Preclinical Studies

Preclinical toxicology indicates that GA is safe, nonmutagenic, and not carcinogenic at up to 15 times the human therapeutic dose. No toxic fetal loss, fetal abnormalities, or postnatal developmental abnormalities occurred in animal reproduction studies at doses up to 36 times the human equivalent. In vivo studies showed only hypotensive effects following high-dose intravenous GA boluses.

Clinical Safety

Safety data on > 3,500 subjects (70% female patients) collected from controlled and uncontrolled studies show adverse experiences leading to therapy withdrawal in 8.4%. Most often cited were dyspnea and vasodilation (~2% each). No patients withdrew for laboratory abnormalities. Local injection site reactions are the most common adverse experiences, described as erythema (41.6%), pain (37%), inflammation (24.5%), pruritus (19.5%), and swelling (12.8%), without skin necrosis. Localized lipoatrophy occurs after a year or more of treatment in some cases (88,89). In a recent review of 76 prior or current GA users identified by chart review and then follow-up examination in a single clinic, 43% had evidence of some regional lipoatrophy, which was rated severe in five women (90). Other adverse events reported by more than 5% of patients include vasodilation (14%), dyspnea (10%), pain (10%), headache (10%), asthenia (10%), urinary infections (8%), paresthesia (7%), rash (7%), depression (6%), nausea (5%), anxiety (5%), backache (5%), and fever (5%).

A postinjection systemic reaction happens in 10% to 15% of GA-treated patients. Affected patients report a variable combination of flushing, chest tightness, palpitations, dyspnea, tachycardia, and anxiety within seconds or minutes of the injection. Portions of or the entire symptom complex last several minutes to several hours, and resolve spontaneously. Most patients who experience this reaction have a single episode, but some have additional episodes at irregular intervals. The cause of the reaction is unknown.

Two of 3,736 patients treated with GA in clinical trials experienced drug-related, nonfatal anaphylactic reactions (data on file, Teva Pharmaceutical Industries, Nordau, Netanya, Israel). There is no evidence of relevant drug interactions.

GA does not induce hematological abnormalities, elevation of hepatic enzymes, flu-like symptoms, depression, or abnormalities of blood pressure. Fatigue may even decrease for some on GA therapy (91). Overall, adverse events observed during GA treatment are few and mild. No medication guide is required by the U.S. Food and Drug Administration (FDA) to accompany its use. Extensive experience with GA in > 40,000 patients shows that it is well-tolerated and local adverse events rarely limit treatment (92).

Pregnancy

Among 253 of 421 reported pregnancies with exposure to GA and known outcome were 187 healthy births, 47 spontaneous abortions, 11 elective abortions, one ectopic pregnancy, and one stillbirth (86). Six cases involved congenital anomalies including failure to thrive, finger anomaly, cardiomyopathy, urethrostenosis, anencephaly, and left adrenal cyst. The remaining 168 cases had not yet reached their due date or were lost to follow-up. Major congenital anomalies occur in 3% of the general population and spontaneous abortion in 15% to 20%. Thus, the rate of these outcomes in women exposed to GA for varying intervals surrounding conception and gestation is within that of the general population. However, GA is viewed as a Pregnancy Category B drug (93).

CONCLUSIONS

MS typically begins with symptoms that can resolve completely or leave residual deficits, with a clinical course that spans years; untreated, it is usually a progressively disabling disease. While the immunopharmacology of GA is complex and not completely understood, the drug appears to have both anti-inflammatory and neuroprotective effects. Controlled studies demonstrate the benefits of GA therapy on the clinically relevant outcomes of reduced relapse rate, delayed accumulation of disability, and on major MRI-monitored measures of disease pathology, with some indication that it may retard the progression of clinical disability that occurs in the absence of defined relapses. The drug has a favorable side effect profile. GA may be most effective when begun in the early phases of the disease and its effects appear to persist over long-term treatment. GA appears a

reasonable first-choice therapy for relapsing MS, and a logical alternative for patients who must switch from a beta-interferon due to intolerable side effects or apparent lack of efficacy.

REFERENCES

1. Lublin FD, Baier M, Cutter G. Effect of relapses on development of residual deficit in multiple sclerosis. *Neurology* 2003;61:1528–32.
2. Lublin FD, Reingold SC. Defining the clinical course of multiple sclerosis: results of an international survey. National Multiple Sclerosis Society (USA) Advisory Committee on Clinical Trials of New Agents in Multiple Sclerosis. *Neurology* 1996;46:907–911.
3. Miller DH, Khan OA, Sheremata WA, et al. A controlled trial of natalizumab for relapsing multiple sclerosis. *N Engl J Med* 2003;348:15–23.
4. Hartung H-P, Gonsette R, König N, et al. Mitoxantrone in progressive multiple sclerosis: a placebo-controlled, double-blind, randomised, multicentre trial. *Lancet* 2002;360:2018–2025.
5. Goodin DS, Arnason BG, Coyle PK, et al. The use of mitoxantrone (Novantrone) for the treatment of multiple sclerosis: report of the Therapeutics and Technology Assessment Subcommittee of the American Academy of Neurology. *Neurology* 2003;61:1332–1338.
6. Dhib-Jalbut S. Glatiramer acetate (Copaxone) therapy for multiple sclerosis. *Pharmacol Ther* 2003;98:245–255.
7. Wolinsky JS. Glatiramer acetate for the treatment of multiple sclerosis. *Expert Opin Pharmacother* 2004;5:875–891.
8. Arnon R. The development of Cop 1 (Copaxone), an innovative drug for the treatment of multiple sclerosis: personal reflections. *Immunol Lett* 1996;50:1–15.
9. Fridkis-Hareli M, Neveu JM, Robinson RA, et al. Binding motifs of copolymer 1 to multiple sclerosis- and rheumatoid arthritis-associated HLA-DR molecules. *J Immunol* 1999;162:4697–4704.
10. Gauthier L, Smith KJ, Pyrdol J, et al. Expression and crystallization of the complex of HLA-DR2 (DRA, DRB1*1501) and an immunodominant peptide of human myelin basic protein. *Proc Natl Acad Sci USA* 1998;95:11828–11833.
11. Aharoni R, Teitelbaum D, Arnon R, et al. Copolymer 1 acts against the immunodominant epitope 82–100 of myelin basic protein by T cell receptor antagonism in addition to major histocompatibility complex blocking. *Proc Natl Acad Sci USA* 1999;96:634–639.
12. Sela M, Teitelbaum D. Glatiramer acetate in the treatment of multiple sclerosis. *Expert Opin Pharmacother* 2001;2:1149–1165.
13. Arnon R, Sela M, Teitelbaum D. New insights into the mechanism of action of copolymer 1 in experimental allergic encephalomyelitis and multiple sclerosis. *J Neurol* 1996;243:S8–S13.
14. Neuhaus O, Farina C, Wekerle H, et al. Mechanisms of action of glatiramer acetate in multiple sclerosis. *Neurology* 2001;56:702–708.
15. Neuhaus O, Farina C, Yassouridis A, et al. Multiple sclerosis: comparison of copolymer-1-reactive T cell lines from treated and untreated subjects reveals cytokine shift from T helper 1 to T helper 2 cells. *Proc Natl Acad Sci USA* 2000;97:7452–7457.
16. Chen M, Gran B, Costello K, et al. Glatiramer acetate induces a Th2-biased response and crossreactivity with myelin basic protein in patients with MS. *Mult Scler* 2001;7:209–219.
17. Miller A, Shapiro S, Gershtein R, et al. Treatment of multiple sclerosis with copolymer-1 (Copaxone): implicating mechanisms of Th1 to Th2/Th3 immune-deviation. *J Neuroimmunol* 1998;92:113–121.
18. Duda PW, Schmied MC, Cook SL, et al. Glatiramer acetate (Copaxone) induces degenerate, Th2-polarized immune responses in patients with multiple sclerosis. *J Clin Invest* 2000;105:967–976.
19. Dhib-Jalbut S, Chen M, Said A, et al. Glatiramer acetate-reactive peripheral blood mononuclear cells respond to multiple myelin antigens with a Th2-biased phenotype. *J Neuroimmunol* 2003;140:163–171.
20. Duda PW, Krieger JI, Schmied MC, et al. Human and murine CD4 T cell reactivity to a complex antigen: recognition of the synthetic random polypeptide glatiramer acetate. *J Immunol* 2000;165:7300–7307.
21. Brenner T, Arnon R, Sela M, et al. Humoral and cellular immune responses to Copolymer 1 in multiple sclerosis patients treated with Copaxone(R). *J Neuroimmunol* 2001;115:152–160.
22. Rieks M, Hoffmann V, Aktas O, et al. Induction of apoptosis of CD4+ T cells by immunomodulatory therapy of multiple sclerosis with glatiramer acetate. *Eur Neurol* 2003;50:200–206.
23. Chen M, Conway K, Johnson KP, et al. Sustained immunological effects of Glatiramer acetate in patients with multiple sclerosis treated for over 6 years. *J Neurol Sci* 2002;201:71–7.
24. Biernacki K, Prat A, Blain M, et al. Regulation of Th1 and Th2 lymphocyte migration by human adult brain endothelial cells. *J Neuropathol Exp Neurol* 2001;60:1127–1136.
25. Aharoni R, Teitelbaum D, Arnon R, et al. Copolymer 1 inhibits manifestations of graft rejection. *Transplantation* 2001;72:598–605.
26. Aharoni R, Kayhan B, Eilam R, et al. Glatiramer acetate-specific T cells in the brain express T helper 2/3 cytokines and brain-derived neurotrophic factor in situ. *Proc Natl Acad Sci USA* 2003;100:14157–14162.
27. Chen M, Valenzuela RM, Dhib-Jalbut S. Glatiramer acetate-reactive T cells produce brain-derived neurotrophic factor. *J Neurol Sci* 2003;215:37–44.
28. Yong VW. Differential mechanisms of action of interferon-beta and glatiramer acetate in MS. *Neurology* 2002;59:802–808.
29. Angelov DN, Waibel S, Guntinas-Lichius O, et al. Therapeutic vaccine for acute and chronic motor neuron diseases: implications for amyotrophic lateral sclerosis. *Proc Natl Acad Sci USA* 2003;100:4790–4795.
30. Benner EJ, Mosley RL, Destache CJ, et al. Therapeutic immunization protects dopaminergic neurons in a mouse model of Parkinson's disease. *Proc Natl Acad Sci USA* 2004;101:9435–9440.
31. Moalem G, Leibowitz-Amit R, Yoles E, et al. Autoimmune T cells protect neurons from secondary degeneration after central nervous system axotomy. *Nat Med* 1999;5:49–55.
32. Kipnis J, Yoles E, Porat Z, et al. T cell immunity to copolymer 1 confers neuroprotection on the damaged

optic nerve: possible therapy for optic neuropathies. *Proc Natl Acad Sci USA* 2000;97:7446–451.
33. Schori H, Kipnis J, Yoles E, et al. Vaccination for protection of retinal ganglion cells against death from glutamate cytotoxicity and ocular hypertension: implications for glaucoma. *Proc Natl Acad Sci USA* 2001;98:3398–3403.
34. Gilgun-Sherki Y, Panet H, Holdengreber V, et al. Axonal damage is reduced following glatiramer acetate treatment in C57/bl mice with chronic-induced experimental autoimmune encephalomyelitis. *Neurosci Res* 2003;47:201–207.
35. Parkinson JF, Mitrovic B, Merrill JE. The role of nitric oxide in multiple sclerosis. *J Mol Med* 1997;75:174–186.
36. Kayhan B, Aharoni R, Arnon R. Glatiramer acetate (Copaxone) regulates nitric oxide and related cytokine secretion in experimental autoimmune encephalomyelitis *Immunol Lett* 2003;88:185–192.
37. Thoenen H. Neurotrophins and neuronal plasticity. *Science* 1995;270:593–598.
38. Ziemssen T, Kumpfel T, Klinkert WE, et al. Glatiramer acetate-specific T-helper 1- and 2-type cell lines produce BDNF: implications for multiple sclerosis therapy. Brain-derived neurotrophic factor. *Brain* 2002;125:2381–2391.
39. Stadelmann C, Kerschensteiner M, Misgeld T, et al. BDNF and gp145trkB in multiple sclerosis brain lesions: neuroprotective interactions between immune and neuronal cells? *Brain* 2002;125:75–85.
40. Chabot S, Yong FP, Le DM, et al. Cytokine production in T lymphocyte-microglia interaction is attenuated by glatiramer acetate: a mechanism for therapeutic efficacy in multiple sclerosis. *Mult Scler* 2002;8: 299–306.
41. Kim HJ, Ifergan I, Antel JP, et al. Type 2 monocyte and microglia differentiation mediated by glatiramer acetate therapy in patients with multiple sclerosis. *J Immunol* 2004;172:7144–153.
42. Weber MS, Starck M, Wagenpfeil S, et al. Multiple sclerosis: glatiramer acetate inhibits monocyte reactivity in vitro and in vivo. *Brain* 2004;127:1370–1378.
43. Teitelbaum D, Aharoni R, Sela M, et al. Cross-reactions and specificities of monoclonal antibodies against myelin basic protein and against the synthetic copolymer 1. *Proc Natl Acad Sci USA* 1991;88:9528–9532.
44. Ure DR, Rodriguez M. Polyreactive antibodies to glatiramer acetate promote myelin repair in murine model of demyelinating disease. *FASEB J* 2002;16:1260–1262.
45. Farina C, Vargas V, Heydari N, et al. Treatment with glatiramer acetate induces specific IgG4 antibodies in multiple sclerosis patients. *J Neuroimmunol* 2002;123:188–192.
46. Teitelbaum D, Brenner T, Abramsky O, et al. Antibodies to glatiramer acetate do not interfere with its biological functions and therapeutic efficacy. *Mult Scler* 2003;9:592–599.
47. Salama HH, Hong J, Zang YC, et al. Blocking effects of serum reactive antibodies induced by glatiramer acetate treatment in multiple sclerosis. *Brain* 2003;126:2638–2647.
48. Bornstein MB, Miller A, Slagle S, et al. A pilot trial of Cop 1 in exacerbating-remitting multiple sclerosis. *N Engl J Med* 1987;317:408–414.
49. Johnson KP, Brooks BR, Cohen JA, et al. Copolymer 1 reduces relapse rate and improves disability in relapsing-remitting multiple sclerosis: results of a phase III multicenter, double-blind placebo-controlled trial. The Copolymer 1 Multiple Sclerosis Study Group. *Neurology* 1995;45:1268–1276.
50. Johnson KP, Brooks BR, Cohen JA, et al. Extended use of glatiramer acetate (Copaxone) is well tolerated and maintains its clinical effect on multiple sclerosis relapse rate and degree of disability. Copolymer 1 Multiple Sclerosis Study Group. *Neurology* 1998;50:701–708.
51. Johnson KP, Brooks BB, Ford CC, et al. Results of the long term (eight-year) prospective, open-label trial of glatiramer acetate for relapsing multiple sclerosis. *Neurology* 2002;58:A458.
52. Johnson KP, Brooks BR, Ford CC, et al. Glatiramer acetate (Copaxone): comparison of continuous versus delayed therapy in a six-year organized multiple sclerosis trial. *Mult Scler* 2003;9:585–591.
53. Weinshenker BG. The natural history of multiple sclerosis. *Neurol Clin* 1995;13:119–146.
54. Ford C, Johnson K, Brooks B, et al. Sustained efficacy and tolerability of Copaxone (glatiramer acetate) in relapsing-remitting multiple sclerosis patients treated for over 10 years. *Mult Scler* 2003;9:120.
55. Comi G, Filippi M, Wolinsky JS. European/Canadian multicenter, double-blind, randomized, placebo-controlled study of the effects of glatiramer acetate on magnetic resonance imaging—measured disease activity and burden in patients with relapsing multiple sclerosis. European/Canadian Glatiramer Acetate Study Group. *Ann Neurol* 2001;49:290–297.
56. Boneschi FM, Rovaris M, Johnson KP, et al. Effects of glatiramer acetate on relapse rate and accumulated disability in multiple sclerosis: meta-analysis of three double-blind, randomized, placebo-controlled clinical trials. *Mult Scler* 2003;9:349–355.
57. Wolinsky JS, Johnson KP, Comi G, et al. The effects of glatiramer acetate on sustained accumulated disability in relapsing multiple sclerosis are evident within one year: meta-analysis results of three double-blind, placebo-controlled clinical trials. *Mult Scler* 2003;9:120.
58. Munari L, Lovati R, Boiko A. Therapy with glatiramer acetate for multiple sclerosis. *Cochrane Database Syst Rev* 2004;CD004678.
59. Bornstein MB, Miller A, Slagle S, et al. A placebo-controlled, double-blind, randomized, two-center, pilot trial of Cop 1 in chronic progressive multiple sclerosis. *Neurology* 1991;41:533–539.
60. Aharoni R, Meshorer A, Sela M, et al. Oral treatment of mice with copolymer 1 (glatiramer acetate) results in the accumulation of specific Th2 cells in the central nervous system. *J Neuroimmunol* 2002;126:58–68.
61. Maron R, Slavin AJ, Hoffmann E, et al. Oral tolerance to copolymer 1 in myelin basic protein (MBP) TCR transgenic mice: cross-reactivity with MBP-specific TCR and differential induction of anti-inflammatory cytokines. *Int Immunol* 2002;14:131–138.
62. Wolinsky JS. The diagnosis of primary progressive multiple sclerosis. *J Neurol Sci* 2003;206:145–152.
63. Wolinsky JS, Pardo L, Stark Y, et al. Effect of glatiramer acetate on primary progressive multiple sclerosis: initial analysis of the completed PROMiSe Trial. *Neurology* 2004;62:A97–A98.
64. Mancardi GL, Sardanelli F, Parodi RC, et al. Effect of copolymer-1 on serial gadolinium-enhanced MRI in

relapsing remitting multiple sclerosis. *Neurology* 1998;50:1127–1133.
65. Ge Y, Grossman RI, Udupa JK, et al. Glatiramer acetate (Copaxone) treatment in relapsing-remitting MS: quantitative MR assessment. *Neurology* 2000;54:813–817.
66. Wolinsky JS, Narayana PA, Johnson KP. United States open-label glatiramer acetate extension trial for relapsing multiple sclerosis: MRI and clinical correlates. Multiple Sclerosis Study Group and the MRI Analysis Center. *Mult Scler* 2001;7:33–41.
67. Wolinsky JS, Comi G, Filippi M, et al. Copaxone's effect on MRI-monitored disease in relapsing MS is reproducible and sustained. *Neurology* 2002;59:1284–1286.
68. Filippi M, Rovaris M, Rocca MA, et al. Glatiramer acetate reduces the proportion of new MS lesions evolving into "black holes." *Neurology* 2001;57:731–733.
69. Rovaris M, Comi G, Rocca MA, et al. Short-term brain volume change in relapsing-remitting multiple sclerosis: effect of glatiramer acetate and implications. *Brain* 2001;124:1803–1812.
70. Sormani MP, Rovaris M, Valsasina P, et al. Measurement error of two different techniques for brain atrophy assessment in multiple sclerosis. *Neurology* 2004;62:1432–1434.
71. Carra A, Onaha P, Sinay V, et al. A retrospective, observational study comparing the four available immunomodulatory treatments for relapsing-remitting multiple sclerosis. *Eur J Neurol* 2003;10:671–676.
72. Khan OA, Tselis AC, Kamholz JA, et al. A prospective, open-label treatment trial to compare the effect of IFN beta-1a (Avonex), IFNbeta-1b (Betaseron), and glatiramer acetate (Copaxone) on the relapse rate in relapsing-remitting multiple sclerosis. *Eur J Neurol* 2001;8:141–148.
73. Khan OA, Tselis AC, Kamholz JA, et al. A prospective, open-label treatment trial to compare the effect of IFNbeta-1a (Avonex), IFNbeta-1b (Betaseron), and glatiramer acetate (Copaxone) on the relapse rate in relapsing–remitting multiple sclerosis: results after 18 months of therapy. *Mult Scler* 2001;7:349–353.
74. Haas J. Onset of clinical benefit of glatiramer (Copaxone) acetate in 255 patients with relapsing-remitting multiple sclerosis. *Neurology* 2003;60:A480.
75. Flechter S, Vardi J, Pollak L, et al. Comparison of glatiramer acetate (Copaxone) and interferon beta-1b (Betaferon) in multiple sclerosis patients: an open-label 2-year follow-up. *J Neurol Sci* 2002;197:51–55.
76. Flechter S, Kott E, Steiner-Birmanns B, et al. Copolymer 1 (glatiramer acetate) in relapsing forms of multiple sclerosis: open multicenter study of alternate-day administration. *Clin Neuropharmacol* 2002;25:11–15.
77. Khan O, Caon C, Zvartau-Hind M, et al. Clinical course before and after change of immunomodulating therapy in relapsing remitting MS. *Neurology* 2001;56:A355.
78. Caon C, Din M, Zvartau-Hind M, et al. Three-year follow-up and clinical course after change of immunomodulatory therapy in relapsing-remitting MS. *J Neurology* 2003;250[Suppl 2]:190.
79. Zwibel H, for the Copaxone Treatment IND Study Group. Benefit of Copaxone demonstrated in patients with relapsing-remitting multiple sclerosis (RRMS) previously treated with interferon. *J Neurology* 2001;248[Suppl 2]:P521.
80. Dhib-Jalbut S. Mechanisms of action of interferons and glatiramer acetate in multiple sclerosis. *Neurology* 2002;58:S3–S9.
81. Yong VW. Differential mechanisms of action of interferon-a and glatiramer acetate in MS. *Neurology* 2002;59:802–808.
82. Simpson D, Noble S, Perry C. Glatiramer acetate: a review of its use in relapsing-remitting multiple sclerosis. *CNS Drugs* 2002;16:825–850.
83. Milo R, Panitch H. Additive effects of copolymer-1 and interferon beta-1b on the immune response to myelin basic protein. *J Neuroimmunol* 1995;61:185–193.
84. Lublin F, Cutter G, Elfont R, et al. A trial to assess the safety of combining therapy with interferon beta-1a and glatiramer acetate in patients with relapsing MS. *Neurology* 2001;56:A148.
85. Farina C, Wagenpfeil S, Hohlfeld R. Immunological assay for assessing the efficacy of glatiramer acetate (Copaxone) in multiple sclerosis. A pilot study. *J Neurol* 2002;249:1587–1592.
86. Coyle PK, Johnson KP, Pardo L, et al. Pregnancy outcomes in patients with multiple sclerosis treated with glatiramer acetate (Copaxone). *Mult Scler* 2003; 9:P160.
87. Kornek B, Bernert G, Balassy C, et al. Glatiramer acetate treatment in patients with childhood and juvenile onset multiple sclerosis. *Neuropediatrics* 2003;34: 120–126.
88. Mancardi GL, Murialdo A, Drago F, et al. Localized lipoatrophy after prolonged treatment with copolymer 1. *J Neurol* 2000;247:220–221.
89. Hwang L, Orengo I. Lipoatrophy associated with glatiramer acetate injections for the treatment of multiple sclerosis. *Cutis* 2001;68:287–288.
90. Edgar CM, Brunet DG, Fenton P, et al. Lipoatrophy in patients with multiple sclerosis on glatiramer acetate. *Can J Neurol Sci* 2004;31:58–63.
91. Metz LM, Patten SB, Archibald CJ, et al. The effect of immunomodulatory treatment on multiple sclerosis fatigue. *J Neurol Neurosurg Psychiatry* 2004;75:1045–1047.
92. Ziemssen T, Neuhaus O, Hohlfeld R. Risk-benefit assessment of glatiramer acetate in multiple sclerosis. *Drug Saf* 2001;24:979–990.
93. Ferrero S, Pretta S, Ragni N. Multiple sclerosis: management issues during pregnancy. *Eur J Obstet Gynecol Reprod Biol* 2004;115:3–9.

Psychopharmacology (2005) 181: 118–125
DOI 10.1007/s00213-005-2229-z

ORIGINAL INVESTIGATION

Tatyana Poltyrev · Elena Gorodetsky · Corina Bejar · Donna Schorer-Apelbaum · Marta Weinstock

Effect of chronic treatment with ladostigil (TV-3326) on anxiogenic and depressive-like behaviour and on activity of the hypothalamic–pituitary–adrenal axis in male and female prenatally stressed rats

Received: 28 September 2004 / Accepted: 6 February 2005 / Published online: 14 April 2005
© Springer-Verlag 2005

Abstract *Objective:* The aim of the study is to investigate the effect of ladostigil, a cholinesterase and brain-selective monoamine oxidase (MAO) inhibitor, on anxiogenic and depressive-like behaviour and the response of the hypothalamic–pituitary–adrenal axis to stress in prenatally stressed (PS) male and female rats. *Methods:* Ladostigil (17 mg/kg/day) was administered daily for 6 weeks to control and PS rats aged 6 weeks. Behaviour was assessed in the elevated plus maze (EPM) and forced swim tests (FST). Plasma corticosterone (COR) was measured before, 30 and 90 min after exposure to stress. *Results:* Ladostigil inhibited brain MAO-A and B by more than 60%, significantly reduced hyperanxiety of male and female PS rats in the EPM and depressive-like behaviour in the FST without affecting that of controls and restored the delayed return to baseline of plasma COR in PS rats after exposure to stress to that of control rats. *Conclusions:* A novel brain-selective MAO inhibitor, ladostigil can selectively reverse the behavioural and neurochemical effects induced by prenatal stress without affecting the behaviour of controls.

Keywords Elevated plus maze · Forced swim test · Ladostigil · Monoamine oxidase inhibitor · Plasma corticosterone · Prenatal stress

T. Poltyrev · E. Gorodetsky · C. Bejar · D. Schorer-Apelbaum · M. Weinstock (✉)
Department of Pharmacology,
Hebrew University Hadassah School of Medicine,
Ein Kerem, Jerusalem, 91120, Israel
e-mail: martar@md.huji.ac.il
Tel.: +972-2-6758731
Fax: +972-2-6758741

Introduction

Thompson (1957) was the first to report that subjection of a pregnant rat to psychological stress increases emotional behaviour of the offspring. His findings have been confirmed and extended in numerous studies in which it was found that prenatal stress impairs learning and memory (Lemaire et al. 2000; Gué et al. 2004), reduces play behaviour (Morley-Fletcher et al. 2003b), exacerbates anxiety in intimidating situations (Archer and Blackman 1971; Fride et al. 1986; Fride and Weinstock 1988) and induces depressive-like behaviour or learned helplessness more readily than in controls (Secoli and Teixeira 1998). While memory deficits (Gué et al. 2004) and hyperanxiety (Fride and Weinstock 1988; Zimmerberg and Blaskey 1998) induced by prenatal stress are seen in rats of each gender, other behavioural and neurochemical changes are more readily seen in female than in male rat offspring. These include the increased propensity for depressive-like behaviour in the forced swim test (FST) (Alonso et al. 1991; Frye and Wawrzycki 2003) and the greater activation of the hypothalamic–pituitary–adrenal (HPA) axis in response to acute stress in adulthood (Weinstock et al. 1992; McCormick et al. 1995; Szuran et al. 2000). Prenatal stress also causes a bigger reduction in hippocampal benzodiazepine receptors in female than in male rats (Fride et al. 1985). While a reduction in the number of hippocampal cells is seen in female offspring after a single exposure of pregnant rats to stress (Schmitz et al. 2002), repeated exposure to stress during the last week of gestation is required in order to reduce hippocampal synapses in male offspring (Hayashi et al. 1998). This could explain why it may be easier to detect depressive-like behaviour in prenatally stressed (PS) female rats, since a role for hippocampal cell loss and inhibition of neurogenesis has been

posited in the aetiology of depression in human subjects (Jacobs et al. 2000). It is possible that female rats are more sensitive than males to alterations in neuronal programming induced by maternal stress hormones and, like women, could be more prone than males to develop depressive symptomatology (Blehar 1995).

The improvement of mood in some depressed human subjects by antidepressant drugs has been associated with a restoration of the feedback regulation of the HPA axis indicated by a normalization of the dexamethasone-suppression test (Holsboer and Barden 1996; Heuser et al. 1996). Furthermore, several classes of antidepressants are at least as effective as benzodiazepines in the treatment of generalized anxiety disorder (Lenox-Smith and Reynolds 2003; Sheehan and Mao 2003) that may precede or accompany depressive symptoms (Breslau et al. 1995). However, antidepressants generally do not improve cognitive impairment that is present in a significant proportion of elderly depressed patients (Nebes et al. 2003) and may even increase it because of anticholinergic activity (Teri et al. 1991). In an attempt to address this problem, a new drug ladostigil (TV-3326, [*N*-propargyl-(3R)-aminoindan-5-yl]-ethyl methyl carbamate) has been developed that has cholinesterase inhibitory activity like drugs currently used for the treatment of dementia and also shows anxiolytic and antidepressant-like activity in rats (Weinstock et al. 2003). Ladostigil was shown to improve cognitive deficits in aged monkeys (Buccafusco et al. 2003). It inhibits brain acetyl and butyryl cholinesterase after acute administration but needs to be given chronically in order to inhibit monoamine oxidase (MAO) A and B selectively in the brain (Weinstock et al. 2002c).

Although many attempts have been made to demonstrate anxiolytic activity of antidepressants in rodent models of hyperanxiety, most have failed to do so even when the drugs were administered chronically (Cassella and Davis 1985; Cole and Rodgers 1995; Van Dijken et al. 1992). In all these experiments, only male rats were used, in spite of the fact that chronic anxiety states and depression are more common in women than in men (Kuehner 1999). In a recent study, we found that chronic treatment with amitriptyline selectively reduced the hyperanxiety of PS females in the elevated plus maze (EPM test) (Poltyrev and Weinstock 2004). This treatment was only effective in PS males after cessation of drug administration either because of gender differences in the mode of action or metabolism of amitriptyline (Masubuchi et al. 1996) or because of its motor depressant effect, which was more prominent in males. Nevertheless, the finding showed that PS female rats are a suitable model for detecting an anxiolytic effect of antidepressant drugs.

The aim of the present study was to determine whether ladostigil has anxiolytic and antidepressant-like activity in PS rats of both sexes. Since the antidepressant effect of different classes of drugs in humans was shown to be associated with restoration of the impaired feedback regulation of the HPA axis, we also determined the effect of ladostigil on changes in plasma corticosterone (COR) in response to acute stress in the same animals.

Materials and methods

Animals

All the experiments were carried out according to the guidelines of the University Committee for Institutional Animal Care, based on those of the National Institutes of Health, USA. Female pathogen-free (SPF) Sprague–Dawley rats weighing 280–300 g (Harlan, Biotec, Jerusalem) on day 1 of pregnancy (detected by the presence of a vaginal plug) were randomly allocated to stress (six) and control (six) groups and housed singly in the animal house at an ambient temperature of 22±1°C and a 12-h diurnal light cycle (lights on at 0700 h, off at 1900 h). Food and water were provided ad libitum, and the cages were changed twice weekly. Control pregnant females were left undisturbed in their home cages. From days 15 to 20 of gestation, rats were placed three times daily for 45 min in transparent cylindrical restrainers, 8 cm in diameter and 20 cm long in normal light at room temperature, 21–22°C. The mothers gave birth between the 21st and 22nd day. In another group of pregnant rats run at the same time, plasma COR was measured between 0900 and 1000 h as described below in control rats and 30 min after the restraint procedure. The total numbers of pups that were available for the subsequent experiments are as follows: C males, 20; C females 20; PS males, 21; PS females, 20. It was shown in previous studies on this strain of rat that maternal restraint stress did not significantly alter birth weight (Herzog-Raalbag 2002). The pups were weaned at 3 weeks of age, distributed according to their sex and prenatal treatment and housed in groups of four per cage at the same ambient temperature and light cycle as shown above.

Drug administration

From the age of 6 weeks, all the rat offspring were housed two per cage, and ladostigil (17 mg/kg) was added to the drinking water until the completion of all the experiments 6 weeks later. This was the highest amount of the drug that could be given in the drinking water that did not alter food or fluid intake by the rats. In order to compute the dose of drug to be given, daily fluid intake was measured and the rats were weighed once a week when their cages were cleaned to avoid unnecessary handling that could influence their behaviour. Previous experiments in control (C) and PS rats in our laboratory had provided fairly accurate information about their fluid intake and weight gain at this age (Poltyrev and Weinstock 2004). The disadvantage of the method is that one cannot ensure that each rat receives the same amount of drug. This could have been accomplished either by housing them singly or administering the drug by oral gavage or parenteral injection. However, both single housing (Lopes Da Silva et al. 1996) and the stress of repeated daily drug administration (Bodnoff et al. 1988) alone have been shown to cause hyperanxiety and could therefore have masked the difference in behaviour between PS and C rats.

Behavioural tests

Behavioural experiments were carried out in PS and C rats aged 11–12 weeks between 1500 and 1900 h in a room adjacent to that in which the rats were housed and having the same conditions of temperature and humidity. All rats were tested in the elevated plus maze (EPM) as previously described (Weinstock et al. 2002c). The experiment was performed under bright light to minimize the variability in the behaviour of females in this test according to the stage of the oestrus cycle (Mora et al. 1996). Rats were tested 2 days later in the FST. EPM and FST were performed in ten rats of each sex and prenatal treatment group given tap water or ladostigil. Five to 6 days after the FST, six to eight rats of each group were randomly selected for measurement of their HPA axis response to novelty stress while still receiving ladostigil. Two to three of the remaining untreated males and females and of those given ladostigil were sacrificed, and the brains were rapidly removed for measurement of MAO activity as previously described (Weinstock et al. 2002a).

Elevated plus maze

The EPM was made of dark wood and consisted of two open arms opposite each other crossed by two enclosed arms (40-cm-high walls) each 50 cm long and 10 cm wide, with a centre square of 10 cm^2. The EPM stood 60 cm above the floor. Rats were placed in the centre of the maze and allowed to explore for 5 min. An observer, unaware of the type of treatment each rat had undergone, recorded the amount of time spent in the open and closed arms and the number of entries into open and closed arms. An open-arm entry was recorded when all four paws were inside the open arm. The maze was cleaned with detergent and dried after each rat.

Forced swim

The FST is a behavioural assay in which rats are exposed to a 15-min pretest in a cylinder of water from which they cannot escape followed 24 h later by a 5-min re-exposure that has been shown to predict the efficacy of potential antidepressants. Antidepressant drugs are usually injected once or three times between the first and second test (Borsini and Meli 1988). Rats typically assume an immobile floating posture, the duration of which is significantly reduced by different types of antidepressants (Porsolt et al. 1978). More recent studies have focussed also on the individual components of active behaviour, such as swimming and attempts to climb the walls, and have shown that these are sensitive to drugs that increase serotoninergic and noradrenergic transmission, respectively (Lucki 1997). It has also been reported that some antidepressants are more effective in altering behaviour of rats in the FST if they are administered chronically rather than acutely between the two tests (Kitada et al. 1981; Borsini and Meli 1988). Since we found that it was necessary to administer ladostigil (26 mg/kg/day) for at least 2 weeks in order to inhibit MAO by more than 60% (Weinstock et al. 2002a), we evaluated the effect of the drug on the behaviour of the rats during both the first and second exposures while the rats were under its influence. The rats were placed individually for 15 min into a glass cylinder, 19 cm in diameter and 60 cm in height, containing 30 cm of water maintained at 25°C, and the duration of each of the following behaviours was recorded during the first 5 min: immobility (floating in the water without active movements of forepaws), climbing or struggling (active movements with forepaws usually directed towards the walls) and swimming (active movements of fore or hindlegs across the top of the water). The rats were removed from the water, were dried gently and were returned to their home cages. On the following day, the rats were re-exposed to the cylinder for 5 min, and the above measurements were repeated.

Corticosterone measurement

For measurement of plasma COR in the rats, blood (50 μl) was rapidly collected after a small incision was made in the tail at 0800 h while the rat remained in its home cage. Sixty minutes later, the rat was placed in a brightly lit open field for 5 min. It was then returned to the home cage, and further blood samples were taken 25 and 85 min later. Plasma COR levels were all assayed at the same time in duplicates using a [^{3}H] corticosterone radioimmunoassay kit (ICN Biomedicals, Inc., California, USA). The sensitivity of the assay was 0.02 ng/tube, and cross-reactivity of the antiserum to other steroids was less than 0.4%. The inter-assay coefficients of variation were 6%.

Drugs

The drug used was ladostigil tartrate (TV3326, Teva Pharmaceuticals Ltd, Israel). Doses are expressed in mg/kg of the salt.

Statistical analysis

The EPM data were analyzed by ANOVA for factors Maternal (stress or control), Gender and Offspring treatment (water or ladostigil). FST data were analyzed by ANOVA for factors Experiment (first or second exposure to the FST), Gender, Maternal and Offspring treatment. The plasma COR data were analyzed by GLM for repeated measures three times and factors Maternal, Gender and Offspring treatment (water or ladostigil) and also independently by GLM at three separate measures of time and using SPSS (version 11) statistical package. Duncan's post hoc test was used when appropriate, and a difference of $P<0.05$ was considered to be statistically significant.

Results

Maternal plasma COR

Plasma COR measurements of control and stressed mothers measured on day 17 of gestation were 52.3±9.3 and 522±55 ng/ml, respectively.

Elevated plus maze

There were no significant differences in the time spent in the open arms of the EPM, the total number of arm entries or entries into the open arms between naive C and PS rats given water. This may have been due to the relatively high intensity of illumination in the room in which the experiment was performed which lowered the general activity of the rats. There was a significant effect of Offspring treatment ($F_{1,79}$=7.98, P<0.01) and a Maternal × Offspring treatment interaction for time spent in open arms ($F_{1,79}$= 8.95, P<0.005), the number of open-arm entries ($F_{1,79}$= 10.11, P<0.001) and the ratio of open/total entries ($F_{1,79}$=8.20, P<0.01), but no significant Gender × Maternal or Gender × Offspring treatment interactions. Thus, under the influence of ladostigil, PS rats of both sexes spent significantly more time in the open arms of the maze without showing an increase in general activity, indicating that the drug specifically reduced anxiety. By contrast, ladostigil had no effect on the behaviour of C rats in the EPM in spite of the fact that their behaviour in this test did not differ from that of PS rats when given water (Fig. 1). Unlike amitriptyline (Poltyrev and Weinstock 2004), ladostigil did not reduce the number of entries into closed arms, indicating that it did not inhibit general exploratory activity in the dose given.

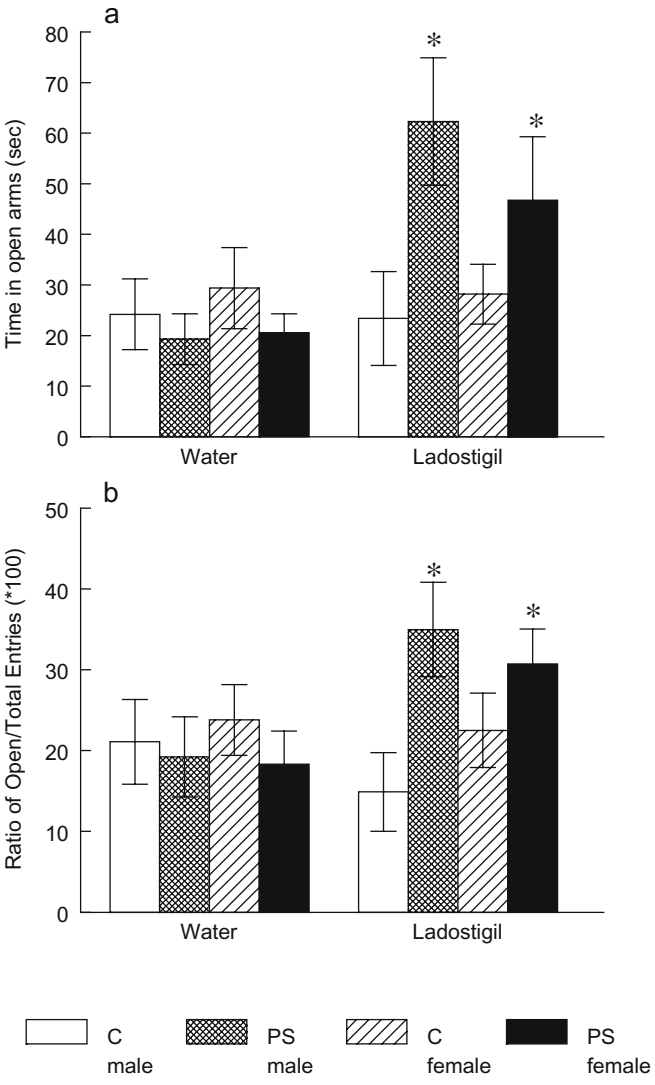

Fig. 1 Effect of ladostigil on behavior of PS and C rats in EPM. **a** Time in open arms; **b** ratio open/total arm entries×100. Data reflect mean and SEM. *Significantly different from water, P<0.05

Forced swim

Analysis of the behaviour of untreated rats during the first and second exposures to the FST revealed the following main effects. For Experiment, there were significant differences between the first and second experiments in immobility ($F_{1,159}$=32.4, P<0.0001), climbing ($F_{1,158}$=32.5, P<0.0001) and swimming ($F_{1,159}$=10.30, P<0.002). There were also significant Gender differences in immobility ($F_{1,159}$=30.5, P<0.0001), climbing ($F_{1,159}$=19.2, P<0.0001) and swimming ($F_{1,159}$=15.1, P<0.0001) since females spent more time in active behaviours than males during the first exposure to the test (Fig. 2). A significant Experiment × Maternal treatment interaction was only found for swimming ($F_{1,158}$=4.11, P<0.05), which was reduced more in PS than in C rats, but there was no Gender × Maternal treatment interaction. Offspring treatment with ladostigil resulted in significant main effects on immobility ($F_{1,158}$=13.2, P<0.0001), climbing ($F_{1,79}$=9.66, P<0.0025) and swimming ($F_{1,158}$=5.74, P<0.02). Maternal × Offspring treatment interactions were significant for all three behavioural paradigms, immobility ($F_{1,79}$=13.2, P<0.0001), climbing ($F_{1,79}$=5.24, P<0.025) and swimming ($F_{1,158}$=9.01, P< 0.005), since ladostigil significantly affected the behaviour of PS but not that of C rats during the first and second exposures. There were significant Experiment × Gender × Offspring treatment interactions for immobility ($F_{1,158}$= 7.71, P<0.01) and swimming ($F_{1,158}$=7.69, P<0.01). Although ladostigil altered all three types of behaviour of PS males in the first experiment, only the decrease in immobility reached statistical significance. Ladostigil selectively increased climbing more in PS than in C females. In the second swim test, ladostigil selectively decreased immobility and increased swimming and climbing of PS rats but not that of controls (Fig. 2). The effect of ladostigil was more evident in PS females than in males.

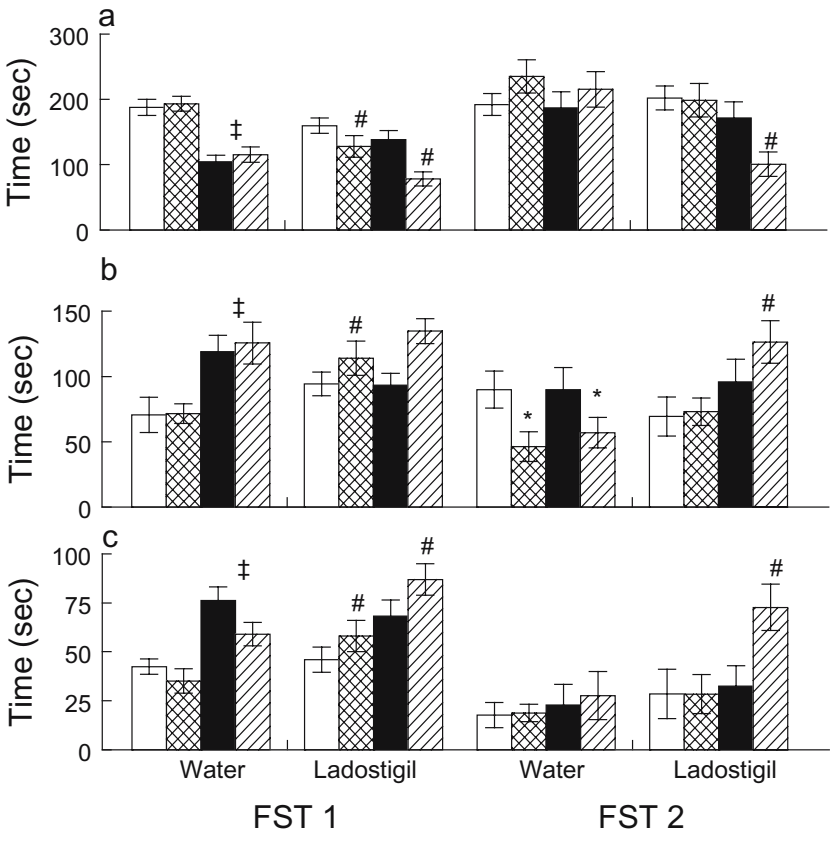

Fig. 2 Effect of ladostigil on the behaviour of PS and C rats during 5 min of first and second exposures to FST. **a** Duration of immobility; **b** duration of swimming; **c** duration of climbing. Data reflect mean and SEM. *Open bars*: C males; *black bars*: C females; *cross-hatched bars*: PS males; *hatched bars*: PS females. First FST: ‡significant gender difference in immobility, swimming and climbing, $P<0.0025$. Second FST: *significant effect of prenatal stress, $P<0.05$. Ladostigil treatment: #significant effect in PS rats on immobility, swimming and climbing, $P<0.025$

Plasma corticosterone in response to novelty stress

Repeated-measures analysis revealed the following significant effects: Time ($F_{1,51}=54.0$, $P<0.0001$) and Time × Maternal treatment ($F_{1,51}=6.9$, $P<0.025$), indicating that the overall response to stress over time differed in PS and C rats. However, there were no Time × Gender or Time × Gender × Maternal treatment interactions, indicating that the change of COR levels did not differ in males and females. There were also no Time × Offspring treatment or Time × Maternal × Offspring treatment interactions. Basal levels of plasma COR were significantly higher in females than in males, Gender ($F_{1,56}=31.7$, $P<0.0001$), but there were no differences between the levels in PS and C rats and there were no Maternal × Offspring treatment interactions as the effect of ladostigil did not differ in PS and C rats at this time (Table 1). There was a significant Gender × Offspring treatment interaction ($F_{1,56}=4.82$, $P<0.05$) since ladostigil decreased resting plasma COR levels in males and increased them in females. The Gender difference was still present 30 min after exposure to the open field ($F_{1,56}=13.72$, $P<0.001$), but there was no longer a Gender × Offspring treatment interaction. The Maternal × Offspring treatment interaction failed to reach statistical significance ($F_{1,56}=3.24$, $P=0.07$). At 90 min, there were significant effects of Gender ($F_{1,56}=9.14$, $P<0.005$) and of Maternal treatment ($F_{1,56}=10.57$, $P<0.0025$) since COR values of PS rats given water were higher than those of controls. There was also a Maternal × Offspring treatment interaction ($F_{1,56}=5.68$, $P<0.025$) because ladostigil reduced plasma COR levels in PS rats but increased them in C rats. The data are summarized in Table 1.

Monoamine oxidase inhibition

Monoamine oxidase A and B inhibition after chronic treatment with ladostigil 17 mg/kg/day for 6 weeks did not differ in whole brain homogenates of two PS and two C male and two PS and two C female rats. The data were

Table 1 Effect of chronic treatment with ladostigil on response of HPA axis of PS and control rats to novelty stress

Treatment	Time (min)	Plasma corticosterone (ng/ml)			
		Male		Female	
		Control	PS	Control	PS
Water		$n=7$	$n=8$	$n=6$	$n=8$
Ladostigil		$n=8$	$n=8$	$n=6$	$n=6$
Water	0	50.6±6.8	58.4±8.3	103±31‡	99.1±19.0‡
Ladostigil	0	28.1±2.3	40.4±9.3	151±32‡	130±34‡
Water	30	203±32	278±37	308±37‡	452±71‡
Ladostigil	30	251±20	245±28	422±81‡	368±104‡
Water	90	87.1±18.1	187±36*	128±20‡	405±64‡*
Ladostigil	90	140±38#	176±46#	219±65#	238±50#

‡Significant gender difference, $P<0.005$
*Significant effect of maternal treatment, $P<0.025$
#Significant interaction between maternal and ladostigil treatment

therefore pooled, and inhibition of MAO-A was 62.0±3.2% and MAO-B 66.8±2.9%.

Discussion

In the present study, we found that ladostigil, a novel potential antidepressant with cholinesterase inhibitory activity, reduced hyperanxiety in both male and female PS rats in the EPM and depressive-like behaviour in the FST without affecting the behaviour of controls. This selective effect of ladostigil in the EPM occurred in spite of the fact that PS rats did not show significantly greater anxiety than controls under the conditions of the test, probably because it was performed in a well-lit room in order to avoid an influence of different stages of the oestrus cycle on behaviour. Under these conditions, control rats also spend little time in the open arms of the maze. The lack of an anxiolytic effect of ladostigil in the EPM concurs with that of others who treated control rats chronically with antidepressants, in contrast to diazepam, which induced a clear reduction in anxiety (Cole and Rodgers 1995; File et al. 1999; Weinstock et al. 2002b). The selective sensitivity of PS rats to the effect of ladostigil in the EPM indicates that there are neurochemical differences underlying the behaviour of PS and C rats. These include, among others, a reduction in hippocampal benzodiazepine receptors (Fride et al. 1986), alterations in glutamate and dopamine receptor subtypes in different forebrain regions (Berger et al. 2002) and in genes associated with subunits NR1 and NR2A of glutamate NMDA receptors (Kinnunen et al. 2003). Unlike amitriptyline in a previous study (Poltyrev and Weinstock 2004), ladostigil had an anxiolytic effect in PS rats of both sexes. This observation makes it unlikely that the lack of effect of amitriptyline in PS males was due to an innate gender difference in anxiogenic behaviour but suggests that it resulted from a difference in the metabolism of amitriptyline in male and female rats (Masubuchi et al. 1996) and to the greater depression caused by the drug in motor activity in males.

In addition to predicting antidepressant potential of drugs, the FST has been used to detect depressive-like behaviour induced in rats by prenatal stress (Alonso et al. 1991; Drago et al. 1999; Frye and Wawrzycki 2003). While some studies reported a difference in the behaviour of PS and control males in this test (Drago et al. 1999; Morley-Fletcher et al. 2003a), others only detected a greater degree of depressive-like activity in PS females (Alonso et al. 1991). This may be because C males were immobile for more than 70% of the time during the second exposure to the test in the latter study, making it difficult to obtain significantly higher levels in PS males. In the present study, a gender difference was seen in the behaviour of rats in the FST. During the first exposure to the test, male rats developed an immobile posture for a greater period of time than females. Such a gender difference has been reported in some (Alonso et al. 1991; Barros and Ferigolo 1998) but not other rat strains (Frye and Wawrzycki 2003) and appears to vary according to the stage of the oestrous cycle. Re-exposure to the FST increased the duration of immobility in females to that in males.

As in the EPM test, untreated PS rats did not differ significantly from controls in any measure of behaviour in the FST test. Nevertheless, ladostigil significantly affected the behaviour of PS rats during both the first and second exposures, thereby confirming the difference in the neurochemical basis underlying their behaviour mentioned above. The effect of ladostigil on swimming and climbing in PS rats resulted from a more than 60% inhibition of brain MAO-A and B, which had been shown to enhance both serotoninergic (Weinstock et al. 2002b) and noradrenergic transmission (Sagi et al. 2003). The selective effect of ladostigil on the behaviour of PS rats in this test is reminiscent of that of other antidepressants, desipramine and nomifensine in the WKY rat (Tejani-Butt et al. 2003), a genetic model of depressive behaviour (Lahamame et al. 1997). These drugs had no effect on the behaviour of normal Wistar or Sprague–Dawley rats. The data of the present study and those of Tejani-Butt et al. (2003) serve to demonstrate the difference in the response to drugs of rats with an anxiety-depression state induced by genetic or environmental factors from that of control animals.

Hyperactivity of the HPA axis with elevation of cortisol at rest and in response to stress is consistently found in patients with major depression and can be explained by impaired corticosteroid receptor signalling (Holsboer 2001). HPA axis function can be normalized by clinically effective treatment with antidepressants (Heuser et al. 1996). A similar impairment in the regulation of the HPA axis associated with a reduction of GR and MR receptors has been reported for PS rats (Weinstock et al. 1992; Henry et al. 1994; McCormick et al. 1995). The present study confirmed previous findings that prenatal stress caused a greater alteration in the activity of the response of the HPA axis to stress. This was shown by the slower return of plasma COR to baseline levels after exposure to novelty stress. Although present in rats of both sexes, the effect was more marked in females which are generally more reactive to stress.

Ladostigil did not significantly effect resting or peak levels of plasma COR in C or PS rats after exposure to the open field. However, at 90 min after stress exposure, the difference between C and PS rats in the rate of return to control levels of plasma COR was no longer seen. This suggests that the rate of recovery of the response of HPA axis to stress may have been increased in PS rats by ladostigil. It would be of interest to determine if this effect of the drug is related to an increase towards normal in hippocampal GR receptors, as has been shown for chronic treatment of rats and human subjects with other antidepressants (Budziszewska 2002; Calfa et al. 2003).

In conclusion, this study showed that the EPM test can be used to detect the potential anxiolytic effect of ladostigil, a novel AChE and MAO inhibitor, in both male and female PS rats. Prenatal stress significantly disrupted the response of the HPA axis to stress in adult rats, resulting in an increased duration of the elevation of plasma COR in response to stress. Chronic treatment with ladostigil at

a dose that inhibited MAO-A and B by more than 60% selectively increased swimming and struggling behaviour of PS rats in the FST, a finding compatible with an elevation of both brain 5HT and NA. The ability of ladostigil to improve cognitive dysfunction because of cholinesterase inhibition and also to decrease anxiety and depressive symptoms may make it a potentially valuable drug for the treatment of elderly depressive with cognitive impairment that do not respond to known antidepressant medications.

Acknowledgements The authors gratefully acknowledge the financial support of Teva Pharmaceuticals Ltd and Ms. Aviva Gross for MAO activity measurements. Dr. T. Poltyrev thanks the Israel Ministry of Absorption for financial support.

References

Alonso SJ, Arevalo R, Afonso D, Rodriguez M (1991) Effects of maternal stress during pregnancy on forced swimming test on behaviour of the offspring. Physiol Behav 50:511–517

Archer J, Blackman D (1971) Prenatal psychological stress and offspring behavior in rats and mice. Dev Psychobiol 4:193–248

Barros HMT, Ferigolo M (1998) Ethopharmacology of imipramine in the forced swimming test: gender differences. Neurosci Biobehav Rev 22:279–287

Berger MA, Barros VG, Sarchi MI, Tarazi FI, Antonelli MC (2002) Long-term effects of prenatal stress on dopamine and glutamate receptors in adult rat brain. Neurochem Res 27:1525–1533

Blehar MC (1995) Gender differences in risk factors for mood and anxiety disorders: implications for clinical treatment research. Psychopharmacol Bull 31:687–691

Bodnoff SR, Suranyi-Cadotte B, Aitken DH, Quirion R, Meaney MJ (1988) The effects of chronic antidepressant treatment in an animal model of anxiety. Psychopharmacology 95:298–302

Borsini F, Meli A (1988) Is the forced swimming test a suitable model for revealing antidepressant activity? Psychopharmacology 94:147–160

Breslau N, Schultz L, Peterson E (1995) Sex differences in depression: a role for preexisting anxiety. Psychiatry Res 58:1–12

Buccafusco JJ, Terry AV Jr, Goren T, Blaugrun E (2003) Potential cognitive actions of TV3326, a novel neuroprotective agent, as assessed in old rhesus monkeys in their performance of versions of a delayed matching task. Neuroscience 119:669–678

Budziszewska B (2002) Effect of antidepressant drugs on the hypothalamic–pituitary–adrenal axis activity and glucocorticoid receptor function. Pol J Pharmacol 54:343–349

Calfa G, Kademian S, Ceschin D, Vega G, Rabinovich GA, Volosin M (2003) Characterization and functional significance of glucocorticoid receptors in patients with major depression: modulation by antidepressant treatment. Psychoneuroendocrinology 28:687–701

Cassella JV, Davis M (1985) Fear-enhanced acoustic startle is not attenuated by acute or chronic imipramine treatment in rats. Psychopharmacology 87:278–282

Cole JC, Rodgers RJ (1995) Ethological comparison of the effects of diazepam and acute/chronic imipramine on the behaviour of mice in the elevated plus-maze. Pharmacol Biochem Behav 52:473–478

Drago F, Di Leo F, Giardina L (1999) Prenatal stress induces body weight deficit and behavioural alterations in rats: the effect of diazepam. Eur Neuropsychopharmacol 9:239–245

File SE, Ouagazzal AM, Gonzalez LE, Overstreet DH (1999) Chronic fluoxetine in tests of anxiety in rat lines selectively bred for differential 5-HT1A receptor function. Pharmacol Biochem Behav 62:695–701

Fride E, Weinstock M (1988) Prenatal stress increases anxiety-related behavior and alters cerebral lateralization of dopaminergic activity. Life Sci 42:1059–1065

Fride E, Dan Y, Gavish M, Weinstock M (1985) Prenatal stress impairs maternal behavior in a conflict situation and reduces hippocampal benzodiazepine receptors. Life Sci 36:2103–2109

Fride E, Dan Y, Feldon J, Halevy G, Weinstock M (1986) Effects of prenatal stress on vulnerability to stress in prepubertal and adult rats. Physiol Behav 37:681–687

Frye CA, Wawrzycki J (2003) Effect of prenatal stress and gonadal hormone condition on depressive behaviors of female and male rats. Horm Behav 44:319–326

Gué M, Bravard A, Meunier J, Veyrier R, Gaillet S, Recasens M, Maurice T (2004) Sex differences in learning deficits induced by prenatal stress in juvenile rats. Behav Brain Res 150:149–157

Hayashi A, Nagaoka M, Yamada K, Ichitani Y, Miake Y, Okado N (1998) Maternal stress induces synaptic loss and developmental disabilities of offspring. Int J Dev Neurosci 16:209–216

Henry C, Kabbaj M, Simon H, Le Moal M, Maccari S (1994) Prenatal stress increases the hypothalamic–pituitary–adrenal axis response to stress in young and adult rats. J Endocrinol 6:341–345

Herzog-Raalbag P (2002) Effect of antidepressants on the behavioural abnormalities and alterations in circadian rhythm induced by prenatal stress in rats. M.Sc. Thesis, Hebrew University, Jerusalem, Israel

Heuser I, Schweiger U, Gotthardt U, Schmider J, Lammers CH, Dettling M, Yassouridis A, Holsboer F (1996) Pituitary–adrenal-system regulation and psychopathology during amitriptyline treatment in elderly depressed patients and normal comparison subjects. Am J Psychiatry 153:93–99

Holsboer F (2001) Stress, hypercortisolism and corticosteroid receptors in depression: implications for therapy. J Affect Disord 62:77–91

Holsboer F, Barden N (1996) Antidepressants and hypothalamic–pituitary–adrenocortical regulation. Endocr Rev 17:187–205

Jacobs BL, Praag H, Gage FH (2000) Adult brain neurogenesis and psychiatry: a novel theory of depression. Mol Psychiatry 5: 262–269

Kinnunen AK, Koenig JI, Bilbe G (2003) Repeated variable prenatal stress alters pre- and postsynaptic gene expression in the rat frontal pole. J Neurochem 86:736–748

Kitada Y, Miyauchi T, Satoh A, Satoh S (1981) Effect of antidepressants in the rat forced swim test. Eur J Pharmacol 72: 145–152

Kuehner C (1999) Gender differences in the short-term course of unipolar depression in a follow-up sample of depressed inpatients. J Affect Disord 56:127–139

Lahamame A, del Arco C, Pazos A, Yritia M, Amario A (1997) Are Wistar–Kyoto rats a genetic model of depression resistant to antidepressant drugs? Eur J Pharmacol 337:115–123

Lemaire V, Koehl M, Le Moal M, Abrous DN (2000) Prenatal stress produces learning deficits associated with an inhibition of neurogenesis in the hippocampus. Proc Natl Acad Sci U S A 97:11032–11037

Lenox-Smith AJ, Reynolds A (2003) A double-blind, randomised, placebo controlled study of venlafaxine XL in patients with generalised anxiety disorder in primary care. Br J Gen Pract 53:772–777

Lopes Da Silva N, Ferreira VMM, Carobrez AP, Morato GS (1996) Individual housing from rearing modifies the performance of young rats on the elevated plus-maze apparatus. Physiol Behav 60:391–396

Lucki I (1997) The forced swimming test as a model for core and component behavioral effects of antidepressant drugs. Behav Pharmacol 8:523–532

Masubuchi Y, Iwasa T, Fujita S, Suzuki T, Horie T, Narimatsu S (1996) Regioselectivity and substrate concentration-dependency of involvement of the CYP2D subfamily in oxidative metabolism of amitriptyline and nortriptyline in rat liver microsomes. J Pharm Pharmacol 48:925–929

McCormick CM, Smythe JW, Sharma S, Meaney MJ (1995) Sex-specific effects of prenatal stress on hypothalamic–pituitary–adrenal responses to stress and brain glucocorticoid receptor density in adult rats. Dev Brain Res 84:55–61

Mora S, Dussaubat N, Diaz-Veliz G (1996) Effects of the estrous cycle and ovarian hormones on behavioral indices of anxiety in female rats. Psychoneuroendocrinology 21:609–620

Morley-Fletcher S, Darnaudery M, Koehl M, Casolini P, Van Reeth O, Maccari S (2003a) Prenatal stress in rats predicts immobility behavior in the forced swim test: effects of a chronic treatment with tianeptine. Brain Res 989:246–251

Morley-Fletcher S, Rea M, Maccari S, Laviola G (2003b) Environmental enrichment during adolescence reverses the effects of prenatal stress on play behaviour and HPA axis reactivity in rats. Eur J Neurosci 18:3367–3374

Nebes RD, Pollock BG, Houck PR, Butters MA, Mulsant BH, Zmuda MD, Reynolds CF (2003) Persistence of cognitive impairment in geriatric patients following anti-depressant treatment: a randomized double-blind clinical trial with nortriptyline and paroxetine. J Psychiatric Res 37:99–108

Poltyrev T, Weinstock M (2004) Gender difference in the prevention of hyperanxiety in adult prenatally-stressed rats by chronic treatment with amitriptyline. Psychopharmacology 171:270–276

Porsolt RD, Anton G, Blavet N, Jalfre M (1978) Behavioral despair in rats: a new model sensitive to antidepressant treatments. Eur J Pharmacol 47:379–391

Sagi Y, Weinstock M, Youdim MBH (2003) Attenuation of MPTP-induced dopaminergic neurotoxicity by TV3326, a cholinesterase-monoamine oxidase inhibitor. J Neurochem 86:290–297

Schmitz C, Rhodes ME, Bludau M, Kaplan S, Ong P, Ueffing I, Vehoff J, Korr H, Frye CA (2002) Depression: reduced number of granule cells in the hippocampus of female, but not male, rats due to prenatal restraint stress. Mol Psychiatry 7:810–813

Secoli SR, Teixeira NA (1998) Chronic prenatal stress affects development and behavioral depression in rats. Stress 2:273–280

Sheehan DV, Mao CG (2003) Paroxetine treatment of generalized anxiety disorder. Psychopharmacol Bull 37(Suppl 1):64–75

Szuran TF, Pliska V, Pokorny J, Welzl H (2000) Prenatal stress in rats: effects on plasma corticosterone, hippocampal glucocorticoid receptors, and maze performance. Physiol Behav 71: 353–362

Tejani-Butt S, Kluczynski J, Paré WP (2003) Strain-dependent modification of behavior following antidepressant treatment. Prog Neuro-Psychopharmacol Biol Psychiatry 27:7–14

Teri L, Reifler BV, Veith RC, Barnes R, White E, McLean P, Raskind M (1991) Imipramine in the treatment of depressed Alzheimer's patients: impact on cognition. J Gerontol 46:P372–P377

Thompson WR (1957) Influence of prenatal maternal anxiety on emotionality in young rats. Science 15:698–699

Van Dijken HH, Tilders FJ, Olivier B, Mos J (1992) Effects of anxiolytic and antidepressant drugs on long-lasting behavioural deficits resulting from one short stress experience in male rats. Psychopharmacology 109:395–402

Weinstock M, Matlina E, Keshet GI, Rosen H, McEwen BS (1992) Prenatal stress selectively alters the reactivity of the hypothalamic–pituitary adrenal system in the female rat. Brain Res 595: 195–200

Weinstock M, Gorodetsky E, Wang R-H, Gross A, Weinreb O, Youdim MBH (2002a) Limited potentiation of blood pressure response to oral tyramine by brain-selective monoamine oxidase A-B inhibitor, TV-3326 in conscious rabbits. Neuropharmacology 43:999–1005

Weinstock M, Poltyrev T, Bejar C, Sagi Y, Youdim MBH (2002b) TV3326, a novel cholinesterase and MAO inhibitor for Alzheimer's disease with co-morbidity of Parkinson's disease and depression. In: Mizuno Y, Fisher A, Hanin I (eds) Mapping the progress of Alzheimer's and Parkinson's disease. Kluwer Academic/Plenum Publishers, New York, pp 199–204

Weinstock M, Poltyrev T, Bejar C, Youdim MBH (2002c) Effect of TV3326, a novel monoamine–oxidase–cholinesterase inhibitor, in rat models of anxiety and depression. Psychopharmacology 160:318–324

Weinstock M, Gorodetsky E, Poltyrev T, Gross A, Sagi Y, Youdim MBH (2003) A novel cholinesterase and brain-selective monoamine oxidase inhibitor for the treatment of dementia co-morbid with depression and Parkinson's disease. Prog Neuro-Psychopharmacol Biol Psychiatry 27:555–561

Zimmerberg B, Blaskey LG (1998) Prenatal stress effects are partially ameliorated by prenatal administration of the neurosteroid allopregnanolone. Pharmacol Biochem Behav 59:819–827

Neuroscience 119 (2003) 669–678

POTENTIAL COGNITIVE ACTIONS OF (*N*-PROPARGLY-(3*R*)-AMINOINDAN-5-YL)-ETHYL, METHYL CARBAMATE (TV3326), A NOVEL NEUROPROTECTIVE AGENT, AS ASSESSED IN OLD RHESUS MONKEYS IN THEIR PERFORMANCE OF VERSIONS OF A DELAYED MATCHING TASK

J. J. BUCCAFUSCO,[a,c]* A. V. TERRY, JR.,[a,b,c] T. GOREN[d] AND E. BLAUGRUN[d]

[a]*Alzheimer's Research Center, Medical College of Georgia, Augusta, GA 30912-2300, USA*

[b]*UGA College of Pharmacy, Medical College of Georgia, Augusta, GA 30912-2300, USA*

[c]*Veterans Administration Medical Center, Augusta, GA 30912, USA*

[d]*TEVA Pharmaceutical Industries Ltd, P.O. Box 8077, Industrial Zone Kiryat Nordau, Netanya, Israel*

Abstract—(*N*-propargyl-(3*R*)-aminoindan-5-yl)-ethyl, methyl carbamate (TV3326), a known neuroprotective agent exhibiting the properties of both an inhibitor of monoamine oxidase (brain selective) and an inhibitor of acetylcholinesterase was administered to seven old rhesus monkeys well trained to perform versions of a delayed matching-to-sample (DMTS) task. An increasing dose regimen of TV3326 was administered orally according to a schedule that allowed the animals to perform the standard DMTS task and a self-titrating version of the DMTS task each week during the study. A distractor version of the task was administered during two of the doses of TV3326. Under the conditions of this experiment TV3326 failed to significantly affect accuracy on the standard DMTS task; however, the drug was very effective in improving the ability of subjects to titrate to longer-duration delay intervals in the titrating version of the task. The maximal drug-induced extension of the self-titrated delay interval amounted to a 36.7% increase above baseline. This increase in maximum delay duration occurred without a significant change in overall task accuracy. TV3326 also significantly improved task accuracy during distractor (interference) sessions. The compound was effective enough to return group performance efficiency to standard DMTS vehicle levels of accuracy. These results were independent of whether trials were associated with a distractor or non-distractor delay interval, and they were independent of delay interval. The lack of delay selectivity in task improvement by TV3326 may not be consistent with a selective effect on attention. TV3326 was not associated with any obvious side effect or untoward reaction of the animals to the drug. Thus, TV3326 may be expected to offer a significant positive cognitive outcome in addition to its reported neuroprotective action. **© 2003 IBRO. Published by Elsevier Science Ltd. All rights reserved.**

Key words: memory, attention, MAO inhibitor, cholinesterase inhibitor, operant task, delayed response task.

The well-known selective vulnerability of basal forebrain acetylcholine-containing neurons in Alzheimer's disease has underscored the importance of this neurotransmitter system in certain components or types of working memory and perhaps in other behavioral and cognitive functions affected by the disease. Among the host of degenerative processes occurring in Alzheimer's disease, reproducible cholinergic deficits have been consistently reported, they appear early in the disease process, and correlate well with the degree of dementia (for review, Francis et al., 1999). Moreover, abnormalities in cholinergic function are frequently reported in other degenerative conditions such as Parkinson's disease, diffuse Lewy body dementia and Huntington's disease. As in Alzheimer's disease, such cholinergic deficits often correlate with memory decline and dementia. The use of cholinesterase inhibitors such as donepezil and rivastigmine provide the bulk of the clinical armamentarium for the treatment of cognitive symptoms in the treatment of Alzheimer's disease. These drugs have provided reasonable effectiveness in mild to moderate cases, improving quality of life and a delay in symptomatic progression of the disease, in the case of donepezil, by up to 55 weeks (Taylor, 2001). Despite their effectiveness as cognition enhancers, thus far cholinesterase inhibitors have not been shown to significantly impact the neurodegenerative process itself. Other disease-modifying approaches to the treatment of Alzheimer's disease are under intense investigation (see Jacobsen, 2002; Taylor et al., 2002). One of these includes the ability to offer a degree of neuroprotection, i.e. to support and possibly repair dystrophic neurons, and to enhance neuronal outgrowth and synaptic sprouting. Whereas the use of selective monoamine oxidase-B (MAO-B) inhibitors such as selegiline have been tested in Parkinson's patients and found to be only partially effective in slowing the progress of the disease (Parkinson Study Group, 1989), this class of agent may offer neuroprotection in Alzheimer's disease (Sano et al., 1997; Knoll, 2000; Pratico and Delanty, 2000). TV3326 is a compound combining properties as a CNS-selective MAO inhibitor and a cholinesterase inhibitor. Initial preclinical studies with the parent compound, rasagiline, revealed potent cytoprotective activity *in vitro*, that

*Correspondence to: J. J. Buccafusco, Alzheimer's Research Center, Medical College of Georgia, 1120 15th Street, Augusta, GA 30912-2300, USA. Tel: +1-706-721-6355; fax: +1-706-721-9861.
E-mail address: jbuccafu@mail.mcg.edu (J. J. Buccafusco).

Abbreviations: DMTS, delayed matching-to-sample; MAO, monoamine oxidase; TV3326, (*N*-propargyl-(3*R*)-aminoindan-5-yl)-ethyl, methyl carbamate.

0306-4522/03$30.00+0.00 © 2003 IBRO. Published by Elsevier Science Ltd. All rights reserved.
doi:10.1016/S0306-4522(02)00937-5

Table 1. Subject demographics

Monkey identification	Age (y)	Sex	Weight (kg)	Short delay (s)	Medium delay (s)	Long delay (s)
350	27	M	9.8	5	10	20
667	28	F	10.2	3	6	15
802[a]	23	M	10.4	5	10	20
671	28	F	5.0	5	10	20
7nv[a]	24	M	8.0	5	7	10
C4n[a]	22	F	9.4	5	7	10
23	17	M	9.2	30	90	180
Mean±S.E.M.	24.1±1.50		8.8±0.71	8.3±3.63	20.0±11.7	39.3±23.5

[a] These subjects refused to consume doses after the first 6 mg/kg dose in the series (see text).

was attributed to an anti-apoptotic activity (Maruyama et al., 2001). The anti-apoptotic and neuroprotective actions of rasagiline and TV3326 were shown to be independent of their ability to inhibit MAO-B, but dependent upon the propargyl moiety component of their structure (Youdim et al., 2001). In the same study, administration of TV3326 to mice was demonstrated to reduce the edema and behavioral deficits produced by closed head injury in mice. Chronic administration of the drug also reversed the specific damage to the neurons in the fornix and corpus callosum produced after central injection of streptozotocin in rats (Weinstock et al., 2000a). In view of the multi-potential (neuroprotectant and cholinesterase inhibitor) of TV3326, the purpose of this study was to determine whether the drug could improve age-dependent cognitive impairment in aged non-human primates.

A wide variety of animal models and behavioral techniques has been applied to the study of drugs that affect memory. Animals of advanced age, usually rodents and non-human primates, have provided a good level of predictability for the clinical efficacy of proposed therapeutics (Arnsten et al., 1996; Paule et al., 1998; Bartus, 2000). In fact, many drug-discovery programs continue to use rodents in general screening procedures for identifying potential cognitive enhancing agents, electing to continue testing potential lead compounds in non-human primates. Our experience has been that evaluation of such compounds in non-human primates allows for a greater level of predictability in terms of clinical potency and efficacy as compared with lower species (Buccafusco and Terry, 2000). Various operant tasks, usually food-motivated, allow for the measurement of abilities which are relevant to human aging such as attention, strategy formation, reaction time in complex situations and memory for recent events (e.g. Irle, 1987; Paule et al., 1998; Paule, 2001). Aged monkeys generally are impaired in their ability to attain efficient performance of these tasks, and they often exhibit a reduced level of task efficiency relative to their younger cohorts (Buccafusco et al., 2002). TV3326 was administered as a chronic escalating regimen by voluntary oral administration to seven aged rhesus monkeys. The animals were well trained in the performance of three versions of the delayed matching-to-sample (DMTS) task with the object of assessing the effect of the drug on working memory, attention, and psychomotor speed.

EXPERIMENTAL PROCEDURES

Study subjects

Seven rhesus macaques were well trained (>100 individual sessions) in the DMTS task. The animals were maintained on tap water (unlimited) and standard laboratory monkey chow (Harlan Teklad Laboratory 20% monkey diet, Madison, WI, USA) supplemented with fruits and vegetables. The animals were maintained on a feeding schedule such that approximately 15% of their normal daily (except weekends) food intake was derived from 300 mg reinforcement food pellets (commercial composition of standard monkey chow and banana flakes, Noyes Precision food pellets, P. J. Noyes Co., Lancaster, NH, USA) obtained during experimental sessions. The remainder was made available following each test session. On weekends the animals were fed twice per day. At least a 4-week washout period preceded the initiation of this study. The monkeys were maintained on a 12-h light/dark cycle and were tested each weekday between 09:00 and 14:00 h. Room temperature and humidity were maintained at 72±1 °C and 52±2%, respectively. All experimental procedures were reviewed and approved by the Medical College of Georgia Institutional Animal Care and Use Committee and are consistent with AAALAC guidelines. The minimal number of animals was used and every effort was taken to minimize their discomfort during the study. Subject demographics are presented in Table 1. In addition to the information provided in Table 1, each of the subjects had participated in one or more previous studies in which potential cognitive enhancing agents were evaluated. The drugs in question were proprietary agents and so no description of their pharmacological properties can be disclosed, other than they were short-acting compounds, and they were administered during acute studies no more than twice per week. No side effects or long-lasting effects were associated with any of these earlier studies, and all animals were provided at least a 4-week washout period prior to the present series. Finally, the aged female animals in the study were perimenopausal, i.e. still cycling, but infrequently. All testing was administered between menstrual cycles.

Drug administration

The solid compound (*N*-propargyl-(3*R*)-aminoindan-5-yl)-ethyl, methyl carbamate (TV3326) was stored in a tightly stoppered polypropylene vial in a desiccator cabinet at room temperature. No other precautions were used for compound storage. On each day of the experiment, appropriate amounts of drug were weighed to the nearest 0.1 mg and placed in a cocoa mixture for oral administration. Previous experience has shown that a cocoa mixture helps to disguise the potential taste and texture of test compound, and the animals readily consume the dose. To prepare the cocoa mixture, approximately 4 g baking cocoa (commercial supermarket brand) is combined with 9 g of confectioner's powdered sugar.

Water is added to consistency (1–1.5 ml). Test compound is added directly to the mixture that is formed into a ball (soft, non-sticky consistency) of about 2 cm in diameter. In each instance drug or vehicle administration occurred 2 h prior to DMTS testing. Initially administration of an 8 mg/kg test dose resulted in several subjects refusing to consume this dose, and certain of our test subjects were able to detect the presence of drug in the vehicle at about the 6 mg/kg level. In order to maintain dosing, we used two strategies: (1) to divide the dose into two vehicle administrations within 5 min of each other; or (2) to provide the drug in about 15 ml of orange juice. Despite our best efforts, only four subjects completed the entire regimen. The other three animals refused to consume the dose as soon as they detected the taste and/or texture of the drug in the mixture. For data presentation in the following figures, the change from N=seven to N=four is always noted.

Standard DMTS task

All test panels, computer interfaces, and computer software for data acquisition were developed and are maintained by the Medical College of Georgia Department of Biomedical Engineering (Augusta, GA, USA). Animals were tested simultaneously in their home cages using a computer-automated training and testing system which measures and categorizes the percent correct at each delay, and the latency of response at each step of each matching problem. The computer and operator were isolated from the subjects. Daily sessions consisted of 96 trials. A trial began by illumination of a sample key with one of three colored discs. Monkeys were trained to depress the illuminated sample key to initiate a trial. This action also terminated the illumination of the sample key during a computer-specified delay interval. Following the delay interval, the two choice keys, but not the sample key, were illuminated. One of the two choice keys is presented as the same color as the sample key had been prior the delay, while the other (incorrect) choice key is presented as one of the two remaining colors. If the monkey matched (i.e. pressed the choice key whose color matched that of the stimulus key), that response was rewarded. The inter-trial interval was always 5 s. Several testing precautions were incorporated into the presentation of the matching problem. First, the various combinations of stimulus color (red, green, yellow) were arranged so that each of the three colors appeared an equal number of times as a sample, each color appeared an equal number of times on the two choice keys, and each color appeared an equal number of times in combination with each other color. Likewise, when two colors (e.g. green/yellow) appeared in combination, each color was counterbalanced between left and right in a non-predictable pattern. Thus, correct responses were arranged so that simplistic strategies such as position preference, left/right alternation, or even double left/right alternation resulted in performance at precisely the chance (50%) level. Finally, all stimulus counterbalancing procedures were matched to length of delay. Monkeys exhibit individual capabilities to maintain matching performance following various delay intervals, and the longest delay chosen for a particular monkey is that which consistently allows correct matching at just above chance levels (approximately 60% correct). In general, the length of delay interval was adjusted until three levels of performance difficulty were found: 1) the least difficult zero delay (mean=85–100% correct); 2) a short delay interval (means ranging from 75–84% correct); 3) a medium delay interval (means ranging from 65–74% correct) and 4) a long delay interval representing each animal's limit in terms of DMTS performance (55–64% correct). "Zero"-delay is included as a control to monitor for changes in reference memory and/or other potential non-mnemonic changes in task performance. Values obtained for each difficulty level were averaged and recorded as the mean percent correct for the respective interval. Baseline data were obtained following the administration of drug vehicle.

Titrating version of the DMTS task

The paradigm requires the animals to perform a 96-trial session. Subjects begin the first trial with a 0-s delay interval. If that trial was answered correctly, the next trial presented a 1-s delay interval. The 1-s incremental progression was maintained until the subject made an incorrect match. The delay interval for the trial after an incorrect match was always decreased by 1 s. After an incorrect match, if the next trial was answered correctly, then the subsequent trial presented a delay interval 1 s longer in duration. Dependent variables included the overall percentage of trials answered correctly, the number of trials to reach the maximal delay interval attained, and the maximum and average delay interval attained (in seconds).

DMTS with distractor trials

Test sessions with distractors (interference sessions) were conducted on three occasions during the study (during vehicle administration, and during administration of the 5 and 7 mg/kg doses of TV3326). Distractor sessions were kept to a minimum so as to avoid the animals becoming tolerant to the distractor (Prendergast et al., 1998a). Distractor stimuli were presented to the test subject on 18 of the 96 trials completed during distractor DMTS sessions. The stimuli were presented simultaneously on the sample and choice keys for 3 s and they consisted of a random pattern of the three colored lights flashing in an alternating manner. The distractor lights were comprised of the same three colors used for sample and choice stimuli presentation. The total duration of onset for a given colored light was 0.33 s. Immediately as one colored light was extinguished, a different colored light was presented. Thus, during presentation of the distractor, each color was presented in random order on each key three separate times. Distractor stimuli were present an equal number of times on trials with short, medium, and long delay intervals. The remaining trials were completed with no delay interval or distractor and they are randomly placed throughout the test session.

Statistical analyses

The following parameters were recorded for all trials during all test sessions (i.e. 96 trials per session): percent correct on trials with zero, short, medium, and long delay intervals and task latencies. Data for percent correct were subdivided according to delay interval for each 24-trial delay component of the session. Four task latencies (collapsed across delays) for trials associated with correct and incorrect choices were recorded: sample latencies (time interval between presentation of the sample stimulus and the subject pressing the sample key) and choice latencies (time interval between presentation of the choice stimuli and the subject pressing a choice key). For the titrating version of the task additional variables included the number of trials to maximum delay interval, the maximal delay interval attained, and the average delay interval attained. All statistical analyses were performed on raw data (percent trials correct or median latencies in seconds). Data were analyzed by use of a multi-factorial analysis of variance with repeated measures (SAS Institute Inc., Cary, NC, USA, JMP statistical software package). The effects of drug, dose, delay interval, time of testing (i.e. the time elapsed between drug administration and DMTS testing), and all crosswise interactions were assessed. An orthogonal multi-comparison test was used to compare individual means. For each table/figure (below) error values denoted by $\pm$ indicate the S.E.M. Differences between means from experimental groups were considered significant at the $P<0.05$ level (two-sided test). For DMTS sessions that were not completed by subjects, those with 20 or fewer total trials were not considered valid for statistical analysis.

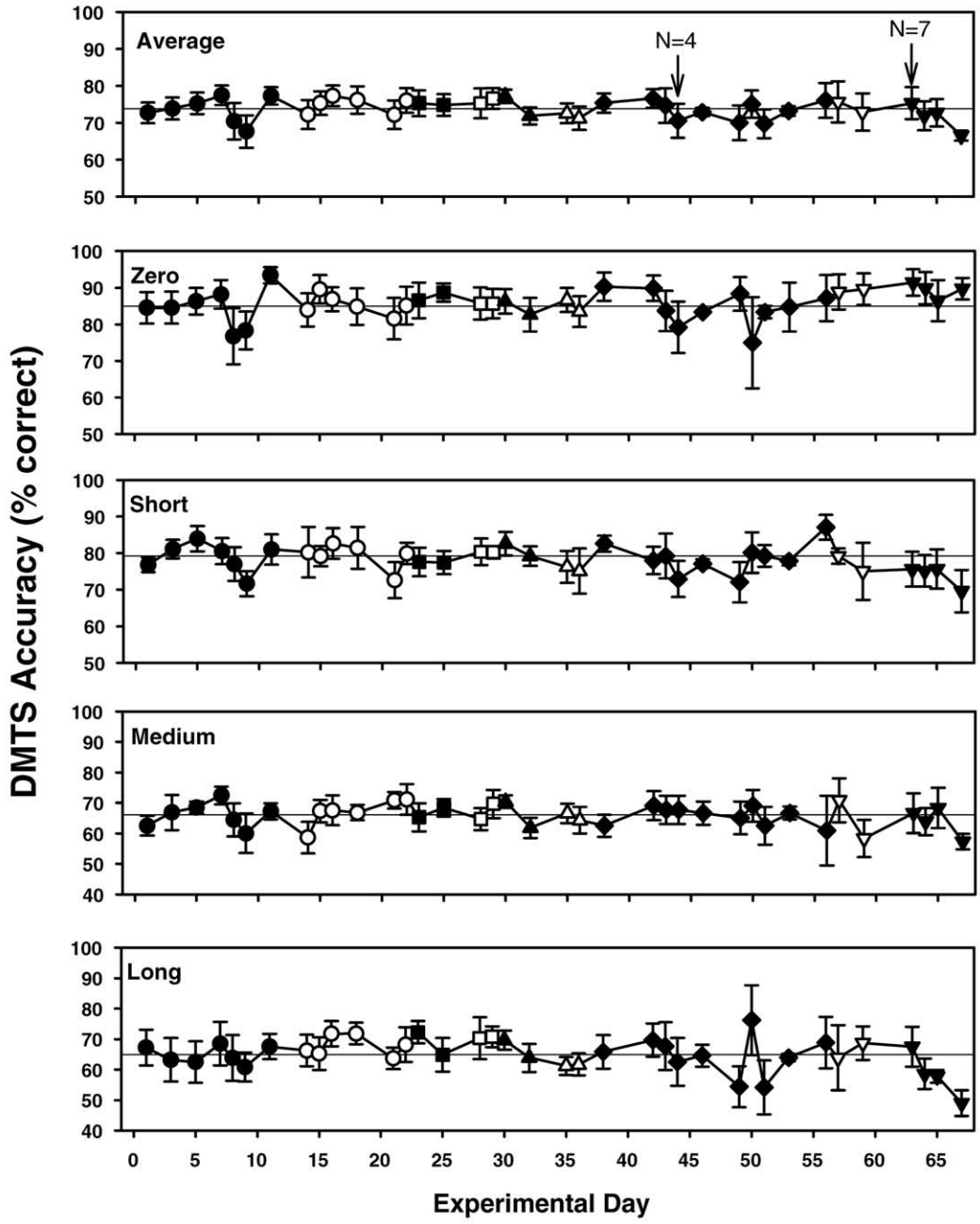

Fig. 1. Effect of daily single dose administration of TV3326 on standard DMTS task performance measured 2 h after drug administration categorized by delay interval (note: Average indicates the mean of all completed trials in the session). Symbols are coded to indicate the dose of TV3326 that was administered on that experimental day: vehicle (filled circles); 1 mg/kg (open circles); 2 mg/kg (filled squares); 3 mg/kg (open squares); 4 mg/kg (filled upward triangles); 5 mg/kg (open upward triangles); 6 mg/kg (filled diamonds); 7 mg/kg (open downward triangles); washout (closed downward triangles). *N*=four with arrow indicates the experimental day where only four animals continued to consume the dose. *N*=seven with arrow indicates the washout period after drug discontinuation. Horizontal lines indicate the combined average for the first seven and the last four data points. There was no significant effect of drug treatment ($F_{36,814}=0.84$, $P=0.74$), nor was there a significant interaction between treatment and delay interval ($F_{108,814}=0.55$, $P=0.99$).

RESULTS

Standard DMTS

Fig. 1 presents the performance efficiencies (percentage of the trials completed that were correctly answered) exhibited by the subjects tested 2 h after administration of vehicle as the first seven data points (Table 2). Increasing the duration of delay (retention) intervals from Zero to Long was associated with the expected decrement in performance efficiency (also shown in Table 2). Task accuracy over consecutive days was relatively stable across all delay intervals. Fig. 1 also shows the composite data set for

Table 2. Average baseline performance efficiency for the seven study subjects by delay interval

Delay intervals				
Average	Zero	Short	Medium	Long
73.8±1.26	85.0±1.78	79.2±1.32	66.2±1.59	64.9±2.25

Each value represents the mean±S.E.M. for 49 determinations (seven per subject). Average refers to the average level of accuracy determined from all completed trials in a session. For the standard delayed matching-to-sample task, including all sessions together, there was a significant effect of "delay interval," independent of treatment ($F_{3,814}=6.90$, $P<0.0001$).

the effects of TV3326 given by oral administration on DMTS performance efficiency categorized by delay interval. Despite daily administration of TV3326, there were no obvious changes in ongoing levels of task accuracy. This was confirmed by statistical analysis in that there was no significant effect of drug treatment ($F_{36,814}=0.84$, $P=0.74$), nor was there a significant interaction between treatment and delay interval ($F_{108,814}=0.55$, $P=0.99$).

In addition to the effect of drug treatment on task accuracy, aspects of working memory associated with the DMTS task, the two task latencies, also were determined. These values are presented in Table 3. There was a trend

Table 3. Effect of TV3326 on median delayed matching-to-sample task latencies (in seconds)

Sample correct			Choice correct		Sample incorrect		Choice incorrect		Dose (mg/kg)
Day	Average	S.E.M.	Average	S.E.M.	Average	S.E.M.	Average	S.E.M.	
1	1.29	0.23	2.29	0.51	1.66	0.47	2.71	0.53	0
3	1.36	0.44	2.34	0.48	1.13	0.21	2.59	0.53	0
5	1.09	0.20	2.17	0.46	1.26	0.20	2.59	0.42	0
7	0.92	0.11	2.17	0.51	0.83	0.10	2.70	0.71	0
8	2.22	0.97	2.58	0.62	1.78	0.56	2.75	0.57	0
9	1.24	0.27	1.90	0.11	1.68	0.50	2.64	0.23	0
11	1.51	0.32	2.47	0.59	1.70	0.51	2.93	0.61	0
14	1.20	0.19	2.13	0.50	1.26	0.24	2.77	0.80	1
15	1.97	0.66	2.52	0.42	1.77	0.51	2.87	0.49	1
16	1.37	0.24	2.23	0.46	1.20	0.19	5.29	2.50	1
18	1.49	0.42	2.26	0.44	1.14	0.20	2.70	0.47	1
21	1.36	0.15	2.19	0.47	1.47	0.36	2.60	0.58	1
22	1.49	0.20	2.21	0.53	2.16	0.78	2.70	0.58	1
23	1.52	0.27	2.37	0.45	1.33	0.16	2.95	0.68	2
25	1.27	0.19	2.21	0.44	1.44	0.35	2.53	0.49	2
28	1.10	0.12	2.11	0.46	1.16	0.16	2.59	0.61	3
29	1.36	0.23	2.07	0.33	1.81	0.50	2.61	0.46	3
30	1.33	0.28	2.03	0.33	1.57	0.49	2.59	0.50	4
32	1.32	0.22	2.42	0.41	1.38	0.25	2.85	0.55	4
35	1.73	0.29	2.33	0.55	1.70	0.38	2.63	0.47	5
36	1.29	0.19	2.17	0.49	1.57	0.23	2.73	0.60	5
38	1.24	0.20	2.07	0.47	1.40	0.22	2.49	0.53	6
42	1.13	0.17	2.16	0.48	1.24	0.26	2.69	0.69	6
43	1.43	0.24	2.60	0.70	1.53	0.43	3.03	1.03	6
44	0.90	0.09	2.35	0.72	0.95	0.17	2.78	0.81	6
46	1.20	0.08	2.58	0.68	1.15	0.26	3.03	0.93	6
49	1.18	0.15	2.50	0.52	1.35	0.26	3.15	0.75	6
50	1.07	0.06	2.93	1.03	0.90	0.09	4.17	1.71	6
51	1.10	0.08	2.55	0.62	1.35	0.16	2.83	0.83	6
53	1.10	0.18	2.97	0.98	1.00	0.13	4.13	1.50	6
56	1.03	0.18	2.63	0.70	0.93	0.10	3.23	1.01	6
57	0.90	0.05	2.80	0.91	0.90	0.05	3.53	1.28	7
59	1.13	0.15	2.63	0.71	0.93	0.05	3.23	1.00	7
63	0.94	0.14	2.06	0.49	0.89	0.06	2.66	0.68	0
64	1.31	0.11	2.37	0.66	1.41	0.18	3.04	0.85	0
65	1.33	0.28	2.73	0.60	0.95	0.08	3.18	0.83	0
67	1.78	0.30	1.85	0.13	2.35	0.56	2.35	0.10	0

Each value represents the mean±S.E.M. for seven subjects except for days 43–59 which were derived from only four subjects (numbers 350, 667, 671, and 23). There was a trend towards a significant difference in the latency category, independent of drug treatment ($F_{3,814}=2.53$, $P<0.065$), but there was no significant effect related to drug treatment ($F_{36,814}=0.84$, $P=0.74$).

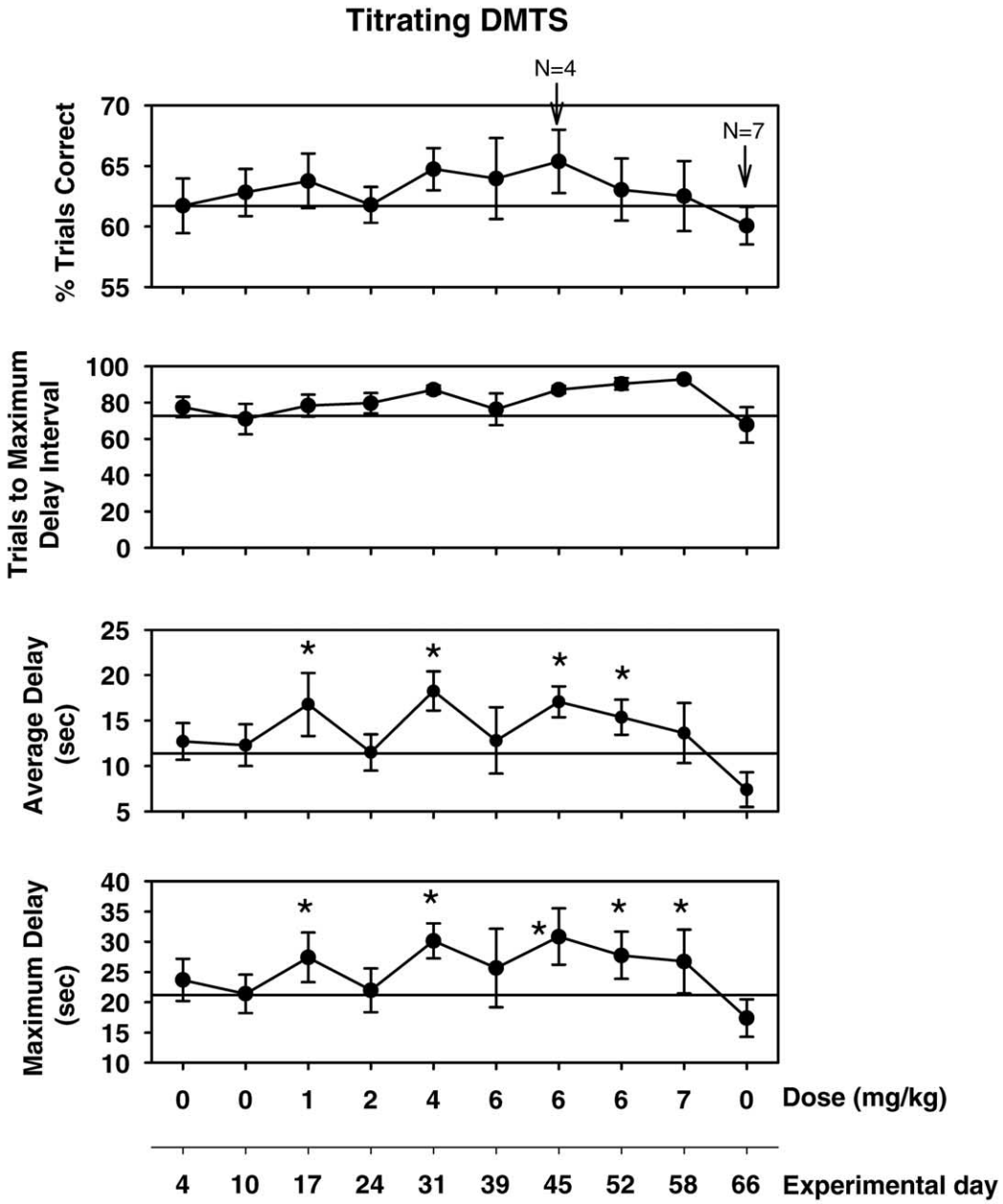

Fig. 2. Effect of daily single dose administration of TV3326 on performance of the titrating version of the DMTS task measured 2 h after drug administration presented as a function of dose (and experimental day). Task accuracy (percent trials correct) during treatment sessions did not exhibit a significant difference from vehicle (0 mg/kg) days ($F_{9,44}=1.77$, $P=0.10$), nor was there a significant effect of treatment for the number of trials to attain the maximal delay interval ($F_{9,44}=1.36$, $P=0.24$). In contrast, TV3326 treatment resulted in self-titration to increased durations of both the average and the maximum delay intervals ($F_{9,44}=3.73$, $P=0.0015$ and $F_{9,44}=3.67$, $P=0.0017$, respectively). * indicates a significant difference from vehicle (0 dose) means (at least $P<0.04$). For the last three doses, $N=4$.

toward a significant difference in the latency category, independent of drug treatment ($F_{3,814}=2.53$, $P<0.065$). Perusal of the data indicates that, on average, there was an increase in choice latencies associated with incorrect choices over choice latencies associated with correct choices. The observation that subjects take longer to make incorrect choices relative to correct choices is a common finding in these types of studies. Drug treatment did not significantly alter this relationship ($F_{36,814}=0.84$, $P=0.74$).

Titrating DMTS

Fig. 2 summarizes the data derived from testing during sessions in which subjects were required to self-titrate to a maximum delay interval. Task accuracies (percent trials correct) exhibited by the study group during treatment sessions were not significantly different from vehicle (0 mg/kg) sessions ($F_{9,44}=1.77$, $P=0.10$). This finding paralleled the lack of effect on task accuracy obtained during

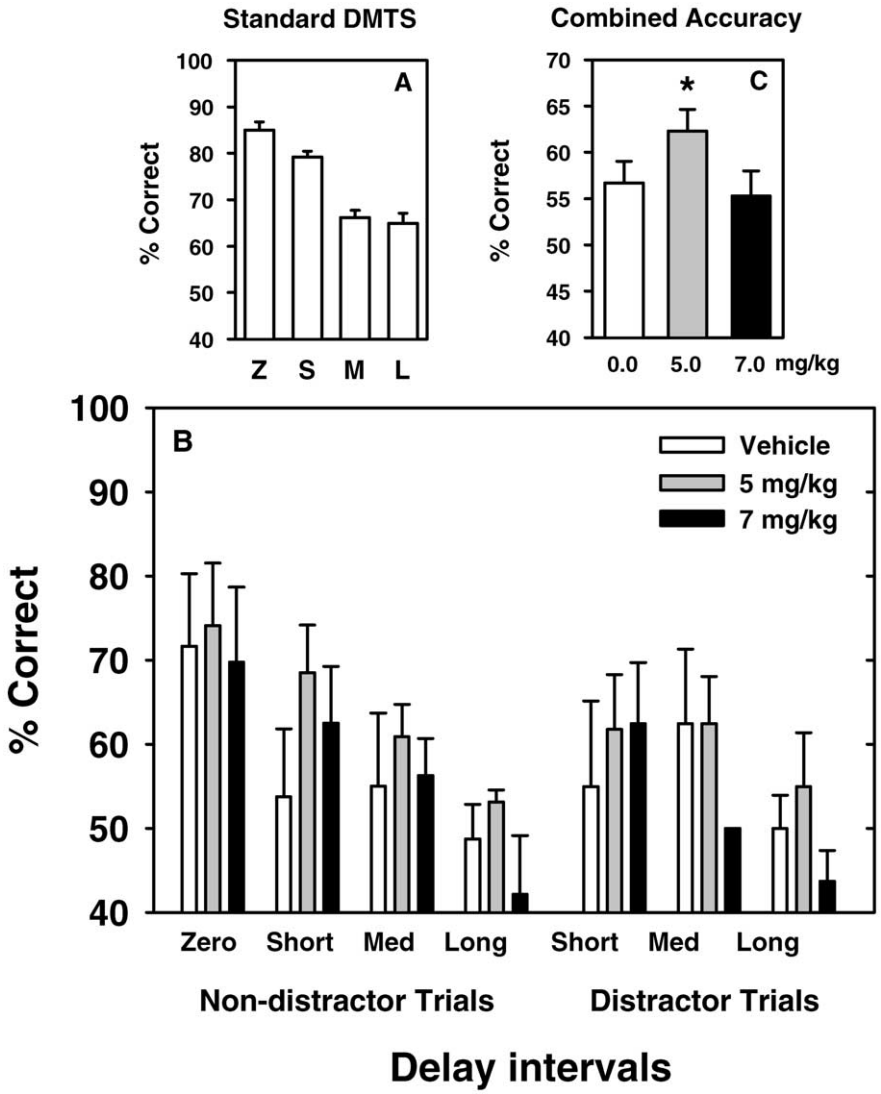

Fig. 3. Effect of daily single dose administration of TV3326 on performance of the distractor version of the DMTS task measured 2 h after drug administration categorized by delay interval (Z=Zero, S=Short, M or Med=Medium, L=Long). Data are presented for Non-distractor Trials and for Distractor Trials (3-s duration initiated 1 s after the start of the delay interval). Although the dosing schedule was as described in Figs. 1 and 2, this version of the task was administered only during one vehicle session (experimental day 2), during one of the 5 mg/kg doses (experimental day 37), and during one of the 7 mg/kg doses (experimental day 60). Note: only 4 subjects received in the 7 mg/kg dose. For comparison purposes, the baseline accuracy for the standard version of the DMTS task is presented in Panel A. The results derived from distractor sessions run after the two doses are presented in Panel B. There was no significant effect of drug treatment either alone, or as a factor with delay interval. There was a trend (*) toward improvement in overall accuracy ($F_{2,87}=2.85$, $P=0.064$), i.e. combined distractor and non-distractor trials, and independent of delay (Panel C).

the standard DMTS sessions. Although there was a gradual increase in the average number of trials to attain the maximal delay interval (particularly during the higher-dose sessions) the effect of drug treatment again was not statistically significant ($F_{9,44}=1.36$, $P=0.24$). In contrast, TV3326 treatment resulted in self-titration to significantly increased durations as reflected in both the average and the maximum delay intervals attained ($F_{9,44}=3.73$, $P=0.0015$ and $F_{9,44}=3.67$, $P=0.0017$, respectively). This increase in task performance was generally sustained from 4-7 mg/kg. The final titrating session was run with no drug administered prior to the task. The data show a rapid return to baseline levels of titrated delay duration (Fig. 2), supporting the concept that the enhanced response obtained during the TV3326 regimen was not simply an artifact, and, that the drug did not maintain its pharmacological effect long after discontinuation of the chronic regimen.

Distractor DMTS

Fig. 3 summarizes the effect of TV3326 on subjects' performance of the distractor version of the DMTS task. Data are presented for non-distractor trials and for distractor trials (3-s duration initiated 1 s after the start of the delay interval). Although the dosing schedule was as described in Figs. 1 and 2, this version of the task was administered only during one vehicle session (experimental day 2), dur-

ing one of the 5 mg/kg doses (experimental day 37), and during one of the 7 mg/kg doses (experimental day 60). For these three sessions the non-distractor trials appeared to be performed as inefficiently (decrements in accuracy relative to standard DMTS levels of performance efficiency) as were the 18 randomly presented distractor trials. We have noted carryover of the distractor-related impairment to non-distractor trials within the same session on other occasions, but the effect seems to be more pronounced in older subjects. Therefore, the results obtained under these conditions should be interpreted with care. Notwithstanding this cautionary note, sessions run after administration of TV3326, independent of dose, independent of delay interval, and independent of trial type (distractor versus non-distractor) showed a trend toward a significant level of improvement in overall accuracy ($F_{2,87}=2.85$, $P=0.064$).

DISCUSSION

Although MAO inhibitors have been examined for their ability to protect against the development of MPTP-induced parkinsonian symptoms or in reversing symptoms in these animals (e.g. Andringa and Cools, 2000; Kupsch et al., 2001), very little is known regarding the effects of these compounds on cognitive function in non-human primates. It is known, however, that noradrenergic neurons are necessary for certain frontal lobe-mediated cognitive processes. These include attention and the prevention of distraction in the presence of irrelevant stimuli (Robbins and Everitt, 1995). A normal level of noradrenergic neural activity appears to be necessary for optimal function of the prefrontal cortex. Agonists at α_{2A} receptors (e.g. clonidine, guanfacine) have been shown to improve prefrontal cortical function in non-human primates whereas antagonists at α_2 receptors (e.g. yohimbine) have been shown to impair function and to antagonize the positive mnemonic actions of agonists (see Mao et al., 1999). Thus, the susceptibility to distracting stimuli known to occur in Alzheimer's disease patients may be improved by compounds designed to optimize noradrenergic activity within the prefrontal cortex. Because of the behavioral effects of amphetamine and its derivatives, it is unlikely that this class of drugs could be used as a treatment adjunct in Alzheimer's disease. However, the mood-elevating aspects and potential cognitive enhancing effects of MAO inhibitors may prove more appropriate in this setting. To suggest this possibility for TV3326 are the results of behavioral studies in rats in which chronic administration of TV3326 reversed immobility in the forced swim test (antidepressant activity) and the drug antagonized scopolamine-induced impairment of spatial memory (Weinstock et al., 2000b). It is undetermined whether this potential positive effect on cognition in these animals was mediated through brain MAO inhibition or through cholinesterase inhibition, or by the combination of effects. Studies in rats (Haroutunian et al., 1990) and macaques (Buccafusco et al., 1992; Terry et al., 1993) have indicated the advantage of combining the effects of central α_2 adrenergic receptor stimulation (clonidine) with cholinesterase inhibition (physostigmine).

It also has not been determined whether the pharmacological actions of TV3326 would include increased brain noradrenergic, dopaminergic, or serotonergic activity at clinically relevant doses. However, in this study, the drug appeared to behave less like a noradrenergic agonist (Jackson and Buccafusco, 1991), and more like a dopaminergic agonist (Prendergast et al., 1998a). This is because TV3326 was more effective in improving task accuracy in the distractor version of the DMTS task as compared with the standard version. The role of brain dopaminergic pathways in attentional aspects of cognition is well known. In fact, normal dopaminergic function appears to be necessary for the successful performance of memory tasks that rely on the function of the prefrontal cortex. For example, a narrow range of the D_1 selective agonists A77636 and SKF81297 were reported to improve performance of a spatial working memory task in aged monkeys (Cai and Arnsten, 1997). For MAO inhibitors, the mechanism for their effects on cognition is even less obvious, in that they may be mediated through mechanisms other than inhibition of the MAO enzyme (Gelowitz et al., 1994; Shankaranarayana et al., 1999).

The increase in self-titrated maximal delay interval from vehicle levels (22.6 s) to those obtained after administration of the second of the 6 mg/kg doses (30.9 s) in the titrating version of the DMTS task amounted to a 36.7% increase above baseline (in fact, the improvement over baseline that was sustained by the 4–7 mg/kg doses in the titrating version of the DMTS task averaged 25.2±4.96% of control). This increase in maximum delay duration occurred with a small, but non-significant, increment in the number of trials needed to attain the longer intervals associated with drug treatment. Also, overall task accuracy was unchanged. The observation that subjects self-titrated to longer delay intervals without a significant change in overall accuracy may indicate that the drug enhanced the motivational aspects of the task. Other behavioral approaches would be needed to confirm this conjecture. Because the average titrated delay interval increased concomitantly with the maximal delay, it is likely that once the maximal delay was attained, accuracy was not sustained for the next few trials, thus maintaining accuracy constant. Nevertheless, we have demonstrated that the titrating DMTS task is more sensitive to age-related task deficits than is the standard DMTS task. Even within the titrating DMTS the scores for session accuracy were not as well correlated with age as was the number of trials to reach the maximal delay interval (Buccafusco et al., 2002). Thus we interpret an increase in titrated delay interval (as long as accuracy does not decrease) as a positive effect on task performance.

TV3326 also significantly improved task accuracy during distractor sessions. The compound was effective enough to return group performance efficiency to standard DMTS vehicle levels of accuracy. These results were independent of whether trials were associated with a distractor or non-distractor trial, and they were independent of

delay interval. Because of the profound carryover effect of the distractor-impaired performance to the non-distractor trials, the positive overall effect produced by the compound on task accuracy is difficult to interpret. Drugs like methylphenidate and nicotine generally affect task accuracy selectively during Short delay trials in the distractor task (Prendergast et al., 1998a,b) although like TV3326, nicotine improved task accuracy for both distractor and non-distractor trials. Despite the lack of a significant delay-dependent effect of drug treatment, on average, TV3326 improved accuracy most consistently during Short delay trials (Fig. 3) both for non-distractor and distractor trials. TV3326 does appear to have at least one advantage over methylphenidate in this task. Whereas methylphenidate exhibited clear efficacy in reversing distractor-induced decrements in task accuracy in young monkeys, the amphetamine derivative was unable to reverse distractor-induced performance decrements by aged subjects (Prendergast et al., 1998a).

It is difficult to provide a level of comparison of the mnemonic effects of TV3326 relative to other drugs tested at this center owing to the lack of effect of the drug on task accuracy. However, the 25% improvement over baseline that was sustained in the titrating version of the DMTS task is in keeping with the most effective drugs that we have tested on an acute basis for improvements in standard DMTS accuracy. We have yet to determine whether such comparisons based on improvement over baseline performance for different task variables are valid. Where a more direct comparison may be made, is with regard to the most improved degree of accuracy associated with a delay interval (Short) for the non-distractor trials in the distractor version of the DMTS task. On average, the improvement amounted to 27.5% relative to vehicle levels of performance. Notwithstanding this limitation, these data provide at least a proof of concept that development of drugs with multiple targets and multiple pharmacological properties may prove superior to either monotherapy, or to combining drugs with varying pharmacokinetic properties in the treatment of neurodegenerative diseases. TV3326 represents a new class of drug at least potentially suited to the treatment of Alzheimer's disease patients who require therapies that will delay the progression of the disease, and who suffer from impaired attention, impaired memory, and depression. The combination of the properties attributed to an adrenergic agonist and to a cholinesterase inhibitor may derive benefit from their combined cognitive enhancing properties, as well as from the ability of adrenergic receptor activation to limit the side effects of cholinesterase inhibition (Buccafusco, 1992; Buccafusco and Terry, 2000; Paule, 2001).

Acknowledgements—This work was partly supported by TEVA Pharmaceutical Industries Ltd, by Prime Behavior Testing Laboratories, Inc., and by the Alzheimer's Association. The authors would like to recognize the excellent primate behavior technical assistance provided by Ms Nancy Kille, and Ms Ritu Duhan.

REFERENCES

Andringa G, Cools (2000) The neuroprotective effects of CGP 3466B in the best in vivo model of Parkinson's disease, the bilaterally MPTP-treated rhesus monkey. J Neural Trans Suppl 60:215–225.

Arnsten AF, Steere JC, Hunt RD (1996) The contribution of α2-noradrenergic mechanisms of prefrontal cortical cognitive function: potential significance for attention-deficit hyperactivity disorder. Arch Gen Psychiatry 53:448–455.

Bartus RT (2000) On neurodegenerative diseases, models, and treatment strategies: lessons learned and lessons forgotten a generation following the cholinergic hypothesis. Exp Neurology 163:495–529.

Buccafusco JJ (1992) Neuropharmacologic and behavioral actions of clonidine: interactions with central neurotransmitters. Int Rev Neurobiol 33:55–107.

Buccafusco JJ, Jackson WJ, Terry AV Jr (1992) Effects of concomitant cholinergic and adrenergic stimulation on learning and memory performance by primates. Life Sci 51:7–12.

Buccafusco JJ, Terry AV Jr (2000) Multiple CNS targets for eliciting beneficial effects on memory and cognition. J Pharmacol Exp Ther 295:438–446.

Buccafusco JJ, Terry AV Jr, Murdoch PB (2002) A computer assisted cognitive test battery for aged monkeys. J Mol Neurosci 19:187–193.

Cai JX, Arnsten AFT (1997) Dose-dependent effects of the dopamine D1 receptor agonists A77636 or SKF81297 on spatial working memory in aged monkeys. J Pharmacol Exp Ther 283:183–189.

Francis PT, Palmer AM, Snape M, Wilcock GK (1999) The cholinergic hypothesis of Alzheimer's disease: a review of progress. J Neurol Neurosurg Psychiatry 66:137–147.

Gelowitz DL, Richardson JS, Wishart TB, Yu PH, Lai CT (1994) Chronic L-deprenyl or L-amphetamine: equal cognitive enhancement, unequal MAO inhibition. Pharmacol Biochem Behav 47:41–45.

Haroutunian V, Kanof PD, Tsuboyama G, Davis KL (1990) Restoration of cholinomimetic activity by clonidine in cholinergic plus noradrenergic lesioned rats. Brain Res 507:261–266.

Irle E (1987) Primate learning tasks reveal strong impairment in patients with presenile dementia of the Alzheimer type. Brain Cogn 6:429–449.

Jackson WJ, Buccafusco JJ (1991) Clonidine enhances delayed matching-to-sample performance by young and aged monkeys. Pharmacol Biochem Behav 39:79–84.

Jacobsen JS (2002) Alzheimer's disease: an overview of current and emerging therapeutic strategies. Curr Topics Med Chem 2:343–352.

Knoll J (2000) (−)Deprenyl (Selegiline): past, present and future. Neurobiology (Budapest) 8:179–199.

Kupsch A, Sautter J, Grotz ME, Breithaupt W, Schwarz J, Youdim MB, Riederer P, Gerlach M, Oertel WH (2001) Monoamine oxidase–inhibition and MPTP-induced neurotoxicity in the non-human primate: comparison of rasagiline (TVP 1012) with selegiline. J Neural Trans 108:985–1009.

Mao Z-M, Arnsten AFT, Li B-M (1999) Local infusion of an α-1 adrenergic agonist into the prefrontal cortex impairs spatial working memory performance in monkeys. Biol Psychiatry 46:1259–1265.

Maruyama W, Youdim MBH, Naof M (2001) Antiapoptotic properties of rasagiline, N-proparglyamine-1(R)-aminoindan, and its optical (S)-isomer, TV1022. Ann NY Acad Sci 939:320–329.

Parkinson Study Group (1989) DATATOP: a multicenter controlled clinical trial in early Parkinson's disease. Arch Neurol 46:1052–1060.

Paule MG, Bushnell PJ, Maurissen JPJ, Wenger GR, Buccafusco JJ, Chelonis JJ, Elliott R (1998) Symposium overview: the use of delayed matching-to-sample procedures in studies of short-term memory in animals and humans. Neurotoxicol Teratol 20:493–502.

Paule MG (2001) Validation of a behavioral test battery for monkeys.

In: Methods of behavior analysis in neuroscience (Buccafusco JJ, ed), pp 281–294. New York: CRC Press.

Pratico D, Delanty N (2000) Oxidative injury in diseases of the central nervous system: focus on Alzheimer's disease. Am J Med 109: 577–585.

Prendergast MA, Jackson WJ, Terry AV Jr, Kille NJ, Arneric SP, Buccafusco JJ (1998a) Age-related: differences in distractibility and response to methylphenidate in monkeys. Cereb Cortex 8:164–172.

Prendergast MA, Jackson WJ, Terry AV, Decker MW, Arneric SA, Buccafusco JJ (1998b) Central nicotinic receptor agonists ABT-418, ABT-089, and (−)-nicotine reduce distractibility in young-adult monkeys. Psychopharmacology 136:50–58.

Robbins T, Everitt B (1995) Arousal systems and attention. In: The cognitive neurosciences (Gazzangia M, ed), pp. 703–720. Cambridge, MA: MIT Press.

Sano M, Ernesto C, Thomas RG, Klauber MR, Schafer K, Grundman M, Woodbury P, Growdon J, Cotman CW, Pfeiffer E, Schneider LS, Thal LJ (1997) A controlled trial of selegiline, alpha-tocopherol, or both as treatment for Alzheimer's disease: the Alzheimer's Disease Cooperative Study. N Engl J Med 336:1216–1222.

Shankaranarayana Rao BS, Lakshamana MK, Meti BL, Raju TR (1999) Chronic (−)deprenyl administration alters dendritic morphology of layer III pyramidal neurons in the prefrontal cortex of adult Bonnett monkeys. Brain Res 821:218–223.

Taylor P (2001) Anticholinesterase agents. In: Goodman and Gilman's pharmacological basis of therapeutics, 10th edition (Hardman JG, Limbird LE, Gilman AG, eds), pp 175–191. New York: McGraw-Hill.

Taylor JP, Hardy J, Fischbeck KH (2002) Toxic proteins in neurodegenerative disease. Science 296:1991–1995.

Terry AV Jr, Jackson WJ, Buccafusco JJ (1993) Effects of concomitant cholinergic and adrenergic stimulation on learning and memory performance by young and aged monkeys. Cereb Cortex 3:304–312.

Weinstock M, Kirschbaum-Slager N, Lazarovici P, Bejar C, Youdim MBH, Shoham S (2000a) Neuroprotective effects of novel cholinesterase inhibitors derived from rasagiline as potential anti-Alzheimer drugs. Ann NY Acad Sci 939:148–161.

Weinstock M, Bejar C, Wang RH, Poltyrev T, Gross A, Finberg JP, Youdin MB (2000b) TV3326, a novel neuroprotective drug with cholinesterase and monoamine oxidase inhibitory activities for the treatment of Alzheimer's disease. J Neural Trans Suppl 60:157–169.

Youdim MBH, Wadia A, Tatton W, Weinstock M (2001) The anti-Parkinson drug rasagiline and its cholinesterase inhibitor derivatives exert neuroprotection unrelated to MAO inhibition in cell culture and in vivo. Ann NY Acad Sci 939:450–458.

(Accepted 30 October 2002)

Rationale for considering that propargylamines might be neuroprotective in Parkinson's disease

C. Warren Olanow, MD, FRCPC

Abstract—A neuroprotective therapy that slows or stops disease progression is the major unmet medical need in Parkinson's disease (PD). Current evidence indicates that cell death in PD occurs, at least in part, by way of a signal-mediated apoptotic process. This raises the possibility that anti-apoptotic agents might be neuroprotective in PD. Propargylamines have been demonstrated to be potent anti-apoptotic agents in both in vitro and in vivo studies, presumably by maintaining glyceraldehyde-3-phosphate dehydrogenase (GAPDH) as a dimer and thereby preventing its nuclear translocation where it blocks upregulation of anti-apoptotic proteins. Selegiline is a monamine oxidase type B (MAO-B) inhibitor that incorporates a propargyl ring within its molecular structure. It was shown to delay the need for symptomatic therapy in untreated PD patients in the DATATOP study, but interpretation is confounded by its symptomatic effects. Rasagiline is another MAO-B inhibitor that contains a propargyl ring and has protective effects in laboratory models. A clinical trial utilizing a delayed start design demonstrated that patients initiated on rasagiline at baseline are improved at one year in comparison to patients initiated on placebo and switched to rasagiline at 6 months even though both groups were on the same treatment for the last 6 months of the study. These results argue against the benefit being due to a symptomatic effect and are consistent with rasagiline having a protective effect.

NEUROLOGY 2006;66(Suppl 4):S69–S79

Parkinson's disease (PD) is an age-related neurodegenerative disorder that is characterized by degeneration of dopaminergic neurons in the substantia nigra pars compacta (SNc) coupled with intracytolasmic proteinaceous inclusions or Lewy bodies.[1] Neurodegeneration is not restricted to dopaminergic neurons of the SNc but also occurs in norepinephrine neurons of the locus coeruleus (LC), cholinergic neurons of the nucleus basalis of Meynert (NBM), serotonin neurons of the dorsal raphe (DR), and neurons of the dorsal motor nucleus of the vagus (DMV) and the olfactory and peripheral autonomic systems.[2] The cardinal clinical features of PD are resting tremor, rigidity, bradykinesia, and gait disturbance with postural instability. Current therapy primarily employs a dopamine replacement strategy using levodopa and dopamine agonists.[3] This approach provides benefits to virtually all PD patients, particularly in the early stages of their disease. However, long-term therapy is complicated by the development of motor complications in the majority of patients. In addition, patients can experience disability due to the emergence of freezing, falling, postural instability, autonomic dysfunction, sleep disturbances, mood disorders, and dementia, which probably reflect degeneration of non-dopaminergic neurons.[3,4] These problems are not well controlled with currently available therapies, such that many PD patients experience intolerable disability despite the many treatment advances in the disorder. The development of a neuroprotective therapy that slows, stops, or reverses disease progression and prevents the development of clinical disability is an urgent priority in PD. Among the many candidate agents that might be neuroprotective in PD,[5,6] propargylamines are among the most promising. Propargylamines are molecules that incorporate a propargyl ring and typically inhibit MAO-B. They include several agents that have been studied in PD, such as selegiline, TCH346, and rasagiline.[7] Many preclinical studies have demonstrated the capacity of propargylamines to block apoptosis in in vitro and in vivo models of PD independent of their capacity to inhibit MAO-B. This review considers the experimental data and the theoretical basis supporting a role for propargylamine-containing molecules as putative neuroprotective agents in PD, and examines clinical trials with these agents that have been performed in PD to date.

From the Department of Neurology, Mount Sinai School of Medicine, New York, New York.

Publication of this supplement was supported by an educational grant from Teva Neuroscience and Eisai, Inc.

Disclosure: The sponsor has provided the author with personal honoraria (in excess of $10,000) during his professional career.

Address correspondence and reprint requests to Dr. C. Warren Olanow, Department of Neurology, Mount Sinai School of Medicine, Annenberg 14–94, One Gustave L. Levy Place, Box 1137, New York, NY 10029; e-mail: warren.olanow@mssm.edu

Neurology supplements are not peer-reviewed. Information contained in *Neurology* supplements represents the opinions of the authors and is not endorsed by nor does it reflect the views of the American Academy of Neurology, Editorial Board, Editor-in-Chief, or Associate Editors of *Neurology*.

Copyright © 2006 by AAN Enterprises, Inc.

Copyright © by AAN Enterprises, Inc. Unauthorized reproduction of this article is prohibited.

Apoptosis and PD. Knowledge of the etiopathogenesis of PD would greatly facilitate the development of a neuroprotective therapy. The precise etiology of PD is not known, except for a small number of familial cases with a genetic mutation,[8] and it is possible that sporadic cases result from a complex interplay between genetic and environmental factors that are not necessarily the same in all patients. Oxidative stress, mitochondrial dysfunction, inflammation, excitotoxicity, and protein aggregation have been implicated in the pathogenesis of cell death in PD.[9,10] However, the role played by these factors in the cell death process is not known, nor is it clear if each of these factors contributes equally to neurodegeneration in all PD patients. Increasing evidence suggests that they act as a network whereby inhibition of any one factor might not be sufficient to prevent neuronal degeneration. A body of evidence suggests that cell death in PD occurs, at least in part, by way of signal-mediated apoptosis in all PD patients.[11-14] If apoptosis is common to all of the different forms of PD, it is possible that anti-apoptotic agents might provide neuroprotective effects in each of the different types of PD.

Apoptosis is a gradual form of cell death that is characterized by cell shrinkage, chromatin condensation, and fragmentation of nuclear DNA with preservation of plasma membranes and absence of an inflammatory response.[15] This contrasts with necrosis, which is a rapid form of cell death characterized by massive ionic fluxes across the plasma membrane, mitochondrial disruption with a complete loss of ATP production, disruption of subcellular organelles with rupture of the plasma membrane, an inflammatory response, and relative preservation of nuclear DNA. Although apoptosis was first described as a counterbalance for excess cell replication in developing organisms, it is now appreciated that neuronal apoptosis can result from a variety of toxic insults, many of which are relevant to PD.[15]

A number of genes and their protein products are known to be involved in neuronal apoptosis.[16] These include the bax/bcl family (bax, bcl-2, bcl-x_L), the interleukin 1β converting enzyme (ICE) family (ice, ich-1_L, and ich-1_S) or caspases, and p53. Increased expression of p53, bax, or caspase promotes apoptosis, whereas increased expression of bcl-2 or bcl-x_L promotes survival. In addition, the early gene c-jun promotes neuronal apoptosis, whereas activation of ERK and the PI3 kinase/AKT pathway decreases neuronal apoptosis.[17,18]

Apoptosis was classically identified by the finding of "laddering" on DNA electrophoresis due to symmetrical cleavage of nuclear DNA by endonucleases. However, this technique requires fragmented DNA from large numbers of cells and is useful only when thousands of cells enter into apoptosis in a synchronized manner. This is not the case in neurodegenerative diseases such as PD, in which degenerating nerve cells most likely enter into apoptosis in a desynchronized manner over a prolonged period of time. Furthermore, DNA markers of apoptosis persist for a relatively short period of time, probably only a matter of hours. The identification of apoptosis in postmortem brain tissue of patients with PD became feasible with the advent of techniques that attach a chromogen or a fluorochrome to the endonuclease-cleaved ends of nuclear DNA (e.g., TUNEL or BODIPY/fluorescein dUTP) and by fluorescent DNA-binding dyes that label regions of chromatin condensation (e.g., YOYO).

Mitochondria can play a major role in some forms of apoptosis.[16,19] A fall in the mitochondrial membrane potential ($\Delta\Psi_M$) caused by a rise in cytosolic calcium or oxidative stress is associated with opening of a mitochondrial megapore [also known as the permeability transition pore (PTP)]. This results in the free diffusion of solutes and small proteins across the mitochondrial membrane, swelling and fracture of the mitochondrial membrane, and the release of factors such as cytochrome c from the mitochondrion that signal for the initiation of apoptosis.[16,19,20] Agents that maintain closure of the PTP, such as BCL-2, SOD, or cyclosporine A, preserve the $\Delta\Psi_M$ and are anti-apoptotic, whereas agents that promote opening of the pore, such as BAD and BAX are pro-apoptotic.[16,21] It is now evident that $\Delta\Psi_M$ is reduced early in the apoptotic process, well before evidence of chromatin condensation and DNA fragmentation. With the use of laser confocal microscopy, these findings have been extended to neuronal models of apoptosis, and it has been confirmed that $\Delta\Psi_M$ decreases before nuclear DNA fragmentation.[22] Apoptosis has also been implicated in other neurodegenerative diseases, such as Alzheimer's disease, amyotrophic lateral sclerosis, and Huntington's disease (reviewed in references 15 and 16).

A substantial body of evidence indicates that cell death in PD occurs by way of apoptosis,[11] although there are reports to the contrary.[23] Apoptosis has been identified in PD with electron microscopy,[24] but most reports have relied on the TUNEL technique to detect fragmented DNA.[13,14] Based on these techniques, it has been estimated that approximately 1% to 2% of SNc neurons in PD have nuclei that stain positively for markers of apoptosis. These percentages seem high, given the short life span of nuclei with detectable DNA strand breaks and the likelihood that nerve cell death in PD occurs asynchronously over the course of many years. This has raised concerns of false-positive results with TUNEL approaches. However, Tatton et al.[14] demonstrated that apoptotic neurons in the PD nigra stained positively for both DNA fragmentation and chromatin condensation, whereas this finding was rarely encountered in controls. This study strongly supports the concept that at least some SNc neurons undergo apoptosis in PD. In further support of this concept, pro-apoptotic changes in BCL-2, SOD, and GAPDH, as well as increased caspase 3 and Bax immunoreactivity, have been detected in surviving SNc neurons in PD patients.[25,26] These findings support the notion that apoptosis occurs in PD and the possibility

Copyright © by AAN Enterprises, Inc. Unauthorized reproduction of this article is prohibited.

that anti-apoptotic drugs might have a neuroprotective effect.

Evidence that propargylamines are neuroprotective agents. Many agents have been demonstrated to have anti-apoptotic properties in PD model systems. Among the most potent and promising of these are the propargylamines.[7] The best studied of these is selegiline (*N*-propynyl-methamphetamine). Selegiline is a relatively selective irreversible inhibitor of MAO-B. It originally attracted attention as a possible neuroprotective therapy for PD based on its capacity to inhibit the MAO-B oxidation of MPTP to MPP+ and thereby to block the development of MPTP-induced parkinsonism.[27] Selegiline also has the potential to prevent the formation of reactive oxygen species derived from the MAO-B oxidation of dopamine, which have been implicated in the pathogenesis of PD.[28,29] In the laboratory, in vitro and in vivo experiments have shown that picomolar doses of selegiline protect dopamine and other motor neurons from many PD-related toxic events, including peroxide, glutamate, MPTP, glutathione depletion, and trophic withdrawal.[30,31] Interestingly, it has now become apparent that selegiline neuroprotection is due to an anti-apoptotic effect and occurs independent of MAO-B inhibition.[32,33] For example, selegiline protects dopamine neurons from the toxic effects of MPP+, the toxic byproduct of MPTP metabolism by MAO-B. This cannot be explained by inhibition of MAO-B and cannot be achieved with MAO-B inhibitors that do not include a propargyl ring.[33] It is also evident that selegiline derives its protective benefit from its metabolite, desmethylselegiline (DMS). DMS provides greater protective effects than selegiline at all concentrations, and P450 inhibitors, which prevent DMS formation, block selegiline-induced neuroprotection.[34,35]

TCH 346 (also referred to in the literature as CGP 3466) is another propargylamine-containing molecule, but unlike selegiline it does not inhibit MAO-B. In the laboratory it has powerful neuroprotective effects on dopamine and other motor neurons in both in vitro and in vivo studies, even when employed at very low concentrations.[36-38] Importantly, TCH has been shown to block MPTP toxicity and the development of parkinsonism in non-human primates, respectively, despite the fact that it does not inhibit MAO-B activity.[39]

Rasagiline [*N*-propargyl-(1*R*)-aminoindan] is an irreversible and potent MAO-B inhibitor that also incorporates a propargyl ring within its molecular structure.[40] It has been demonstrated to provide antiparkinsonian benefits when used as monotherapy or as an adjunct to levodopa,[41,42] and has now been approved for use in many countries. Rasagiline differs from selegiline in that it has a closed ring structure, is metabolized to form an aminoindan, and avoids the amphetamine metabolites associated with selegiline. Like other propargylamines, rasagiline has been demonstrated to provide anti-apoptotic effects in the laboratory that are independent of MAO-B inhibition.[43] In vitro, rasagiline protects against a variety of toxins, including the nitric oxide donor 3-morpholinosydnonimine hydrochloride (SIN-1), glutamate, 6-hydroxydopamine (6-OHDA), MPTP, β-amyloid, 1,2,3,4-tetrahydroisoquinoline, and serum and growth factor deprivation.[44-51] Rasagiline has specifically been shown to increase survival of cultured fetal mesencephalic dopaminergic neurons[44,45] and to protect the dopamine cell line SH-SY5Y against apoptotic cell death induced by the tetrahydroisoquinoline-related dopaminergic neurotoxin *N*-methyl-(*R*)salsolinol.[50,51]

Rasagiline has also been shown to provide neuroprotective effects in a variety of in vivo models. Rasagiline protects dopamine neurons from the toxic effects of a unilateral injection of 6-OHDA[52] and significantly reduces apomorphine-induced rotational behaviors. In this model, pretreatment with rasagiline prevents the loss of tyrosine hydroxylase (TH)-positive dopaminergic neurons in the SNc and the loss of dopamine terminals in the striatum by approximately 35%. This study demonstrates the capacity of chronic treatment with rasagiline to protect against the behavioral and pathologic consequences of a dopamine lesion. The drug has also been reported to protect non-dopaminergic motor neurons. After closed head injury in the mouse, rasagiline promotes recovery of motor function and spatial memory and reduces cerebral edema.[53] Rasagiline also improved neurologic severity score and reduced the volume of necrotic brain tissue after middle cerebral artery occlusion in the rat.[54] Benefits have also been observed in rats with degeneration of vasopressin-containing neurons in the paraventricular nucleus (PVN) of the hypothalamus, which experience spontaneous hypertension.[55] Rasagiline reduced PVN neuronal cell loss, reduced systolic blood pressure, reduced the risk for stroke, and increased cumulative survival from 56.09 ± 1.77 days to 73.6 ± 2.22 days ($p < 0.0001$). Rasagiline treatment also increased survival of the G93A Cu/Zn SOD transgenic mouse model of familial ALS and extended the duration of benefit induced by riluzole.[56]

In these studies, several factors suggest that rasagiline might be a preferred neuroprotective agent in comparison with selegiline. First, in comparative studies neuroprotection is generally greater with rasagiline than with selegiline. Second, rasagiline itself is protective, whereas its metabolite aminoindan is less protective than the parent drug. In contrast, selegiline neuroprotection is dependent on its conversion to its desmethyl metabolite, and benefits are lost if metabolism is impaired. Finally, rasagiline is not metabolized to form amphetamines, which have been suggested to inhibit neuroprotective effects.

A summary of the models and toxins in which rasagiline has shown neuroprotective effects is provided in table 1.

Mechanism of action of propargylamines. Increasing evidence indicates that protection associ-

Copyright © by AAN Enterprises, Inc. Unauthorized reproduction of this article is prohibited.

Table 1 *Neuroprotective activity of rasagiline*

In Vitro	
Cell type	Toxin
SH-SY5Y cells	Salsolinol
PC12 cells	Trophic withdrawal
PC12 cells	Anoxia and glucose deprivation
Mesencephalic dopamine neurons	Enhances survival
Hippocampal neurons	Glutamate
In Vivo	
Benefit	Toxin/injury
Surviving nigral neurons in rat	6-OHDA
Facial neurons in rat pups	Axotomy
Survival	Transgenic SOD mouse
Motor function, lesion size	MCA occlusion
PVN of hypothalamus	Increased survival, reduced blood pressure

ated with propargylamines is not related to MAO-B inhibition but rather to an anti-apoptotic effect that is dependent on transcriptionally-mediated new protein synthesis.[32,33,57] Apoptosis in trophically withdrawn cells is associated with increased levels of pro-apoptotic molecules such as c-Jun (which activates the caspase cascade) and Bax (which promotes apoptosis by inducing opening of the PTP and loss of the $\Delta\Psi_M$).[58] In contrast, treatment with propargylamines results in downregulation of these molecules coupled with upregulation of anti-apoptotic molecules such as SOD-1, SOD-2, BCL_2, and BCL_{XL}.[33] There is now substantial evidence indicating that propargylamines exert anti-apoptotic effects by way of an interaction with glyceraldehyde-3-phosphate dehydrogenase (GAPDH). GAPDH is an intermediary enzyme in glycolytic metabolism that is also involved in protein translation, and normally exists in a tetrameric form bound to AUUA-rich (stem loop) regions of RNA within the cytoplasm (figure). Increased expression of GAPDH and its translocation from the cytoplasm to the nucleus have been shown to be associated with apoptosis.[59,60] In cases of mitochondrial stress, NAD+ levels are increased and displace GAPDH from its binding site, where it then translocates to the nucleus and promotes apoptosis. Carlile et al.[61] used confocal laser microscopy and size- exclusion chromatography to demonstrate that propargylamines exert protection by fitting into the channel formed by the GAPDH tetramer (see figure) and maintaining the molecule as a dimer.[61] In this form, GAPDH does not translocate to the nucleus and apoptosis does not occur. The precise mechanism whereby GAPDH in the nucleus leads to apoptosis is believed to involve inhibition of transcriptional upregulation of anti-apoptotic molecules, thereby preventing upregulation of cell defenses and consequent cell death. Propargylamines, by preventing the nuclear translocation of GAPDH, permit the cell to upregulate levels of protective molecules such as bcl-2, SOD, and GSH and thereby to prevent oxidative stress, maintain the mitochondrial membrane potential, and block apoptosis. In support of this concept, propargylamines have been shown to stabilize mitochondrial membrane potential, reduce cytosolic levels of cytochrome c, reduce levels of caspase 3, and prevent the development of DNA markers of apoptosis.[58]

Similar observations have been reported with rasagiline. Rasagiline prevents the nuclear translocation of GAPDH[62] and is associated with upregulation of the anti-apoptotic proteins/mRNAs Bcl-2, Bcl-x_L, and SOD, and downregulation of the pro-apoptotic molecules/ mRNAs Bax and Bad.[49,62-65] Furthermore, rasagiline prevents the fall in mitochondrial membrane potential, release of cytochrome c, activation of caspases, and DNA fragmentation that characterize apoptosis.[63,66,67] Recent studies further indicate that rasagiline protection involves the PKC/MAP kinase pathway, which is involved with BCL-2 activation, and that protection is blocked by

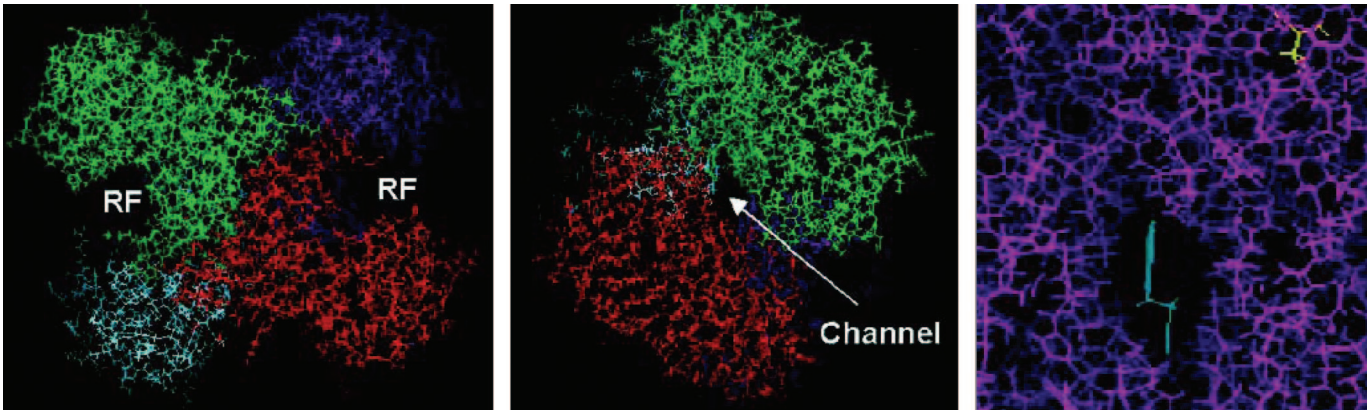

Figure. Models of the rat GAPDH tetramer showing the four identical monomers that make up the GAPDH tetramer in different colors (left panel) the binding channel formed by the site where the four monomers join (center panel), and a schematic representation of a propargylamine located within the channel so as to maintain the molecule as a dimer and prevent nuclear translocation with the development of apoptosis (right panel). Figures adapted from Carlile et al.[61]

Copyright © by AAN Enterprises, Inc. Unauthorized reproduction of this article is prohibited.

Table 2 *Evidence that rasagiline provides protection through an anti-apoptotic mechanism*

Prevents GAPDH translocation to the nucleus
Enhances BCL-2 upregulation
Preserves mitochondrial membrane potential
Prevents upregulation of cytochrome c
Prevents upregulation of caspase 3
Prevents DNA fragmentation and chromatin clumping

GF109203X, a broad-spectrum inhibitor of PKC.[49,64] These findings suggest that a PKC/BCL-2 interaction mediates the neuroprotection induced by rasagiline. Rasagiline (100 nM) has also been shown to induce a marked upregulation of glial cell line-derived neurotrophic factor (GDNF) in SH-SY5Y, which might also contribute to its protective effects.[68]

A summary of factors indicating that rasagiline acts as an anti-apoptotic agent is provided in table 2. The capacity of propargylamines such as rasagiline to block apoptosis make these drugs promising agents for testing as putative neuroprotective agents in PD, in which substantial evidence indicates that cell death occurs by way of apoptosis (table 3).

Clinical trials testing propargylamines in PD. Several clinical trials have examined the potential of propargylamine-containing compounds to have neuroprotective and disease-modifying effects in PD. The first of these was the DATATOP study.[69] This trial assessed the capacity of selegiline to slow the development of disability necessitating the introduction of levodopa therapy in comparison with placebo in otherwise untreated PD patients. The hypothesis underlying this study was based on the potential of selegiline to inhibit the MAO-B oxidation of toxins such as MPTP or to prevent the formation of free radicals derived from the MAO-B oxidation of dopamine. That selegiline, and more specifically its metabolite DMS, might have anti-apoptotic effects was not appreciated at that time. In this study, selegiline significantly delayed the need for levodopa in comparison to placebo, consistent with the drug having a protective effect. However, the study also demonstrated that selegiline had symptomatic effects associated with the introduction and withdrawal of the drug. This confounded interpretation of the trial and prevented a clear determination as to whether or not selegiline was protective. In other words, it was not possible to ascertain if the selegiline benefit was due to a protective effect, with slowing of neurodegeneration, or a symptomatic effect which simply masked ongoing cell death.[70] It is noteworthy, however, that long-term follow-up in the DATATOP study showed that patients who had been originally randomized to receive treatment with selegiline had less freezing than did those originally randomized to placebo.[71]

Table 3 *Evidence of apoptosis in PD*

DNA fragmentation
Chromatin condensation
DNA fragmentation and chromatin condensation in same cells
GAPDH translocation to the nucleus
BCL-2 overexpression

The SINDEPAR study used change in motor score between an untreated baseline and a final visit performed after drug wash-out as the primary endpoint in an attempt to test the putative neuroprotective effects of selegiline.[72] This study also showed a significant benefit in favor of selegiline in comparison to placebo, although here the potential of a confound due to a long-duration symptomatic effect of the drug could not be excluded. These studies suggest that selegiline might be protective in addition to having symptomatic effects, although it still cannot be ascertained with certainty if any of the benefits associated with selegiline treatment are due to neuroprotection.

The propargylamine TCH346 has also been studied as a possible neuroprotective effect in a prospective, double-blind, placebo-controlled trial. Much was expected of this agent because it is a very potent neuroprotective agent in the laboratory. In addition, it does not inhibit MAO-B and is therefore unlikely to have the confounding symptomatic effects that have limited interpretation of studies with selegiline. Unfortunately, at the three doses tested TCH346 had no beneficial effect on the primary endpoint (time to need for levodopa) or on any of the prespecified secondary endpoints, and no further studies are planned with this agent.

More promising are the results with rasagiline. The TEMPO study employed a delayed start design to try and avoid confounding symptomatic effects associated with drugs that inhibit MAO-B.[73] In the delayed-start design, untreated PD patients are randomized to initiate therapy with the study intervention or placebo during the first treatment phase. During the second treatment phase, all patients, including those originally on placebo, receive the active study intervention. Benefits observed with the study drug compared with placebo at the end of the first phase of the study could be due to either symptomatic or protective effects or to a combination of both. However, at the end of the second phase all patients are receiving the same treatment, and symptomatic effects should therefore be comparable. Therefore, it is thought that any benefit between the study intervention and the placebo group at the end of the study cannot be due to a symptomatic effect and is consistent with a neuroprotective effect due to treatment with the study intervention during the first phase of the study.[74-76] The TEMPO study used this design to compare rasagiline with placebo. At the end of the first stage of the study (6 months), rasagiline-treated patients had significant improvement in UPDRS motor scores in comparison with patients in the placebo group, consistent with the drug having a protective and/or symptomatic effect. However, these benefits persisted at the end of the second stage of the study (12 months) when all patients had

Copyright © by AAN Enterprises, Inc. Unauthorized reproduction of this article is prohibited.

been receiving rasagiline for at least 6 months. This difference cannot be explained simply by a symptomatic effect of the drug because patients in both groups were on the same medication, and is consistent with rasagiline having a protective effect in PD patients. A larger study to evaluate initial treatment with rasagiline versus placebo using a delayed-start design (the Adagio Study) is now under way.

Summary. Neuroprotection is the single most important unmet medical need in PD. A body of evidence suggests that cell death in PD occurs by way of apoptosis, raising the possibility that drugs that interfere with pro-apoptotic signals might have disease-modifying effects. Propargylamine-containing molecules are anti-apoptotic and have been shown to protect dopamine and other motor neurons from a variety of toxins. Substantial evidence indicates that these agents act by binding to GAPDH, maintaining it as a dimer and preventing its translocation to the nucleus, where it interferes with transcriptional upregulation of anti-apoptotic proteins. Clinical trials of these agents have not yet established that they are neuroprotective in PD. However, the delayed-start design study showed that initiating treatment with rasagiline provided benefits in comparison to placebo that could not be attained when the drug was initiated at a later time point. These findings are consistent with a neuroprotective effect and warrant further investigation.

Discussion

DR. SCHAPIRA: How strong do you think the evidence is that selegiline is neuroprotective in PD?

DR. OLANOW: It is hard to say. Don't forget that the DATATOP study was positive, and patients on selegiline had a highly significant delay in their need for levodopa. Unfortunately, the study was confounded by the symptomatic effect of the drug, but this does not mean that there wasn't a neuroprotective component to this effect. Long-term studies also show that patients originally randomized to selegiline had reduced freezing compared to those originally treated with placebo. There have also been many laboratory studies showing that selegiline, by way of its desmethyl metabolite, protects dopamine and other motor neurons in a wide variety of in vitro and in vivo model systems. Plus the mechanism of action of how it could provide neuroprotective effects is very well worked out. So it is certainly possible.

DR. SCHAPIRA: Were there primate studies as well?

DR. OLANOW: There were. Selegiline blocked the effect of MPTP in primates, but this was most likely because of its MAO-B inhibiting properties. Still, studies in other model systems have shown that MAO-B inhibition is not necessary for selegiline to exert a protective effect, and it is possible that some of the benefit in monkeys is due to a protective effect.

DR. MCNAUGHT: These studies were done for the most part before studies on the role of the ubiquitin proteasome system (UPS) in PD. Have any of the models that have been studied looked at the effect of selegiline on proteasomal function, ubiquitination, or protein aggregation?

DR. OLANOW: Catherine Mytilineou and I looked at the effect of selegiline on lactocystin-induced toxicity, and we did not find protection in this model.

DR. JENNER: I don't want to bait you, but we have looked at the effects of selegiline in cell lines exposed to a range of toxic insults and we have been unable to show many of the neuroprotective effects that are reported in the literature.

DR. SCHAPIRA: Maybe it was where you got your selegiline.

DR. JENNER: We also tried other agents that were said to be neuroprotective and could not replicate what was reported in the literature.

DR. OLANOW: There are dozens of excellent investigators who have published on the neuroprotective effects of selegiline. What cell line did you use?

DR. JENNER: The work was done with SHSY-5Y cells.

DR. OLANOW: We have never worked with SHSY-5Y cells, and maybe there are differences in the cell lines.

DR. JENNER: But didn't you and Kevin show that selegiline didn't protect against proteasomal inhibition in cultured cells?

DR. MCNAUGHT: That's correct. It didn't work in primary cultures, but in fact we did some work with Bill Tatton and showed that it did protect against a proteasome inhibitor in PC12 cells.

DR. OLANOW: Do you know if primary cultures have P450 in order to metabolize selegiline to the active propargylamine?

DR. JENNER: My understanding is that primary cultures don't have P450, and now I need to find out if SHSY-5Y cells have it. That might explain the differences in our findings from other groups.

DR. OLANOW: I know that rasagiline is protective against many toxins in primary cultures. I think it would be interesting to see if rasagiline gives you protection in your model, Peter, because it does not require metabolism to provide protection. It is also

Copyright © by AAN Enterprises, Inc. Unauthorized reproduction of this article is prohibited.

worth pointing out that the literature is confusing as to which P450 metabolizes selegiline, with conflicting results having been reported.

DR. MCNAUGHT: I am curious to know if there's differential expression of P450 in PC12 cells compared to primary cultures.

DR. SIDEROWF: How much of a problem is it that positive results are published and negative results tend not to be?

DR. OLANOW: There is a bias that journals don't like to publish negative results, but if you were to report that you tried a series of agents that had previously been reported to be neuroprotective and couldn't get them to work and the methodologies that you used were sound, I think you could get that work published. Have you tried to publish your results, Peter?

DR. JENNER: We haven't published them yet because we were so worried that we couldn't reproduce what was in the literature and we want to confirm them. The more we discuss this, the more I think that results can be system-dependent. This illustrates why it is important to discuss negative as well as positive results.

DR. KIEBURTZ: How do you block the metabolism of selegiline?

DR. OLANOW: With P450 inhibitors, which block the demethylation of selegiline to DMS. And interestingly this blocks the protection, indicating that it is the DMS metabolite that is primarily responsible for this effect. This is further supported by the finding of reduced benefits with selegiline compared with DMS at the same concentration.

DR. POEWE: What about with rasagiline?

DR. OLANOW: It is different with rasagiline. Here the neuroprotective benefit is greater with rasagiline than with its metabolite, aminoindan, and blocking rasagiline metabolism does not block its protective effects.

DR. HAUSER: What accounts for this difference?

DR. OLANOW: It probably has to do with the capacity of the molecule to fit into the channel formed by the GAPDH tetramers and its ability to maintain GAPDH as a dimer so that it doesn't go to the nucleus and prevent the protective response that blocks apoptosis. It is likely that DMS and rasagiline fit, whereas selegiline per se does not. Bill Tatton showed that if you employ antibodies to the proteins that make up the canal, you lose the protective effects that are seen with propargylamines.

DR. SCHAPIRA: What was the basis for determining that propargylamines maintain GAPDH as a dimer?

DR. OLANOW: This was work done by Graham Carlile and Bill Tatton. They used size-exclusion chromatography and showed that GAPDH normally exists as a tetramer, but when a propargylamine is added it predominantly exists as a dimer.

DR. HAUSER: If you block the metabolism of selegiline to desmethyl selegiline, do you still get a fair amount of protection?

DR. OLANOW: No, you lose the protection.

DR. KIEBURTZ: And this has nothing to do with MAO-B inhibition?

DR. OLANOW: That's correct. Bill Tatton showed in the trophic withdrawal model that the selegiline benefit was not seen with other MAO-B inhibitors. Subsequently, Catherine Mytilineou and I reproduced these results. These were the original studies that led us to believe that the selegiline benefits were related to its propargyl ring and based on an anti-apoptotic effect.

DR. JENNER: How did you establish that it was anti-apototic?

DR. OLANOW: First, we selected models that result in apoptosis, such as trophic withdrawal, and showed that propargylamines prevent the development of the DNA markers indicative of apoptosis. Tatton and Ishitani and others also showed that apoptosis was associated with upregulation of GAPDH and downregulation of BCL-2, SOD-1, and SOD-2, while the addition of a propargylamine such as DMS prevented the upregulation of GAPDH and induced upregulation of BCL-2, SOD-1, and SOD-2. These findings indicate that propargylamines act by interfering with pro-apoptotic signals.

DR. KIEBURTZ: I think I am beginning to see how this works. Presumably propargylamines exert anti-apoptotic effects by interacting with GAPDH and preventing it from promoting pro-apoptotic signals in response to minor or inappropriate cell stresses.

DR. OLANOW: Exactly.

DR. SIDEROWF: What exactly does GAPDH do?

DR. OLANOW: It has several functions. It is well known to be an intermediary in glycolytic metabolism. It also sits on stem loops of RNA and plays an important role in RNA translation into proteins. And it is also involved in signaling for apoptosis under conditions of mitochondrial stress.

DR. SIDEROWF: How is it that GAPDH plays such an important role in signaling for apoptosis?

Copyright © by AAN Enterprises, Inc. Unauthorized reproduction of this article is prohibited.

DR. OLANOW: GAPDH is involved in fundamental glycolytic metabolism and is probably a sensor of mitochondrial function. When mitochondria are under stress, this is reflected by excessive release of NAD+ from mitochondria, which displaces tetrameric GAPDH from stem loops where it translocates to the nucleus, inhibits the normal protective response of the cell, and promotes apoptosis. It is interesting to speculate that this might occur as a way of avoiding necrotic cell death, which is associated with inflammation that might have an adverse effect on neighboring healthy cells.

DR. POEWE: What are the differences between selegiline and rasagiline?

DR. OLANOW: Rasagiline is similar to selegiline but there are a few important differences. First, it is a more potent MAO-B inhibitor. Second, the ring here is closed so that it is metabolized to form an aminoindan and does not generate amphetamine metabolites. It is similar to selegiline in that it incorporates a propargyl ring, but protection comes from the parent molecule and not from a metabolite. Finally, it provides protection in laboratory models and has been better studied as an antiparkinsonian agent in double-blind controlled trials. Therefore, at least in my opinion, it warrants trial in PD as a putative neuroprotective drug, particularly in view of the results of the delayed-start component of the TEMPO study.

DR. POEWE: Do rasagiline and selegiline show comparable protection in the laboratory?

DR. OLANOW: More or less, although at the same concentration rasagiline tends to show slightly more protection. The selegiline story has been nicely worked out, and there is a nice body of work showing that rasagiline, like other propargylamines, can protect a variety of cells in vitro, including dopaminergic and non-dopaminergic cells. In vivo, you can see quite extensive protection in a variety of models, including 6-hydroxydopamine, axotomy, ALS, MCA occlusion, head injuries, and so on. Interestingly, Mousa Youdim did gene microarray studies before and after rasagiline and showed that mRNAs that were upregulated by rasagiline included those that have the potential to be anti-apoptotic or protective, whereas those that were downregulated were pro-apoptotic, such as caspase-3.

DR. MCNAUGHT: You reported that buthionine sulfoxamine induces cell death. How does it do that?

DR. OLANOW: It kills cells by blocking the formation of glutathione, but you have to deplete it by quite a lot, about 70 percent. We were surprised because the GSH depletion in PD is only about 40 percent.

DR. SCHAPIRA: Cells tend to conserve mitochondrial glutathione, which is perhaps why you need to deplete it so much.

DR. KIEBURTZ: How does TCH346 differ from rasagiline and selegiline?

DR. OLANOW: TCH346 is also a propargylamine, but it has minimal if any MAO-B inhibition.

DR. JENNER: But it was supposed to have shown excellent protective effects in the laboratory, is that not correct?

DR. OLANOW: It did. That is why the negative clinical trial was especially disappointing because the drug would likely not have had a symptomatic confound and any benefit could have been attributed to neuroprotection.

DR. JENNER: On the other hand, doesn't the negative trial with this agent suggest that benefits seen with drugs such as selegiline and rasagiline are due to MAO-B inhibition rather than protection?

DR. OLANOW: I suppose that is correct, but it is also possible that we picked the wrong dose to test. TCH346 worked in the laboratory at concentrations of 10^{-10} but had a U-shaped curve and didn't work at higher or lower concentrations. It is also 99% protein-bound. So it was hard to pick the correct dose, and we may have gotten it wrong.

DR. STERN: What do you think is the best animal model to test putative neuroprotective therapies for PD?

DR. OLANOW: That's a problem. The animal models we have such as MPTP and 6-OHDA don't really reflect PD, and positive results in these models doesn't necessarily mean you will get positive results in PD patients. The transgenic animals offer the best opportunity because these animals carry the specific mutation that causes the human disease. However, the same mutation that causes PD in humans may not be harmful to the animal model, and in fact most transgenic or knockout animals do not replicate PD behavior or pathology. I like the proteasome inhibition model because it is progressive and has dopamine and non-dopamine lesions. But many groups are having difficulty reproducing this model, and we can't rely on this model until we resolve these issues. It is interesting that, in tissue culture, many of the agents that we think might be neuroprotective in PD are ineffective in the proteasome inhibition model. Ideally, I would like to test a drug in PD that works in this model.

DR. KIEBURTZ: That's a real problem, isn't it? How do we take a drug from the laboratory to humans? If it works in a laboratory model, does that mean it will work in humans? Is that a good predictor? Did we look at the

Copyright © by AAN Enterprises, Inc. Unauthorized reproduction of this article is prohibited.

right models? Have we got a drug that never would have worked in humans and we could have known this had we looked at the correct models? Or would this have worked in any system but we used the wrong dose, or perhaps we didn't deliver it to the correct target. Or perhaps we used the wrong study design? Maybe we didn't address compensation adequately, and maybe we should have looked for longer in order to tell if a drug is protecting nerve cells? Of course I don't know the answers to any of these questions. Given all we know, a confounded study with selegiline and a negative trial with TCH346, are you still a fan of propargylamines as neuroprotective agents?

DR. OLANOW: I still am optimistic because the mechanism is so well worked out, because they protect at very low concentrations that can be obtained physiologically, and because they protect in so many different model systems. Another big question that remains is whether you can design a trial that can show slowing of disease progression.

DR. KIEBURTZ: It's always hard to know whether it's a failed drug or a failed trial. Even if it was the right trial design, was it implemented incorrectly? Is there something funny about the characteristics and the behavior of the patients who are enrolled? I think we could learn a lot by exploring negative studies such as the riluzole, the cephalon mixed-lineage kinase inhibitor, and TCH studies to see if we can learn anything.

DR. JENNER: One of the problems I have is that these companies frequently go right to phase III studies without doing phase II dosing studies.

DR. KIEBURTZ: It's often hard to know what dose to use in a neuroprotective study, because there is no biomarker to indicate activity. In which case, you might as well look at dosing, tolerability, safety, and efficacy in a pivotal phase IIb trial. In the cephalon study we went right to a pivotal study looking at three doses and hoped that one of them would be the right dose.

DR. OLANOW: That study was another disappointment because there is a good rationale for testing Jun kinase inhibitors based on evidence that protein aggregation promotes cell death by way of Jun kinase activation.

DR. MCNAUGHT: Let's suppose you are successful with an anti-apoptotic drug and you reduce the number of cells going into apoptosis. What happens to those cells in the long run?

DR. OLANOW: That's a very good question. We know the short-term but not the long-term consequences of these therapies. We show reduced cell death with reduced markers of apoptosis at 24 or 48 hours, but we don't know what happens to the cells afterwards and whether they behave like healthy cells. What would be bad is if these drugs converted cells from undergoing apoptosis to dying by necrosis, which could be worse for the organism. The situation might be different, though, if there were a problem such as a complex I defect where the mitochondrial membrane potential was set abnormally low. Here, anti-apoptotic drugs could help to maintain closure of the pore and reset the resting membrane potential and eliminate the cell's vulnerability. This might be the case in PD, where there is evidence at postmortem that GAPDH has translocated to the nucleus in some cells and the cell is perhaps in a pro-apoptotic state. Propargylamines might take a cell that was getting ready to die and restore it to a more normal function. In other words, you may be taking a vulnerable cell and making it less vulnerable.

DR. SCHAPIRA: Yes, less vulnerable to die. But the issue is, is that cell able to function normally?

DR. KIEBURTZ: Tim Greenamyre took normal and HD fiberblasts and subjected them to repetitive calcium challenges. He found that resting mitochondrial membrane potential dropped and then recovered between challenges with normal fibroblasts, while with HD fiberblasts the mitochondrial potential continued to fall until the cells died. So he was trying to get at not only do they die but could they recover function.

DR. OLANOW: Bill Tatton did a similar experiment in which he showed that fibroblasts from PD patients had a low mitochondrial membrane potential and were very sensitive to rotenone in comparison to controls. If that were to be the state of nigral neurons in PD, then I think propargylamines might be helpful by restoring mitochondrial membrane potential in an otherwise intact cell that is vulnerable to undergo apoptosis when exposed to ordinarily non-lethal stresses.

DR. HAUSER: One of my concerns is that, by the time you start a treatment, irreversible events may have already occurred.

DR. OLANOW: That's a fair concern. Venu Nair in our group showed that, after exposure to hydrogen peroxide, cultured cells very quickly express markers indicating whether or not they will undergo apoptosis, even though DNA markers of apoptosis may not be seen for another 24 to 48 hours. I think of propargylamines as a way to promote the likelihood that the cell will survive. As you imply, there are probably many factors that determine whether a cell will ultimately die or survive. And if we could, for example, through a propargylamine drug like rasagiline preserve the mitochondrial membrane potential, that would mean that some cells might tolerate a stress they otherwise might not, and a greater percentage of cells would survive. Whether that will translate into a clinically meaningful effect I don't know. One of the jobs in the laboratory is to define

Copyright © by AAN Enterprises, Inc. Unauthorized reproduction of this article is prohibited.

reasonable hypotheses, find targets, and develop candidate drugs that show protection in models. In the final analysis, you have to do a clinical trial to know if it really works in PD.

DR. SIDEROWF: I was impressed when you described the many different systems where rasagiline exerted a protective effect. And it made me think that, in Parkinson's disease, only part of the degeneration is in the nigrostriatal dopaminergic system, but many other extranigral neurons also degenerate, and deficits are not just in motor function but in cognition and mood. Given the capacity of rasagiline to protect so many different cell types in the laboratory, does that make it more promising to study in PD and does it suggest specific trial designs and endpoints that should be employed?

DR. KIEBURTZ: I think you make a good point, and that trial designs that look at non-dopaminergic feature as a measure of protection are potentially very valuable because they are less likely to be confounded by the dopaminergic agents we use to treat PD today. I personally would feel much more comfortable that a therapy was neuroprotective if it slowed the development of non-dopaminergic features, such as postural instability or dementia. And even if it turned out to be a symptomatic mechanism it would still be a boon for patients, since such therapies are not currently available.

DR. JENNER: Certainly, very little research has taken place outside the nigra in PD to date, and I think more information in this area could be very helpful to clinicians designing neuroprotection trials.

DR. OLANOW: To take that one point further, if we had a good model of PD based on etiopathogenesis, positive results in such a model would be very helpful in determining that positive results in a clinical trial were due to protection, as no current clinical endpoint can be totally relied on as yet.

DR. KIEBURTZ: I think it's also important for clinical trialists to inform basic scientists about what body of evidence they want to see before starting a trial, sort of like a venture capitalist. We're not going to invest our time and efforts in doing a trial of that drug until we see this array of information. This would help in selecting a compound to study—why rasagiline, why minocycline, why creatine, why coenzyme Q10? Well, we should have equivalent bits of information for all of them and choose the best one. The other reason is that the basic science helps to contextualize the clinical findings and strengthen a possible neuroprotective association.

DR. JENNER: Another thing we should be doing is measuring plasma levels of the drug, because it would be very useful to know the plasma level at which these effects are being achieved in order to try to plan doses for clinical trials.

DR. OLANOW: One problem is whether the plasma level in the rat or monkey means the same thing in a human.

DR. JENNER: I don't know about the story with neuroprotective drugs, but I can tell you we use plasma levels in the common marmoset to predict doses for PD patients and find that these are a very good guide to getting the dose right in the clinic.

References

1. Forno LS. Neuropathology of Parkinson's disease. J Neuropathol Exp Neurol 1996;55:259–272.
2. Braak H, Tredici KD, Rub U, de Vos RA, Jansen Steur EN, Braak E. Staging of brain pathology related to sporadic Parkinson's disease. Neurobiol Aging 2003;24:197–211.
3. Olanow CW, Watts RL, Koller WC. An algorithm (decision tree) for the management of Parkinson's disease (2001): treatment guidelines. Neurology 2001;56(suppl 5):1–88.
4. Olanow CW. The scientific basis for the current treatment of Parkinson's disease. Annu Rev Med 2004;55:41–60.
5. Ravina BM, Fagan SC, Hart RG, et al. Neuroprotective agents for clinical trials in Parkinson's disease: a systematic assessment. Neurology 2003;60:1234–1240.
6. Marsden CD, Olanow CW. Neuroprotection in Parkinson's disease: the causes of Parkinson's disease are being unravelled and rational neuroprotective therapy is close to reality. Ann Neurol 1998;44:189–196.
7. Boulton AA. Symptomatic and neuroprotective properties of the aliphatic propargylamines. Mech Ageing Dev 1999;111:201–209.
8. Schapira AHV. Etiology of Parkinson's disease. Neurology 2006; 66(Suppl 4):S10–S23.
9. Jenner P, Olanow CW. The pathogenesis of cell death in Parkinson's disease. Neurology 2006;66(Suppl 4):S24–S36.
10. McNaught K St.P, Jackson T, Jnobaptiste R, Kapustin A, Olanow CW. Proteasomal dysfunction in sporadic Parkinson's disease. Neurology 2006;66(Suppl 4):S37–S49.
11. Hirsch EC, Hunot S, Faucheux B, et al. Dopaminergic neurons degenerate by apoptosis in Parkinson's disease. Mov Disord 1999;14:383–385.
12. Agid Y. Aging, disease and nerve cell death. Bull Acad Natl Med 1995;179:1193–1203.
13. Mochizuki H, Goto K, Mori H, Mizuno Y. Histochemical detection of apoptosis in Parkinson's disease. J Neurol Sci 1996;131:120–123.
14. Tatton NA, Maclean-Fraser A, Tatton WG, Perl DF, Olanow CW. A fluorescent double-labeling method to detect and confirm apoptotic nuclei in Parkinson's Disease. Ann Neurol 1998;44(suppl 1):142–148.
15. Olanow CW, Tatton WG. Etiology and pathogenesis of Parkinson's disease. Annu Rev Neurosci 1999;22:123–144.
16. Tatton WG, Olanow CW. Apoptosis in neurodegenerative disease: the role of mitochondria. Biochim Biophys Acta 1999;1410:195–213.
17. Nair VD, Olanow CW, Sealfon SC. Activation of phosphoinositide 3-kinase by D2 receptor prevents apoptosis in dopaminergic cell lines. Biochem J 2003;373:25–32.
18. Nair VD, Yuen T, Olanow CW, Sealfon S. Early single cell bifurcation of pro- and anti-apoptotic states during oxidative stress. J Biol Chem 2004;25:27494–27501.
19. Susin SA, Zamzami N, Kroemer G. The cell biology of apoptosis: evidence for the implication of mitochondria. Apoptosis 1996;1:231–242.
20. Liu XS, Kim CN, Yang J, Jemmerson R, Wang XD. Induction of apoptotic program in cell-free extracts: requirement for dATP and cytochrome c. Cell 1996;86:147–157.
21. Susin SA, Zamzami N, Castedo M, et al. Bcl-2 inhibits the mitochondrial release of an apoptogenic protease. J. Exp Med 1996;184:1331–1341.
22. Wadia JS, Chalmers-Redman RME, Ju WJH, et al. Mitochondrial membrane potential and nuclear changes in apoptosis caused by trophic withdrawal: time course and modification by (-) deprenyl. J Neurosci 1996;18:932–947.
23. Jellinger KA. Cell death mechanisms in neurodegeneration. J Cell Mol Med 2001;5:1–17.
24. Anglade P, Vyas S, Javoy-Agid F, et al. Apoptosis and autophagie in nigral neurons of patients with Parkinson's disease. Histol Histopathol 1997;12:25–31.
25. Mogi M, Harada M, Kondo T, et al. BCL-2 protein is increased in the brain of Parkinson patients. Neurosci Lett 1996;215:137–139.
26. Tatton NA. Increased caspase 3 and Bax immunoreactivity accompany

Copyright © by AAN Enterprises, Inc. Unauthorized reproduction of this article is prohibited.

nuclear GAPDH translocation and neuronal apoptosis in Parkinson's disease. Exp Neurol 2000;166:29–43.
27. Cohen G, Pasik P, Cohen B, et al. Pargyline and deprenyl prevent the neurotoxicity of 1-methyl-4-phenyl-1,2,3,6-tetrahydropyridine (MPTP) in monkeys. Eur J Pharmacol 1985;106:209–210.
28. Heikkila RE, Manzino L, Duvoisin RC, Cabbat FS. Protection against the dopaminergic neurotoxicity of 1-methyl-4-phenyl-1,2,3,6-tetrahydropyridine (MPTP) by monoamine oxidase inhibitors. Nature 1984;311:467–469.
29. Olanow CW. Oxidation reactions in Parkinson's disease. Neurology 1990;40:32–37.
30. Olanow CW, Mytilineou C, Tatton WH. Status of selegiline as a neuroprotective agent in Parkinson's disease. Mov Disord 1998;13(suppl): 55–58.
31. Jenner P. Preclinical evidence for neuroprotection with monoamine oxidase-B inhibitors in Parkinson's disease. Neurology 2004;63(7 suppl 2):S13–22.
32. Mytilineou C, Radcliffe P, Leonardi EK, Werner P, Olanow CW. L-deprenyl protects mesencephalic dopamine neurons from glutamate receptor-mediated toxicity. J Neurochem 1997;68:33–39.
33. Tatton WG, Chalmers-Redman RME. Modulation of gene expression rather than monoamine oxidase inhibition: (-)deprenyl-related compounds in controlling neurodegeneration. Neurology 1996;47:171–183.
34. Mytilineou C, Radcliffe PM, Olanow CW. L-(-)-Desmethylselegiline, a metabolite of L-(-)-selegiline, protects mesencephalic dopamine neurons from excitotoxicity *in vitro*. J Neurochem 1997;68:434–436.
35. Mytilineou C, Leonardi EK, Radcliffe P, et al. Deprenyl and desmethylselegiline protect mesencephalic neurons from toxicity induced by glutathione depletion. J Pharmacol Exp Ther 1998;284:700–706.
36. Waldmeier PC, Spooren WP, Hengerer B. CGP 3466 protects dopaminergic neurons in lesion models of Parkinson's disease. Naunyn Schmiedebergs Arch Pharmacol 2000;362:526–537.
37. Matarredona ER, Meyer M, Seiler RW, Widmer HR. CGP 3466 increases survival of cultured fetal dopaminergic neurons. Restor Neurol Neurosci 2003;21:29–37.
38. Andringa G, van Oosten RV, Unger W, et al. Systemic administration of the propargylamine CGP 3466B prevents behavioural and morphological deficits in rats with 6-hydroxydopamine-induced lesions in the substantia nigra. Eur J Neurosci 2000;12:3033–3043.
39. Andringa G, Eshuis S, Perentes E. TCH346 prevents motor symptoms and loss of striatal FDOPA uptake in bilaterally MPTP-treated primates. Neurobiol Dis 2003;14:205–217.
40. Youdim MD, Gross A, Finberg JP. Rasagiline [*N*-propargyl-1*R*(+)-aminoindan], a selective and potent inhibitor of mitochondrial monoamine oxidase B. Br J Pharmacol 2001;132:500–506.
41. Parkinson Study Group. A randomized placebo-controlled trial of rasagiline in levodopa-treated patients with Parkinson disease and motor fluctuations: the PRESTO study. Arch Neurol 2005;62:241–248.
42. Rascol O, Brooks DJ, Melamed E, et al. Rasagiline as an adjunct to levodopa in patients with Parkinson's disease and motor fluctuations (LARGO, Lasting effect in Adjunct therapy with Rasagiline Given Once daily, study): a randomised, double-blind, parallel-group trial. Lancet. 2005;365:947–954.
43. Weinreb O, Amit T, Bar-Am O, Chillag-Talmor O, Youdim MB. Novel neuroprotective mechanism of action of rasagiline is associated with its propargyl moiety: interaction of Bcl-2 family members with PKC pathway. Ann NY Acad Sci 2005;1053:348–355.
44. Finberg JP, Takeshima T, Johnston JM, Commissiong JW. Increased survival of dopaminergic neurons by rasagiline, a monoamine oxidase-B inhibitor. Neuroreport 1998;9:703–707.
45. Goggi J, Theofilipoulos S, Riaz SS, Jauniaux E, Stern GM, Bradford HF. The neuronal survival effects of rasagiline and deprenyl on fetal human and rat ventral mesencephalic neurons in culture. Neuroreport 2000;11:3937–3941.
46. Naoi M, Maruyama W. Future of neuroprotection in Parkinson's disease. Parkinsonism Relat Disord 2001;8:139–145.
47. Bar Am O, Amit T, Youdim M. Contrasting neuroprotective and neurotoxic actions of respective metabolites of anti-Parkinson drugs rasagiline and selegiline. Neurosci Lett 2004;355:169–172.
48. Bonneh-Barkay D, Ziv N, Finberg JPM. Characterization of the neuroprotective activity of rasagiline in cerebellar granule cells. Neuropharmacology 2005;48:406–416.
49. Mandel S, Weinreb O, Amit T, Youdim MBH. Mechanism of neuroprotection of the anti-Parkinson drug rasagiline and its derivatives. Brain Res Brain Res Rev 2005;48:379–387.
50. Maruyama W, Akao Y, Youdim MB, Naoi M. Neurotoxins induce apoptosis in dopamine neurons: protection by N-propargylamine-1(R)- and (S)-aminoindan, rasagiline and TV1022. J Neural Transm Suppl 2000; 60:171–186.
51. Naoi M, Maruyama W, Youdim MBH, Yu P, Boulton AA. Antiapoptotic function of propargylamine inhibitors of type-B monoamine oxidase. Inflammopharmacology 2003:11:175–181.
52. Blandini F, Armentero MT, Fancellu R, Blaugrund E, Nappi G. Neuroprotective effects of rasagiline in a rodent model of Parkinson's disease. Exp Neurol 2004;187:455–459.
53. Huang W, Chen Y, Shohami E, Weinstock M. Neuroprotective effect of rasagiline, a selective a monoamine oxidase-B inhibitor, against closed head injury in the mouse. Eur J Pharmacol 1999;366:127–135.
54. Speiser Z, Mayk A, Eliash S, Cohen S. Studies with rasagiline, a MAO-B inhibitor, in experimental focal ischemia. J Neural Transm 1999;106:593–606.
55. Eliash S, Speiser Z, Cohen S. Rasagiline and its (S) enantiomer increase survival and prevent stroke in salt-loaded stroke-prone spontaneously hypertensive rats. J Neural Transm 2001;108:909–923.
56. Waibel S, Reuter A, Malessa S, Blaugrund E, Ludolph AC. Rasagiline alone and in combination with riluzole prolongs survival in an ALS mouse model. J Neurol 2004;251:1080–1084.
57. Tatton WG, Ju WY, Holland DP, Tai C, Kwan M. (-)-Deprenyl reduces PC12 cell apoptosis by inducing new protein synthesis. J Neurochem 1994;63:1572–1575.
58. Wadia JS, Chalmers-Redman RME, Ju WJH, Carlile GW, Phillips JL, Tatton WG. Mitochondrial membrane potential and nuclear changes in apoptosis caused by trophic withdrawal: time course and modification by (-) deprenyl. J Neurosci 1998;18:932–947.
59. Sawa A, Khan AA, Hester LD, Snyder SH. Glyderaldehyde-3-phosphate dehydrogenase: nuclear translocation participates in neuronal and non-neuronal cell death. Proc Natl Acad Sci USA 1997;94: 11669–11674.
60. Ishitani R, Kimura M, Sunaga K, Katsube N, Tanaka M, Chuang DM. An antisense oligonucleotide to glyderaldehyde-3-phosphate dehydrogenase blocks age-induced apoptosis of mature cerebro-cortical neurons in culture. J Pharmacol Exp Ther 1996;278:447–454.
61. Carlile GW, Chalmers-Redman RME, Tatton NA, Pong A, Borden KE, Tatton WG. Reduced apoptosis after nerve growth factor and serum withdrawal: conversion of tetrameric glyceraldehyde-3-phosphate dehydrogenase to a dimer. Mol Pharmacol 2000;57:2–12.
62. Maruyama W, Akao Y, Youdim MBH, Davis BA, Naoi M. Transfection-enforced Bcl-2 overexpression and an anti-Parkinson drug, rasagiline, prevent nuclear accumulation of glyceraldehyde-3-phosphate dehydrogenase induced by an endogenous dopaminergic neurotoxin, N-methyl(R)salsolinol. J Neurochem 2001;78:727–735.
63. Youdim MBH, Bar-Am O, Yogev-Falach, et al. Rasagiline: neurodegeneration, neuroprotection, and mitochondrial permeability transition. J Neurosci Res 2005;79:172–179.
64. Weinreb O, Bar-Am O, Amit T, Chillag-Talmor O, Youdim MBH. Neuroprotection via pro-survival protein kinase C isoforms associated with Bcl-2 family members. FASEB J 2004;18:1471–1473.
65. Akao Y, Maruyama W, Yi H, Shanoto-Nagai M, Youdim M, Naoi M. An anti-Parkinson's disease drug, *N*-propargyl-1(*R*)-aminoindan (rasagiline), enhances expression of anti-apoptotic Bcl-2 in human dopaminergic SH-SY5Y cells. Neurosci Lett 2002;326:105–108.
66. Akao Y, Maruyama W, Shimizu S, et al. Mitochondrial permeability transition mediates apoptosis induced by N-methyl(R)salsolinol, an endogenous neurotoxin, and is inhibited by Bcl-2 and rasagiline, N-propargyl-1(R)-aminoindan. J Neurochem 2002;82:913–923.
67. Youdim MBH, Amit T, Bar-Am O, Weinstock M, Yogev-Falach. Amyloid processing and signal transduction properties of antiParkinson-antiAlzheimer neuroprotective drugs rasagiline and TV3326. Ann NY Acad Sci 2003:993:378–386.
68. Maruyama W, Nitta A, Shamoto-Nagai M, et al. N-Propargyl-1 (R)-aminoindan, rasagiline, increases glial cell line-derived neurotrophic factor (GDNF) in neuroblastoma SH-SY5Y cells through activation of NF-kappaB transcription factor. Neurochem Int 2004;44:393–400.
69. Parkinson's Study Group. Effects of tocopherol and deprenyl on the progression of disability in early Parkinson's disease. N Engl J Med 1993;328:176–183.
70. Olanow CW, Calne D. Does selegiline monotherapy in Parkinson's Disease act by symptomatic or protective mechanisms? Neurology 1991;42:41–48.
71. Shoulson I, Oakes D, Fahn S, et al. The impact of sustained deprenyl (selegiline) in levodopa-treated Parkinson's disease: a randomized placebo-controlled extension. Ann Neurol 2002;51:604–612.
72. Olanow CW, Hauser RA, Gauger L, et al. The effect of deprenyl and levodopa on the progression of signs and symptoms in Parkinson's disease. Ann Neurol 1995;38:771–777.
73. The Parkinson Study Group. A controlled, randomised, delayed-start study of rasagiline in early Parkinson disease. Arch Neurol 2004;61: 561–566.
74. Youdim MB, Weinstock M. Molecular basis of neuroprotective activities of rasagiline and the anti-Alzheimer drug TV3326 [(N-propargyl-(3R)aminoindan-5-YL)-ethyl methyl carbamate]. Cell Mol Neurobiol 2001;21:555–573.
75. Tatton WG, Chalmers-Redman RM, Ju WJ, et al. Propargylamines induce antiapoptotic new protein synthesis in serum- and nerve growth factor (NGF)-withdrawn, NGF-differentiated PC-12 cells. J Pharmacol Exp Ther 2002;301:753–764.
76. Youdim MB, Amit T, Falach-Yogev M, Am OB, Maruyama W, Naoi M. The essentiality of Bcl-2, PKC and proteasome-ubiquitin complex activations in the neuroprotective-antiapoptotic action of the anti-Parkinson drug, rasagiline. Biochem Pharmacol 2003;66:1635–1641.

Copyright © by AAN Enterprises, Inc. Unauthorized reproduction of this article is prohibited.

A peptide based on the complementarity-determining region 1 of an autoantibody ameliorates lupus by up-regulating $CD4^+CD25^+$ cells and TGF-β

Amir Sharabi*, Heidy Zinger*, Maya Zborowsky*, Zev M. Sthoeger†, and Edna Mozes*‡

*Department of Immunology, Weizmann Institute of Science, Rehovot 76100, Israel; and †Department of Medicine B, Kaplan Hospital, Rehovot 76100, Israel

Communicated by Michael Sela, Weizmann Institute of Science, Rehovot, Israel, April 25, 2006 (received for review March 2, 2006)

Systemic lupus erythematosus is an autoimmune disease characterized by autoantibodies and systemic clinical manifestations. A peptide, designated hCDR1, based on the complementarity-determining region (CDR) 1 of an autoantibody, ameliorated the serological and clinical manifestations of lupus in both spontaneous and induced murine models of lupus. The objectives of the present study were to determine the mechanism(s) underlying the beneficial effects induced by hCDR1. Adoptive transfer of hCDR1-treated cells to systemic lupus erythematosus-afflicted $(NZB\times NZW)F_1$ female mice down-regulated all disease manifestations. hCDR1 treatment up-regulated (by 30–40%) $CD4^+CD25^+$ cells in association with $CD45RB^{low}$, cytotoxic T lymphocyte antigen 4, and Foxp3 expression. Depletion of the $CD25^+$ cells diminished significantly the therapeutic effects of hCDR1, whereas administration of the enriched $CD4^+CD25^+$ cell population was beneficial to the diseased mice. Amelioration of disease manifestations was associated with down-regulation of the pathogenic cytokines (e.g., IFN-γ and IL-10) and up-regulation of the immunosuppressive cytokine TGF-β, which substantially contributed to the suppressed autoreactivity. TGF-β was secreted by $CD4^+$ cells that were affected by hCDR1-induced immunoregulatory cells. The hCDR1-induced $CD4^+CD25^+$ cells suppressed autoreactive $CD4^+$ cells, resulting in reduced rates of activation-induced apoptosis. Thus, hCDR1 ameliorates lupus through the induction of $CD4^+CD25^+$ cells that suppress activation of the autoreactive cells and trigger the up-regulation of TGF-β.

cytokines | Foxp3 | immunomodulating peptide | regulatory T cells | systemic lupus erythematosus

Systemic lupus erythematosus (SLE) is an autoimmune disease characterized by the production of Ab against nuclear antigens and damage to multiple organs including kidneys, CNS, joints, and skin (1). Several strains of mice that spontaneously develop an SLE-like disease were reported, of which the $(NZB\times NZW)F_1$ female mice are the most widely used (2, 3). In addition, our laboratory has established a model of experimentally induced SLE in different susceptible strains of mice (4–6).

A peptide, designated hCDR1, based on the complementarity-determining region (CDR) 1 (7) of a human anti-DNA mAb, was shown to ameliorate the serological and clinical manifestations in both the spontaneous and induced models of SLE and to reduce the secretion and expression of the pathogenic cytokines IFN-γ, IL-10, IL-1β, and TNF-α (the latter in the induced model) while up-regulating the immunosuppressive cytokine TGF-β (8).

It has become increasingly evident that peripheral tolerance is mediated by suppressor T cells with a regulatory function (9, 10). The best-characterized are the $CD4^+CD25^+$ cells, which constitute 5–10% of the $CD4^+$ cells (11). $CD4^+CD25^+$ cells are naturally occurring, whereas adaptive regulatory $CD4^+CD25^-$ cells with suppressive capacity may be induced in the periphery in response to tolerogenic stimuli (11, 12). Nevertheless, several *in vitro* and *in vivo* studies indicated that $CD25^+$ cells might also be generated in the periphery (13–20). Recently it was reported that the number of $CD4^+CD25^+$ cells is diminished in patients with SLE as well as in $(NZB\times NZW)F_1$ female mice with established lupus (21–23), thus suggesting a role for these cells in regulating the disease.

In the present study we attempted the elucidation of the mechanism(s) underlying the ameliorating effects of treatment with hCDR1 on SLE manifestations. We demonstrated that the inhibitory effects of hCDR1 can be adoptively transferred to mice with established lupus by cells originating from young, healthy $(NZB\times NZW)F_1$ female mice that were treated with hCDR1. $CD4^+CD25^+$ cells were up-regulated in the hCDR1-treated cell population and were found to play a crucial role in ameliorating the serological and clinical parameters of SLE. This improvement was achieved by suppressing the activation of the $CD4^+$ cells and by triggering the up-regulated secretion of TGF-β, which was shown to play a key role in down-regulating SLE manifestations.

Results

Adoptive Transfer of Spleen Cells from Mice Treated with hCDR1 to $(NZB\times NZW)F_1$ Mice with Established Disease Is Beneficial. To determine whether the beneficial effects of hCDR1 can be transferred by cells of treated mice, we first performed adoptive transfer experiments. Thus, 2-mo-old, disease-free, $(NZB\times NZW)F_1$ mice were injected with hCDR1 s.c. (50 μg per mouse) for 3 alternating days. Two control groups of young mice were treated with the vehicle or with a scrambled (control) peptide. Splenocytes (20×10^6 per mouse) from the different groups were injected i.p. to respective groups of 8-mo-old $(NZB\times NZW)F_1$ mice with established disease. Disease severity of the recipient mice was similar in all groups as assessed by their anti-dsDNA autoantibody titers and proteinuria levels. Fig. 1 summarizes the clinical effects of the transferred cells on lupus-like manifestations at the end of a 2-wk follow-up and represents one experiment of five performed. As demonstrated, the production of dsDNA-specific autoantibodies as well as elevated proteinuria levels and the formation of glomerular immune complex deposits (ICD) were significantly reduced in SLE-afflicted mice that were injected with the hCDR1-treated spleen cells compared with recipients of cells treated with the scrambled peptide or with the vehicle.

Treatment with hCDR1 Results in an Up-Regulation of $CD4^+CD25^+$ Cells. Because $CD4^+CD25^+$ cells are the most characterized immunoregulatory T cells and because these cells were shown to be protective against autoimmune responses, we studied their possible role in the mode of action of hCDR1. For this purpose, three groups of 2-mo-old $(NZB\times NZW)F_1$ mice were treated with hCDR1, the vehicle, or a scrambled peptide. In all experiments the magnitude of $CD4^+CD25^+$ cells ranged between 3% and 9%. Treatment with

Conflict of interest statement: M.S. serves on the Board of Directors of Teva Pharmaceutical Industries, which supported this study.

Abbreviations: CDR, complementarity-determining region; CTLA-4, cytotoxic T lymphocyte antigen 4; FasL, Fas ligand; ICD, immune complex deposits; SLE, systemic lupus erythematosus; PE, phycoerythrin.

‡To whom correspondence should be addressed. E-mail: edna.mozes@weizmann.ac.il.

© 2006 by The National Academy of Sciences of the USA

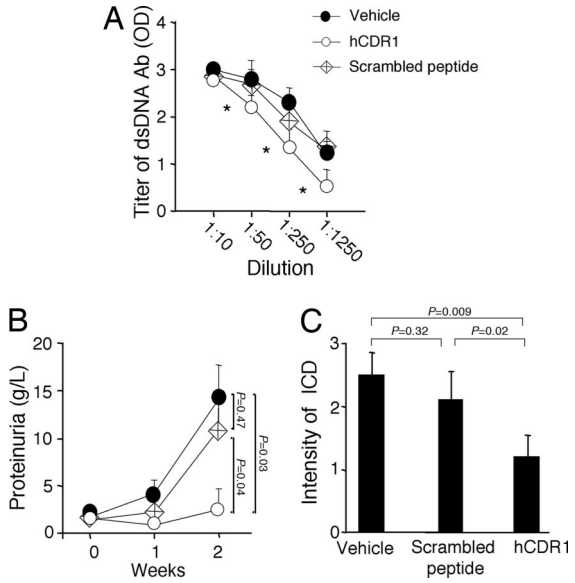

Fig. 1. Amelioration of murine lupus by adoptive transfer of cells from hCDR1-treated mice. Two-month-old (NZB×NZW)F_1 female mice were treated with three s.c. injections of hCDR1, the vehicle, or a scrambled control peptide. Splenocytes of the different groups were injected i.p. (20×10^6 per mouse) to respective groups of 8-mo-old (NZB×NZW)F_1 mice with established lupus. (*A*) Titers (mean OD ± SD) of dsDNA-specific Ab (*, $P < 0.05$) in individual sera of recipient mice ($n = 6$–10 mice per group) 2 wk after cell transfer. (*B*) Kinetics of proteinuria levels (mean grams per liter ± SD) in the recipient mice. (*C*) Mean intensity ± SD of ICD of kidney sections of all recipient mice per treatment group. Results represent one of five independent experiments.

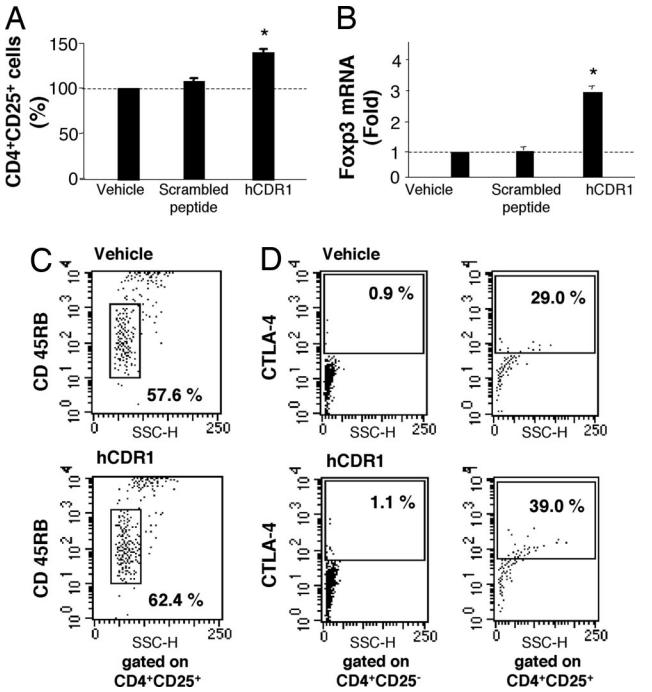

Fig. 2. Induction and characterization of $CD4^+CD25^+$ cells after treatment with hCDR1. Two-month-old (NZB×NZW)F_1 female mice ($n = 3$ mice per group) were treated with three s.c. injections of hCDR1, the vehicle, or a scrambled peptide. Spleen cells were then pooled and examined for cell-surface and intracellular markers by flow cytometry. (*A*) Percentage of $CD4^+CD25^+$ cells compared with that of vehicle-treated mice that was considered as 100%. Shown are results of five experiments (mean percentage ± SD). (*B*) Foxp3 mRNA expression. Shown are mean ± SD values of five independent experiments. Results were normalized to β-actin expression and are presented relative to the vehicle-treated mice (represented by the dashed line). (*C*) Expression of $CD45RB^{low}$ in $CD4^+CD25^+$ cells. (*D*) Expression of CTLA-4 on $CD4^+CD25^-$-gated and $CD4^+CD25^+$-gated cells. *, $P < 0.05$.

hCDR1, unlike treatment with the scrambled peptide, up-regulated these cells by 1–2%. The latter was associated with a 1.5- to 2-fold increase in mean fluorescence intensity. Fig. 2*A*, which represents the mean values of five experiments, indicates a 30–40% up-regulation of $CD4^+CD25^+$ cells compared with the vehicle-treated population. The latter was also accompanied by a 3-fold increase in the mRNA expression of Foxp3 (Fig. 2*B*), which indicated the development of $CD4^+CD25^+$ regulatory T cells (24, 25). The expression of regulatory characteristic markers [$CD45RB^{low}$ and cytotoxic T lymphocyte antigen 4 (CTLA-4)] on $CD4^+$ cells was higher as a result of hCDR1 treatment. Triple staining of the $CD4^+CD25^+$ cell population with the latter two markers indicated that their up-regulation was associated with an increase of $CD4^+CD25^+$ cells (Fig. 2 *C* and *D*). As shown in Fig. 2*D*, CTLA-4 was expressed almost exclusively on $CD4^+CD25^+$ cells, and its levels were higher in hCDR1-induced $CD4^+CD25^+$ cells. Thus, it appears that treatment with hCDR1 up-regulates the immunoregulatory $CD4^+CD25^+$ cells.

hCDR1-Induced $CD4^+CD25^+$ Cells Play an Important Role in Ameliorating Lupus-Like Manifestations. Because treatment with hCDR1 resulted in an up-regulation of $CD4^+CD25^+$ cells, it was of major importance to determine whether the hCDR1-induced $CD4^+CD25^+$ cells play a role in ameliorating lupus manifestations. To this end, we performed experiments for depletion and enrichment of $CD25^+$ cells that were further transferred into SLE-afflicted recipient mice. Splenocytes of hCDR1-treated mice, as well as the latter, depleted of or enriched with $CD25^+$ cells, were transferred into old SLE-afflicted (NZB×NZW)F_1 mice. Splenocytes of five control groups of donors were used as well (Fig. 3): untreated mice, scrambled peptide-treated mice, vehicle-treated mice, vehicle-treated mice depleted of $CD25^+$ cells, and vehicle-treated mice enriched with $CD25^+$ cells. Fig. 3*A*, which represents the results of six independent experiments, demonstrates that the up-regulated $CD4^+CD25^+$ cells of the hCDR1-treated mice (lane f) or enrichment of $CD4^+CD25^+$ cells of the latter origin (lane h) were accompanied by 3- and 8-fold increased Foxp3 mRNA expression, respectively, compared with the vehicle-treated cells (Fig. 3*A*, lane c). Foxp3 mRNA was also up-regulated in enriched $CD4^+CD25^+$ cells of the vehicle-treated mice (Fig. 3*A*, lane e), although to a lesser extent.

The above eight cell populations were injected (20×10^6 cells per mouse) into respective groups of 8-mo-old (NZB×NZW)F_1 mice with established manifestations of lupus. A representative experiment shows a significant decrease in the dsDNA Ab as well as down-regulated secretion of IFN-γ and IL-10 in the groups of old mice that were injected with hCDR1-treated splenocytes, or the latter enriched with $CD4^+CD25^+$ cells (Fig. 3 *B* and *C*, lanes f and h). Depletion of $CD4^+CD25^+$ cells abrogated the inhibitory effects of hCDR1 (Fig. 3 *B* and *C*, lane g). Administration of $CD4^+CD25^+$-enriched cells of vehicle-treated mice (Fig. 3*A*, lane e) did not diminish the levels of dsDNA-specific Ab (Fig. 3*B*, lane e) or the secretion of the pathogenic cytokines (Fig. 3*C*, lane e). In addition, depletion of the $CD4^+CD25^+$ cells from the vehicle-treated cells (Fig. 3*A*, lane d) did not substantially modulate autoantibody titers or the levels of secreted cytokines (Fig. 3 *B* and *C*, lane d versus lanes a–c). The kidney function of the diseased mice was similarly affected. SLE-afflicted mice that were administered with cells of the three control groups (Fig. 3 *D* and *E*, groups a–c) had high levels of proteinuria and glomerular ICD. In contrast, adoptive transfer of hCDR1-treated cells, as well as of hCDR1-treated cells enriched with $CD4^+CD25^+$ cells, significantly lowered the proteinuria levels

IMMUNOLOGY

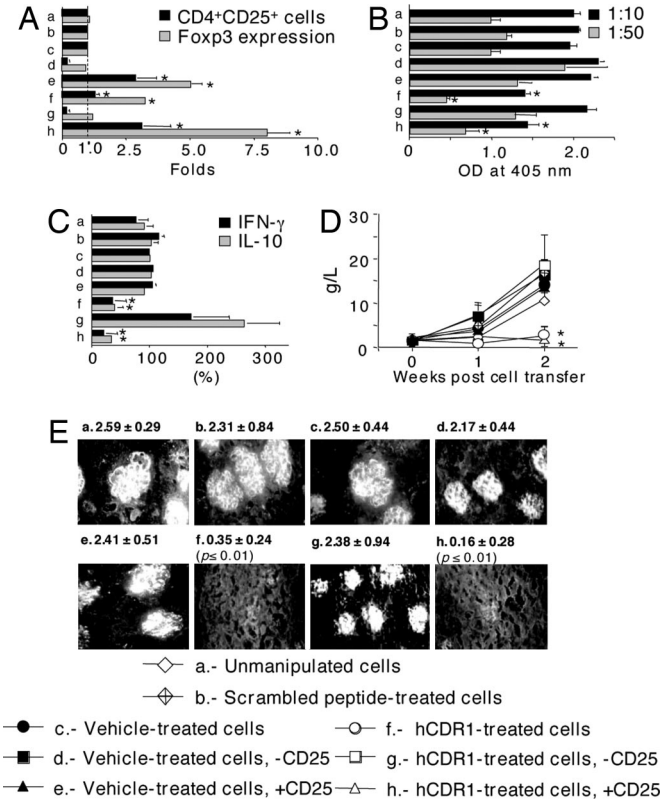

Fig. 3. Ameliorating effects of hCDR1-induced $CD4^+CD25^+$ cells. Cells of hCDR1- or vehicle-treated mice were either unmanipulated or depleted or enriched for CD25 cells and then transferred to SLE-afflicted (NZB×NZW)F_1 mice. (*A*) Donor $CD4^+CD25^+$ cells and Foxp3 mRNA expression. Shown are mean ± SD values of six independent experiments. Results are presented relative to the vehicle-treated mice (represented by the dashed line). (*B*) Titers (mean OD ± SD) of dsDNA-specific Ab in sera (diluted 1:10 and 1:50) obtained from recipient mice of each of the eight groups described ($n = 5$–8 mice per group) 2 wk after the cell transfer. Results represent one of six independent experiments performed. (*C*) Constitutive secretion of IFN-γ and IL-10. Results are relative to levels measured in the supernatants of splenocytes from mice that were injected with the vehicle-treated cells (100% = 210 ± 23 pg/ml for IFN-γ and 415 ± 32 pg/ml for IL-10). Shown are mean values ± SD of four independent experiments. (*D*) Kinetics of proteinuria levels (mean grams per liter ± SD) in the recipient mice. Results represent one of six independent experiments. (*E*) Immunohistology of kidney sections of representative mice of each group are demonstrated. (Magnification: ×400.) Also shown are the mean intensity values ± SD of kidney sections of all mice per treatment group. *, $P \leq 0.05$.

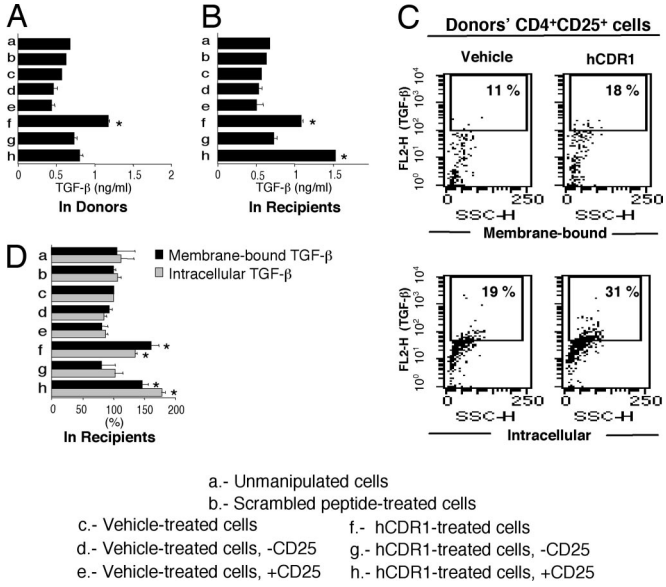

Fig. 4. The status of TGF-β in $CD4^+CD25^+$ and in affected $CD4^+$ cells. Levels of secreted TGF-β were determined in the supernatants of splenocytes of the donor treatment groups (*A*, $n = 5$ mice per group) and the different groups (*B*, $n = 5$–8 mice per group) of recipient mice. (*C*) Staining of donor splenocytes of hCDR1- and vehicle-treated mice for the presence of membrane-bound and intracellular TGF-β in $CD4^+CD25^+$-gated cells. Dot plots are representative of one of two experiments performed. (*D*) Splenocytes of the different groups of recipient mice were stained for membrane-bound and intracellular TGF-β in $CD4^+$ cells. Percentages of stained cells were compared with those found on cells of recipients of vehicle-treated cells (considered as 100% and determined to be 9.5 ± 0.1% for membrane-bound TGF-β and 40.0 ± 4.0% for intracellular TGF-β). *, $P \leq 0.05$.

and the intensity of glomerular ICD (Fig. 3 *D* and *E*, groups f and h). The efficacy of the enriched hCDR1-induced $CD4^+CD25^+$ cells was demonstrated in dose-dependent experiments. Thus, as low as 10^6 and 10^5 enriched $CD4^+CD25^+$ cells down-regulated proteinuria to levels observed after transfer of 20 and 10 million splenocytes of hCDR1-treated cells, respectively. Furthermore, the latter was confirmed by the significant reduction of ICD determined in the kidneys of recipients of 10^6 and 10^5 enriched $CD4^+CD25^+$ cells. No significant difference could be observed in the sustained high levels of proteinuria and ICD after the transfer of either enriched or depleted $CD4^+CD25^+$ cells originating from vehicle-treated cells (Fig. 3 *D* and *E*, groups d and e).

hCDR1-Induced $CD4^+CD25^+$ Cells Promote the Secretion of TGF-β by Recipient-Derived $CD4^+$ Cells. It was of interest to find out whether the up-regulated TGF-β in hCDR1-treated mice could be related to the hCDR1-induced $CD4^+CD25^+$ cells. Fig. 4*A* shows the levels of TGF-β in the supernatants of splenocytes of the donor (disease-free) mice. It can be seen that splenocytes of donor mice, which were treated with hCDR1, secreted elevated levels of TGF-β, as compared with those of control groups. Depletion of $CD4^+CD25^+$ cells led to diminished secretion of the latter; however, enrichment with $CD4^+CD25^+$ cells did not result in a significant increase of this cytokine. Nevertheless, when the treated cells were injected into old SLE-afflicted mice, splenocytes of the recipients of the enriched (hCDR1-treated) $CD4^+CD25^+$ cell population secreted the highest levels of TGF-β (Fig. 4*B*). Hence, it appears that $CD4^+CD25^+$ cells originating from hCDR1-treated mice affect another subset or subsets of cells to secrete TGF-β rather than secreting elevated levels of this cytokine by themselves. Nevertheless, the hCDR1-induced $CD4^+CD25^+$ cells had a significantly ($P \leq 0.05$) higher expression of both membrane-bound and intracellular TGF-β as compared with the expression by $CD4^+CD25^+$ cells of vehicle-treated mice (Fig. 4*C*).

To find the cell source of the elevated TGF-β levels, we determined the expression of membrane-bound and intracellular TGF-β in potential producers. In comparison to the control groups, significantly higher levels of expression of both membrane-bound and intracellular TGF-β could be observed mainly in $CD4^+$ cells from recipients of hCDR1-treated cells and from recipients of hCDR1-treated cells that were enriched with $CD4^+CD25^+$ cells (Fig. 4*D*). The expression of TGF-β in macrophages and in apoptotic cells was not affected in the eight groups of the recipient mice described. Because $CD4^+$ cells from the recipients of hCDR1-treated cells or of the enriched hCDR1-induced $CD4^+CD25^+$ cells expressed high levels of TGF-β, it is likely that these $CD4^+$ cells also secreted TGF-β.

Suppression by hCDR1-Induced $CD4^+CD25^+$ Cells Is Mediated by Means of TGF-β. To further assess the suppressive efficacy of hCDR1-induced $CD4^+CD25^+$ immunoregulatory cells, we used enriched $CD4^+CD25^+$cells from either hCDR1- or vehicle-treated

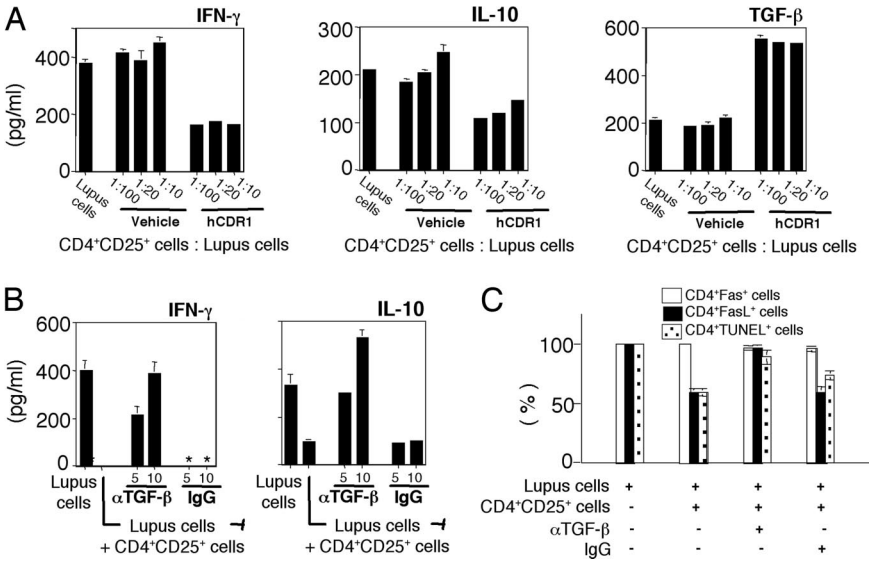

Fig. 5. Suppression by hCDR1-induced $CD4^+CD25^+$ cells is mediated by means of TGF-β. Triplicate of spleen cells (10^5 cells, designated lupus cells) of 8-mo-old $(NZB\times NZW)F_1$ female mice ($n = 5$) were cocultured with various numbers of hCDR1-induced or vehicle-induced $CD4^+CD25^+$ cells. (*A*) Lupus cells (10^5 cells) were cultured alone or together with various numbers of hCDR1-induced or vehicle-induced $CD4^+CD25^+$ cells for 36 h. Supernatants were collected and assessed for secreted cytokines. Lupus cells (10^5 cells) were cocultured with hCDR1-induced $CD4^+CD25^+$ cells (1,000 cells) for 36 h in the presence of anti-TGF-β neutralizing mAb (5 or 10 μg/ml) or its IgG isotype control. (*B*) Effect on cytokine secretion. (*C*) Effect on activation-induced apoptosis.

mice. Each of the two groups of enriched $CD4^+CD25^+$ cells was coincubated (in three different ratios) with splenocytes (designated "lupus cells") of 8-mo-old $(NZB\times NZW)F_1$ mice with established lupus. Fig. 5*A* shows that coincubation with hCDR1-induced $CD4^+CD25^+$ cells resulted in a significant decrease of the pathogenic cytokines IFN-γ and IL-10, whereas the levels of the immunosuppressive cytokine TGF-β were elevated (Fig. 5*A*). This effect was achieved with all three concentrations of the hCDR1-induced $CD4^+CD25^+$ cells, the lowest being 1:100. Coincubation with vehicle-induced $CD4^+CD25^+$ cells had no effect on the cytokine profile.

To determine the role of TGF-β in the inhibitory effect of the hCDR1-induced $CD4^+CD25^+$ cells, lupus cells (10^5 cells) were coincubated with 10^3 hCDR1-induced $CD4^+CD25^+$ cells for 36 h with or without anti-TGF-β neutralizing mAb (5 or 10 μg/ml) and its IgG isotype control. Fig. 5*B* demonstrates that both concentrations of anti-TGF-β mAb abrogated the ability of the hCDR1-induced $CD4^+CD25^+$ cells to down-regulate IFN-γ and IL-10, whereas the isotype control used did not interfere with the activity of hCDR1-induced $CD4^+CD25^+$ cells. Furthermore, it can be seen in Fig. 5*C* that suppression of $CD4^+$ lupus cells by the hCDR1-induced $CD4^+CD25^+$ cells, as indicated by a significant ($P < 0.0001$) reduction of Fas ligand (FasL) and apoptosis (determined by TUNEL), was also mediated by TGF-β.

hCDR1-Induced $CD4^+CD25^+$ Cells Suppress the Activation of Lupus $CD4^+$ Cells *in Vivo*. We further measured the expression of Fas and FasL (26) and the rate of apoptosis and in $CD4^+$ cells of the different groups of recipient mice to confirm the effect of $CD4^+CD25^+$ cells on activation-induced apoptosis of the $CD4^+$ cells of SLE-afflicted mice. Administration of hCDR1-treated cells or the latter enriched with $CD4^+CD25^+$ cells significantly down-regulated the rate of TUNEL[+] (Fig. 6*A*) and FasL expression (Fig. 6*B*) on $CD4^+$ cells in comparison with the control groups. In contrast, when lupus-afflicted mice were injected with hCDR1-treated cells that were depleted of $CD4^+CD25^+$ cells, the rate of apoptotic $CD4^+$ cells and FasL-expressing cells was remarkably high (Fig. 6). None of these changes occurred in response to depletion or enrichment with the $CD4^+CD25^+$ cells of the vehicle-treated mice. These results were reproduced in three independent experiments.

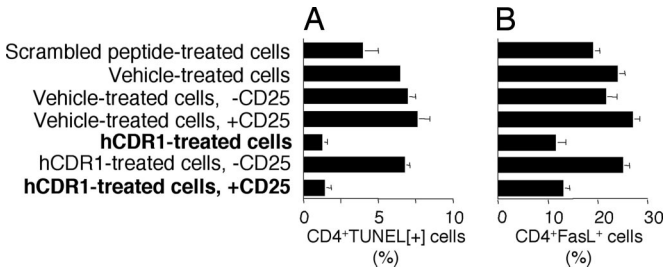

Fig. 6. hCDR1-induced $CD4^+CD25^+$ cells reduce activation-induced cell death of $CD4^+$ cells. (*A*) Two weeks after the transfer of the various cell populations, the mice ($n = 5$–8 mice per group) were killed, and $CD4^+$ spleen-derived cells were stained for apoptosis by using the TUNEL technique. (*B*) Cells from each group were double-stained for CD4 and FasL. Shown are representative results of one experiment of three performed.

Discussion

The main findings of this study are that amelioration of the clinical and serological manifestations of SLE after treatment with hCDR1 is, at least partially, the consequence of the induction of immunoregulatory $CD4^+CD25^+$ cells. These cells were found to suppress $CD4^+$ cells not through their deletion by apoptosis but rather by down-regulating their state of activation and by up-regulating the secretion of the immunosuppressive cytokine TGF-β by $CD4^+$ cells of the recipient mice. This cascade of events is triggered directly by the hCDR1-induced $CD4^+CD25^+$ cells. Thus, this study is an *in vivo* demonstration of the induction of $CD4^+CD25^+$ immunoregulatory cells by a CDR-based peptide that ameliorates lupus manifestations in association with cytokine immunomodulation.

We showed here that cells of hCDR1-treated mice could actively transfer the inhibitory capacity of hCDR1 into mice with established lupus. The latter suggested the presence of a subpopulation of regulatory cells with suppressive activity in the splenocytes of hCDR1-injected mice. Several types of regulatory cells of the immune system are recognized. The $CD4^+CD25^+$ regulatory T cells are the best characterized and are known to be protective against the development of autoimmunity. We therefore studied the mechanistic role of $CD4^+CD25^+$ regulatory T cells regarding the ameliorative effects of hCDR1 on SLE. Indeed, treatment with hCDR1 resulted in the up-regulation of $CD4^+CD25^+CD45RB^{low}$ cells (Figs. 2 and 3*A*) with regulatory characteristics such as CTLA-4 and TGF-β and of Foxp3 mRNA, which is selectively expressed in these cells (24, 25). In light of the fact that treatment with the scrambled control peptide, as well as with the vehicle, had no effect on the magnitude of the $CD4^+CD25^+$ cell population, and because a 3-fold-higher expression of Foxp3 mRNA was determined exclusively in the hCDR1-treated cells, our data suggest that

IMMUNOLOGY

treatment with hCDR1 results in the peripheral generation of $CD4^+CD25^+$ immunoregulatory cells.

The relevance and importance of hCDR1-induced $CD4^+CD25^+$ cells were demonstrated in *in vitro* and *in vivo* settings. Thus, the clinical amelioration combined with the reduction of activated $CD4^+$ lupus cells and of the pathogenic cytokines IFN-γ and IL-10 occurred only in the presence of hCDR1-induced $CD4^+CD25^+$ cells. This effect was also demonstrated after a 10-wk direct treatment with hCDR1 of SLE-afflicted $(NZB\times NZW)F_1$ mice (A.S. and E.M., unpublished data). In agreement, previous reports have shown the induction of $CD4^+CD25^+$ cells with regulatory functions in other systems, including models of lupus (13–20). The hCDR1-induced $CD4^+CD25^+$ cells reported in the present study are highly effective because as little as 10^5 enriched cells were still protective after transfer to SLE-afflicted recipient mice.

Antigenic specificity of $CD4^+CD25^+$ regulatory cells was reported under both autoimmune and infectious conditions (19, 20, 27–29). The specificity of hCDR1-induced $CD4^+CD25^+$ cells is presumed for several reasons. First, injection of $CD4^+CD25^+$ cells of either naïve (healthy) donors or of mice treated with a control peptide into mice with established lupus had no beneficial effects. Furthermore, treatment of SLE-afflicted mice with an enriched $CD4^+CD25^+$ cell population from vehicle-treated donors neither improved the clinical condition of the mice nor modulated their pattern of cytokine secretion or state of cellular activation. These results rule out the possibility of a quantitative replenishment in the number of regulatory cells as an explanation for lupus amelioration. In contrast, a small number of hCDR1-induced $CD4^+CD25^+$ cells effectively suppressed the clinical manifestations and the secretion of pathogenic cytokines. Furthermore, whereas adoptive transfer of cells from vehicle-treated donors that were depleted of $CD25^+$ cells did not affect the severity of the disease, the transfer of hCDR1-treated cells that were depleted of $CD4^+CD25^+$ cells resulted in a more severe kidney disease in the recipient mice, associated with an up-regulated secretion of IFN-γ and IL-10 (Fig. 3 *C* and *D*). Moreover, in another model of experimental SLE, inhibition of the specific *in vitro* proliferation of cells from mice immunized with an anti-DNA mAb that bears an idiotype designated 16/6Id (4–6) could be achieved only by the transfer of splenocytes from mice that were treated with hCDR1, but not with a dual altered peptide ligand (18), which was reported to down-regulate myasthenogenic manifestations (H.Z. and E.M., unpublished data). Collectively, these data indicate that the hCDR1-induced $CD4^+CD25^+$ cells have unique qualitative characteristics that enable them to specifically suppress lupus-associated manifestations.

Treatment with hCDR1 has always been associated with an up-regulation of the secretion and expression of the immunosuppressive cytokine TGF-β (8). The latter correlated with the amelioration of lupus manifestations. Here we have shown that the secretion of TGF-β depends on the presence of hCDR1-induced $CD4^+CD25^+$ cells (Fig. 4 *A* and *B*). Although $CD4^+CD25^+$ cells were reported in some studies to function independent of TGF-β (28, 29), others showed that immune suppression *in vivo* depended on the presence of TGF-β (30–33). Furthermore, Thompson and Powrie (34) reported that *in vivo* suppression by $CD4^+CD25^+$ cells from TGF-$\beta^{-/-}$ donor mice could still be achieved when TGF-β, clearly derived from other cell types, was present. Indeed, only in the presence of other cell types, shown here to be $CD4^+$ cells of the recipient mice (Fig. 4*D*), were the levels of TGF-β elevated, as demonstrated after the transfer of either hCDR1-treated cells or the latter enriched with $CD4^+CD25^+$ cells. Neutralization of TGF-β abrogated the effects of hCDR1-induced $CD4^+CD25^+$ cells on the secretion of cytokines and activation-induced apoptosis (Fig. 5 *C* and *D*), thus supporting a central role for TGF-β in mediating the suppression.

It is possible that the hCDR1-induced $CD4^+CD25^+$ cells, by means of membrane-bound or soluble forms of TGF-β and/or by means of engagement of CTLA-4, may raise the threshold for TCR activation, reported to be lower in lupus cells (35). We therefore suggest that hCDR1-induced $CD4^+CD25^+$ cells cause the "silencing" of $CD4^+$ cells as indicated by reduced expression of FasL, consequently with a reduced rate of activation-induced apoptosis (26), rather than causing the depletion of the latter by means of apoptosis. Taken together, our results indicate a key role for $CD4^+CD25^+$ cells in the mechanism of action of hCDR1, although other cell types and mechanisms (36, 37) may be involved as well. Based on the present report, we suggest that inhibition by the hCDR1-induced $CD4^+CD25^+$ cells is mediated through TGF-β, which is secreted by other T cells that are affected by the immunoregulatory cells. The up-regulated secretion of TGF-β and the down-regulation of activated $CD4^+$ cells are associated with a decrease in the pathogenic cytokines IFN-γ and IL-10. Eventually, the suppression of $CD4^+$ lupus cells by the hCDR1-induced $CD4^+CD25^+$ cells enables the clinical improvement of the SLE-afflicted mice.

Materials and Methods

Mice. Female $(NZB\times NZW)F_1$ mice were purchased from The Jackson Laboratory. All experiments were approved by the Animal Care and Use Committee of the Weizmann Institute of Science.

Synthetic Peptides. A peptide, GYYWSWIRQPPGKGEEWIG, designated hCDR1, based on the CDR1 of the human anti-DNA mAb that bears a major idiotype, 16/6Id (7, 38), was synthesized (solid-phase synthesis by F-moc chemistry) by Polypeptide Laboratories (Torrance, CA) and used in this study. A peptide containing the same amino acids as hCDR1, with a scrambled order (scrambled peptide), SKGIPQYGGWPWEGWRYEI, was used as a control. hCDR1 (Edratide) is currently under clinical development for the treatment of human SLE by Teva Pharmaceutical Industries (Netanya, Israel).

Treatment of Mice with hCDR1. Two-month-old $(NZB\times NZW)F_1$ female mice were treated with s.c. injections of hCDR1 (50 μg per mouse) a total of three times on alternating days. Control groups of young mice were treated with the scrambled peptide or with the vehicle alone [Captisol, sulfobutylether β-cyclodextrin, a solvent designed by CyDex (Lenexa, KS) to enhance the solubility and stability of drugs].

Depletion and Enrichment of $CD4^+CD25^+$ Cells. Depletion and enrichment of $CD25^+$ cells were performed by using the StemSep system (StemCell Technologies). Briefly, splenocytes (100×10^6) of mice treated with hCDR1 (50 μg per mouse) were incubated with anti-CD25-biotinylated mAb (clone 7D4; Southern Biotechnology Associates). The cells were further incubated with an anti-biotin tetrameric complex (StemCell Technologies) followed by incubation with magnetic beads (StemCell Technologies). The cells that were eluted from a column (StemCell Technologies), which was placed within a magnet stand, were collected. Depletion rate of $CD25^+$ cells was >90%. Next, the column was removed from the magnet stand and washed, and the eluted cells (≈80% $CD4^+CD25^+$ cells) were collected.

Measurement of dsDNA-Specific Ab. Briefly, Maxisorb microtiter plates (Nunc) were coated with polyL-lysine (5 μg/ml) (Sigma) followed by coating with λ phage dsDNA (5 μg/ml) (Boehringer Mannheim). After the plates were blocked, the sera were added. Goat anti-mouse IgG (γ-chain-specific) conjugated to horseradish peroxidase (Jackson ImmunoResearch) was added. Plates were incubated with the substrate 2,2′-azino-bis(3-ethylbenzthiazoline-6-sulfonic acid) (Sigma) and read at 405 nm with an ELISA reader.

Proteinuria. Proteinuria was measured by a standard semiquantitative test by using an Albustix kit (Bayer).

Immunohistology. For the detection of ICD, frozen cryostat kidney sections (6 μm) were incubated with FITC-conjugated goat anti-mouse IgG (γ-chain-specific) (Jackson ImmunoResearch). Staining was visualized by using a fluorescence microscope. The intensity of the ICDs was graded as follows: 0, no ICDs; 1, low intensity; 2, moderate intensity; 3, high intensity of immune complexes. ICD analysis was performed by two persons blinded to whether mice belong to control or experimental groups.

Ab and Reagents. The following antibodies were used in the study: anti-CD4-phycoerythrin (PE) (clone GK1.5), anti-CD4-allophycocyanin (clone L3T4), anti-CD25-FITC (clone 7D4), anti-CTLA-4-PE (clone 1B8), anti-CD8-FITC (clone 53-6.7), and their matched isotype controls (obtained from Southern Biotechnology Associates). Anti-CD45RB-PE (clone 16A), anti-Fas-PE (clone Jo2), anti-FasL-PE (clone MFL3), and their matched isotype controls were purchased from Pharmingen. Anti-TGF-β1-PE Ab (clone TB21) was obtained from IQ Products (Groningen, The Netherlands). Biotinylated chicken anti-TGF-β1 and anti-TGF-β1, -β2, and -β3 neutralizing mAb (clone 1D11) and its isotype control were purchased from R & D Systems. Streptavidin labeled with PE or FITC and anti-F 4/80 Ab (clone CI:A3-1) with its matched isotype control were obtained from eBioscience (San Diego). Fixation and permeabilization solutions for intracellular staining were obtained from Serotec.

Cytokine Detection by ELISA. Splenocytes (5×10^6 cells per well) were incubated in enriched medium for 48 h and 72 h. IFN-γ and IL-10 were determined in the supernatants by ELISA using OptEIA sets (Pharmingen) according to the manufacturer's instructions. For the detection of TGF-β, the plates were coated with a recombinant human TGF-β sRII/Fc chimera (R & D Systems). Supernatants were added after activation of latent TGF-β1 to immunoreactive TGF-β1, a biotinylated anti-human TGF-β1 Ab was added thereafter, and the assay was developed according to the manufacturer's instructions (R & D Systems).

Flow Cytometry. Briefly, splenocytes (1×10^6 cells) were incubated with the relevant Ab and analyzed by FACS. For intracellular staining, the cells were incubated with a fixation solution, washed, and resuspended in permeabilization solution (Serotec).

TUNEL Assay. Apoptosis, as demonstrated by fragmented DNA, was determined by using the *In Situ* Death Detection Kit (Roche, Indianapolis) based on TUNEL technology, according to the protocol supplied by the manufacturer. Cells were analyzed by FACS.

***In Vitro* Assays.** Enriched ($\approx$80%) $CD4^+CD25^+$ cells obtained from mice treated with either hCDR1 or the vehicle were coincubated (in different ratios) for 18–48 h with splenocytes (10^5 cells) taken from 8-mo-old (NZB$\times$NZW)F_1 female mice with established lupus.

Real-Time RT-PCR. The mRNA levels of Foxp3 were analyzed by real-time RT-PCR by using LightCycler (Roche, Mannheim, Germany). Total RNA was isolated from splenocytes, and then RNA was reverse-transcribed to prepare cDNA by using Moloney murine leukemia virus reverse transcriptase (Promega). The resulting cDNA was subjected to real-time PCR according to the manufacturer's instructions. Briefly, a 20-μl reaction volume contained 3 mM $MgCl_2$, LightCycler HotStart DNA SYBR Green I mix (Roche), specific primer pairs, and 5 μl of cDNA. PCR conditions were as follows: 10 min at 95°C followed by 35–50 cycles of 15 s at 95°C, 15 s at 60°C, and 15 s at 72°C. Primer sequences (forward and reverse, respectively) were used as follows: Foxp3, 5′-taccacaatatgcgaccc-3′ and 5′-ctcaaattcatctacggtcc-3′; β-actin, 5′-gacgttgacatccgtaaag-3′. The relative expression of Foxp3 normalized to β-actin levels was determined.

Statistical Analysis. Mann–Whitney and unpaired Student's *t* tests were used for evaluating the significant differences between treated and untreated groups. Values of $P \leq 0.05$ were considered significant.

This work was supported by Teva Pharmaceutical Industries.

1. Hahn, B. H. (1993) in *Dubis' Lupus Erythomatosus*, eds. Wallace, D. J. & Hahn, B. H. (Williams & Wilkins, Philadelphia), pp. 69–76.
2. Theofilopoulos, A. N. (1992) in *Systemic Lupus Erythematosus*, ed. Lahita R. G. (Churchill Livingston, New York), pp. 121–194.
3. Morel, L. & Wakeland, E. K. (1998) *Curr. Opin. Immunol.* **10,** 718–725.
4. Mendelovic, S., Brocke, S., Fricke, H., Shoenfeld, Y., Bakimer, R. & Mozes, E. (1990) *Immunology* **69,** 228–236.
5. Mendlovic, S., Brocke, S., Shoenfeld, Y., Ben Bassat, M., Meshorer, A., Bakimer, R. & Mozes, E. (1988) *Proc. Natl. Acad. Sci. USA* **85,** 2260–2264.
6. Waisman, A., Mendlovic, S., Ruiz, J. P., Zinger, H., Meshorer, A. & Mozes, E. (1993) *Int. Immunol.* **5,** 1293–1300.
7. Waisman, A., Shoenfeld, Y., Blank, M., Ruiz P. J. & Mozes, E. (1995) *Int. Immunol.* **7,** 689–696.
8. Luger, D., Dayan, M., Zinger, H., Liu, J. P. & Mozes, E. (2004) *J. Clin. Immunol.* **24,** 579–590.
9. Sakaguchi, S. (2000) *Cell* **101,** 455–458.
10. Shevach, E. M. (2000) *Annu. Rev. Immunol.* **18,** 423–449.
11. Sakaguchi, S., Sakaguchi, N., Asano, M., Itoh, M. & Toda, M. (1995) *J. Immunol.* **155,** 1151–1164.
12. Groux, H., O'Garra, A., Bigler, M., Rouleau, M., Antonenko, S., de Vries, J. E. & Roncarolo, M. G. (1997) *Nature* **389,** 737–742.
13. Asano, M., Toda, M., Sakaguchi, N. & Sakaguchi, S. (1996) *J. Exp. Med.* **184,** 387–396.
14. Jonuleit, H., Schmitt, E., Schuler, G., Knop, J. & Enk, A. H. (2000) *J. Exp. Med.* **192,** 1213–1222.
15. Thorstenson, K. M. & Khoruts, A. (2001) *J. Immunol.* **167,** 188–195.
16. Zhang, X., Izikson, L., Liu, L. & Weiner, H. L. (2001) *J. Immunol.* **167,** 4245–4253.
17. Gregori, S., Casorati, M., Amuchastegui, S., Smiroldo, S., Davalli, A. M. & Adorini, L. (2001) *J. Immunol.* **167,** 1945–1953.
18. Paas-Rozner, M., Sela, M. & Mozes, E. (2003) *Proc. Natl. Acad. Sci. USA* **100,** 6676–6681.
19. La Cava, A., Ebling, F. M. & Hahn, B. H. (2004) *J. Immunol.* **173,** 3542–3548.
20. Kang, H.-K., Michaels, M. A., Berner, B. R. & Datta, S. K. (2005) *J. Immunol.* **174,** 3247–3255.
21. Crispin, J. C., Martinez, A. & Alcocer-Varela, J. (2003) *J. Autoimmun.* **21,** 273–276.
22. Liu, M.-F., Wang, C.-R., Fung, L.-L. & Wu, C.-R. (2004) *Scand. J. Immunol.* **59,** 198–202.
23. Wu, H. Y. & Staines, N. A. (2004) *Lupus* **13,** 192–200.
24. Hori, S., Nomura, T. & Sakaguchi, S. (2003) *Science* **299,** 1057–1061.
25. Fontenot, J. D., Gavin, M. A. & Rudensky, A. Y. (2003) *Nat. Immunol.* **4,** 330–336.
26. Green, D. R., Droin, N. & Pinkoski, M. (2003) *Immunol. Rev.* **193,** 70–81.
27. Belkaid, Y., Piccirillo, C. A., Mendez, S., Shevach, E. M. & Sacks, D. L. (2002) *Nature* **420,** 502–507.
28. Kullberg, M. K., Jankovic, D., Gorelick, P. L., Caspar, P., Letterio, J. J., Cheever, A. W. & Sher, A. (2002) *J. Exp. Med.* **196,** 505–515.
29. Piccirillo, C. A., Letterio, J. J., Thornton, A. M., McHugh, R. S., Mamura, M., Mizuhara, H. & Shevach, E. M. (2002) *J. Exp. Med.* **196,** 237–245.
30. Parijs, L. V. & Abbas, A. K. (1998) *Science* **280,** 243–248.
31. Nakamura, K., Kitani, A. & Strober, W. (2001) *J. Exp. Med.* **194,** 629–644.
32. Chen, W. & Wahl, S. M. (2003) *Cytokine Growth Factor Rev.* **14,** 85–89.
33. Peng, Y., Laouar, Y., Li, M. O., Green Allison, E. & Flavell, R. A. (2004) *Proc. Natl. Acad. Sci. USA* **101,** 4572–4577.
34. Thompson, C. & Powrie, F. (2004) *Curr. Opin. Pharmacol.* **4,** 408–414.
35. Tsokos, G. C., Nambiar, M. P., Tenbrock, K. & Juang, Y. T. (2003) *Trends Immunol.* **24,** 259–263.
36. Cortesini, R., LeMaoult, J., Ciubotariu, R. & Cortesini, N. S. (2001) *Immunol. Rev.* **182,** 201–206.
37. Mevorach, D. (2003) *Clin. Rev. Allergy Immunol.* **25,** 49–60.
38. Sthoeger, Z., Dayan, M., Tcherniack, A., Green, L., Toledo, S., Segal, R., Elkayam, O. & Mozes, E. (2003) *Clin. Exp. Immunol.* **131,** 385–392.

Clinical Immunology (2006) 119, 146–155

available at www.sciencedirect.com

SCIENCE DIRECT®

www.elsevier.com/locate/yclim

Amelioration of murine lupus by a peptide, based on the complementarity determining region-1 of an autoantibody as compared to dexamethasone: Different effects on cytokines and apoptosis

Amir Sharabi, Asher Haviv, Heidy Zinger, Molly Dayan, Edna Mozes*

Department of Immunology, The Weizmann Institute of Science, Rehovot 76100, Israel

Received 4 July 2005; accepted with revision 14 January 2006
Available online 28 February 2006

KEYWORDS
Apoptosis;
Cytokines;
Dexamethasone;
Fas pathway;
Immunomodulation;
(NZBxNZW)F1 mice;
Peptides;
Systemic lupus erythematosus

Abstract A peptide (hCDR1) based on the sequence of the complementarity-determining region-1 of an anti-DNA autoantibody ameliorates clinical manifestations of lupus. We analyzed the beneficial effects of hCDR1 when given alone or in combination with dexamethasone, while comparing the mechanisms of action of the latter. Treatment with either hCDR1 or dexamethasone, or a combination of the latter significantly reduced titers of dsDNA-specific autoantibodies, levels of proteinuria, and intensity of glomerular immune complex deposits. Both drugs down-regulated the secretion and expression of IFN-γ and IL-10, but only treatment with hCDR1 up-regulated TGF-β. While both drugs reduced the expression of Fas ligand (FasL) and caspase 8, treatment with hCDR1 resulted in reduced whereas dexamethasone administration resulted in increased rate of apoptosis. Furthermore, down-regulation of FasL appeared to play a role in cytokine modulation. We conclude that specific treatment with hCDR1 ameliorates murine lupus via distinct mechanisms of action than those of dexamethasone.
© 2006 Elsevier Inc. All rights reserved.

Abbreviations: CDR, complementarity-determining region; hCDR1, human CDR1; FasL, Fas ligand; Id, idiotype; NZB, New Zealand Black; NZW, New Zealand White; SLE, systemic lupus erythematosus; TUNEL, terminal deoxynucleotidyltransferase-mediated dUTP nick end labeling.

* Corresponding author. Fax: +972 8 9344141.
E-mail address: edna.mozes@weizmann.ac.il (E. Mozes).

1521-6616/$ – see front matter © 2006 Elsevier Inc. All rights reserved.
doi:10.1016/j.clim.2006.01.007

Introduction

Systemic lupus erythematosus (SLE) is an autoimmune disease characterized by the dysregulation of immune responses mediated by T and B cell lymphocytes. This results in the vast production of autoantibodies against several self antigens and further development of immune complexes, which deposit within the kidneys and other organs as well [1]. Our laboratory established a model of murine SLE induced in naive mice by active immunization with a pathogenic anti-DNA monoclonal antibody that bears the 16/6 idiotype (Id) of either human or mouse origin [2,3]. The immunized mice develop a clinical SLE-like disease manifested by high levels of autoantibodies, including anti-dsDNA antibodies [2]. Leukopenia, proteinuria, and immune-complex glomerular kidney disease are also observed in the immunized mice [2,3]. Further, mice with experimental SLE, shared common features with (New Zealand Black (NZB) × New Zealand White (NZW)) F1 mice that are known to develop the disease spontaneously. High homology was found between the variable regions coding for the heavy and light chains of anti-DNA monoclonal antibody of the mice with induced SLE and (NZBxNZW)F1 mice [4].

Peptides based on the sequences of the complementarity-determining region (CDR)-1 and 3 of either a murine (5G12) or human anti-DNA, 16/6Id$^+$ monoclonal antibodies [5,6] were designed and synthesized. The peptides, shown to interact and affect T cells, were capable of down-regulating autoimmune responses associated with SLE [5,7,8]. Furthermore, the peptides were capable of either preventing or treating an established disease that was either induced or developed spontaneously [7,9–11]. Moreover, hCDR1 and hCDR3 were shown to inhibit efficiently and specifically the 16/6Id-induced in vitro proliferation and interleukin (IL)-2 production of peripheral blood lymphocytes of SLE patients [12]. hCDR1 was shown to immunomodulate the cytokine profile found in SLE-afflicted mice by down-regulating the secretion and expression of the pathogenic cytokines IL-1, IL-10, interferon (IFN)-γ, and tumor necrosis factor (TNF)-α, and by up-regulating the secretion of the immunosuppressive cytokine transforming-growth factor (TGF)-β [7]. Furthermore, hCDR1 was demonstrated to affect specifically T cell adhesion, chemotaxis, and proliferation [8,13].

Currently, glucocorticosteroids are frequently used for the treatment of lupus. Their down-regulating effects are generally explained by their ability to suppress immune responses that are mediated by T and B cell lymphocytes as well as effector functions of monocytes and neutrophils [14]. The main disadvantage of steroids, however, is their broad immunosuppressive effect as well as the development of serious adverse side effects following their long-term use. In contrast, treatment with CDR-based peptides is highly specific and is aimed at down-regulating the SLE-associated autoreactive responses only.

In the present study, we investigated the effects and mechanisms of action of the well-studied specific immunomodulator hCDR1 by comparing it to those of the commonly used long acting steroid, dexamethasone. While treatment with hCDR1 is as effective as dexamethasone in ameliorating clinical manifestations of SLE, both means of treatment differ in their mechanisms of action as demonstrated by the resultant cytokine profiles, rates of apoptosis, and both apoptotic and non-apoptotic functions of Fas ligand (FasL).

Materials and methods

Mice

Female (NZBxNZW)F1 mice were purchased from the Jackson Laboratory (Bar Harbor, ME, USA), and BALB/c female mice were purchased from Harlan (Jerusalem, Israel). The study has been approved by the Animal Care and Use committee of the Weizmann Institute of Science.

Synthetic peptide

A peptide with the following sequence GYYWSWIRQPPGK-GEEWIG (hCDR1) based on the CDR1 of the human anti-DNA monoclonal antibody [6] bearing the 16/6Id was synthesized (solid phase synthesis by F-moc chemistry) by Polypeptide laboratories (LA, USA) and used in this study. A peptide with scrambled order of the amino acids of the hCDR1, SKGIP-QYGGWPWEGWRYEI ('scrambled peptide') was synthesized and used as a control. hCDR1 (TV-4710, Edratide) is currently under clinical development for human SLE by Teva Pharmaceutical Industries Ltd.

Monoclonal antibody

The human anti-DNA 16/6Id (IgG1/k) was secreted by hybridoma cells [6] that were grown in culture and was purified by a protein G-Sepharose column (Pharmacia, Fine Chemicals, Uppsala, Sweden).

Treatment of mice with hCDR1 and dexamethasone

A preliminary dosing study using 0.5, 1, and 2 μg/mouse of dexamethasone indicated that, although the 3 doses used down-regulated SLE-associated responses, the 2 μg dose demonstrated the most efficient and reproducible inhibitory effect and therefore was used in this study.

(NZBxNZW)F1 female mice at the age of 6 months were divided into 6 groups (n = 7–12 mice/group) and treated with 10 weekly subcutaneous injections as follows: vehicle Captisol® (Sulfobutylether beta cyclodextrin that has been designed by CyDex to enhance the solubility and stability of drugs), hCDR1 (50 μg/mouse), scrambled peptide (50 μg/mouse), dexamethasone [(9α-Fluoro-16α-methylprednisolone); Sigma; 2 μg/mouse], hCDR1 and dexamethasone, a 5-week treatment with a combination of hCDR1 and dexamethasone followed by a 5-week treatment with hCDR1 alone. In the short-term experiment, BALB/c mice were immunized intradermal with the human anti-DNA monoclonal antibody, 16/6Id (1 μg/mouse, in CFA) concomitant with the injection of either hCDR1 (50 μg/mouse, in PBS), dexamethasone (2 μg/mouse), or both.

Proliferation of lymph node-derived cells of 16/6Id-immunized BALB/c mice

All assays were performed in triplicate in flat-bottomed microtiter plates (Falcon, Becton Dickinson, Oxnard, CA,

USA). Popliteal lymph node cells (5×10^5/well) from each treatment group were cultured in enriched RPMI-1640, supplemented with 1% normal mouse serum in the presence of various concentrations (0.1–10 μg/well) of the 16/6Id. The cultures were incubated in 7.5% CO_2 at 37°C for 96 h before [^{3}H] thymidine (0.5 μCi of 5 Ci/mmol) (Nuclear Research Center, Negev, Israel) was added, and 16 h later plates were harvested and radioactivity was counted.

Cytokine production and detection by ELISA

Spleen cells (5×10^6/ml) of (NZBxNZW)F1 mice or lymph node cells (3×10^6/ml) of BALB/c mice that were immunized with the 16/6Id were incubated with either enriched medium or hCDR1 (25 μg/ml), or the 16/6Id for the immunized mice (25 μg/ml). Supernatants were removed after 48 h and 72 h and analyzed for cytokine content. IFN-γ and IL-10 were determined by ELISA using OptEIA sets (PharMingen, San Diago, CA) and according to the manufacturer's instructions. For the detection of TGF-β, plates were coated with a recombinant human TGF-β sRII/Fc chimera (R&D Systems, Minneapolis, USA). Supernatants were added after activation of latent TGF-β1 to immunoreactive TGF-β1 according to the manufacturer (R&D Systems, Minneapolis, USA). Thereafter, a biotinylated anti-human TGF-β1 antibody was added and the assay was developed according to the manufacturer's instructions (R&D Systems, Minneapolis, USA).

ELISA for the detection of anti-dsDNA antibodies

Maxisorb microtiter plates (Nunk, Denmark) were coated with poly-L-lysine (5 μg/ml) (Sigma, St Louis, MO), followed by coating with lambda phage dsDNA (5 μg/ml) (Boehringer, Mannheim). After incubation with different dilutions of sera, horseradish peroxidase-labeled goat anti-mouse IgG (γ chain-specific; Jackson Immuno Research, West Grove, PA) was added to the plates, followed by the addition of the substrate, ABTS (Sigma). Results were read at 405 nm using an ELISA reader.

Real-time PCR

Levels of mRNA of cytokines were analyzed by quantitative real-time RT-PCR using LightCycler (Roche, Germany). Total RNA was isolated from spleen cells that were pooled (n = 9–12 mice) from each treatment group of the (NZBxNZW)F1 mice. RNA was reverse-transcribed to prepare cDNA using M-MLV reverse transcriptase (Promega, Madison, WI). The resultant cDNA was subjected to real-time PCR according to the manufacturer's instructions. Briefly, 20 μl reaction volume contained 3 mM $MgCl_2$, LightCycler HotStart DNA SYBR Green I mix (Roche), specific primer pairs, and 5 μl of cDNA. PCR conditions were as follows: 10 min at 95°C followed by 35–50 cycles of 15 s at 95°C, 15 s at 60°C, and 15 s at 72°C. Cytokine primer sequences (forward and reverse, respectively) were used as follows: β-actin (5′-gtgacgttgacatccg-3′, 5′-cagtaacagtccgcct-3′), caspase 8 (5′-acataacccaactccgaa-3′, 5′-gtgggataggatacagcaga-3′), IFN-γ (5′-gaacgctacacactgc-3′, 5′-ctggacctgtgggttg-3′), IL-10 (5′-aacctcgtttgtacctct-3′, 5′-caccatagcaaagggc-3′), and TGF-β 5′-gaacccccattgctgt-3′, 5′-gccctgtattccgtct-3′). β-actin levels were used for normalization while calculating the expression levels of all other genes.

Terminal deoxynucleotidyltransferase-mediated dUTP nick end labeling (TUNEL) assay

Apoptosis, as evidenced by fragmented DNA, was determined using the In Situ Death Detection Kit (Roche, Indianapolis, IN) based on TUNEL technology, according to the protocol supplied by the manufacturer. Cells were analyzed by FACS, with forward and side scatter gates adjusted to include all cells and to exclude debris. Each sample was accompanied by a negative control, consisted of UTP labeled with fluorescein, and a positive control, consisted of DNase I, grade I (Roche) that was added prior to the TUNEL staining.

Staining with antibodies to Fas and FasL

Spleen cells (1×10^6 cells/tube) were stained with monoclonal antibody to PE-conjugated Fas (CD95, clone Jo2) or PE-conjugated FasL (CD178, clone MFL3, Pharmingen) for 30 min at 4°C. Each sample was also stained with the appropriate IgG isotype control (Pharmingen). Cells were thereafter analyzed by FACS.

In vitro assays

Spleen cells (0.5×10^6 cells) taken from 8-month-old (NZBxNZW)F1 female mice with established lupus were co-incubated either with anti-mouse FasL monoclonal antibody (C57BL/6 gld anti-mFasL-transfected L5178Y T lymphoma, clone Kay-10, Pharmingen), or with splenocytes (in a 1:25 ratio) obtained from 2-month-old (NZBxNZW)F1 female mice subcutaneously treated with hCDR1 (50 μg/mouse, 3 injections in 1 week), or with both anti-mouse FasL monoclonal antibody and the hCDR1-treated cells, during 36 h and thereafter assessed for content of secreted cytokines.

Detection of proteinuria

Proteinuria was measured by a standard semi-quantitative test, using an Albustix kit (Bayer Diagnostic, Newbury, UK). Results were graded according to the manufacturer as: negative, + = 0.3 g/l, ++ = 1 g/l, +++ = 3 g/l, or ++++ = ≥20 g/l.

Immunohistology

Mice were sacrificed 2–3 weeks after the end of treatment, and kidneys were removed and frozen immediately in liquid nitrogen. Frozen cryostat sections (6 μm) were air-dried and fixed in acetone. For the detection of Ig deposits, sections were incubated with FITC-conjugated goat anti-mouse IgG (γ chain-specific) (Jackson Immuno Research). Staining was visualized using a fluorescence microscope.

Statistical analysis

To evaluate the significance of the differences between groups, the Student's t test and the non-parametric Mann–Whitney test were used. Values of $P \leq 0.05$ were considered significant.

Results

hCDR1 and dexamethasone have similar beneficial effects on lupus manifestations

Female (NZBxNZW)F1 mice at the age of 6 months (when lupus-like manifestations are already present) were treated weekly during a 10 week period with subcutaneous injections of the hCDR1 (50 μg/mouse), dexamethasone (2 μg/mouse), or both. An additional group received both hCDR1 and dexamethasone for 5 weeks whereas for the rest of the treatment period, hCDR1 only was administered to the mice. A control group of mice was treated with the vehicle alone. Fig. 1 demonstrates results of a representative experiment. It can be seen in the figure that treatment with hCDR1 resulted in a reduction in the titers of anti-dsDNA autoantibodies as did the treatment with dexamethasone alone, when compared to mice treated with the vehicle or the control (scrambled) peptide (Fig. 1A). Co-treatment with hCDR1 and dexamethasone (either a 5 or a 10 week course) also decreased the levels of anti-dsDNA autoantibodies.

The effect of the different treatment protocols on the kidney disease of the mice was assessed by measuring the levels of proteinuria and by analyzing the kidneys for the presence of immune complex deposits. Fig. 1B shows that while proteinuria in vehicle or in control peptide-treated mice increased with time, its levels remained low in all groups of hCDR1- and/or dexamethasone-treated mice, and the differences were statistically significant after the fifth weekly treatment. In addition, Fig. 2 demonstrates that the improvement in proteinuria was associated with a significant reduction in the intensity of the glomerular immune complex deposits in the hCDR1 and/or dexamethasone-treated groups.

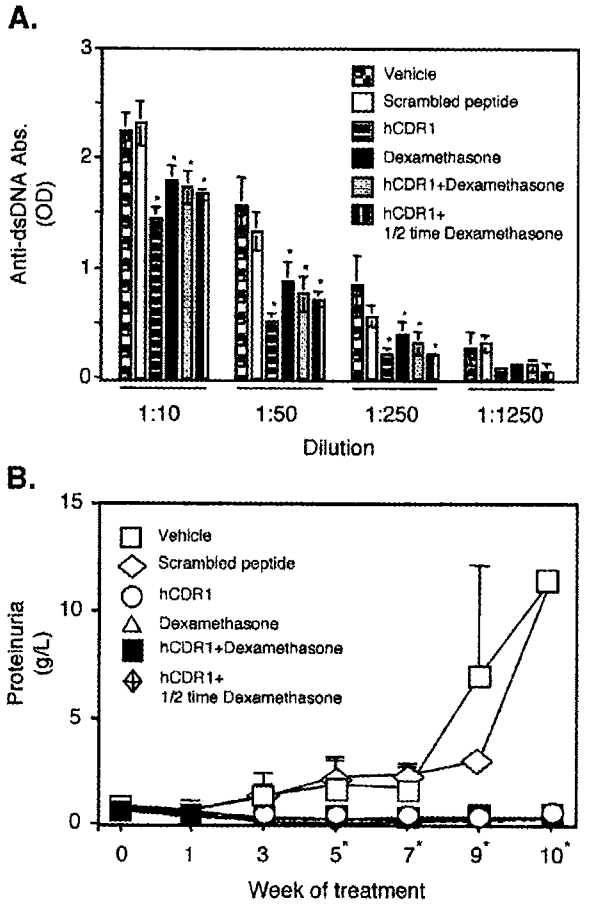

Figure 1 Clinical effects of hCDR1 and dexamethasone in (NZBxNZW)F1 female mice. (A) Sera of individual mice (n = 9–12 mice/group) were obtained at the end of a 10-week treatment and tested for anti-dsDNA antibodies. (B) Proteinuria levels were obtained from individual mice in each treatment group and the mean g/l levels (±SEM) were calculated for each group. Proteinuria was always measured at the same time of day, and all mice in an experimental cohort were tested together. *P < 0.05 for all treatment groups (except for scrambled peptide-treated) in comparison to the vehicle-treated group. Results are of one representative experiment out of four performed.

The effects of treatment with hCDR1 and/or dexamethasone on the pattern of secreted and expressed cytokines

It was of interest to compare the effect of treatment with hCDR1, dexamethasone, or both on the cytokine profile of the treated mice. The results presented in Fig. 3 summarize 4 experiments performed and demonstrate that the high secreted levels of IFN-γ and IL-10 (Fig. 3A) in mice with established SLE decreased dramatically after treatment with hCDR1, dexamethasone, or both means given in combination. The reduction of the latter cytokines by hCDR1 was specific since treatment with a control (scrambled) peptide resulted in an increase rather than a decrease of IFN-γ and IL-10 levels. Fig. 3A depicts also the levels of TGF-β secreted by splenocytes of mice of the different groups. It can be seen that whereas splenocytes of hCDR1-treated mice secreted significantly ($P \leq 0.003$) higher levels of TGF-β than splenocytes of the vehicle-treated mice, treatment with dexamethasone affected minimally the secretion of the latter cytokine. The combined treatment of hCDR1 and a 5-week administration of dexamethasone resulted in a significant higher secretion of TGF-β than in the control groups (Fig. 3A). Treatment with a control peptide did not modulate the secretion of TGF-β. To further confirm the above results of cytokines secretion, each group of cells was assessed for mRNA expression of the relevant cytokines. Results of cytokine gene expression demonstrated in Fig. 3B are in agreement with the cytokine secretion data.

hCDR1 and dexamethasone down-regulate the proliferative responses of BALB/c mice and immunomodulate cytokine secretion

The effect of dexamethasone was compared to that of hCDR1 in an additional model, namely in BALB/c mice

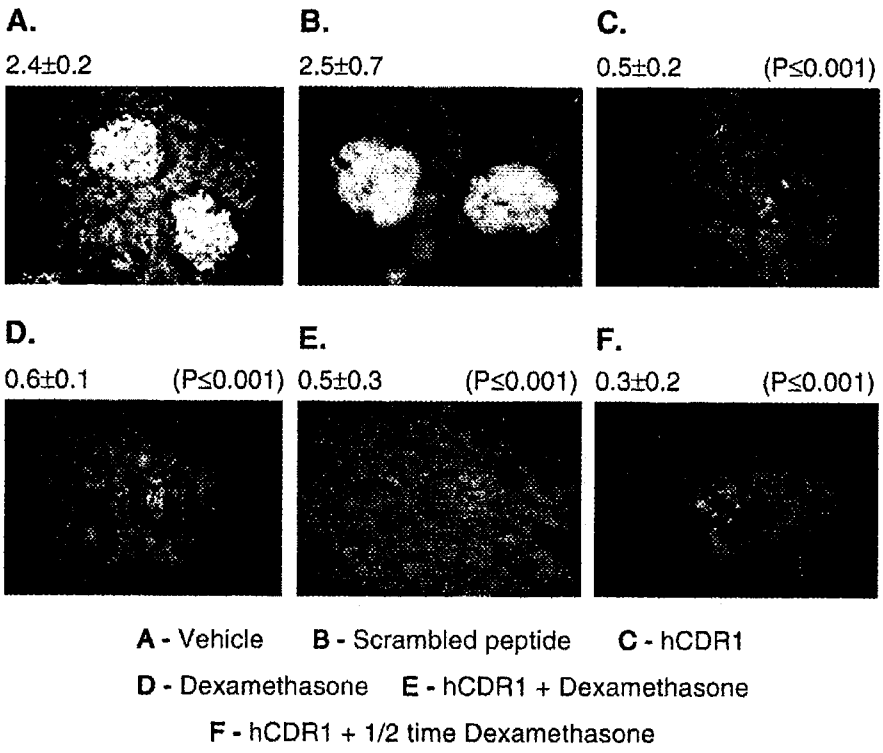

Figure 2 Immunohistology of kidney sections obtained from (NZBxNZW)F1 female mice. Kidney sections were obtained at the end of 10 weeks of treatment and analyzed for the presence of immune complex deposits. The stained samples were graded on a scale of 0–3 as follows: 0–no immune complex deposits; 1–low intensity; 2–moderate intensity, and 3–high intensity of immune complexes. Representative kidney sections (×400) are shown. Results are expressed as mean (±SD) intensity of immune complex deposits of all mice within a group (n = 9–12 mice/group). Results are of one representative experiment out of four performed.

that were immunized with the monoclonal anti-DNA 16/6Id shown to be capable of inducing experimental SLE [2]. The immunized mice were treated concomitantly with subcutaneous injections of hCDR1 (50 μg/mouse, administered in PBS), dexamethasone (2 μg/mouse), or both drugs. Lymph node-derived cells were taken from the experimental mice 10 days later and their ability to proliferate in vitro in the presence of the 16/6Id or to secrete cytokines following in vitro triggering with the 16/6Id was tested. Fig. 4A shows that treatment with hCDR1 or with dexamethasone concomitant with the immunization with 16/6Id resulted in a significant inhibition of cell proliferation. Co-treatment with both hCDR1 and dexamethasone led to the most prominent inhibition. Both hCDR1 and dexamethasone reduced the levels of IFN-γ (Fig. 4B). However, hCDR1, but not dexamethasone up-regulated TGF-β levels (Fig. 4C). As shown in Fig. 4C, dexamethasone alone did not affect the secretion of TGF-β as compared to mice immunized with the 16/6Id. It is also shown in the figure that levels of TGF-β in supernatants of lymph node cells of mice treated with dexamethasone and hCDR1 were similar to those of mice injected with hCDR1 alone. Thus, the results of the short-term experiments in BALB/c mice confirmed the data of long-term experiments of treatment of the SLE-prone (NZBxNZW)F1 mice indicating that only hCDR1 up-regulated TGF-β.

hCDR1 reduces whereas dexamethasone increases rates of apoptosis

A disruption of apoptosis and subsequent clearance of cellular debris are hypothesized to be in the essence of the pathogenesis of some autoimmune diseases, including SLE. In order to determine the effect of treatment on apoptosis in SLE-afflicted mice, we documented the frequency of cells undergoing apoptosis and the involvement of the Fas pathway. Fig. 5A shows that the expression of Fas was comparable for both young and old (diseased) mice. However, a significant enhanced expression (of about 40%) in FasL was determined in old SLE-afflicted mice in comparison to young healthy mice. The latter was reproducible in 4 individual experiments. Concerning the effect of treatments, neither hCDR1 nor dexamethasone caused a significant change in the surface expression of Fas (Fig. 5A). Nevertheless, FasL expression was reduced in all treatment groups (Fig. 5A; c–f versus a) but not in the group treated with the control peptide (Fig. 5A; b versus a). As can be seen in Fig. 5B, the rate of apoptosis as determined by TUNEL was 2–3-fold higher in SLE-afflicted mice than in young healthy controls. A reduced number of TUNEL[+] cells was determined in spleens of hCDR1-treated mice as compared to vehicle-treated mice (Fig. 5B; a versus c). Treatment with the control peptide did not affect the rate of apoptosis (Fig. 5B; a versus b). However, the number of TUNEL[+] cells was

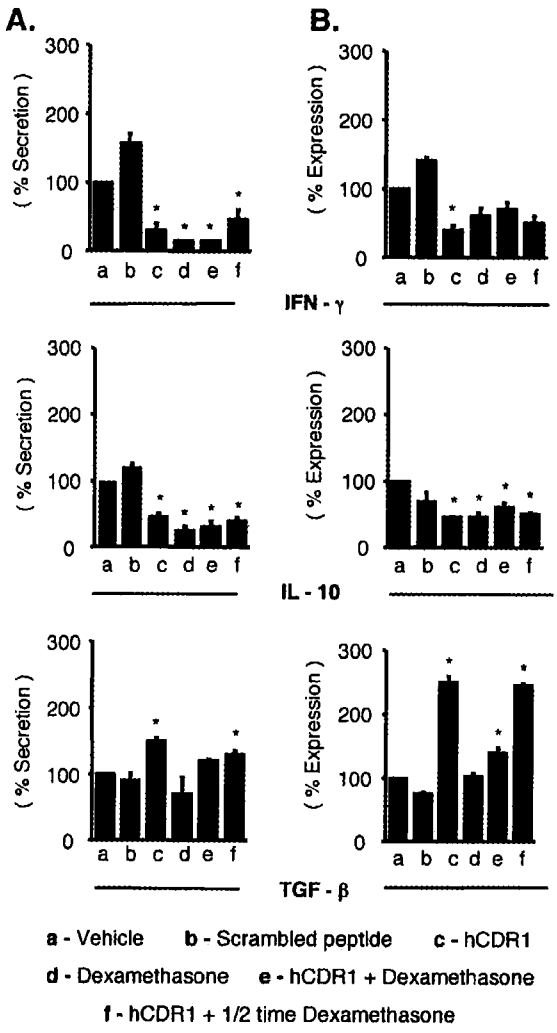

Figure 3 The effect of treatment with hCDR1 and dexamethasone on the cytokine profile in (NZBxNZW)F1 mice. Splenocytes originating from each treatment group (n = 9–12 mice/group) were incubated in enriched medium and the supernatants were collected after 48–72 h and tested for secreted and expressed cytokines by ELISA and real-time PCR, respectively. Mean results (±SD) are expressed relatively to vehicle-treated group, which was defined as 100%. (A) Cytokine secretion of IFN-γ (100% = 671 ± 275 pg/ml), IL-10 (100% = 2647 ± 1339 pg/ml), and TGF-β (100% = 821 ± 67 pg/ml). (B) Cytokine mRNA expression. Results were first normalized as percentage of β-actin and further normalized to the values of vehicle-treated group defined as 100%. Statistical analysis was based on four individual experiments (*$P < 0.05$).

increased after treatment with dexamethasone (Fig. 5B; a versus d). Co-treatment of both drugs resulted in an intermediate number (but lower than in the old mice) of TUNEL[+] cells (Fig. 5B; e). Discontinuation of dexamethasone for half the time of treatment while continuing with hCDR1 treatment led to a number of TUNEL[+] cells that was lower than that observed for vehicle or control peptide treatments (Fig. 5B; f versus a and b). These results were reproducible in four individual experiments. To confirm the effect of FasL on the rate of apoptosis, we measured mRNA expression of caspase 8. As demonstrated in Fig. 5C, all treatment groups had a lower expression of caspase 8 mRNA as compared to the vehicle or scrambled peptide-treated groups. Indeed, the expression of caspase 8 was associated with that of FasL. Thus, treatment with hCDR1 led to a decrease, whereas treatment with dexamethasone resulted in an increase in the rate of apoptosis.

The hCDR1-mediated reduction of FasL plays a role in the cytokine secretion

Since FasL is suggested to be involved not only in the apoptotic process, and because treatment with hCDR1 resulted in a 40% decrease in FasL expression, it was of interest to find out whether the latter affects cytokine secretion. To this end, splenocytes (5×10^5 cells) originating from 8-month-old SLE-afflicted mice ('lupus' cells) were co-incubated for 36 h with splenocytes (2×10^4 cells) from 2-month-old (NZBxNZW)F1 mice that were pre-treated with hCDR1 (50 μg/mouse, 3 subcutaneous injections in 1 week). As can be seen in Fig. 6 (left end), co-incubation with hCDR1-treated cells resulted in down-regulation of IFN-γ and IL-10, and in up-regulation of TGF-β, in comparison to incubation of 'lupus' cells alone. Fig. 6, right end, shows that incubation of 'lupus' cells in the presence of different concentrations of anti-FasL neutralizing monoclonal antibody (0.3, 1.5, 3, or 15 μg) resulted in a cytokine modulation similar to that observed following incubation with hCDR1-treated cells. No such effects were observed when the isotype control was present in the medium (Fig. 6, right end). Further, no additive effect, to that of hCDR1-treated cells, could be determined when the anti-FasL monoclonal

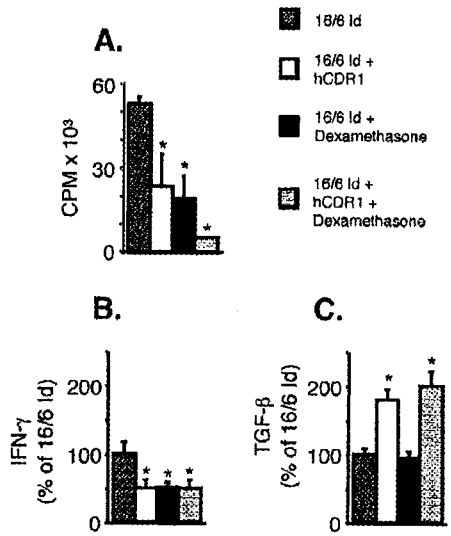

Figure 4 The proliferative capacity and cytokine profile in BALB/c mice immunized with the 16/6Id and concomitantly treated with either hCDR1, dexamethasone, or both. (A) Proliferation of lymph node-derived cells. (B and C) Mean results (±SEM) of cytokines expressed relatively to the 16/6 Id-immunized group of mice, which was defined as 100%. (B) IFN-γ (100% = 2393 ± 313 pg/ml); (C) TGF-β (100% = 902.3 ± 94.8 pg/ml). Statistical analysis was based on three individual experiments (*$P < 0.05$).

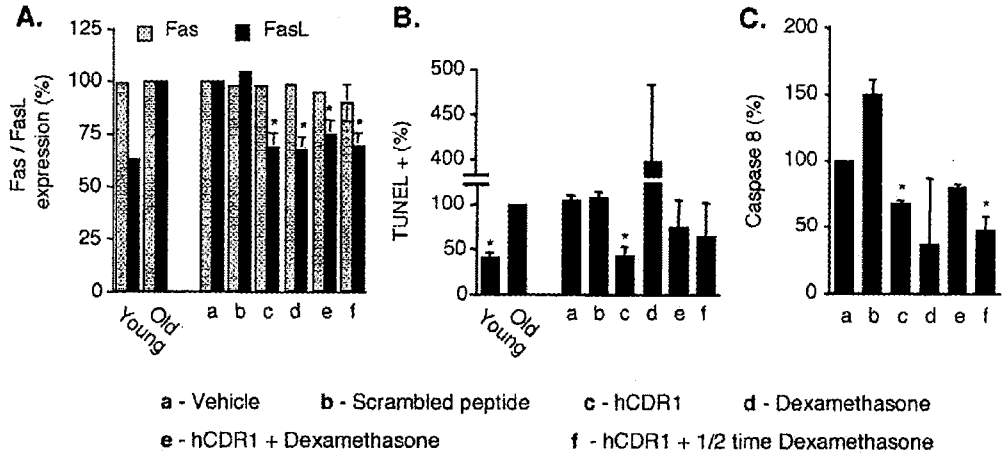

Figure 5 The effect of treatment with hCDR1 and dexamethasone on apoptosis in (NZBxNZW)F1 mice. (A) Spleens from each group were pooled and thereafter splenocytes were depleted from red blood cells and stained with Fas or FasL. Mean values of 4 individual experiments for Fas and FasL expressing splenocytes originating from young and old (NZBxNZW)F1 mice, and from the 6 treatment groups (n = 9–12 mice/group). All results are expressed as percentage of splenocytes of old mice (Fas, 100% = 87.90 ± 0.05%; FasL, 100% = 38.22 ± 0.15%). (B) Spleens from each group were pooled and thereafter splenocytes were depleted from red blood cells and stained according to the TUNEL technique. Mean values of 4 individual experiments for TUNEL[+] splenocytes originating from young and old (NZBxNZW)F1 mice, and from the 6 groups of treatment (n = 9–12 mice/group). All results are expressed as percentage splenocytes of old mice (100% = 4.4 ± 0.1%). (C) Caspase 8 mRNA expression in splenocytes of each of the 6 treatment groups described. Representative results of one experiment out of 4 were normalized to β-actin and are relative to the vehicle-treated group defined as 100% (*$P < 0.05$).

antibody was present in the co-culture of 'lupus' cells and hCDR1-treated cells (Fig. 6, right end). It, thus, appears that FasL that is reduced by hCDR1 treatment is also involved in the down-regulation of IFN-γ and IL-10, and the up-regulation of TGF-β.

Discussion

The main findings of this study are that the specific treatment with hCDR1 is at least as effective as that with dexamethasone. The mechanisms underlying the therapeutic effects of the two drugs are partially distinct. Under the combined treatment of hCDR1 and dexamethasone, the latter drug does not interfere with hCDR1 activity. Both drugs down-regulate the secretion of IFN-γ and IL-10. Yet, treatment with hCDR1 results in an up-regulated TGF-β secretion whereas treatment with dexamethasone has a minor effect on the latter cytokine. Both drugs reduce the expression of FasL; however, hCDR1 decreases whereas dexamethasone increases the rate of apoptosis. Further, in addition to the apoptosis-related effects of FasL, neutralization of FasL is demonstrated to reverse the pathogenic profile of cytokines as achieved with hCDR1 treatment.

Anti-DNA antibodies are involved in the pathogenesis of the immune glomerulonephritis in SLE in mice and in human patients [15,16]. Here, we demonstrated that treatment with hCDR1 resulted in lower titers of anti-DNA antibodies in the sera as did treatment with dexamethasone, or with a combination of both means (Fig. 1A). Further, all treatment groups responded with a significant reduction of proteinuria levels and of immune complex deposits in the kidneys in comparison to the untreated mice (Figs. 1B and 2).

Cytokines have been suggested to play a central role in the immune dysregulation observed in experimental models of SLE, in lupus-prone mice, and in SLE patients [17–19]. Both IFN-γ and IL-10 were reported to be involved in the pathogenesis of lupus in SLE models as well as in patients [18,20–24]. In this study, we showed that treatment with either hCDR1 or dexamethasone, and a combined treatment with both drugs reduced significantly the levels of IFN-γ and IL-10 (Fig. 3). Indeed, steroids were reported to down-regulate the latter cytokines, although they mainly affect the secretion of the Th1 type cytokines [25,26].

The importance of TGF-β in SLE was shown in several studies. In SLE patients, the high levels of IgG were attributed, in part, to the low levels of TGF-β [27]. Likewise, TGF-β gene knockout mice were shown to rapidly develop a lethal syndrome of lymphocyte hyperactivity and autoantibodies together with lupus-like disease [28,29]. Moreover, in MRL/lpr/lpr mice, this cytokine was capable of decreasing the production of autoantibodies [30], and in (NZBxNZW)F1 mice, the improvement in clinical manifestations was correlated with increased mRNA expression of TGF-β [31]. In the present study, we demonstrate that the production of TGF-β is influenced differently by the two types of drugs. Thus, while hCDR1 treatment resulted in the up-regulation of TGF-β, dexamethasone treatment resulted in unchanged or reduced levels of the latter cytokine (Fig. 3). This particular pattern was demonstrated in supernatants as well as in mRNA expression. It was also confirmed in short-term experiments in BALB/c mice immunized with the SLE inducing autoanibody, 16/6Id (Fig. 4), and in mice with experimental SLE induced by the 16/6Id that were treated with hCDR1 [7]. Further, treatment of naive BALB/c mice and young, free-of-disease (NZBxNZW)F1 mice with hCDR1 markedly up-regulated the secretion of TGF-β by splenocytes of the treated mice (unpublished data). Furthermore, up-regulated levels of TGF-β following treatment

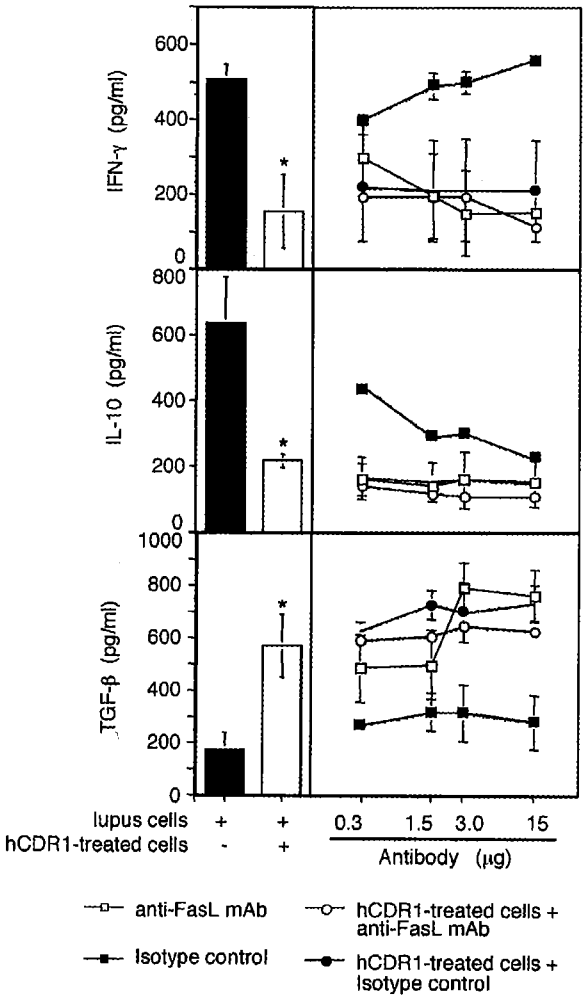

Figure 6 Down-regulated expression of FasL by hCDR1 is associated with modulation of cytokines profile. Triplicate of spleen cells (5×10^5) from 8-month-old (NZBxNZW)F1 mice (n = 3), designated as 'lupus' cells, were co-incubated for 36 h with splenocytes (2×10^4 cells) from 2-month-old mice (n = 3) that were pre-treated subcutaneously with hCDR1 (50 μg/mouse, 3 injections in 1 week), or with the latter in the presence or absence of either anti-FasL neutralizing monoclonal antibody or its isotype control. Levels of secreted cytokines in the supernatants were measured by ELISA for each concentration of antibody (presented in logarithmic scale). Results are of one representative experiment out of two performed.

with hCDR1 were shown to be involved in the inhibition of T cell migration, adhesion, and proliferation [8,13], and in mediating the suppressive effects of hCDR1-induced $CD4^+CD25^+$ regulatory cells (unpublished data). Thus, whereas TGF-β is not involved in the mechanism of action of dexamethasone, this immunosuppressive cytokine plays a central role in mediating the ameliorative effects of hCDR1.

Dysregulated apoptosis has been demonstrated for autoimmune diseases, including SLE. Thus, administration of apoptotic lymphocytes to (NZBxNZW)F1 mice resulted in accelerated onset of SLE-like manifestations in these mice [32]. Further, lymphocytes of SLE patients exhibited increased rate of apoptosis that was also correlated with disease activity [33,34]. We showed here an increased rate of apoptosis that was associated with increased expression of FasL in SLE-afflicted (NZBxNZW)F1 mice (Fig. 5). In agreement, several reports indicated high levels of functional FasL in activated T cells originated from SLE patients [35]. In hCDR1-treated mice, amelioration in clinical status was associated with a reduction in rate of apoptosis, as reflected by TUNEL staining. Analyzing the Fas/FasL system indicated that this could be explained, at least partially, by the reduced expression of FasL, as the expression of caspase 8 was reduced too while no changes were observed in the levels of Fas (Fig. 5). Dexamethasone, which also caused a reduced FasL expression, still resulted in higher rates of apoptosis. This finding strikingly presents the dual role of FasL as a trigger for apoptosis in T lymphocytes [36], but also as a pro-inflammatory signal [37–40]. Thus, administration of steroids, which are pro-apoptotic and anti-inflammatory agents, leads to reduced expression of the pro-inflammatory FasL but with increased rate of apoptosis, which further supports in this case the involvement of apoptotic signaling pathways other than the Fas/FasL system. In agreement, studies in knockout mice demonstrated differences between corticosteroid-induced apoptosis and Fas-induced apoptosis [41]. Thus, although the two apoptosis pathways are caspase-dependent, the Fas-induced apoptosis requires the involvement of caspase 8 whereas the corticosteroid-induced apoptosis may depend alternatively on caspase 3.

FasL, in addition to its involvement in the apoptotic process, plays a role in the modulation of cytokine profile. Indeed, neutralization of FasL affected splenocytes of SLE-afflicted (NZBxNZW)F1 mice to reduce the secretion of IFN-γ and IL-10 and to enhance the secretion of TGF-β (Fig. 6). The same effect could be achieved by co-incubation of hCDR1-treated cells and 'lupus' cells, thus suggesting that the cytokine modulation by hCDR1 is likely to be affected by the reduced expression of FasL. Likewise, FasL was reported to affect the kidney disease of (NZBxNZW)F1 mice because

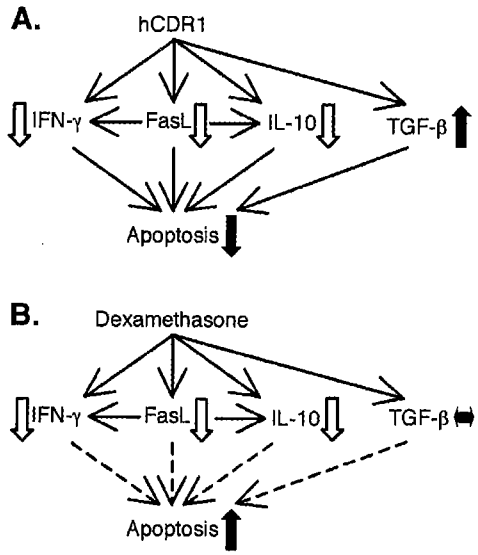

Figure 7 Schematic illustration of the effects of hCDR1 and dexamethasone. (A) Effects of hCDR1. (B) Effects of dexamethasone. Dashed line arrows represent alternative pathways.

its neutralization prevented the development of lupus nephritis [42].

The rate of apoptosis may be influenced not only by FasL expression but also by modulation of the cytokine profile. For instance, in SLE patients with active disease, the high levels of IL-10 were reported to augment T cell death in vivo [43]. In addition, IFN-γ, which is up-regulated in lupus, was shown to mediate its responses through the induction of subset of genes, namely, IFN-stimulated-genes that are involved, among other biological responses, in the apoptotic process [44]. Hence, the reduction of the latter cytokines by hCDR1 may lead to the observed lower apoptosis rates. In contrast, in the case of dexamethasone, apoptosis was unaffected by the down-regulated IL-10 and IFN-γ, and the observed higher rates may be attributed to the classic genomic activation [41]. In addition, TGF-β was shown to inhibit the expression of FasL and to reduce Fas-induced apoptosis [45,46]. Also, T cells of TGF-β1-deficient mice were reported to undergo increasing rates of apoptosis [47]. Therefore, the up-regulation of TGF-β by hCDR1 may mediate the reduction of apoptosis as well. In contrast, TGF-β does not play a role in the mechanisms of action of dexamethasone since this drug minimally affected its secretion and expression. Hence, it appears that the down-regulation of IFN-γ and IL-10 and the up-regulation of TGF-β, in addition to the reduced expression of FasL, may contribute to the reduced rate of apoptosis following treatment with hCDR1.

In summary, in the present study, we demonstrate that hCDR1 and dexamethasone down-regulate lupus manifestations by different mechanisms of action. As illustrated in Fig. 7, treatment with either hCDR1 or dexamethasone results in reduced secretion of IFN-γ and IL-10, but only treatment with hCDR1 leads to an increased secretion of TGF-β. The effect on cytokine secretion may be, at least in part, due to the reduced expression of FasL. The combined effect of cytokine modulation and FasL reduction leads to the decrease in the apoptosis rate in the lupus-afflicted mice, in response to treatment with hCDR1. In contrast, treatment with dexamethasone, which also down-regulated IFN-γ and IL-10 but did not affect TGF-β, leads to an increase in the apoptosis rate suggesting the existence of another pathway that is different from that of hCDR1 (Fig. 7B, dashed line). The mechanism of action as well as its specificity distinguishes treatment with hCDR1 from that with dexamethasone. Thus, hCDR1 is an effective specific candidate for the treatment of SLE.

References

[1] B.H. Hahn, An overview of the pathogenesis of systemic lupus erythematosus, in: D.J. Wallace, B.H. Hahn (Eds.), Dubis' Lupus Erythomatosus, Williams and Wilkins, Philadelphia, PA, 1993, p. 69.

[2] S. Mendlovic, S. Brocke, Y. Shoenfeld, M. Ben Bassat, A. Meshorer, R. Bakimer, E. Mozes, Induction of a systemic lupus erythematosus-like disease in mice by a common human anti-DNA idiotype, Proc. Natl. Acad. Sci. U. S. A. 85 (1988) 2260-2264.

[3] A. Waisman, S. Mendlovic, J.P. Ruiz, H. Zinger, A. Meshorer, E. Mozes, The role of the 16/6 idiotype network in the induction and manifestation of systemic lupus erythematosus, Int. Immunol. 5 (1993) 1293-1300.

[4] A. Waisman, E. Mozes, Variable regions sequences of autoantibodies from mice with experimental systemic lupus erythematosus, Eur. J. Immunol. 23 (1993) 1566-1573.

[5] A. Waisman, P.J. Ruiz, E. Israeli, E. Eilat, S. Konen-Waisman, H. Zinger, M. Dayan, E. Mozes, Modulation of murine systemic lupus erythematosus with peptides based on complementarity determining regions of a pathogenic anti-DNA monoclonal antibody, Proc. Natl. Acad. Sci. U. S. A. 94 (1997) 4620-4625.

[6] A. Waisman, Y. Shoenfeld, M. Blank, P.J. Ruiz, E. Mozes, The pathogenic human monoclonal anti-DNA that induces experimental systemic lupus erythematosus in mice is encoded by a VH4 gene segment, Int. Immunol. 7 (1995) 689-696.

[7] D. Luger, M. Dayan, H. Zinger, J.P. Liu, E. Mozes, A Peptide based on the complementarity determining region 1 of a human monoclonal autoantibody ameliorates spontaneous and induced lupus manifestations in correlation with cytokine immunomodulation, J. Clin. Immunol. 24 (2004) 579-590.

[8] U. Sela, R. Hershkoviz, L. Cahalon, O. Lider, E. Mozes, Down-regulation of stromal cell-derived factor-1alpha-induced T cell chemotaxis by a peptide based on the complementarity-determining region 1 of an anti-DNA autoantibody via up-regulation of TGF-beta secretion, J. Immunol. 174 (2005) 302-309.

[9] E. Eilat, H. Zinger, A. Nyska, E. Mozes, Prevention of lupus-erythematosus-like disease in (NZBxNZW) F1 mice by treating with CDR1 and CDR3-based peptides of a pathogenic autoantibody, J. Clin. Immunol. 20 (2000) 268-278.

[10] E. Eilat, M. Dayan, H. Zinger, E. Mozes, The mechanism by which a peptide based on the complementarity determining region-1 of a pathogenic anti-DNA autoantibody ameliorates experimental SLE, Proc. Natl. Acad. Sci. U. S. A. 98 (2001) 1148-1153.

[11] H. Zinger, E. Eilat, A. Meshorer, E. Mozes, Peptides based on the complementarity-determining regions of a pathogenic autoantibody mitigate lupus manifestations of (NZBxNZW) F1 mice via active suppression, Int. Immunol. 15 (2003) 205-214.

[12] Z.M. Sthoeger, M. Dayan, A. Tcherniack, L. Green, S. Toledo, R. Segal, O. Elkayam, E. Mozes, Modulation of autoreactive responses of peripheral blood lymphocytes of patients with systemic lupus erythematosus by peptides based on human and murine anti-DNA autoantibodies, Clin. Exp. Immunol. 131 (2003) 385-392.

[13] U. Sela, N. Mauermann, R. Hershkoviz, H. Zinger, M. Dayan, L. Cahalon, J.P. Liu, E. Mozes, O. Lider, The inhibition of autoreactive T cell functions by a peptide based on the CDR1 of an anti-DNA autoantibody is via TGF-beta-mediated suppression of LFA-1 and CD44 expression and function, J. Immunol. 175 (2005) 7255-7263.

[14] W.W. Chatham, R.P. Kimberly, Treatment of lupus with corticosteroids, Lupus 10 (2001) 140-147.

[15] A.N. Theofilopoulos, Murine models of lupus, in: R.G. Lahita (Ed.), Systemic Lupus Erythematosus, Churchill Livingston, New York, 1992, p. 121.

[16] B.H. Hahn, Antibodies to DNA, N. Engl. J. Med. 338 (1998) 1359-1368.

[17] R. Segal, B.L. Bermas, M. Dayan, F. Kalush, G.M. Shearer, E. Mozes, Kinetics of cytokine production in experimental systemic lupus erythematosus: involvement of T helper cell 1/T helper cell 2-type cytokines in disease, J. Immunol. 158 (1997) 3009-3016.

[18] A.N. Theofilopoulos, B.R. Lawson, Tumer necrosis factor and other cytokines in murine lupus, Ann. Rheum. Dis. 58 (1999) 149-155 (Suppl).

[19] G.S. Dean, J. Tirrell-Price, E. Crawley, D.A. Isenberg, Cytokines and systemic lupus erythematosus, Ann. Rheum. Dis. 59 (2000) 243-251.

[20] C.O. Jacob, P.H. van der Meide, H.O. McDevitt, In vivo treatment of (NZBxNZW) F1 lupus-like nephritis with mono-

clonal antibody to gamm interferon, J. Exp. Med. 166 (1987) 798-803.
[21] D. Balomenos, R. Rumold, A.N. Theofilopoulos, Interferon-γ is required for lupus-like disease and lymphoaccumulation in MRL-*lpr* mice, J. Clin. Invest. 101 (1998) 364-371.
[22] S.L. Peng, J. Moslehi, J. Craft, Roles of interferon-γ and interleukin-4 in murine lupus, J. Clin. Invest. 99 (1997) 1936-1946.
[23] H. Ishida, T. Muchamuel, S. Sakaguchi, S. Andrade, S. Menson, M. Howard, Continuous administration of anti-interleukin 10 antibodies delays onset of autoimmunity in NZB/W F1 mice, J. Exp. Med. 179 (1994) 305-310.
[24] L. Llorente, W. Zou, Y. Levy, J. Richaud-Patin, J. Wijdenes, J. Alcocer-Varela, B. Morel-Fourrier, J.C. Brouet, D. Alarcon-Segovia, P. Galanaud, et al., Role of interleukin 10 in the B lymphocyte hyperactivity and autoantibody production of human systemic lupus erythematosus, J. Exp. Med. 181 (1995) 839-844.
[25] R.J. ten Berge, H.P. Sauerwein, S.L. Yong, P.T. Schellekens, Administration of prednisolone in vivo affects the ratio of OKT4/OKT8 and the LDH isoenzyme pattern of human T-lymphocytes, Clin. Immunol. Immunopathol. 30 (1984) 91-103.
[26] J.D. Slade, B. Hepburn, Prednisone induced alterations of circulating human lymphocytes subsets, J. Lab. Clin. Med. 101 (1983) 479-487.
[27] K. Ohtsuka, J. Dixon Gray, M.M. Stimmler, B. Toro, D.A. Horwitz, Decreased production of TGF-β by lymphocytes from patients with systemic lupus erythematosus, J. Immunol. 160 (1998) 2539-2545.
[28] L. Yaswen, A.B. Kulkarni, T. Fredrickson, B. Mittleman, R. Schiffmann, S. Payne, G. Longenecker, E. Mozes, S. Karlsson, Autoimmune manifestations in transforming growth factor-β1 knockout mouse, Blood 87 (1996) 1439-1445.
[29] J.J. Letterio, A.B. Roberts, Regulation of immune responses by TGF-beta, Annu. Rev. Immunol. 16 (1998) 137-161.
[30] E. Raz, A. Watanabe, S.M. Baird, R.A. Isenberg, T.B. Parr, M. Lotz, T.J. Kipps, D.A. Carson, Systemic immunological effects of cytokine genes injected into skeletal muscle, Proc. Natl. Acad. Sci. U. S. A. 90 (1993) 4523-4527.
[31] M.N. Sato, P. Minoprio, S. Avrameas, T. Teninck, Changes in the cytokine profile of lupus-prone mice (NZB/NZW)F_1 induced by *Plasmodium chaubaudi* and their implications in the reversal of clinical symptoms, Clin. Exp. Immunol. 119 (2000) 333-339.
[32] H. Trebeden-Negre, B. Weill, C. Fournier, F. Batteux, B cell apoptosis accelerates the onset of murine lupus, Eur. J. Immunol. 33 (2003) 1603-1612.
[33] E. Emlen, J. Nieber, R. Kadera, Accelerated in vitro apoptosis of lymphocytes from patients with systemic lupus erythematosus, J. Immunol. 152 (1994) 3685-3692.
[34] M. Bijl, G. Horst, P.C. Limburg, C.G. Kallenberg, Fas expression on peripheral blood lymphocytes in systemic lupus erythematosus (SLE): relation to lymphocyte activation and disease activity, Lupus 10 (2001) 866-872.
[35] B. Kovacs, S.N. Liossis, G.J. Dennis, G.C. Tsokos, Increased expression of functional Fas-ligand in activated T cells from patients with systemic lupus erythematosus, Autoimmunity 25 (1997) 213-221.
[36] T.S. Griffith, T. Brunner, S.M. Fletcher, D.S. Green, T.A. Ferguson, Fas ligand-induced apoptosis as a mechanism of immune privilege, Science 270 (1995) 1189-1192.
[37] M.R. Alderson, R.J. Armitage, E. Maraskovsky, T.W. Tough, E. Roux, K. Schooley, F. Ramsdell, D.H. Lynch, Fas transduces activation signals in normal human T lymphocytes, J. Exp. Med. 178 (1993) 2231-2235.
[38] H. Arai, D. Gordon, E.G. Nabel, G.J. Nabel, Gene transfer of Fas ligand induces tumor regression vivo, Proc. Natl. Acad. Sci. U. S. A. 94 (1997) 13862-13867.
[39] K. Seino, N. Kayagaki, K. Okumura, H. Yagita, Antitumor effect of locally produced CD95 ligand, Nat. Med. 3 (1997) 165-170.
[40] K. Miwa, M. Asano, R. Horai, Y. Iwakura, S. Nagata, T. Suda, Caspase 1-independent IL-1β release and inflammation induced by apoptosis inducer Fas ligand, Nat. Med. 4 (1998) 1287-1292.
[41] C.W. Distelhorst, Recent insights into the mechanism of glucocorticosteroid-induced apoptosis, Cell Death Differ. 9 (2002) 6-19.
[42] A. Nakajima, H. Hirai, N. Kayagaki, S. Yoshino, S. Hirose, H. Yagita, K. Okumura, Treatment with lupus in NZB/WF1 mice with monoclonal antibody against Fas ligand, J. Autoimmun. 14 (2000) 151-157.
[43] L. Goergescu, R.K. Vakkalanka, K.B. Elkon, M.K. Crow, Interleukin-10 promotes activation-induced cell death of SLE lymphocytes mediated by FasL, J. Clin. Invest. 100 (1997) 2622-2633.
[44] M. Chawla-Sarker, D.J. Linder, Y.F. Liu, B.R. Williams, G.C. Sen, R.H. Silverman, E.C. Borden, Apoptosis and interferons: role of interferon-stimulated genes as mediators of apoptosis, Apoptosis 8 (2003) 237-249.
[45] A. Cerwenka, H. Kovar, O. Majdic, W. Holter, Fas- and activation-induced apoptosis are reduced in human T cells preactivated in the presence of TGF-beta, J. Immunol. 156 (1996) 459-464.
[46] L. Genestier, S. Kasibhatla, T. Brunner, D.R. Green, Transforming growth factor β1 inhibits Fas ligand expression and subsequent activation-induced cell death in T cells via down-regulation of c-Myc, J. Exp. Med. 189 (1999) 231-239.
[47] W. Chen, W. Jin, H. Tian, P. Sicurello, M. Frank, J.M. Orenstein, S.M. Wahl, Requirement for transforming growth factor beta1 in controlling T cell apoptosis, J. Exp. Med. 194 (2001) 439-453.

Clin Exp Immunol 2004; 137:513–520 doi:10.1111/j.1365-2249.2004.02559.x

Amelioration of lupus manifestations by a peptide based on the complementarity determining region 1 of an autoantibody in severe combined immunodeficient (SCID) mice engrafted with peripheral blood lymphocytes of systemic lupus erythematosus (SLE) patients

N. MAUERMANN*†, Z. STIHOEGER†‡, H. ZINGER* & E. MOZES* *Department of Immunology, The Weizmann Institute of Science, Rehovot, Israel and †‡Department of Medicine 'B', Kaplan Hospital, Rehovot, Israel

(Accepted for publication 2 June 2004)

SUMMARY

A peptide based on the complementarity determining region (CDR)1 of a human monoclonal anti-DNA autoantibody (hCDR1) was shown to either prevent or treat an already established murine lupus in systemic lupus erythematosus (SLE)-prone mice or in mice with induced experimental SLE. The present study was undertaken to determine the therapeutic potential of hCDR1 in a model of lupus in severe combined immunodeficient (SCID) mice engrafted with peripheral blood lymphocytes (PBL) of patients with SLE. To this end, PBL obtained from lupus patients were injected intraperitoneally into two equal groups of SCID mice that were treated either with the hCDR1 (50 μg/mouse) once a week for 8 weeks, or with a control peptide. Mice were tested for human IgG levels, anti-dsDNA autoantibodies, anti-tetanus toxoid antibodies and proteinuria. At sacrifice, the kidneys of the successfully engrafted mice were assessed for human IgG and murine complement C3 deposits. Of the 58 mice transplanted with PBL of SLE patients, 38 (66%) were engrafted successfully. The mice that were treated with the control peptide developed human dsDNA-specific antibodies. Treatment with hCDR1 down-regulated the latter significantly. No significant effect of the treatment on the levels of anti-tetanus toxoid antibodies could be observed. Treatment with hCDR1 resulted in a significant amelioration of the clinical features manifested by proteinuria, human IgG complex deposits as well as deposits of murine complement C3. Thus, the hCDR1 peptide is a potential candidate for a novel specific treatment of SLE patients.

Keywords lupus PBL of patients peptide treatment SCID mice

INTRODUCTION

Systemic lupus erythematosus (SLE) is a non-organ-specific, T cell-dependent autoimmune disease that is characterized by the production of high-titre affinity-matured IgG anti-dsDNA autoantibodies. Other targets of the autoimmune response include nuclear proteins. The disease affects mainly women of childbearing age. Due to the systemic availability of the autoantigens, many tissues and organs are afflicted in SLE patients (e.g. dermal, haematological, renal, neurological, musculoskeletal manifestations are observed) [1,2]. There are several animal models for this disease, most of which are genetically based, where mouse strains develop spontaneously a SLE-like disease. The SLE-prone mice include (NZB×NZW) F1, MRL-lpr/lpr, *Palmerston* North (PN) and BXSB [3,4].

SLE can be induced in naive (not lupus-prone) mice by an active immunization with the human monoclonal anti-DNA antibody that bears the 16/6 idiotype (Id) or with the murine monoclonal anti-DNA 16/6Id, 5G12 antibody [5,6]. Immunized mice develop high levels of autoantibodies, and show SLE-related clinical manifestations (leukopenia, thrombocytopenia and renal impairment) [5,6]. It is noteworthy that high homologies were found between anti-dsDNA autoantibodies isolated from SLE-prone mice [(NZB×NZW) F_1] and autoantibodies from 16/6Id immunized diseased mice [7].

Two peptides, based on the sequence of the complementarity determining regions (CDR) 1 and 3 of the pathogenic murine anti-DNA 16/6Id were synthesized. The peptides were shown to be immunodominant T cell epitopes in non-autoimmune (e.g. BALB/c, SJL) and in lupus-prone (NZB×NZW) F_1 mice [8–10]. Treatment with the peptides ameliorated clinical manifestations

Correspondence: Edna Mozes PhD, Department of Immunology, The Weizmann Institute of Science, Rehovot 76100, Israel.
E-mail: *edna.mozes@weizmann.ac.il*
†N. M. and Z. S. contributed equally to this study.

© 2004 Blackwell Publishing Ltd

and decreased autoantibody production of spontaneous and induced SLE [11–13]. Amelioration of clinical manifestations following treatment with the CDR-based peptides was associated with down-regulation of interferon (IFN)-γ, interleukin (IL)-10 and tumour necrosis factor (TNF)-α (the latter in the induced model of BALB/c mice) and with an up-regulation of the immunosuppressive cytokine transforming growth factor (TGF)-β [11,13].

As a result of the above findings two peptides (hCDR1 and hCDR3), based on the CDRs of the human anti-DNA 16/6Id, were synthesized [14]. All CDR-based peptides (of either murine or human origin) were shown to inhibit the *in vitro* proliferation of human peripheral blood lymphocytes (PBL) of SLE patients to stimulation with 16/6Id. The inhibition correlated with a reduction in IL-2 secretion and an up-regulated secretion of the immunosuppressive cytokine TGF-β [14], suggesting a mechanism of inhibition similar to that observed for the animal models [11,13].

Several studies have been published in which attempts were made to create a human SLE model by transferring peripheral blood lymphocytes (PBL) of lupus patients into severe combined immunodeficient (SCID) mice [15–17]. We have reported recently the successful development of two reproducible models of human SLE [18]. One model has been of human PBL engrafted severe combined immunodeficient (SCID) mice, whereas the second model of human/mouse chimera was based on the previously reported studies of Lubin *et al.* [19]. Some of the SLE serological (human anti-DNA antibodies) and clinical manifestations (proteinuria, immune complex deposits in kidneys) of SLE were observed in the successfully engrafted mice of both models [18]. Thus these models allow the evaluation of potential therapies for the treatment of lupus patients.

In the present study we investigated the *in vivo* immunomodulating effect of the peptide based on the CDR1 of the human anti-DNA 16/6Id (hCDR1) on SLE-like disease in SCID mice transplanted with PBL of SLE patients. We report here the beneficial specific therapeutic effects of weekly injections of the hCDR1 on the serological (human dsDNA-specific antibodies) and clinical (proteinuria, human IgG and mouse complement C3 deposits in the kidney) manifestations.

MATERIALS AND METHODS

Mice

Female SCID mice (BALB/c background) 5–8 weeks old, were obtained from the Jackson Laboratory (Bar Harbor, ME, USA). The Animal Care and Use Committee of the Weizmann Institute of Science approved the study.

Synthetic peptides

A peptide (designated hCDR1) with the amino acid sequence GYYWSWIRQPPGKGEEWIG, based on the complementarity determining region 1 (CDR1) of the human monoclonal anti-DNA autoantibody that bears the 16/6Id, was synthesized (solid phase synthesis by F-moc chemistry) by Polypeptide Laboratories (LA, USA). A peptide with the amino acids of the hCDR1 synthesized in a scrambled order ('scrambled peptide'), SKGIPQYGGWPWEGWRYEI, was used as a control. hCDR1 (TV4710) is currently under clinical development for human SLE by Teva Pharmaceutical Industries Ltd.

SLE patients

Seven female SLE patients participated in this study. All fulfilled at least four of the ACR revised diagnostic criteria for SLE [20]. Patients were between 24 and 56 years old (mean 40·5 ± 13·4 years). All SLE patients had high levels of antinuclear antibodies (ANA) and anti-dsDNA antibodies in their sera at the time of the study. All patients (100%) had arthritis; six of them (86%) had haematological disturbances (two patients with haemolytic anaemia, two with thrombocytopenia and four with leukopenia). Three of the patients (43%) had renal involvement at some stage of their disease.

At the time of the study the disease activity index (SLEDAI [21]), was between 2 and 14 (mean 5·7 ± 5·12). One patient had active renal disease, two demonstrated lymphopenia, one thrombocytopenia and two had arthritis. Treatment modalities at the time of the study were prednisone (10–30 mg/day) in four patients, Plaquenil (400 mg/day) in two patients and methotrexate (7·5–10 mg/week) in two patients. All patients signed an informed consent form prior to their participation in the study, which was approved by the Ethics Committee of the Kaplan Medical Center, Rehovot, Israel.

Transplantation of human PBL and treatment

PBL obtained from SLE patients were injected intraperitoneally (i.p.) into 8–10-week-old recipient SCID mice at a concentration of 30×10^6 cells in 0·5 ml phosphate buffered saline (PBS). PBL of each donor were transferred into six to eight mice that were divided equally into two groups. One group was treated once a week, starting at the day of cell transfer with 50 μg hCDR1 given subcutaneously (s.c.) in PBS, whereas a control group was injected with the scrambled peptide. Mice were bled periodically and the sera were evaluated for the presence of human IgG, human anti-dsDNA antibodies and anti-tetanus toxoid (TT) antibodies.

Determination of human IgG

Levels of human IgG were measured by enzyme-linked imunosorbent assay (ELISA) [18], using a goat $F(ab)_2$ purified antihuman IgG (Jackson ImmunoResearch Laboratories, West Grove, PA, USA) as the capture antibody and peroxidase-conjugated goat antihuman Ig (Jackson) as the detection antibody. Human IgG at a known concentration was used as a standard in all assays.

ELISA for human antibodies

For determination of human anti-dsDNA antibodies in the recipient mouse sera maxisorb 96-well microtitre plates were coated with poly L-lysine (5 μg/ml, Sigma, St. Louis, MO, USA), followed by coating with lambda phage dsDNA (5 μg/well, Boehringer Mannheim, Germany). Plates were then blocked with 10% fetal calf serum (FCS) in PBS, and the sera (diluted 1 : 5–1 : 40) were incubated for 2 h. Plates were washed and incubated with a goat-antihuman IgG antibody conjugated to horseradish peroxidase (Jackson) for 90 min. Following washing, plates were incubated with the substrate ABTS (2·2'azino-bis-3-ethylbenzthiazoline-6-sulphonic acid; Sigma) and read at 405 nm using an ELISA reader (Tecan Spectra Classic, Austria).

For the detection of human tetanus, toxoid-specific antibodies purified TT (5 μg/ml, kindly provided by RAFA Laboratories Ltd, Israel) was used for coating of microtitre plates (Nunc Roskilde, Denmark). Plates were then washed, blocked, incubated with serum samples (diluted 1 : 10–1 : 1280) and developed with a

goat-antihuman IgG Fc-specific antibody conjugated to horseradish peroxidase. Plates were developed with ABTS. Results of anti-dsDNA and anti-TT are presented as OD per 1 mg of human IgG [18]. Positive and negative murine sera for dsDNA reactivity were further tested by Hep 2 (ANA) and by *Crithidia luciliae* (dsDNA) assays [18].

Proteinuria

Proteinuria was measured semiquantitively by using Albustix dipsticks (Ames Division, Bayer Diagnostics, Newbury, UK) on the following scale: 0 = undetectable, 1 = 0·3 g/l, 2 = 1 g/l, 3 = 3 g/l, 4 = ≥20 g/l.

Immunohistology of kidneys

Kidneys of sacrificed mice were frozen immediately in vials containing 0·5 ml isopentan (2-methylbutan) in liquid nitrogen. Kidney sections (6 micron) were air-dried and fixed in acetone. Staining with FITC-conjugated goat-antihuman IgG- (Jackson) and FITC-conjugated goat-antimouse complement C3 antibodies (Cappel, ICN Pharmaceuticals Inc., Aurora, OH, USA) were performed. Sections were visualized and graded, using a fluorescence microscope (Zeiss Axioskop 2, Germany).

Cytokine secretion and detection

Spleen cells (5×10^6/ml) of the tested mice were incubated with enriched medium and supernatants were removed after 48 h (for IFN-γ and IL-10) and 72 h (for TGF-β). Cytokine levels were measured by ELISA as described previously [13].

Statistical analysis

To test statistical significance for anti-dsDNA antibody production, proteinuria and kidney stainings between the treatment groups, the Mann–Whitney test with a two-tailed P-value and Fisher's exact test with two-sided P-value were performed.

RESULTS

Engraftment of PBL of SLE patients

Three separate experiments were performed in which SCID mice were injected i.p. with 30×10^6 PBL/mouse obtained from seven SLE patients. The recipients of PBL of each SLE patient were divided equally into two treatment groups that received weekly s.c. injections of either 50 μg hCDR1 or the control scrambled peptide (50 μg). Altogether, 58 recipient mice were injected with PBL of SLE patients. Engraftment of the human PBL in mice was determined based on the levels of human IgG in the mouse sera. Levels equal or above 100 μg/ml of human IgG indicated successful engraftment. Of the 58 mice transplanted with human PBL, 38 (66%) were engrafted successfully. Figure 1 demonstrates that the mean levels of human IgG produced by the engrafted PBL were about 500 μg/ml. It is also shown in Fig. 1 that the levels of human IgG were similar in the sera of mice that were treated with hCDR1 or scrambled peptide.

dsDNA-specific autoantibodies

During treatment of SCID mice, the titre of human anti-dsDNA antibodies was determined periodically. Figure 2 shows the kinetic of anti-dsDNA antibody production for two representative mice engrafted with PBL of the same lupus patient, one treated with hCDR1 and the other with the control peptide. It can be seen that the dsDNA-specific antibody levels peaked between

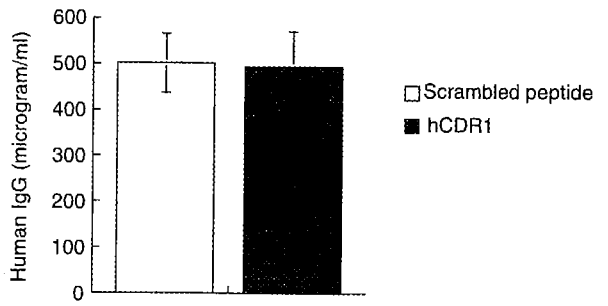

Fig. 1. Levels of total human IgG in sera of successfully engrafted SCID mice. Mean (± s.e.) levels of human IgG in sera of SCID mice 4–5 weeks following administration of human PBL.

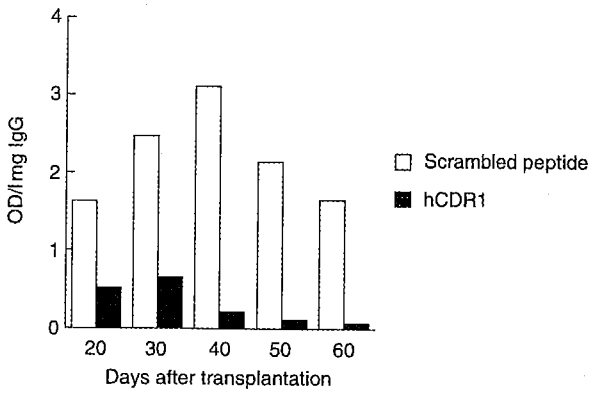

Fig. 2. Kinetics of anti-dsDNA specific antibody production. Kinetics of human anti-dsDNA antibody production, shown for two representative mice transplanted with PBL of the same lupus patient that were treated either with hCDR1 or with the control peptide. Mice were bled every 10 days and human anti-dsDNA antibody levels were determined by ELISA. The results are presented as OD/1 mg of human IgG determined for the same sera samples.

days 30 and 40 following cell transplantation and then started to decline. Figure 2 also shows that treatment with hCDR1 down-regulated significantly the production of the human anti-dsDNA antibodies. Figure 3a shows the mean anti-dsDNA antibody levels (OD/1 mg human IgG) in the sera of all mice in the two groups at the time that antibody levels peaked. As can be seen, anti-dsDNA antibody titres were significantly lower ($P = 0{\cdot}0053$) in the sera of the hCDR1-treated mice compared to sera of the control, scrambled peptide-treated mice. It is noteworthy that sera of 10 of the 21 (48%) SCID mice that were treated with the control peptide had levels of anti-dsDNA antibodies that were higher than 1 OD/1 mg of human IgG. In contrast, an OD of 1·03/1 mg IgG was observed in serum of only one of the 17 (6%) successfully engrafted mice that were treated with hCDR1. It should be noted that the results for dsDNA reactivity measured by ELISA correlated with the clinical assays for ANA and dsDNA reactivity measured by Hep 2 and *C. luciliae* assays. Thus, 90% of the sera determined to be positive for dsDNA reactivity by ELISA were determined to be positive by the clinical assays for ANA and dsDNA (≥ + +). Furthermore, as shown by ELISA, serum of only one mouse treated by hCDR1 was positive for ANA by the Hep 2 assay.

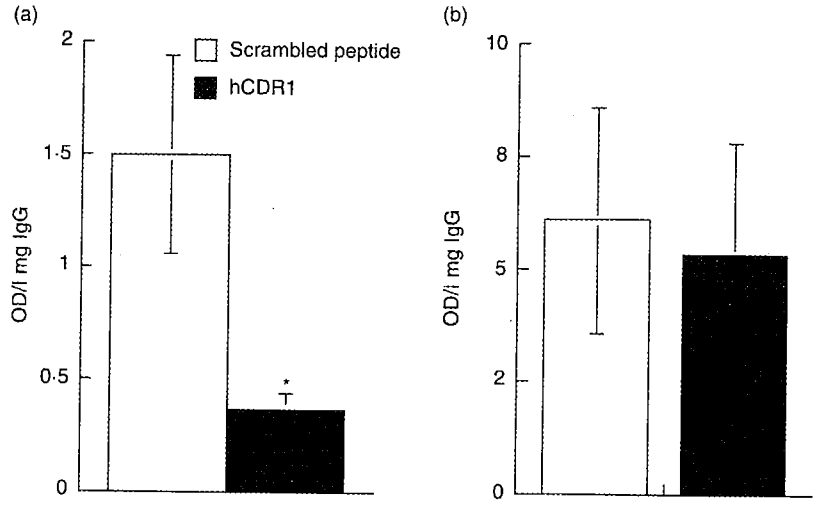

Fig. 3. Human anti-dsDNA and anti-tetanus toxoid antibodies in sera of SCID mice. Titres of human anti-dsDNA (a) and anti-tetanus toxoid (b) antibodies were determined by ELISA on the same sera samples (~ 40 days following cell transplantation). Shown are values of the mean OD/1 mg human IgG (± s.e.) for the two groups of mice, treated with either hCDR1 or the control peptide. $*P = 0{\cdot}0053$.

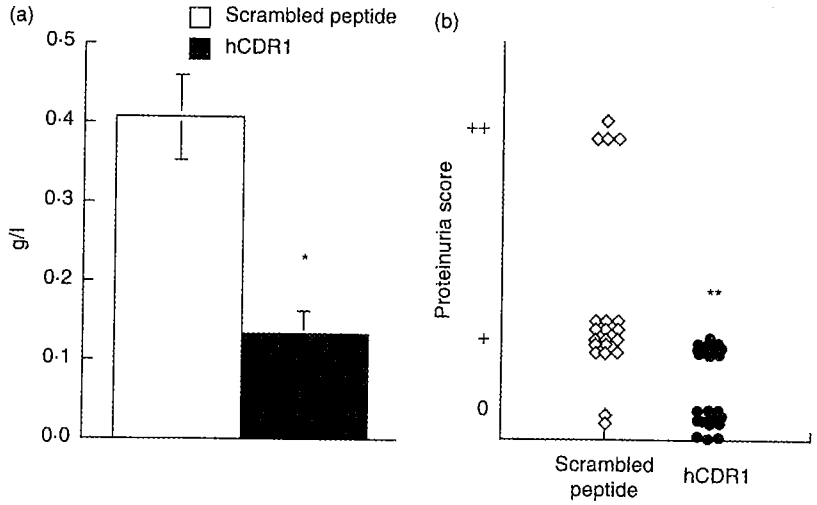

Fig. 4. Proteinuria in SCID mice engrafted with PBL of SLE patients. Levels of proteinuria were measured before sacrifice (~ 60 days following cell transfer). Results are expressed as (a). Mean (± s.e.) proteinuria (g/l) for all mice within a treatment group $*P = 0{\cdot}0002$. (b) Proteinuria score for individual mice in both treatment groups. $**P = 0{\cdot}0017$

Anti-tetanus toxoid antibodies

In order to determine whether hCDR1 treatment is specific to SLE-associated antibodies and does not affect other immune responses, we studied its effect on anti-TT antibody levels. Figure 3b shows levels of the anti-TT antibodies in the sera of mice from both treatment groups. The results indicate that there was no significant decrease in the antibody titres specific to TT, when sera samples of hCDR1-treated SCID mice were compared to those of control peptide-treated mice. Thus, the effect of hCDR1 is restricted to SLE-associated responses.

Cytokine secretion

Supernatants of splenocytes obtained from mice of the two treatment groups were tested for the secretion of IFN-γ, IL-10 and TGF-β. The secreted levels of IFN-γ and IL-10 were low (below the detectable sensitivity of the assay, 15 pg/ml for both IFN-γ and IL-10).

However, the secretion of TGF-β was higher (1102 ± 249 pg/ml) in supernatants of splenocytes of hCDR1-treated mice than in supernatants obtained from cells of scrambled peptide-treated mice (751 ± 62 pg/ml). Although the differences between groups did not reach significance, an increased secretion of TGF-β following hCDR treatment was demonstrated clearly.

SLE-associated clinical manifestations

The levels of proteinuria were determined periodically in the SCID mice. Although the measured levels were relatively low (up to 1 g/l) in both treatment groups, Fig. 4 shows a significant ($P = 0{\cdot}0002$) reduction in the mean proteinuria levels (Fig. 4a) and in the number of mice with detectable proteinuria (Fig. 4b) following treatment with hCDR1 ($P = 0{\cdot}0017$).

Table 1. Human Ig and murine complement C3 deposits in kidney sections of SCID mice engrafted with PBL of SLE patients and treated with hCDR1

Human IgG deposits		Murine C3 deposits	
Scrambled peptide 66% (14/21)	hCDR1 5·8% (1/17) $P = 0.0001$	Scrambled peptide 52% (11/21)	hCDR1 5·8% (1/17) $P = 0.0023$

Frozen cryostat sections (6 micron) of kidneys were stained with FITC-labelled goat antihuman IgG (γ-chain specific) or with FITC-goat-antimouse complement C3.

Kidney sections of all successfully engrafted mice were analysed for human IgG and mouse complement C3 depositions. The results summarized in Table 1 indicate that immune complex deposits were determined in 14 of 21 (66%) mice treated with the control peptide. In contrast, in kidney sections of only one of 17 (6%) mice treated with hCDR1 were human Ig immune complex deposits detected ($P = 0.0001$). The human IgG deposits in the glomeruli were associated with inflammatory glomerulonephritis, as demonstrated by the presence of murine complement C3 deposits. As also shown in Table 1 kidney sections of 11 of 21 (52%) control peptide-treated mice compared to only one of 17 (6%) hCDR1-treated mice had murine complement C3 deposits in their kidneys ($P = 0.0023$). It is noteworthy that the only kidney in the hCDR1-treated group that was positively stained for both human Ig and mouse complement C3 was that of the only mouse determined to have high dsDNA-specific antibody titre (1·03OD/1 mg of human IgG). The representative kidney sections which are shown in Fig. 5 demonstrate the absence of human Ig (Fig. 5d,e) and murine complement C3 (Fig. 5f) deposits in a kidney of a mouse treated with hCDR1 compared to the positive staining of the kidney of a control peptide-treated mouse (human Ig deposits Fig. 5a,b; murine complement C3 deposits, Fig. 5c).

DISCUSSION

The main findings of the present report are that a peptide based on the complementarity determining region (CDR)1 of a human monoclonal anti-dsDNA antibody that bears the 16/6Id is capable of ameliorating disease manifestations in SCID mice engrafted with PBL of SLE patients. Thus the peptide, hCDR1, has beneficial effects on a disease model that is the closest possible to human SLE.

We have reported previously successful attempts to establish an SLE model in SCID mice [18], showing then that engraftment with the PBL of SLE patients was successful in 71% of the recipient SCID mice. Similar results were obtained in the present study, where engraftment was successful in 66% of the recipients. The percentage of recipients with successful engraftment as well as the levels of human IgG measured in the engrafted mice was the same for mice that were treated either with the hCDR1 or with the control scrambled peptide (Fig. 1).

Production of dsDNA-specific antibodies is one of the hallmarks of SLE. Weekly injections of as little as 50 μg/mouse of the hCDR1 down-regulated significantly the levels of dsDNA-specific antibodies in the treated mice compared to mice engrafted with PBL of the same lupus donors that were treated with the control scrambled peptide (Figs 2 and 3a). The down-regulating effect of the hCDR1 on the human autoantibody levels was demonstrated further by using the standard clinical assays for ANA (Hep 2) and dsDNA (*C. luciliae*)-specific antibodies.

The optimal treatment for SLE, as well as for other autoimmune diseases, should down-regulate specifically SLE-associated responses without affecting other unrelated arms of the immune system. To this end, in the present study we tested the levels of the acquired antibody activity in the sera of recipient SCID mice to tetanus toxoid. The production of antibodies specific to tetanus toxoid by SCID mice engrafted with human PBL has been shown previously [18,22]. We showed here that treatment with hCDR1 did not affect the antibody levels to tetanus toxoid. Thus a comparable binding activity was determined in sera of recipients of PBL of the same donors that were treated with either hCDR1 or with the control scrambled peptide (Fig. 3b), suggesting that the down-regulating effect by the hCDR1 is indeed specific.

One of the major manifestations of lupus is kidney involvement. In the present study, 14 of the 21 (66%) successfully engrafted recipient mice that were treated with the control peptide developed immune complexes of human IgG in their kidneys. In the group that was treated once a week with 50 μgof hCDR1, only one of the 17 recipient mice developed immune complex deposits. Thus, treatment with hCDR1 abolished almost completely the kidney involvement in SCID mice with the lupus-like disease. No correlation could be determined between kidney disease in the lupus donor patients, in the past or at the time of the study, and the immune complex deposits in the recipient mice. These results are in agreement with our previous publication [18]. The human IgG deposits in the glomeruli were associated with inflammatory glomerulonephritis as suggested by the presence of proteinuria (Fig. 4a,b) which correlated with the glomerular IgG deposits. In addition, deposits of murine complement C3 were detected in the kidneys of 11 of the 14 SCID mice that were treated with the scrambled control peptide and had human IgG immune complexes (Table 1, Fig. 5). The ability of human Ig deposits to cause inflammatory glomerulonephritis by the interaction with mouse complement C3 in kidneys of SCID mouse/human model of lupus was reported previously by Duchosal *et al.* [15] as well as by us [18].

Previous studies utilizing the human/SCID mouse model dealt mainly with the production of anti-DNA antibodies and a limited number of other clinical symptoms that are characteristic for SLE [15–17]. As for treating SCID mice with lupus manifestations, it has been reported previously that anti-IL-10 monoclonal antibodies inhibited the production of anti-DNA antibodies in SCID mice engrafted with PBL of SLE patients [23]. Similarly, Kalechman *et al.* reported the reduction in autoantibody levels in a lupus model in SCID mice, following treatment with AS101 that down-regulates IL-10 [24]. The two latter studies utilized non-specific means that indeed down-regulated total immunoglobulin production, whereas the treatment with hCDR1 used in the present study inhibited specifically SLE-related responses without affecting antibody reactivity to tetanus toxoid and total IgG. More recently, Suzuki *et al.* reported the therapeutic effect of the chemically modified ribozyme (RZ-1) to target the V3-7 gene. In the reported model, PBL of patients with active lupus nephritis were treated *in vitro* with RZ-1 prior to their transfer to SCID mice. Beneficial effects were observed on the serological and clinical manifestations [25]. Unlike the *in vitro* manipulation performed in the latter report, treatment with

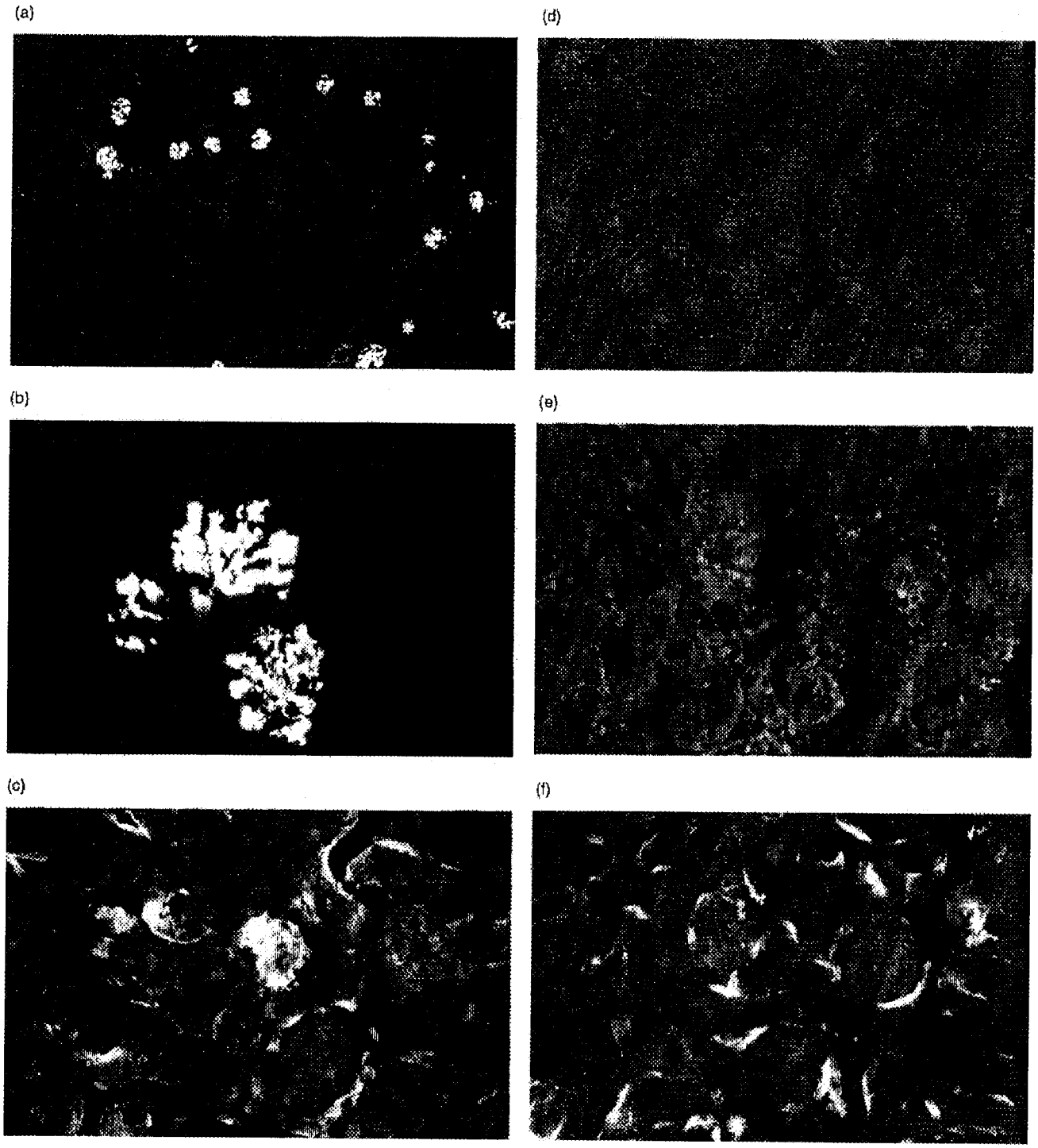

Fig. 5. Deposits of human IgG and mouse complement C3 in kidney sections of SCID mice engrafted with PBL of SLE patients. Frozen cryostat sections (6 micron) of kidneys (taken ~ 60 days following cell transfer) were air-dried, fixed with acetone and stained with either (a, b,d, e) FITC-labelled goat antihuman IgG (γ-chain specific) or (c, f) FITC-labelled goat antimouse complement C3 antibodies. Shown are representative kidney sections of two mice, engrafted with PBL of the same SLE patient. (a, b, c) Kidney sections of a mouse treated with the control scrambled peptide; (d, e, f) kidney sections of a mouse treated with hCDR1 (a, d ×100 and b, e, c, f ×400).

hCDR1 was given *in vivo* by s.c. injections resembling possible treatment protocols of patients.

The peptides that are based on the CDR of the murine anti-DNA 16/6Id autoantibody as well as the hCDR1 were shown by us to be capable of ameliorating experimental SLE in induced and spontaneous animal models [8,11–13 and Luger *et al.*, unpublished data]. Other laboratories have also reported the beneficial effects of peptides based on variable regions of autoantibodies or

of a consensus peptide based on amino acid sequences of murine anti-DNA monoclonal antibodies on experimental models of SLE [26–30]. The latter reports as well as ours support the crucial role of peptides derived from heavy chain variable regions in the immunomodulation of murine lupus. We have shown previously that peptides based on the murine or human anti-DNA monoclonal autoantibodies down-regulated the *in vitro* anti-DNA-specific proliferative responses of PBL of SLE patients [14]. The present study shows that the hCDR1 is also efficient in the *in vivo* amelioration of disease symptoms manifested by PBL of SLE patients.

The mechanism by which the hCDR1 ameliorates SLE characteristic manifestations is currently studied. We have shown previously that treatment of SLE-afflicted mice with the CDR-based peptides down-regulates IFN-γ, IL-10 and proinflammatory cytokines (TNF-α, IL-1β). In contrast, the treatment leads to an up-regulated production of the immunosuppressive cytokine TGF-β [11,13]. We have shown further that the inhibition of proliferative responses of PBL of SLE patients is associated with an increase in the secretion of TGF-β [18]. In agreement, in the present study treatment with hCDR1 also up-regulated the secretion of TGF-β, suggesting that this immunosuppressive cytokine plays an important role in the mechanism by which the hCDR1 ameliorates SLE. Our recent studies indicate that hCDR1 up-regulates a population of $CD4^+CD25^+$ immunoregulatory cells that play a key role in the inhibitory activity of the hCDR1 (Mauermann *et al.*, unpublished data). These cells may either secrete TGF-β by themselves or they may trigger other regulatory T cell populations to secrete this suppressive cytokine. Nevertheless, as shown here treatment with hCDR1 is beneficial in an *in vivo* model of human lupus. The hCDR1 is therefore a novel potential candidate for the specific treatment of SLE patients.

ACKNOWLEDGEMENT

This work was supported by Teva Pharmaceutical Industries, Ltd, Israel.

REFERENCES

1 Hahn BH. An overview of the pathogenesis of systemic lupus erythematosus. In: Wallace DJ, Hahn BH, eds. Dubois' lupus erythematosus. Philadelphia: Williams & Wilkins, 1993:69–76.

2 Winchester RJ. Systemic lupus erythematosus pathogenesis. In: Koopman WJ, ed. Arthritis and allied conditions. Birmingham, AL: Williams & Wilkins, 1996: 69–76.

3 Steinberg AD. Systemic lupus erythematosus: insight from animal models. Ann Int Med 1984; **100**:714–27.

4 Theofilopoulos AN, Dixon FJ. Murine models of systemic lupus erythematosus. Adv Immunol 1985; **27**:269–390.

5 Mendlovic S, Brocke S, Shoenfeld Y *et al.* Induction of a systemic lupus erythematosus-like disease in mice by a common human anti-DNA idiotype. Proc Natl Acad Sci USA 1988; **85**:2260–4.

6 Waisman A, Mendlovic S, Ruiz PJ, Zinger H, Meshorer A, Mozes E. The role of the 16/6 idiotype network in the induction and manifestation of systemic lupus erythematosus. Int Immunol 1993; **5**:1293–300.

7 Waisman A, Mozes E. Variable region sequences of autoantibodies from mice with experimental systemic lupus erythematosus. Eur J Immunol 1993; **23**:1566–73.

8 Waisman A, Ruiz PJ, Israeli E *et al.* Modulation of murine systemic lupus erythematosus with peptides based on complementarity determining regions of a pathogenic anti-DNA monoclonal antibody. Proc Natl Acad Sci USA 1997; **94**:4620–5.

9 Brosh N, Eilat E, Zinger H, Mozes E. Characterization and role in experimental systemic lupus erythematosus of T-cell lines specific to peptides based on complementarity-determining region-1 and complementarity-determining region-3 of a pathogenic anti-DNA monoclonal antibody. Immunology 2000; **99**:257–65.

10 Brosh N, Dayan M, Fridkin M, Mozes E. A peptide based on the CDR3 of an anti-DNA antibody of experimental SLE origin is also a dominant T-cell epitope in (NZB×NZW) F1 lupus-prone mice. Immunol Lett 2000; **72**:61–8.

11 Eilat E, Dayan M, Zinger H, Mozes E. The mechanism by which a peptide based on the complementarity-determining region-1 of a pathogenic anti-DNA auto-Ab ameliorates experimental systemic lupus erythematosus. Proc Natl Acad Sci USA 2001; **98**:1148–53.

12 Eilat E, Zinger H, Nyska A, Mozes E. Prevention of systemic lupus erythematosus-like disease in (NZB×NZW) F_1 mice by treating with CDR-1 and CDR-3 based peptides of a pathogenic autoantibody. J Clin Immunol 2000; **20**:268–78.

13 Zinger H, Eilat E, Meshorer A, Mozes E. Peptides based on the complementarity-determining regions of a pathogenic autoantibody mitigate lupus manifestations of (NZB×NZW) F_1 mice via active suppression. Int Immunol 2003; **15**:205–14.

14 Sthoeger ZM, Dayan M, Tcherniak A *et al.* Modulation of autoreactive responses of peripheral blood lymphocytes of patients with systemic lupus erythematosus by peptides based on human and murine anti-DNA autoantibodies. Clin Exp Immunol 2003; **131**:385–92.

15 Duchosal MA, McConahey PJ, Robinson CA, Dixon FJ. Transfer of human systemic lupus erythematosus in severe combined immunodeficient (SCID) mice. J Exp Med 1990; **172**:985–8.

16 Ashany D, Hines J, Gharavi A, Moiradian J, Elkon KB. Analysis of antibody production in SCID-systemic lupus erythematosus (SLE) chimeras. Clin Exp Immunol 1992; **88**:84–90.

17 Vladutiu AO. The severe combined immunodeficient (SCID) mouse as a model for the study of autoimmune diseases. Clin Exp Immunol 1993; **93**:1–8.

18 Sthoeger Z, Zinger H, Dekel B, Arditi F, Reisner Y, Mozes E. Lupus manifestations in severe combined immunodeficient (SCID) mice and in human/mouse radiation chimera. J Clin Immunol 2003; **23**:91–9.

19 Lubin I, Segall H, Marcus H *et al.* Engraftment of human peripheral blood lymphocytes in normal strains of mice. Blood 1994; **83**:2368–81.

20 Tan EM, Cohen AS, Fries JF *et al.* The 1982 revised criteria for the classification of systemic lupus erythematosus. Arthritis Rheum 1982; **25**:1271–7.

21 Bombardier C, Gladman DD, Urowitz MB, Caron D, Chang CH. Derivation of the SLEDAI. A disease activity index for lupus patients. The Committee on Prognosis Studies in SLE. Arthritis Rheum 1992; **35**:630–40.

22 Somasundaram R, Jacob L, Herlyn D. Tetanus toxoid-specific T cell responses in severe combined immunodeficiency (SCID) mice reconstituted with human peripheral blood lymphocytes. Clin Exp Immunol 1995; **101**:94–9.

23 Llorente L, Zou W, Levy Y *et al.* Role of interleukin 10 in the B lymphocyte hyperactivity and autoantibody production of human systemic lupus erythematosus. J Exp Med 1995; **181**:839–44.

24 Kalechman Y, Da Gafter UJP, Albeck M, Alarcon-Segovia D, Sredni B. Delay in the onset of systemic lupus erythematosus following treatment with the Immunomodulator AS101. J Immunol 1997; **159**:2658–67.

25 Suzuki Y, Funato T, Munakata Y *et al.* Chemically modified ribozyme to Vgene inhibits anti-DNA production and the formation of immune deposits caused by lupus lymphocytes. J Immunol 2000; **165**:5900–5.

26 Singh RR, Ebling FM, Sercarz EE, Hahn BH. Immune tolerance to autoantibody-derived peptides delays development of autoimmunity in murine lupus. J Clin Invest 1995; **96**:2990–6.

27 Singh RR, Kumar V, Ebling FM *et al.* T cell determinants from autoantibodies to DNA can upregulate autoimmunity in murine systemic lupus erythematosus. J Exp Med 1995; **181**:2017–27.

28 Kaliyaperumal A, Michaels MA, Datta SK. Antigen-specific therapy of murine lupus nephritis using nucleosomal peptides. Tolerance spreading impairs pathogenic function of autoimmune T and B cells. J Immunol 1999; **162**:5775–83.

29 Jouanne C, Avrameas S, Payelle-Brogard B. A peptide derived from a polyreactive monoclonal anti-DNA natural antibody can modulate lupus development in (NZB×NZW) F_1 mice. Immunology 1999; **96**:333–9.

30 Hahn BH, Singh RR, Wong WK, Tsao BP, Bulpitt K, Ebling FM. Treatment with a consensus peptide based on amino acid sequences in autoantibodies prevents T cell activation by autoantigens and delays disease onset in murine lupus. Arthritis Rheum 2001; **44**:432–41.

NEUROLOGY

Neuroprotective agents for clinical trials in ALS: A systematic assessment

B. J. Traynor, L. Bruijn, R. Conwit, F. Beal, G. O'Neill, S. C. Fagan and M. E. Cudkowicz

Neurology 2006;67;20-27
DOI: 10.1212/01.wnl.0000223353.34006.54

This information is current as of September 12, 2006

The online version of this article, along with updated information and services, is located on the World Wide Web at:
http://www.neurology.org/cgi/content/full/67/1/20

Neurology is the official journal of AAN Enterprises, Inc. A bi-monthly publication, it has been published continuously since 1951. Copyright © 2006 by AAN Enterprises, Inc. All rights reserved. Print ISSN: 0028-3878. Online ISSN: 1526-632X.

AMERICAN ACADEMY OF NEUROLOGY

Downloaded from www.neurology.org by MICHAEL FETELL on September 12, 2006

Neuroprotective agents for clinical trials in ALS

A systematic assessment

B.J. Traynor, MD, MRCPI; L. Bruijn, PhD; R. Conwit, MD; F. Beal, MD; G. O'Neill, MD, MRCPI; S.C. Fagan, PharmD, FCCP; and M.E. Cudkowicz, MD, MSc

Abstract—*Background:* Riluzole is currently the only Food and Drug Administration–approved treatment for ALS, but its effect on survival is modest. *Objective:* To identify potential neuroprotective agents for testing in phase III clinical trials and to outline which data need to be collected for each drug. *Methods:* The authors identified 113 compounds by inviting input from academic clinicians and researchers and via literature review to identify agents that have been tested in ALS animal models and in patients with ALS. The list was initially narrowed to 24 agents based on an evaluation of scientific rationale, toxicity, and efficacy in previous animal and human studies. These 24 drugs underwent more detailed pharmacologic evaluation. *Results:* Twenty drugs were selected as suitable for further development as treatments for patients with ALS. Talampanel and tamoxifen have completed early phase II trials and have demonstrated preliminary efficacy. Other agents (ceftriaxone, minocycline, ONO-2506, and IGF-1 polypeptide) are already in phase III trials involving large numbers of patients with ALS. Remaining agents (AEOL 10150, arimoclomol, celastrol, coenzyme Q10, copaxone, IGF-1–viral delivery, memantine, NAALADase inhibitors, nimesulide, scriptaid, sodium phenylbutyrate, thalidomide, trehalose) require additional preclinical animal data, human toxicity and pharmacokinetic data including CNS penetration prior to proceeding to large scale phase III human testing. Further development of riluzole analogues should be considered. *Conclusions:* Several potential neuroprotective compounds, representing a wide range of mechanisms, are available and merit further investigation in ALS.

NEUROLOGY 2006;67:20–27

Riluzole is the only Food and Drug Administration (FDA)–approved drug for ALS, but it has only a modest affect on survival. ALS has a median survival of 3 to 5 years.[1] A number of mechanisms are thought to initiate and propagate the neurodegenerative process in ALS, including oxidative stress, mitochondrial dysfunction, excitotoxicity, apoptosis, inflammation, and glial activation.[2] These advances in ALS research, together with the application of high throughput drug screening such as the National Institute of Neurologic Disorders and Stroke Neurodegeneration Drug Screening Consortium,[3] have yielded a large number of drug candidates that may be neuroprotective. However, only a small number of drug candidates can be tested at any one time, as resources available to the ALS community are limited both in terms of eligible research participants and funds. A transparent and rational selection process is required to determine which candidate agents should be prioritized for clinical trial development. A systematic approach to drug selection, rather than pursuing the latest "hot" compound, is important both for ALS and for the broader issue of research strategy in neurodegenerative disorders.

We describe the drug identification and review processes and outline attractive neuroprotective candidates for future ALS clinical trials. Priority was given to making the drug selection process explicit, transparent, and reproducible. We also identify data to be collected for each drug prior to proceeding to

Additional material related to this article can be found on the *Neurology* Web site. Go to www.neurology.org and scroll down the Table of Contents for the July 11 issue to find the title link for this article.

From the Neurology Clinical Trials Unit (B.J.T., M.E.C.), Department of Neurology, Massachusetts General Hospital, Boston; The ALS Association (L.B.), Palm Harbor, FL; National Institute of Neurological Diseases and Stroke (NINDS) (R.C.), Bethesda, MD; Department of Neurology (F.B.), Weill Medical College of Cornell University, New York, NY; Biogen Idec Inc. (G.O.), Cambridge, MA; and University of Georgia College of Pharmacy and Medical College of Georgia (S.C.F.), Augusta.

Disclosure: The authors report no conflicts of interest.

Received August 23, 2005. Accepted in final form March 10, 2006.

Address correspondence and reprint requests to Dr. Bryan J. Traynor, SDGE, NIMH, Building 35, Room 1A110, 35 Convent Drive, Bethesda, MD 20892-3720; e-mail: traynorb@mail.nih.gov

 Copyright © 2006 by AAN Enterprises, Inc.

Downloaded from www.neurology.org by MICHAEL FETELL on September 12, 2006

Copyright © by AAN Enterprises, Inc. Unauthorized reproduction of this article is prohibited.

Table 1 *Evaluation criteria for potential neuroprotective agents in ALS**

Criteria	Operational definition
Scientific rationale	Consistency of preclinical data; credible mechanism relevant to ALS although mechanism may be unknown in many cases
Safety and tolerability	Safe and tolerable in humans in the dose and route of administration needed for the proposed effect. Further safety data may be required before use in ALS
Efficacy in relevant animal	Efficacy in rodent model of ALS or other relevant models of disease
Indication of benefit in human clinical studies	Evidence from previous trials that is suggestive of a neuroprotective effect or epidemiologic data fulfilling criteria for causal inference

*Developed from criteria for evaluation of neuroprotective agents in Parkinson disease.[4]

phase III efficacy testing enrolling large numbers of patients with ALS.

Methods. *Drug selection process.* We first identified a wide spectrum of potential therapeutic agents and a broad range of strategies that could potentially slow disease progression and prolong survival in patients with ALS. We incorporated 1) therapies with mechanisms of action relevant to ALS pathogenesis, 2) agents that have already been tested in ALS animal models or clinical trials, and 3) medications approved or under consideration for neurodegenerative diseases other than ALS. Input was obtained from academic scientists, clinicians, and patient groups to capture the broadest range of available compounds. We also searched Medline to identify publications concerning agents that had been tested in ALS animal models (table E-1 on the *Neurology* Web site at www.neurology.org) or in human trials (table E-2).

Selection of drugs for detailed pharmacologic and safety assessment. We identified 113 therapeutic agents as potentially beneficial in patients with ALS (table E-3). Each therapeutic intervention was assessed by the authors (B.J.T., L.B., R.C., F.B., G.O., M.E.C.) according to the following criteria established at the February 2004 meeting: 1) scientific rationale (i.e., an effect on a pathway implicated in ALS), 2) drug safety and tolerability in humans, 3) indication of benefit in human clinical studies, and 4) efficacy of the drug in ALS animal models. The assessment criteria were developed from those previously employed in evaluating neuroprotective agents in Parkinson disease (PD) (table 1).[4] The inability of ALS animal models to predict beneficial effects in human trials is recognized[5] and consequently data from $SOD1^{G93A}$ mouse model were only one of several preclinical data points examined in the drug evaluation process. Data from cell-based screening were included where relevant, though an in-depth review of drug discovery techniques is beyond the scope of this article. Both published and unpublished information was considered. To maintain transparency of the process, expand discussion, and further scientific rigor, we circulated the list of 113 therapeutic agents (table E-3) within the ALS research community. Twenty-four drugs judged to be the most promising agents were selected for further analysis. The reasons for not selecting the remaining 89 drugs for detailed review are also listed in table E-3.

Detailed pharmacologic and safety assessment of proposed agents. A clinical pharmacologist (S.F.) with expertise in neurologic drugs performed a detailed pharmacokinetic and safety assessment of the 24 selected drugs (table E-4). The complete pharmacokinetic, tolerability, and preclinical data sets were employed to select neuroprotective candidates for future ALS clinical trials using a scorecard method (table 2). The pharmaceutical company or academic scientist directly responsible for developing that agent was contacted to obtain further data.

TCH346 was excluded from the final list based on negative results of phase III studies that were not available during the initial review.[6] Vitamin E was excluded based on the results of two negative clinical trials.[7,8] Adverse side effects and unfavorable pharmacokinetics eliminated NBQX. Nimodipine was eliminated due to insufficient scientific rationale to support its development as an ALS therapy. Through this process we determined that 20 drugs are viable candidates to be explored in ALS clinical trials in the future (figure and table 3).

Annual reassessments of newly published data on existing and novel neuroprotective agents will also be provided on the ALS Association Web site and will be presented at the International ALS/MND Symposium on a yearly basis.

Description of priority agents. *AEOL 10150 (Aeolus Science Inc.).* Oxidative damage mediated by toxic free radicals has been implicated in the pathogenesis of ALS[9] and a variety of antioxidants have been tested in patients with ALS (table E-2). AEOL 10150 is a manganoporphyrin antioxidant that catalytically neutralizes superoxide, hydrogen peroxide, and peroxynitrite, and inhibits lipid peroxidation.[10] Administration of AEOL 10150 to transgenic mice with the glycine 93 to alanine SOD1 mutation ($SOD1^{G93A}$) commencing at symptom onset improved the survival interval (the time from symptom onset to death) by 196% (26.5 days).[11] The compound has to be administered IV or by subcutaneous injection. A phase I single dose escalating study enrolling 30 patients with ALS is underway to determine pharmacokinetic, optimum dose, and safety properties of this novel drug class.

Arimoclomol (Cytrx Corporation). Motor neurons have an intrinsically higher threshold for activation of the heat shock protein pathway[12] and agents that upregulate this pathway may be neuroprotective. Arimoclomol is a hydroxylamine derivative that co-induces heat shock protein (HSP) expression,[13] a powerful cytoprotective mechanism under acute stress conditions. Treatment with arimoclomol prolonged the lifespan of $SOD1^{G93A}$ mice by 22% (28 days).[14] The beneficial effect was independent of whether the treatment was started pre-symptomatically or at symptom onset. Arimoclomol was well tolerated in a phase I study of healthy volunteers (http://www.cytrx.com/prDetail.cfm?pr_id= 164&showcspr=1). Safety, optimum dose, and pharmacokinetics of arimoclomol (including ability to cross blood–brain barrier [BBB]) are unknown for patients with ALS. A multicenter, dose ranging, phase II study of arimoclomol in ALS has commenced enrollment (n = 80, www.clinicaltrials.gov, NCT00244244).

Ceftriaxone (Roche Laboratories). Glutamate-mediated excitotoxicity arising from repetitive firing or elevation of intracellular calcium by calcium-permeable glutamate receptors is likely to be an important contributor to motor neuronal death in ALS.[1] Glutamate levels are increased in CSF of patients with sporadic ALS[15] and clearance of glutamate from neuromuscular synapses is also diminished in patients with ALS due to loss of the astroglial glutamate transporter EAAT2.[16] Furthermore, spinal motor neurons are relatively reduced in intracellular calcium-binding components,[17] which may account for their selective vulnerability.[2]

The antiexcitatory and antioxidant properties of cephalosporins were identified by the Neurodegeneration Drug Screening Consortium that screened 1040 FDA-approved drugs for efficacy in in vitro models of neurodegenerative diseases.[18] Cephalosporins increase EAAT2 promoter activ-

Downloaded from www.neurology.org by MICHAEL FETELL on September 12, 2006
Copyright © by AAN Enterprises, Inc. Unauthorized reproduction of this article is prohibited.

Table 2 *Scorecard outlining detailed pharmacologic and safety assessment of 24 neuroprotective drugs in patients with ALS*

Agent	Mechanism of action	PK	ALS mouse model	Human safety	Benefits in ALS
AEOL 10150	Antioxidant	0	++	0	0
Arimoclomol	HSP inducer	0	+	+	0
Ceftriaxone	Antioxidant and antiglutamate	+	+	+++	0
Celastrol	Antioxidant and anti-inflammatory	0	+	0	0
CoQ10	Antioxidant and mitochondrial factor	+	++	++	0
Copaxone	Immunomodulatory	0	–/+	+++	0
IGF-1	Neurotrophic	0	+ (wobbler)	++	+/–
IGF-1-AAV	Neurotrophic	0	+	0	0
Memantine	Antiglutamate	++	0	+++	0
Minocycline	Antiapoptotic	++	++	+++	0
Naaladase inhibitor	Antiglutamate	0	+	0	0
NBQX	Antiglutamate	0	+	–	0
Nimesulide	Anti-inflammatory and antioxidant	0	–	+++	0
Nimodipine	Ca^{2+} channel blocker	++	+	+++	–
ONO-2506	Glial modulator and antiglutamate	0	0	0	0
Riluzole	Antiglutamate and Na channel inactivation	+	++	++++	+++
Scriptaid	Antiaggregation	0	0	0	0
Phenylbutyrate	HDAC inhibitor	0	+	+++	0
Talampanel	Antiglutamate	+	+	++	+
Tamoxifen	Protein kinase C inhibitor	+	+ (viral model)	+++	+
TCH346	Antiapoptotic	+	–/+	++	–
Thalidomide	Immunomodulatory and antiangiogenic	+	+	+++	0
Trehalose	Antiaggregation	0	0	+++	0
Vitamin E	Antioxidant	+	+	+++	–

Pharmacokinetics: 0 = data on ability of drug to penetrate CSF are unknown; + = drug known to penetrate CSF; ++ = drug has excellent CSF penetration. ALS mouse model: 0 = effect on ALS mouse model unknown to us; – = one mouse study with negative effect on survival; + = one mouse study with a positive effect on survival; ++ = two mouse studies with positive effects on survival; ½ = two animal studies performed, one showed beneficial effect, the other displayed a negative effect on survival. Human safety: 0 = safety in humans not known; + = one human trial that showed drug was relatively safe; ++ = two human trials that showed drug was relatively safe; +++ = FDA/EMEC approved for chronic use in other disorders; ++++ = FDA/EMEC approved as an ALS drug. Benefits in ALS: 0 = unknown; – = negative trial in well-designed studies; + = positive (or trend) efficacy in phase II trials; +++ = FDA/EMEC approved as an ALS drug.

ity and protect motor neurons from glutamate toxicity in culture.[18] The third generation ceftriaxone was selected for human studies because of its superior CNS penetration and long half-life.[19] $SOD1^{G93A}$ transgenic mice treated with ceftriaxone at symptom onset lived 8% (10 days) longer than control animals.[18] Ceftriaxone is generally well tolerated,[20] though experience with long term IV administration (beyond 6 weeks) is limited. A combined phase II and III study will commence enrollment in the near future.

Celastrol (generic). Neuroinflammation occurs in the brainstem and spinal cord of patients with ALS[21] and $SOD1^{G93A}$ mice suggesting that anti-inflammatory agents may be effective in treating this disease.[22] Celastrol is a potent anti-inflammatory and antioxidant triterpene that suppresses TNFα, IL-1β, and inducible nitric oxide production[23] and induces a heat shock protein response.[24] Administration of celastrol from 4 weeks of age improved weight loss, rotorod performance, and survival of $SOD1^{G93A}$ mice.[25] Further data concerning the ability of the drug to cross the BBB, toxicity, and safety in patients with ALS

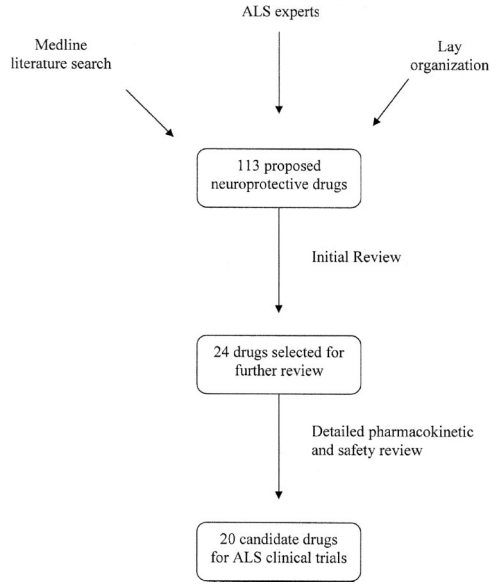

Figure. Drug identification and assessment sequence.

Downloaded from www.neurology.org by MICHAEL FETELL on September 12, 2006
Copyright © by AAN Enterprises, Inc. Unauthorized reproduction of this article is prohibited.

Table 3 *Priority list for phase III ALS clinical trials*

A. Suitable for phase III trials in the near future
   1. Talampanel
   2. Tamoxifen

B. Already in phase III trials involving large number of human subjects
   1. Ceftriaxone
   2. IGF-1 polypeptide
   3. Minocycline
   4. ONO-2506

C. More data required prior to phase III testing
   1. AEOL 10150†‡§
   2. Arimoclomol*†‡§
   3. Celastrol*†‡§
   4. Coenzyme Q10‡§
   5. Copaxone*§
   6. IGF-1–viral delivery*†‡§
   7. Memantine*†‡§
   8. NAALADase inhibitors*†‡§
   9. Nimesulide*‡§
   10. Scriptaid*†‡§
   11. Sodium phenylbutyrate†‡§
   12. Thalidomide†‡§
   13. Trehalose*‡§

D. Already Food and Drug Administration approved as ALS therapy
   1. Riluzole and related benzothiazole drugs (see text for further details)

*Transgenic efficacy animal studies.
†Human toxicology.
‡CNS pharmacokinetic studies.
§Dose-ranging studies.

and optimum dose remain to be collected prior to phase III testing.

Coenzyme Q10 (generic). The high metabolic load of motor neurons and the consequent dependence of these cells on oxidative phosphorylation may make them particularly vulnerable to the loss of mitochondrial function.[1] Coenzyme Q10 is an antioxidant and an essential mitochondrial cofactor facilitating electron transfer in the respiratory chain.[26] This commonly used nutraceutical is being tested in neurodegenerative conditions in which mitochondrial dysfunction has been implicated including ALS, Huntington disease (HD), and PD. Low dose coenzyme Q10 prolonged median survival of $SOD1^{G93A}$ transgenic mice by only 4.4% (6 days),[27] but higher doses are more effective (Flint Beal, personal communication). Doses up to 3,000 mg per day are safe and well tolerated in patients with ALS.[28] Coenzyme Q10 is lipophilic and effectively crosses the BBB.[29] A phase II study in ALS has commenced enrollment (NCT00243932).

Copaxone/glatiramate (Teva Pharmaceuticals). Previous clinical trials of immunosuppressant therapies failed to slow progression in ALS,[30] but immunomodulation may be more effective at preventing neuronal apoptosis.[31] Copaxone evokes a neuroprotective T cell-mediated response and may protect against glutamate toxicity.[31] Low copy number $SOD1^{G93A}$ ALS mice immunized at 60 days of age followed by oral dosing of copolymer-1 experienced a 24.6% (52 day) increase in lifespan and delayed disease onset,[31] though these findings have not been replicated in high copy $SOD1^{G93A}$ mice treated with a copaxone derivative.[32] Additional preclinical data are required to determine reproducibility and optimum dosing schedule to achieve immunomodulation.

Insulin-like growth factor 1 (IGF-1, Cephalon). Neurotrophic factors selectively regulate survival and differentiation of nerve cells and maintain neuronal structural integrity. Of all neurotrophic factors tested in ALS to date (table E-2), only IGF-1 slowed the rate of functional decline by 26% in a North American phase III trial (n = 266).[33] In contrast, a European IGF-1 trial was negative (n = 183)[34] and so a third phase III trial of this neurotrophic factor is currently underway (n = 330, NCT00035815) to conclusively determine efficacy. IGF-1 is well tolerated, though the large size of the IGF-1 polypeptide may prevent BBB penetration. There are no published reports of the effect of IGF-1 on mutant $SOD1^{G93A}$ mouse survival.

IGF-1—viral delivery (Ceregene, Inc.). Adeno-associated virus engineered to contain the gene for IGF-1 (AAV-IGF1) allows targeted delivery of IGF-1 to motor neurons. After IM injection, the gene vector is transported to the neuronal cell body by retrograde axonal transport along motor neurons.[35] AAV-IGF-1 prolongs median survival by 30% (37 days) when administered before disease onset.[35] Human safety, dose schedule, and pharmacokinetics have not yet been established for this novel gene therapy, though AAV-factor IX vector has proven safe in patients with hemophilia.[36] A small phase IIa trial of AAV-IGF-1 is planned for the near future. Expansion of the viral vector production capacity will be required before proceeding to large scale trials.

Memantine (Forest Laboratories, Inc.). The higher expression of calcium-permeable α-amino-3-hydroxy-5-methyl-4-isoxazole propionic acid (AMPA) glutamate receptors on motor neurons may explain the selective vulnerability of this cell type to glutamate excitotoxicity.[37] Memantine (an amino adamantine derivative) is an AMPA receptor antagonist licensed as a neuroprotective agent for Alzheimer disease (AD). The drug exhibits excellent CNS penetration[38] and is well tolerated by patients with AD, but there are no published studies of the survival effect of in ALS animal models and additional data to support the rationale for testing in patients with ALS are needed.

Minocycline (generic). The role of apoptosis in motor neuron degeneration is increasingly recognized. In SOD1-mediated ALS, motor neurons probably die through the formation of insoluble mutant SOD1 aggregates that bind to and deplete motor neurons of the antiapoptotic protein Bcl-2 allowing activation of caspases.[39,40] Although apoptosis is a late event in the degeneration of motor neurons, inhibition of programmed cell death might ameliorate ALS.[1] Minocycline is a second generation tetracycline antibiotic that prevents microglial activation[41] and inhibits caspase activation.[42] Four SOD1 transgenic mouse studies show enhanced median survival ranging between 6.4% and 16%.[41-44] Two small phase II studies demonstrated safety and tolerability of minocycline in patients with ALS (n =

Downloaded from www.neurology.org by MICHAEL FETELL on September 12, 2006
Copyright © by AAN Enterprises, Inc. Unauthorized reproduction of this article is prohibited.

19 and 23).[45] Typical side effects include gastrointestinal upset, vertigo, and cumulative dose-dependant photosensitivity. A phase III efficacy trial of minocycline is currently enrolling 400 patients (NCT00047723). The ability of the drug to penetrate uninflamed meninges should be determined.

N-acetylated alpha-linked acidic dipeptidase (NAALADase, Guilford Inc.). Inhibition of glutamate carboxypeptidase 2 (GCP2) may be neuroprotective by simultaneously decreasing glutamate production and inhibiting glutamate release.[46] Median survival of $SOD1^{G93A}$ ALS mice was prolonged by 15% (29 days) by administration of the GCP2 inhibitor 2-(3-mecaptopropyl) pentanedioic acid. GCP2 inhibition is attractive as a therapeutic target because the effects only occur during excessive glutamate stimulation avoiding glutamate receptor antagonist side effects.[46] NAALADase inhibitors have not yet been administered to humans and there are no data on pharmacokinetics and tolerability.

Nimesulide (generic). The enzyme COX-2 is an attractive therapeutic target because of its marked increase in ALS spinal cord stimulating astrocytic glutamate release.[47,48] Nimesulide is a preferential COX-2 inhibitor with additional antioxidant properties.[49] Nimesulide administration decreased PG-E2 levels in the spinal cord of $SOD1^{G93A}$ mice and preserved motor skill integrity.[50] However, the COX-2 inhibitor celecoxib failed to show benefit in a phase II/III trial.[51] Furthermore, safety concerns surrounding long-term administration of this medication class may limit use in patients with ALS.[52]

ONO-2506 (Ono Pharmaceutical Co. Ltd). Chimeric mice with both normal and mutant SOD1-expressing cells indicate that glia play a role in motor neuron degeneration.[53] Possible mechanisms include microglial-mediated neuroinflammation, loss of neurotrophic support,[2] and diminished clearance of glutamate from neuromuscular synapses by the astrocytic glutamate transporter EAAT2.[16] ONO-2506 is an enantiomeric homologue of valproate that restores normal astrocyte functions after brain damage by preventing reactive astrocytosis, by activating astrocytic $GABA_A$ receptors and suppressing GABA transferase.[54] This agent has additional antiglutamate[55] and anti-inflammatory COX-2 inhibitor properties.[56] Results of a completed phase II trial of 1,200 mg per day oral formulation (cereact) are pending. A phase III trial of the parent compound valproate has commenced enrollment in Europe (n = 173, NCT00136110).

Riluzole (Sanofi-Aventis). Riluzole remains the only FDA-approved drug for ALS based on the 3-month improvement in survival observed in two large clinical trials.[57,58] Riluzole has a broad range of pharmacologic effects including inhibition of glutamate release, postsynaptic glutamate receptor activation, and voltage-sensitive sodium channels inactivation. It was identified before the SOD1 mouse model became available by studying toxicity of CSF from patients with ALS on neuronal cell cultures.[59] Subsequently, riluzole was found to have a modest effect on $SOD1^{G93A}$ mouse survival (prolonged median survival by 11%, 14 days).[60]

Riluzole has been included in the final list not to suggest that further trials of this drug are required, but rather to emphasize the surprising lack of effort to build on the modest success of riluzole. Related benzothiazoles have not been tested in ALS animal models or patients. A collaborative effort between academic scientists and industry may rejuvenate development of this drug class.

Scriptaid (Alexis Biochemicals). Abnormal protein aggregates have been described in neurodegenerative diseases including AD, PD, and HD. Ubiquitin inclusions are present in motor neurons and astrocytes of patients with ALS.[61] It is not known if these aggregates damage or protect motor neurons, though several possible toxic mechanisms have been proposed including aberrant chemistry, loss of normal proteins through sequestration within aggregates, and inhibition of mitochondria, peroxisomes, or proteosomeal function overwhelmed with indigestible, misfolded protein.[2] Agents that decrease aggregation have been hypothesized to be neuroprotective. Scriptaid was identified in a screen for small molecules that disrupt in vitro aggresome formation in cultured COS cells transfected with mutant SOD1-GFP.[62] Safety, optimum dose, and pharmacokinetic animal and human data remain to be determined for this drug.

Sodium phenylbutyrate (Scandinavian formulas). Sodium phenylbutyrate (NaPB) is FDA-approved for chronic treatment of hyperammonia and has been tested as a treatment of spinomuscular atrophy.[63] Its potential benefit in ALS is based on its ability to inhibit histone deacetylase (HDAC) leading to increased gene transcription.[64] This aromatic short-chain fatty acid extends median survival of $SOD1^{G93A}$ ALS mice by 21.9% (27.5 days).[64] NaPB has a short half life (45 minutes), though changes in gene expression induced by the drug may be more persistent. CNS distribution of NaPB has been determined by MR spectroscopy.[65] An open label, dose-escalation study enrolling 40 patients with ALS is underway to determine human safety (NCT00107770).

Talampanel (8-methyl-7H-1,3-dioxolo(2,3)benzodiazepine, IVAX Corporation). Talampanel is a noncompetitive modulator of AMPA glutamate receptors primarily under development as an antiepileptic agent. Talampanel has been shown to prolong $SOD1^{G93A}$ mouse median survival (Jeffrey Rothstein, personal communication). ALSFRS and TQNE scores declined at a slower rate in a 9-month phase II study of talampanel in 60 patients with ALS though the study was not powered to detect efficacy (Robert Pascuzzi, personal communication). The most common side effects were ataxia and sedation. The antiepileptic properties of talampanel indicate that the drug crosses the BBB.

Tamoxifen (Astra Zeneca). Tamoxifen may be neuroprotective in ALS because of its ability to inhibit protein kinase C, which mediates inflammation in spinal cords of patients with ALS.[66] Tamoxifen extended survival in a virally induced ALS mouse model.[67] A phase II study of 60 patients with ALS prolonged survival at 10 mg, 20 mg, 30 mg, and 40 mg daily doses (Ben Brooks, personal communication). The drug penetrates the CNS and is generally well tolerated. The effect of the drug on survival of $SOD1^{G93A}$ mice needs to be evaluated and the results of the phase II study should be peer-reviewed. However, if these results are favorable, planning for a phase III study may be expedited.

Thalidomide (Celgene). Angiogenic factors controlling the growth and permeability of blood vessels have been implicated in the pathogenesis of ALS. Mice bearing a deletion of the vascular endothelial cell growth factor

Downloaded from www.neurology.org by MICHAEL FETELL on September 12, 2006
Copyright © by AAN Enterprises, Inc. Unauthorized reproduction of this article is prohibited.

(VEGF) gene develop an ALS-like phenotype[68] and polymorphisms of the VEGF promoter region increase the risk of ALS.[69] Coding mutations of a related gene angiogenin have also been linked to the disease.[70] Thalidomide is a non-barbiturate sedative that was withdrawn from the world market in 1961 on discovery of its teratogenic effects. It has been selectively reintroduced for a variety of conditions including progressive body weight loss related to advanced cancer and AIDS.[71] The drug has anti-angiogenic activity and immunomodulatory properties.[71] Oral thalidomide reduced TNFα, attenuated weight loss, and increased survival in $SOD1^{G93A}$ mice.[72] Thalidomide crosses the BBB, as indicated by its sedative effects. Peripheral neuropathy has been observed in 8% of patients with HIV and can become irreversible if thalidomide is not discontinued.[73] Lenalidomide, a novel 4 amino-glutarimide analogue, shows the same efficacy in animal studies without the neurotoxic and teratogenic effects.[72,74] An open-label, phase II trial is currently recruiting patients (n = 24, NCT00140452).

Trehalose (Cargill, Inc.). Trehalose is a natural disaccharide used in freeze-dried products to prevent protein denaturation. Trehalose may prevent formation of mutant SOD1 aggregates in ALS by stabilizing mutant proteins.[75] The agent has a long history of human use and the FDA has issued a "letter of no objection" (GRAS No. GRN 000045). However, there are no data on toxicity in patients with ALS, the ability of the drug to penetrate the CNS is unknown, and its effect in transgenic ALS mouse model remains to be evaluated.

Discussion. We identified and assessed potential compounds for clinical trials in patients with ALS. Academic clinicians and scientists identified 113 compounds, of which 24 were selected for more detailed pharmacokinetic and safety analysis. Twenty were chosen as the most promising agents that should be studied in phase III clinical ALS trials. Two agents on the priority list (talampanel and tamoxifen) show preliminary efficacy in phase II ALS clinical studies. Other agents (ceftriaxone, minocycline, ONO-2506, and IGF-1 polypeptide) are already in phase III trials involving large numbers of patients. Most agents on the final priority list require additional data (preclinical animal data, human toxicity, and pharmacokinetic data [including CNS penetration]) prior to proceeding to large scale human testing (see table 3).

While a detailed attempt was made to make the review process explicit, qualitative judgments had to be prepared about the relative value and weighting of different types of information. The most problematic issues were the evaluation of unpublished data and the authors' biases. Although considerable effort was made to obtain information from investigators developing an agent, not all data were available to the authors. The initial screen was performed by investigators in the field, which may have resulted in bias toward agents studied in their laboratories. To ensure transparency all data relevant to this article were made available to the ALS community throughout the selection process.

Animal drug-screening studies in ALS almost exclusively utilize the mutant $SOD1^{G93A}$ mouse (table E-1), but the ability of this model to predict drug efficacy in humans is ambiguous. Several drugs that prolong survival in animal studies have not shown efficacy in human trials (celebrex,[51,76] creatine,[77,78] gabapentin,[60,79] N-acetylcysteine[80,81]). This discrepancy may be due to intraspecies differences in pharmacokinetics and the difficulty in establishing dose equivalence to achieve the same biologic activity in humans as observed in mice. It may also be that this mouse model of familial ALS does not predict drug effect in patients with sporadic ALS and that development of alternative models should be prioritized.

Interpretation of animal drug screening studies is complicated by varying experimental designs between laboratories. For example, mouse strain and sex,[82] as well as environmental factors such as access to exercise, affect survival.[83] There is a need to establish consensus guidelines to ensure ALS animal drug studies are conducted in a uniform manner. Experimental design issues that warrant standardization include the type of animal models, number of animals and sex distribution required to reliably detect an effect, as well as the timing and method of drug delivery. The selection of appropriate survival and motor function endpoints is essential. Guidelines on the publication of negative results and the establishment of an online database of ALS animal drug studies should be a priority. Most importantly, guidelines should be established outlining the magnitude and the reproducibility of drug effect in different laboratories and animal models required to proceed to human clinical testing.

The pharmacokinetic profile, the safety/toxicity properties, and the most efficacious dose of the drug in humans must be adequately established prior to phase III studies. There has been a tendency for potentially beneficial candidates to move rapidly to large ALS clinical trials. Although this approach has demonstrated that certain drugs are ineffective, it has been unsuccessful at identifying useful therapies. The ability of a drug to cross the human BBB to reach its target ligand should be determined prior to starting phase II studies. Tolerability of a dose in healthy patients should not be taken as indication that the same dose will be safe in patients with ALS. The frequency of adverse events was significantly higher in patients with ALS receiving topiramate than was seen in patients with epilepsy, possibly related to dehydration and malnutrition in patients with ALS.[84] Dose-ranging studies are a prerequisite to phase III studies to determine the most effective and safe dosage. Focusing on early clinical safety, dose-finding, and pharmacokinetic testing will increase a drug's early development costs, but will maximize its chance of success in large phase III efficacy studies.

Multiple pathways have been implicated in the pathogenesis of ALS.[2] A medication or combination

Downloaded from www.neurology.org by MICHAEL FETELL on September 12, 2006
Copyright © by AAN Enterprises, Inc. Unauthorized reproduction of this article is prohibited.

of medications that targets more than one pathogenic pathway may slow disease progression in an additive or synergistic fashion. Such combination therapy has been successful in oncology, though multiple drug interactions and increased incidence of drug side effects should be considered. More detailed animal toxicology studies of combination therapies are required than for therapies given alone. Drug resistance must also be considered when a medication is administered for prolonged periods (months). Upregulation of multidrug resistance proteins has been reported in astrocytes and BBB of patients with neurodegenerative diseases with neuroinflammatory components, such as ALS. These transporters extrude endogenous toxins (such as medications) from CNS from the cells and may nullify a drug's bioactivity.[85]

In this article we evaluated existing drugs for their potential development in ALS in an explicit, systematic, and transparent manner. The selection process is intended to prioritize interventions for phase III trials in patients with ALS and to identify data that need to be collected prior to clinical studies involving large numbers of human subjects. The ALS Association has issued a request for applications building on the final list published in this article.[86] More candidate drugs will be identified as academic researchers adopt high throughput screening techniques and study candidate neuroprotective drugs in new animal models of ALS. Thus, the need to rationally select agents for clinical testing in patients with ALS will increase and the current approach can be extended to evaluate new therapies as they emerge. New data on both existing and novel neuroprotective agents will be assessed annually and updates made available on the ALS Association Web site and presented at the annual International ALS/MND Symposium.

Acknowledgment

The authors thank Vincent Meininger, MD, Robert G. Hart, MD, and Davide Trotti, PhD, for advice on the manuscript and Susanna Benn, PhD, for help constructing the table of animal studies. The authors thank attendees of the ALS Association-hosted conference to discuss candidates for ALS clinical trials: Stanley Appel, MD, Robert Brown, MD, Jill Heemskerk, PhD, Tom Maniatis, PhD, Bernard Ravina, MD, Jeff Rothstein, MD, PhD, and Paul Sheehy, PhD.

References

1. Rowland LP, Shneider NA. Amyotrophic lateral sclerosis. N Engl J Med 2001;344:1688–1700.
2. Bruijn LI, Miller TM, Cleveland DW. Unraveling the mechanisms involved in motor neuron degeneration in ALS. Annu Rev Neurosci 2004; 27:723–749.
3. Heemskerk J. High throughput drug screening. Amyotroph Lateral Scler Other Motor Neuron Disord. 2004;5(suppl 1):19–21.
4. Ravina BM, Fagan SC, Hart RG, et al. Neuroprotective agents for clinical trials in Parkinson's disease: a systematic assessment. Neurology 2003;60:1234–1240.
5. Rothstein JD. Of mice and men: reconciling preclinical ALS mouse studies and human clinical trials. Ann Neurol 2003;53:423–426.
6. Miller RG, Bradley W, Cudkowicz M, et al. Phase II/III controlled trial of TCH 346 in patients with amyotrophic lateral sclerosis. Amyotroph Lateral Scler Other Motor Neuron Disord 2005; 6(suppl 1):13.
7. Desnuelle C, Dib M, Garrel C, Favier A. A double-blind, placebo-controlled randomized clinical trial of alpha-tocopherol (vitamin E) in the treatment of amyotrophic lateral sclerosis. ALS Riluzole-Tocopherol Study Group. Amyotroph Lateral Scler Other Motor Neuron Disord 2001;2:9–18.
8. Graf M, Ecker D, Horowski R, et al. High dose vitamin E therapy in amyotrophic lateral sclerosis as add-on therapy to riluzole: results of a placebo-controlled double-blind study. J Neural Transm 2005; 112:649–660
9. Cleveland DW. From Charcot to SOD1: mechanisms of selective motor neuron death in ALS. Neuron 1999;24:515–520.
10. Patel M, Day BJ. Metalloporphyrin class of therapeutic catalytic antioxidants. Trends Pharmacol Sci 1999; 20:359–364.
11. Crow JP, Calingasan NY, Chen J, Hill JL, Beal MF. Manganese porphyrin given at symptom onset markedly extends survival of ALS mice. Ann Neurol 2005;58:258–265.
12. Batulan Z, Shinder GA, Minotti S, et al. High threshold for induction of the stress response in motor neurons is associated with failure to activate HSF1. J Neurosci 2003;23:5789–5798.
13. Hargitai J, Lewis H, Boros I, et al. Bimoclomol, a heat shock protein co-inducer, acts by the prolonged activation of heat shock factor-1. Biochem Biophys Res Commun 2003;307:689–695.
14. Kieran D, Kalmar B, Dick JR, et al. Treatment with arimoclomol, a coinducer of heat shock proteins, delays disease progression in ALS mice. Nat Med 2004;10:402–405.
15. Rothstein JD, Tsai G, Kuncl RW, et al. Abnormal excitatory amino acid metabolism in amyotrophic lateral sclerosis. Ann Neurol 1990;28:18–25.
16. Rothstein JD, Van Kammen M, Levey AI, Martin LJ, Kuncl RW. Selective loss of glial glutamate transporter GLT-1 in amyotrophic lateral sclerosis. Ann Neurol 1995;38:73–84.
17. Ince P, Stout N, Shaw P, et al. Parvalbumin and calbindin D-28k in the human motor system and in motor neuron disease. Neuropathol Appl Neurobiol 1993;19:291–299.
18. Rothstein JD, Patel S, Regan MR, et al. Beta-lactam antibiotics offer neuroprotection by increasing glutamate transporter expression. Nature 2005;433:73–77.
19. Nau R, Prange HW, Muth P, et al. Passage of cefotaxime and ceftriaxone into cerebrospinal fluid of patients with uninflamed meninges. Antimicrob Agents Chemother 1993;37:1518–1524.
20. Guglielmo BJ, Luber AD, Paletta D Jr., Jacobs RA. Ceftriaxone therapy for staphylococcal osteomyelitis: a review. Clin Infect Dis 2000;30:205–207.
21. Kawamata T, Akiyama H, Yamada T, McGeer PL. Immunologic reactions in amyotrophic lateral sclerosis brain and spinal cord tissue. Am J Pathol 1992;140:691–707.
22. McGeer PL, McGeer EG. Inflammatory processes in amyotrophic lateral sclerosis. Muscle Nerve 2002;26:459–470.
23. Allison AC, Cacabelos R, Lombardi VR, Alvarez XA, Vigo C. Celastrol, a potent antioxidant and anti-inflammatory drug, as a possible treatment for Alzheimer's disease. Prog Neuropsychopharmacol Biol Psychiatry 2001;25:1341–1357.
24. Westerheide SD, Bosman JD, Mbadugha BN, et al. Celastrols as inducers of the heat shock response and cytoprotection. J Biol Chem 2004; 279:56053–56060.
25. Kipiani K, Kiaei M, Chen J, Calingasan NY, Beal MF. Celastrol blocks motor neuron cell death and extends life in transgenic mouse model of amyotrophic lateral sclerosis. J Neurochem 2004; 90(suppl 1):92.
26. Do TQ, Schultz JR, Clarke CF. Enhanced sensitivity of ubiquinone-deficient mutants of Saccharomyces cerevisiae to products of autoxidized polyunsaturated fatty acids. Proc Natl Acad Sci USA 1996;93: 7534–7539.
27. Matthews RT, Yang L, Browne S, Baik M, Beal MF. Coenzyme Q10 administration increases brain mitochondrial concentrations and exerts neuroprotective effects. Proc Natl Acad Sci USA 1998;95:8892–8897.
28. Ferrante KL, Shefner J, Zhang H, et al. Tolerance of high-dose (3,000 mg/day) coenzyme Q10 in ALS. Neurology 2005;65:1834–1836.
29. Crone C, Gabriel G, Wise TN. Non-herbal nutritional supplements-the next wave: a comprehensive review of risks and benefits for the C-L psychiatrist. Psychosomatics 2001;42:285–299.
30. Haverkamp LJ, Smith RG, Appel SH. Trial of immunosuppression in amyotrophic lateral sclerosis using total lymphoid irradiation. Ann Neurol 1994;36:253–254.
31. Angelov DN, Waibel S, Guntinas-Lichius O, et al. Therapeutic vaccine for acute and chronic motor neuron diseases: implications for amyotrophic lateral sclerosis. Proc Natl Acad Sci USA 2003;100:4790–4795.
32. Perez NB, Haenggeli C, Rothstein JD. Vaccination with COP1 derivative does not alter disease progression in a SOD1 G93A transgenic ALS mouse. Abstr Soc Neurosci 2005;213.9. Abstract.
33. Lai EC, Felice KJ, Festoff BW, et al. Effect of recombinant human insulin-like growth factor-I on progression of ALS. A placebo-controlled study. The North America ALS/IGF-I Study Group Neurology 1997;49: 1621–1630.
34. Borasio GD, Robberecht W, Leigh PN, et al. A placebo-controlled trial of insulin-like growth factor-I in amyotrophic lateral sclerosis. European ALS/IGF-I Study Group. Neurology 1998;51:583–586.
35. Kaspar BK, Llado J, Sherkat N, Rothstein JD, Gage FH. Retrograde viral delivery of IGF-1 prolongs survival in a mouse ALS model. Science 2003;301:839–842.

Downloaded from www.neurology.org by MICHAEL FETELL on September 12, 2006
Copyright © by AAN Enterprises, Inc. Unauthorized reproduction of this article is prohibited.

36. Manno CS, Chew AJ, Hutchison S, et al. AAV-mediated factor IX gene transfer to skeletal muscle in patients with severe hemophilia B. Blood 2003;101:2963–2972.
37. Terro F, Yardin C, Esclaire F, Ayer-Lelievre C, Hugon J. Mild kainate toxicity produces selective motoneuron death with marked activation of CA(2+)-permeable AMPA/kainate receptors. Brain Res 1998;809:319–324.
38. Kornhuber J, Quack G. Cerebrospinal fluid and serum concentrations of the N-methyl-D-aspartate (NMDA) receptor antagonist memantine in man. Neurosci Lett 1995;195:137–139.
39. Pasinelli P, Belford ME, Lennon N, et al. Amyotrophic lateral sclerosis-associated SOD1 mutant proteins bind and aggregate with Bcl-2 in spinal cord mitochondria. Neuron 2004;43:19–30.
40. Pasinelli P, Houseweart MK, Brown RH Cleveland DW. Caspase-1 and -3 are sequentially activated in motor neuron death in Cu,Zn superoxide dismutase-mediated familial amyotrophic lateral sclerosis. Proc Natl Acad Sci USA 2000;97:13901–13906.
41. Kriz J, Nguyen MD, Julien JP. Minocycline slows disease progression in a mouse model of amyotrophic lateral sclerosis. Neurobiol Dis 2002;10:268–278.
42. Zhu S, Stavrovskaya IG, Drozda M, et al. Minocycline inhibits cytochrome c release and delays progression of amyotrophic lateral sclerosis in mice. Nature 2002;417:74–78.
43. Zhang W, Narayanan M, Friedlander RM. Additive neuroprotective effects of minocycline with creatine in a mouse model of ALS. Ann Neurol 2003;53:267–270.
44. Van Den BL, Tilkin P, Lemmens G, Robberecht W. Minocycline delays disease onset and mortality in a transgenic model of ALS. Neuroreport 2002;13:1067–1070.
45. Gordon PH, Moore DH, Gelinas DF, et al. Placebo-controlled phase I/II studies of minocycline in amyotrophic lateral sclerosis. Neurology 2004;62:1845–1847.
46. Slusher BS, Vornov JJ, Thomas AG, et al. Selective inhibition of NAALADase, which converts NAAG to glutamate, reduces ischemic brain injury. Nat Med 1999;5:1396–1402.
47. Almer G, Guegan C, Teismann P, et al. Increased expression of the pro-inflammatory enzyme cyclooxygenase-2 in amyotrophic lateral sclerosis. Ann Neurol 2001;49:176–185.
48. Bezzi P, Carmignoto G, Pasti L, et al. Prostaglandins stimulate calcium-dependent glutamate release in astrocytes. Nature 1998;391:281–285.
49. Facino RM, Carini M, Aldini G. Antioxidant activity of nimesulide and its main metabolites. Drugs 1993;46(suppl 1):15–21.
50. Pompl PN, Ho L, Bianchi M, et al. A therapeutic role for cyclooxygenase-2 inhibitors in a transgenic mouse model of amyotrophic lateral sclerosis. FASEB J 2003;17:725–727.
51. Cudkowicz ME, Shefner JM, Schoenfeld D, et al. Clinical trial of celecoxib in subjects with amyotrophic lateral sclerosis. Amyotroph Lateral Scler Other Motor Neuron Disord 2004;5(suppl 2):25–26.
52. FitzGerald GA. Coxibs and cardiovascular disease. N Engl J Med 2004;351:1709–1711.
53. Clement AM, Nguyen MD, Roberts EA, et al. Wild-type nonneuronal cells extend survival of SOD1 mutant motor neurons in ALS mice. Science 2003;302:113–117.
54. Nilsson M, Hansson E, Ronnback L. Interactions between valproate, glutamate, aspartate, and GABA with respect to uptake in astroglial primary cultures. Neurochem Res 1992;17:327–332.
55. Katsumata S, Tateishi N, Kagamiishi Y, et al. Inhibitory effect of ONO-2506 on GABAA receptor disappearance in cultured astrocytes and ischemic brain. Abstr Soc Neurosci 1999;843:11. Abstract.
56. Shimoda T, Tateishi N, Shintaku K, et al. ONO-2506, a novel astrocyte modulating agent, suppresses the increase of COX-2 and iNOS mRNA expression in cultured astrocytes and ischemic brain. Abstr Soc Neurosci 1998;384:13. Abstract.
57. Bensimon G, Lacomblez L, Meininger V. A controlled trial of riluzole in amyotrophic lateral sclerosis. ALS/Riluzole Study Group. N Engl J Med 1994;330:585–591.
58. Lacomblez L, Bensimon G, Leigh PN, Guillet P, Meininger V. Dose-ranging study of riluzole in amyotrophic lateral sclerosis. Amyotrophic Lateral Sclerosis/Riluzole Study Group II. Lancet 1996;347:1425–1431.
59. Couratier P, Sindou P, Esclaire F, Louvel E, Hugon J. Neuroprotective effects of riluzole in ALS CSF toxicity. Neuroreport 1994;5:1012–1014.
60. Gurney ME, Cutting FB, Zhai P, et al. Benefit of vitamin E, riluzole, and gabapentin in a transgenic model of familial amyotrophic lateral sclerosis. Ann Neurol 1996;39:147–157.
61. Leigh PN, Anderton BH, Dodson A, Gallo JM, Swash M, Power DM. Ubiquitinated deposits in anterior horn cells in motor neurone disease. Neurosci Lett 1988; 93:197–203.
62. Corcoran LJ, Mitchison TJ, Liu Q. A novel action of histone deacetylase inhibitors in a protein aggresome disease model. Curr Biol 2004;14:488–492.
63. Mercuri E, Bertini E, Messina S, et al. Pilot trial of phenylbutyrate in spinal muscular atrophy. Neuromuscul Disord 2004;14:130–135.
64. Ryu H, Smith K, Camelo SI, et al. Sodium phenylbutyrate prolongs survival and regulates expression of anti-apoptotic genes in transgenic amyotrophic lateral sclerosis mice. J Neurochem 2005;93:1087–1098.
65. Barker PB, Artemov D, Raymond GV, Horská A, Moser HW. Detection of 4-phenylbutyrate in the human brain by in vivo Proton MR Spectroscopy. Proceedings of the ISMRM 8th Scientific Meeting and Exhibition; Denver, CO; 2000.
66. Hu JH, Zhang H, Wagey R, Krieger C, Pelech SL. Protein kinase and protein phosphatase expression in amyotrophic lateral sclerosis spinal cord. J Neurochem 2003;85:432–442.
67. Brooks B, Sanjak M, Roelke K, et al. Phase 2B randomized dose-ranging clinical trial of tamoxifen, a selective estrogen receptor modulator [SERM], in ALS: sensitivity analyses of discordance between survival and functional outcomes with long-term follow-up. Amyotroph Lateral Scler Other Motor Neuron Disord 2005;6(suppl 1):118.
68. Oosthuyse B, Moons L, Storkebaum E, et al. Deletion of the hypoxia-response element in the vascular endothelial growth factor promoter causes motor neuron degeneration. Nat Genet 2001;28:131–138.
69. Lambrechts D, Storkebaum E, Morimoto M, et al. VEGF is a modifier of amyotrophic lateral sclerosis in mice and humans and protects motoneurons against ischemic death. Nat Genet 2003;34:383–394.
70. Greenway MJ, Andersen PM, Russ C, et al. ANG mutations segregate with familial and 'sporadic' amyotrophic lateral sclerosis. Nat Genet 2006 Feb 26 [Epub ahead of print].
71. Mujagic H, Chabner BA, Mujagic Z. Mechanisms of action and potential therapeutic uses of thalidomide. Croat Med J 2002;43:274–285.
72. Kiaei M, Petri S, Kipiani K, et al. Thalidomide and lenalidomide extend survival in a transgenic mouse model of amyotrophic lateral sclerosis. J Neurosci 2006;26:2467–2473.
73. Alexander LN, Wilcox CM. A prospective trial of thalidomide for the treatment of HIV-associated idiopathic esophageal ulcers. AIDS Res Hum Retroviruses 1997;13:301–304.
74. List A, Kurtin S, Roe DJ, et al. Efficacy of lenalidomide in myelodysplastic syndromes. N Engl J Med 2005;352:549–557.
75. Romisch K. A cure for traffic jams: small molecule chaperones in the endoplasmic reticulum. Traffic 2004;5:815–820.
76. Drachman DB, Frank K, Dykes-Hoberg M, et al. Cyclooxygenase 2 inhibition protects motor neurons and prolongs survival in a transgenic mouse model of ALS. Ann Neurol 2002;52:771–778.
77. Klivenyi P, Ferrante RJ, Matthews RT, et al. Neuroprotective effects of creatine in a transgenic animal model of amyotrophic lateral sclerosis. Nat Med 1999;5:347–350.
78. Groeneveld GJ, Veldink JH, van dT I, et al. A randomized sequential trial of creatine in amyotrophic lateral sclerosis. Ann Neurol 2003;53:437–445.
79. Miller RG, Moore DH, Gelinas DF, et al. Phase III randomized trial of gabapentin in patients with amyotrophic lateral sclerosis. Neurology 2001;56:843–848.
80. Andreassen OA, Dedeoglu A, Klivenyi P, Beal MF, Bush AI. N-acetyl-L-cysteine improves survival and preserves motor performance in an animal model of familial amyotrophic lateral sclerosis. Neuroreport 2000;11:2491–2493.
81. Kuther G, Struppler A. Therapeutic trial with N-acetylcysteine in amyotrophic lateral sclerosis. Adv Exp Med Biol 1987;209:281–284.
82. Cudkowicz ME, Pastusza KA, Sapp PC, et al. Survival in transgenic ALS mice does not vary with CNS glutathione peroxidase activity. Neurology 2002;59:729–734.
83. Kirkinezos IG, Hernandez D, Bradley WG, Moraes CT. Regular exercise is beneficial to a mouse model of amyotrophic lateral sclerosis. Ann Neurol 2003;53:804–807.
84. Cudkowicz ME, Shefner JM, Schoenfeld DA, et al. A randomized, placebo-controlled trial of topiramate in amyotrophic lateral sclerosis. Neurology 2003;61:456–464.
85. Kirkinezos IG, Hernandez D, Bradley WG, Moraes CT. An ALS mouse model with a permeable blood-brain barrier benefits from systemic cyclosporine A treatment. J Neurochem 2004;88:821–826.
86. ALS Association. Clinical research pilot study request for proposals. Available at: http://www.alsa.org/news/article.cfm?id=682&CFID=1785756&CFTOKEN=32724346

Downloaded from www.neurology.org by MICHAEL FETELL on September 12, 2006
Copyright © by AAN Enterprises, Inc. Unauthorized reproduction of this article is prohibited.

Neuroprotective agents for clinical trials in ALS: A systematic assessment
B. J. Traynor, L. Bruijn, R. Conwit, F. Beal, G. O'Neill, S. C. Fagan and M. E. Cudkowicz
Neurology 2006;67;20-27
DOI: 10.1212/01.wnl.0000223353.34006.54

This information is current as of September 12, 2006

Updated Information & Services	including high-resolution figures, can be found at: http://www.neurology.org/cgi/content/full/67/1/20
Supplementary Material	Supplementary material can be found at: http://www.neurology.org/cgi/content/full/67/1/20/DC1
Permissions & Licensing	Information about reproducing this article in parts (figures, tables) or in its entirety can be found online at: http://www.neurology.org/misc/Permissions.shtml
Reprints	Information about ordering reprints can be found online: http://www.neurology.org/misc/reprints.shtml

AMERICAN ACADEMY OF NEUROLOGY

Downloaded from www.neurology.org by MICHAEL FETELL on September 12, 2006

NEUROLOGY

Randomized controlled phase II trial of glatiramer acetate in ALS

P. H. Gordon, C. Doorish, J. Montes, R. L. Mosley, B. Diamond, R. B. MacArthur, L. H. Weimer, P. Kaufmann, A. P. Hays, L. P. Rowland, H. E. Gendelman, S. Przedborski and H. Mitsumoto

Neurology 2006;66;1117-1119
DOI: 10.1212/01.wnl.0000204235.81272.e2

This information is current as of September 12, 2006

The online version of this article, along with updated information and services, is located on the World Wide Web at:
http://www.neurology.org/cgi/content/full/66/7/1117

Neurology is the official journal of AAN Enterprises, Inc. A bi-monthly publication, it has been published continuously since 1951. Copyright © 2006 by AAN Enterprises, Inc. All rights reserved. Print ISSN: 0028-3878. Online ISSN: 1526-632X.

AMERICAN ACADEMY OF NEUROLOGY

Downloaded from www.neurology.org by MICHAEL FETELL on September 12, 2006

Randomized controlled phase II trial of glatiramer acetate in ALS

Abstract—The authors conducted a randomized controlled trial to test the safety and immunology of glatiramer acetate in ALS. Twenty treated patients were randomly assigned to daily or biweekly injections. Ten control patients were selected from another trial and followed up concurrently. Injection reactions were the only common adverse event ($p = 0.01$). Treated patients showed enhanced lymphocyte proliferation ($p = 0.02$). The safety profile and immune effects support conducting larger trials of dose selection and efficacy.

NEUROLOGY 2006;66:1117–1119

P.H. Gordon, MD; C. Doorish, BA; J. Montes, PT, MA; R.L. Mosley, PhD; B. Diamond, PhD; R.B. MacArthur, PharmD; L.H. Weimer, MD; P. Kaufmann, MD, MS; A.P. Hays, MD; L.P. Rowland, MD; H.E. Gendelman, MD; S. Przedborski, MD, PhD; and H. Mitsumoto, MD, DSci

Inflammation in ALS may be a secondary response to neuronal injury by genetic, biochemical, or environmental insults. Inflammatory cells surround degenerating neurons,[1] leading to the accumulation of proinflammatory cytokines and free radicals that likely contribute to neurodegeneration.[2] Modulation of inflammation may reduce cell death.

The term *vaccination* can be used for an intervention that leads to the induction of an immune response, which then slows the underlying disease. Vaccination with glatiramer acetate (GA) boosts regulatory T cell–mediated immunity. GA is approved by the US Food and Drug Administration for treatment of multiple sclerosis (MS)[3] and delays disease progression in animal models of ALS and neurodegeneration.[4,5]

We now report a trial designed to test the safety, tolerability, and immunogenicity of different doses of GA in human ALS.

Methods. A detailed description of the methods (appendix E-1) and a figure (figure E-1) outlining the patient flow are available on the *Neurology* Web site at www.neurology.org. In brief, we conducted a 6-month prospective, randomized controlled phase II trial. The primary aim was to determine whether GA is safe and tolerated by patients with ALS. In vitro assays were used to determine whether ALS patients show altered T-cell proliferation before or after administration of GA.

Twenty patients were randomly assigned to receive 20 mg subcutaneous GA daily (Group 1) or 20 mg subcutaneous GA biweekly (Group 2). Ten control patients (Group 3) were selected from consecutive participants in a blinded trial of minocycline in ALS. All patients signed consent forms and were evaluated monthly. The design provided 80% power ($\alpha = 0.05$) to detect a 48% difference in the rates of adverse events (AEs) and a 16% difference in T-cell responses between groups. T-cell proliferative activities were determined in response to GA (5 to 10 μg/mL) and phytohemagglutinin (PHA; 3 μg/mL), a mitogenic control. Stimulation indices were calculated as the counts per million from treated, stimulated samples divided by counts per million of background, unstimulated samples.

Additional material related to this article can be found on the *Neurology* Web site. Go to www.neurology.org and scroll down the Table of Contents for the April 11 issue to find the title link for this article.

Results. Thirty patients were enrolled and 10 were assigned to each group (see figure E-1) between June and September 2004. All were included in the intent-to-treat analysis. Twenty-six patients completed the trial (9 in Group 1, 9 in Group 2, and 8 controls). Four patients died; none withdrew from the study or discontinued medication for other reasons. The baseline characteristics of the patients (table E-1) were well matched between groups.

Five patients in each GA treatment group had at least one injection site reaction ($p = 0.01$). The reactions occurred multiple times in nine patients. There were no other differences in safety measures between groups, or in GA-treated patients overall compared with controls (tables E-2 and E-3). There were six serious AEs (two in Group 1, one in Group 2, and three in Group 3; table E-4); none were considered to be related to drug. Four patients (one in Group 1, one in Group 2, and two in Group 3) died of progressive respiratory failure due to ALS.

Systemic postinjection reactions (SPIRs) consisting of palpitations, dyspnea, flushing, and thoracic tightness occurred in three GA-treated patients ($p = 0.15$). Two patients had multiple SPIRs. All described the event as anxiety provoking or frightening. One patient was monitored during a SPIR. A cardiologist reviewed four EKGs taken before, during, and after the event. There were no changes except increased heart rate.

Baseline lymphoproliferative responses were similar in all three groups. Even though some control patients presumably took active minocycline, there were no differences from baseline in responses for controls under each culture condition at any time point.

From the Departments of Neurology (P.H.G., C.D., J.M., L.H.W., P.K., L.P.R., S.P., H.M.), Pharmacology (R.B.M.), Pathology (A.P.H.), and Biostatistics at the General Clinical Research Center (B.D.), Columbia University, NY; and the Department of Pharmacology and Experimental Neuroscience, Center for Neurovirology and Neurodegenerative Disorders (R.L.M., H.E.G.), University of Nebraska Medical Center, Omaha, NE.

Supported by GCRC Grant # 3301, NIH P01 NS11766-27A1, P01 NS43985, R21 NS049264, MDA Wings Over Wall Street, and Michael Gluck, Marsha and Alan Baer, and the Frani and Louis Blumkin Foundations, 2R37 NS36126. Drs. Gordon and Mitsumoto received a single consulting honorarium of less than $10,000 following the trial.

Disclosure: Study was partially funded by Teva Pharmaceuticals. The authors report no conflicts of interest.

Received September 12, 2005. Accepted in final form December 27, 2005.

Address correspondence and reprint requests to Dr. Paul H. Gordon, Eleanor and Lou Gehrig MDA/ALS Research Center, Neurological Institute, 9th Floor, 710 West 168th Street, New York, NY 10032; e-mail: phg8@columbia.edu

Copyright © 2006 by AAN Enterprises, Inc.

Downloaded from www.neurology.org by MICHAEL FETELL on September 12, 2006
Copyright © by AAN Enterprises, Inc. Unauthorized reproduction of this article is prohibited.

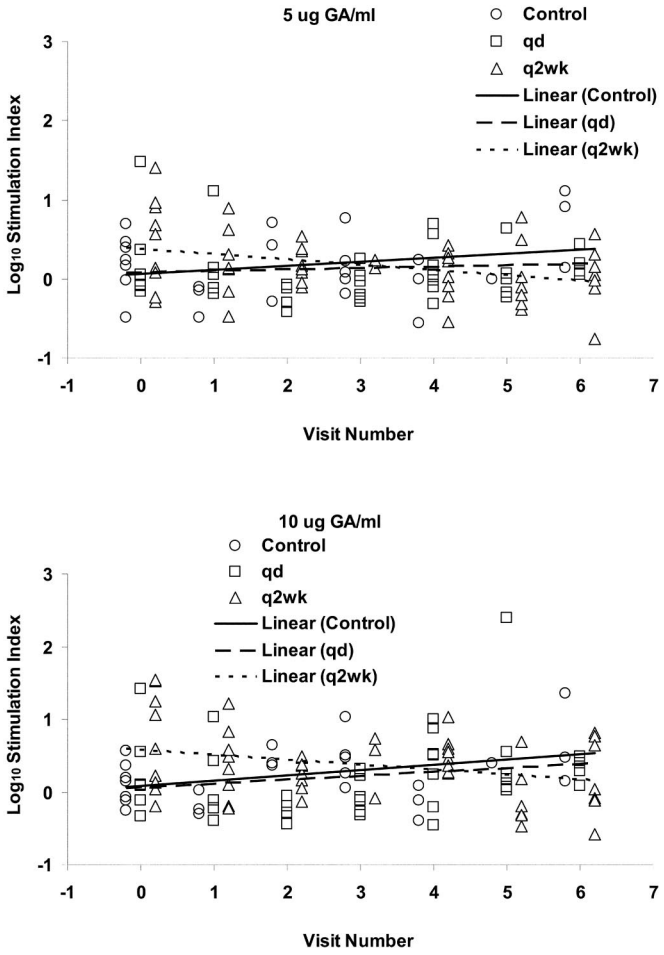

Figure. Immune changes: T-cell proliferation. The top figure shows the monthly proliferative indices in response to stimulation with 5 μg/mL glatiramer acetate (GA), and the bottom figure shows the monthly indices in response to stimulation with 10 μg/mL GA. qd = daily; q2wk = every other week.

T-cell proliferation changed with time in both GA-treated groups compared with controls ($p = 0.02$; figure); the responses diminished progressively in the treated groups and remained level in control patients. The findings were most significant in the less frequent dosing group ($p = 0.01$; see figure). Response to PHA was similar in treated and control subjects.

Autopsy, performed in one patient who died during the trial, showed severe loss of motor neurons and Bunina bodies within the surviving nerve cells typical of ALS. Inflammatory cells, consisting of CD68-positive microglia/macrophages, were present diffusely within the spinal cord including the corticospinal tracts, vicinity of anterior horn cells, and dorsal columns. The brain exhibited numerous neurofibrillary tangles in limbic regions and sparse neuritic plaques in the neocortex.

Discussion. Modulation of inflammation is one potential means of limiting neurodegeneration in ALS. Vaccination with GA induces highly cross-reactive anti-inflammatory Th2 cells.[6] Th2 cells migrate to sites of inflammation as part of their normal surveillance functions, where they serve as a source of anti-inflammatory cytokines and neurotrophic factors, thereby reducing inflammation and promoting neuronal survival.[7] GA has prolonged life span in the murine model of ALS,[4] although this is unconfirmed.[8]

The purpose of this trial was to test the safety and tolerability of GA over prolonged periods in subjects with ALS and to test the impact on measures of immune function. The most common AE was injection-site reaction. There were no other differences in AEs or the ability to complete the trial between groups. SPIRs, reported in approximately 10% of patients with MS,[9] also occurred in this trial. The mechanism is unknown, but EKG monitoring, performed because of concerns that the symptoms might mimic those of cardiac ischemia, showed no evidence of cardiotoxicity. Even though our patients described the events as frightening, none discontinued treatment because of the SPIR.

We administered GA as 20-mg daily or biweekly injections. Daily dosing, currently suggested for treatment of MS,[9] may induce both Th1 and Th2 responses.[10] Less frequent dosing regimens could favor a predominantly Th2 response, theoretically preferable in ALS. A control group, selected from participants in a blinded trial of minocycline in ALS, did not show changes in immune responses, either in comparison to pretreatment measures or over time. That is, we could detect no impact of minocycline on T-cell proliferation in control patients.

In contrast, patients with ALS mounted T-cell proliferative responses to GA. These responses differed significantly from those of control patients at both doses, indicating that immune function can be modulated in patients with ALS in ways similar to those in MS. The difference was more marked in patients given infrequent doses, and resulted from significant diminution with time, possibly as a result of global reduction of T-cell populations, loss of antigen-specific effector T cells, increases in anergic T cells, or induction of regulatory T cells.

One of our four patients who died of progressive ALS had an autopsy, which was unusual for several reasons. First, there was a diffuse microglial response in the spinal cord involving the dorsal columns as well as the motor nerves. Posterior column degeneration occurs only rarely in sporadic ALS. One possible explanation for the finding is that the microglia were more widespread in response to GA. Second, pathologic findings were consistent with the consensus criteria for stage III or IV AD. Most cases of dementia in ALS are now attributed to frontotemporal dementia, but this autopsy shows that findings of AD and ALS can coexist.

The trial established the clinical and immunologic scientific interaction in the study of vaccination in human ALS. We could measure immunologic changes in ALS patients, setting the stage for future trials in which clinical outcomes may be compared with immune responses. The small sample size and limited duration of the trial

Downloaded from www.neurology.org by MICHAEL FETELL on September 12, 2006
Copyright © by AAN Enterprises, Inc. Unauthorized reproduction of this article is prohibited.

render it premature to draw conclusions about efficacy. The tolerability of GA was acceptable and the immune response was sufficiently meaningful to support proceeding to larger trials of dose selection and efficacy.

References

1. Hirano A. Cytopathology in amyotrophic lateral sclerosis. Adv Neurol 1991;56:91–101.
2. Shaw P, Ince P, Falkous G, Mantel D. Oxidative damage to protein in sporadic motor neuron disease spinal cord. Ann Neurol 1995;38:691–695.
3. Goodin DS, Frohman EM, Garmany GP, et al. Disease modifying therapies in multiple sclerosis: report of the Therapeutics and Technology Assessment Subcommittee of the American Academy of Neurology and the MS Council for Clinical Practice Guidelines. Neurology 2002;58:169–178.
4. Angelov DN, Waibel S, Guntinas-Lichius et al. Therapeutic vaccine for acute and chronic motor neuron diseases: implications for amyotrophic lateral sclerosis. Proc Nat Acad Sci USA 2003;100:4790–4795.
5. Benner EJ, Mosley RL, Destache CJ, et al. Therapeutic immunization protects dopaminergic neurons in a mouse model of Parkinson's disease. Proc Natl Acad Sci USA 2004;101:9435–9440.
6. Wiesemann E, Klatt J, Sonmez D, Blasczyk R, Heidenreich F, Windhagen A. Glatiramer acetate (GA) induces IL-13/IL-5 secretion in naïve T cells. J Neuroimmun 2001;119:137–144.
7. Ziemssen T, Kumpfel T, Klinkert WE, Neuhaus O, Hohlfeld R. Glatiramer acetate-specific T-helper 1- and 2-type cell lines produce BDNF: implications for multiple sclerosis therapy. Brain 2002;125:2381–2391.
8. Haenggeli D, Perez N, Rothstein JD. Copaxone lacks efficacy in the G93A SOD1 transgenic ALS mouse: a dose-response analysis. Ann Neurol 2005;58:S28.
9. Johnson KP, Brooks BR, Cohen JA, et al. Copolymer 1 reduces relapse rate and improves disability in relapsing-remitting multiple sclerosis: results of a phase III multicenter, double-blind, placebo-controlled trial. Neurology 1995;45:1268–1276.
10. Farina C, Wagenpfeil S, Hohlfeld R. Immunological assay for assessing the efficacy of glatiramer acetate (Copaxone) in multiple sclerosis: a pilot study. J Neurol 2002;249:1587–1592.

GET VITAL INFORMATION ON NEW MEDICARE PART D PRESCRIPTION DRUG COVERAGE

Open enrollment for Medicare Part D prescription drug coverage continues through May 15, 2006. Visit www.aan.com/partd for timely information and resources to help your patients understand this new program.

Downloaded from www.neurology.org by MICHAEL FETELL on September 12, 2006

Copyright © by AAN Enterprises, Inc. Unauthorized reproduction of this article is prohibited.

Randomized controlled phase II trial of glatiramer acetate in ALS
P. H. Gordon, C. Doorish, J. Montes, R. L. Mosley, B. Diamond, R. B. MacArthur, L. H. Weimer, P. Kaufmann, A. P. Hays, L. P. Rowland, H. E. Gendelman, S. Przedborski and H. Mitsumoto
Neurology 2006;66;1117-1119
DOI: 10.1212/01.wnl.0000204235.81272.e2

This information is current as of September 12, 2006

Updated Information & Services	including high-resolution figures, can be found at: http://www.neurology.org/cgi/content/full/66/7/1117
Supplementary Material	Supplementary material can be found at: http://www.neurology.org/cgi/content/full/66/7/1117/DC1
Subspecialty Collections	This article, along with others on similar topics, appears in the following collection(s): **Amyotrophic lateral sclerosis** http://www.neurology.org/cgi/collection/amyotrophic_lateral_sclerosis_ **All Clinical trials** http://www.neurology.org/cgi/collection/all_clinical_trials **Clinical trials Randomized controlled (CONSORT agreement)** http://www.neurology.org/cgi/collection/clinical_trials_randomized_controlled_consort_agreement
Errata	An erratum has been published regarding this article. Please see next page or: http://www.neurology.org/cgi/content/full/67/5/920
Permissions & Licensing	Information about reproducing this article in parts (figures, tables) or in its entirety can be found online at: http://www.neurology.org/misc/Permissions.shtml
Reprints	Information about ordering reprints can be found online: http://www.neurology.org/misc/reprints.shtml

AMERICAN ACADEMY OF NEUROLOGY

Downloaded from www.neurology.org by MICHAEL FETELL on September 12, 2006

Sudden deafness from stroke

To the Editor: We would like to add to the correspondence about the possibility of an auditory Anton's syndrome in the report of sudden bilateral deafness from stroke.[1] While Anton's eponymous syndrome is most closely associated with denial of blindness, in one seminal article, "About the perception of focal brain lesions by patients with cortical blindness and deafness," two of three reported cases were of denial of deafness.[2]

We saw a patient who, like those described by Anton, did not respond to voice or loud noises but insisted he was not deaf. As with Anton's original patients, communication was accomplished by writing down queries to which the patient would respond verbally. Our patient was a 72-year-old man with alcohol-associated dementia who was brought into the emergency room for odd behavior. He confabulated reasons why he could not hear (e.g., "the radio's on too loud," "the fan is on"). He was cheerful and engaging and told a consistent and detailed story of his migration from South Carolina to New York City decades prior, but gave vague and confabulatory answers to questions about the recent past.

He reported drinking Heavenly Hill Bourbon 80 proof, "one glass in the morning and one at night," every day for decades. Oddly, the only evidence of preserved hearing was that he coughed when he heard others cough, even when he could not see them. One of us (J.C.M.B.) dubbed this the "Metropolitan Opera Reflex." His ear examination was normal but he was uncooperative with BAERs and formal audiometry. MRI of the brain showed only generalized atrophy and evidence of microvascular disease.

The mechanisms of contagious coughing or yawning are unclear. We propose that our patient was cortically deaf and the preservation of acoustic cough response was mediated by pathways known to exist between the cochlear nucleus, the inferior colliculus, and descending acousticomotor pathways involved in acoustic reflexes and vocalization.[3]

Laura S. Boylan, Robert Staudinger, John C.M. Brust, *New York, NY*

Disclosure: The authors report no conflicts of interest.

Reply from the Author: I found Boylan et al.'s description of their patient with auditory Anton's syndrome quite fascinating, especially because this patient, though cortically deaf, responds mimetically to people coughing. This must involve a subcortical loop, as the authors suggest, but may also entail the activation of the precuneus or posterior cingulate regions, parts of the brain probably subserving self-reference and empathy, and which are known to be implicated in contagious yawning.[4,5]

It is also valuable to be reminded that Anton originally described auditory as well as visual syndromes, for most textbooks refer only to the visual form.

Oliver Sacks, MD, *New York, NY*

Disclosure: The author reports no conflict of interest.

Copyright © 2006 by AAN Enterprises, Inc.

References

1. Sacks OW, Naumann M, Reiners K. Sudden deafness from stroke. Neurology 2006;66:293.
2. Anton G. Über die Selbstwahrnehmung der Herderkrankungen des Gehirns durch den Kranken bei Rindenblindheit und Rindentaubheit. Archiv Psychiatrie Nervenkrankheiten 1899;32:86–127.
3. Huffman RF, Henson OW Jr. The descending auditory pathway and acousticomotor systems: connections with the inferior colliculus. Brain Res Rev 1990;15:295–323.
4. Perreiol MP, Monaca C. One person yawning sets off everyone else. J Neurol Neurosurgery Psychiatry 2006;77:3.
5. Platek SM, Mohamed FN, Gallup GG. Contagious yawning and the brain. Cogn Brain Res 2005;23:448–452.

Brain death worldwide: Accepted fact but no global consensus in diagnostic criteria

To the Editor: I recently read the article by Dr. Wijdicks, who comprehensively reviewed brain death status and guidelines worldwide.[1] Unfortunately, Table 1A provides mistaken information about the guidelines in Taiwan due to the incorrect extraction of the data from the cited article of Hung and Chen.[2] The following should be corrected:

1. The law regulating brain death was passed by Taiwan government in 1987. Thus the law is present instead of "absent" as summarized in the table.
2. The number of physicians is two instead of one.
3. The observation time is 12 hours instead of 6 hours.
4. The law requires another 4 hours for defining brain death, and thus a confirmatory test is mandatory.

I hope *Neurology* can provide corrected information to the readers.

Sung-Tsang Hsieh, *Taipei, Taiwan*

Disclosure: The author reports no conflicts of interest.

Reply from the Author: I appreciate the comments by Dr. Hsieh and I apologize if I misread the legal document. The Chinese version of the legal document available to me states that two physicians are needed and in Taiwan an additional 4 hours of observation is needed after the diagnosis of brain death is made. This is in addition to the 12 hours of observation on the ventilator of a patient with a structural brain lesion before the first full brain death examination.

In my article,[1] I referred to laboratory tests as confirmatory tests and it is my understanding that laboratory tests remain optional and not mandatory. Since my article was published in 2002, I have also noticed—in conversations with physicians from other countries—that there is sometimes confusion between what physicians think they should do and what the law dictates.

Eelco F.M. Wijdicks, *Rochester, MN*

Disclosure: The author reports no conflicts of interest.

Copyright © 2006 by AAN Enterprises, Inc.

References

1. Wijdicks EFM. Brain death worldwide: accepted fact but no global consensus in diagnostic criteria. Neurology 2002;58:20–25.
2. Hung TP, Chen ST. Prognosis of deeply comatose patients on ventilators. J Neurol Neurosurg Psychiatry 1995;58:75–80.

Different degrees of right-to-left shunting predict migraine and stroke: Data from 420 patients

To the Editor: The authors of this article[1] suggest only embolism as a possible explanation of their findings that the size of right-to-left shunt predicts the occurrence of migraine and of stroke.

It has recently been proposed[2] that migraine may be a physiologic response to hypoxia, as evidenced by its high incidence in a wide variety of hypoxia-provoking circumstances. This hypothesis would predict that increasing degrees of right-to-left shunting would, by increasing the levels of hypoxia, inflate the frequency and intensity of migraine attacks.

Downloaded from www.neurology.org by MICHAEL FETELL on September 12, 2006
Copyright © by AAN Enterprises, Inc. Unauthorized reproduction of this article is prohibited.

It is possible that the authors' data include pO_2 levels on each of the 420 patients reported and that a strong inverse correlation might be found between pO_2 levels and migraine frequency and intensity. If so, it is possible that oxygen inhalation by these patients could reduce the incidence and severity of migraine attacks yet not alter the occurrence of putative embolism.

Gordon J. Gilbert, *St. Petersburg, FL*

Disclosure: The author reports no conflicts of interest.

Reply from the Authors: We appreciate Dr Gilbert's suggestion that right-to-left shunts may facilitate migraine through the mechanism of increasing hypoxia.[1,2] It is not our policy to routinely measure pO_2 saturation in patients undergoing transcranial Doppler (TCD) testing for right-to-left shunt unless desaturation is clinically suspected, which was not the case in the patients included in the study.

Comparing TCD with arterial blood gas measurement in patients without obvious pulmonary disease has yielded disappointing results in terms of the correlation between blood oxygen content and degree of the shunt,[3] which means that the amount of the shunted blood is many times too small to induce a clinically significant hypoxia.

However, both the patients of Devuyst et al. and our patients were examined in the recumbent position,[1,3] whereas right-to-left shunt may increase to a significant extent on standing, not only in patients with the platypnea- orthodeoxia syndrome[4] but also in normal individuals.[5]

Dr. Gilbert's hypothesis needs to be properly tested in prospective studies aimed at assessing the variation of both pO_2 and right-to-left shunt from the recumbent to the upright position.

Gian Paolo Anzola, Eustaquio Onorato, Eva Morandi, Francesco Casilli, *Brescia, Italy*

Disclosure: The authors report no conflicts of interest.

Copyright © 2006 by AAN Enterprises, Inc.

References

1. Anzola GP, Morandi E, Casilli F, Onorato E. Different degrees of right-to-left shunting predict migraine and stroke: data from 420 patients. Neurology 2006;66:765–767.
2. Gilbert GJ. The purpose of migraine. Florida Med Assn Quart J 2005; Oct:26–27.
3. Devuyst G, Piechowski-Józwiak B, Karapanayiotides T, et al. Controlled contrast transcranial Doppler and arterial blood gas analysis to quantify shunt through patent foramen ovale. Stroke 2004;35:859–863.
4. Cheng TO. Platypnea-orthodeoxya syndrome: etiology, differential diagnosis, and management. Cathet Cardiovasc Interv 1999;47:64–66.
5. Telman G, Kouperberg E, Sprecher E, Yarnitsky D. The positions of the patients in the diagnosis of patent foramen ovale by transcranial Doppler. J Neuroimaging 2003;13:356–358.

Corrections

Randomized controlled phase II trial of glatiramer acetate in ALS

In the Brief Communication "Randomized controlled phase II trial of glatiramer acetate in ALS" (*Neurology* 2006;66:1117–1119) by P.H. Gordon, C. Doorish, J. Montes, et al., the fourth author's name is misspelled. It should be R.L. Mosley.

This error was corrected on www.neurology.org on August 21, 2006. The publisher regrets the error.

Diagnostic performance of spectroscopic and perfusion MRI for distinction of brain tumors

In the article "Diagnostic performance of spectroscopic and perfusion MRI for distinction of brain tumors" (*Neurology* 2006;66:1899–1906) by M.A. Weber, S. Zoubaa, M. Schlieter, et al., on page 1901, line 9 "...the serial T2-weighted images..." should read "...the serial T2*-weighted images..." On page 1903, Table 2, an asterisk is missing at the top of the "Cho/Cr" column.

Downloaded from www.neurology.org by MICHAEL FETELL on September 12, 2006
Copyright © by AAN Enterprises, Inc. Unauthorized reproduction of this article is prohibited.

NEUROLOGY

A crossover, add-on trial of talampanel in patients with refractory partial seizures

A. S. Chappell, J. W. Sander, M. J. Brodie, D. Chadwick, A. Lledo, D. Zhang, J. Bjerke, G. M. Kiesler and S. Arroyo

Neurology 2002;58;1680-1682

This information is current as of September 12, 2006

The online version of this article, along with updated information and services, is located on the World Wide Web at:
http://www.neurology.org/cgi/content/full/58/11/1680

Neurology is the official journal of AAN Enterprises, Inc. A bi-monthly publication, it has been published continuously since 1951. Copyright © 2002 by AAN Enterprises, Inc. All rights reserved. Print ISSN: 0028-3878. Online ISSN: 1526-632X.

AMERICAN ACADEMY OF NEUROLOGY

Downloaded from www.neurology.org by MICHAEL FETELL on September 12, 2006

A crossover, add-on trial of talampanel in patients with refractory partial seizures

Abstract—The authors report a double-blind, placebo-controlled, crossover study of talampanel in 49 patients with refractory partial seizures. Three doses of talampanel were investigated based on differences in patients' concomitant antiepileptic drug usage. Talampanel showed efficacy in reducing seizure frequency ($p = 0.001$) with a median seizure reduction of 21%. Eighty percent of patients had fewer seizures on talampanel than on placebo. Dizziness (52%) and ataxia (26%) were the only significant adverse events.

NEUROLOGY 2002;58:1680–1682

A.S. Chappell, MD; J.W. Sander, MD, PhD; M.J. Brodie, MD; D. Chadwick, DM, FRCP; A. Lledo, MD, PhD; D. Zhang, PhD; J. Bjerke, RPh, MBA; G.M. Kiesler, RPh; and S. Arroyo, MD, PhD

Talampanel (®-7Acetyl-5-(4-aminophenyl)-8,9-dihydro-8-methyl-7H-1,3-dioxolo[4,5-hour][2,3] benzodiazepine) or LY300164 (formerly known as GYKI 53773) is a potent member of a novel class of pharmacologic agents.[1-3] It is an orally active, noncompetitive antagonist of the AMPA (α-amino-3-hydroxy-5-methyl-4-isoxazeoleproprionic acid) subtype of glutamate excitatory amino acid receptors.

Anticonvulsants that directly block glutamate transmission may exert their antiseizure effect by limiting neuronal hyperexcitability and preventing glutamate-driven neuronal damage. This dual mechanism might offer an advantage in terms of efficacy over traditional antiepileptic drugs (AED) that act via γ-aminobutyric acid agonism or sodium channel blockade.

Talampanel is effective in animal models of seizures. It both blocks the spread of seizures and increases the threshold for seizure at doses lower than those that produce motor impairment.[4] Talampanel was well tolerated in healthy human subjects. The maximum tolerated single dose was 100 mg, the no-effect dose 20 mg, and the half-life 6.8 hours. Drowsiness and ataxia were the most common adverse events.[5]

Pharmacokinetics was explored in patients with epilepsy who were taking other, concomitant anticonvulsants. Whereas concomitant therapy with hepatic enzyme inducers such as carbamazepine increases talampanel clearance by a factor of three, concomitant therapy with valproate reduces it.

From Eli Lilly and Company (Drs. Chappell, Lledo, Zhang, Bjerke, and Kiesler), Lilly Corporate Center, Indianapolis, IN; Department of Clinical and Experimental Epilepsy (Dr. Sander), Institute of Neurology, University College London, United Kingdom; Epilepsy Unit (Dr. Brodie), University Department of Medicine and Therapeutics; Walton Hospital (Dr. Chadwick), United Kingdom; and Epilepsy Unit (Dr. Arroyo), Hospital Clinic de Barcelona, Spain.

This article concerns a clinical trial sponsored by Eli Lilly and Company to test the efficacy in epilepsy of talampanel. The authors were either Eli Lilly employees (A.S.C., J.B., A.L., G.M.K., and Z.D.Z.) or trial investigators (S.A., M.J.B., D.C., and J.W.S.). Trial investigators were paid according to how many patients they recruited into the trial.

Received May 10, 2001. Accepted in final form February 16, 2002.

Address correspondence and reprint requests to Dr. Amy S. Chappell, Eli Lilly and Company, Lilly Corporate Center, Indianapolis, IN 46285; e-mail: aschappell@lilly.com

Subjects and methods. *Subjects.* Patients were 18 to 65 years old with a diagnosis of partial seizures with or without generalization according to the seizure classification of the International League Against Epilepsy.[6] For the 3 months before the study, patients were required to have had at least 4 or more partial seizures per month with no 4-week seizure-free period. For the 2 months prerandomization and for the duration of the study, no changes in AED dose could be made other than those to maintain AED serum levels within 30% of baseline trough levels.

Design and procedure. This was a multicenter, crossover, double-blind, randomized, placebo-controlled trial to evaluate three target doses of talampanel—25, 60, or 75 mg by mouth three times a day—for three groups formed based on differences in patients' concomitant AED usage.

Patients taking phenobarbital, phenytoin, carbamazepine, or primidone (the induced group) received up to 75 mg by mouth three times a day. Those taking valproic acid alone (the inhibited group)received up to 25 mg by mouth three times a day. Patients taking hepatic enzyme-inducing AED and valproic acid or taking gabapentin, vigabatrin, topiramate, lamotrigine, diazepam, clobazam, clonazepam, or ethosuximide (the balanced group) received up to 60 mg by mouth three times a day. A crossover design was used to reduce the number of patients exposed to a yet-unproven drug.

Study protocol and consent forms were approved by Institutional Review Boards at each center, and the study was conducted in accordance with the Declaration of Helsinki.

The study consisted of a 4-week lead-in period and two 14-week treatment periods (Treatment Periods I and II) separated by a 4-week washout. At their first visit patients were screened for eligibility, seizure frequency was documented, and informed consent was obtained. After a lead-in period of 4 weeks, patients who met entry criteria were randomized to placebo or talampanel (Treatment Period I).

Patients were titrated to the maximum allowable dose based on their concomitant AED regimen. If they could not tolerate this maximum allowable dose, they were titrated down to the highest dose they could tolerate. During the ensuing 10 weeks they remained at this dose, and efficacy was evaluated. Patients were tapered off drug (or placebo) during weeks 13 and 14. After a 4-week washout, the process was repeated during Treatment Period II.

Measurement of efficacy and safety. Patients recorded date and time of each seizure and description of seizure

 Copyright © 2002 by AAN Enterprises, Inc.
Downloaded from www.neurology.org by MICHAEL FETELL on September 12, 2006

Table 1 *Baseline characteristics for all randomized patients*

Characteristic	Talampanel/ placebo, n = 26	Placebo/ talampanel, n = 23	Total, n = 49
Sex			
F	6 (23)	9 (39)	15 (31)
M	20 (77)	14 (61)	34 (69)
Origin			
Caucasian	26 (100)	22 (96)	48 (98)
East/Southeast Asian	0	1 (4)	1 (2)
Mean age, y	39.3 (9.1)	38.4 (11)	38.9 (10)
AED group classification			
Induced	23 (89)	21 (91)	44 (90)
Balanced	2 (8)	1 (4)	3 (6)
Inhibited	1 (4)	1 (4)	2 (4)
Seizure history			
Simple partial	8 (31)	10 (43)	18 (37)
Complex partial	22 (85)	19 (83)	41 (84)
Secondarily generalized	23 (88)	19 (83)	42 (86)
Seizure syndrome			
Symptomatic	23 (89)	20 (87)	43 (88)
Unknown	3 (11)	3 (13)	6 (12)
Patients receiving AED			
1	3 (12)	3 (13)	6 (12)
2	18 (69)	16 (70)	34 (69)
>2	5 (19)	4 (17)	9 (19)
Patients receiving			
Carbamazepine	19 (73)	13 (57)	32 (65)
Lamotrigine	6 (23)	6 (26)	12 (25)
Base seizures per week			
Mean	12.6	9.9	11.3
Median	4.2	3.4	3.7

Values expressed as n (%) unless otherwise indicated.

AED = antiepileptic drugs.

type. Investigators classified each patient seizure event as simple partial, complex partial, or secondarily generalized. Simple partial seizures had to have a motor component to be counted.

The primary efficacy variable was the percent reduction in average weekly seizure rate (all types total). Secondary efficacy variables included percent of seizure-free days, clinical global impression of improvement, patient global impression of improvement, and changes in the Bond Lader Mood Rating Scale,[7] the Purdue Pegboard Test,[8] and the National Hospital Seizure Severity Scale.

Statistical analysis. Primary efficacy analysis was on the logarithmic transformation of seizure frequency, which was analyzed by the crossover analysis of variance.[9] The analysis of variance included investigator, sequence, and patient nested within investigator and sequence combination, period treatment, and investigator-by-treatment interaction. Carryover effect was assessed using the F-test of sequence. Additional crossover analyses were performed on secondary efficacy variables.

Table 2 *Treatment emergent adverse events (TEAE) among >5% of patients receiving talampanel*

TEAE	Talampanel, n = 46	Placebo, n = 45
Dizziness	24 (52.2)	7 (15.6)
Ataxia	12 (26.1)	1 (2.2)
Headache	6 (13.0)	5 (11.1)
Somnolence	6 (13.0)	4 (8.9)
Accidental injury	5 (10.9)	0
Asthenia	5 (10.9)	5 (11.1)
Abnormal gait	5 (10.9)	2 (4.4)
Pharyngitis	5 (10.9)	6 (13.3)
Infection	4 (8.7)	2 (4.4)
Pain	4 (8.7)	1 (2.2)
Incoordination	4 (8.7)	3 (6.7)
Nystagmus	4 (8.7)	3 (6.7)
Diplopia	4 (8.7)	2 (4.4)
Rhinitis	3 (6.5)	1 (2.2)

Values expressed as n (%).

Results. Demographic data for the 49 randomized patients are shown in table 1. Forty-two (86%) completed Treatment Period I whereas 38 (75%) completed the entire trial.

For the three dosing groups, the mean daily talampanel dosages were 60 mg for the induced group (44 patients), 58 mg for the balanced group (3 patients), and 23 mg for the inhibited group (2 patients).

There was a treatment effect in favor of talampanel ($p = 0.001$). Carryover effect was not significant ($p = 0.706$). Overall median percent reduction in total seizure frequencies was 21% with a 95% CI of 8 to 30%. The figure shows the numbers of patients experiencing the indicated percentage change in total seizure frequency. Thirty of 41 patients who had comparable data from both periods showed an improvement with talampanel compared with placebo. Among the 38 patients who completed the study, 30 had fewer seizures while taking talampanel.

Analyses by frequency of seizure type yielded improvement for simple partial seizures ($p = 0.001$). Seizure frequency reduction was not significant for complex partial seizures and secondarily generalized seizures ($p = 0.217$ and 0.235). There were no treatment-related differences in secondary endpoints.

Patients taking two hepatic enzyme-inducing AED (n = 7) had a mean plasma level of 66 ng/mL; patients taking one hepatic enzyme-inducing AED (n = 42) had a mean plasma level of 155 ng/mL; patients taking no inducing drugs (n = 5) had a mean plasma level of 372 ng/mL.

The most common treatment emergent adverse events are shown in table 2.

Discussion. Talampanel was effective in reducing seizures in this treatment-refractory population. Site 1, which enrolled the most patients (n = 22), saw a

Downloaded from www.neurology.org by MICHAEL FETELL on September 12, 2006

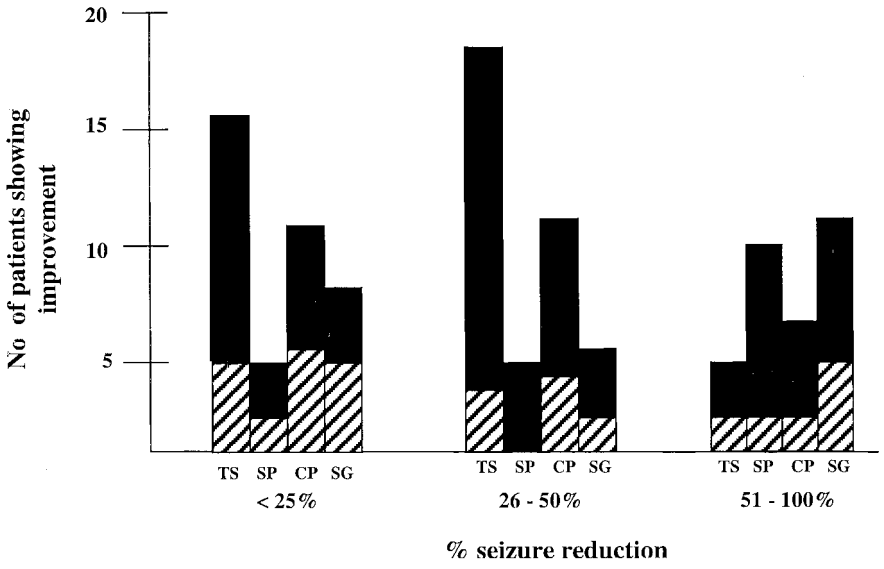

Figure. Number of patients showing improvement. Striped bars = placebo; black bars = talampanel. TS = total seizures; SP = simple partial; CP = complex partial; SG = secondarily generalized.

median reduction of 31% in seizure frequency. Two other sites that enrolled 12 and 3 patients had median reductions of 26 and 11%. A fourth site, whose patients had the most refractory seizures, enrolled 12 patients and showed 0% reduction.

Six patients taking carbamazepine required dose reductions to maintain plasma levels within 30% of baseline. However, efficacy could not be attributed to drug interaction because seizure reduction was the same as overall seizure reduction—21%—in patients not taking carbamazepine.

Plasma levels were highly variable. No correlation was seen between plasma levels and efficacy, possibly because some patients in the trial had seizures so refractory as to be unaffected by any plasma level of talampanel. The large impact on plasma levels of two inducing agents was not anticipated. In retrospect, patients taking two inducing drugs should have received higher doses of talampanel or should have been excluded from the study.

Dizziness was generally mild to moderate, transient, and associated with peak plasma levels. Ataxia, which had not been seen in a study of patients with ALS, may have been caused by pharmacodynamic interaction with concomitant AED.

In this study, talampanel had antiepileptic activity when added to standard therapies in patients with treatment-refractory partial seizures. Talampanel promises not only antiseizure efficacy via a unique mechanism but also the prospect of much-needed neuroprotection in patients with seizures. Additional trials are warranted.

Acknowledgment

The authors thank Carol Mitchell, MD, Nika Butler, and Faith Wilhite for editorial assistance.

References

1. Vizi ES, Mike A, Tarnawa I. 2,3-Benzodiazepines (GYKI 52466 analogs): negative allosteric modulators of AMPA receptors. CNS Drug Reviews 1996;2:91–126.
2. Bleakman D, Ballyk B, Schoepp D, et al. Activity of 2,3-benzodiazepines at native rat and recombinant human glutamate receptors in vitro: stereospecificity and selectivity profiles. Neuropharmacology 1996;35:1689–1702.
3. Lodge D, Bond A, O'Neill MJ, Hicks CA, Jones MG. Stereoselective effects of 2,3-benzodiazepines in vivo: electrophysiology and neuroprotection studies. Neuropharmacology 1996;35:1681–1688.
4. Kallman MJ, Tizzano JP, Modlin DL, et al. Behavioral characterization of a noncompetitive AMPA antagonist LY300164. Soc Neurosci Abstr 1995;21(Pt 1):350.
5. Jewell H, Lucas R, Schaefer H, Mant T. LY300164 initial experience in healthy subjects. Clin Pharmacol Ther 1998;63:188.
6. Commission on Classification and Terminology of the International League Against Epilepsy. Proposal for revised classification of epilepsies and epileptic syndromes. Epilepsia 1989;30:389–399.
7. Bond A, Lader M. The use of analogue scales in rating subjective feelings. Br J Med Psychol 1974;47:211–218.
8. Tiffin J, Asher EJ. The Purdue pegboard: norms and studies of reliability and validity. J Appl Psychol 1948;32:234–247.
9. Grizzle JE. The two-period change over design and its use in clinical trials. Biometrics 1965;21:467–480.

Downloaded from www.neurology.org by MICHAEL FETELL on September 12, 2006

A crossover, add-on trial of talampanel in patients with refractory partial seizures
A. S. Chappell, J. W. Sander, M. J. Brodie, D. Chadwick, A. Lledo, D. Zhang, J. Bjerke, G. M. Kiesler and S. Arroyo
Neurology 2002;58;1680-1682

This information is current as of September 12, 2006

Updated Information & Services	including high-resolution figures, can be found at: http://www.neurology.org/cgi/content/full/58/11/1680
Subspecialty Collections	This article, along with others on similar topics, appears in the following collection(s): **All Clinical trials** http://www.neurology.org/cgi/collection/all_clinical_trials **Clinical trials Observational study (Cohort, Case control)** http://www.neurology.org/cgi/collection/clinical_trials_observational_study_cohort_case_control **Antiepileptic drugs** http://www.neurology.org/cgi/collection/antiepileptic_drugs **Partial seizures** http://www.neurology.org/cgi/collection/partial_seizures **Complex partial seizures** http://www.neurology.org/cgi/collection/complex_partial_seizures
Permissions & Licensing	Information about reproducing this article in parts (figures, tables) or in its entirety can be found online at: http://www.neurology.org/misc/Permissions.shtml
Reprints	Information about ordering reprints can be found online: http://www.neurology.org/misc/reprints.shtml

AMERICAN ACADEMY OF NEUROLOGY

Downloaded from www.neurology.org by MICHAEL FETELL on September 12, 2006

Available online at www.sciencedirect.com
SCIENCE DIRECT
Cancer Letters 229 (2005) 217–222
CANCER Letters
www.elsevier.com/locate/canlet

BAT monoclonal antibody immunotherapy of human metastatic colorectal carcinoma in mice

Britta Hardy[a,*], Sara Morgenstern[b], Annat Raiter[a], Galina Rodionov[a], Ludmilla Fadaeev[a], Yaron Niv[c]

[a]*Felsenstein Medical Research Center, Tel Aviv University School of Medicine, Rabin Medical Center, Beilinson Campus, Petah Tikva 49100, Israel*
[b]*Departments of Pathology, Rabin Medical Center, Beilinson Campus, Petah Tikva 49100, Israel*
[c]*Gastroenterology, Rabin Medical Center, Beilinson Campus, Petah Tikva 49100, Israel*

Received 20 March 2005; accepted 14 June 2005

Abstract

BAT monoclonal antibody exhibited anti-tumor activity mediated by T and NK cells. We have evaluated the efficacy of murine and humanized BAT for the treatment of human colorectal carcinoma liver metastases in nude mice. HM7, a human colorectal carcinoma was injected into the spleen to colonize the liver. A single intravenous administration of both BAT antibodies significantly reduced the number of metastases and liver weights. Histological examinations demonstrated lymphocyte accumulation near remnant tumors and in tumor-free tissues of BAT treated mice. The efficacy of humanized BAT in the regression of hepatic metastases in human colorectal carcinoma has potential clinical use.
© 2005 Elsevier Ireland Ltd. All rights reserved.

Keywords: Cancer immunotherapy; BAT monoclonal antibody; Mice tumor model; Metastatic colorectal carcinoma; liver metastases; Liver histopathology

1. Introduction

Colorectal cancer (CRC) is a major cause of cancer-associated morbidity and mortality in developed countries [1–3]. Primary colorectal carcinoma becomes life threatening when it metastasizes to the liver [4–5]. Surgery alone may be curative in the early stages but adjuvant therapy is needed at later stages [6]. Unfortunately, in cases diagnosed in advanced stages, cure with either surgery or chemotherapy is not efficient [7–8]. Immunotherapy is used in cancer treatment to modulate the immune system response to kill tumor cells. Several types of immunotherapy based on different humoral and cell-immunity factors are currently undergoing preclinical and clinical trials. One approach involves the use of monoclonal antibodies that selectively bind to a specific determinant on T cells, thereby either initiating an activation pathway or inducing an inhibitory effect [9–11].

We have described a monoclonal antibody (mAb) which we termed BAT, that induces regression of

* Corresponding author. Tel.: 972 3 9376782; fax: 972 3 9216979.
E-mail address: bhardy@post.tau.ac.il (B. Hardy).

0304-3835/$ - see front matter © 2005 Elsevier Ireland Ltd. All rights reserved.
doi:10.1016/j.canlet.2005.06.046

murine tumors in the lungs of mice (B16 melanoma, 3LL Lewis lung carcinoma or MCA fibrosarcoma) [12] and of human tumors (SK-28 melanoma) in lungs of SCID mice engrafted with human lymphocytes [13]. However, BAT differs from other agonistic antibodies, such as anti-CD3 and anti-CTLA4, in that its anti-tumor activity involves the stimulation of both T cells and natural killer (NK) cells. BAT induces proliferation of $CD4^+$T cells and secretion of interferon-gamma [14]. BAT mAb is directed against a determinant on Daudi cells, a human Burkitt lymphoma cell line which stimulates murine lymphocytes and human peripheral blood T cells [15]. The murine BAT mAb has been humanized for clinical trials. Humanized antibodies are important because they bind to the same antigen as the original antibodies, but are less immunogenic when injected into humans [16]. The aim of the present study was to investigate the effect of both humanized BAT mAb (HuBAT) and murine BAT in the treatment of hepatic metastases of human CRC in mice.

2. Materials and Methods

2.1. BAT antibody production

BAT is a murine mAb developed in our laboratory as previously described [12]. Murine BAT was used at 10 μg/mouse, which was previously found to be an optimal anti-tumor concentration in mice [12]. HuBAT mAb was prepared by Aeres Ltd., (London, England) by recombinant DNA technology in which complementary-determining regions (CDRs) from the murine BAT, converts donor murine BAT immunoglobulin into a human-like immunoglobulin, by CDR grafting [16].

2.2. Binding of BAT mAb and HuBAT to Daudi cells.

Murine BAT mAb and HuBAT were added at different concentrations (10, 20, 40 and 80 μg/ml) to 0.5×10^6 Daudi cells samples for 2 h on ice. After washing the cells, anti-mouse or anti-human fluorescein (Sigma, Rehovot, Israel) were added to the samples for 30 minutes on ice. Mean fluorescent intensity (MFI) was evaluated by FACS analysis, using FACSCalibur flow cytometer (Becton Dickinson, Esembodegem, Belgium).

2.3. Human CRC cell line HM7

HM7 is a sub-clone of the human CRC cell line LS174T. It was selected for its high mucin synthesis and metastatic potential [17]. The cells were obtained as a generous gift from Professor Robert S. Breselier (MD Andersen, USA). They were grown in DMEM supplemented with 10% FCS, L-glutamine (2mM), Na-pyruvate (1nMol), penicillin (100 units/ml), streptomycin sulfate (0.1 mg/ml) and nystatin (12.5 μg/ml). Cultures were maintained at 37 °C in a humidified 5% CO2 incubator.

A large stock of cells was prepared to maintain the homogeneity and tumorigeneity of the cell lines. The stock was prepared by subcutaneous injection of 10^6 HM7 cells to nude mice, the resulting tumor at 0.5 cm diameter was removed, followed by tumor disruption, suspension and growth in vitro for about 1 week in large bottles and then frozen.

2.4. In vivo studies

We used a previously published human CRC liver metastatic tumor model [17]. In brief, BALB/c nude mice were anesthetized and their spleens were exposed. The tumor cell line, HM7 (2×10^6 cells in 0.250 ml PBS), was injected into the exposed spleen; after 1 minute, spleens were removed and the excisions closed. Mice were sacrificed 24 days after tumor inoculation.

HM7 cells retained their ability to colonize the liver as bulky metastatic nodules. BAT (10 μg/mouse) in PBS was injected intravenously 12 days after tumor inoculation. HuBAT was injected at 1 μg/mouse (effective concentration determined in preliminary experiments). Control mice were injected with mouse IgG3 at 10 μg/mouse. The livers were weighed, and the number of tumor nodules was counted.

2.5. Histological examinations

Liver specimens were fixed in 4% buffered formalin, embedded in paraffin blocks, sectioned in 4-micron thick layers and stained with hematoxilin and eosin. Liver sections were examined for

the presence of tumor metastases; special attention was addressed to the liver-metastasis interface in the involved parenchyma and to the presence of lymphocytes and histiocytes.

3. Results

3.1. Comparative binding of BAT and HuBAT to Daudi cells

Binding of HuBAT to that of murine BAT mAb to Daudi cells were compared by FACS analysis. As can be seen in Fig. 1, increasing concentrations of murine BAT mAb or HuBAT bound Daudi cells in a similar fluorescent intensity. The percent of mean fluorescence intensity (%MFI) was calculated as the fluorescent intensity per maximal fluorescent intensity x100, for each concentration of antibody used in this assay.

3.2. BAT treatment of CRC liver metastases in mice injected with human HM7 cells

Nude mice injected with human HM7 cells were divided into 3 groups: (1) injected 12 days after tumor inoculation with BAT mAb at a concentration of 10 μg/mouse; (2) injected with humanized BAT (HuBAT) at a concentration of 1 μg/mouse; (3) injected with 10 μg/mouse of normal mouse IgGs (controls). All mice were sacrificed 24 days after inoculation and the anti-tumor effect of HuBAT was compared to that of the BAT mAb and the control mice (Fig. 2). Both BAT and HuBAT exhibited anti tumor effect on hepatic metastasis, as manifested by the reduced number of liver tumor nodules and the reduced liver weight. Livers obtained from 11 untreated nude mice injected with human colon carcinoma, had an average weight 3.58 ± 1.66gr, whereas livers obtained from mice given a single

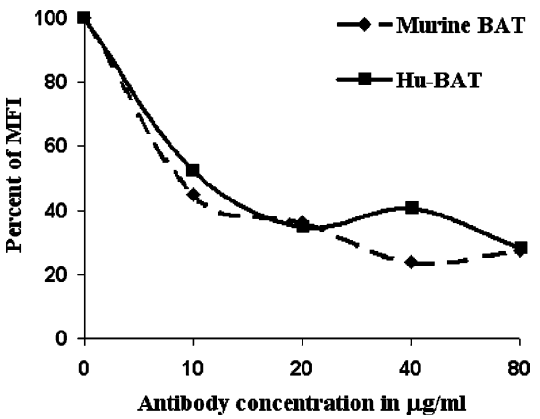

Fig. 1. Comparative study of murine and HuBAT monoclonal antibodies HuBAT or murine BAT mAbs were added in different concentrations to Daudi cells. Percent of mean fluorescence intensity (%MFI) was determined by FACS analysis. Increasing concentrations of murine BAT mAb or HuBAT bind Daudi cells in a similar fluorescent intensity to Daudi cells.

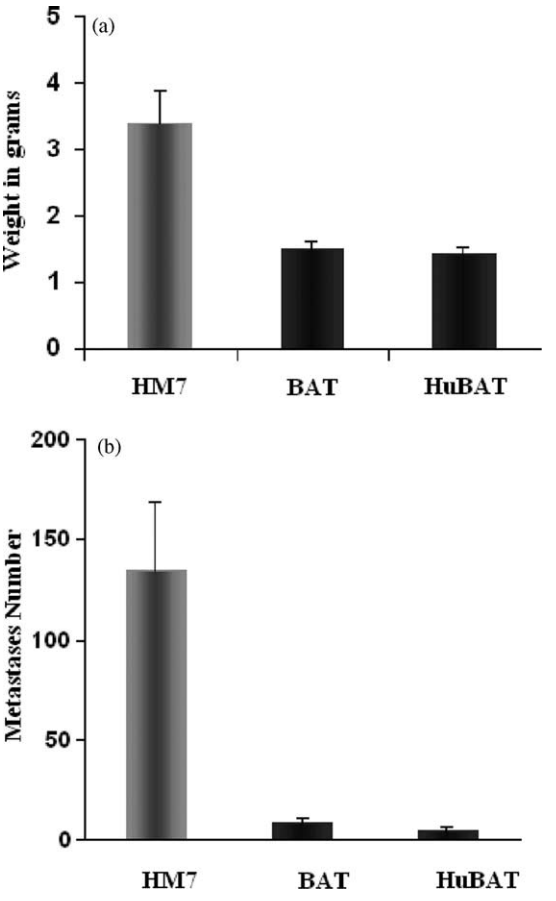

Fig. 2. Mice injected with HM7 cells and treated with BAT Nude mice injected with human colorectal cancer HM7 cells were divided into 3 groups 12 days later: (1) injected with BAT ($n=8$); (2) injected with HuBAT ($n=8$); (3) injected with normal mouse IgG 3 ($n=11$). Mice were sacrificed 24 days after tumor inoculation. The livers were weighed (Fig. 2a) and the number of tumor nodules was counted (Fig. 2b).

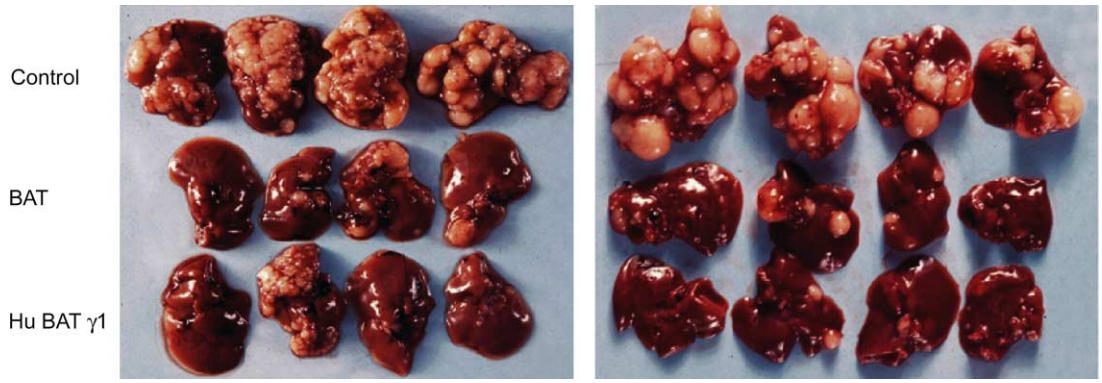

Fig. 3. Photograph of colorectal cancer metastases in livers Livers contain bulky pale nodules, which are the tumor lesions, encompassing most of the liver volume in non-treated mice. BAT and HuBAT antibodies induced a decrease in tumor metastases. Control mice received normal mouse IgG3.

injection of either antibody were within the normal weight range: 1.51 ± 0.2gr in the BAT antibody treated group and 1.43 ± 0.2gr in the HuBAT antibody group ($n = 8$). Separate comparisons of the number of metastases and weights of the liver among the three groups, using the Tukey-Kramer HSD statistical test, yielded significant differences between the BAT and HuBAT groups and the control group ($P \leq 0.01$). The livers of the untreated mice contained tumor lesions, bulky pale nodules (Fig. 3) that filled liver volume, whereas the livers from the BAT and HuBAT-treated group were of a normal shape and color.

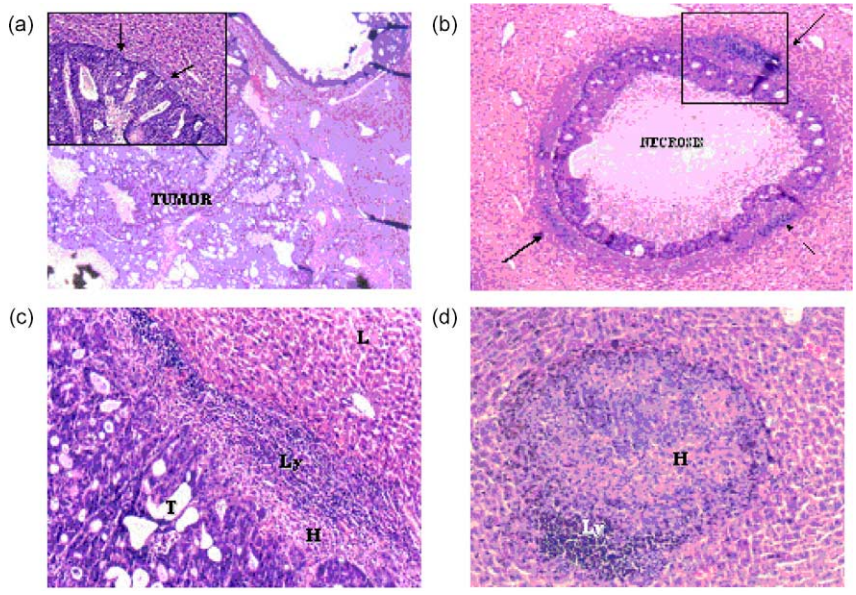

Fig. 4. Histological examination of sections from livers. (a): Mice that were not treated with BAT (injected with control IgG3) developed large liver metastatic colorectal tumors. Note extensive metastatic involvement of liver parenchyma (×40). (b): Section shows liver parenchyma of a mouse treated by BAT. The largest metastasis measured 0.15 cm and was surrounded by a granulomatous reaction consisting of histiocytes and a dense lymphocytic ring (arrows) (H&E ×40). (c): Higher magnification (H&E ×200) showing the malignant glands (M) separated from liver tissue (L) by histiocytes (H) in a palisade arrangement, and lymphocytes. (d): Lymphocytic infiltrate in liver of tumor-free (BAT-treated) nude mouse.

3.3. Histological study of BAT-treated mice livers demonstrates small necrotic tumor lesions surrounded by dense lymphocytes

Histological examinations of the livers were performed on day 24 after tumor inoculation. Sections through the liver parenchyma of the untreated mice demonstrated massive tumor involvement (Fig. 4a). In contrast, the liver parenchyma of BAT-treated mice was either free of tumors or contained only micrometastatic tumors. In some of the small necrotic tumors (Fig. 4b), the cells were surrounded by a granulomatous reaction consisting of histiocytes and a dense lymphocyte ring (Fig. 4c). Furthermore, in the liver parenchyma of the BAT-treated mice, we noted epithelioid granuloma formed by histiocytes and surrounded by lymphocyte infiltrate (Fig. 4d).

4. Discussion

Most cases of human CRC are diagnosed in advanced stages and cannot be cured by surgery or chemotherapy. Immunotherapy is being developed as an alternative treatment modality, which may change this fatal outcome. In this study we treated hepatic metastases of CRC with a single administration of either murine or human BAT mAb. BAT-treated mice exhibited a significantly lower development rate of hepatic metastases, compared to control mice. This observation supports the efficacy of immunotherapy and demonstrates, in vivo, the anti-tumor and anti-metastatic effects of BAT antibodies.

We have previously reported that BAT exhibited anti-tumor properties in mice bearing a variety of murine and human tumors in lungs [12–13]. To evaluate the potential clinical use of this antibody in human CRC, we tested BAT injection to nude mice in which human CRC tumors developed in the livers, similar to the disease pattern in human CRC patients. In this study both BAT and HuBAT induced anti-CRC tumor activity in the metastatic livers. The reduction of the number of metastases and the correlating liver weights were similar in BAT and HuBAT treatments. On pathological examinations of BAT treated mouse livers, we confirmed the anti tumor activity against metastases accompanied by granulomatous reactions consisting of histiocytes and dense lymphocytic rings. We have previously analyzed the lymphocyte subpopulations in these athymic mice. We found that injection of BAT mAb in nude mouse induced lymphopoiesis and a 20% increase in CD3 and CD4 T cells. The proportion of NK cells also increased due to BAT administration [18]. These findings provide an explanation of the BAT anti metastatic activity in the nude mouse. The efficacy of humanized BAT in the regression of hepatic metastases in human colorectal carcinoma suggest potential development into therapy for clinical use.

References

[1] R.S. Bresalier, Gastrointestinal and Liver Disease, seventh ed., Saunders, Philadelphia, PA, 2002. pp. 2215–2269 (Sleisenger & Fordtran).
[2] D. Parkin, P. Pisani, J. Ferlay, Global cancer statistics, CA Cancer J. Clin. 49 (1999) 33–64.
[3] L.A. Ries, P.A. Wingo, D.S. Miller, H.L. Howe, H.K. Weir, H.M. Rosenberg, et al., The annual report to the nation on the status of cancer 1973–1977 with a special section on colorectal cancer, Cancer 15 (2000) 2398–2424.
[4] M. Lise, P.P. Da Pian, D. Nihi, P.L. Pilati, C. Prevaldi, Colorectal metastases to the liver: present status of management, Dis. Colon Rectum 33 (1990) 688–694.
[5] P.M. Murphy, Chemokines and the molecular basis of cancer metastasis, N. Engl. J. Med. 345 (2001) 833–835.
[6] C.G. Moertel, T.R. Fleming, J.S. Mc Donald, D.G. Haller, J.A. Laurie, P.J. Goodman, et al., Levamisole and fluorouracil for adjuvant therapy of resected colon carcinoma, N. Engl. J. Med. 322 (1990) 352–358.
[7] N. Wolmark, H. Rockette, E. Mamounas, J. Jones, S. Wiland, D.L. Wickerham, et al., Clinical trial to assess the relative efficacy of fluorouracil, fluorouracil and leucovorin, fluorouracil and levamisole, and fluorouracil, leucovorin, and levamisole in Dukes' B and C carcinoma of the colon: results from the national adjuvant breast and bowel project C-04, J. Clin. Oncol. 17 (1999) 3553–3559.
[8] M.J. O'Connell, D.M. Nagorney, A.M. Bernath, G. Schroeder, R.J. Fitzgibbons, J.A. Mailliard, et al., Prospectively randomized trial of postoperative adjuvant chemotherapy in patients with high-risk colon cancer, J. Clin. Oncol. 16 (1998) 295–300.
[9] S. Dickman, Cancer therapy-antibodies stage a comeback in cancer treatment, Science 280 (1998) 1196–1197.
[10] G. Kohler, C. Milstein, Continuous cultures of fused cells secreting antibody of predefined specificity, Nature 256 (1995) 495–497.
[11] E.A. Clark, J.A. Ledbetter, Amplification of the immune response by agonistic antibodies, Immunol. Today 7 (1986) 267–269.

[12] B. Hardy, I. Yampolski, R. Kovjazin, M. Galli, A. Novogrodski, A monoclonal antibody against a human B lymphoblastoid cell line induces tumor regression in mice, Cancer Res. 54 (1994) 5793–5796.
[13] B. Hardy, R. Kovjazin, A. Raiter, N. Ganor, A. Novogrodsky, Lymphocyte-activating monoclonal antibody induces regression of human tumors with severe combined immunodeficient mice, Proc. Natl Acad. Sci. USA 94 (1997) 5756–5760.
[14] A. Raiter, G. Rodionov, A. Novogrodsky, B. Hardy, CD4+T lymphocytes as primary cellular target for BAT mAb stimulation, Int. Immunol. 12 (2000) 1623–1628.
[15] B. Hardy, M. Galli, E. Rivlin, L. Goren, A. Novogrodsky, Activation of human lymphocytes by a monoclonal antibody to B lymphoblastoid cells; molecular weight and distribution of binding protein, Cancer Immunol. Immunother. 40 (1995) 376–382.
[16] M.M. Bending, Humanization of rodent monoclonal antibodies by CDR grafting methods: a comparison to methods in enzymology, 8 (1995) 83–93.
[17] R.S. Bresalier, Y. Niv, J.C. Byrd, Q.Y. Duh, N.W. Toribara, R.W. Rockwell, et al., Mucin production by human colonic carcinoma cells correlates with their metastatic potential in animal models of colon cancer metastasis, J. Clin. Invest. 87 (1991) 1037–1045.
[18] B. Hardy, Y. Niv, L. Fadaeev, A. Raiter, BAT mAb induces lymphopoiesis in nude mice, Int. Immunol. 17 (2005) 615–619.

The European Hematology Association 10th Annual Congress, Stockholm, Sweden, June 2-5, 2005

Abstract nr.: 471

PHASE I CLINICAL TRIAL OF CT-011, A HUMANIZED MONOCLONAL ANTIBODY DIRECTED AGAINST A B7 FAMILY-ASSOCIATED PROTEIN, IN PATIENTS WITH ADVANCED HEMATOLOGICAL MALIGNANCIES

Author: Nagler, A , Chaim Sheba Medical Center, Ramat Gan, Israel
Co-author(s):
Kneller, A., Chaim Sheba Medical Center, Ramat Gan, Israel
Avigdor, A., Chaim Sheba Medical Center, Ramat Gan, Israel
Leiba, M., Chaim Sheba Medical Center, Ramat Gan, Israel
Koren, R., CureTech Ltd., Yavne, Israel
Klapper, L.N., CureTech Ltd., Yavne, Israel
Schickler, M., CureTech Ltd., Yavne, Israel
Shimoni, A., Chaim Sheba Medical Center, Ramat Gan, Israel

Topic: 26. Vaccination / Dendritic cells, cellular, immunotherapy
Keywords*:* Immunotherapy, CT-011, B7 receptor family, Phase I

Background: CT-011, a humanized monoclonal antibody that is directed against a B7 family-associated protein, was previously shown to efficiently elicit anti-cancer immune response against a wide range of murine and human tumors (Hardy et al PNAS 94:5756-5760, 1997; Hardy et al. Intl. J. Oncol. 19: 897-902, 2001). Its interaction with both NK cells and CD4+CD45+RO T cells culminates in NK- and T- cell dependent immune responses. CT-011 target-antigen operates through the PI3K pathway to extend the survival of effector/memory T cells and to promote the generation of tumor-specific memory T cells.

Aims: The purpose of this first in human clinical study was to evaluate the safety and determine the maximal tolerated dose (MTD) of CT-011 single intravenous administration in pts with advanced stage hematological malignancies.

Methods: We studied the safety profile of CT-011 in 17 pts with advanced hematological malignancies. All pts failed several lines of conventional chemotherapy and radiotherapy as well as allo (n=6) or auto SCT (n=3). Eleven of the pts were females and six were males with a median age of 55 (20-77, range) years. Eight had AML, four NHL, three CLL, one MM and one HD. CT-011 was given in a single 5h IV infusion in escalating doses starting at 0.2 mg/kg up to 6.0 mg/kg (3 pts at each dose level). One pt at the lowest dose level was re-enrolled five months after the first administration at a higher dose level for a total of 16 administered treatments.

Results: CT-011 was safe and well tolerated with no treatment-related toxicities. Common adverse events included minimal allergic reactions and low grade fever. No single dose MTD was found in this study. One AML pt with resistant leukemia that was platelet-dependent with plt < 10x10^9/L is currently 9 months post first CT- 011 infusion in partial response and is platelet transfusion-independent. Two other pts (CLL-1, HD-1) remain with stable disease with no disease progression for more than 8 months and two

additional pts (NHL) exhibit minimal response to treatment . Four other pts are alive with active disease with a median follow up of 3 (1-6) months, while seven pts died from their advanced resistant disease. Accrual to this study as well as pts follow up continues.

Conclusions: A single administration of CT-011 is safe and well tolerated in pts with advanced hematological malignancies. The observed anti-tumor activity may be related to CT-011 interaction with the B7 receptor family-associated protein resulting in enhancement of tumor-specific immune response. Future studies will evaluate the combination of donor lymphocyte infusion and CT-011 for pts with hematological malignancies having minimal residual disease after stem cell transplantation.

Treatment with BAT monoclonal antibody decreases tumor burden in a murine model of leukemia/lymphoma

BRITTA HARDY[1], LEONORA INDJIIA[1], GALINA RODIONOV[1], ANNAT RAITER[1] and AIDA INBAL[2]

[1]Felsenstein Medical Research Center, Tel-Aviv University Sackler Faculty of Medicine, Rabin Medical Center, Beilinson Campus, Petach Tikva; [2]Hematology Department, Sheba Medical Center, Tel Hashomer, Tel Aviv University Sackler Faculty of Medicine, Israel

Received July 20, 2001; Accepted August 16, 2001

Abstract. BAT is a monoclonal antibody produced against membranes of Daudi cells that induces anti-tumor activity in mice against a variety of solid murine and human tumors, mediated by its immune stimulatory properties on murine and human lymphocytes. The present study analyzes the effect of BAT on leukemia/lymphoma using the BCL1 model of leukemia/lymphoma in BALB/C mice. BAT antibody binds to BCL1 leukemia cells and recognizes a 48 kDa protein similar to the antigen on Daudi cells. Mice inoculated with leukemia cells were treated either by direct BAT injections or by adoptive transfer of lymphocytes from BAT-injected mice. Administration of BAT monoclonal antibody was either once, on day 14, or daily on days 10-13 post tumor inoculation. A single injection of BAT resulted in reduction of peripheral blood tumor cells, however additional injections further decreased the tumor cell number reaching a 95-fold reduction on day 20 post tumor inoculation. Anti-tumor effect was also obtained when animals were injected with splenocytes from BAT-treated donor mice. A significant prolongation of survival of BAT-treated mice was observed although with no cure. The results of this study indicate that BAT might be used for reducing the tumor burden in leukemia for immunotherapy and in combination with other treatment modalities.

Introduction

BAT, a monoclonal antibody, produced by us against membranes of a Burkitt lymphoma B cells, binds and stimulates T lymphocytes. BAT also exhibits anti-tumor properties in mice bearing a variety of solid tumors. A single intravenous administration of BAT to mice resulted in regression of the tumors and prolongation of their survival (1,2). BAT also induced regression of human tumors inoculated into SCID mice that had been implanted with human lymphocytes (3). The anti-tumor activity of BAT was related to its immune stimulatory properties, as was manifested by the regression of tumors in mice previously transplanted with lymphocytes from BAT treated mice (1). Selective depletion in mice or selective engraftment of T or NK cells into SCID mice indicated that both NK and T cells mediate the anti-tumor activity of BAT (3). The immune stimulation of selected lymphocyte sub-populations indicated that CD4 T cells responded to BAT activation by proliferation and IFN-γ secretion (4). In order to study the effect of BAT on non-solid tumors we investigated its anti-tumor activity in mice bearing BCL1, a B-cell leukemia/lymphoma (5).

The clinical features of the disease are characterized by infiltration of spleen, liver, lymph nodes by leukemic cells followed by appearance of the tumor cells in the peripheral blood. The clinical characteristics of BCL1 in mice resemble the pro-lymphocytic form of chronic lymphocytic leukemia (PLL) in humans (6). BCL1 tumor cells express IgM λ and IgD λ that share a common idiotype (7,8). This mouse leukemia/lymphoma model offers a number of advantages in the fields of anti-idiotypic therapy (9), idiotypic vaccination (10,11), tumor dormancy (12,13) and in different aspects of monoclonal antibody therapy of B-cell lymphomas (14,15). Leukemia/lymphoma cells express tumor specific antigens. However, they generally lack expression of costimulatory surface molecules such as B7, which are necessary for induction of T cell responses thus leading to T cell anergy. Some of the leukemia/lymphoma cells, however, express the CD40 antigen that upon binding to a ligand or a monoclonal anti-CD40 antibody, induces stimulatory responses that consequently resulted in anti-tumor activity (16).

In the present study, we analyzed the direct or adoptive transfer-induced effect of BAT on the tumor burden in the murine model of leukemia/lymphoma.

Materials and methods

Flow cytometry of BAT binding to BCL1 lymphoma/leukemia tumor cells. Peripheral blood mononuclear cells and splenocytes from BCL1 lymphoma/leukemia bearing mice

Correspondence to: Dr Britta Hardy, Felsenstein Medical Research Center, Rabin Medical Center, Beilinson Campus, Petah-Tikva 49100, Israel
E-mail: brittah@netvision.net.il

Key words: tumor regression, lymphocyte stimulation, BAT monoclonal antibody, BCL1 lymphoma/leukemia, adoptive transfer

were washed twice with PBS containing 0.5% BSA and 0.05% azide. Aliquots of $0.5x10^6$ cells were used for double labeling assays. Cells were incubated with a saturated amount of biotin bound BAT for 45 min at 4°C. After washing, the cells were incubated with streptavidin labeled Phycoerythrine (PE) for 30 min. The cells were then stained by the BCL1 anti-idiotype antibody labeled with FITC (a generous gift from Professor M.J. Glennie, Southampton, UK). The cell samples were analyzed by a FACScan (Becton-Dickinson). Side Scatter and Forward Scatter determined the gate of the cells. Streptavidin-PE plus anti-mouse-IgG-FITC were used as isotype control.

Western blot analysis of BAT binding antigen on BCL1 tumor cells. Splenocytes from mice bearing BCL1 leukemia/lymphoma were mixed with 50 µl of lysis buffer (10 mM Tris-HCl buffer, pH 7.6 with 5 mM EDTA, 0.14 M NaCl, 0.1 mM phenylmethylsulfonyl fluoride, 10 mM NaF and 0.5% NP-40) and incubated for 30 min at 0°C. The mixtures were centrifuged and the supernatants were collected. Samples of splenocytes 14 and 28 days post BCL1 inoculation were used. Daudi cell lysate was used for comparison at 10 µg/lane. Proteins were separated by SDS-PAGE (10%) and then transferred to nitrocellulose membranes. Detection of the BAT-binding protein was done by incubation with BAT monoclonal antibody overnight at 4°C followed by incubation for 45 min with anti-mouse IgG-peroxidase conjugated (Sigma Chemical Co., Germany) and by chemiluminescent substrate (Pierce, USA).

Tumor model. BALB/C female mice 7-8 weeks old were supplied by Harlan Laboratories (Jerusalem) and maintained at the local Animal Facility, in accordance with the Animal Care Committee of Rabin Medical Center. BCL1 mouse B-cell leukemia/lymphoma cells were maintained *in vivo* in BALB/C mice. Enlarged spleens were taken at the terminal stage of disease (21-28 days) and single cell suspensions were prepared as previously described (5). BALB/C mice were inoculated (i.p.) with BCL1 cells at various concentrations, as indicated in the results.

Determination of tumor growth. The extent of tumor growth was evaluated by physical palpation (13). Determination of the number of tumor cells in blood circulation was done by morphological assessment of percent of tumor cells in 200 white blood cells in smears stained with May-Grunwald-Giemsa, multiplied by the total number of leukocytes. Anti-BCL1 anti-idiotype (the kind gift of Professor Martin J. Glennie, Southampton, UK) was used for fluorocytometric determination of percent of tumor cells to compare the morphological determination. Tumor cell numbers determined by morphological assessments were also compared to the number of large unstained cells (LUC) obtained by automatic counter hematologic system (ADVIA 120). Survival of mice bearing tumors and either treated or used as controls were studied.

BAT was generated and purified as previously described (1,2). BAT was injected i.v. into BALB/C mice at various concentrations and at different days after tumor injections, according to the experimental design. We used a single injection of 10 µg/mouse on day 14 (post tumor inoculation), or multiple injections on days 10-13.

Adoptive transfer experiments: Splenocytes ($6-8x10^7$) from mice that had been injected with 10 µg/mouse of BAT 10 days prior to removal of spleen, were use for adoptive transfer into recipient mice - 14 days post inoculation with BCL1 lymphoma cells. Adoptive transfer of normal splenocytes to the tumor-bearing mice was used as a control in addition to non-treated mice. All animals were sacrificed 26 days post tumor inoculation.

Statistical analysis. Experiments in mice injected with BAT were analysed by ANOVA (Analysis of Variance), with groups (the 4 treatment conditions) and days (the two days considered in the analysis), along with their interaction (as independent factors) and tumor cell counts (as the dependent variable). The specific questions of interest, namely various comparisons to controls, or between groups, and between groups and days, were constructed and tested as preplanned contrasts within the ANOVAs. JMP (SAS Institute, Cary, NC, USA) was employed for statistical analyses. Survival experiments of BCL1-bearing mice without and with BAT treatment using different protocols, was statistically analyzed by Kaplan-Meier life table analysis and tested by log-rank and Wilcoxon tests.

Results

BAT binding to BCL1 lymphoma/leukemia tumor cells. BAT monoclonal antibody produced against membranes of Daudi cells, a Burkitt lymphoma human cell line, was also found to bind other EBV-transformed B-lymphoblastoid cells such as Raji cell line (17), thus, it was of interest to establish whether BAT binds murine BCL1 lymphoma cells. Double staining of tumor cells from peripheral blood and spleen with BAT and BCL1 anti-idiotype demonstrated that BAT binds to the tumor BCL1 cells, a murine lymphoma/leukemia cells among the murine peripheral blood cells. Half of the tumor cells in the peripheral blood were stained with BAT. A higher percent (>80%) of splenocytes obtained from mice with a fully progressed disease binds BAT/anti-Id (Fig. 1).

BAT antibody recognizes a 48 kDa protein similar to the antigen on Daudi cells. Western blot analysis of splenocytes from mice bearing BCL1 for 14 and 28 days post inoculation were tested. A 48-50 kDa band was detected by BAT antibody. The sample prepared from splenocytes removed from mice 28 days post tumor inoculation shows a more prominent band probably due to the relative increase in the numbers of tumor cells in this preparation. It should be noted that this band is similar to that recognized by BAT on Daudi cells (Fig. 2).

Treatment of BCL1-bearing mice with BAT monoclonal antibody. Four groups of BALB/C mice were studied (Table I). Each mouse was injected intraperitoneally (i.p.) with $5x10^4$ BCL1 cells. One group (A) was not treated following the injection of tumor cells. The second group of mice (B) was treated with a single intravenous injection of 10 µg/mouse of BAT monoclonal antibody 14 days

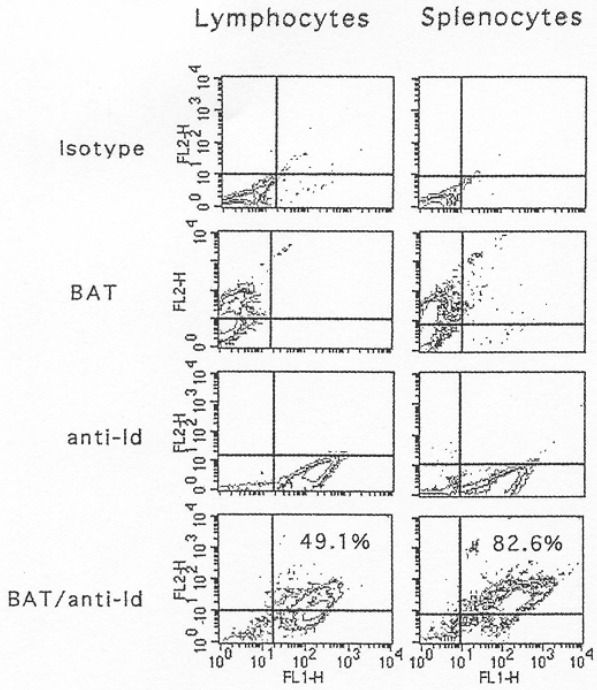

Figure 1. FACS analysis of BCL1 leukemia/lymphoma cells labeled with anti-idiotype and BAT. Double staining of peripheral blood lymphocytes and of splenocytes from BALB/C mice, 21 days post BCL1 tumor cell inoculation. Streptavidin-PE plus anti-mouse-IgG-FITC were used as isotype control. BAT was labeled with biotin followed by streptavidin-PE. BCL1 anti-idiotype antibody was labeled with FITC. The lower panel contour plots show the double staining of anti-BCL1 anti-idiotype-FITC with BAT-PE.

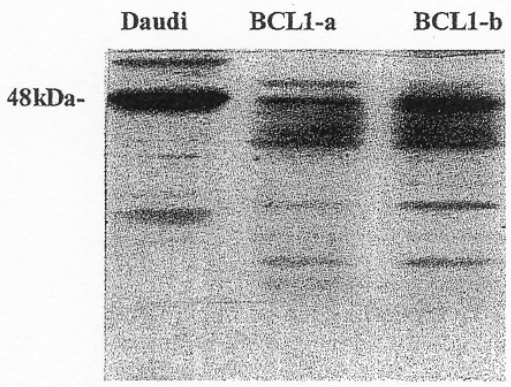

Figure 2. Western blot analysis of BAT binding antigen on BCL1 tumor cells. Lysates from spleen cells removed from mice 14 and 28 days post BCL1 tumor inoculations were separated by SDS-PAGE (samples of 10 µg protein) and then transferred to nitrocellulose membranes. Detection of the BAT-binding protein was done by BAT monoclonal antibody. Daudi binding protein was used as control. A 48-50 kDa band on BCL1 tumor cells was detected.

following the tumor cell injection. The third group (C) was treated with a series of 4 daily injections of BAT starting with i.v. - injection of 10 µg on day 10, followed by 3 i.p.

Table I. Clinical parameters of leukemia/lymphoma (BCL1) in mice treated with BAT.

Group	Tumor cells (x10^6/ml) Day 20	Day 25	P-value
Control BCL1 injected mice[a]	19.0±4.7	26.0±3.9	
BAT (T14)[b]	5.0±3	18.5±4.6	<0.005
BAT (T10, 11, 12, 13)[c]	0.42±0.1	12.4±3.2	<0.0001
BAT (T10, 11, 12, 13)[d]	0.2±0.03	4.6±2.6	<0.001

[a]BALB/C mice were injected i.p. with 5x10^4 BCL1 lymphoma cells. [b]BAT (10 µg), administered i.v. by a single injection on day 14 post tumor inoculation. [c]BAT (10 µg), administered i.v. on day 10, followed by an additional 3 administrations of 1 µg BAT i.p., on days 11, 12 and 13 post tumor inoculation. [d]BAT (10 µg) was administered i.v. to mice on day 10, followed by 10 µg i.p on days 11, 12 and 13 post tumor inoculation.

Table II. Assessment of tumor cells from peripheral blood of affected mice by Coulter counter, flow cytometry and morphological analyses.

	Total WBC[a] (x10^6/ml)	LUC cells[b] (x10^6/ml)	Anti-idiotype[c] (x10^6/ml)	Morphology[d] (x10^6/ml)
Normal mice	10.36±1.4	0.36±0.1	0	0
BCL1-bearing mice	75.23±25.7	19±11	19.19±0.8	19±4.7

[a]WBC, white blood cells determined by counter. [b]LUC, large unstained cells, denotes tumor cells determined by counter. [c]Anti-idiotype, FITC binding to BCL1 cells by FACS analysis. [d]Assessment by microscope as outlined in Materials and methods.

injections of 1 µg each on days 11, 12 and 13. In the last group (D) the injections on days 11, 12 and 13 were 10 µg each. The number of tumor cells on days 20 and 25 after inoculation, were estimated for each group, as described in Materials and methods. In group A, an increase in tumor cells in peripheral blood from 0 to 19±4.7 on day 20 was observed (Table I). Further increase in tumor cells was observed on day 25. In contrast, in the group treated with single BAT injection (B) the increase in tumor cells was smaller ($p<0.005$). Similarly, the number of tumor cells was significantly fewer in the third group (C), where repeated injections of BAT were administered. This anti-tumor effect of BAT was even more pronounced in group D, where higher doses of BAT were injected. In this group the number of tumor cells was almost undetectable, 20 days post tumor inoculation ($p<0.001$ by ANOVA).

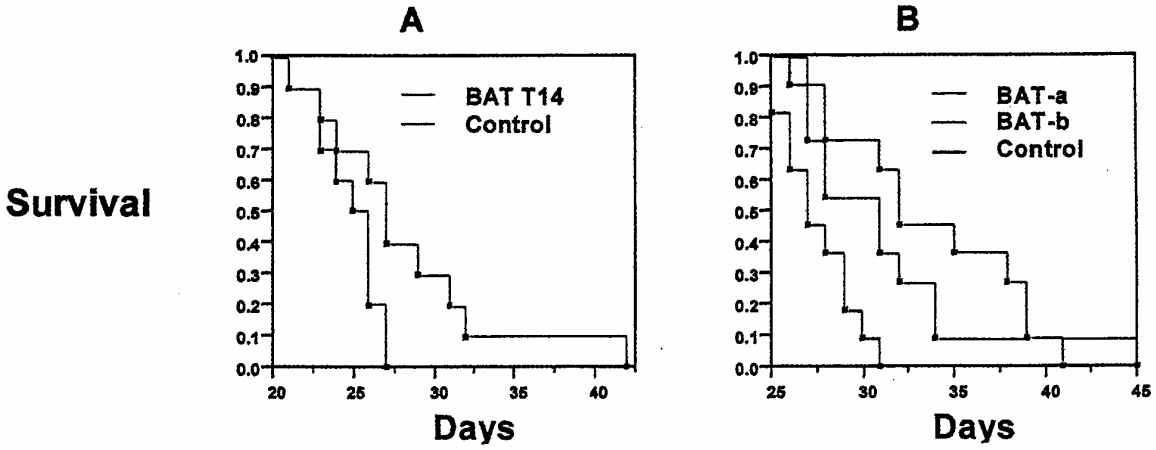

Figure 3. Survival curves of BCL1 leukemia/lymphoma-bearing mice. (A), Comparison between BCL1 injected and untreated mice (control) and those treated with a single injection of 10 μg BAT on day 14 post tumor inoculation. (B), Comparison between 3 groups of mice: BCL1 injected and untreated (control) and BAT-a: treated with 10 μg BAT (i.v.) on day 10 followed by 1 μg i.p. on days 11, 12 and 13 post tumor inoculation BAT-b: treated with 10 μg BAT (i.v.) on day 10 followed by 10 μg i.p. on days 11, 12 and 13 post tumor inoculation.

Table III. Adoptive transfer of splenocytes from BAT injected mice, to mice with BCL1 leukemia/lymphoma.

Group	Mice (n)	Tumor cells (x10^6/ml) Day 20	Tumor cells (x10^6/ml) Day 25	Significance P-value
Control mice injected with BCL1[a]	12	17.3±2	49.8±14	
Mice treated by BAT on day 14[b]	9	5.0±3	21.2±9	0.003
Adoptive transfer of normal splenocytes[c]	12	15.1±6	29.2±7	
Adoptive transfer of splenocytes from BAT injected mice[d]	12	0.1±0.02	4.6±1.6	0.001

[a]Control mice were inoculated i.p. with BCL1 5x10^4/mouse. [b]Mice injected (i.v.) with BAT (10 μg/mouse) 14 days post BCL1 inoculation. [c]Adoptive transfer of normal splenocytes (7x10^7 cells/mouse) was performed 14 days post BCL1 cell inoculation. [d]Splenocytes isolated from mice 10 days post BAT injection (10 μg/mouse) i.v. were used for adoptive transfer (7x10^7 cells/mouse) into recipient mice 14 days after BCL1 inoculation. All mice were sacrificed on day 26 post BCL1 inoculation.

In order to confirm the quantitative assessments of tumor cells performed by morphological evaluation described in Materials and methods, peripheral blood cells of mice from group A were also analyzed by a Coulter counter and flow cytometry using anti-BCL1 anti-idiotype. The comparison between the morphological assessment of the number of tumor cells, the number of tumor cells counted by automatic counter and that obtained by flow cytometry is presented in Table II. It appears that the number of tumor cells assessed by all three methods was almost identical.

The survival of each group is shown in Fig. 3. Survival analysis performed by Kaplan-Meier life table analysis and tested by log-rank, demonstrated an increase in survival in the group treated with single BAT injection on day 14, as compared to the untreated group. The difference was statistically significant (p=0.046, Fig. 3A). The increase in survival of mice treated by four daily injections of BAT (1 μg or 10 μg on days 10, 11, 12, and 13 (BAT-a or BAT-b, respectively) compared to controls is demonstrated in Fig. 3B. The difference in survival between the groups treated by either protocol and the untreated group was highly significant (p=0.0014 by log-rank and p= 0.0035 by Wilcoxon). It should be noted, however, that all treated mice died by day 45.

Treatment of leukemia/lymphoma mice by adoptive transfer of lymphocytes from BAT injected mice. We have previously shown that adoptive transfer of splenocytes from mice that have been injected with BAT into tumor-bearing recipients, induced anti-tumor activity (1). We therefore injected (i.v.) BALB/C mice with 10 μg of BAT, followed by adoptive transfer of their splenocytes to recipients 10 days later. The recipients were inoculated with BCL1 prior to treatment and then treated with either direct injection of BAT or adoptive transfer on day 10 post tumor cell inoculation. Table III,

summarizes the results of two experiments in which the effect on the number of tumor cells, of direct treatment with BAT or treatment by adoptive transfer of lymphocytes from BAT injected animals is compared. Both modalities of treatment induced significant decrease in the tumor burden. A single BAT injection induced a 3.5- and 2.3-fold decrease in the number of tumor cells on days 20 and 25, respectively ($p=0.003$). The treatment of splenocytes from BAT-treated mice, by adoptive transfer as compared to adoptive transfer of normal splenocytes, induced a 151- and 6.3-fold decrease in the number of tumor cells on day 20 and 25, respectively ($p=0.001$). It should be noted that adoptive transfer of non-stimulated normal splenocytes to the tumor-bearing recipient mice demonstrated a therapeutic effect only on day 25 (1.7-fold reduction) which was, however, not statistically significant.

Discussion

In the present study, the anti-tumor activity of BAT monoclonal antibody in a murine model of BCL1 leukemia/lymphoma, was demonstrated. A significant reduction in the number of tumor cells reaching a nadir at day 20, was observed following either direct BAT injections or adoptive transfer of mice splenocytes treated prior with BAT. In addition, the size of the spleen of the treated animals was smaller than the untreated controls (data not presented). The anti-tumor activity was also reflected by a significant increase in the survival of BAT-treated mice compared to the untreated group.

The anti-tumor effect of BAT was dose-dependent. A single injection of BAT reduced the number of tumor cells almost 4-fold. Moreover, repeated low doses of BAT caused a remarkable reduction in tumor cells (45-fold). In addition, treatment with repeated increased doses of BAT resulted in almost complete disappearance of tumor cells from peripheral blood of the animals (95-fold reduction). BAT monoclonal antibody was previously shown to bind T cells, normal and transformed and EBV transformed B cells like Daudi - a Burkitt lymphoma cell line and Raji - an EBV transformed B cell line (17). BCL1 tumor cells, a murine B cell leukemia/lymphoma, bind BAT antibody (Fig. 1) and recognize a similar antigen on these cells (Fig. 2). The nature of the antigen is not yet clear but seems to be similar in mouse and human cells and present on various tumor cells. Binding of the antibody to the tumor cells might induce a first signal for activation of the immune system. However, the anti-tumor effect is mediated by the antibody stimulated lymphocytes as was demonstrated by the 173-fold reduction in leukemia cells that was observed in mice bearing tumors injected with splenocytes from mice pretreated with BAT, whereas normal splenocytes had no effect on tumor cell reduction (Table III). However, despite the significant reduction in leukemia cells 20 days after BAT treatment, a gradual extension of the tumor was observed thereafter. It may be that in malignancies such as lymphoma, the disease progression is associated with a decrease in critical number of normal T cells that BAT stimulates, explaining the limitation of BAT's anti-tumor effect in lymphoma in contrast to the solid tumors (1). The anti-tumor activity by BAT against BCL1 leukemia might be also induced by IFN-γ. We have previously demonstrated that BAT stimulates $CD4^+$ T cells to proliferate and secrete INF-γ (4). IFN-γ alone or in combination with reagents to cross-link the surface immunoglobulins, induces both cell cycle arrest and apoptosis in BCL1 cell line (18). A similar approach of treating mice bearing BCL1 lymphoma with anti-CD40 immunostimulatory antibody, has been undertaken by Glennie's group (15). They demonstrated that injection with anti-CD40 eradicated the lymphoma and provided protection against tumor rechallenge, without further antibody treatment (16). This difference in outcome may stem from the differences in the cell types activated. Anti-CD40 acts on dentritic cells and BAT activates T cells. Apart from BAT and anti-CD40, additional antibodies have been found to be therapeutically active in mice B-cell lymphomas (15).

In contrast to agents like anti-CD20 and anti-CD33, which target the affected lymphoma or leukemia cell (19,20), BAT enhances the host's natural anti-tumor response. Thus, it could be used in conjunction with agents like these two monoclonal antibodies as well as with chemotherapy/irradiation.

Acknowledgements

We would like to express our appreciation to Mr. Elliot Sprecher for the statistical analysis. Our gratitude to Professor Nehama Haran-Gera and Dr Alfa Peled from the Weizmann Institute of Science for their help in initiation of this study and to Mrs. S.P. Dominitz for editorial assistance.

References

1. Hardy B, Yampolski I, Kovjazin R, Galli M and Novogrodsky A: A monoclonal antibody against a human B lymphoblastoid cell line induced tumor regression in mice. Cancer Res 54: 5793-5796, 1994.
2. Hardy B, Galli M, Rivlin E, Goren L and Novogrodsky A: Activation of human and lymphocytes by a monoclonal antibody to B lymphoblastoid cells; molecular weight and distribution of binding protein. Cancer Immunol Immunother 40: 376-382, 1995.
3. Hardy B, Kovjazin R, Raiter A, Ganor N and Novogrodsky A: A lymphocyte-activating monoclonal antibody induces regression of human tumors in severe combined immunodeficient mice. Proc Natl Acad Sci USA 94: 5756-5760, 1997.
4. Raiter A, Rodionov G, Novogrodsky A and Hardy B: $CD4^+$ T lymphocytes as a primary cellular target for BAT monoclonal antibody stimulation. Int Immunol 12: 1623-1628, 2000.
5. Slavin S and Strober S: Spontaneous murine B-cell leukaemia. Nature 272: 624-626, 1978.
6. Krolick KA, Isakson PC, Uhr JW and Vitetta ES: BCL1, a murine model for chronic lymphocytic leukemia: use of the surface immunoglobulin idiotype for the detection and treatment of tumor. Immunol Rev 48: 81-106, 1979.
7. Vitetta E, Yuan D, Krolick K, Isakson P, Knapp M, Slavin S and Strober S: Characterization of the spontaneous murine B cell leukemia (BCL1) III evidence for monoclonality by using an anti-idiotype antibody. J Immunol 122: 1649-1654, 1979.
8. Knapp M, Jones P, Black S, Vitetta E, Slavin S and Strober S: Characterization of spontaneous murine B cell leukemia (BCL1). I cell surface expression of IgM, IgD, Ia and FcR. J Immunol 123: 992-999, 1979.
9. George A, Tutt A and Stevenson F: Anti-idiotype mechanisms involved in suppression of a mouse B cell lymphoma, BCL1. J Immunol 138: 628-634, 1987.
10. George AJ and Stevenson FK: Prospects for the treatment for B cell tumors using idiotypic vaccination. Int Rev Immunol 4: 271-310, 1989.

11. George A, Folkard S, Hamblin T and Stevenson F: Idiotypic vaccination as a treatment for a B cell lymphoma. J Immunol 141: 2168-2174, 1988.
12. Uhr JW, Tucker T, May RD, Siu H and Vitetta ES: Cancer dormancy studies of the murine BCL1 lymphoma. Cancer Res 51 (Suppl.): 5045S-5053S, 1991.
13. Vitetta ES, Tucker TF, Racila E, Huang Y-W, Marches R, Lane N, Scheuermam RH, Street NE, Watanabe T and Uhr JW: Tumor dormancy and cell signaling. V. Regrowth of the BCL1 tumor after dormancy is established. Blood 89: 4425-4436, 1997.
14. George A, McBride H, Glennie M, Smith L and Stevenson F: Monoclonal antibodies raised against the idiotype of the murine B cell lymphoma,BCL1, act primarily with heavy chain determinants. Hybridoma 10: 219-227, 1991.
15. Tutt AL, French RR, Illidge TM, Honeychurch J, McBride HM, Penfold CA Fearon DT, Parkhouse ME, Klaus GGB and Glennie MJ: Monoclonal antibody therapy of B cell lymphoma: signalling activity on tumor cells appears more important than recruitment of effectors. J Immunol 161: 3176-3185, 1998.
16. French RR, Chan CHT, Tutt AL and Glennie MJ: CD40 antibody evokes a cytotoxic T-cell response that eradicates lymphoma and bypasses T-cell help. Nat Med 5: 548-545, 1999.
17. Raiter A, NovogrodskyA and Hardy B: Activation of lymphocytes by BAT and anti CTLA-4: comparison of binding to T and B cells. Immunol Lett 69: 247-251, 1999.
18. Farrar JD, Katz KH, Windsor J, Thrush G, Scheuermann RH, Uhr JW and Street NE: Cancer dormancy. VII. A regulatory role for $CD8^+$ T cells and IFN-gamma in establishing and maintaining the tumor-dormant state. J Immunol 162: 2842-2849, 1999.
19. Hainsworth JD, Burris HA III, Morrissey LH, Litchy S, Scullin DC Jr, Bearden JD III, Richards P and Greco FA: Rituximab monoclonal antibody as initial systemic therapy for patients with low grade non-Hodgkin lymphoma. Blood 95: 3052-3056, 2000.
20. Maloney DG, Grillo-Lopez AJ, White CA, Bodkin D, Shilder JR, Neidhart JA, Janakiraman N, Foon KA, Liles TM, Dallaire BK, Wey K, Royston I, Davis T and Levy R: IDEC-C2B8 (rituximab) anti-CD20 monoclonal antibody therapy in patients with relapsed low grade non-Hodgkin lymphoma. Blood 90: 2188-2195, 1997.

Proc. Natl. Acad. Sci. USA
Vol. 94, pp. 5756–5760, May 1997
Immunology

A lymphocyte-activating monoclonal antibody induces regression of human tumors in severe combined immunodeficient mice

(human melanoma/tumor regression/immune stimulation/nude and beige mice/T or NK cell depletion)

BRITTA HARDY*, RIVA KOVJAZIN, ANNAT RAITER, NIRIT GANOR, AND ABRAHAM NOVOGRODSKY

Felsenstein Medical Research Center, Rabin Medical Center, Belinson Campus, Petah Tikva 49100, Israel, and Sackler School of Medicine, Tel Aviv University, Tel Aviv 69978, Israel

Communicated by Richard A. Lerner, The Scripps Research Institute, La Jolla, CA, March 25, 1997 (received for review August 7, 1996)

ABSTRACT **Monoclonal antibodies were raised against Daudi B-lymphoblastoid cell line membranes. An mAb (BAT) was selected for its ability to stimulate human and murine lymphocyte proliferation. BAT induced cytotoxicity in human and murine lymphocytes against natural killer cell-sensitive and -resistant tumor cell lines. A single intravenous administration of BAT to mice that had been inoculated with various murine tumors (e.g., B16 melanoma, 3LL carcinoma, and methylcholanthrene fibrosarcoma) resulted in striking antitumor effects as manifested by complete tumor regression and prolonged survival of the treated mice. BAT exhibited a diminished but significant antitumor effect in athymic nude mice, which are deficient in T lymphocytes, and in beige mice, which are deficient in NK cells. Furthermore, selective depletion of T or NK cells in mice reduced the response to the antitumor effect of BAT. These data indicate a dual role for T and NK cells in mediating the antitumor activity of BAT. We report here on the antitumor activity of BAT mAb on human tumor xenografts in mice. BAT demonstrated an antitumor effect in nude mice bearing human colon carcinoma (HT29) xenografts. It failed, however, to inhibit established lung metastases in severe combined immunodeficient (SCID) mice that had been inoculated (i.v.) with SK28 human melanoma. Engraftment of human lymphocytes into SCID mice bearing human melanoma xenografts rendered them responsive to the antitumor effect of BAT. The efficacy of BAT in the regression of human tumors by activation of human lymphocytes indicates its potential clinical use.**

Monoclonal antibodies (mAbs) directed against various T cell determinants were previously reported to induce proliferation and differentiation of T cells (1). The most remarkable among them is the mAb against CD3 determinant, which was able to induce clonal proliferation, elicit mitogenic activity, and also trigger the cytolytic process in T lymphocytes (2–4). Additional immunostimulatory mAbs were found to react with CD5 (5), CD69 (6), and CD28. The latter, an antigen on the T cell that interacts with its ligand, B7, present on antigen presenting cells including tumor cells (7–9). *In vivo* antitumor activity of anti-CD3 and of anti-CD28 was previously reported (10, 11). Activation of T cells, which elicit a variety of effector functions, results from interaction of antigen with the T cell antigen receptor and a costimulation directed to additional surface determinants such as the CD28 (12).

We previously reported a mAb directed against human B-lymphoblastoid cell membranes (BAT) that stimulates human lymphocytes, as manifested by enhanced murine and human lymphocyte proliferation and cytolytic activity against tumor cells *in vitro* (13). BAT binding protein was identified as a 48- to 50-kDa monomeric protein (13). BAT was found to induce murine tumor regression in C57BL mice that was mediated by its immune stimulatory properties (14).

In the present study, we evaluated the antitumor activity of BAT in nude mice carrying human tumor xenografts and in severe combined immunodeficient (SCID) mice engrafted with human lymphocytes and inoculated with human tumor cells (15, 16).

MATERIALS AND METHODS

Monoclonal Antibodies. BAT was generated and purified as described (14). In brief, BALB/c mice were immunized with membranes from Daudi cells. Spleen cells were fused with myeloma NS-O cells. BAT was selected by its ability to bind Daudi cells and by its ability to induce proliferation of human peripheral blood mononuclear cells (PBMC). Cells were grown in RPMI 1640 medium supplemented with fetal calf serum (10%), sodium pyruvate, glutamine, and antibiotics and incubated at 37°C in a humidified atmosphere containing 5% CO_2. BAT was purified on a protein G Sepharose column according to manufacturer's instructions (Pharmacia).

Cell Preparations for Engraftment to SCID Mice. Human PBMC were obtained from blood of healthy donors by Ficoll/Hypaque density centrifugation. Cells were washed and suspended in PBS. Cells (5×10^7) were injected i.p. to each SCID mouse to construct a human immune system in these mice.

Splenocytes were obtained from either untreated C57BL mice or from mice 24 h after injection of 100 μg/mouse of anti CD3 (PharMingen) or anti-asialoGM1 (ASGM1) (Wako Chemicals, Dallas). Cells (5×10^7) were injected i.p. to each SCID mouse.

Activation of Lymphocytes by Tumor Cells and BAT. Human PBL (2×10^6/ml) were incubated on HT29 human colon carcinoma cells monolayers for 1 day. Peripheral blood lymphocyte (PBL) cells were then removed from the tumor cell monolayer, washed twice with medium, and suspended at the initial concentration. Splenocytes obtained from tumor-inoculated mice were suspended at 2×10^6/ml, and BAT at 0.1 μg/ml was added for 3 days *in vitro*.

Proliferation Assay of Lymphocytes upon Incubation with BAT. PBLs were separated from PBMC by removing the adherant monocytes after 1-h incubation on plastic Petri dishes. Aliquots of 2×10^6 PBL (200 μl) in culture medium containing 5% human type AB serum were incubated for 3 days in 96-well flat-bottom plates with and without BAT at 0.1 μg/ml. [^{3}H]Thymidine (1 μCi/well; 1 Ci = 37 GBq) was added for 20 h before harvesting. Cultures were harvested into glass

The publication costs of this article were defrayed in part by page charge payment. This article must therefore be hereby marked "*advertisement*" in accordance with 18 U.S.C. §1734 solely to indicate this fact.

Copyright © 1997 by THE NATIONAL ACADEMY OF SCIENCES OF THE USA
0027-8424/97/945756-5$2.00/0
PNAS is available online at **http://www.pnas.org**.

Abbreviations: SCID mice, severe combined immunodeficient mice; PBMC, peripheral blood mononuclear cells; PBL, peripheral blood lymphocyte.

*To whom reprint requests should be addressed at: Felsenstein Medical Research Center, Beilinson Campus, Petah Tikva 49100, Israel.

filters and radioactivity was counted using a liquid β-scintillation counter.

Mouse Tumor Models. Five to six female mice, obtained from Harlan Laboratories (Jerusalem), 6–8 weeks old were used in each group for every experiment. SCID mice were maintained in sterile conditions at a controlled temperature.

B16 murine melanoma cells (5×10^4) were injected i.v. into C57BL wild type, nude mice (C57BL nu/nu), beige mice, or SCID mice that had been engrafted with murine splenocytes. BAT was injected i.v. at 10 μg/mouse 14 days later. Twenty-four days after tumor inoculation, mice were killed and lungs metastases were counted and scored by number, size, and lung weight.

HT29 human colon carcinoma cells were injected s.c. at 10^6/mouse at the axillary region of wild-type or nude mice. BAT (10 μg/mouse) was injected i.p. at days 7, 14, and 21 posttumor inoculation. Beginning at 7 days posttumor inoculation, the tumor size was measured daily until day 30 posttumor inoculation, when the untreated mice died.

SK-mel 28 (SK28), a human melanoma-derived cell line (originally obtained from Sloan–Kettering Institute, New York) was injected i.v. into SCID mice at 5×10^5/mouse. We found that i.v. injection of these cells resulted in tumor lesions in the lungs. SK28 melanoma cells were inoculated 1 day following i.p. administration of anti-ASGM1 (35 μg/mouse) (Wako Chemicals). Anti-ASGM1 is a rabbit polyclonal antibody that binds to murine NK cells and depletes these cells when injected i.p. into mice (17). This antibody was previously used to enhance engraftment of human PBMC into SCID mice (17). Human PBMC (5×10^7/mouse) were engrafted i.p. to SCID mice. Treatment with BAT was done by a single i.v. injection (10 μg/mouse) 14 days posttumor inoculation or at different times as indicated in the tables. Twenty-four days posttumor inoculation, the mice were killed, the lungs removed, melanoma metastases were counted, and lung weight was determined.

RESULTS

We evaluated the antitumor activity of BAT in mice bearing human tumors. Initially we studied the antitumor effect of BAT in athymic nude mice bearing murine B16 melanoma. As demonstrated in Table 1, BAT was found to be effective in this tumor model although to a lesser extent than in the wild-type mice. C57BL mice inoculated with murine B16 melanoma and treated with BAT had zero or only 1 ± 1 melanoma lesion compared with the nude mice that had numerous tumor metastases. The antitumor effect of BAT in nude mice that are deficient in T cells, suggests that non-T cells could mediate its antitumor activity. Similar experiments using beige mice (Table 1) which are deficient in NK cells (18), showed similar results, namely, a reduced number of tumor lesions in the lungs of BAT-treated beige mice although not to the same extent as was observed in the wild-type mice. In the following experiment, C57BL mice were depleted of T or NK cells by *in vivo* administration of the appropriate antibodies. As seen in Table 2, depletion of either T cells or NK cells increased the tumor resistance to BAT. However prolonged administration of the antibodies as in experiment 1 (Table 2) indicates that NK depletion was effective in rendering mice resistant to the antitumor activity of BAT.

Table 1. Antitumor activity of BAT in nude and beige mice bearing B16 melanoma

	No. of metastases			
	Exp. 1		Exp. 2	
BAT treatment	−	+	−	+
	Effect of BAT in nude mice			
C57BL	>200	0	>200	1 ± 1
Nude	>200	48 ± 25	95 ± 45	10 ± 3
	Effect of BAT in beige mice			
C57Bl	141 ± 8	0	49 ± 8	0
Beige	>200	47 ± 39	140 ± 47	101 ± 44

Mice were injected (i.v.) with B16 melanoma (5×10^4) cells and 14 days later with BAT (10 μg/mouse). Mice were sacrificed 24 days posttumor inoculation and the number of lung metastases were scored. More than 200 represents confluent tumor growth in the lungs. Five mice were used in each group in each experiment, and the results are expressed as mean ± SD.

Table 2. The effect of T- or NK cell-depletion in mice bearing B16 melanoma on the antitumor activity of BAT

	Number of metastases			
	Exp. 1		Exp. 2	
BAT treatment	−	+	−	+
Nondepleted	113 ± 80	0.5 ± 1	>200	0
T cells depleted	>200	56 ± 9	>200	37 ± 23
NK cells depleted	>200	>200	>200	160 ± 60

C57BL mice were injected i.p. with either anti-CD3 (100 μg) or anti-asialo GM1 (35 μg) 1 day prior to B16 melanoma injection and on days 7, 14, and 21 days posttumor inoculation. Experiment 1: Mice injected with anti-CD3 or anti-asialoGM1 on day 12 and 22 posttumor inoculation. Experiment 2: Five mice were used in each group. Animals were sacrificed on day 24 posttumor injection and the numbers of metastases were scored. Results are expressed as the means ± SD.

The antitumor activity of BAT in nude mice implanted s.c. with human colon carcinoma (HT29), was also demonstrated (Fig. 1). The growth of the tumor in these mice treated with BAT was delayed up to 24 days posttumor inoculation and was half the size on day 46 compared with the tumor size in untreated mice.

We have investigated whether BAT is capable of inducing human tumor regression via the stimulation of human lymphocytes. SCID mice injected with murine or human tumors failed to respond to BAT treatment and died within 14 days posttumor inoculation. We then established that engraftment of murine splenocytes enabled BAT to induce regression of murine B16 melanoma in the SCID mice (Table 3). BAT was administered 14 days posttumor inoculation, the time at which BAT was previously found to be most effective in inducing regression of murine tumors in wild-type mice (14). BAT treatment in the engrafted SCID mice reduced the number of lung metastases from 217 ± 65 to an average of only 7 ± 3. Engraftment of splenocytes from C57BL mice, which had been

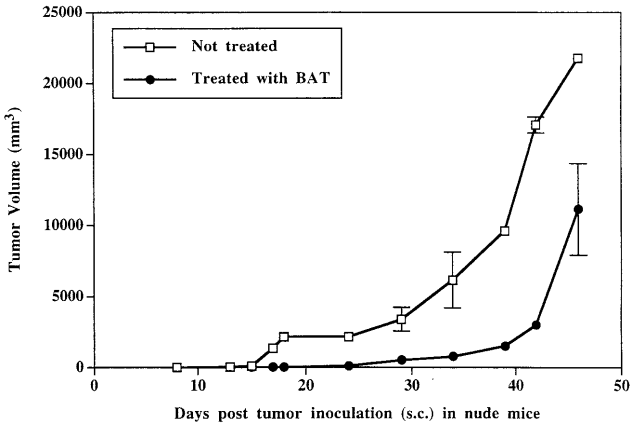

FIG. 1. BAT treatment of human colon carcinoma (HT29) growth in nude mice. Nude mice were injected (s.c.) with human HT29 cells (10^6/mouse) and treated with BAT (10 μg/mouse). BAT was injected i.p. at days 7, 14, and 21 posttumor inoculation.

Table 3. Regression of murine B16 melanoma in SCID mice engrafted with murine splenocyte subpopulations and treated with BAT

	No. of metastases per BAT treatment	
Splenocyte engraftment	−	+
Nonengrafted	>250	>250
Nondepleted	217 ± 65	7 ± 3
CD3 depleted	>250	>250
NK depleted	>250	84 ± 38

SCID mice were engrafted i.p. with splenocytes (5×10^7/mouse) from C57BL mice or from C57BL mice that were injected with anti-CD3 (100 μg/mouse) or anti-asialoGM1 (100 μg/mouse) 1 day prior to isolation of splenocytes for engraftment. B16 melanoma cells were injected i.v. 5 days later. BAT (10 μg/mouse) was injected i.v. 10 days following tumor administration. Mice were sacrificed 24 days posttumor inoculation and the number of lung metastases was determined. Five SCID mice were used in each group and the results are expressed as the mean ± SD.

Table 4. Number of lung metastases and lung weight in SCID mice engrafted with human lymphocytes, inoculated with human melanoma (SK28), and treated 14 days later with BAT

	Nonengrafted,	Engrafted with human PBMC	
BAT treatment	−	−	+
No. lung metastases	>250 (n = 13)	174 ± 53 (n = 25)	8 ± 9 (n = 32)
Lung weight, mg	867 ± 82 (n = 12)	702 ± 140 (n = 22)	206 ± 17 (n = 32)

SCID mice were injected with anti-GM1 (25 μg/mouse). On the following day, human PBMC (5×10^7/mouse) were injected i.p. Human melanoma cells (SK28) were inoculated i.v. 3–5 days later at $5–7 \times 10^5$/mouse. Mice were treated with BAT (10 μg/mouse) in a single injection i.v. 14 days posttumor inoculation. Mice were sacrificed on day 24 posttumor inoculation, and the extent of lung metastases was evaluated by scoring the number of metastases and lung weights. Average lung weight of untreated mice is 210 ± 10 mg. n, The total number of mice studied in five different experiments.

depleted of CD3, rendered the SCID mice recipients resistant to the antitumor effect of BAT. In contrast, engraftment of NK-depleted splenocytes rendered the SCID mice only partially resistant to BAT treatment (Table 3).

We extended these studies to evaluate the antitumor effect of BAT against human tumors. SCID mice were engrafted i.p. with human PBMC along with an inoculation i.v. of human melanoma (SK28) cells. Inoculation i.v. of human SK28 melanoma cells led to development of tumor lesions in the lungs (similar to the previously reported model of established lung metastases using a variety of syngeneic murine tumors) (14). Administration of BAT to these mice, 14 days after tumor inoculation, resulted in a marked regression of tumor lesions in the lungs (Table 4, Fig. 2). Ten out of the 32 mice in five different experiments treated as above were tumor-free. Illustrations of the lungs of BAT-treated mice compared with the lungs of untreated mice are presented in Fig. 2. The distribution of human lymphocyte subpopulations in the lungs of SCID mice engrafted with human PBMC and treated with BAT was investigated. Some 15% of the cells in the lungs were human CD3-positive, whereas 13% were human CD56-positive. Some 7% were CD3- and CD56-positive. The antitumor effect of BAT in the SCID mice was dependent upon the engrafted human lymphoid cells. In these mice, treatment by BAT reduced the number of metastases from an average of 174 ± 53 to 8 ± 9 and lung weight from 702 ± 140 mg to a normal weight of 206 ± 17 mg. It should be noted that the engraftment of the human lymphoid cells by themselves had a slight antitumor effect (Table 4). Treatment with anti-asialoGM1 of nonengrafted mice, which were inoculated with SK28 melanoma, did not change their response to the antitumor effect of BAT. Nonengrafted mice treated or untreated by anti-asialoGM1 died 10–13 days posttumor inoculation.

We previously demonstrated that the antitumor activity of BAT against murine B16 melanoma was maximally pronounced upon administration of the antibody between days 10 and 14 posttumor inoculation (14). Similar effects of BAT's antitumor activity, when administered on day 14 posttumor inoculation, in SCID mice engrafted with human PBMC and inoculated with SK28 melanoma, were achieved. Administration of BAT 3 days after tumor inoculation had only a marginal nonsignificant antitumor effect, whereas administration of the

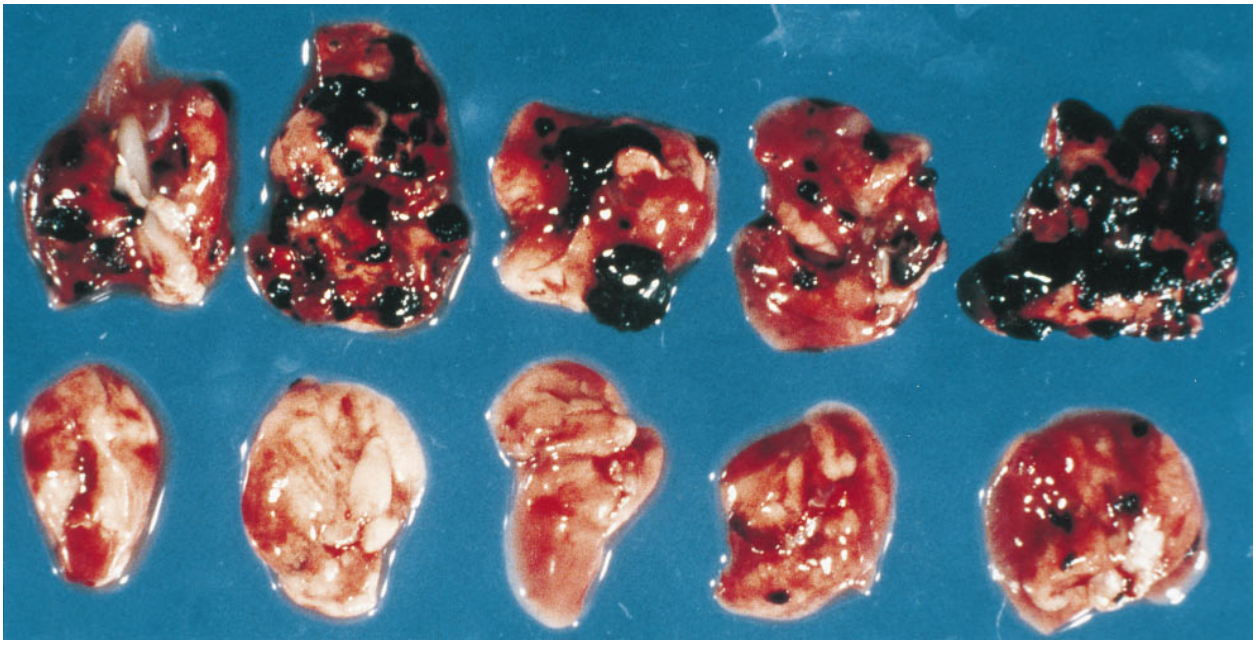

FIG. 2. Lungs from SCID mice bearing human melanoma treated with BAT. (*Upper*) Lungs from human PBMC engrafted SCID mice 24 days postinoculation with SK28 human melanoma. (*Lower*) Lungs from human PBMC engrafted SCID mice 24 days postinoculation with SK28 human melanoma and 10 days posttreatment with BAT.

antibody after 14 days reduced metastases from confluence to an average of 10 ± 17. BAT administered 5 days and 10 days posttumor inoculation was also effective and reduced metastases to 89 ± 7 and 35 ± 12, respectively (Table 5).

To study whether BAT elicited its antitumor effect as a result of a stimulatory signal provided by the tumor cells, we conducted experiments in which splenocytes isolated from mice bearing tumors exhibited an enhanced response *in vitro* to stimulation by BAT (Fig. 3). Splenocytes of C57BL mice injected with B16 melanoma, were co-cultured in the presence of BAT (1 μg/ml) *in vitro* and the [^{3}H]thymidine uptake was measured. As can be seen, uptake of thymidine in splenocytes from mice bearing tumors for 5 days increased (26633 ± 872) in the presence of BAT, compared with the splenocytes of tumor-free mice (13156 ± 447). To further examine the mechanism of BAT activation, we studied the stimulatory effect of BAT *in vitro* on human PBLs that were preincubated on HT29 human colon carcinoma cell monolayers. Results of 4 experiments using 4 different human PBLs are shown in Fig. 4. Exposure of lymphocytes to the tumor cells *in vitro* led to a significant increase in their proliferative response ranging from a 12- to 22-fold increase in [^{3}H]thymidine uptake. Moreover, in lymphocytes that were pre-exposed to tumor cells and then cultured with BAT, thymidine uptake increased 22- to 44-fold. Lymphocytes that were incubated on allogeneic macrophage monolayers did not acquire the enhanced sensitivity to stimulation by BAT (data not shown).

The cell surface markers (CD3 for T cells and CD56 for NK cells) of the lymphocytes from the different experimental groups described in Fig. 4 were analyzed by fluorescence cell analyzer. The percent of CD3/CD56-positive double-labeled cells increased to 25 ± 2 following preincubation on tumor monolayers and incubation with BAT. The percent of CD3/CD56 cells of the lymphocytes that were incubated on tumor cells alone was 17 ± 1%, whereas it was 9 ± 3% of the lymphocytes treated with BAT alone. In control untreated group 6 ± 1% of CD3/CD56-positive cells were detected.

DISCUSSION

The BAT mAb generated against human B-lymphoblastoid cell line was found to bind to and stimulate human T cells. The stimulation was manifested by induction of cell proliferation and cytolytic activity to NK-resistant and NK-sensitive tumor target cells (13). This antibody also stimulated murine splenocytes *in vitro* and was found to induce *in vivo* regression of a variety of murine tumors (14). Tumor regression was related to the immune-stimulatory properties of the antibody. This conclusion is strongly supported by the observation that the antitumor activity could be transferred with splenocytes from mice treated with the antibody. Furthermore, mice bearing tumors that had been cured by treatment with BAT were refractory to a tumor rechallenge (14).

Table 5. BAT treatment at different times following human melanoma inoculation of SCID mice engrafted with human lymphocytes

BAT treatment, day	No. metastases	Lung weight, mg
None	>250	750 ± 70
3	206 ± 75	665 ± 150
5	89 ± 7	315 ± 8
10	35 ± 12	219 ± 1
14	10 ± 17	217 ± 6

BAT was administered (10 μg/mouse) at different times in relation to tumor inoculation at day 0. Human PBMC were engrafted i.p. at 5 × 10^7/cells per mouse, 1 day postinjection of anti-GM1 (25 μg/mouse). Tumor cells were injected i.v. 3–5 days later at 7 × 10^5 cells/mouse. Twenty-four-day posttumor inoculation mice were sacrificed and the number of lung metastases and weights were determined. Average lung weight of untreated mice is 210 ± 10 mg.

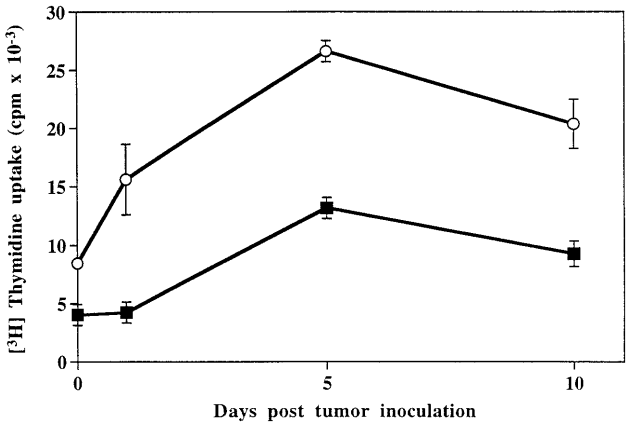

FIG. 3. Proliferation of splenocytes from B16 melanoma bearing mice in the presence and absence of BAT. Splenocytes obtained from C57BL mice at various days postinjection with murine B16 melanoma cells were cultured in the presence of BAT (1 μg/ml) for 3 days (○) and without BAT for 3 days (■). [^{3}H]Thymidine uptake was determined as described.

To evaluate the potential clinical use of this antibody in human cancer, experiments were initiated in mice bearing human tumors. First, we investigated whether BAT would elicit an antitumor effect in nude mice, which are commonly employed for studies involving human tumor xenografts (19). Nude mice are deficient in T cells, and the question was raised whether BAT would induce antitumor activity in these immune-compromised animals. As observed in Table 1, BAT exhibited antitumor activity in nude mice bearing the B16 melanoma. This effect, however, was incomplete as compared with the curing effect that was attained in wild-type (C57BL) animals bearing the same tumor. A similar incomplete antitumor effect of BAT was also observed in nude mice implanted subcutaneously with human colon carcinoma (Fig. 1).

The lymphocyte cell type that mediates the antitumor effect in nude mice may involve NK cells that are present in these mice. This possibility was further supported by the experiment

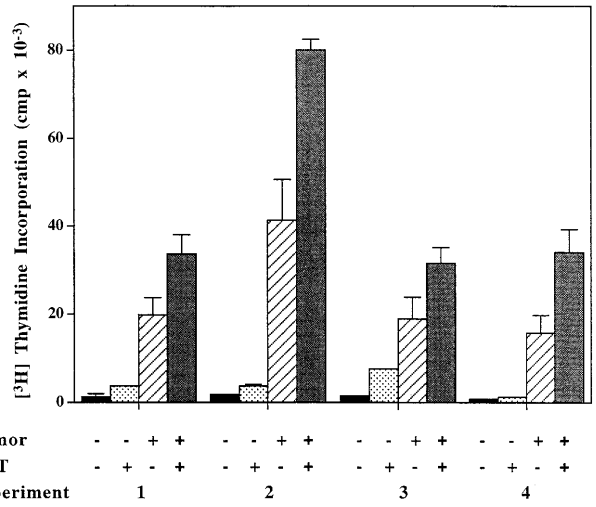

FIG. 4. Thymidine uptake in human PBLs incubated on human HT29 colon carcinoma cells in the presence and absence of BAT. Four experiments using four different human PBLs are shown. PBLs were cocultured on HT29 human colon cells. The lymphocytes were removed after 1 day, washed, and resuspended to 2 × 10^6/ml. Lymphocytes were cultured in the absence and presence of BAT at 0.1 μg/ml for 3 more days and [^{3}H]thymidine uptake was determined as described.

depicted in Table 2, which indicated that continuous depletion of NK cells diminishes the antitumor effect of BAT. However the possibility that T cells could mediate the antitumor effect of BAT is indicated from experiments (Table 1) demonstrating that BAT exhibited antitumor response in the beige mouse that is deficient in NK cells (18). Supporting this view are experiments in which SCID mice bearing murine B16 melanoma engrafted with splenocytes depleted of CD3 lymphocytes failed to respond to BAT (Table 3). In these experiments engraftment of splenocytes which were NK-depleted rendered the SCID mice partially responsive to BAT. Recent studies have shown that CD3/CD56-positive lymphocytes exhibited a potent antitumor activity (20–23). We have found that CD3/CD56-positive cells are generated *in vitro* upon stimulation of human lymphocytes by BAT and human tumor cells. Thus it is possible that this cell type plays a role in the antitumor effect induced by BAT. Taken together, it is possible that either NK or T cells can mediate the antitumor effect of BAT. Furthermore cross talk between these sub-populations (24) may also play an important role in mediating the effect of BAT.

A question of utmost clinical importance was whether BAT could induce human tumor regression mediated by activation of human lymphocytes. To address this question, we evaluated the effect of BAT in SCID mice engrafted with human lymphocytes and inoculated with human SK28 melanoma cells. BAT alone failed to induce tumor regression in SCID mice. Engraftment of PBL alone into SCID mice had a slight antitumor effect, which most probably is related to the genetic disparity between the tumor and the engrafted PBLs. The most pronounced antitumor effect was achieved when BAT was administered into the SCID mice that had been engrafted with human PBLs. In contrast to the curative effect that was attained in the wild strain of mice, the antitumor effect in the SCID mouse engrafted with PBL, although most pronounced, was incomplete in a few cases. This may result from the incomplete reconstitution of the immune system in the SCID mice (25) and was also demonstrated in the experiment in SCID mice that had been inoculated with B16 melanoma and engrafted with syngeneic splenocyctes (Table 3).

Our previous results in normal C57BL mice bearing murine tumors indicated that maximal antitumor effect was obtained upon administration of BAT late after tumor inoculation. A similar effect was also observed when BAT was administered to human PBMC-engrafted SCID mice at different times after inoculation of SK28 human melanoma. It is possible that lymphocytes sensitization by the tumor cells led to their enhanced response to BAT. Support for this notion was obtained from experiments in which the stimulatory response to BAT was assessed *in vitro* in splenocytes derived from tumor bearing mice and was also demonstrated in our *in vitro* experiments which showed that human lymphocytes sensitized by human tumor cells increased proliferation in the presence BAT (Fig. 4).

The nature of the two signals elicited by the tumor cells and by BAT is not known. It is possible that the first signal elicited by the tumor involves the presentation of a tumor antigen to the T cell receptor. The second signal provided by BAT may represent an accessory signal. The finding that BAT induced regression of human tumors mediated by activation of human lymphocytes points to its therapeutic potential in cancer patients.

We thank Dr. Yehuda Shoenfeld for helpful discussions and his critical review of the manuscript. We thank Mrs. Sara Domintz for the preparation of the manuscript.

1. Clark, E. A. &. Ledbetter, J. A. (1986) *Immunol. Today* **7,** 267–270.
2. Meurer, S. C., Hussey, R. E., Cantrel, D. A., Hodgdon, J. C., Schlossman S. F., Smith, K. A. & Reinherz, E. L. (1984) *Proc. Natl. Acad. Sci. USA* **81,** 1509–1513.
3. Van Wauwe, J. P., DeMey, J. P. & Goossens, J. G. (1980) *J. Immunol.* **124,** 2708–2713.
4. Jung, G., Martin D. E. & Muller-Eberhard, J. H. (1987) *J. Immunol.* **139,** 639–644.
5. Ledbetter, J. A., Martin P. J., Spooner, C. E., Wofsy, D., Tsu, T. T., Beatty, P. G. & Gladstone, P. (1985) *J. Immunol.* **135,** 2331–2336.
6. Moretta, A., Poggi, A., Pende D., Tripodi, G., Orengo, A. M., Pella, N., Augugliaro, R., Bottino, C., Ciccone, E. & Moretta, L. (1991) *J. Exp. Med.* **174,** 1393–1398.
7. Razi-Wolf, Z., Freeman, G. J., Galvin, F., Benacerraf, B., Nadler, L. & Reiser, J. (1992) *Proc. Natl. Acad. Sci. USA* **89,** 4210–4214.
8. Norton, S. D., Zuckerman, L., Urdahl, K. B., Shefner, R., Miller, J. & Jenkins, M. K. (1992) *J. Immunol.* **149,** 1556–1561.
9. Li, Y., McGowan, P., Hellstrom, I., Hellstrom, K. E. & Chen, L. (1994) *J. Immunol.* **153,** 421–428.
10. Ellenhorn, J. D., Hirsch, R., Schreiber, H. & Bluestone, J. A. (1988) *Science* **242,** 569–571.
11. Townsend, S. E. & Allison J. P. (1993) *Science* **259,** 368–380.
12. Jenkins M. K. Taylor, P. S., Norton, S. D. & Urdahl, K. B. (1991) *J. Immunol* **147,** 2461–2466.
13. Hardy, B., Galli, M., Rivlin, E., Goren L. & Novogrodsky, A. (1995) *Cancer Immunol. Immunother.* **40,** 376–382.
14. Hardy, B., Yampolski, I., Kovjazin, R., Galli, M. & Novogrodsky, A. (1994) *Cancer Res.* **54,** 5793–5796.
15. Mueller, B. M. & Reisfeld R. A. (1991) *Cancer Metastasis Rev.* **10,** 1930–200.
16. Sandhu, J., Shpitz, B., Gallinger, S. & Hozumi, N. (1994) *J. Immunol.* **152,** 3806–3813.
17. Shpitz, B., Chambers, C. A., Singhal, A. B., Hozumi, N., Fernandes, B. J., Roifman, C. M., Weiner, L. M., Roder, J. C. & Gallinger, S. (1994) *J. Immunol. Methods* **169,** 1–15.
18. Stutman, O. & Cuttito, M. J. (1981) *Nature (London)* **290,** 254–257.
19. Garofalo, A., Chirivi, R. G. S., Scanziani, E., Mayo, J. G., Vecchi, A. & Giavazzi, R. (1993) *Invasion Metastasis* **13,** 82–91.
20. Lu, P.-H. & Negrin, R. S. (1994) *J. Immunol.* **153,** 1687–1696.
21. Schmidt-Wolf, I. G. H., Lefterova, P., Johnston, V., Huhn, D., Blum, K. G. & Negrin, R. S. (1994) *Br. J. Haematol.* **87,** 453–458.
22. Mehta, B. A., Schmidt-Wolf, G. H., Weissman, I. L. & Negrin, R. S. (1995) *Blood* **86,** 3493–3499.
23. Takeda, K. & Dennert, G. (1994) *Transplantation* **58,** 496–504.
24. Kurosawa, S., Harada, M. Matsuzaki, G. Shinomiya, Y. Terao, H. Kobayashi, N. & Nomoto, K. (1995) *Immunology* **85,** 338–346.
25. Hendrickson, E. A. (1993) *Am. J. Pathol.* **143,** 1511–1522.

Transplantation of Cord Blood Expanded Ex Vivo with Copper Chelator

E Shpall [1], M de Lima [1], K Chan [1], R Champlin [1], A Gee [2], P Thall [1], K Komanduri [1], D Couriel [1], B Andersson [1], C Hosing [1], S Giralt [1], S Karandish [1], T Sadeghi [1], B Muriera [1], T Peled [3], F Grynspan [3], A Nagler [4] and J McMannis [1].

[1] BMT, The M.D. Anderson Cancer Center, Houston, TX, United States, 77030; [2] Center for Cell and Gene Therapy, Baylor College of Medicine, Houston, TX, United States, 77030; [3] Gamida Cell Ltd, Jerusalem, Israel and [4] BMT, Chaim Sheba Med Center, Ramat Gan, Israel.

Introduction: Cord blood (CB) is used to restore hematopoiesis in transplant patients lacking marrow donors. CB is associated with higher rates of delayed/failed engraftment. Peled et al. (Br J Haematol. 2002 Mar;116(3):655-61) developed an expansion technology using the copper chelator tetraethylenepentamine (TEPA), which enhanced the expansion of primitive CB populations when combined with early acting cytokines.

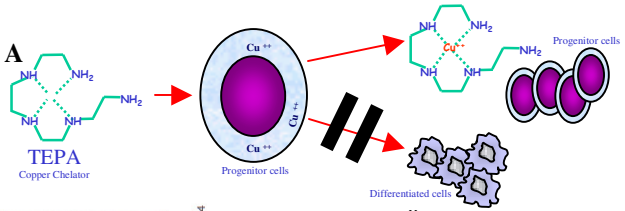

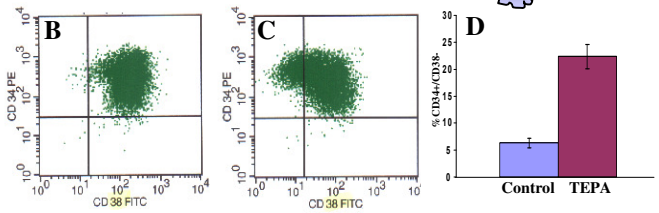

Fig 1. Expansion of progenitor/stem cells by the copper chelator tetraethylenepentamine (TEPA). A. addition of TEPA to HSC's promote self renewal divisions over differentiation. B and C. FACS analysis of 3-week cultures treated with cytokines alone (B) or with cytokines+TEPA (C). D. %CD34+CD38- in Control and TEPA cultures, n=72, p<0.001

Methods: A phase I/II clinical trial employing this technology was initiated (Figure 3). 10 patients with high-risk, heavily pre-treated hematologic malignancies have been enrolled with CB units that were cryopreserved in 2 fractions. 21 days prior to infusion, AC133+ cells were isolated from the smaller (if unequal) or 50% CB fractions using the CliniMACS device and cultured for 21 days in media containing 10% FBS and SCF, FLT-3, IL6, TPO plus the copper chelator TEPA (Gamida). Patients received a total (expanded plus unmanipulated) median of 1.8 (range 1.3-6.6) $x10^7$ TNC/kg and $1.6x10^5$ (range 0.4-49.9) CD34+ cells/kg. Myeloablative and Prophylaxis regiments are shown in Figure 2. Clinical Data is presented in Table 1. Progenitor enrichment scale derived from the total number of CD34+ cells transplanted from both fractions divided by the calculated number of AC133+ cells present in the entire unmanipulated unit

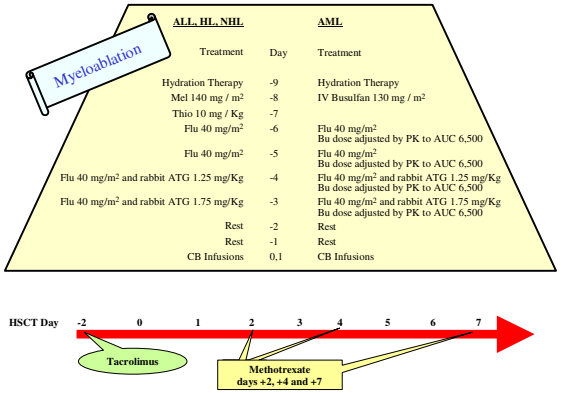

Fig 2. GvHD prophylaxis was methotrexate 5mg/m² days 2, 4, 7, and tacrolimus for 6 months.

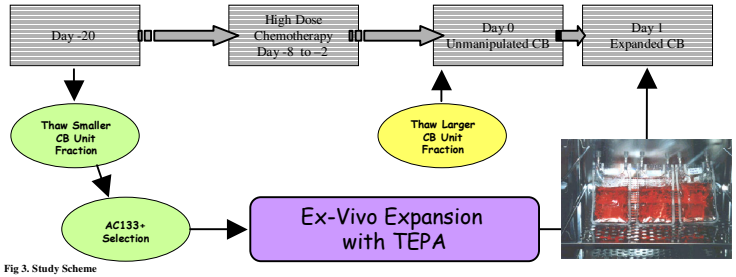

Fig 3. Study Scheme

Results:

	Patient			Cord Blood Unit		Expansion			Engraftment		GvHD	Status
	Indication	*Age*	*Weight*	*HLA*	*Fractions*	*Frozen fraction ($x10^6$)*	*Expanded ($x10^6$)*	*TNC Fold Expansion*	*ANC ≥0.5x10^9/L for 3 days*	*Platelet ≥20x10^9/L for 7 days*		
1	AML	22	53	5/6	60/40	791	30	74	auto			DEC, AML Progression (d167)
2	ALL, CNS relapse	18	70	4/6	50/50	1107	148	421	Day 22	Day 96	G2, skin (d16)	CR
3	HD	25	75	4/6	60/40	972	30	231	Day 33			DEC, ARDS/Sepsis (d93)
4	ALL, ph+	12	55	4/6	60/40	968	126	207	Day 37	Day 53	Chronic, Skin/GI (d113)[d]	CR
5	HD, previous auto-trans	20	74	4/6	80/20	1240	69	61	Day 27	Day 42		CR
6	ALL	44	83	5/6	80/20	1008	68	105	Day 46[c]			DEC, ARDS (d121)
7	AML	51	67	4/6	60/40	924	393	414	Day 22	Day 105	G2, skin (d21)	CR
8	ALL	12	51	4/6	50/50	1773	1638	616	Day 16	Day 27	Chronic, Skin/Occular (d125)[f]	CR
9	ALL	7	31	4/6	60/40	1482	2[b]	2[b]	Day 33	Day 50		CR
10	NHL	52	64	4/6	50/50	NA[a]	48	36	Day 34			CR

Table 1. Clinical Data

[a]: Non-volume reduced Cord Blood unit required change in protocol. [b]: CFU at time/cell of unit: #10B0. [c]: Delayed engraftment due to bacteria administration. [d]: Post-100 days events are presented but not entered into 100-day analysis.

PARAMETER		Phase I/II StemEx® Trial
Graft Failure		0%
Transplant-Related Mortality (day 100)		10%[b]
GvHD	Acute II – IV	20%
	Acute III – IV	0%
	Chronic	0%
Median Time to Engraftment[a]	Platelet	52 Days
	ANC	27 days

Table 2. Data summary, analysis for 100-day follow up

[a]: Excludes patients 6 and 10; [b]: death at day 93, event unrelated to study drug.

Conclusions:

- ✓There is no toxicity associated with infusion of TEPA-expanded Cord Blood cells.
- ✓Pivotal study recommended to solidify the efficacy of this approach
- ✓Future directions include the expansion of the entire Cord Blood unit and the removal of methotrexate from the GVHD regimen to improve time to engraftment
- ✓The Pivotal Study will include a fractionated one-unit strategy and a 2-unit back-up (100% expanded + non expanded) for patients without an identified fractionated unit.

ELSEVIER

EXPERIMENTAL HEMATOLOGY

Experimental Hematology 33 (2005) 1092–1100

Chelatable cellular copper modulates differentiation and self-renewal of cord blood–derived hematopoietic progenitor cells

Toni Peled[a], Elina Glukhman[a], Nira Hasson[a], Sophie Adi[a], Harel Assor[a], Dima Yudin[a], Chana Landor[a], Julie Mandel[a], Efrat Landau[a], Eugenia Prus[c], Arnon Nagler[b], and Eitan Fibach[c]

[a]*Gamida Cell Ltd., Jerusalem, Israel;*
[b]*Chaim Sheba Medical Center, Tel-Hashomer, Israel;*
[c]*Hadassah–Hebrew University Medical Center, Jerusalem, Israel*

(Received 3 February 2005; revised 2 June 2005; accepted 2 June 2005)

Objectives. **We have demonstrated epigenetic modulation of $CD34^+$ cell differentiation by the high-affinity copper (Cu) chelator tetraethylenepentamine (TEPA). TEPA slowed down the rate of $CD34^+$ cell differentiation and increased their engraftability in SCID mice. TEPA biological activity was attributed to its effect on cellular Cu levels as (a) treatment with TEPA resulted in reduction of cellular Cu, and (b) excess of Cu reversed TEPA's activity and accelerated differentiation. In the present study we further evaluated the role of cellular Cu in TEPA's biological activity.**

Methods. **The effects of Cu-chloride, TEPA, TEPA/Cu mixtures at various ratios, and a synthesized, stable, TEPA-Cu complex on short- and long-term cord blood–derived $CD34^+$ cell cultures as well as on the overall and chelatable cellular Cu were investigated.**

Results. **Addition of TEPA, TEPA/Cu mixtures at up to equimolar concentrations, and the TEPA-Cu complex to $CD34^+$ cell cultures resulted in inhibition of differentiation and enhancement of long-term self-renewal. Measurement of the overall cellular Cu by atomic absorption spectrophotometry showed 20 to 40% decrease by TEPA while the TEPA-Cu mixture and the TEPA-Cu complex increased cellular Cu by 10- to 20-fold, as did $CuCl_2$. However, measurement of the cellular pool of labile Cu showed similar reduction (50% from the control) by all the TEPA forms, while $CuCl_2$ increased it. Thus, inhibition of differentiation and enhancement of self-renewal of $CD34^+$ cells was correlated with reduction in the cellular chelatable Cu content.**

Conclusion. **The results suggest that decreasing of the chelatable Cu pool, rather than overall Cu, is the mechanism that stands behind TEPA's biological activity.** © **2005 International Society for Experimental Hematology. Published by Elsevier Inc.**

Introduction

Metal ions such as iron (Fe), calcium (Ca), magnesium (Mg), and zinc (Zn) are known to play important roles in basic cell functions such as cell survival, proliferation, and differentiation. Relatively little attention, however, has been drawn to the role of copper (Cu) in key cellular functions, despite well-documented and significant clinical manifestations of Cu deficiency [1–3]. The symptoms of such deficiency involve several organ systems, yet of particular relevance to this study is the fact that Cu deficiency is often associated with hematopoietic cell differentiation arrest, which results in anemia, neutropenia, and thrombocytopenia [1–3]. These pathological manifestations are unresponsive to iron therapy but are rapidly reversed following Cu supplementation [1–5]. Morphological and functional evaluation of the bone marrow (BM) of neutropenic, Cu-deficient patients demonstrates the striking absence of mature cells (''maturation arrest'') along with the presence of intact progenitor cells. This finding suggests that the shortage of functional circulating blood cells in these patients is due to a block in development of the hematopoietic stem/progenitor cells (HSPCs) in a Cu-deficient microenvironment [1].

Further insight into the role of Cu in hematopoiesis comes from studies with established cell lines. Bae and Percival [6] have demonstrated that retinoic acid–induced

Offprint requests to: Dr. Toni Peled, Gamida-Cell, Ltd., Research and Development, 5 Nahum Hfzadi St., Ofer Building, Jerusalem 95484, Israel; E-mail: Tony@gamida-cell.com

0301-472X/05 $–see front matter. Copyright © 2005 International Society for Experimental Hematology. Published by Elsevier Inc.
doi: 10.1016/j.exphem.2005.06.015

HL-60 cell differentiation was associated with accelerated uptake of Cu during the early stages of differentiation. Accordingly, addition of excess Cu to the culture medium sensitized the cells to retinoic acid–induced differentiation [7]. Ceruloplasmin, the main Cu-binding protein in serum, was demonstrated in vitro [8] and in vivo [9] to be a potent inducer of hematopoietic cell differentiation. In this context, it is interesting to note that ceruloplasmin has been shown to have a therapeutic effect in patients with aplastic anemia [9]. While excess Cu was associated with enhanced differentiation, Cu-deficient cells displayed suboptimal responses to several differentiation signals; reduction of Cu in U937 cells by the polyamine Cu-chelator triethylenetetramine was shown to inhibit cell differentiation induced by 1,25-dihydroxyvitamin D3 and phorbol 12-myristate 13-acetate [10].

To gain insight into the role of Cu in the regulation of HSPC proliferation and differentiation, we used cultures of cord blood (CB)-derived purified $CD34^+$ cells grown in cytokine-supplemented liquid medium. Cellular Cu concentration was moderately modulated by addition of Cu or a Cu chelator, tetraethylenepentamine (TEPA) [11]. Treatment with TEPA resulted in enrichment of progenitor subsets ($CD34^+CD38^-$ and $CD34^+CD38^-Lin^-$) that displayed prolonged ex vivo expansion of CFUc and $CD34^+$ cells and an enhanced capacity to repopulate NOD/SCID mice [12,13]. In contrast, treatment with Cu chloride resulted in a marked decrease in $CD34^+$ cells and the early subsets and, consequently, in their long-term culture potential. These results suggested that changes in the cellular Cu mediated the biological effects of these reagents. Indeed, we demonstrated that only Cu, but not other transitional metal ions, could reverse TEPA's effect [11]. However, this reversal was achieved only with excess of Cu. At equimolar ratio, Cu did not quench TEPA's effect.

In the present study, we reevaluate the role of Cu in HSPC self-renewal and differentiation. For this purpose, we synthesized a stable TEPA-Cu complex and compared its effect on CD34 cells to that of the TEPA:Cu (1:1) mixture and TEPA. The results indicated similar biological activity for all these reagents. Yet, measurement of the overall cellular Cu content indicated that while TEPA decreased it, the TEPA:Cu (1:1) mixture and the complex, as well as Cu chloride, which has an opposite biological activity, decreased it.

Cellular Cu is mostly bound to various cellular components such as ceruloplasmin and various enzymes such as Cu/Zn superoxide dismutase. Very little exists as loosely bound, labile ions. The labile form of Cu can be quantified by its ability to bind to cell-permeable chelators, and thus it is operationally characterized as chelatable Cu. We determined the chelatable Cu pool by its effect on the fluorescence of the cell-permeable chelator calcein acetoxymethyl ester as measured by flow cytometry. The results indicated that TEPA in all its forms decreased this Cu pool, while Cu chloride increased it. These results suggest that reduction in the chelatable Cu pool rather than that of the overall Cu content is the mechanism that stands behind the effect of TEPA on cord blood–derived $CD34^+$ cells.

Materials and methods

Purification of cord blood–derived CD34 cells

Cells were separated from umbilical cord blood obtained from normal full-term deliveries from Chaim Sheba Medical Center, Tel Hashomer, Israel (informed consent was given). Samples were collected and frozen according to Rubinstein et al. [14] within 24 hours postpartum. Prior to use, the cells were thawed, and $CD34^+$ cells purified by immunomagnetic bead separation using a Mini-MACS CD34 progenitor cell isolation kit (Miltenyi Biotec, Bergisch Gladbach, Germany), according to the manufacturer's recommendations.

Ex vivo expansion

Purified $CD34^+$ cells were cultured in culture bags (American Fluoroseal Co., Gaithersburg, MD, USA) at a concentration of 1×10^4 cells/mL in MEMα/10% FCS containing the following human recombinant cytokines: thrombopoietin, interleukin-6, FLT-3 ligand, stem cell factor (each at a final concentration of 50 ng/mL), and interleukin-3 at 20 ng/mL (Pepro Tech, Inc., Rocky Hill, NJ, USA), and incubated at 37°C in a humidified atmosphere of 5% CO_2 in air. The cultures were topped weekly with the same volume of fresh medium up to week 3, and then up to the termination of the experiment the cultures were weekly demi-depopulated.

The two-phase culture assay

To evaluate the biological effect of various forms of tetraethylenepentamine (TEPA) and Cu chloride (Aldrich, Milwaukee, WI, USA), cultures were treated for 3 weeks (treatment phase) with a specific reagent or combination of these reagents, as indicted, in addition to cytokines, while control cultures were treated with cytokines only. From week 3 on, both experimental and control cultures were treated with cytokines only for an additional 5 weeks (assay phase). CFUc and $CD34^+$ cells were assayed as previously described [12] to determine the effect of specific treatment on the long-term culture potential.

Immunostaining and flow cytometry

The cells were washed with a phosphate-buffered saline (PBS) solution containing 1% bovine serum albumin (BSA), and stained (at 4°C for 30 minutes) with fluorescein isothiocyanate (FITC)- or phycoerythrin (PE)-conjugated antibodies. The cells were then washed in the above buffer and analyzed using a FACScalibur flow cytometer (Becton-Dickinson, San Jose, CA, USA). The cells were passed at a rate of up to 1000 cells/second, using a 488-nm argon laser beam as the light source for excitation. Emission of 10^4 cells was measured using logarithmic amplification, and analyzed using CellQuest software (Becton-Dickinson). Cells stained with FITC- and PE-conjugated isotype control antibodies were used to determine background fluorescence.

Determination of $CD34^+$ cell content after expansion

$CD34^+$ cells were measured in a purified, reselected fraction, using the MiniMACS CD34 progenitor cell isolation kit as described above (purification of cord blood–derived CD34 cells). $CD34^+$ cell content of the entire culture was calculated as follows: Number of $CD34^+$ cells recovered following repurification $\times$ culture volume / volume of the portion of the culture subjected to repurification. Up to week 3 the cultures were topped weekly with fresh medium; therefore, the culture volume was measured directly. From week 3 on, the culture volume was calculated by multiplying the actual volume by the number of passages. Fold expansion was calculated by dividing the $CD34^+$ cell content of the culture by the number of inoculated $CD34^+$ cells.

Determination of early $CD34^+$ cell subsets

The percentages of the early $CD34^+$ cell subsets were determined from the repurified $CD34^+$ cell fraction. Cells were washed and immuno-stained as described above with FITC anti-CD38 and PE anti-CD34 antibodies for determination of $CD34^+CD38^-$ cells and FITC anti-CD34 and PE anti–lineage-specific antibodies (anti CD38, CD33, CD14, CD15, CD3, CD61, CD19) (Becton-Dickinson) for determination of $CD34^+CD38^-Lin^-$ cells. Results are given as percentage of $CD34^+$ cells. Absolute numbers of $CD34^+CD38^-$ and $CD34^+CD38^-Lin^-$ cells in the culture were calculated from the total number of $CD34^+$ cells recovered following the repurification step.

Preparation of the TEPA-Cu complex

TEPA·5 HCl (3 mmol, 1.1 g, obtained from Sigma) was treated with a 15-mL solution of 1 N NaOH in methanol. The precipitate of NaCl was separated by centrifugation at 3000 rpm for 5 minutes. The solution of TEPA base was diluted with 120 mL methanol and a light blue 30-mL solution of 3 mM $CuCl_2$ in H_2O was added. A bright blue color solution was formed. The reaction solution was evaporated under vacuum at 25 to 30°C. The residue was diluted with 100 mL methanol and again evaporated under vacuum to remove water. This process was repeated twice. The residue was dissolved in isopropanol (15 mL) and the resulting NaCl precipitate was removed by filtration. The filtrate solution was diluted with diethyl ether (45 mL) and the resulting solution was recrystallized at 8 to 10°C for 2 weeks to obtain the crystallized TEPA-Cu complex. The solution was filtered out, and the resulting recrystallized solid material (dark blue precipitate) on the walls of the flask was washed with diethyl ether (50 mL). The ether was removed and the solid product was dried under vacuum, yielding 0.74 g of dark blue solid TEPA-Cu complex product. No traces of residual free Cu or TEPA were detected by fast atom bombardment mass spectrometry (FAB-MS) [15].

Cu determination

Overall cellular Cu content was determined as previously described [7]. In brief, cells were harvested and washed with PBS. Aliquots of 2×10^6 cells in metal-free Eppendorf tubes were pelleted and dissolved with 0.03 mol/L ultra-pure nitric acid (Mallinckrodt Baker B.V., Deventer, Holland). Samples were sonicated and then analyzed by graphite furnace atomic absorption spectrophotometry using a model 460 spectrophotometer with a HGA 2200 controller (Perkin Elmer, Norwalk, CT, USA).

Cellular chelatable Cu was measured as follows: cells were washed twice with saline and incubated at a density of 0.5 to 1 $\times$ 10^6/mL with 0.25 mM calcein acetoxymethyl ester (CA-AM) for 15 minutes at 37°C. Then, the cells were washed twice and exposed to either TEPA, the TEPA:Cu (1:1) mixture, the TEPA-Cu complex, or none, as indicated. Cellular fluorescence was measured after incubation with CA-AM and 3 hours thereafter by flow cytometry using a 488-nm argon laser for excitation and the FL1 PMT for measuring emission. Unstained cells served to determine background fluorescence. CellQuest software (Becton-Dickinson) was used to calculate the mean fluorescence channel of the studied cell population in arbitrary fluorescence units.

The procedure is based on the ability of CA-AM to enter viable cells and to become fluorescent upon hydrolysis [16,17]. Following binding of Cu calcein fluorescence is quenched. This quenching is much greater than that caused by iron or any other metal ion [18,19]. The decrease in fluorescence under different conditions measures, in relative terms, the chelatable Cu pool.

Statistics

The nonparametric test (Wilcoxon Rank Test) was applied for testing differences between the study groups for quantitative parameters. All tests applied were two-tailed, and p value of 5% or less was considered statistically significant. The data were analyzed using SAS software (SAS Institute, Cary, NC, USA).

Results

The effect of Cu on $CD34^+$ cell cultures

CB-derived $CD34^+$ cells were treated with cytokines and 10 μM Cu chloride during the first 3 weeks of the culture (treatment phase) and then with cytokines only for additional 5 weeks (assay phase). Analysis of the cultures at the end of the treatment phase indicated that the number of total nuclear cells (TNC) was similar in cultures treated or untreated with Cu (Fig. 1A). The CFUc content of the Cu-treated cultures was 1.6-fold lower than in the untreated cultures (170 ± 78 vs 272 ± 172, respectively, $n = 3$), but this difference did not reach statistical significance ($p > 0.05$) (Fig. 1B). At the end of the assay phase (week 8), significantly lower CFUc were found in Cu-treated cultures than in control cultures ($43 \pm 11 \times 10^3$ vs $124 \pm 9 \times 10^3$, respectively, $n = 3$, $p < 0.05$ (Fig. 1C). FACS analysis of the subset cell composition on week 3 of cultures treated with different concentrations of Cu (5–20 μM) revealed remarkably lower absolute numbers of $CD34^+$, $CD34^+CD38^-$, and $CD34^+CD38^-Lin^-$ cells in Cu-treated cultures (Fig. 2A–C). Notably, at all the tested concentrations, Cu chloride treatment did not adversely affect the TNC number during the treatment phase (Fig. 2D), suggesting that the Cu treatment specifically impaired the proliferation of progenitor cells.

The effect of simultaneous treatment with Cu and TEPA on $CD34^+$ cell cultures

Next, we tested the effect of simultaneous treatment with TEPA and Cu on CFUc content (Fig. 3) and cell immunophenotype (Fig. 4). At up to equimolar concentration, Cu did not attenuate TEPA's effect on long-term

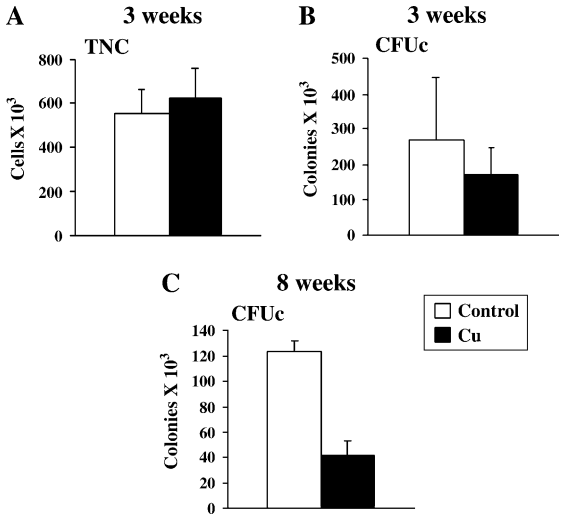

Figure 1. The effect of Cu on CD34$^+$ cell cultures. CD34$^+$ cell cultures (n = 3), grown in the presence of cytokines, were treated for 3 weeks with or without 10 μM Cu chloride. The numbers of TNC **(A)** and CFUc **(B)** were determined. From week 3 on, the cultures were grown with cytokines alone. CFUc content was determined on week 8 **(C)**. Cumulative numbers are shown.

(8-week) CFUc. Surprisingly, even at equimolar ratio (TEPA:Cu 1:1) the CFUc content of the cultures was comparable to that of only-TEPA-treated cultures and was significantly above that of control (nontreated) cultures. Only excess Cu (TEPA:Cu 1:2) overrode TEPA's effect

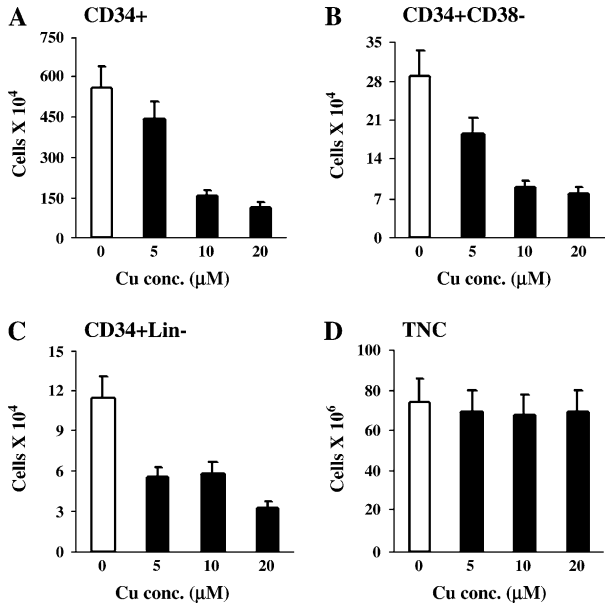

Figure 2. Analysis of the cell composition of 3-week cultures treated with Cu. CD34$^+$ cell cultures (n = 3), grown in the presence of cytokines, were treated for 3 weeks with or without different concentrations of Cu chloride. Absolute numbers of CD34$^+$ **(A)**, CD34$^+$CD38$^-$ **(B)**, and CD34$^+$CD38$^-$Lin$^-$ cells **(C)**, stained, analyzed, and calculated as described in Materials and methods, are demonstrated. TNC numbers are shown in **D**.

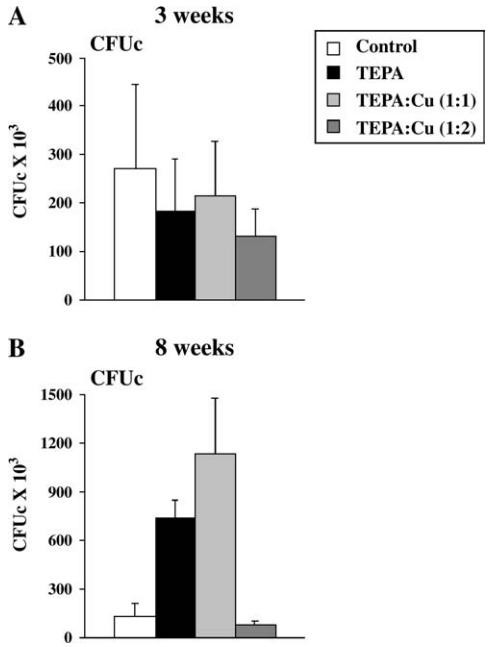

Figure 3. Effect of simultaneous treatment with TEPA and Cu at 1:1 and 1:2 molar ratios on short- and long-term CFUc expansion. CD34$^+$ cell cultures (n = 3), grown in the presence of cytokines with 10 μM TEPA, 10 μM TEPA + 10 μM Cu chloride (1:1), 10 μM TEPA + 20 μM Cu chloride (1:2), or none. From week 3 on, the cultures were grown with cytokines alone. CFUc were determined on weeks 3 **(A)** and 8 **(B)**. Cumulative numbers were calculated as described in Materials and methods.

(Fig. 3B). Notably, on week 3, the CFUc (Fig. 3A) and CD34$^+$ cell content (Fig. 4C) were comparable in control and treated cultures. In sharp contrast, at this time CD34$^+$ early cell subsets (CD34$^+$CD38$^-$ and CD34$^+$Lin$^-$) were higher in cultures treated with either TEPA:Cu 1:1 or TEPA alone compared to control cultures (Fig. 4A,B).

The effect of a TEPA-Cu complex on CD34$^+$ cell cultures

In order to further explore the effects of TEPA and Cu, we synthesized a stable TEPA-Cu complex. Mass-spectra analysis of the TEPA-Cu-complex in solution (Fig. 5A) indicated the presence of two peaks of TEPA-Cu complex with molecular mass of 252 and 287, which correspond to TEPA-Cu complex and TEPA–Cu chloride complex, respectively. The two-dimensional chemical structure of the ionized form is shown in Figure 5B. Peaks of free Cu (MW=63) and free TEPA (MW=190) as well as other analogs of the TEPA-Cu complex were not detected. A similar pattern was observed after one month incubation at 37°C, indicating the stability of the synthesized compound.

To evaluate its biological activity, CD34$^+$ cell cultures were treated for 3 weeks with cytokines in the absence or presence of various concentrations (15–40 μM) of the TEPA-Cu complex. Analysis of cultures on week 8 demonstrated a dose-related increase in CFUc in cultures pretreated with the TEPA-Cu complex at times when control cultures declined (Fig. 6A). The CD34$^+$ cell

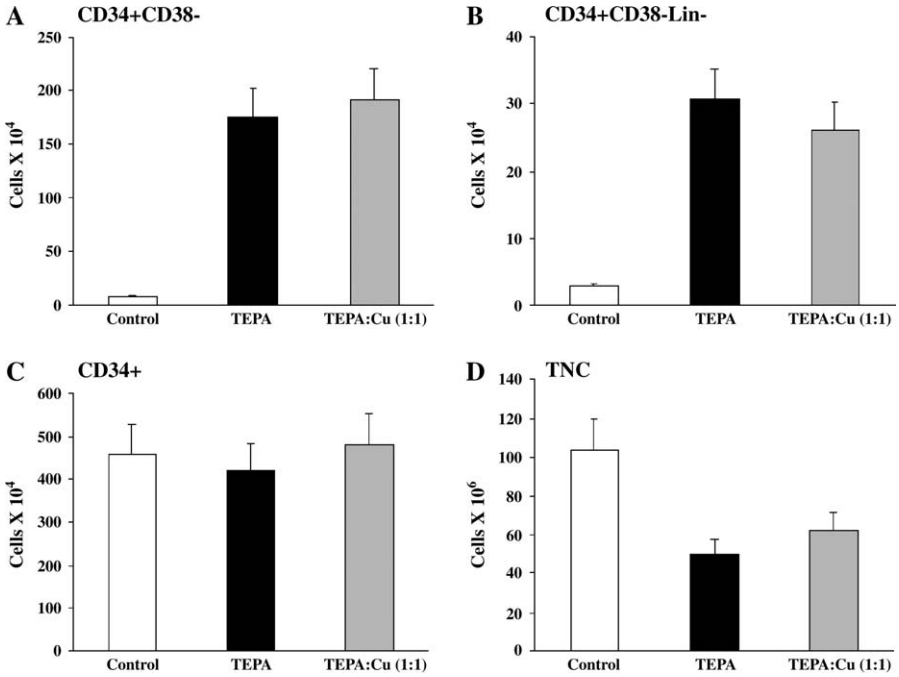

Figure 4. Effect of simultaneous treatment with Cu and TEPA on short-term expansion of $CD34^+$ cells. $CD34^+$ cells were treated for 3 weeks with 10 μM TEPA, 10 μM TEPA + 10 μM Cu chloride (1:1), or cytokines alone (n = 3). For FACS analysis of early progenitor subsets, $CD34^+CD38^-$ **(A)** and $CD34^+CD38^-Lin^-$ **(B)**, purified $CD34^+$ cells were stained, analyzed, and cumulative numbers were calculated as described in Materials and methods. Numbers of purified $CD34^+$ cells and TNC numbers are shown in **C** and **D**, respectively.

content of 8-week cultures treated with optimal concentrations of TEPA-Cu complex (40 μM) and TEPA (10 μM) were comparable ($27 \pm 10 \times 10^6$ and $27 \pm 9 \times 10^6$, respectively), and significantly above that of control cultures ($4 \pm 2 \times 10^6$, n = 4, $p < 0.05$) (Fig. 6B).

Phenotype analysis of 3-week cultures (Fig. 7A–C) demonstrated that the fold expansion of $CD34^+CD38^-$ cells in the treated cultures was significantly ($p < 0.05$) above that of control cultures (169 ± 40 and 21 ± 6, respectively). Similar results were obtained with $CD34^+CD38^-Lin^-$ cells (153 ± 26 and 37 ± 14, respectively), while $CD34^+$ cell expansion remained comparable to control cultures. To determine the specificity of the TEPA-Cu complex for TEPA's biological effects, we prepared and analyzed a TEPA-Zn complex. The preparation of this molecule was similar to that of the TEPA-Cu complex. Its biological analysis indicated no effect on CD34 cells (data not shown).

The effect of TEPA, TEPA:Cu (1:1), TEPA-Cu complex, and Cu chloride on cellular Cu content

Determination of the total cellular Cu content after treatment with TEPA, Cu-chloride, and the TEPA-Cu complex at various concentrations was performed by

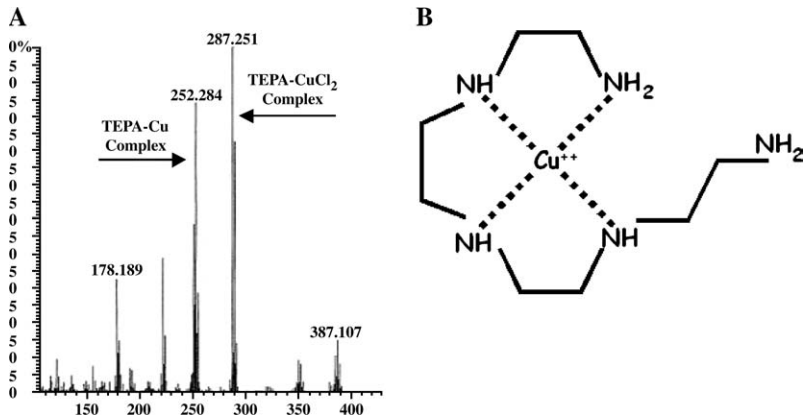

Figure 5. Mass spectrum analysis of the TEPA-Cu complex. Mass spectrum analysis of TEPA-Cu complex maintained in solution **(A)** and the two-dimensional structure of the TEPA-Cu complex **(B)** are shown.

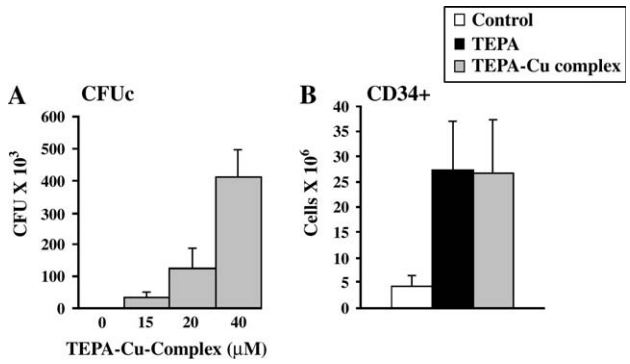

Figure 6. The biological activity of the TEPA-Cu complex. $CD34^+$ cell cultures (n = 4), grown in the presence of cytokines, were treated for 3 weeks with the indicated concentrations of the TEPA-Cu complex. From week 3 on, the cultures were grown with cytokines alone. On week 8, cultures were analyzed for their CFUc content. Cumulative numbers are shown **(A)**. $CD34^+$ cells were treated with 40 μM TEPA-Cu complex, 10 μM TEPA, or cytokines alone for 3 weeks. From week 3 on, all cultures were treated with cytokines only. At week 8, $CD34^+$ cells were repurified and enumerated (n = 4). Cumulative numbers are shown **(B)**.

atomic absorption spectrophotometry as described in Materials and methods. This technique measures total cell-associated Cu and does not discriminate between chelatable and tightly bound Cu. The results indicated that TEPA, at 5 and 10 μM, reduced overall cellular Cu by 20% and 40%, respectively, whereas the TEPA-Cu complex (25–100 μM) or Cu-chloride (5–20 μM) resulted in a dose-related increase in overall cellular Cu (Fig. 8A–C).

To determine the effect of the different culture conditions on the chelatable Cu pool, cells were loaded with CA-AM, as described in Materials and methods, followed by a 3-hour incubation with TEPA, TEPA:Cu (1:1), TEPA-Cu complex, Cu chloride, 20 μM each, or none (control). Cellular fluorescence was measured before the incubation with the above reagents and 3 hours later. The results show that the fluorescence of control cells following 3-hour incubation dropped by about 50% while the decrease in fluorescence of cells treated with TEPA, TEPA-Cu (1:1), or the TEPA-Cu complex dropped by 20% only (Fig. 9A).

Thus, the overall cellular Cu content was profoundly elevated by treatment with TEPA:Cu (1:1), TEPA-Cu complex, and Cu, while TEPA reduced it (Fig. 9B). In contrast, the chelatable Cu pool was reduced by all the TEPA reagents, while Cu chloride significantly increased it (Fig. 9A).

Discussion

In vitro expansion of HSPCs is constrained by commitment and differentiation [20]. In order to maximize the ex vivo expansion of HSPCs for research and therapeutic (transplantation) purposes attempts are constantly being made to overcome this limitation by defining epigenetic modulators that favor HSPC self-renewal with only limited differentiation [21–23]. We have previously reported data suggesting that cellular Cu content modulates self-renewal and differentiation of HSPCs [11]. Short-term (3 weeks) treatment with the Cu chelator TEPA resulted in enrichment of cord blood–derived progenitor subsets ($CD34^+CD38^-$ and $CD34^+CD38^-Lin^-$) that displayed prolonged ex vivo expansion of CFUc and $CD34^+$ cells and an enhanced capacity to repopulate NOD/SCID mice [12,13]. In contrast, 3-week treatment with Cu chloride resulted in a marked decrease in $CD34^+$ cells and the early subsets. During the treatment with Cu chloride the number of TNC and CFUc were comparable to control cultures, but the long-term potential of these cultures was impaired.

The results of these experiments suggested that changes in the cellular Cu mediated the biological effects of these

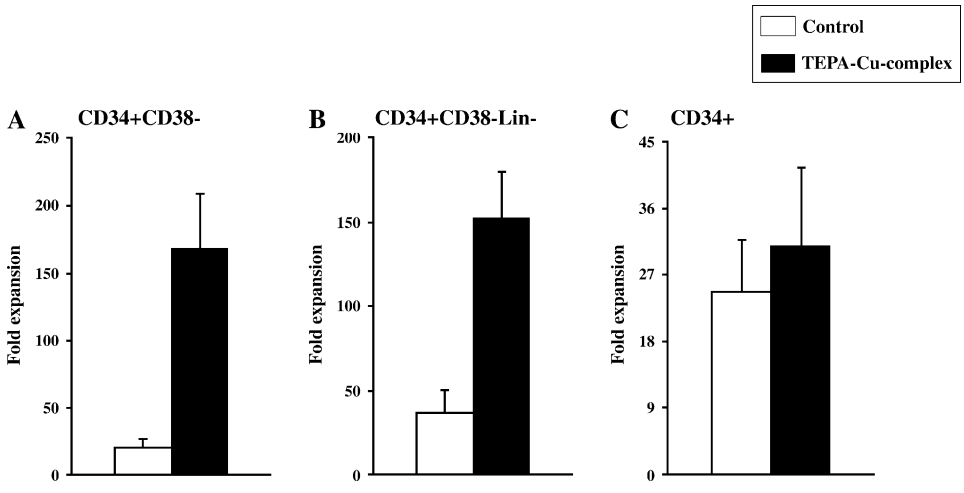

Figure 7. The effect of the TEPA-Cu complex on 3-week expansion of $CD34^+$ cell subsets. $CD34^+$ cells were treated with the TEPA-Cu complex (40 μM) or with cytokines alone. Purified $CD34^+$ cells were stained for CD34/CD38 **(A)** and CD34/Lin/CD38/L in **(B)** and analyzed by FACS. $CD34^+$ cells are shown in **C** (n = 3). Fold expansion was calculated as described in the Materials and methods.

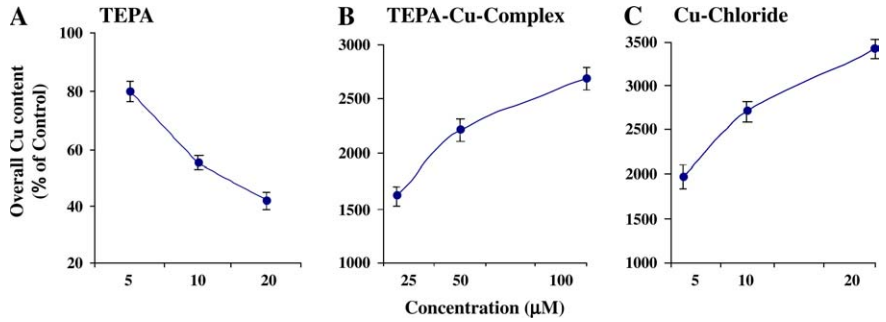

Figure 8. Measurement of overall cellular Cu content. $CD34^+$ cells were treated with the indicated concentrations of TEPA **(A)**, the TEPA-Cu complex **(B)**, Cu chloride **(C)**, or cytokines alone (control). Cellular Cu was determined by atomic absorption spectrophotometry as described in Materials and methods. Results of the Cu content are shown as percentages of control, cytokine-treated cultures.

reagents. Indeed, we demonstrated that only Cu, but not other transitional metal ions, could reverse the TEPA's effect [11]. However, this reversal was achieved only with excess of Cu. Contrary to studies in other cell systems [24,10], in our experiments, at equimolar concentration (TEPA:Cu 1:1), Cu did not quench the TEPA's effect. These surprising results prompted us to reevaluate the role of Cu in self-renewal and differentiation. For this purpose, we synthesized a stable TEPA-Cu complex at 1:1 molar ratio and evaluated its effect on CD34 cells. The results indicated that the complex had biological activity similar to the TEPA:Cu (1:1) mixture as well as TEPA.

We next determined the effect of these reagents on the overall Cu content of CD34 cells using atomic absorption spectrophotometry. The results indicated that TEPA reduced it whereas the TEPA-Cu mixture and complex or Cu chloride increased it (Figs. 8 and 9B).

Cu is present in cells in at least two various forms: one which is firmly bound to compounds such as ceruloplasmin and various enzymes such as Cu/Zn superoxide dismutase and the other a more loosely bound, labile pool, possibly involved in the synthesis of Cu proteins [25,26]. Under physiological conditions the amount of the labile pool is quite small [26], but it may have a significant biological role. To measure the cytosolic pool of labile Cu we utilized a novel flow cytometry method that makes use of a cell-permeable Cu chelator: calcein. The change in calcein fluorescence under different culture conditions measures the amount of calcein-bound Cu that in turn reflects the relative levels of cellular chelatebale Cu. We demonstrated that a 3-hour treatment with TEPA, TEPA:Cu (1:1), and TEPA-Cu complex of calcein preloaded cells reduced by 50% the decrease in fluorescence, relative to the decrease in the fluorescence of untreated cells (Fig. 9A), suggesting

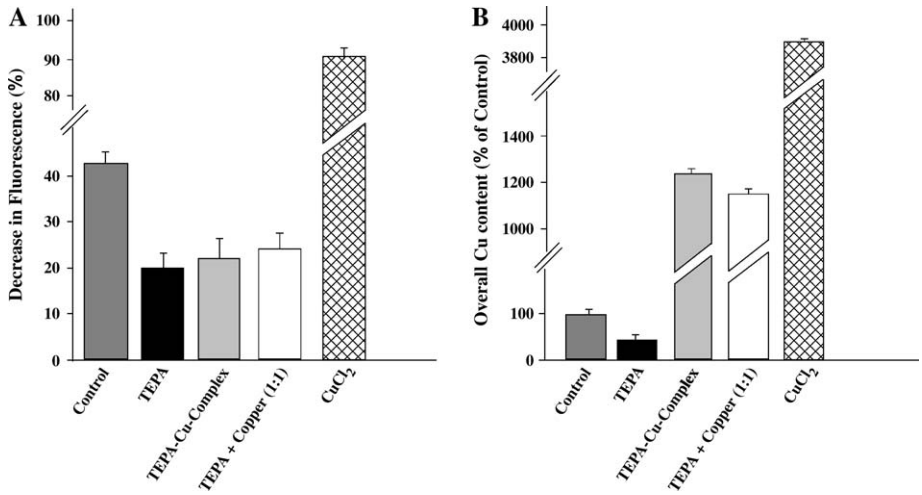

Figure 9. The effect of TEPA, TEPA:Cu (1:1), TEPA-Cu complex, and Cu chloride on chelatable **(A)** and overall **(B)** cellular Cu. Cells were loaded with calcein, then washed twice and exposed for 3 hours to either TEPA, the TEPA:Cu (1:1) mixture, the TEPA-Cu complex, and Cu chloride (20 μM each) or none (control), as indicated. Cellular fluorescence was measured after incubation with calcein (T0) and 3 hours thereafter (T3) by flow cytometry as described in Materials and methods. Percentage decrease in fluorescence during 3-hour incubation was calculated relative to the fluorescence of calcein-loaded cells (T0) as follows: fluorescence at T3 × 100/fluorescence at T0 **(A)**. The decrease in fluorescence represents, in relative terms, the available chelatable Cu pool. In parallel, overall Cu content of cells treated with 20 μM of the above-mentioned reagents was measured by atomic absorption spectrophotometry as described in Materials and methods **(B)**.

that all these reagents reduce the availability of chelatable Cu. Thus, although the overall cellular Cu content was profoundly elevated by treatment with TEPA:Cu (1:1) mixture and complex, as well as Cu chloride, and TEPA reduced it, the chelatable Cu was reduced by all the TEPA reagents, while Cu chloride significantly increased it.

At least two mechanisms may account for the biological effects of TEPA; the first suggests that a TEPA-Cu chelate is the specific active intermediate responsible for TEPA's biological activity. Since TEPA has the strongest binding affinity for Cu (its stability constants for Cu, Zn, Co, Fe, Mn are 23, 15, 13, 10, 7, respectively) [27], it is expected to form a chelate, similar to the synthesized TEPA-Cu complex [25]. The chelate, as well as the complex, acts directly to affect pathways involved in self-renewal and differentiation of CD34 cells. This mechanism does not require reduction of cellular Cu since the TEPA:Cu (1:1) mixture and the TEPA-Cu complex, which display biological activity similar to TEPA, have opposite effect on the overall Cu content. This mechanism also fails to explain the effect of Cu chloride on self-renewal and CD34 cell differentiation. The second mechanism involves changes in the levels of the chelateble Cu pool. All the TEPA reagents were found to reduce this pool while Cu chloride was found to increase it. This correlates with their effect on self-renewal and differentiation.

Intracellular Cu was reported to regulate gene expression [28–31] and cell differentiation [32,33] by a variety of pathways. It modifies the function of transcription factors and the activities of Cu enzymes such as S-adenosylhomocysteine hydrolase and protein arginine methyltransferase 1, which are involved in protein methylation. Cu chelation by TEPA deactivates these enzymes, resulting in protein hypomethylation and inhibition of neurite differentiation [24]. Cu has also been shown to suppress the enzyme histone acetyl transferase, resulting in a decrease in overall and specific histone acetylation; Cu chelators, in contrast, had an opposite effect [34]. Reversible histone acetylation/deacetylation plays a pivotal role in transcriptional modulation of cell fate [35,36]. Histone deacetylase inhibitors were reported to increase the self-renewal of hematopoietic $CD34^+$ cells in vitro and their engraftability in vivo [37]. Cu may be involved in hematopoietic cell regulation by modulating cellular post-translational modification activities.

The results of the present study support the notion that reduction of the chelatable Cu pool rather than a specific TEPA-Cu chelate mediates the mechanism of TEPA's activity on $CD34^+$ cells. Further studies are in progress to clarify this mechanism.

Acknowledgments

We thank Dr. Yaron Daniely for helpful discussions during the preparation of the manuscript.

References

1. Zidar BL, Shadduck RK, Zeigler Z, Winkelstein A. Observations on the anemia and neutropenia of human Cu deficiency. Am J Hematol. 1977;3:177–185.
2. Hirase N, Abe Y, Sadamura S, Yufu Y. Anemia and neutropenia in a case of copper deficiency: Role of copper in normal hematopoiesis. Acta Haematol. 1992;87:195–197.
3. Banno S, Niita M, Kikuchi M. Anemia and neutropenia in elderly patients caused by copper deficiency for long-term eternal nutrition. Rinsho Ketsueki. 1994;35:1276–1281.
4. Wasa M, Satani M, Tanano H. Copper deficiency with pancytopenia during total parenteral nutrition. J Parenter Enteral Nutr. 1994;18:190–192.
5. Gregg XT, Reddy V, Prchal JT, et al. Copper deficiency masquerading as myelodysplastic syndrome. Blood. 2002;100:1493–1495.
6. Bae B, Percival SS. Copper uptake and intracellular distribution during retinoic acid–induced differentiation of HL-60 cells. J Nutr Biochem. 1994;5:457–461.
7. Bae B, Percival SS. Retinoic acid–induced HL-60 cell differentiation is augmented by Cu supplementation. J Nutr. 1993;123:997–1002.
8. Peled T, Treves AJ, Rachmilewitz EA, et al. Identification of a serum-derived differentiation-inducing activity as the copper-binding protein ceruloplasmin. Blood. 1998;92:618a.
9. Shimizu M. Clinical results on the use of human ceruloplasmin in aplastic anemia. Transfusion. 1979;19:742–748.
10. Huang ZL, Failla ML, Reeves PG. Differentiation of human U937 promonocytic cells is impaired by moderate copper deficiency. Exp Biol Med (Maywood). 2001;226:222–228.
11. Peled T, Landau E, Prus E, et al. Cellular copper content modulates differentiation and self-renewal in cultures of cord blood–derived $CD34^+$ cells. Br J Haematol. 2002;116:655–661.
12. Peled T, Landau E, Mandel J, et al. Linear polyamine copper chelator tetraethylenepentamine augments long-term ex vivo expansion of cord blood–derived $CD34^+$ cells and increases their engraftment potential in NOD/SCID mice. Exp Hematol. 2004;32:547–555.
13. Peled T, Mandel J, Goudsmid RN, et al. Pre-clinical development of cord blood–derived progenitor cell graft expanded ex vivo with cytokines and the polyamine copper chelator tetraethylenepentamine. Cytotherapy. 2004;6:344–355.
14. Rubinstein P, Dobrila L, Rosenfield RE, et al. Processing and cryopreservation of placental/umbilical cord blood for unrelated bone marrow reconstitution. Proc Natl Acad Sci U S A. 1995;92:10119–10122.
15. Grodzicki M, Chrzaszez M, Kachniarz E, Piszezek P, Rozploch F. Spectral and magnetic properties of some copper (II) carboxylate compounds with hexamethylenetetramine. Pol J Chem. 1994;68:445–452.
16. Weston SA, Parish CR. New fluorescent dyes for lymphocyte migration studies. Analysis by flow cytometry and fluorescence microscopy. J Immunol Methods. 1990;133:87–97.
17. Weston SA, Parish CR. Calcein: A novel marker for lymphocytes which enter lymph nodes. Cytometry. 1992;13:739–749.
18. Dean KE, Klein G, Renaudet O, Reymond JL. A green fluorescent chemosensor for amino acids provides a versatile high-throughput screening (HTS) assay for proteases. Bioorg Med Chem Lett. 2003;13:1653–1656.
19. Luo W, Ma YM, Quinn PJ, Hider RC, Liu ZD. Design, synthesis and properties of novel iron (III)-specific fluorescent probes. J Pharm Pharmacol. 2004;56:529–536.
20. Von Drygalski A, Alespeiti G, Ren L, et al. Murine bone marrow cells cultured ex vivo in the presence of multiple cytokine combinations lose radioprotective and long-term engraftment potential. Stem Cells Dev. 2004;13:101–111.

21. Zheng X, Beissert T, Kukoc-Zivojnov N, et al. γ-catenin contributes to leukemogenesis induced by AML-associated translocation products by increasing the self-renewal of very primitive progenitor cells. Blood. 2004;103:3535–3543.
22. Amsellem S, Pflumio F, Bardinet D, et al. Ex vivo expansion of human hematopoietic stem cells by direct delivery of the HOXB4 homeoprotein. Nat Med. 2003;9:1423–1427.
23. Willert K, Brown JD, Danenberg E, et al. Wnt proteins are lipid-modified and can act as stem cell growth factors. Nature. 2003;423: 448–452.
24. Birkaya B, Aletta JM. NGF promotes copper accumulation required for optimum neurite outgrowth and protein methylation. J Neurobiol. 2005;63:49–61.
25. McArdle HJ, Gross SM, Vogel HM, Ackland ML, Danks DM. The effect of tetrathiomolybdate on the metabolism of copper by hepatocytes and fibroblasts. Biol Trace Elem Res. 1989;22:179–188.
26. Rosenzweig AC. Copper delivery by metallochaperone proteins. Acc Chem Res. 2001;34:119–128.
27. Smith RM, Martell AE. Critical stability constants. New York: Plenum Press; 1975. Vol. 2.
28. Hainaut P, Rolley N, Davies M, et al. Modulation by copper of p53 conformation and sequence-specific DNA binding: role for Cu (II)/Cu (I) redox mechanism. Oncogene. 1995;10:27–32.
29. Kudrin AV. Trace elements in regulation of NF-κb activity. J Trace Elem Med Biol. 2000;14:129–142.
30. Vanacore RM, Eskew JD, Morales PJ, et al. Role for copper in transient oxidation and nuclear translocation of MTF-1, but not of NF-κb, by the heme-hemopexin transport system. Antioxid Redox Signal. 2000;2:739–752.
31. Ostrakhovitch EA, Lordnejad MR, Schliess F, et al. Copper ions strongly activate the phosphoinositide-3-kinase/Akt pathway independent of the generation of reactive oxygen species. Arch Biochem Biophys. 2002 Jan 15;397:232–239.
32. Nakamura H, Nakamura K, Yodoi J. Redox regulation of cellular activation. Annu Rev Immunol. 1997;15:351–369.
33. Iseki A, Kambe F, Okumura K, Hayakawa T, Seo H. Regulation of thyroid follicular cell function by intracellular redox-active copper. Endocrinology. 2000;141:4373–4382.
34. Kang J, Lin C, Chen J, et al. Copper induces histone hypoacetylation through directly inhibiting histone acetyltransferase activity. Chem Biol Interact. 2004;148:115–123.
35. Akashi K, He X, Chen J, et al. Transcriptional accessibility for genes of multiple tissues and hematopoietic lineages is hierarchically controlled during early hematopoiesis. Blood. 2003;101:383–389.
36. Lehrmann H, Pritchard LL, Harel-Bellan A. Histone acetyltransferases and deacetylases in the control of cell proliferation and differentiation. Adv Cancer Res. 2002;86:41–65.
37. Milhem M, Mahmud N, Lavelle D, et al. Modification of hematopoietic stem cell fate by 5aza 2′deoxycytidine and trichostatin A. Blood. 2004;103:4102–4110.

Please select Print from the file menu to print your Abstract.

Please print, sign and fax this Official Print-Out to Marathon Multimedia at US 507-334-0126
before August 10, 2004, 11:59 PM EDT.

46th ASH Annual Meeting

Filename: 551903
Presenting Author E Shpall

Department/Institution: Department of Blood and Marrow Transplantation, University of Texas M.D. Anderson Cancer Center

Address: 1515 Holcombe Blvd., Unit 423

City/State/Zip/Country: Houston, TX, 77030, United States

Phone: 1-713-745-2803 **Fax:** 1-713-794-4902 **E-mail:** eshpall@mail.mdanderson.org

Presenting author is member of the American Society of Hematology: No

Presenting author is an Associate Member of ASH (member in training): No

Sponsoring Member: Elizabeth Shpall, MD

Department/Institution: Department of Blood and Marrow Transplantation, M D Anderson Cancer Center

Address: 1515 Holcombe blvd. unit 423

City/State/Zip/Country: Houston, TX, 77030, United States

Phone: 713-792-8750 **Fax:** 713-792-8503 **E-mail:** eshpall@mail.mdanderson.org

Abstract Category: 732. Clinical Results - Allogeneic Mismatched or Unrelated Transplantation

Presentation format preference: No preference
Publication preference: Publish in *Blood* if not accepted for presentation.
Special consideration: No.

Award Category: No award

Disclosure Statement: Disclosure information pertinent to the abstract: Research support from Gamida Cell

Will your presentation include information or discussion of off-label use of products? There is no information to disclose

Keywords:
Ex vivo expansion; Cord blood; Cord blood transplant

Title: Transplantation of Cord Blood Expanded Ex Vivo with Copper Chelator

E Shpall [1]*, M de Lima [1], K Chan [1], R Champlin [1], A Gee [2], P Thall [1], K Komanduri [1], D Couriel [1], B Andersson [1], C Hosing [1], S Giralt [1], S Safa Karandish [1]*, T Tara Sadeghi [1]*, B Muriera [1]*, T Peled [3]*, F Grynspan [3]*, A Nagler [4]* and J McMannis [1]. [1] BMT, The M.D. Anderson Cancer Center, Houston, TX, United States, 77030; [2] Center for Cell and Gene Therapy, Baylor College of Medicine, Houston, TX, United States, 77030; [3] Gamida Cell Ltd, Jerusalem, Israel and [4] BMT, Chaim Sheba Med Center, Ramat Gan, Israel.

Cord blood (CB) is used to restore hematopoiesis in transplant patients lacking marrow donors. CB is associated with higher rates of delayed/failed engraftment. Peled et al developed an expansion technology using the copper chelator tetraethylenepentamine (TEPA), which enhanced the expansion of primitive CB populations when combined with early acting cytokines. A phase I clinical trial employing this technology was initiated. 10 patients with high-risk, heavily pre-treated hematologic malignancies (AML-2, ALL-5, HD-2, and NHL-1) have been enrolled with CB units that were cryopreserved in 2 fractions [20:80% (n=2), 40:60% (n=5) or 50:50% (n=3)]. 21days prior to infusion, AC133+ cells were isolated from the smaller (if unequal) or 50% CB fractions using the CliniMACS device and cultured for 21 days in media containing 10% FBS and SCF, FLT-3, IL6, TPO plus the copper chelator TEPA (Gamida). Patients then received myeloablative therapy with ATG and either fludara and busulfan (AML), or fludara, melphalan, thiotepa (ALL, HD, NHL) with infusion of the unmanipulated CB fraction on day 0, and the expanded fraction on day +1. GVHD prophylaxis was methotrex 5 mg/m^2 days 2, 4 ,7, and tacrolimus for 6 months. The median age was 21 (range 7-51) and weight 69 (range 31-156) kg. The CB units were matched at 4/6 (n=8) or 5/6 (n=2) HLA antigens. The pre-thaw total nucleated cell (TNC) dose of the CB units was a median of 2.5x10^7/kg with post-thaw TNC of 2.4 x10^7/kg. Following AC133-selection, the manipulated CB fractions were a median of 73 (range 38-95)% AC133+ with a median of 0.650 (range 0.16-2.7) x10^6 TNCs, which were placed in culture. After 21 days of culture the expanded fraction had 69 (range 2-1638) x10^6 TNCs representing a 207 (range 2-616) fold TNC expansion. Patients received a total (expanded plus

fold TNC expansion. Patients received a total (expanded plus unmanipulated) median of 1.8 (range 1.1-6.1) $x10^7$ TNC/kg and $1.6x10^5$ (range 0.4-49.9) CD34+ cells/kg. Two patients have CB cultures in progress. Of the 8 patients transplanted, 1 had autologous recovery with relapse of AML on day 30 and death. Of the remaining patients, 7 were evaluable for neutrophil engraftment and 4 of them for platelet engraftment (2 too early for platelet evaluation and 1 early death). The median time to engraftment was 27 days for neutrophils (range 16-46) and 48 days for platelets (range 27-96). Preliminary analysis suggest a correlation between a shorter time to neutrophil engraftment and total TNC/kg infused (p=0.02), and a trend for CD34+ cells/kg infused (p=0.09). Three patients have developed grade $\leq$2 acute skin GVHD and one had chronic extensive GVHD of the skin and GI tract; all resolved with steroids. One patient (without GVHD) died of a systemic viral infection on day 56, despite adequate neutrophil recovery (not platelets). All of the remaining patients are all alive and free of malignancy at a median follow-up of 4 (range 1-16) months. **Conclusion:** There was no toxicity associated with infusion of the TEPA-expanded CB cells. Additional data is necessary to determine the efficacy of this approach. Future directions include the expansion of the entire CB unit and removal of methotrex from the GVHD regimen to improve time to neutrophil engraftment, as well as comprehensive assessment of immune reconstitution.

Certification for Human Subjects: I certify that this study abides by the rules of the appropriate internal review board and the tenets of the Helsinki protocol, if human subjects were involved.
Agree

Signature of Presenting Author:

_____

E Shpall

Sponsoring ASH Member:

_____

Elizabeth Shpall

Close Window

International Society for Cellular Therapy ISCT

Cytotherapy (2004) Vol. 6, No. 4, 344–355

Taylor & Francis healthsciences

Pre-clinical development of cord blood-derived progenitor cell graft expanded *ex vivo* with cytokines and the polyamine copper chelator tetraethylenepentamine

T Peled[1], J Mandel[1], RN Goudsmid[1], C Landor[1], N Hasson[1], D Harati[1], M Austin[1], A Hasson[1], E Fibach[2], EJ Shpall[3] and A Nagler[4]

[1]Gamida-Cell Ltd, Jerusalem, Israel, [2]Hadassah–Hebrew University Medical Center, Jerusalem, Israel, [3]MD Anderson, Houston, Texas, USA, and [4]Chaim Sheba Medical Center, Tel Hashomer, Israel

Background

We have previously demonstrated that the copper chelator tetraethylenepentamine (TEPA) enables preferential expansion of early hematopoietic progenitor cells ($CD34^+ CD38^-$, $CD34^+ CD38^- Lin^-$) in human umbilical cord blood (CB)-derived $CD34^+$ cell cultures. This study extends our previous findings that copper chelation can modulate the balance between self-renewal and differentiation of hematopoietic progenitor cells.

Methods

In the present study we established a clinically applicative protocol for large-scale ex vivo *expansion of CB-derived progenitors. Briefly, $CD133^+$ cells, purified from CB using Miltenyi Biotec's (Bergisch Gladbach, Germany) CliniMACS separation device and the anti-CD133 reagent, were cultured for 3 weeks in a clinical-grade closed culture bag system, using the chelator-based technology in combination with early-acting cytokines (SCF, thrombopoietin, IL-6 and FLT-3 ligand). This protocol was evaluated using frozen units derived from accredited cord blood banks.*

Results

Following 3 weeks of expansion under large-scale culture conditions that were suitable for clinical manufacturing, the median output value of $CD34^+$ cells increase by 89-fold, $CD34^+ CD38^-$ increase by 30-fold and CFU cells (CFUc) by 172-fold over the input value. Transplantation into sublethally irradiated non-obese diabetic (NOD/SCID) mice indicated that the engraftment potential of the ex vivo *expanded $CD133^+$ cells was significantly superior to that of unexpanded cells: $60 \pm 5.5\%$ vs. $21 \pm 3.5\%$ $CD45^+$ cells, $P = 0.001$, and $11 \pm 1.8\%$ vs. $4 \pm 0.68\%$ $CD45^+ CD34^+$ cells, $P = 0.012$, $n = 32$, respectively.*

Discussion

Based on these large-scale experiments, the chelator-based ex vivo *expansion technology is currently being tested in a phase 1 clinical trial in patients undergoing CB transplantation for hematological malignancies.*

Keywords

ex vivo *large-scale expansion, pre-clinical development, tetraethylenepentamine.*

Introduction

Cord blood (CB) is a valuable source of stem cells. Transplanted CB hematopoietic stem/progenitors cells (HPC) can treat malignant and non-malignant disorders [1–3]. However, the major clinical limitation of CB transplantation is the low number of HPC in comparison with mobilized peripheral blood or BM grafts. This limitation may explain the slower time to engraftment and higher rate of engraftment failure following CB transplantation [4,5]. To overcome this limitation, *ex vivo* expansion of CB progenitors with a cocktail of growth factors has been attempted [6]. It was shown that a

Correspondence to: **Professor Arnon Nagler**, Director of Hematology Division, Bone Marrow Transplantation & Cord Blood Bank, Chaim Sheba Medical, Tel Hashomer, Israel.

© *2004 ISCT*

DOI: 10.1080/14653240410004916

combination of early- and late-acting cytokines, including SCF, thrombopoietin (TPO), G-CSF and IL-3, resulted in only a marginal-fold expansion of late ($CD34^+$) and early ($CD34^+CD38^-$) progenitor cells, probably due the fact that the late-acting cytokines drive the cultures mainly toward accelerated differentiation [7–9]. On the other hand, cultures with only early-acting cytokines (SCF, TPO, IL-6 and FLT-3 ligand) resulted in better and prolonged expansion of both late and early progenitors [10,11], which are important for short-term early trilineage engraftment [12–14].

We have previously demonstrated that short-term (3 weeks) treatment with the polyamine copper chelator tetraethylenepentamine (TEPA) augmented the long-term expansion potential of CB-derived progenitor cells [15]. During the treatment period, TEPA inhibited the onset of cytokine-driven differentiation of early progenitor cells, resulting in a robust accumulation of $CD34^+CD38^-$ and $CD34^+Lin^-$ cells, with no effect on proliferation and differentiation of more mature committed cells [$CD34^+Lin^+$ and CFU culture (CFUc)] [16]. These results strongly suggest that TEPA supports the self-renewal division cycle without compromising differentiation capacity of hematopoietic stem cells.

In view of these results, the TEPA-based expansion procedure was adapted to comply with current good manufacturing practice (cGMP) standards required for clinical trials. In the present study we describe the development of a clinical-scale procedure using Miltenyi Biotec's (Bergisch Gladbach, Germany) CliniMACS separation device, and the anti-CD133 reagent for progenitor cell enrichment and 3-week expansion in culture bags, using the chelator-based technology with an early-acting cytokine cocktail (FLT-3 ligand, IL-6, TPO, SCF).

Methods

CB samples

Cells were obtained from neonatal umbilical cord blood after normal full-term delivery (informed consent was given). Samples were collected and frozen in our laboratories according to Rubinstein *et al.* [17] within 24 h postpartum, or kindly provided by the New York Blood Bank (New York, NY) and the Duke University Medical Center Cord Blood Bank (Durham, NC).

Thawing procedure and CliniMACS separation of $CD133^+$ and $CD34^+$ cells

The cells were thawed by doubling the volume of the blood sample in 2.5% dextran (Sigma, St Louis, MO) and 1.25% HSA (Bayer Co., Elkhart, IN). Prior to centrifuging an additional 40 mL of 10% dextran was added.

The cells were resuspended in 40 mL of 2.5% dextran/1.25% HSA and then filled to 100 mL with PBS (Biological Industries, Beit-HaEmek, Israel) containing 0.4% sodium citrate solution (Baxter HealthCare Co., Deerfield, IL) and 1% HSA. The pellet was incubated with 0.15% w/v intravenous immunoglobulin (IvIg; Omrix Biopharmaceuticals, Nes-Ziona, Israel) for 10 min at room temperature before centrifugation, and then resuspended in PBS containing 0.4% sodium citrate solution and 1% HAS, and 0.25 mg/mL recombinant human deoxyribonuclease (rHu-Dnase) added. Subsequently, the cells were labeled with Miltenyi's anti-CD133 (clone 1) or anti-CD34 CliniMACS reagent (Miltenyi Biotec) and separated by CliniMACS (according to the manufacturer's instructions). Following separation, cells were stained with trypan blue, counted, assayed for CFUc and immunophenotyped to determine purity.

Purity determination of CD34– and CD133–enriched cell fractions

The cells were washed with a PBS solution containing 1% BSA (PBS/1%BSA), and stained (at 4°C for 30 min) with FITC-conjugated anti-CD45 (Becton Dickinson, San Jose, CA) and either PE-conjugated anti-CD34 (DAKO, Glostrup, Denmark) or PE anti-CD133 (Miltenyi Biotec) Ab. In addition, the percentage of cells exhibiting both the CD133 and CD34 markers was measured by staining the cells with FITC–anti-CD34 (IQ Products, Groningen, the Netherlands) and PE–anti-CD133 (Miltenyi Biotec) Ab. The cells were then washed in the above buffer and analyzed using a FACScalibur® flow cytometer (Becton Dickinson, Immunofluorometry Systems, Mountain View, CA). The cells were passed at a rate of up to 1000 cells/second, using a 488-nm argon laser beam as the light source for excitation. Emission of 5000 cells was measured using logarithmic amplification, and analyzed using the CellQuest software (Becton Dickinson). Cells stained with FITC- and PE-conjugated isotype control Ab were used to determine background fluorescence.

Cell counting

The number of total nucleated cells (TNC) was determined by diluting the cells 1:2 with trypan blue and differentially counting viable and dead cells using a hemocytometer under an upright microscope at 100 × magnification.

Assay for CFUc

Cells, 1000 ($CD34^+$ or $CD133^+$) before culture and 1500 following culture, were added per 3 mL semisolid minimal essential alpha medium (MEMα), containing methylcellulose (Sigma), 30% FCS, 1% BSA, 1×10^{-5} M β-mercaptoethanol (Sigma), 1 mM glutamine (Biological Industries), 2 IU/mL erythropoietin (Eprex, Cilag AG Int., Schaffhausen, Switzerland), SCF and IL-3, both at 20 ng/mL, G-CSF and GM-CSF, both at 10 ng/mL (Perpo Tech Inc., Rocky Hill, NJ), and 2 μm hemin (Sigma). Following stirring, the mixture was divided into two 35-mm dishes and incubated for 14 days at 37°C in a humidified atmosphere of 5% CO_2 in air. At the end of the incubation period, colonies (both myeloid and erythroid) were counted under an inverted microscope at 40 × magnification. CFUc content was calculated as the following: number of scored colonies per two dishes × total cell number/1500 or 1000. The number of cells was determined by multiplying the number of cells/mL by the culture volume. CFUc frequency was calculated as number of colonies divided by the number of cells seeded.

Ex vivo expansion

Purified $CD34^+$ or $CD133^+$ cells were cultured at 1×10^4 cells/mL in MEMα and 10% FCS (Biological Industries) containing the following human recombinant cytokines: TPO, IL-6, FLT-3 ligand and SCF, each at a final concentration of 50 ng/mL (Pepro Tech Inc.), and 5 μm TEPA (Aldrich, Milwaukee, WI). VueLife Teflon PEP culture bags (American Fluoroseal Co., Gaithersburg, MD) were used: 72-mL bags were used for up to 20×10^4 initiating cells, and 270-mL bags were used for up to $20-70 \times 10^4$ cells. The cultures were incubated for 3 weeks (unless otherwise stated) at 37°C in a humidified atmosphere of 5% CO_2 in air. Cultures were topped weekly with the same volume of fresh medium, FCS, cytokines and TEPA. At the termination of the experiment, cells were counted following staining with trypan blue, assayed for CFUc and immunophenotyped for surface antigens.

Surface antigen analysis of cultured cells

The cells were washed with PBS/1%BSA and stained (at 4°C for 30 min) with both FITC–anti-CD45 and PE–anti-CD34 (both from DAKO) Ab for determination of $CD34^+$ cells, with FITC–anti-CD38 and PE–anti-CD34 for determination of $CD34^+CD38^-$ cells and with FITC–anti-CD45 and PE–Ab to lineage specific antigens (Becton Dickinson). The cells were then washed and analyzed as described above.

Clinical grade reagents

During the development phase, the research grade ingredients were replaced by clinical grade ingredients as follows.

Thawing procedure and CliniMACS separation: Gentran-40, a ready-made 10% w/v dextran solution, HSA and IvIg (all from Baxter), Dnase (Genentech Inc., San Francisco, CA) and PBS (Hyclone, Logan, UT). CFUc assay: MethoCult™, a methylcellulose-based medium (StemCell Technologies, Vancouver, Canada). *Ex vivo* expansion: MEMα and FCS (gamma-irradiated defined fetal bovine serum batch), from Hyclone.

TEPA was purchased from NovaSep (Boothwyn, PA). The cytokines TPO, IL-6, SCF and FLT-3 ligand were from R&D Systems (Minneapolis, MN). They are human recombinant cytokines from non-mammalian origin (derived from either *Escherichia coli* or Sf-21 cells). FLT-3 ligand and TPO were purified on affinity columns containing MAb. The cytokines were filtered through a 0.2-micron membrane, packaged under aseptic conditions and tested for endotoxin. Cytokine batches used in the study were tested for sterility by Charles River Laboratories (Rockville, MD) according to the ICH guideline *Viral safety evaluation of biotechnology products derived from cell lines of human or animal origin* adopted by the ICH Steering Committee (March 5, 1997) and the Code of Federal Regulations (April 1, 2003).

Reselection of cultured $CD34^+$ cells

To purify the $CD34^+$ cells, cultured cells were harvested and subjected to two cycles of immunomagnetic bead separation, using a MiniMACS CD34 progenitor cell isolation kit (Miltenyi Biotec) according to the manufacturer's recommendations. The purity of the $CD34^+$ population thus obtained was 90–98%, as evaluated by flow cytometry. The eluted cells were then counted and dually stained with PE–anti-CD34 and FITC–anti-CD38 Ab for determination of the percentage of $CD34^+CD38^-$

cells. $CD34^+$ cell content of the entire culture was calculated as follows: number of $CD34^+$ cells recovered following repurification × culture volume/volume of the portion of the culture subjected to repurification. Fold expansion of $CD34^+$ cells was calculated by dividing the $CD34^+$ cell content of the culture by the number of inoculated $CD34^+$ cells. The $CD34^+CD38^-$ cell content of the entire culture was calculated from the total $CD34^+$ cells. Fold expansion was calculated by dividing the total $CD34^+CD38^-$ cell number following culture by the number of inoculated cells.

Stability tests of the expanded graft

Following 3-week expansion, the cells were harvested, washed twice with PBS/EDTA–HSA solution, resuspended in transfusion solution (PBS/EDTA–HSA buffer) at $1-1.5 \times 10^6$ cells/mL and transferred (at least 30 mL) into a transfusion bag (Transfer bag-Terumo, Teruflex T-150, Tokyo, Japan). Closure clamps were used to prevent foaming. The bags were kept in a shipping container (Styrofoam) at 22 ± 4°C. Data loggers were put inside the container and its inner surface fastened for temperature monitoring. The bags were sampled to assess the number of viable cells and CFUc at 0, 6, 10 and 24 h.

Transplantation of human CB-derived $CD133^+$ cells into NOD/SCID mice

Each CB unit was frozen in two portions. $CD133^+$ cells purified from the first portion were cultured for 3 weeks with TEPA, as described above. The second portion of each unit was kept frozen until the day of transplantation (non-cultured cells). Mice were transplanted either with the progeny of 5×10^4 cultured $CD133^+$ cells or with 10×10^6 non-cultured mononuclear cells. Control mice were injected with medium only.

NOD/SCID mice, aged 10–11 weeks, bred and maintained at the Department of Immunology, the Weizmann Institute of Science, Rehovot, Israel, were injected intravenously with the above cells 1 day after they had been irradiated at 375 cGy.

The mice were killed 4 weeks post transplantation; BM was collected from both femurs and tibiae. The BM cells were washed in PBS/1%BSA and stained (at 4°C for 30 min) with PE-conjugated Ab to human CD45 (DAKO) and FITC-conjugated Ab to human CD34 (IQ Products), CD41, CD61, glycophorin A (DAKO), CD14, CD15, CD33 and CD19 (Becton Dickinson). Following incubation, the suspension was treated with FACS lysing solution (Becton Dickinson) to remove red blood cells, washed in PBS/1%BSA and analyzed by flow cytometry, as described above.

Calculations

Ex vivo expansion of TNC, CD34, $CD34^+CD38^-$ cells and CFUc are reported either as total numbers (number of cells per mL multiplied by the final culture volume) or as fold-expansion (total numbers divided by initial seeding cell number).

Statistics

The following statistical tests were used. The non-parametric test (Wilcoxon rank test) was applied for testing differences between the study groups for quantitative parameters. The data was analyzed using the SAS software (SAS version 8.2; SAS Institute Inc., Cary, NC).

Results

Progenitor cell purification

As a first step toward large-scale experiments and a clinical trial, we replaced the research-grade CD34-based separation device with the clinical grade CD133-based device. For this purpose, we compared the anti-CD34 and anti-CD133 CliniMACS reagents, using the CliniMACS separation device, with respect to the yield (number of cells) (Figure 1a) and purity (percent of $CD34^+$ or $CD133^+$ cells) (Figure 1b). The results indicated no statistically significant difference. Most ($>90\%$) of the cells in the enriched populations were double positive for both CD133 and CD34. A representative FACS analysis is shown in Figure 1c. A comparison of the fractions with respect to their CFUc frequency also produced similar results, $0.2 \pm 0.1\%$ and $0.12 \pm 0.07\%$, respectively.

Clinical-scale *ex vivo* expansion

To optimize the duration of the expansion procedure, we compared 2- vs. 3-week cultures. Cultures were initiated with 1×10^4 cells/mL purified by the CliniMACS utilizing the anti-CD133 reagent. The cells were grown in 290-mL culture bags (initial culture volume/bag, 25 mL) in alpha medium supplemented with FCS, a combination of four cytokines (SCF, TPO, IL-6 and FLT-3 ligand, 50 ng/mL each) and 5 μm TEPA. The cultures were topped up weekly with an equal volume of fresh medium.

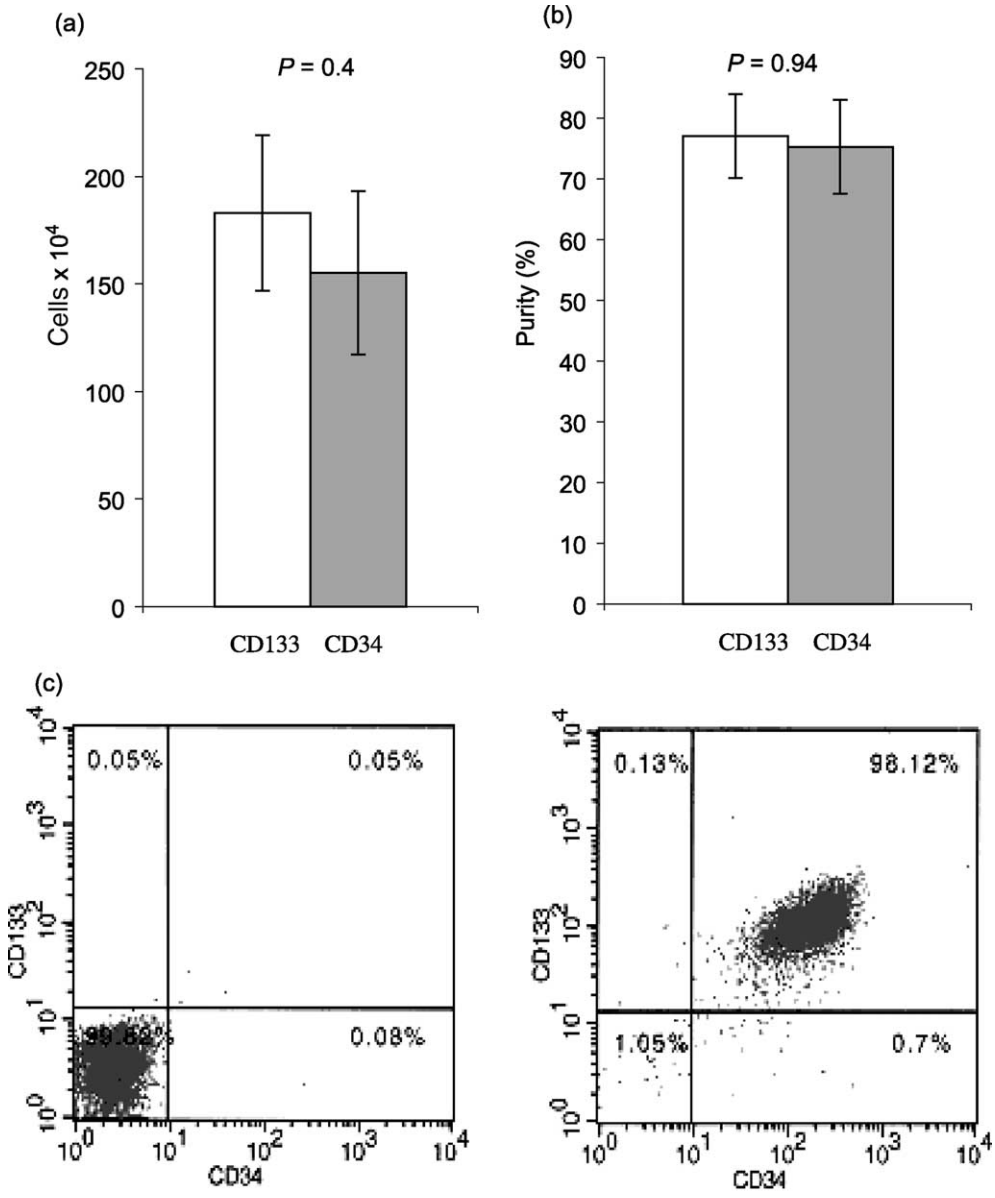

Figure 1. *Comparison between anti-CD133 and anti-CD34 CliniMACS enrichment reagents. Frozen CB units (*n = 6*) were thawed, divided into two equal portions and enriched for progenitor cells using anti-CD133 or anti-CD34$^+$ reagents and CliniMACS separation device. Cell yield (a) was determined by counting the number of viable cells in the positive fraction. Purity (b) was determined by FACS analysis of double stained cells with PE–anti-CD45 and either anti-CD34 or FITC–anti-CD133 Ab. A representative FACS analysis dot-plot of CD133-enriched cells is shown in (c). The eluted cells were double stained with isotype controls (left panel) or with both PE–anti-CD133 and FITC–anti-CD34 Ab (right panel). The percentage of cells in each quadrant is indicated.*

Figure 2 shows that the cumulative numbers ($\times 10^6$) of TNC, CD34$^+$ and CD34$^+$CD38$^-$ cells were significantly higher following 3-week expansion compared with 2 weeks: 84 ± 7 vs. 34 ± 3, 22 ± 2 vs. 11 ± 2, and 5.4 ± 1 vs. 2.6 ± 0.4, respectively. Only limited expansion was observed following the first week of culturing (data not shown).

We then compared the expansion potential of cells purified from the same CB unit with either the anti-CD133$^+$ or the anti-CD34$^+$ reagents. The cultures ($n = 4$) were initiated with 2.5×10^5 cells and grown for 3 weeks. The yield of TNC was $1065 \pm 124 \times 10^5$ and $760 \pm 75 \times 10^5$ ($P = 0.19$), CFUc 81 ± 9 and $83 \pm 11 \times 10^5$ ($P = 0.66$), CD34$^+$ cells $43 \pm 7 \times 10^5$ and $39 \pm 9 \times 10^5$

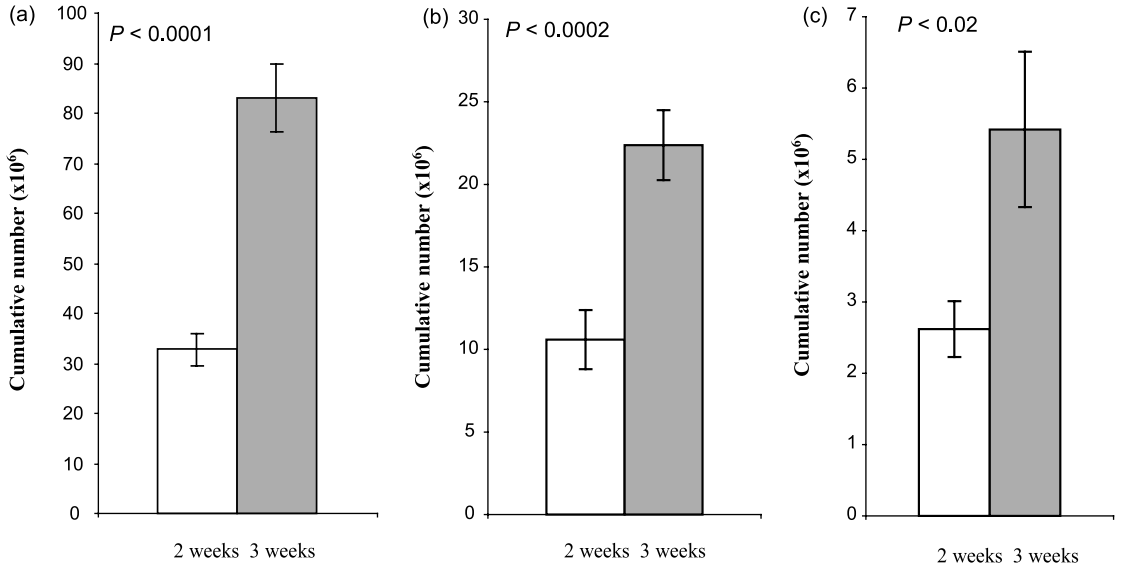

***Figure 2**. Optimization of the expansion duration. Cultures* (n = *18) were initiated with purified CD133$^+$ cells. TNC (a), CD34$^+$ (b) and CD34$^+$CD38$^-$ (c) cells were determined after 2 and 3 weeks. Cumulative numbers were calculated as described in the Methods.*

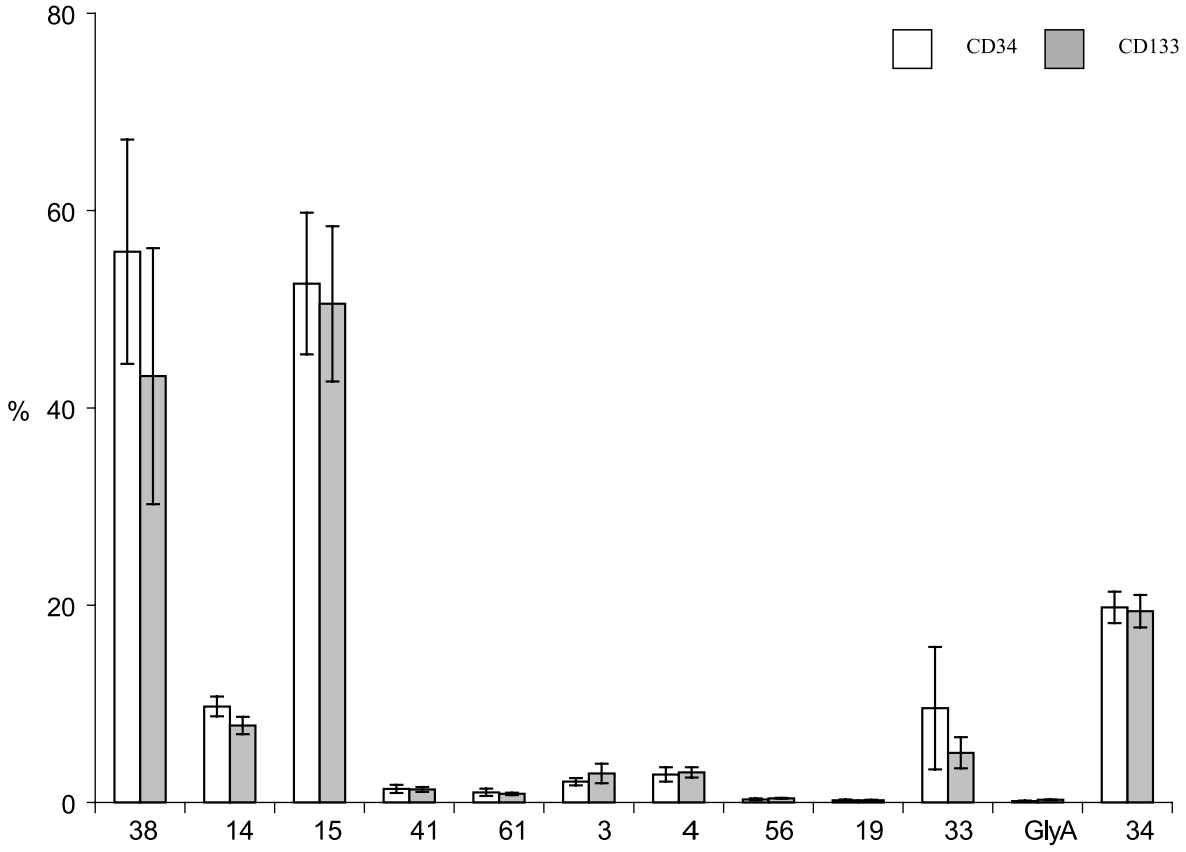

***Figure 3**. Phenotype analysis of 3-week cultures. Cultures were initiated with either CD133$^+$ or CD34$^+$ cells. After 3 weeks cultured cells* (n = *18) were double stained with PE– anti-CD45 and FITC– anti-lineage specific Ab and analyzed by FACS. The percentages of cells expressing CD38, myeloid (CD14, CD15, CD33), lymphoid (CD3, CD4, CD19, CD56), erythroid, (GlyA) and megakaryocytic (CD41, CD61) antigens as well as that expressing the progenitor cell antigen (CD34) are shown.*

($P = 0.89$), $CD34^+CD38^-$ cells $12 \pm 3.6 \times 10^5$ and $5.6 \pm 1.3 \times 10^5$ ($P = 0.11$), in cultures initiated with $CD133^+$ cells and with $CD34^+$ cells, respectively. In this set of experiments, $CD34^+$ and $CD34^+CD38^-$ cells were determined following affinity reselection of $CD34^+$ cells, as described in the Methods. Additional immunophenotyping indicated similar proportions of cells expressing myeloid, lymphoid or megakaryocytic phenotype in cultures initiated either with $CD34^+$ or $CD133^+$ cells (Figure 3).

Evaluation of the expansion procedure

Based on the above-described experiments, we carried out a large-scale evaluation of the following expansion procedure. A 20% portion of a CB unit was thawed and progenitor cells were enriched by the CliniMACS anti-CD133 procedure. The purified cells were grown for 3 weeks in culture bags with cGMP components, including cytokines and TEPA. Of the frozen CB units studied, 18 were derived from accredited CB banks (Netcord Düsseldorf, Germany, and COBLT) and 4 units from the Gamida-Cell research-grade CB bank (Jerusalem, Israel). The results showed that the yield of viable cells was in the range of $17-35 \times 10^4$ and the purity 58–97%. The percentages of $CD34^+$ and $CD34^+CD38^-$ cells following 3-week expansion are shown in Figure 4.

The input numbers of $CD34^+$, $CD34^+CD38^-$ and CFU cells as well as the output numbers following 3 weeks expansion are shown in Table 1. The median output value of $CD34^+$ cells increased by 89-fold, $CD34^+CD38^-$ increased by 30-fold and CFUc by 172-fold over the input values.

We then determined the expansion efficacy with regard to the number of cells of different subtypes available for transplantation. For this purpose, the number of cells in the expanded product (derived from 20% of the CB unit) and the number of cells in the non-manipulated 80% portion, were combined and compared with the number of cells in the whole (100%) non-manipulated unit (Table 2). Statistical analysis of the data demonstrated that the numbers of CFUc, $CD34^+$ and $CD34^+CD38^-$ cells in a graft also containing expanded cells were significantly higher than in a non-manipulated graft ($P < 0.025$), whereas the total nuclear cell numbers were comparable ($P = 0.4$).

Stability of the expanded graft

To prepare the expanded cell product for transplantation, the cells are resuspended in infusion buffer and transferred into a transfusion bag. Since there may be a delay of several hours between the completion of the manufacturing process and the infusion of the cells into the patient, we conducted a 24-h stability study as described in the Methods. Cell samples were taken immediately after inoculation of the cells into the transfusion bags, and 6, 10 and 24 h thereafter. The results shown in Table 3 demonstrate that the numbers of viable cells and CFUc during the 24 h were statistically comparable.

NOD/SCID engraftment potential of the expanded graft

The marrow-repopulating ability of the expanded cells in NOD/SCID mice was compared with that of non-

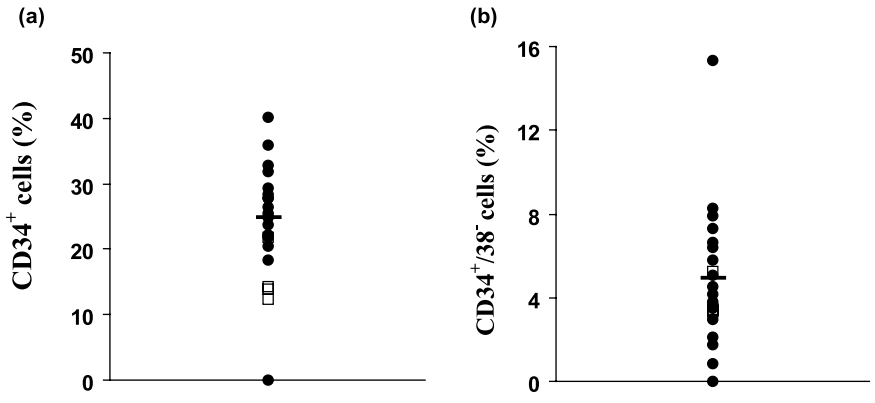

Figure 4. *Large-scale evaluation of the 3-week expansion procedure. Cultures were initiated with $CD133^+$-enriched cells following separation on CliniMACS of 22 CB units [four research-grade units (squares) and 18 clinical-grade units (circles)]. After 3 weeks, the cultured cells were double stained with PE–anti-CD45 and FITC–anti-CD34 (a) or FITC–anti-CD34 and PE–anti-CD38 (b). Percentages of $CD34^+$ and $CD34^+CD38^-$ cells were determined by FACS analysis.*

Table 1. Expansion of cells following 3-week culture

	Input			Output			Median-fold increase
	Range	Median	Mean ± SE	Range	Median	Mean ± SE	
TNC × 10^7				2–20	12	12 ± 3	
$CD34^+$ × 10^4	17–35	25	25 ± 2	131–3061	2224	2120 ± 556	89
$CD34^+CD38^-$ × 10^4	2–17	11	10 ± 3	33–803	335	361 ± 103	30.5
CFU × 10^4	2–7	3	4 ± 1	136–1100	517	537 ± 144	172

The cultures were initiated with $CD133^+$ cells derived from a 20% portion of a CB unit. At the initiation of the cultures (input) and after 3 weeks (output), cells were analyzed for the indicated parameters. Median-fold increase was calculated by dividing the median output by the median input values.

expanded cells, both derived from the same CB unit. Mice were concomitantly transplanted with either 10×10^6 non-expanded mononuclear cells (containing 5×10^4 $CD133^+$ cells) or all the progeny of purified 5×10^4 $CD133^+$ cells following a 3-week large-scale expansion. In all eight experiments, mice injected with cultured cells contained a significantly higher percentage of total human ($CD45^+$) cells (Figure 5a and Table 4), and human progenitor ($CD45^+CD34^+$) cells (Figure 5b), compared with mice injected with non-cultured cells ($P = 0.001$ and $P = 0.012$, respectively). Calculated engraftment efficacy, i.e. the percentage of $CD45^+$ cells in mice transplanted with cultured cells divided by the percentage of $CD45^+$ cells in mice transplanted with non-cultured cells, ranged from 1.7 to 31.

Phenotype analysis demonstrated that the expanded cells maintained the potential to differentiate *in vivo* into various hematopoietic lineages, myeloid (CD14, CD15, CD33), megakaryocyte (CD41 and CD61), erythroid (glycophorin A) and B lymphoid (CD19). The engraftment of all assessed hematopoietic lineages was significantly higher in mice transplanted with expanded cells compared with non-cultured cells (Figure 5b).

Discussion

Umbilical CB has been used successfully as a source of hematopoietic stem cells in allogeneic stem cell transplantation. Advantages of using CB include reduced susceptibility to post-transplant infections and to GvHD, as well as greater availability of a donor. The major limitation of using CB is related to the low cell dose in CB and possibly to some intrinsic properties of CB cells [18]. *Ex vivo* expansion is a strategy to increase the number of cells available for transplantation. Two general protocols suitable for clinical application have been published [19–21]. The first protocol comprises a two-step culture system

Table 2. Number of specific cells available for infusion in the non-expanded vs. expanded graft

No. cells	Treatment	Median	Mean ± SE	*P*-value	Expansion efficacy***
TNC × 10^7	Non-expanded*	76.3	71.8 ± 5.8		
	Expanded**	74.3	69.4 ± 6.6	0.4	0.97
$CD34^+$ cells × 10^4	Non-expanded	124.5	118.3 ± 18		
	Expanded	2345.0	2220 ± 559	0.0025	19
$CD34^+CD38^-$ cells × 10^4	Non-expanded	53.5	46.8 ± − 12.7		
	Expanded	378.0	398.3 ± − 112.2	0.025	7
CFUc × 10^4	Non-expanded*	15.0	17.5 ± 4.3		
	Expanded	528.0	550.7 ± 146	0.009	35

Cells in each CB unit were frozen in two portions of 80% and 20%. The 20% portion was thawed, counted and the CD133 cells purified and cultured for 3 weeks as described in the Methods. The numbers present the cells of the various subsets calculated for the 100% non-expanded cells of the CB unit (*) and a mixture of the 80% non-expanded plus the culture output of the 20% portion (**).

****Calculated by dividing the median expanded cell graft values by the median non-expanded graft values.*

Table 3. Stability of the expanded graft

Exp. #	0 h	6 h	10 h	24 h
(a) No. viable cells $\times 10^4$/mL				
1	77 ± 0.6	73 ± 0.3	77 ± 3.9	91 ± 3.8
2	64 ± 11	50 ± 3.1	54 ± 2.0	37 ± 6.9
3	104 ± 5.2	106 ± 4.8	96 ± 12.1	102 ± 6.9
(b) CFU $\times 10^4$/mL				
1	3.3 ± 0.2	3.6 ± 0.1	4.0 ± 0.4	4.2 ± 0.1
2	2.1 ± 0.3	3.2 ± 0.2	1.6 ± 0.2	2.0 ± 0.4
3	6.9 ± 0.4	7.0 ± 0.4	6.6 ± 0.7	7.3 ± 0.9

Following 3-week expansion, the cells were harvested, washed and transferred into bags as detailed in the Methods. The bags were kept in a shipping container at $22 \pm 4^{\circ}$C and sampled to assess the number of viable cells (a) and CFUc (b) at time 0, 6, 10 and 24 h.

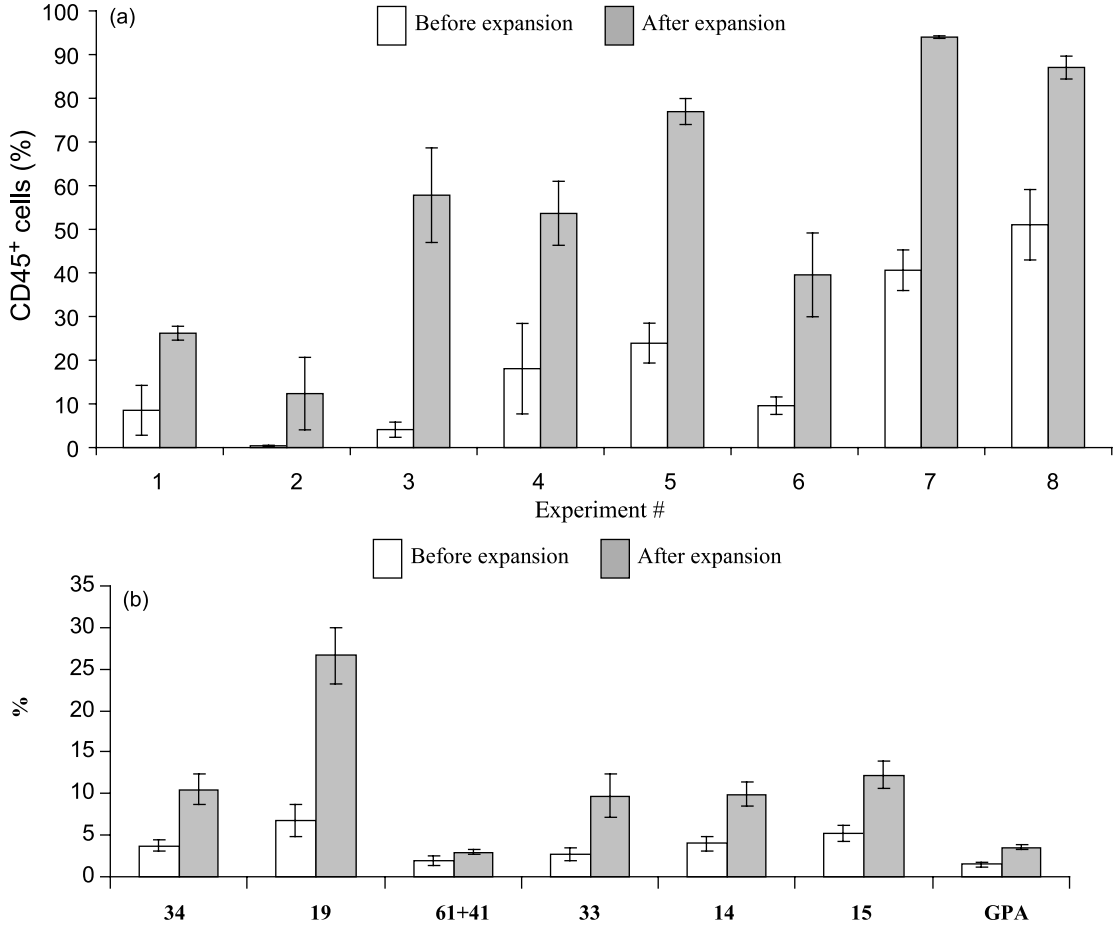

Figure 5. *Engraftment of clinical-grade cultured cells in NOD/SCID mice. Mice (3–5 per experimental group) were transplanted with all the progeny of 5×10^4 CD133$^+$ cells after 3 weeks expansion or with the equivalent fraction of MNC before expansion (10×10^6 cells), both derived from the same CB units. Four weeks after transplantation, human cell engraftment was evaluated by FACS analysis of CD45$^+$ cells (a). Progenitor cells (CD34$^+$) and lineage-specific differentiated cells were evaluated by FACS analysis of cells double stained with PE–anti-human CD45 and FITC–anti-human lineage antigens (b). The data in (a) present the mean $\pm$ SE of each experiment of eight (#1–8) consecutive experiments. The data in (b) present the mean $\pm$ SE of four experiments. GPA = GlycophorinA.*

Table 4. Engraftment of human cells in SCID mice BM

Exp. #	% CD45$^+$ human cells in mouse BM 4 weeks after transplantation													
	Non-cultured cells						Cultured cells							
	Mouse 1	Mouse 2	Mouse 3	Mouse 4	Mouse 5	Average	SE	Mouse 1	Mouse 2	Mouse 3	Mouse 4	Mouse 5	Average	SE
1	20.0	3.6	2.1	–	–	8.6	5.7	28.9	23.3	26.3	–	–	26.2	1.6
2	0.2	0.6	0.4	–	–	0.4	0.1	28.9	5.1	3.1	–	–	12.4	8.3
3	7.5	2.9	1.9	–	–	4.1	1.7	63.5	36.8	73.0	–	–	57.8	10.8
4	37.6	2.4	14.2	–	–	18.1	10.4	61.0	60.9	39.0	–	–	53.6	7.3
5	8.7	26.7	19.0	33.7	31.6	23.9	4.6	78.2	69.4	83.8	76.4	D	77.0	3.0
6	9.0	11.7	14.5	10.2	2.5	9.6	2.0	60.3	14.4	37.5	45.9	D	39.5	9.6
7	46.1	28.4	49.3	38.6	D	40.6	4.7	94.6	94.3	93.2	93.8	D	94.0	0.3
8	43.2	67.5	32.3	61.1	D	51.0	8.1	77.5	86.6	91.8	87.7	91.6	87.0	2.6

The table demonstrates the raw data of the experiments presented in Figure 5a.
D = dead; – = not done.

initiated with CB-derived CD34$^+$ cells. The cells were cultured in Teflon culture bags supplemented with defined medium containing SCF, G-CSF and TPO [9]. The second protocol comprises an automated continuous perfusion culture device developed by Aastrom Biosciences [21]. In this system cultures are initiated with CB-derived mononuclear cells and expanded for 12 days in media supplemented with FBS, horse serum, PIXY321, FLT-3 ligand and erythropoietin [21]. The duration of both clinical applicative protocols is 12–14 days and in both protocols the cultures are supplemented with a mixture of early- and late-acting cytokines. These conditions accelerate cell proliferation and differentiation, resulting in increased expansion of TNC and further maturation of myeloid precursors. Clinical studies performed using these protocols demonstrated that clinical-scale expansion of CB is feasible, and that administration of these cells is well tolerated [19–21].

Our current study presents an applicable protocol for clinical-scale *ex vivo* expansion of CB-derived CD133$^+$ progenitor cells in the presence of early-acting cytokines and the copper chelator TEPA. As opposed to the previously reported expansion protocols, it appears that the present culture conditions enable better expansion of less differentiated cell subsets.

Due to regulatory and proprietary concerns, we utilized the Miltenyi Biotec's CliniMACS apparatus [22] and the anti-CD133 CliniMACS reagent, both of them clinically approved, replacing the research-grade MiniMACS CD34 progenitor cell isolation kit. The CD133 antigen is a novel marker for stem/progenitor cells. Phenotypic and functional studies indicated that the CD133-enriched population could serve as an alternative to CD34$^+$ cell selection and engraftment purposes [23–25]. Furthermore, CD133$^+$ selected cells have already been used in clinical transplantation settings without any safety impairment [26]. In our study, we demonstrated similar yield and purity, crucial parameters for successful transplantation [22], using the CliniMACS instrument in combination with either the anti-CD34 or anti-CD133 reagent.

The duration of most expansion protocols for clinical application is between 10 and 14 days [19–21]. We evaluated the feasibility of the chelator technology to extend the expansion in order to maximize the number of early and late progenitor cells. To this end, we compared 2 vs. 3-week cultures and found that the latter was superior with respect to the yields of TNC, CD34$^+$ and

$CD34^+CD38^-$ cells (Figure 2). Although the technology enables longer expansion [16], it is not desirable in a clinical setting. Following a 3-week large-scale clinical grade expansion, the yield of early progenitor ($CD34^+CD38^-$) cells was higher in cultures initiated with $CD133^+$ cells ($12 \pm 3.6 \times 10^5$) than in cultures initiated with a similar number of $CD34^+$ cells ($5.6 \pm 1.3 \times 10^5$).

Using optimized clinically applicable conditions, e.g. CD133 cell enrichment, CliniMACS separation device and culture bags, we evaluated the procedure on 22 frozen CB units, 18 of which were obtained from accredited CB banks. In spite of the high variability among CB units [27], we demonstrated the efficacy of the procedure to expand early and late progenitor cells. In these experiments the median output value of $CD34^+$ cells increased by 89-fold, $CD34^+CD38^-$ increased by 30-fold and CFUc by 172-fold over the input values.

We then determined the expansion efficacy with regard to the number of cells of different subtypes available for transplantation. Since in clinical trials expanded cells will be given in addition to non-manipulated cells of the same unit, the efficacy depends on the portion of the unit taken for expansion. We calculated the efficacy based on the expanding 20% portion of the unit. The results show (Table 2) that the major contribution of the expanded product is in the numbers of early progenitor cells ($CD34^+CD38^-$) as well as that of late progenitor cells ($CD34^+$, CFUc). Numbers of TNC in the expanded graft were comparable to those in the non-expanded unit.

Finally, we demonstrated that our clinical-scale expanded cells successfully engrafted SCID mice. In eight consecutive experiments, the percentage of engrafted human progenitors as well as that of myeloid and lymphoid cells was significantly superior in mice transplanted with expanded cells to that in mice transplanted with non-expanded cells.

In summary, we describe a 3-week large-scale expansion procedure, utilizing a combination of copper chelator (TEPA) with early-acting cytokines (SCF, TPO, IL-6 and FLT-3 ligand), a clinically approved separation device and clinical grade reagents. Extensive research and development work demonstrated that FCS is suitable for the expansion process. As there is no regulation that prohibits the use of FCS in clinical trials in the USA, the use of a specific lot of FCS and its certificates of analysis were submitted to the FDA as part of Gamida Cell's investigational new drug (IND) application. The expansion procedure, evaluated using CB units derived from accredited CB banks, was demonstrated to produce a high yield of early progenitors with increased SCID engraftment potential. This novel strategy for *ex vivo* expansion of CB progenitors is currently under study in a phase 1 clinical trial.

Acknowledgements

We would like to thank Dr Pablo Rubinstein, director of the National Cord Blood Program (USA) at the New York Blood Center (New York, NY), and Dr Joanne Kurtzberg, Director of Pediatric Bone Marrow and Stem Cell Transplant Program, Duke University Medical Center (Durham, NC), for kindly providing CB units for this study.

References

1 Kurtzberg J, Laughlin M, Graham ML *et al*. Placental blood as a source of hematopoietic stem cells for transplantation into unrelated recipients. *N Engl J Med* 1996;335:157–66.

2 Ballen K, Broxmeyer HE, McCullough J *et al*. Current status of cord blood banking and transplantation in the United States and Europe. *Biol Blood Marrow Transplant* 2001;7:635–45.

3 Risdon G, Gaddy J, Broxmeyer HE. Allogeneic responses of human umbilical cord blood. *Blood Cells* 1994;20:566–70.

4 Barker JN, Wagner JE. Umbilical cord blood transplantation: current state of the art. *Curr Opin Oncol* 2002;14:160–4.

5 Laughlin MJ, Barker J, Bambach B *et al*. Hematopoietic engraftment and survival in adult recipients of umbilical-cord blood from unrelated donors. *N Engl J Med* 2001;344:1815–22.

6 Broxmeyer HE, Hangoc G, Cooper S *et al*. Growth characteristics and expansion of human umbilical cord blood and estimation of its potential for transplantation in adults. *Proc Natl Acad Sci USA* 1992;89:4109–13.

7 McNiece I, Jones R, Cagnoni P *et al*. *Ex vivo* expansion of hematopoietic progenitor cells: preliminary results in breast cancer. *Hematol Cell Ther* 1999;41:82–6.

8 Koller MR, Manchel I, Maher RJ *et al*. Clinical-scale human umbilical cord blood cell expansion in a novel automated perfusion culture system. *Bone Marrow Transplant* 1998;21:653–63.

9 McNiece I, Kudegov D, Kerzic P *et al*. Increased expansion and differentiation of cord blood products using a two-step expansion culture. *Exp Hematol* 2000;28:1181–6.

10 Bruno S, Gammaitoni L, Gunetti M *et al*. Different growth factor requirements for the *ex vivo* amplification of transplantable human cord blood cells in a NOD/SCID mouse model. *J Biol Regul Homeost Agents* 2001;15:38–48.

11 Piacibello W, Gammaitoni L, Bruno S *et al*. Negative influence of IL3 on the expansion of human cord blood in vivo long-term repopulating stem cells. *J Hematother Stem Cell Res* 2000;9:945–56.

12 Henon P, Sovalat H, Becker M *et al*. Primordial role of CD34+ 38- cells in early and late trilineage haemopoietic engraftment after autologous blood cell transplantation. *Br J Haematol* 1998;103:568–81.

13 Henon PH, Sovalat H, Bourderont D. Importance of $CD34^+$ cell subsets in autologous PBSC transplantation: the mulhouse experience using $CD34^+$. *J Biol Regul Homeost Agents* 2001;15:62–7.

14 Ishikawa F, Livingston AG, Minamiguchi H *et al*. Human cord blood long-term engrafting cells are $CD34^+CD38^-$. *Leukemia* 2003;17:960–4.

15 Peled T, Landau E, Prus E *et al*. Cellular copper content modulates differentiation and self-renewal in cultures of cord blood-derived $CD34^+$ cells. *Br J Haematol* 2002;116:655–61.

16 Peled T, Landau E, Mandel J *et al*. Linear polyamine copper chelator tetraethylenepentamine augments long-term *ex vivo* expansion of cord-blood-derived CD34(+) cells and increases their engraftment potential in NOD/SCID mice. *Exp Hematol* 2004;32:547–55.

17 Rubinstein P, Dobrila L, Rosenfield RE *et al*. Processing and cryopreservation of placental/umbilical cord blood for unrelated bone marrow reconstitution. *Proc Natl Acad Sci USA* 1995;92:10119–22.

18 Lewis ID. Clinical and experimental use of umbilical cord blood. *Intern Med J* 2002;32:601–9.

19 Astori G, Malangone W, Adami V *et al*. A novel protocol that allows short-term stem cell expansion of both committed and pluripotent hematopoietic progenitor cells suitable for clinical use. *Blood Cells Mol Dis* 2001;27:715–24, 725–7.

20 Shpall EJ, Quinones R, Giller R *et al*. Transplantation of *ex vivo* expanded cord blood. *Biol Blood Marrow Transplant* 2002;8:368–76.

21 Jaroscak J, Goltry K, Smith A *et al*. Augmentation of umbilical cord blood (UCB) transplantation with *ex vivo*-expanded UCB cells: results of a phase 1 trial using the AastromReplicell System. *Blood* 2003;101:5061–7.

22 McNiece IK, Stoney GB, Keren BP *et al*. $CD34^+$ cell selection from frozen cord blood products using the Isolex 300i and CliniMACS CD34 selection device. *J Hematother* 1998;7:457–61.

23 de Wynter EA, Buck D, Hart C *et al*. $CD34^+CD133^+$ cells isolated from cord blood are highly enriched in long-term culture-initiating cells, NOD/SCID-repopulating cells and dendritic cell progenitors. *Stem Cells* 1998;16:387–96.

24 Yin AH, Miraglia S, Zanjani ED *et al*. CD133, a novel marker for human hematopoietic stem and progenitor cells. *Blood* 1997;90:5002–12.

25 Pasino M, Lanza T, Marotta F *et al*. Flow cytometric and functional characterization of $CD133^+$ cells from human umbilical cord blood. *Br J Haematol* 2000;108:793–800.

26 Koehl U, Esser R, Zimmermann S *et al*. Clinical scale purification of progenitor cells by $CD133^+$ selection: from laboratory experience to the first transplantation of a pediatric patient with relapsed leukemia. *Blood* 2001;98:851a.

27 Encabo A, Mateu E, Carbonell-Uberos F *et al*. $CD34^+CD38^-$ is a good predictive marker of cloning ability and expansion potential of $CD34^+$ cord blood cells. *Transfusion* 2003;43:383–9.

Available online at www.sciencedirect.com
SCIENCE DIRECT
International Journal of Pharmaceutics 312 (2006) 15–23
INTERNATIONAL JOURNAL OF PHARMACEUTICS
www.elsevier.com/locate/ijpharm

Cutaneous gene expression of plasmid DNA in excised human skin following delivery via microchannels created by radio frequency ablation

James Birchall [a,*], Sion Coulman [a], Alexander Anstey [b], Chris Gateley [b], Helen Sweetland [c], Amikam Gershonowitz [d], Lewis Neville [d], Galit Levin [d]

[a] *Gene Delivery Research Group, Welsh School of Pharmacy, Cardiff University, Cardiff CF10 3XF, UK*
[b] *Gwent Healthcare NHS Trust, Royal Gwent Hospital, Cardiff Road, Newport, South Wales NP20 2UB, UK*
[c] *School of Medicine, Cardiff University & University Hospital of Wales, Heath Park, Cardiff CF14 4XN, UK*
[d] *TransPharma Medical Ltd., 2 Yodfat Street, Northern Industrial Zone, Lod 71291, Israel*

Received 8 September 2005; received in revised form 5 December 2005; accepted 5 December 2005
Available online 15 February 2006

Abstract

The skin is a valuable organ for the development and exploitation of gene medicines. Delivering genes to skin is restricted however by the physico-chemical properties of DNA and the stratum corneum (SC) barrier. In this study, we demonstrate the utility of an innovative technology that creates transient microconduits in human skin, allowing DNA delivery and resultant gene expression within the epidermis and dermis layers. The radio frequency (RF)-generated microchannels were of sufficient morphology and depth to permit the epidermal delivery of 100 nm diameter nanoparticles. Model fluorescent nanoparticles were used to confirm the capacity of the channels for augmenting diffusion of macromolecules through the SC. An ex vivo human organ culture model was used to establish the gene expression efficiency of a β-galactosidase reporter plasmid DNA applied to ViaDerm™ treated skin. Skin treated with ViaDerm™ using 50 μm electrode arrays promoted intense levels of gene expression in the viable epidermis. The intensity and extent of gene expression was superior when ViaDerm™ was used following a prior surface application of the DNA formulation. In conclusion, the RF-microchannel generator (ViaDerm™) creates microchannels amenable for delivery of nanoparticles and gene therapy vectors to the viable region of skin.
© 2006 Elsevier B.V. All rights reserved.

Keywords: Radiofrequency-microchannels; Radiofrequency ablation; Plasmid DNA; Skin; Gene therapy

1. Introduction

The ability to target genes directly to the skin provides a strategy for the treatment of certain localised heritable genetic skin diseases (Greenhalgh et al., 1994; Ehrlich et al., 1995), various forms of malignancies (Hart and Vile, 1994) and cutaneous wounds (Byrnes et al., 2004; Lee et al., 2004). Furthermore, 'genetic immunisation' via the skin provides a method of vaccinating patients by introducing DNA into cells, leading to expression of foreign antigen and the subsequent induction of an immune response (Fynan et al., 1993; Raz et al., 1994; Shi et al., 1999). Intra-cutaneous DNA vaccines utilise the highly competent antigen-presenting capabilities of epidermal Langerhans cells in eliciting a systemic immune response, leading to more proficient and cost-efficient vaccination compared with conventional vaccines (Lin et al., 2000). As the immune response is induced by a single gene rather than an entire organism, this approach is also considered to be safer than using live attenuated vaccines (Durrant, 1997).

The challenge of delivering genes to the viable region of skin is a product of the physico-chemical properties of the large hydrophilic DNA molecule, with or without an additional carrier vehicle, and the significant barrier properties of cutaneous tissue. Superficially the skin is regarded as a valuable organ for the development and clinical administration of gene medicines as it is readily accessed, well characterized and easily monitored (Hengge et al., 1996). However, if cutaneous gene therapy is to translate from the laboratory to clinical practice then approaches

* Corresponding author. Tel.: +44 29 20875815; fax: +44 29 20874149.
E-mail addresses: birchalljc@cardiff.ac.uk, birchalljc@cf.ac.uk (J. Birchall).

0378-5173/$ – see front matter © 2006 Elsevier B.V. All rights reserved.
doi:10.1016/j.ijpharm.2005.12.036

must be developed to efficiently and reproducibly transport the delivered transgene to the target cell population. The primary role of the skin however, is to serve as a physical barrier to the invasion of foreign material. In humans, the epidermis, which constitutes the uppermost layer of the skin, is approximately 50–150 μm thick with the non-viable SC layer, approximately 15–20 μm in thickness, representing the principal barrier to penetration and permeation of substances through the skin (Birchall, 2004). Therefore, in order to deliver therapeutic compounds to the epidermis, the underlying dermis or the systemic circulation, delivery strategies must overcome the physical barrier created by the nature of the tightly packed dead cells of the SC. Traditional transdermal formulation strategies aim to enhance the delivery of small therapeutic molecules, less than 500 molecular weight, across the SC by paracellular, transcellular or intracellular routes. However, in order to deliver DNA and proteins, more innovative and radical methods of drug delivery are required. To date, the physico-chemical methods employed to promote therapeutic drug or gene transfer to the skin include the use of direct DNA injection (Hengge et al., 1995, 1996; Chesnoy and Huang, 2002) chemical enhancers (Barry, 1987; Pillai and Panchagnula, 2003), iontophoresis (Green, 1996; Préat and Dujardin, 2001), biolistic particle bombardment (Cheng et al., 1993; Heiser, 1994; Udvardi et al., 1999), electroporation (Prausnitz et al., 1993; Dujardin et al., 2001; Zhang et al., 2002), sonophoresis (Lavon and Kost, 2004), laser ablation (Nelson et al., 1991), microseeding (Eriksson et al., 1998), skin tattooing (Bins et al., 2005) and the recent use of microfabricated microneedles (Henry et al., 1998; McAllister et al., 2000, 2003; Chabri et al., 2004).

Recently, we have developed an innovative technology, coined ViaDerm™, which creates transient microchannels across the SC thereby enabling a more direct and controlled passage of molecules to the underlying viable epidermis and dermis. ViaDerm™ has an intimately spaced array of microelectrodes which are placed against the surface of skin to individually conduct an applied alternating electrical current at radio frequency (RF). Application of this rf electrical current (100–500 kHz) to the tissue elicits a vibration in motion of ions with localized frictional heating of tissue resulting in a rapid obliteration of cells close to the energy source. The intimate and orderly spacing of the microelectrodes therefore drives the orderly generation of functional microchannels. The passage of the electric current through cells in the upper skin strata generates localised ionic vibrations, heating, evaporation and cell ablation to create microchannels.

Previously, we have reported that RF-generated microchannels reside in the epidermis and dermis and are amenable to the effective transdermal delivery of small molecules (Sintov et al., 2003) and proteins (Levin et al., 2005) into the systemic circulation. Furthermore, the microchannels did not impinge on underlying blood vessels and nerve endings thus minimizing skin trauma, bleeding and neural sensations (Sintov et al., 2003). Clearly, the use of electricity for augmenting transcutaneous drug delivery also applies to some of the other aforementioned physical delivery methods, e.g. iontophoresis, electroporation. Unlike these examples however, the technology described in this study leads to the creation of an orderly array of defined microchannels by cell ablation at specific locations (Levin et al., 2005).

The purpose of the present study using the ViaDerm™ technology was two-fold. Firstly, to extensively characterize ViaDerm™-generated microchannels within ex vivo human skin. Secondly, to assess the feasibility of ViaDerm™ in supporting the transdermal delivery of a mammalian expression plasmid with subsequent reporter expression within the target region of the skin.

2. Materials and methods

2.1. Materials

The 7.2 kb pCMVβ plasmid construct containing the β-galactosidase reporter gene and the pEGFP-N1 (4.7 kb) plasmid containing the green fluorescent protein reporter gene were propagated and purified as detailed previously (Birchall et al., 1999). Fluorescein isothiocyante (FITC)-labelled polystyrene nanospheres (L-1280) were obtained from Sigma Chemicals (Poole, UK). OCT embedding medium and Histobond® microscope slides were from RA Lamb Ltd. (Eastbourne, UK). One percent aqueous eosin solution and Harris' haematoxylin solution were from BDH Laboratory Supplies (Dorset, UK). One percent aqueous toludine blue solution was from TAAB Laboratories Equipment Ltd. (Berkshire, UK). Cell culture plastics were obtained from Corning-Costar (High Wycombe, UK). MEM (EAGLES) 25 mM HEPES, Dulbecco's Modified Eagle's Medium (DMEM 25 mM HEPES), foetal bovine serum, penicillin-streptomycin solution and trypsin-EDTA solution 1× were obtained from In-Vitrogen Corporation, Paisley, UK. All other reagents were of analytical grade and purchased from Fisher Scientific UK (Loughborough, UK).

2.2. ViaDerm™ treatment of human skin

Full-thickness human breast skin was obtained from mastectomy or breast reduction with ethical committee approval and informed patient consent. Skin was collected from a variety of donors ranging from 45 to 65 years of age. Matched samples were used for each individual experiment. To maintain structural and cellular viability the skin tissue was transported on ice in MEM (EAGLES) 25 mM HEPES growth media and used within 3 h of excision. All excess adipose tissue was removed by blunt dissection.

The components and operating conditions of the RF-microchannel generator (ViaDerm™, TransPharma Medical, Israel) have been described previously (Sintov et al., 2003). Briefly the ViaDerm™ device comprises an electronic controller unit and a disposable array of stainless steel electrodes (100 or 50 μm in length) at a density of 100 electrodes/cm^2 in a total area of 1.4 cm^2. Thus, application of an RF-activated array (1.2 cm × 1.2 cm) resulted in the generation of 144 microchannels over the 1.4 cm^2 area. Studies were performed using the electrodes at device parameter settings resulting in one, two or five bursts of 700 μs burst length at an applied voltage of 290 or 330 V and an RF frequency of 100 kHz. Control experiments

involved equivalent pressure application of the ViaDerm™ device to human skin in the absence of the RF-generating power source.

2.3. Electron microscopy of full thickness skin

ViaDerm™ treated (100 μm electrode, density of 200 microchannels/cm^2) full thickness human skin samples were fixed with 2.5% glutaraldehyde in 0.1 M sodium cacodylate buffer (pH 7.4) for 60 min at room temperature and washed for 10 min (2 × 5 min) in the same buffer. The samples were post-fixed in 1% osmium tetroxide in 0.1 M cacodylate buffer for 1 h at 4 °C and then dehydrated with a graded series of ethanol concentrations as follows (70% for 10 min at 4 °C, 100% for 10 min at 4 °C, 100% for 10 min at 4 °C, 100% for 10 min at 4 °C). The samples were subsequently transferred to a critical point drier (Samdri 780, Maryland, USA) for 12 h. The samples were mounted on metal stubs and gold sputter coated, using an Edward sputter coater, prior to examination in a Philips XL-20 scanning electron microscope.

2.4. Electron microscopy of epidermal sheets

Following ViaDerm™ treatment (100 μm electrode) of full thickness human skin, epidermal sheets were isolated by a heat separation technique (Christophers and Kligman, 1963). The resulting epidermal sheets were placed in cold distilled water and then gently lifted from the water onto a metal stub. The mounted epidermal sheet was allowed to dry, gold sputter coated and the samples were examined using a scanning electron microscope (Philips Xl-200 SEM) (Electron Microscopy Unit, Cardiff School of Biosciences, Cardiff University, Cardiff, UK).

2.5. Visualisation of microchannels en face

ViaDerm™ treated (100 μm electrode) skin was incubated in media (MEM (EAGLES), 25 mM HEPES) for 24 h at 37 °C. Following two washes in phosphate buffered saline (PBS) the skin was fixed in 0.5% gluataraldehyde for 2 h on ice. Methylene blue staining involved a 5 min surface application of five drops of methylene blue solution on the ViaDerm™ treated skin followed by removal of excessive stain with a brief PBS rinse and an ethanol surface swab. Tissue stained with methylene blue was visualised using an Olympus BX50 microscope and a Schott KL1500 electronic light source.

2.6. Histology of ViaDerm™ treated tissue

Skin was treated with ViaDerm™ using either 50 or 100 μm electrode arrays. Following treatment the skin was washed with PBS and fixed for 4 h in 0.5% glutaraldehyde on ice. Fixed tissue was embedded in OCT and sectioned using a Leica CM3050S Cryostat. Sections were collected on Histobond® microscope slides and stained with either—(i) eosin: 1% aqueous eosin solution for 5 s, (ii) haematoxylin and eosin (H&E): Harris' haematoxylin solution for 5 min followed by 1% aqueous eosin solution for 5 s or (iii) toludine blue: 1% aqueous toludine blue solution for 5 min.

2.7. Diffusion of fluorescent nanoparticles through RF-microchannels™

Non-treated and ViaDerm™ treated (50 and 100 μm electrodes) full thickness human skin was heat separated in order to isolate the epidermal membranes which were subsequently mounted between the donor and receptor compartments of static Franz-type glass diffusion cells. The receptor phase of each cell was filled with phosphate buffered saline (PBS; pH 7.4). The receptor arm was sealed with a foil cap and the donor chamber occluded with NESCO® film to prevent sample evaporation. The cells were placed on a stirring plate in a water-bath maintained at 37 °C, to provide continuous agitation and a skin surface temperature of 32 °C. Prior to addition of the test formulations to the donor chamber, cells were allowed to equilibrate for at least 30 min and the integrity of epidermal membranes was visually inspected.

Fluorescently (FITC) labelled polystyrene nanospheres (100 nm diameter) were used as a size-representative model for the delivery of non-viral gene therapy vectors (Chabri et al., 2004). A volume of 500 μl of a 50 μl/ml dilution of the fluorescent nanosphere stock suspension, concentration 4.57^{10} μl^{-1}, was applied to the surface of ViaDerm™ treated epidermal membranes. Control cells consisted of untreated epidermal membrane with either the nanosphere suspension or PBS applied to the donor phase. At each timepoint 200 μl samples were removed from the receptor arm at regular intervals and replaced with PBS. On completion of the experiment, samples were analysed using a fluorescence spectrophotometer (BMG Fluostar, Aylesbury, UK) with excitation and emission wavelengths set at 485 and 520 nm, respectively. A calibration curve was performed using standard dilutions of the suspension of fluorescent nanoparticles.

2.8. Localised delivery of fluorescent nanoparticles in ViaDerm™ treated human skin

ViaDerm™ treated (100 μm electrode) skin was placed in a six-well cell culture plate and maintained in 1.5 ml MEM (EAGLES) 25 mM HEPES. Fifty microliters of a concentrated (4.57^{10} μl^{-1}) stock of fluorescent red polystyrene nanospheres was applied to the treated skin surface and the sample incubated for 6 h at 37 °C. At 6 h a further 2 ml of media was added the submerged skin was incubated for a further 18 h. Following two washes in PBS the skin was fixed in 0.5% gluataraldehyde for 1 h on ice and embedded in OCT medium prior to tissue sectioning using a Leica CM3050S Cryostat. Sections were either visualised unstained under blue fluorescence or stained with haematoxylin and eosin (H&E) (Olympus BX50 microscope).

2.9. Gene expression in ViaDerm™ treated human skin

Human skin was pre-treated with the ViaDerm™ device, 50 μm electrode arrays, prior to the topical application of 50 μl

of pCMVβ plasmid DNA solution (1 mg/ml) to the skin surface. This area of skin was thereafter post-treated with the ViaDerm™ device at the identical skin location as the first ViaDerm™ application. The treated human skin was placed on lens tissue supported by metal gauze in a six-well cell culture plate containing 7.5 ml media (DMEM 25 mM HEPES supplemented with 5% foetal bovine serum and 1% penicillin/streptomycin) per well. This organ culture maintained the skin at an air–liquid interface for 24 h at 37 °C. Following one wash in PBS/$MgCl_2$ (30 min) the tissue was fixed for 2 h in 2% glutaraldehyde/$MgCl_2$ at 4 °C. Subsequently the tissue was rinsed in a series of PBS/$MgCl_2$ solutions for 2, 3 h and 30 min. The tissue was stained for β-galactosidase expression over 20 h using X-Gal staining solution [X-Gal (5% (v/v) of a 40 mg/ml solution in dimethylformamide), potassium ferricyanide (0.84% (v/v) of a 0.6 M solution), potassium ferrocyanide (0.84% (v/v) of a 0.6 M solution), magnesium chloride (0.2% (v/v) of a 1 M solution), Tris–HCl buffer pH 8.5 (50% (v/v) of a 0.2 M solution), deionised water to 100%]. Tissue was visualised en face using either a Zeiss Stemi 2000C Stereomicroscope with a 2.0× attachment or an Olympus BX50 microscope, both with a Schott KL1500 electronic light source.

For sectioning, the samples were embedded in OCT and sectioned using a Leica CM3050S Cryostat. Tissue sections were collected onto Histobond® microscope slides and stained with H&E.

3. Results and discussion

The surface morphology of the microchannels created in full-thickness breast skin following application of ViaDerm™ was initially investigated using scanning electron microscopy (SEM). Fig. 1 shows a channel created using the 100 μm electrode appearing as a deep invagination into the surface of the skin tissue. Further SEM characterisation of the heat-separated epidermal membrane, comprising of SC and viable epidermis, treated with ViaDerm™ is shown in Fig. 2. These data show that the RF-microchannels either totally or partially penetrate the epidermal membrane. Although the depth of the microchannels was variable, possibly due to variation in thickness of the separated epidermal sheet (Eriksson et al., 1998), the diameter of the microchannels (∼50 μm), was reproducible and consistent

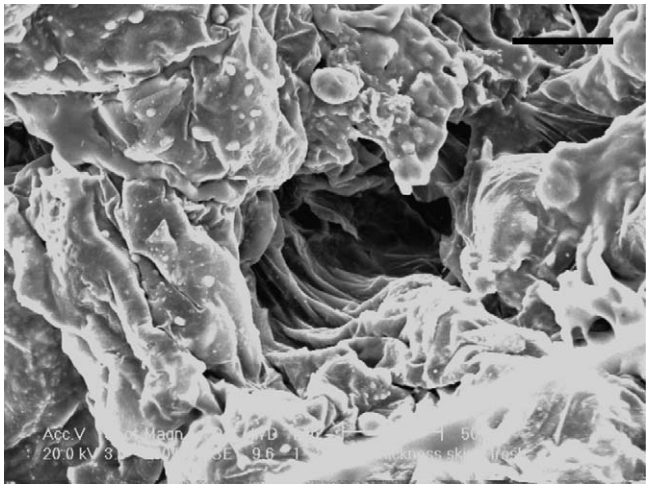

Fig. 1. Scanning electron microscopy of an RF-microchannel in intact human skin. Bar = 50 μm.

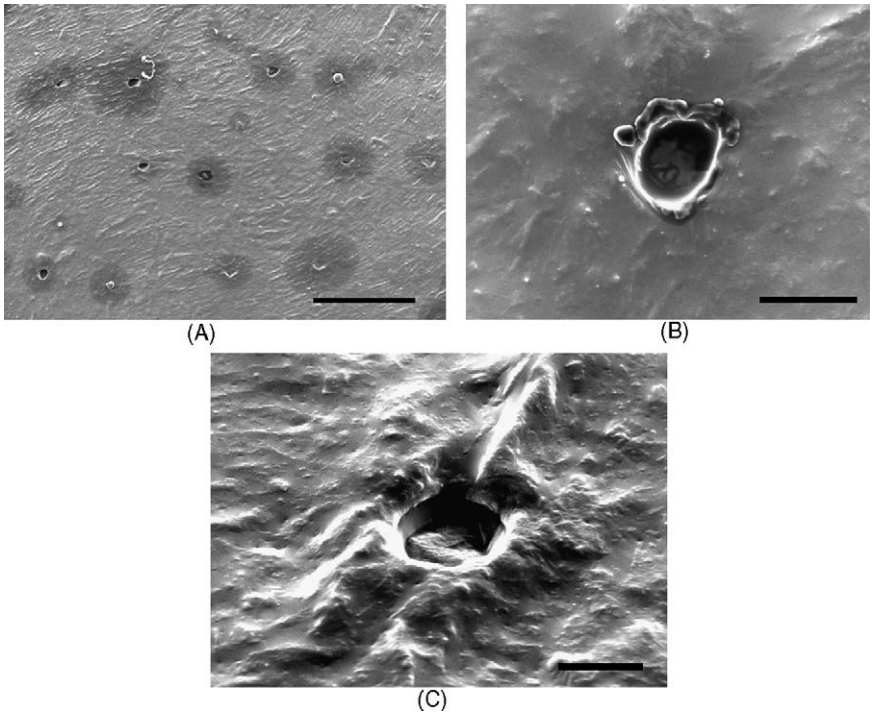

Fig. 2. Scanning electron microscopy of RF-microchannels in heat-separated epidermal membrane. (A) Low magnification showing distribution pattern of channels following two applications of ViaDerm™, bar = 1 mm; (B) high magnification showing dimensions of microchannels, bar = 100 μm; (C) visualisation of microchannel depth using an angled electron beam, bar = 50 μm.

with the microchannel dimensions observed in full-thickness skin (Fig. 1). More accurate determinations of the depth and structural morphology of the microchannels are provided in the histological tissue sections.

The quantity and distribution pattern of microchannels created in ViaDerm™ treated skin is shown in Fig. 3. The distribution pattern of the channels can be visualised through their ability to uptake and retain a low molecular weight marker, i.e. methylene blue (Fig. 3A). At higher magnification the dye appears to diffuse to the periphery of the microchannel (Fig. 3B). The application and considerable potential of this technology for the cutaneous delivery of low molecular weight medicaments has previously been reported (Sintov et al., 2003).

The structural dimension of microchannels created in human breast skin following application of ViaDerm™ was assessed using transverse sectioning. The photomicrographs are representative of the entire population of channels observed. Fig. 4 illustrates the dimensions of RF-microchannels that are created in human breast skin following application of ViaDerm™ with 50 μm electrode arrays at different parameter settings. In the majority of processed skin sections ($n > 100$), the channels are approximately 50 μm in length and 30–50 μm at their widest aperture, extending only to the viable epidermis.

In line with the data depicted in Fig. 4, doubling the electrode length to 100 μm resulted in further penetration through the human epidermis and impingement into the superficial dermal layer (Fig. 5). Representative sections ($n > 100$) show that microchannels were approximately 100 μm in length and 30–50 μm at their widest aperture. Consequently, using isolated human breast skin, the 100 μm electrode arrays can create a microchannel of sufficient length to permit specific cell targeting for localised cutaneous gene therapy applications (Greenhalgh et al., 1994; Sawamura et al., 2002) and genetic vaccination (Dean et al., 2003). Clearly, the exploitation of different electrode lengths for creating microchannels of varying depths underscores the flexibility of ViaDerm™ for permitting controlled delivery of therapeutics to different target cell populations.

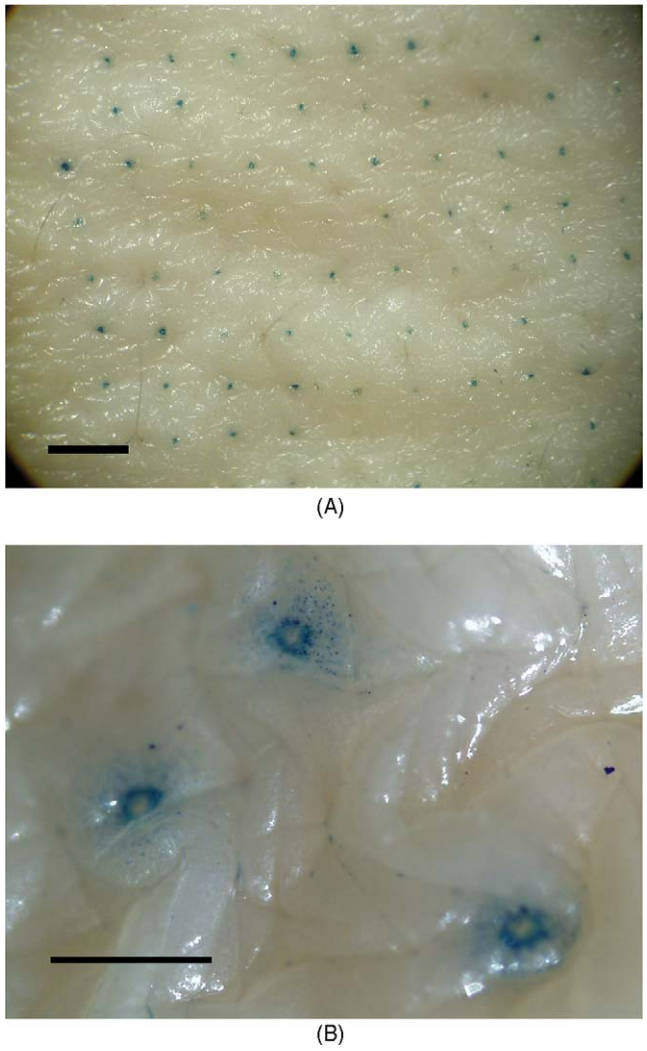

Fig. 3. Light microscopy of methylene blue stained skin following ViaDerm™ treatment. (A) Low magnification, bar = 1 mm; (B) high magnification, original magnification = 40×, bar = 500 μm.

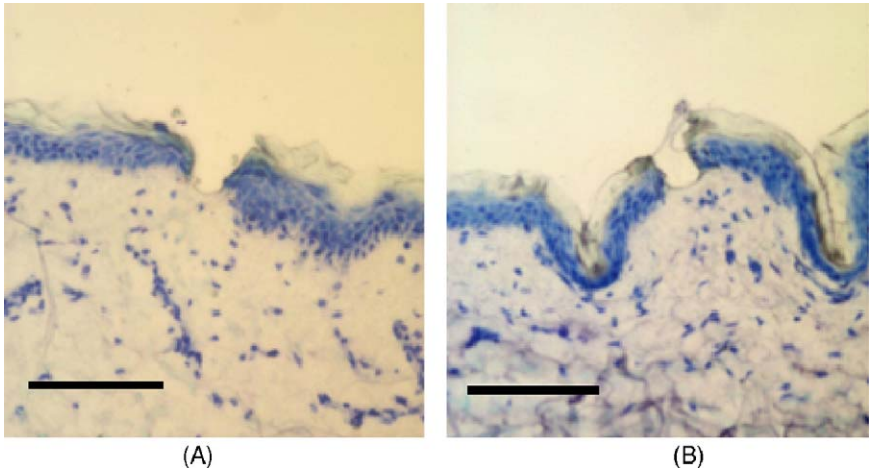

Fig. 4. Light microscopy of human breast skin treated with ViaDerm™ 50 μm electrode arrays. (A) One burst of 700 μs burst length, toludine blue stained; (B) two bursts of 700 μs burst length, toludine blue stained. Original magnification = 200×, bar = 100 μm.

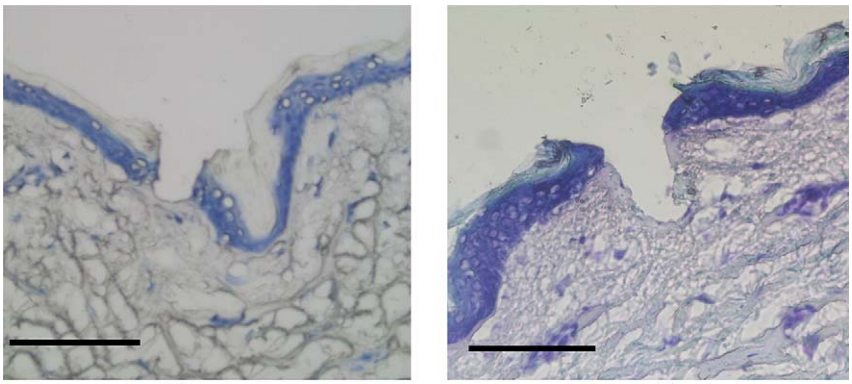

Fig. 5. Light microscopy of human breast skin treated with ViaDerm™ 100 μm electrode arrays. (A) One burst of 700 μs burst length, toludine blue stained; (B) three bursts of 700 μs burst length, toludine blue stained. Original magnification = 200×, bar = 100 μm.

Previously, from ex vivo studies employing a permeation methodology, we have demonstrated the total inability of the ViaDerm™ device to generate microchannels when disconnected from a power source as evidenced by both negative visualization and lack of drug permeation (Sintov et al., 2003). Such findings were totally substantiated in follow up in vivo studies whereby application of drugs at a ViaDerm™ treated skin site in the absence of a power supply resulted in no transdermal drug delivery as compared to robust drug deliveries with a functional power supply (Sintov et al., 2003; Levin et al., 2005). In our histological studies, and subsequent gene delivery experiments, we confirm the previously published ex vivo and in vivo observations (Sintov et al., 2003; Levin et al., 2005) of the total absence of microchannels on the surface skin following the placement of the ViaDerm™ device disconnected from a functional power source.

Following confirmation of the ability of ViaDerm™ to create microchannels in human skin, further experiments were

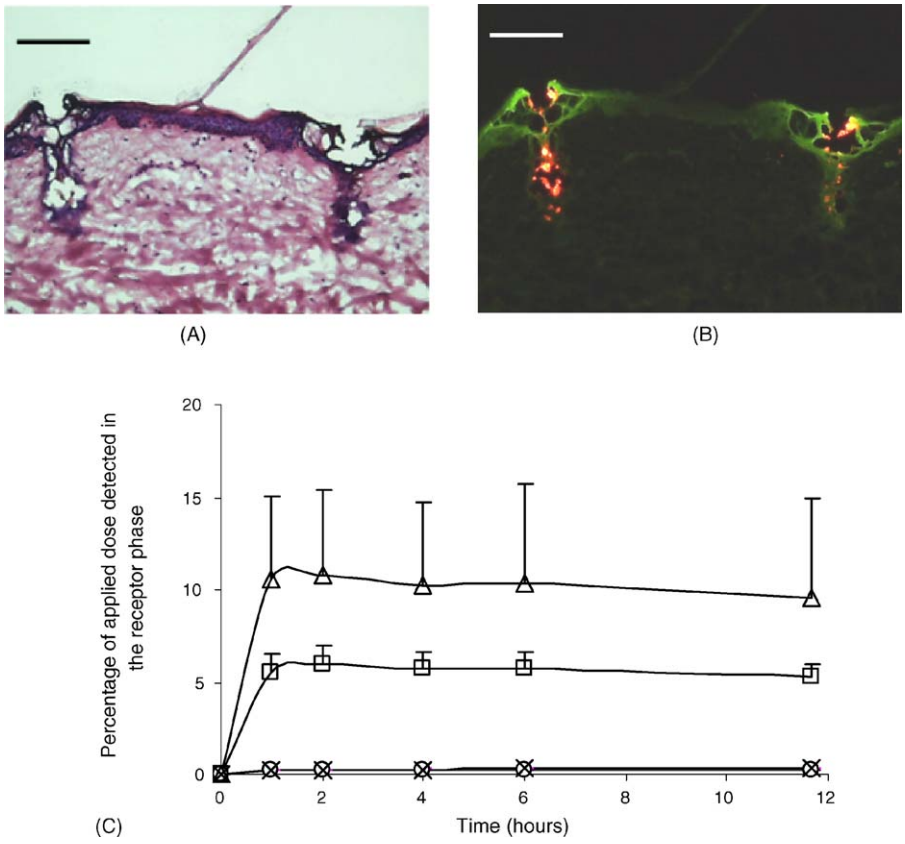

Fig. 6. Light (A) and fluorescent (B) photomicrographs of RF-microchannels containing fluorescent nanoparticles. Original magnification = 100×, bar = 100 μm; (C) diffusion of fluorescent nanoparticles through ViaDerm™ treated epidermal membranes. Data presented as percentage of topical nanoparticle dose detected in the receptor phase of Franz cells over a 12 h period. (◯) Untreated skin—PBS donor phase, (×) Untreated skin—topical nanoparticles, (□) 50 μm array ViaDerm™ treated skin—topical nanoparticles, (△) 100 μm array ViaDerm™ treated skin—topical nanoparticles ($N = 3 \pm$ S.D.).

performed to demonstrate the capability of these microchannels to permit cutaneous delivery of macromolecules or nanoparticulates. To that end, 100 nm fluorescent nanoparticles were selected as an easily detectable and size-representative model nanoparticle delivery system. Indeed, we have previously reported their application as an experimental tool for lipid:polycation:pDNA (LPD) non-viral gene delivery particle studies (Chabri et al., 2004). Fig. 6 confirms that the RF-microchannels created in skin following application of ViaDerm™ are of sufficient dimensions to uptake, entrap and permit the diffusion of 100 nm fluorescent nanoparticles. The channels shown in Fig. 6A and B appear to be larger than those observed in Fig. 5, possibly due to changes in the tissue sample over the incubation period (24 h compared with 0 h). These micrographs imply that the RF-microchannels generated can be considered to be of appropriate dimensions for the cutaneous delivery of macromolecules and non-viral gene therapy vectors.

Fig. 6C shows the data from a Franz-type diffusion experiment designed to determine the transit of the 100 nm nanoparticles through ViaDerm™ treated and control epidermal

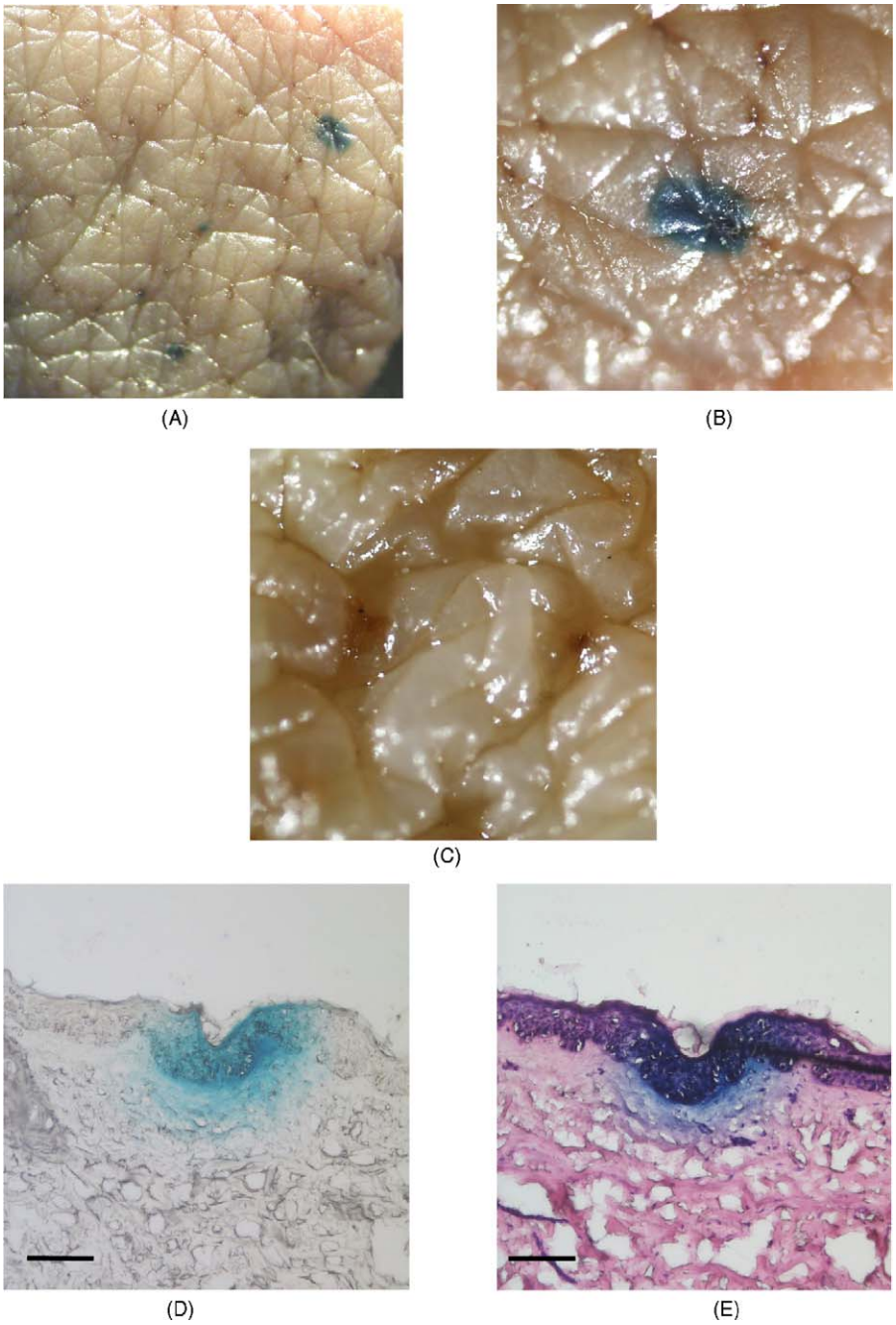

Fig. 7. Photomicrographs of ViaDerm™ treated human skin stained for β-galactosidase expression (50 μm arrays). (A) En face stereomicroscopy; (B) en face light microscopy, original magnification = 40×; (C) en face stereomicroscopy of ViaDerm™ treated human skin treated with the pEGFP-N1 plasmid; (D) unstained cryosection, original magnification = 100×; (E) H&E stained cryosection, original magnification = 100×, bar = 100 μm.

membranes. The non-treated epidermal membranes demonstrate the significant barrier function of this membrane to 100 nm nanoparticles, with undetectable penetration observed following 12 h incubation. Following ViaDerm™ treatment the epidermal membranes demonstrated a significantly enhanced ($p > 0.05$, one-way analysis of variance) permeability to the nanoparticles. Interestingly, whilst application of the 50 μm electrode arrays mediated reproducible permeation of the membrane to facilitate the diffusion of approximately 5% of the surface-applied nanoparticles, appliance of the 100 μm electrode arrays led to enhanced, though more variable, disruption of the membrane, as evidenced by an increase in mean penetration of the 100 nm nanoparticles. A possible mechanism for the more variable permeation of nanoparticles following ViaDerm™ treatment using the 100 μm electrodes is provided by the SEM images in Fig. 2. When the skin is treated with ViaDerm™ using the 50 μm electrodes and the epidermal membrane is subsequently removed by heat separation, it is not guaranteed that the entire membrane, i.e. stratum corneum and viable epidermis, will be punctured although disruption of the outer 15–30 μm will be sufficient to overcome the primary diffusive barrier, the stratum corneum. The observed increase in nanoparticle permeation therefore results from particle transit through the ablated SC channels and subsequent diffusion through the underlying epidermis. As shown in Fig. 2, skin treatment with ViaDerm™ using the 100 μm electrodes can occasionally effect complete penetration through the heat-separated epidermal sheet. Variability will therefore arise from the proportion of complete punctures, which in turn will depend on the thickness of the epidermal membrane following heat separation.

The delivery and expression of plasmid DNA in viable human skin via RF-microchannels has been initially demonstrated using the 50 μm electrode arrays. In these experiments the plasmid was used alone, i.e. without any non-viral carrier system, as numerous studies have shown the ability of naked DNA to undergo efficient expression in vivo (Hengge et al., 1995, 1996; Chesnoy and Huang, 2002). Fig. 7A and B clearly show the presence of intense blue staining, relating to substantial reporter gene expression with no expression evident in skin treated with ViaDerm™ and probed with the pEGFP-N1 plasmid (control; Fig. 7C). The expression is primarily localised in the viable epidermal cells surrounding the RF-microchannel (Fig. 7D and E). Interestingly, when a solution of DNA is applied topically to an area of ViaDerm™ treated skin the resulting epidermal gene expression is relatively low (data not shown). When the skin is treated with ViaDerm™ both prior to and following a topical application of the DNA solution the extent and level of gene expression is demonstrably greater. Consequently, it is reasonable to suggest that the ViaDerm™ might be used not only to create microchannels in the skin but also to enhance the intracellular uptake of the delivered DNA via a mechanism analogous to electroporation (Titomirov et al., 1991; Zhang et al., 2002).

In conclusion, we have demonstrated that the channels created in human breast skin following application of the RF-microchannel generator (ViaDerm™) are of appropriate dimensions, and enhance skin permeability to such a degree, as to permit the delivery of macromolecules and gene therapy vectors to the skin. The ViaDerm™ device represents a significant breakthrough in the challenge of delivering high molecular weight medicaments through the SC barrier. In particular, the ability to facilitate minimally invasive, targeted and controlled delivery of genes to the viable epidermis further supports the experimental and clinical evaluation of this novel transdermal drug delivery technology.

Acknowledgement

The authors acknowledge the support of Dr. Antony Hann, Cardiff School of Biosciences for assistance with electron microscopy.

References

Barry, B.W., 1987. Mode of action of penetration enhancers in human skin. J. Contr. Release 6, 85–97.

Bins, A.D., Jorritsma, A., Wolkers, M.C., Hung, C.F., Wu, T.C., Schumacher, T.N., Haanen, J.B., 2005. A rapid and potent DNA vaccination strategy defined by in vivo monitoring of antigen expression. Nat. Med. 11, 899–904.

Birchall, J.C., 2004. Cutaneous gene delivery. In: Amiji, M.M. (Ed.), Polymeric Gene Delivery: Principles and Applications. CRC Press, Florida, USA, pp. 573–588.

Birchall, J.C., Kellaway, I.W., Mills, S.N., 1999. Physico-chemical characterisation and transfection efficiency of cationic lipid–plasmid DNA gene delivery complexes. Int. J. Pharm. 183, 195–207.

Byrnes, C.K., Malone, R.W., Akhtar, N., Nass, P.H., Wetterwald, A., Cecchini, M.G., Duncan, M.D., Harmon, J.W., 2004. Electroporation enhances transfection efficiency in murine cutaneous wounds. Wound Rep. Reg. 12, 397–403.

Chabri, F., Bouris, K., Jones, T., Barrow, D., Hann, A., Allender, C., Brain, K., Birchall, J.C., 2004. Microfabricated silicon microneedles for nonviral cutaneous gene delivery. Br. J. Dermatol. 150, 869–878.

Cheng, L., Ziegelhoffer, P.R., Yang, N.-S., 1993. In vivo promoter activity and transgene expression in mammalian somatic tissues evaluated by using particle bombardment. Proc. Natl. Acad. Sci. U.S.A. 90, 4455–4459.

Chesnoy, S., Huang, L., 2002. Enhanced cutaneous gene delivery following intradermal injection of naked DNA in a high ionic strength solution. Mol. Ther. 5, 57–62.

Christophers, E., Kligman, A., 1963. Preparation of isolated sheets of human stratum corneum. Arch. Dermatol. 88, 702–704.

Dean, H.J., Fuller, D., Osorio, J.E., 2003. Powder and particle-mediated approacxhes for delivery of DNA and protein vaccines into the epidermis. Comp. Immun. Microbiol. Infect. Dis. 26, 373–388.

Dujardin, N., Van Def Smissen, P., Préat, V., 2001. Topical gene transfer into rat skin using electroporation. Pharm. Res. 18, 61–66.

Durrant, L., 1997. Cancer vaccines. Anticancer Drugs 8, 727–733.

Ehrlich, P., Sybert, V.P., Spencer, A., Stephens, K., 1995. A common keratin 5 gene mutation in Epidermolysis Bullosa Simplex–Weber–Cockayne. J. Invest. Dermatol. 104, 877–879.

Eriksson, E., Yao, F., Svensjö, T., Winkler, T., Slama, J., Macklin, M.D., Andree, C., McGregor, M., Hinshaw, V., Swain, W.F., 1998. In vivo gene transfer to skin and wound by microseeding. J. Surg. Res. 78, 85–91.

Fynan, E.F., Webster, R.G., Fuller, D.H., Haynes, J.R., Santoro, J.C., Robinson, H.L., 1993. DNA vaccines: protective immunization by parenteral, mucosal and gene innoculation. Proc. Natl. Acad. Sci. U.S.A. 90, 11478–11482.

Green, P.G., 1996. Iontophoretic delivery of peptide drugs. J. Contr. Release 41, 33–48.

Greenhalgh, D.A., Rothnagel, J.A., Roop, D.R., 1994. Epidermis: an attractive target tissue for gene therapy. J. Invest. Dermatol. 103, 63S–69S.

Hart, I.R., Vile, R.G., 1994. Targeted therapy for malignant melanoma. Curr. Opin. Oncol. 6, 221–225.

Heiser, W.C., 1994. Gene transfer into mammalian cells by particle bombardment. Anal. Biochem. 217, 185–196.

Hengge, U.R., Chan, E.F., Foster, R.A., Walker, P.S., Vogel, J.C., 1995. Cytokine gene expression in epidermis with biological effects following injection of naked DNA. Nat. Genet. 10, 161–166.

Hengge, U.R., Walker, P.S., Vogel, J.C., 1996. Expression of naked DNA in human, pig and mouse skin. J. Clin. Invest. 97, 2911–2916.

Henry, S., McAllister, D.V., Allen, M.G., Prausnitz, M.R., 1998. Microfabricated microneedles: a novel approach to transdermal drug delivery. J. Pharm. Sci. 87, 922–925.

Lavon, I., Kost, J., 2004. Ultrasound and transdermal drug delivery. Drug Discovery Today 9, 670–676.

Lee, P-Y., Chesnoy, S., Huang, L., 2004. Electroporatic delivery of TFG-β1 gene works synergistically with electric therapy to enhance diabetic wound healing in db/db mice. J. Invest. Dermatol. 123, 791–798.

Levin, G., Gershonowitz, A., Sacks, H., Stern, M., Sherman, A., Rudaev, S., Zivin, I., Phillip, M., 2005. Transdermal delivery of human growth hormone through RF-microchannels. Pharm. Res. 22, 550–555.

Lin, M.T.S., Pulkkinen, L., Uitto, J., 2000. Cutaneous gene therapy: principles and prospects. New Emerg. Therap. 18, 177–188.

McAllister, D.V., Allen, M.G., Prausnitz, M.R., 2000. Microfabricated microneedles for gene and drug delivery. Annu. Rev. Biomed. Eng. 2, 289–313.

McAllister, D.V., Wang, P.M., Davis, S.P., Park, J.H., Canatella, P.J., Allen, M.G., Prausnitz, M.R., 2003. Microfabricated needles for transdermal delivery of macromolecules and nanoparticles: fabrication methods and transport studies. Proc. Natl. Acad. Sci. U.S.A. 100, 13755–13760.

Nelson, J.S., McCullough, J.L., Glenn, T.C., Wright, W.H., Liaw, L.H., Jacques, S.L., 1991. Mid-infrared laser ablation of stratum corneum enhances in vitro percutaneous transport of drugs. J. Invest. Dermatol. 97, 874–879.

Pillai, O., Panchagnula, R., 2003. Transdermal delivery of insulin from ploxamer gel: ex vivo and in vivo skin permeation studies in rat using iontophoresis and chemical enhancers. J. Contr. Release 89, 127–140.

Prausnitz, M.R., Bose, V.G., Langer, R.S., Weaver, J.C., 1993. Electroporation of mammalian skin: a mechanism to enhance transdermal drug delivery. Proc. Natl. Acad. Sci. U.S.A. 90, 10504–10508.

Préat, V., Dujardin, N., 2001. Topical delivery of nucleic acids in the skin. Pharmascience 11, 57–68.

Raz, E., Carson, D.A., Parker, S.E., Parr, T.B., Abai, A.M., Aichinger, G., Gromkowski, S.H., Singh, M., Lew, D., Yankauckas, M.A., Baird, S.M., Rhodes, G.H., 1994. Intradermal gene immunization: The possible role of DNA uptake in the induction of cellular immunity to viruses. Proc. Natl. Acad. Sci. U.S.A. 91, 9519–9523.

Sawamura, D., Yasukawa, K., Kodama, K., Yokota, K., Sato-Matsumura, K.C., Toshihiro, T., Shimizu, H., 2002. The majority of keratinocytes incorporate intradermally injected plasmid DNA regardless of size but only a small proportion of cells can express the gene product. J. Invest. Dermatol. 118, 967–971.

Shi, Z., Curiel, D.T., Tang, D.C., 1999. DNA-based non-invasive vaccination onto the skin. Vaccine 17, 2136–2141.

Sintov, A.C., Krymberk, I., Daniel, D., Hannan, T., Sohn, Z., Levin, G., 2003. Radiofrequency-driven skin microchanneling as a new way for electrically assisted transdermal delivery of hydrophilic drugs. J. Contr. Release 89, 311–320.

Titomirov, A.V., Sukharev, S., Kistanova, E., 1991. In vivo electroporation and stable transformation of skin cells of newborn mice by plasmid DNA. Biochim. Biophys. Acta 1088, 131–134.

Udvardi, A., Kufferath, I., Grutsch, H., Zatloukal, K., Volc-Platzer, B., 1999. Uptake of exogenous DNA via the skin. J. Mol. Med. 77, 744–750.

Zhang, L., Nolan, E., Kreitschitz, S., Rabussay, D.P., 2002. Enhanced delivery of naked DNA to the skin by non-invasive in vivo electroporation. Biochim. Biophys. Acta 1572, 1–9.

Pharmaceutical Research, Vol. 22, No. 4, April 2005 (© 2005)
10.1007/s11095-005-2490-1

Research Paper

Transdermal Delivery of Human Growth Hormone Through RF-Microchannels

Galit Levin,[1,3] Amikam Gershonowitz,[1] Hagit Sacks,[1] Meir Stern,[1] Amir Sherman,[1] Sergey Rudaev,[1] Inna Zivin,[1] and Moshe Phillip[2]

Received August 10, 2004; accepted January 10, 2005

Purpose. To evaluate the bioavailability and bioactivity of human growth hormone (hGH) delivered transdermally through microchannels (MCs) in the skin created by radio-frequency (RF) ablation.
Methods. The creation of MCs was observed in magnified rat and guinea pig skin after staining by methylene blue. Various doses of hGH in a dry form were applied on rat or guinea pig (GP) skin after the formation of MCs. The pharmacokinetic profile of systemic hGH in both animal models was monitored for 15 h post patch application. Bioactivity of the transdermally delivered hGH was verified by measuring IGF-I levels in hypophysectomized rats.
Results. The ordered array of MCs was clearly visible in the magnified rat and guinea pig skin. The MCs were very uniform in diameter and of equal separation. Creation of MCs in the outer layers of the skin enabled efficient delivery of hGH, with a bioavailability of 75% (rats) or 33% (GPs) relative to subcutaneous (s.c.) injection with plasma profiles resembling that of s.c. injection. Elevated levels of systemic insulin-like growth factor-1 (IGF-I) were observed after transdermal delivery of hGH to hypophysectomized rats indicative of the bioactivity of the transdermally delivered hGH *in vivo*.
Conclusions. Formation of RF-microchannels is a well-controlled process. These MCs permitted the transdermal delivery of bioactive hGH in rats and GPs with high bioavailability.

KEY WORDS: transdermal drug delivery; radio-frequency ablation; Via Derm; stratum corneum; human growth hormone.

INTRODUCTION

The number of peptide and protein drugs has increased dramatically in the past decades and is expected to grow further as a result of intense biotechnology research in academia and industry. Elucidation of appropriate delivery methods for this group of active molecules is extremely challenging, and currently most of these drugs are given by injection. However, various alternative strategies are being developed. These include oral methods that overcome the proteolysis in the GI tract (1), nasal delivery, buccal delivery (2), inhalation (3) or transdermal methods (4). Most of the methods developed so far have various limitations, such as drug molecular weight, low deliverable dose, or low bioavailability.

Recently, a new transdermal delivery technology was developed, being adapted from the well-known medical technology of radio-frequency (RF) ablation (5–8). It is based on an electronic device, termed ViaDerm, which generates an electrical current at high frequency in the range of radio frequencies (100–500 kHz). The passage of this current through cells in the upper skin layers, via an array of microelectrodes placed on the skin, brings about ionic vibrations within the skin cells leading to local heating, liquid evaporation, and cell ablation. Consequently, small microchannels (MCs), called RF-microchannels, are formed across the stratum corneum (SC) and epidermis, which are highly amenable to the transdermal delivery of water-soluble drugs into the systemic circulation (9).

Human growth hormone (hGH) is a 22-kDa protein with clinical use in children having short stature due to hGH-deficiency, renal insufficiency, Turner syndrome, and Prader-Willi syndrome. Recently, hGH was also approved by the FDA for children with severely short stature. Additionally, this drug is also indicated in adults who suffer from either acquired or childhood onset hGH-deficiency. hGH therapy, which demands years of good compliance to achieve its therapeutic effects, is currently administered by frequent subcutaneous (s.c.) injections. A depot injection was also developed that reduced the frequency of injection to once or twice a month. However, due to pain and irritation side effects (10), the success of this product is mediocre. Therefore, a user-friendly hGH delivery method is a keenly sought-after therapeutic.

The aim of the current study was to investigate if RF-generated MCs could support the transdermal delivery of hGH in rats and guinea pigs (GPs). Furthermore, *in vivo* bioactivity of hGH was assessed by monitoring the production of IGF-I, a key downstream mediator following hGH receptor activation.

[1] TransPharma Medical, Lod 71291, Israel.
[2] The Felsenstein Medical Research Center, Institute for Endocrinology and Diabetes, National Center for Childhood Diabetes, Schneider Children's Medical Center, Petach Tikva, Israel.
[3] To whom correspondence should be addressed. (e-mail: galitl@transpharma.co.il)

0724-8741/05/0400-0550/0 © 2005 Springer Science+Business Media, Inc.

MATERIALS AND METHODS

Instruments

The device used to produce microchannels in the skin (ViaDerm, TransPharma Medical, Lod, Israel) was previously described in detail (9). The standard array of electrodes that was used produced MCs in the density of 100 MCs/cm^2 in a total area of 1.4 cm^2. In the hGH delivery studies, the device was applied twice on each skin area, so the MC density was 200 MCs/cm^2. Prior to ViaDerm application on the skin of animals, the hair was clipped using an Oster A5 clipper (cat. no. 78005-500, McMinnville, TN, USA), and shaved using a no. 40 blade and a Braun 3615 shaver. Immediately after ViaDerm application, TransEpidermal Water Loss (TEWL) was measured using a Dermalab instrument (Cortex Technology, Hadsund, Denmark).

Visualization of MCs

Fresh rat and guinea pig skin samples (Sprague-Dawley male rat, 350 g; Dunkin Hartley male guinea pig, 600 g; Harlan Laboratories Ltd., Rehovot, Israel) were excised from the animals, immediately pretreated with ViaDerm (100 MCs/cm^2), and then stained with 1% aqueous methylene blue (Carlo Erba Reagenti). The solution was applied for 15 s on the skin site, then wiped with soft tissue paper followed by isopropyl alcohol pads (Webcol, Kendall Company, Mansfield, MA, USA).

The control group consisted of application of the ViaDerm device on the skin in the absence of the power source but held with the same pressure followed by methylene blue staining. A Video Inspection System (S-T Industries Inc. model 20-8600, St. James, MN, USA) equipped with ×10 lens, was used in order to observe the created MCs.

Preparation of hGH Patches

Lyophilized hGH (Genotropin 16 or 36 IU/vial, Pharmacia & Upjohn, Puurs, Belgium) was used for the preparation of "printed" patches, in a proprietary owned process (11). This "print-like" method is based on accurately depositing small droplets of hGH solution on a transdermal backing liner at a total area of 1.4 cm^2 followed by a controlled drying process. This method permits accurate dosing and stable patches that contain a thin uniform layer of the protein in a dry form.

Animals

Study protocols were approved by the Institutional Animal Care and Use Committee of Assaf Harofeh Medical Center (Zriffin, Israel), and all procedures were conducted according to the Principles of Labotarory Animal Care (NIH Publication No. 85-23, revised 1985). Wild-type and hypophysectomized male Sprague-Dawley rats, 200–350 g, as well as wild-type male Dunkin Hartley guinea pigs 500–700 g (Harlan Laboratories Ltd.) were used. They were kept at constant temperature with a 12 h light:12 h dark cycle. Water and pelleted food (Koffolk, Tel Aviv, Israel) were freely available. The hypophysectomized rats were treated daily with s.c. injections of hydrocortisone sodium succinate (500 μg kg^{-1} day^{-1} Solu-Cortef®, (hydrocortisone sodium succinate for injection, USP, Pharmacia & Upjohn) and thyroxine sodium (15 μg kg^{-1} day^{-1}, Eltroxin, Bedford Labs, Bedford, OH, USA) from the day of arrival until beginning of the trial.

Procedures

The animals were anaesthetized by intraperitoneal (i.p.) injection of a combination of ketamine hydrochloride (85 mg/kg for rats and 70 mg/kg for GPs; Ketaset, Fort Dodge, IA, USA) and xylazine (3 mg/kg for rats and 6 mg/kg for GPs, Xyl-M2 veterinary, VMD, Arendonk, Belgium). Anesthesia was maintained using Isoflurane (0.5–1.5%, Isoflurane, Rhodia, Bristol, UK) or Halothane (0.5–2%, Rhodia, Bristol, UK) gas. Animals were placed in a dorsal recumbancy, and the abdominal hair was clipped and shaved. The application site was then wiped using an isopropyl alcohol pads (Webcol, Kendall). Thirty minutes later, TEWL measurements were used to check the skin integrity. Then, ViaDerm treatment was performed and followed by a second TEWL measurement 5 min post ViaDerm treatment. A hGH patch designated for each study protocol was then placed over the 1.4 cm^2 ViaDerm treated area. In each study, one group of animals received an hGH subcutaneous injection and was used as a reference group.

Blood samples were collected over 15–24 h, at time intervals specific for each study protocol, from the tail vein in rats and from a preinserted carotid cannula (PE-50, Portex Hythe, Kent, UK) in guinea pigs. Serum (rats) and plasma (GPs) were separated using a centrifuge (Hsiangtai Machinery Ind. Co. Ltd., Taipei Hsien, Taiwan) for 10 min at 6000 rpm and stored at –20°C until analysis. At the end of the study, the animals were euthanized after intracardial administration of pentobarbitone sodium (140 mg/kg, Pental, CTS Chemical Industries, Hod Hasharon, Israel).

Bioavailability of hGH in Rats and GPs Treated with ViaDerm

In order to study the bioavailability of hGH in rats, transdermal doses of 75, 150, 300, or 450 μg hGH were applied on normal rats' skin pretreated by ViaDerm application. Plasma hGH profiles were compared to those obtained following s.c. administration (150 μg hGH per rat). Each treatment group consisted of six animals. A test similar to the rat study described above was performed with GPs using transdermal doses of 50, 150, 300, and 400 μg per GP and an s.c. dose of 50 μg per animal. Each treatment group consisted of 5–6 animals.

Bioactivity of Transdermal Applied hGH

The bioactivity of the hGH was verified by measurement of IGF-I in hypophysectomized rats. A 200 μg hGH patch was directly applied to the 1.4 cm^2 ($n = 9$) skin area that was pretreated by ViaDerm application. The levels of hGH and IGF-I in the serum of these rats were compared to those found in the s.c. treated group (150 μg hGH, $n = 6$). A nontreated group and hGH on intact skin (800 μg) served as negative controls.

Analytical Methods

The dose of hGH placed on the printed patches was measured using high performance liquid chromatography (HPLC) analysis (EP 5.0, Somatropin assay). Briefly, the active material was extracted with 1 ml of 25 mM buffer phosphate, pH = 7, and was analyzed by size exclusion

(SE) HPLC using 30 cm column (internal diameter = 7.8 mm) TSK Gel G2000 SW 5 μm (TOSOH Bioscience, Stuttgart, Germany), precolumn TSK-Gel 6 cm × Ø 6 mm (TOSOH), phosphate/2-propanol mobile phase (97 volumes of 0.063 M buffer phosphate pH 7.0, with 3 volumes of 2-propanol), and detection at 214 nm.

hGH levels in rats and GP serum or plasma was measured using an enzyme-linked immunosorbent assay (ELISA) commercial kit (DSL-10-1900, Diagnostic Systems Laboratories, Inc., Webster, TX, USA). The kit is specific for human growth hormone and does not detect endogenous GP or rat GH. Areas under the concentration curves (AUCs) were calculated using a trapezoid method. Levels of IGF-1 were measured by the functional separation method, as previously described (12).

RESULTS

The photomicrograph of Fig. 1 shows a magnified image of rat (Fig. 1A) and guinea pig (Fig. 1B) skin samples after formation of MCs by ViaDerm and staining with methylene blue. The ordered pattern of microchannels can be observed. The diameter of all the MCs and the distances between MCs were uniform.

The TEWL values of the skin before and after ViaDerm application on rats and GPs were as follows: 2.9 ± 0.8 and 4.0 ± 0.8 *vs.* 39.2 ± 5.1 and 36.1 ± 5.6 g h^{-1} m^{-2} for rats and GPs before and after ViaDerm application, respectively. A significant increase in the TEWL was observed as a result of the formation of MCs in the skin.

Figure 2 depicts serum or plasma levels of hGH in rats (Fig. 2A) or GPs (Fig. 2B), respectively, after s.c. injection or transdermal delivery from patches containing increasing amounts of hGH. Table I summarizes the AUC and bioavailability level of the various transdermal doses compared to s.c. administration. A dose-dependent increase in the C_{max} and AUC was observed in both animal species up to a dose of 300 μg per 1.4 cm^2. A further increase in the amount of active material on the patch resulted in reduced bioavailability.

The serum hGH and IGF-1 levels are presented in Fig. 3. Delivery of hGH by s.c. injection or by application of hGH patch on ViaDerm treated skin resulted in a peak in the level of the hGH in the serum of the hypophysectomized rats. Both delivery methods resulted also in an increase in IGF-1 level. In the control group, there was no change in the levels of hGH and IGF-1.

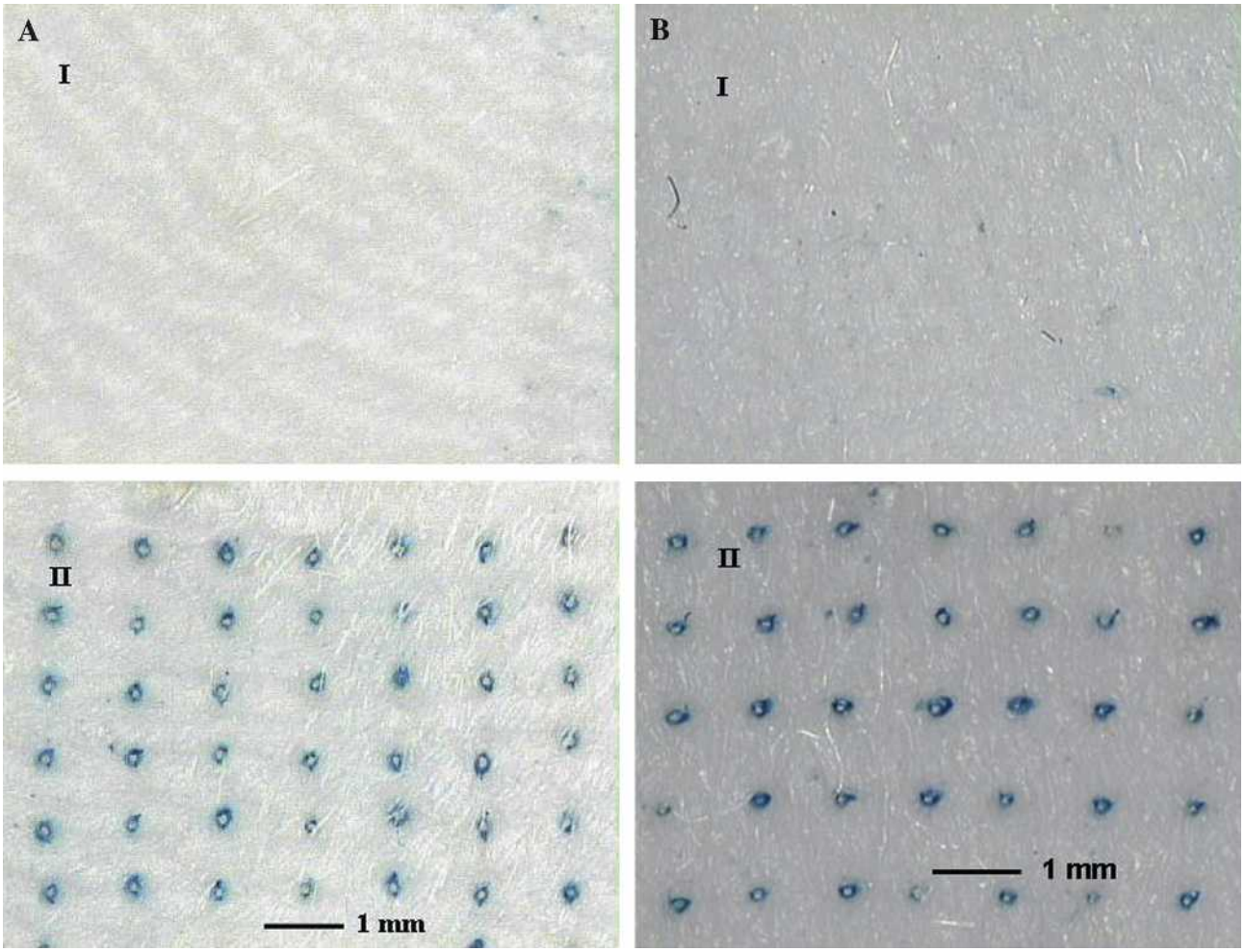

Fig. 1. Microchannels on the surface of ViaDerm treated (A) fresh rat and (B) guinea pig skin samples, after staining with methylene blue solution. The control group consisted of application of the ViaDerm device on the skin in the absence of the power source but held with the same pressure followed by methylene blue staining. (I) Control, (II) ViaDerm treated skin.

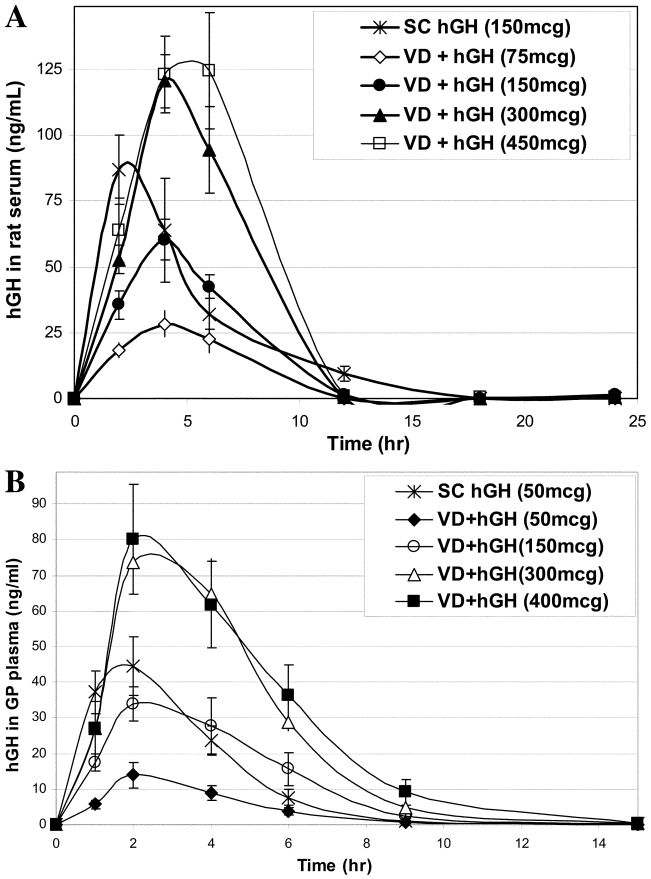

Fig. 2. hGH levels (ng/ml) in serum or plasma after application of increasing doses of transdermal hGH on 1.4 cm^2 ViaDerm treated area and s.c. injection of hGH: (A) Serum levels in rats. (B) Plasma levels in GP. Each data point represents the mean ± SEM of 5–6 animals.

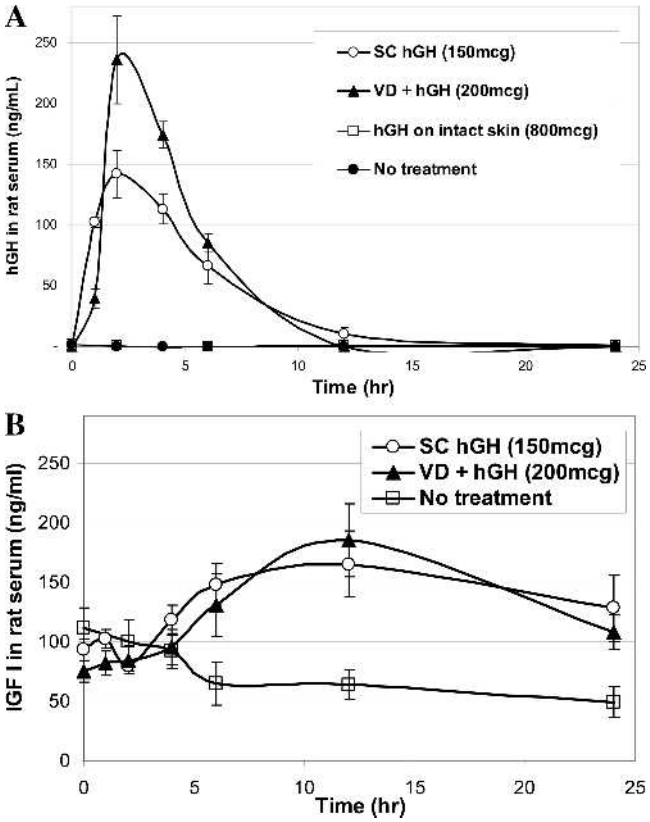

Fig. 3. Serum levels (ng/ml, mean ± SEM) of (A) hGH and (B) IGF-I after application of 200 μg hGH on 1.4 cm^2 ViaDerm treated area (n = 9), s.c. injection of 150 μg hGH (n = 7), or no treatment (n = 9) (control). Serum levels of hGH after application of 800 μg hGH on intact skin served as negative control (A).

DISCUSSION

The orderly pattern of RF-generated MCs in terms of their diameter and separated distances (Fig. 1) lays credence as to the reproducibility of the ViaDerm in creating MCs. Because methylene blue coloration of the MCs was a very rapid process, it would demonstrate the hydrophilic nature of the MCs. Indeed, previous studies showing the presence of extracellular fluid in MCs from porcine skin would support the theory of the hydrophilic nature of the MCs (9).

Table I. Mean AUC and Relative Bioavailability Values in Rats and Guinea Pigs

Mode of delivery	Dose micrograms (mcg)	AUC (ng.hr/ml.)	Bioavailability (% of s.c.)
Rats			
s.c.	150	489	100
Transdermal	75	184	75.3
Transdermal	150	376	76.9
Transdermal	300	727	74.3
Transdermal	450	884	60.3
Guinea pigs			
s.c.	50	176	100
Transdermal	50	57	32.4
Transdermal	150	175	33.1
Transdermal	300	362	34.3
Transdermal	400	404	28.7

The notion of using electricity for enhancement of transdermal drug delivery is not exclusive to the RF-microchannel technology. Iontophoresis uses an electrical field in order to drive ionized drug molecules across the SC barrier (13). In electroporation, short electrical pulses are used to create transient aqueous pores in the SC (14). Neither of these methods creates an orderly array of pores or MCs, by ablation of cells in specific locations, as presented in this study. Moreover, the ViaDerm device is user-friendly and minimally invasive. A human device safety study with 20 subjects was successfully completed with the electric parameters tested in this study. It was found that the ViaDerm device produced only slight irritation responses (minimal erythema and no edema) of a transient nature and the pain levels recorded were within the acceptable range for clinical use (in preparation).

It is important to note that the area covered with MCs is very small compared to the total skin area. MCs were created in a density of 200 MCs per cm^2 and less than 1% of the total treated area consists of MCs. Nevertheless, these MCs are highly amenable to the transdermal delivery of hGH, as non-ViaDerm treated skin is totally impermeable to hGH due to its large molecular size and hydrophilic nature (see also Fig. 3A, hGH on intact skin).

It is known that breaching the SC integrity is accompanied by an elevation in TEWL (15). Therefore, the formation

of MCs in the skin was verified by comparing TEWL values before and after treatment with the ViaDerm. There was a significant enhancement, of about 13- and 9-fold in rats and GPs, respectively, in TEWL values after ViaDerm application, despite the fact that the MCs occupy less than 1% of the skin area. It is also interesting to note that in rats and in guinea pigs the enhancement in TEWL was of a similar magnitude, despite of the differences in thickness of skin layers (16). The increase in TEWL serves as an indication for the creation of MCs, and as a predictor for the enhancement in transdermal drug delivery (17).

Low bioavailability is one of the major obstacles for the development of user-friendly delivery methods for peptides and proteins. The manufacturing processes of these active materials are usually complex with associated high costs. As compared to parenteral methods, this low bioavailability significantly reduces the feasibility of developing these alternative delivery methods as commercial products. If the bioavailability of the protein using the delivery method is low (less than 10–20%), there is a significant loss of protein resulting in higher manufacturing costs. This is despite the fact that more convenient methods will probably increase patient compliance and therefore drug efficacy (4). The bioavailability of hGH in this study relative to s.c. injection was found to be surprisingly high (75% in rats and 33% in GP; Table I). The RF-microchannel technology not only enabled the delivery of a high-molecular-weight protein (hGH) but also permitted a very efficient transdermal delivery of the drug.

This high bioavailability can be explained by the proposed mechanism of absorption of the hGH from a powder form. It is postulated that the highly water soluble hGH is dissolved by fluid that exudes from the created MCs. Consequently, a very high, local concentration of hGH solution is formed *in situ*. The delivery of the dissolved molecules is then mediated through the MCs into the viable tissues of the skin by diffusion across a steep concentration gradient. This leads to a high delivery rate and peak blood profile of the drug. The profile resembles that of s.c. injection, with a small delay in T_{max} that stems from the time required for dissolving the solid hGH and diffusion through MCs.

It is well-known that the SC functions as a rate controlling membrane in the case of transdermal delivery (18). In this study, we have demonstrated a clear increase in AUC in response to increasing amounts of drug on the patch. This dose response was linear up to a dose of 300 μg per 1.4 cm^2 and was observed in both rats and GPs. It is a reasonable hypothesis that following ViaDerm treatment, the SC no longer poses as a barrier to drug penetration through the aqueous microconduits. However, this linear increase in AUC did not persist at doses higher than 300 μg. It would appear that in both animal species, a dose of 300 μg/1.4 cm^2 can be defined as the "maximal efficient dose," at least when using the specific MCs density and electrodes that were used in this study. The factors that limit the delivered dose may be dissolution rate of hGH from the patches, the diffusion rate through the channels, the healing process of the channels and/or metabolism of the protein drug by skin derived proteases. These factors may also explain the differences in bioavailability observed in rats and GPs. It may be that these species differences stem from different healing rate and/or differences in proteases population and activity. This issue, as well as its relevance to human skin, should be further studied.

In addition to bioavailability, it is necessary to evaluate the effect of the processing method and delivery route on the integrity, conformation, and activity of the delivered protein drug (4). In this study, the bioactivity of the transdermally delivered hGH was clearly demonstrated using the hypophysectomized rat model. GH effects on cartilage growth are partly mediated by circulating IGF-1. A deficiency of GH is associated with low levels of IGF-1. In order to demonstrate the bioactivity of the hGH delivered through ViaDerm treated skin, hypophysectomized rats were used. The absence of hypophysa in these rats brings about minimal levels of endogenous GH, with concomitantly very low serum levels of IGF-1. Delivery of exogenous hGH in an active state elicits IGF-I release by the rat liver, which is expressed by a peak in serum IGF-I levels (19,20). Significant hGH doses in the plasma were measured in the ViaDerm treated rats reaching maximum levels within 4 h (Fig. 3A). The elevation in hGH, either in the s.c. or transdermal groups, was followed by an increase in IGF-1 (Fig. 3B), demonstrating that the hGH delivered transdermally was in an active form. The fact that the hGH retained its bioactivity throughout the patch manufacturing process and diffusion through skin layers underscores the notion that this delivery method might be used in a clinical setting.

In conclusion, this study demonstrates the functionality of the RF-microchannel technology as an alternative delivery method to s.c. injection of hGH. The similarities between the two methods in bioavailability, bioactivity, and serum drug profile offer much hope that the development of a commercial product based on this transdermal technology might be feasible.

REFERENCES

1. R. R. B. Shah, F. Ahsan, and M. A. Khan. Oral delivery of proteins: progress and prognostication. *Crit. Rev. Ther. Drug Carrier Syst.* **19**:135–169 (2002).
2. A. P. Sayani and Y. W. Chien. Systemic delivery of peptides and proteins across absorptive mucosae. *Crit. Rev. Ther. Drug Carrier Syst.* **13**:85–184 (1996).
3. R. U. Agu, M. I. Ugwoke, M. Armand, R. Kinget, and N. Verbeke. The lung as a route for systemic delivery of therapeutic proteins and peptides. *Respir. Res.* **2**:198–209 (2001).
4. J. L. Cleland, A. Daugherty, and R. Mrsny. Emerging protein delivery methods. *Curr. Opin. Biotechnol.* **12**:212–219 (2001).
5. S. N. Goldberg. Radiofrequency tumor ablation: principles and techniques. *Eur. J. Ultrasound* **13**:129–147 (2001).
6. L. Solbiati, T. Ierace, M. Tonolini, V. Osti, and L. Cova. Radiofrequency thermal ablation of hepatic metastases. *Eur. J. Ultrasound* **13**:149–158 (2001).
7. F. J. McGovern, B. J. Wood, S. N. Goldberg, and P. R. Mueller. Radiofrequency ablation of renal cell carcinoma via image guided needle electrodes. *J. Urol.* **161**:599–600 (1999).
8. F. Izzo, C. C. Barnett, and S. A. Curley. Radiofrequency ablation of primary and metastatic malignant liver tumors. *Adv. Surg.* **35**:225–250 (2001).
9. A. C. Sintov, I. Krymberk, D. Daniel, T. Hannan, Z. Sohn, and G. Levin. Radiofrequency-driven skin microchanneling as a new way for electrically assisted transdermal delivery of hydrophilic drugs. *J. Control. Release* **89**:311–320 (2003).
10. B. L. Silverman, S. L. Blethen, E. O. Reiter, K. M. Attie, R. B. Neuwirth, and K. M. Ford. A long-acting human growth hormone (Nutropin depot): efficacy and safety following two years of treatment in children with growth hormone deficiency. *J. Pediatr. Endocrinol. Metab.* **15**:715–722 (2002).
11. International Patent Application WO 2004/039428. Transdermal delivery system for dried particulate or lyophilized medications, TransPharma Medical Ltd., Lod, Israel.

12. M. Phillip, G. Maor, S. Assa, A. Silbergeld, and Y. Segev. Testosterone stimulates growth of tibial epiphyseal growth plate and insulin-like growth factor-1 receptor abundance in hypophysectomized and castrated rats. *Endocrine* **16**:1–6 (2001).
13. N. Kanikkannan. Iontophoresis-based transdermal delivery systems. *BioDrugs* **16**:339–347 (2002).
14. B. W. Barry. Novel mechanisms and devices to enable successful transdermal drug delivery. *Eur. J. Pharm. Sci.* **14**:101–114 (2001).
15. G. L. Grove, M. J. Grove, C. Zerweck, and E. Pierce. Comparative metrology of the evaporimeter and the Dermalab TEWL probe. *Skin Res. Technol.* **5**:1–8 (1999).
16. R. Panchagnula, K. Stemmer, and W. A. Ritschel. Animal models for transdermal delivery. *Meth. Find. Exp. Clin. Pharmacol.* **19**: 335–341 (1997).
17. A. Rougier, C. Lotte, and H. I. Maibach. *In vivo* relationship between percutaneous absorption and transepidermal water loss. In: R. L. Bronaugh and H. I. Maibach (eds.), *Percutaneous Absorption*, Marcel Dekker, New York, 1999, pp. 117–132.
18. V. R. Sinha and M. P. Kaur. Permeation enhancers for transdermal drug delivery. *Drug Dev. Ind. Pharm.* **26**:1131–1140 (2000).
19. W. V. J. Wilson, M. Rattray, C. R. Thomas, B. H. Moreland, and D. Schulster. Effects of hypophysectomy and growth hormone administration on the mRNA levels of collagen I,III and insulin-like growth factor-I in rat skeletal muscle. *Growth Horm. IGF Res.* **8**:431–438 (1998).
20. J. Oscarsson, M. Ottosson, K. Vikman-Adolfsson, F. Frick, S. Enerback, H. Lithell, and S. Eden. GH but not IGF-I or insulin increases lipoprotein lipase activity in muscle tissues of hypophysectomised rats. *J. Endocrinol.* **160**:247–255 (1999).

Available online at www.sciencedirect.com
SCIENCE DIRECT
Journal of Controlled Release 89 (2003) 311–320
journal of controlled release
www.elsevier.com/locate/jconrel

Radiofrequency-driven skin microchanneling as a new way for electrically assisted transdermal delivery of hydrophilic drugs

Amnon C. Sintov[a,*], Igor Krymberk[a], Dorit Daniel[b], Talli Hannan[b], Ze'ev Sohn[b], Galit Levin[b]

[a]*The Institutes for Applied Research, Ben Gurion University of the Negev, P.O. Box 653, Beer Sheva 84105, Israel*
[b]*TransPharma Ltd., 3a Geron St., P.O. Box 222, Yehud, Israel*

Received 27 November 2002; accepted 14 February 2003

Abstract

The aim of this study was to increase the skin penetration of two drugs, granisetron hydrochloride and diclofenac sodium, using a microelectronic device based on an ablation of outer layers of skin using radiofrequency high-voltage currents. These radiofrequency currents created an array of microchannels across the stratum corneum deep into the epidermis. The percutaneous penetration studies were first performed in vitro using excised full thickness porcine ear skin. An array of 100 microelectrodes/cm^2 was used in these studies. The skin permeability of both molecules was significantly enhanced after pretreatment with the radiofrequency microelectrodes, as compared to the delivery through the untreated control skin. Steady state fluxes of 41.6 μg/cm^2/h (r=0.997) and 23.0 μg/cm^2/h (r=0.989) were obtained for granisetron and diclofenac, respectively. The enhanced transdermal delivery was also demonstrated in vivo in rats. It was shown that diclofenac plasma levels in the pretreated rats reached plateau levels of 1.22±0.32 μg/ml after 3 h to 1.47±0.33 μg/ml after 6 h, as compared to 0.16±0.04 μg/ml levels obtained after 6 h in untreated rats. Similarly, application of granisetron patches (3% in crosslinked hydrogel) onto rats' abdominal skin pretreated with radiofrequency electrodes resulted in an averaged peak plasma level of 239.3±43.7 ng/ml after 12 h, which was about 30 times higher than the plasma levels obtained by 24-h passive diffusion of the applied drug. The results emphasize, therefore, that the new transdermal technology is suitable for therapeutic delivery of poorly penetrating molecules.
© 2003 Elsevier Science B.V. All rights reserved.

Keywords: Radiofrequency-microchannels; Radiofrequency ablation; Granisetron; Diclofenac; Transdermal delivery; Skin permeation

1. Introduction

The outmost dermal layer, the stratum corneum (SC), forms an effective barrier to the permeation of external chemicals; therefore, the transdermal administration of drugs and other substances is remarkably restricted. Passive penetration of the SC is particularly difficult for hydrophilic and charged molecules. Consequently, transdermal delivery of drugs has been the subject of intensive research. In addition to the vehicle formulations and the chemical enhancers [1,2], physical methods such as microneedles [3,4], iontophoresis and electroosmosis [5–7], electroporation [8–13], and ultrasound [14] have

*Corresponding author. Tel.: +972-8-647-2709; fax: +972-8-647-2960.
E-mail address: asintov@bgumail.bgu.ac.il (A.C. Sintov).

0168-3659/03/$ – see front matter © 2003 Elsevier Science B.V. All rights reserved.
doi:10.1016/S0168-3659(03)00123-8

been investigated. Synergistic interactions between chemical and physical enhancers as well as synergism between two physical means of drug enhancement were also studied [15–17].

Radiofrequency (RF) thermal ablation is a well-known and effective technology for electrosurgery and ablation of malignant tissues. The method involves placing of a thin, needle-like electrode directly into the tumor. During the application of RF energy, a frequency alternating current moves from the tip of the electrode into the tissue surrounding that electrode. As the ions within the tissue attempt to follow the change in the direction of the alternating current, their movements result in frictional heating of the tissue, producing coagulative necrosis and cell ablation. Operations using radiofrequencies are considered safe and convenient during the surgery, since cessation of neuromuscular stimulation occurs at approximately 100 kHz. That is, while the target tissue absorbs the heat energy released during the electrosurgery, the applied high-frequency current does not affect the proximal muscles [18–21]. This technology has been adapted as an optional physical enhancer of drug transport across the skin. Its potential in the creation of aqueous microchannels in the outer layer of the skin was studied.

The present paper is the first report describing this novel method in facilitating the transport of hydrophilic drugs, granisetron hydrochloride (pK_a=9.4, MW=348.9) and diclofenac sodium (pK_a=4.0, MW=318.1), through the SC barrier. We have chosen these drugs because the transdermal administration of charged and polar molecules is difficult due to the intrinsic lipophilicity of the SC. The method of using RF energy is based on creating an array of small microchannels across the SC into the viable epidermis by microablating skin cells. The high frequency electrical current conducted through the aqueous medium of the stratum corneum generates heat that brings about an instant removal of cells beneath the electrode. Due to the high velocity (1 ms per electrode), it is postulated that only heat conduction results in the creation of microchannels, and other mechanisms such as electrochemical reactions do not take place. Skin electroporation, which is operated by low duty cycle, high intensity electric-field pulsing, is also believed to create transient aqueous microchannels [8–13]. The creation of transient aqueous microchannels by RF energy has been evidenced for the first time in the present report. The operating principle of RF-microchanneling formation are shown in Scheme 1. As illustrated,

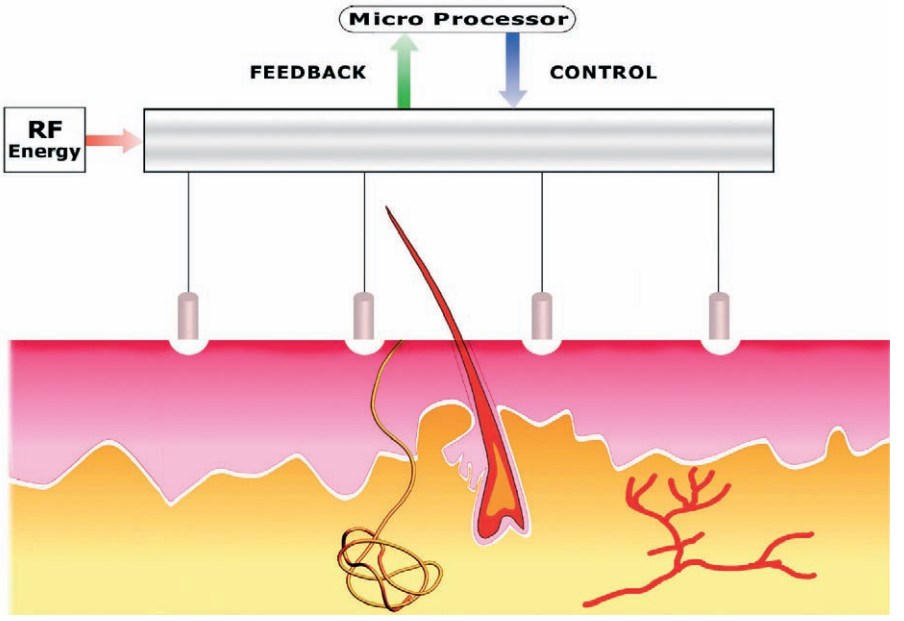

Scheme 1. Schematic presentation of RF-microchannels.

a closely spaced array of tiny electrodes is placed against the skin while an alternating current at radio frequency is applied to each of the microelectrodes. This forms RF-microchannels on the very outer layer of the skin through ablation of cells. The microchannels are designed to penetrate only the outer layers of the skin where there are no blood vessels or nerve endings, resulting in minimal skin trauma and neural sensation.

2. Materials and methods

2.1. Instruments and materials

The RF-microchannels generator (ViaDerm™, Transpharma Ltd, Israel) is illustrated in Scheme 2 [22]. ViaDerm™ generator is made of two primary components: a reusable electronic controller in a size similar to a phone handset, and a disposable array that can snap onto the end of the controller. The controller can communicate with a computer and be reprogrammed to change any of the critical parameters used. The controller is also able to measure and download electrical inputs during the ablation process, such as a peak current, final current, voltage, time and energy. The array is made of a polycarbonate body and stainless steel electrodes of length 100 μm and diameter 40 μm. It has 140 electrodes spaced 1 mm from each other in a square matrix arrangement. In this prototype, each electrode is individually operated. The electrodes are designed to create micro-channels that are 40 μm wide and 70 μm deep. The operation of the RF-microchannel generator is simple and easy. The user holds the controller in his hand and presses the array against the test site on the skin. When a minimum pressure is placed on the skin the RF-generator is activated and the treatment begins automatically. Within seconds (typically less than a millisecond per burst per electrode) the array completes its work. The density of the microelectrode array used in these studies was 100 or 200 microelectrodes/cm^2. Each electrode received a multiple number of bursts of RF energy as programmed. The animal studies (rats) were done with the following conditions: applied voltage: 200 or 250 V; RF frequency: 100 kHz; burst length: 1 ms; number of bursts: 5; time between bursts: 15 ms. Excised porcine skin for in vitro testing and histological observation was treated with an applied

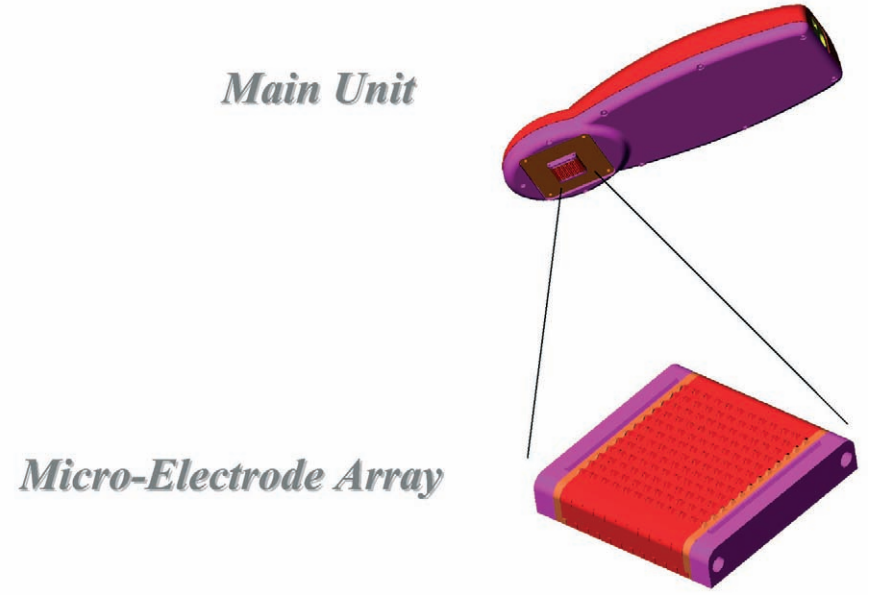

Scheme 2. The handset system and the microelectrodes array (ViaDerm™, Transpharma Ltd.) as designed to facilitate the transdermal drug delivery by transmission of radio frequency currents through the electrodes into the skin, and by the creation of microchannels.

voltage of 380 V and five bursts or with 330 V and two bursts, respectively.

Granisetron hydrochloride was obtained from Natco Pharma, Hyderabad, India. Diclofenac sodium was purchased from Sigma. The drug solutions at a concentration of 1% w/v were freshly prepared. Sodium diclofenac was dissolved in 1:4 ethanol–water, while granisetron HCl was dissolved in distilled water. For the pharmacokinetics experiments, granisetron in solution was soaked into a crosslinked polyethylene oxide wound dressing (Vigilon, Bard Inc.) to obtain a hydrogel patch containing 3% w/v of drug substance. This formulation was prepared and used in vivo instead of 1% w/v concentration utilized in the in vitro studies. All solvents were HPLC grade (Merck, Germany).

2.2. In vitro skin permeation study

The permeability of diclofenac sodium and granisetron hydrochloride through full thickness porcine ear skin was measured in vitro with a flow-through Franz diffusion cell system (Laboratory Glass Apparatus, Berkeley, CA). The diffusion area was 3.1 cm^2. Full-thickness porcine skin was excised from fresh ears of slaughtered white pigs (breeding of Landres and Large White, locally grown in Kibbutz Lahav, Israel). Transepidermal water loss measurements (TEWL, Dermalab® Cortex Technology, Hadsund, Denmark) were performed and only those pieces that the TEWL levels were less than 15 $g/m^2/h$ were mounted in the diffusion cells. Skin microchanneling was performed in cells defined as pretreatment group, then TEWL was measured again to control the operation (see Table 1). The skin pieces were placed on the receiver chambers with the stratum corneum facing upwards, and the donor chambers were clamped in place.

Drug solutions (1% w/v sodium diclofenac or granisetron HCl) were pipetted into the donor chambers (0.5 or 1 ml of granisetron or diclofenac solutions, respectively). Phosphate buffered saline (PBS, pH 7.4) or ethyl alcohol–PBS (1:9) in granisetron or diclofenac experiments, respectively, was passed through the receiver cells at a flow rate of 2 ml/h. Samples from the receiver solutions were collected into tubes (using a fraction collector, Retriever IV, ISCO), at predetermined times for a 24-h period. The samples were kept at 4 °C until analyzed by HPLC.

2.3. HPLC analysis of samples from receiver solutions

2.3.1. Diclofenac

Aliquots of 20 ml from each sample were injected into a HPLC system, equipped with a prepacked C_{18} column (Phenomenex LUNA™, 5 mm, 150×4 mm). The HPLC system (ProStar modules, Varian Inc.) was equipped with an autosampler and a UV detector (Varian's ProStar model 310). The quantification of diclofenac was carried out at 280 nm. The samples were chromatographed using an isocratic mobile phase consisting of acetonitrile–sodium acetate buffer, pH 6.3 (35:65) at a flow rate of 1 ml/min.

2.3.2. Granisetron

Aliquots of 10 ml from each sample were injected into the HPLC system, equipped with a prepacked C_{18} column (Phenomenex LUNA™, 5 mm, 150×4 mm). The detection of granisetron was carried out at 305 nm. The samples were chromatographed using an isocratic mobile phase consisting of acetonitrile–sodium acetate buffer, pH 4.2 (40:60) at a flow rate of 0.75 ml/min.

Data were expressed as the cumulative drug permeation (Q_t) per unit of skin surface area, Q_t/S

Table 1
Summary of TEWL values obtained before and after treatment with RF currents in the overall experiments (values are expressed in $g/m^2/h$)

	Drugs aimed to be tested	Control experiments (without RF treatment)	Tested skin before treatment	Tested skin after treatment
Excised porcine skin	Diclofenac	6.83±0.54	8.22±1.33	17.3±0.99
In vitro	Granisetron	8.38±0.93	10.67±1.2	23.4±2.06
Abdominal rat skin	Diclofenac	5.05±0.65	5.35±1.06	25.38±1.44
In vivo	Granisetron	6.16±0.98	5.7±0.98	23.73±4.33

($S=3.1$ cm^2). The steady-state fluxes (J_{ss}) were calculated by linear regression interpolation of the experimental data.

2.4. Pharmacokinetic studies of transdermal drug in rats

Male Sprague–Dawley rats (400–500 g, Harlan Laboratories Ltd., Jerusalem, Israel) were anesthetized (5 mg/kg ketamine i.p.) and were placed on their back. Anesthesia was maintained with 0.1 ml ketamine (100 mg/ml) along the experiment. The procedure protocol related to animals was reviewed and approved by the Institutional Animal Care and Use Committee.

The abdominal skin hair was trimmed off and shaved carefully, and was cleaned with isopropyl alcohol. After 30 min, the transepidermal water loss was measured to check skin integrity. At this stage, RF-microchannels were generated on the shaved skin of a test group. After generation of RF-microchannels, TEWL was measured again and the obtained values were documented (see Table 1). It was obvious according to the TEWL data that the hair clipping and shaving did not cause apparent damage to the skin. Each test group of the diclofenac pharmacokinetic study consisted of three animals for the whole testing duration, while the test group of the granisetron study consisted of four animals for each time period ($n=4$; five sampling times; total of 20 rats). Each experiment was accompanied by a control group of animals that were not undergoing the pretreatment procedure ($n=6$ for diclofenac, $n=4$ with a total of 20 rats for granisetron application). Drug solutions (1% diclofenac sodium or 3% granisetron hydrochloride in a hydrogel sheet) were then applied on the skin surface. In the case of diclofenac solution, special containers glued to the skin by a silicon rubber were used to hold drug solution over the specified place. Skin surface areas of 1.4 cm^2 or 2.8 cm^2 (1.4 cm$^2\times2$) were covered with granisetron patches and diclofenac solutions, respectively. Blood samples were taken under anesthesia from the tail vein (while monitoring diclofenac) or directly from the heart (while monitoring granisetron) into heparanized tubes. After centrifugation, plasma samples were kept at -20 °C until analyzed for drug concentration.

2.5. HPLC analysis of plasma extracts

2.5.1. Diclofenac

Into 100 ml of plasma, 200 ml of methanol was added and mixed well. After centrifugation, aliquots of 20 ml from each vial were injected into the HPLC system, equipped with a prepacked C_{18} column (Phenomenex LUNA™, 5 mm, 150×4 mm). The HPLC system (Shimadzu VP series) was equipped with an autosampler and a diode array detector. The quantification of diclofenac was carried out at 280 nm. The samples were chromatographed using an isocratic mobile phase consisting of acetonitrile–sodium acetate buffer, pH 6.3 (30:70) at a flow rate of 1.5 ml/min. Calibration curves (peak area vs. drug concentration) were linear over the range 1–20 mg/ml.

2.5.2. Granisetron

The procedure was basically performed according to Kudoh et al. [23]. Into 1 ml plasma, 500 ml of phosphate buffer (pH 7) was added and mixed well. The mixture was transferred on a 500-mg C-2 Bond Elute SPE cartridge pre-washed consecutively with methanol, water and phosphate buffer (pH 7). After plasma application, the SPE cartridge was washed with 2 ml water and 2 ml acetonitrile–water 40:60. The cartridge was dried under vacuum and granisetron was then eluted with 2 ml methanol followed by 2 ml methanol containing 1% trifluoroacetic acid. The combined eluent was dried at 40 °C under nitrogen and the residue was dissolved in 200 ml methanol–water 10:90. Aliquots of 30 ml from each sample were injected into the HPLC system, equipped with a prepacked C_8 column (Hypersil BDS C-8 100×3.0 mm, 3 μm). The HPLC system (1050 HP) was equipped with an autosampler, and a fluorescence detector (Model 1046A). The detection of granisetron was carried out at 305-nm excitation wavelength and 365-nm emission wavelength. The samples were chromatographed using an isocratic mobile phase consisting of acetonitrile–0.1 M acetate buffer (pH 4.7) containing 10 mM hexanesulfonate and 0.23 g/l EDTA (19:81) at a flow rate of 0.3 ml/min. Calibration curves (peak area vs. drug concentration) were linear over the range 2–100 ng/ml.

2.6. Histology

RF-microchannels were created at a density of 200 channels/cm^2 on the dorsal skin of a pig. Skin biopsies were taken immediately after RF-microchannels creation, by a biopsy punch, and preserved in 4% buffered formaldehyde solution. The samples were embedded in paraffin wax, cut to a thickness of 4–5 μm, stained with hematoxylin and eosin (HandE) and examined microscopically.

3. Results

The photomicrograph of Fig. 1 shows the microchannel produced by RF energy of 330 V applied voltage (100 kHz; two bursts). The tissue around the microchannel showed normal epidermal and dermal structure, with no pathological changes. The microchannel produced at these conditions measures about 30 μm in diameter and 70 μm in depth from the epidermal surface into the superficial dermis. The porcine epidermis is usually thinner than human epidermis — 36.9 μm vs. 49.5 μm, respectively [26] — indicating that RF-microchannels would go into the human epidermis without perturbing the dermis.

The permeability of diclofenac sodium and granisetron hydrochloride through excised porcine ear skin was significantly enhanced after pretreatment with RF energy, as compared to the delivery through the untreated control skin (Figs. 2–3). After lag times of 3 and 9 h, pseudo steady state fluxes of 41.6 μg/cm^2/h (r=0.997) and 23.0 μg/cm^2/h (r=0.989) were obtained for granisetron and diclofenac, respectively. These results were compared to fluxes obtained after 24-h penetration through untreated intact skin (passive delivery) — 5.9 μg/cm^2/h (r=0.983) and 6.0 μg/cm^2/h (r=0.988) for granisetron and diclofenac, respectively. The concentration of the drugs in the donor was 10 mg/ml; therefore, the 'apparent permeability coefficients' (J_{ss} divided by donor concentration) after RF-microchanneling were 41.63×10^{-4} and 22.98×10^{-4} cm/h for granisetron and diclofenac respectively (Table 2). The values obtained for granisetron and diclofenac were 7.1 and 3.8 times, respectively, higher than the coefficients

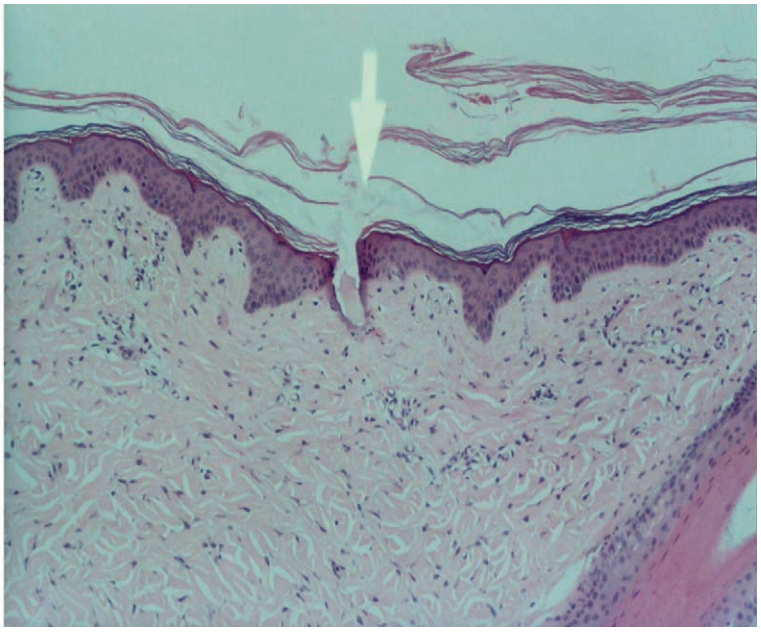

Fig. 1. Photomicrograph of cross-section of porcine skin treated with RF currents (density=200 electrodes/cm^2) of 200 V applied voltage (100 kHz; five bursts) showing a localized microchannel intruding the epidermis into the superficial dermis (70 μm in length), hematoxylin–eosin staining, 400×.

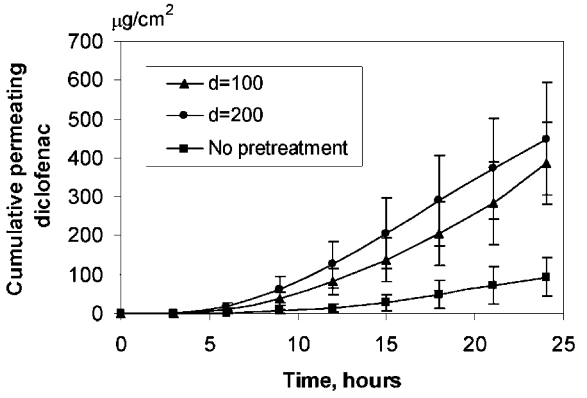

Fig. 2. In vitro percutaneous penetration of diclofenac sodium from 1% hydroalcoholic solution after skin was pretreated with RF currents of 200 V applied voltage (100 kHz; five bursts), using an array of 100 microelectrodes/cm^2 (triangles) and 200 microelectrodes/cm^2 (circles). Passive diffusion through untreated skin is also illustrated (squares). The in vitro testing was performed on porcine ear skin in Franz diffusion cells (n=6).

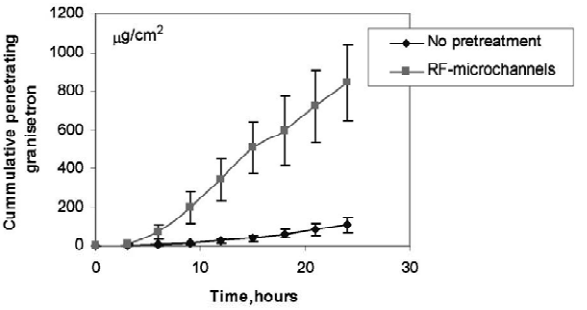

Fig. 3. In vitro percutaneous penetration of granisetron hydrochloride from 1% aqueous solution after skin was pretreated with RF currents of 200 V applied voltage (100 kHz; five bursts), using an array of 100 microelectrodes/cm^2 (squares). Passive diffusion through untreated skin is also illustrated (diamonds). The in vitro testing was performed on porcine ear skin in Franz diffusion cells (n=6).

Table 2
Comparison of the apparent permeability coefficients obtained for granisetron and diclofenac transport through porcine skin

	Permeability coefficient (cm/h)	
	Granisetron	Diclofenac
Intact skin	5.86×10^{-4}	6.05×10^{-4}
RF[a]-treated skin	41.63×10^{-4}	22.98×10^{-4}

[a] RF-microchannels were created using 100 electrodes/cm^2. Applied voltage: 200 or 250 V; RF frequency: 100 kHz; and number of bursts: 5.

obtained after a passive diffusion through the porcine skin. As shown in Fig. 2, by multiplying the density of the electrodes array from 100 to 200 electrodes/cm^2, the in vitro percutaneous penetration of diclofenac changed slightly (apparent permeability coefficient=26.3×10^{-4} cm/h compared to 23.0×10^{-4} cm/h), although it was not statistically significant.

The enhanced transdermal delivery was also demonstrated in vivo in rats. It was shown that diclofenac plasma levels in the pre-treated rats reached plateau levels of 1.22 ± 0.32 μg/ml after 3 h to 1.47 ± 0.33 μg/ml after 6 h, as compared to 0.16 ± 0.04 μg/ml levels obtained after 6 h in untreated rats (Fig. 4). This enhancement was achieved by using an array consisting of 100 electrode/cm^2 and an applied voltage of 250 V. When a power of 200 V was applied, the drug plasma levels were significantly reduced ($P>0.05$), rising to only 0.93 μg/ml after 6 h. Fig. 5 shows the pharmacokinetics profiles of granisetron in rats for 24 h after dermal application of patches containing 3% granisetron. A group of animals that were pretreated with an array of 100 electrodes/cm^2 delivering an RF energy of 250 V applied voltage was compared with the untreated control group (n=4). The plasma levels of granisetron in the pretreated group reached a peak after 12 h with an averaged value of 239.3 ± 43.7 ng/ml. This enhanced con-

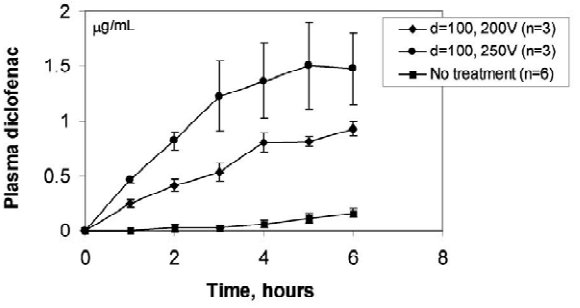

Fig. 4. Plasma levels (μg/ml) of diclofenac in rats after application of 1% hydroalcoholic solution on 2.8 cm^2 skin surface area. The diamond-shaped symbols represent skin pretreatment with RF currents of 250 V applied voltage (100 kHz; five bursts) (n=3), while the circle-shaped symbols represent skin pretreatment with RF currents of 200 V applied voltage (n=3). The pharmacokinetic profile of passive diffusion through untreated skin is represented by the square-shaped symbols (n=6).

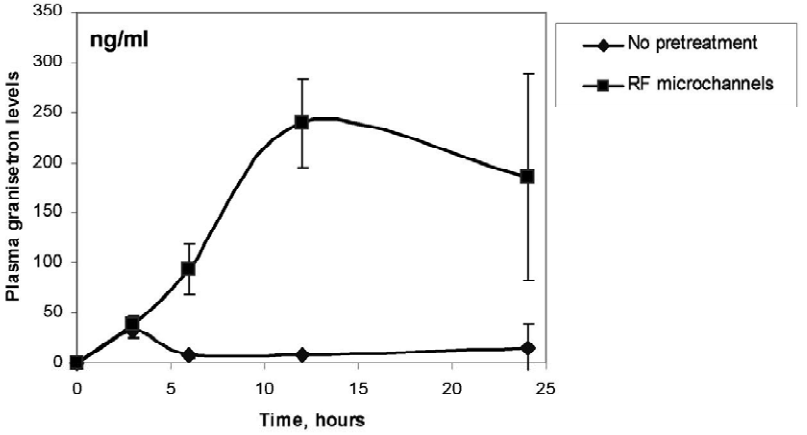

Fig. 5. Plasma levels (ng/ml) of granisetron in rats after application of 3% aqueous solution in Vigilon hydrogel patches on 1.4 cm^2 skin surface area. The square-shaped symbols represent skin pretreatment with RF currents of 200 V applied voltage (100 kHz; five bursts) ($n=4$). The pharmacokinetic profile of passive diffusion through untreated skin is represented by the diamond-shaped symbols.

centration was about 30 times higher than the plasma levels after dermal granisetron application, which passively absorbed to the blood circulation during 24 h, as demonstrated by the pharmacokinetics profile of the control group (Fig. 5).

4. Discussion

It has already been evidenced by many publications that high voltage electric-field pulses significantly increase the transdermal flux of drugs [8–13]. This phenomenon, which is called electroporation (or electropermeabilization), is believed to involve the creation of transient aqueous 'pores' in the lipid bilayers of the SC. While neither visual evidence of these pores has been reported nor the physical nature of the structural skin changes is known, the mechanism by which electroporation increases the transdermal flux is incomplete, thus being explained by theoretical models of transient aqueous pathways in planar lipid bilayer systems [24]. Our study presents for the first time a new method of creating visual pores or microchannels in the skin outer layers by radiofrequency currents. The mechanism by which these visual microchannels (Fig. 1) are created may be explained by the heat released during a fast flow of ions in the epidermis. Based on the known practice of needle ablation of tumors and lesions by RF-electrodes [19], the RF power (<1 MHz) causes oscillatory movement of ions in the tissue with a velocity that is proportional to the electric field intensity. This ionic current results in a frictional energy loss, heating and coagulation necrosis. It has been postulated according to the fact that the immediate surroundings of the microchannel was not damaged that heat is created in the ablated cells themselves, rather than being conducted from an external source. Further mechanistic studies are needed to elucidate how RF currents work on skin tissue.

The fluxes and the permeability coefficients of diclofenac sodium and granisetron hydrochloride through porcine skin in vitro, as shown in Table 2 and Figs. 2–3, demonstrate that granisetron HCl is twice more permeable through RF-pretreated porcine skin than diclofenac sodium. The molecular weights of both drugs are similar (349 and 318 for granisetron and diclofenac salts, respectively), however, in the vehicle and in the physiological environment of the skin they are salts, which possess opposite charges. Since granisetron is a positively charged molecule and diclofenac is negatively charged polar molecule, it may imply that electrostatic attraction/repulsion ratios dictate the migration along the aqueous microchannels. This might also be an indication of a potential gradient that is created by RF microchanneling procedure in which, like ion-

tophoresis, monovalent cations cross the skin more easily than monovalent anions based on the net negative charge of the skin [25]. It is also reasonably postulated that the diffusion through the aqueous microchannels might be easier for the highly water-soluble granisetron hydrochloride (with an octanol/water partition coefficient of $K_{ow}=0.28$) than for the sparingly water-soluble diclofenac sodium ($K_{ow}=13.4$ at pH 7.4 and $K_{ow}=1545$ at pH 5.2).

Finally, RF microchanneling as performed in this study produced no skin damage in rats. There was no evidence of erythema and edema immediately after the pretreatment process, and 6 and 24 h after pretreatment when experiments were terminated. This may be explained by the fact that only a small portion of the total skin area is covered by microchannels. Since in the diameter of a microchannel is approximately 30 μm, its cross-section area is 7×10^{-6} cm^2. By using a given density of 100 or 200 channels per centimeter square, it is found that less than 0.2% of the skin area is occupied by microchannels. Due to this small figure and the relatively low microchanneling depth, no apparent skin reaction was documented. Since toxicological research was beyond the scope of this paper, more studies including long-term follow-up and histopathological examinations should be conducted.

In conclusion, the results obtained in this study have shown that the permeability of polar hydrophilic molecules, which poorly penetrate the lipophilic SC barrier, was significantly enhanced through excised porcine ear skin and through rat skin in vivo by using radiofrequency microelectrodes. The mechanism by which they create microchannels in the outer layers of the skin still remains to be studied.

References

[1] K.A. Walters, Penetration enhancers and their use in transdermal therapeutic systems, in: J. Hadgraft, R.H. Guy (Eds.), Transdermal Drug Delivery, Developmental Issues and Research Initiatives, Marcel Dekker, Inc., New York and Basel, 1989, pp. 197–246.

[2] E.W. Smith, H.I. Maibach (Eds.), Percutaneous Penetration Enhancers, CRC Press, Boca Raton, FL, 1995.

[3] S. Henry, D.V. McAllister, M.G. Allen, M.R. Prausnitz, Microfabricated microneedles: a novel approach to transdermal drug, J. Pharm. Sci. 87 (1998) 922–925.

[4] D.V. McAllister, M.G. Allen, M.R. Prausnitz, Microfabricated microneedles for gene and drug delivery, Ann. Rev. Biomed. Eng. 2 (2000) 298–313.

[5] P. Singh, P. Liu, S.M. Dinh, Facilitated transdermal delivery by iontophoresis, in: R.L. Bronaugh, H.I. Maibach (Eds.), Percutaneous Absorption, Drugs–Cosmetics–Mechanisms–Methodology, 3rd Edition, Marcel Dekker, Inc., New York and Basel, 1999, pp. 633–657.

[6] M.J. Pikal, The role of electroosmotic flow in transdermal iontophoresis, Adv. Drug Del. Rev. 46 (2001) 281–305.

[7] B.D. Bath, H.S. White, E.R. Scott, Visualization and analysis of electroosmotic flow in hairless mouse skin, Pharm. Res. 17 (2000) 471–475.

[8] M.R. Prausnitz, V.G. Bose, R. Langer, J. Weaver, Electroporation of mammalian skin: a mechanism to enhance transdermal drug delivery, Proc. Natl. Acad. Sci. USA 90 (1993) 10504–10508.

[9] R. Vanbever, N. Lecouturier, V. Preat, Transdermal delivery of metoprolol by electroporation, Pharm. Res. 11 (1994) 1657–1662.

[10] J.E. Riviere, N.A. Monteiro-Riviere, R.A. Rogers, D. Bommannan, J.A. Tamada, R.O. Potts, Pulsatile transdermal delivery of LHRH using electroporation: drug delivery and skin toxicology, J. Controlled Release 36 (1995) 229–233.

[11] R. Vanbever, E. Le Boulenge, V. Preat, Transdermal delivery of fentanyl by electroporation. I. Influence of electrical factors, Pharm. Res. 13 (1996) 559–565.

[12] M.R. Prausnitz, A practical assessment of transdermal drug delivery by skin electroporation, Adv. Drug Del. Rev. 35 (1999) 61–76.

[13] Q. Hu, W. Liang, J. Bao, Q. Ping, Enhanced transdermal delivery of tetracaine by electroporation, Int. J. Pharm. 202 (2000) 121–124.

[14] J. Kost, S. Mitragotri, R. Langer, Phonophoresis, in: R.L. Bronaugh, H.I. Maibach (Eds.), Percutaneous Absorption, Drugs–Cosmetics–Mechanisms–Methodology, 3rd Edition, Marcel Dekker, Inc., New York and Basel, 1999, pp. 615–631.

[15] S. Mitragotri, Synergistic effect of enhancers for transdermal drug delivery, Pharm. Res. 17 (2000) 1354–1359.

[16] D. Bommannan, J. Tamada, L. Leung, R.O. Potts, Effect of electroporation on transdermal iontophoretic delivery of luteinizing hormone releasing hormone (LHRH) in vitro, Pharm. Res. 11 (1994) 1809–1814.

[17] S-L. Chang, G.A. Hofmann, L. Zhang, L.J. Deftos, A.K. Banga, The effect of electroporation on iontophoretic transdermal delivery of calcium regulating hormones, J. Controlled Release 66 (2000) 127–133.

[18] F. Izzo, C.C. Barnett, S.A. Curley, Radiofrequency ablation of primary and metastatic malignant liver tumors, Adv. Surg. 35 (2001) 225–250.

[19] S. Nahum Goldberg, Radiofrequency tumor ablation: principles and techniques, Eur. J. Ultrasound 13 (2001) 129–147.

[20] L. Solbiati, T. Ierace, M. Tonolini, V. Osti, L. Cova, Radiofrequency thermal ablation of hepatic metastases, Eur. J. Ultrasound 13 (2001) 149–158.

[21] F.J. McGovern, B.J. Wood, S. Nahum Goldberg, P.R. Mueller, Radiofrequency ablation of renal cell carcinoma via

image guided needle electrodes, J. Urol. 161 (1999) 599–600.
[22] Z. Avrahami, Transdermal Drug Delivery and Analyte Extraction, US Patent No. 6,148,232, (2000).
[23] S. Kudoh, T. Sato, H. Okada, H. Kumakura, H. Nakamura, Simultaneous determination of granisetron and 7-hydroxy-granisetron in human plasma by high-performance liquid chromatography with fluorescence detection, J. Chromatogr. B 660 (1994) 205–210.
[24] J.C. Weaver, Y.A. Chizmadzhev, Theory of electroporation: a review, Bioelectrochem. Bioenerg. 41 (1996) 135–160.
[25] R.R. Burnette, B. Ongpipattanakul, Characterization of the preselective properties of excised human skin during iontophoresis, J. Pharm. Sci. 76 (1987) 765–773.
[26] R. Panchagnula, K. Stemmer, W.A. Ritschel, Animal models for transdermal drug delivery, Meth. Find. Exp. Clin. Pharmacol. 19 (1997) 335–341.